



If you have discovered material in AURA which is unlawful e.g. breaches copyright, (either yours or that of a third party) or any other law, including but not limited to those relating to patent, trademark, confidentiality, data protection, obscenity, defamation, libel, then please read our [Takedown Policy](#) and [contact the service](#) immediately

From Uncontrolled to Control and then "Quasiliving" Cationic Ring-Opening
Polymerisation (C.R.O.P) of Oxetane by Activation Chain- End (A.C.E) Mechanism

by

Hassen Bouchékif

A thesis submitted for Degree

of

Doctor of Philosophy

of

The University of Aston in Birmingham

November 2002

This copy of the thesis has been supplied on condition that anyone who consults it is understood to recognise that its copyright rests with its author and that no quotation from the thesis and no information derived from it may be published without proper acknowledgement

ACKNOWLEDGMENTS

Firstly, I would like to take this opportunity to thank QinetiQ (DERA), whose funding of the project made this work possible.

I would like also to express my sincere thanks to my supervisor Dr. Allan Amass for his help and guidance during the past three years. In addition my thanks are extended to Dr. Mike Perry for running all my NMR samples. I also acknowledge the help received from David and Jane during their placement in the lab.

I also wish to express my gratitude to Drs. Eamon Colclough and Marcia Hohn from QinetiQ at Fort Halstead for their personal support and encouragement.

I also wish to thank all the people I have worked with in the lab including Alex, Bjeom, Cathy, Chris, David, Daphné, Gérald, Graham, Iris, James, Jane, Laurence, Peter, Pierre, Tristan, Olivia, Wendy and Yulia.

Science without virtue is immoral science. — Plato

427 - 347 B.C.E.

From Uncontrolled to Control and then "Quasiliving" Cationic Ring-Opening Polymerisation (C.R.O.P) of Oxetane by Activation Chain- End (A.C.E) Mechanism

Hassen Bouchékif

PhD 2002

SUMMARY

The cationic polymerisation of oxolane (tetrahydrofuran)^[184] and oxepane^[133] are often described as "living". Although studies of these monomers provided indisputable evidence of the absence of termination reactions, they have not allowed complete control over either \overline{Mn} or $\overline{Mw}/\overline{Mn}$ due to the 'ceiling' temperature^[96,102,203,207] and the occurrence of transfer reactions^[210]. The main characteristic of THF polymerisation is also found in the cationic polymerisation of epoxide^[180] and oxetane^[115,182,198] monomers, though transfer reactions occur more significantly. Polymerisation reactions with reversible equilibria between propagating and "dormant" species (so-called quasiliving^[306-313] and controlled^[39,44] polymerisation) are often used to suppress^[306-311] or to reduce^[39] side reactions unfavourable for the control of the polymerisation over \overline{Mn} or $\overline{Mw}/\overline{Mn}$. Our investigations of the mechanism of C.R.O.P of oxetane have shown that the use of ether additive such as 1,4-dioxane as solvent can prevent transfer reactions (back-biting, end-biting and intermolecular transfer reactions) at 35°C. Using a "living monomeric polyoxetane" initiator ($C_6H_5(CH_2)_3O^+(CH_2CH_2)_2O[SbF_6]^-$), polymers with narrow molecular weight distribution ($1.18 < \overline{Mw}/\overline{Mn} < 1.28$) were produced with no cyclic oligomer formation. The \overline{Mn} increased linearly with the monomer conversion and upon addition of further monomer, the existing polymers were extended correspondingly. High molecular weight materials ($\overline{Mn} = 160,000$ g/mol and $\overline{Mw}/\overline{Mn} = 1.2$) were produced successfully. On the basis of the kinetic data, a mechanism of quasiliving polymerisation has been proposed (see figure 1.0) in which the concentration of propagating [1] and dormant [2] species depend on the remaining concentration of oxetane.

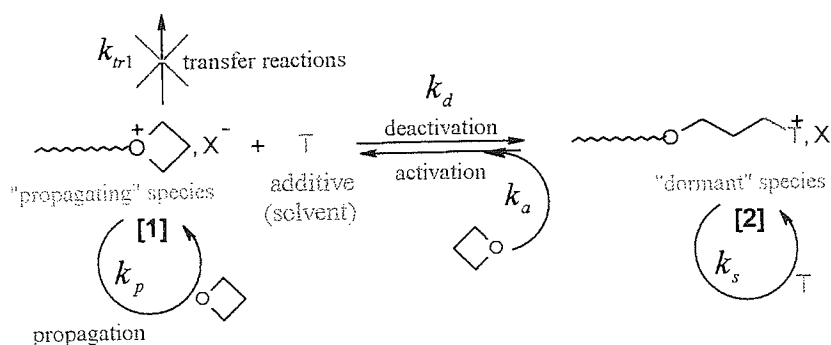


Figure 1.0: Formation of "dormant" species in quasiliving cationic ring-opening polymerisation of oxetane in the presence of ether additive T.

Further investigations showed that oxonium salts ([1] and [2]) in 1,4-dioxane are in the form of tight ions pairs and that the size of the counter-ions plays a significant role in the chemoselectivity of the polymerisation towards propagation, transfer reactions of the propagating species [1] and activation of the "dormant" species [2]. The mechanism of the above process was then discussed when different cationic initiator (alkylating and protonic initiator) and ether additive (tetrahydropyran, diphenyl ether and 1,6-dibenzyl-crown-6-ether) were employed. Other investigation showed that it is also possible to take advantage of the reversible end-capping reaction of the propagating reactions [1] by the ether additive (T) to prepare macrocyclic ether by end-biting reactions.

KEYWORDS: Polyoxetane, active chain end mechanism, cationic ring-opening polymerisation, living, quasiliving and control.

Table of Contents

1.1	Scope of the work.....	23
1.2	General principles of polymerisation	24
1.2.1	Living polymerisation	25
1.2.1.1	Characteristics of living polymerisation.....	26
1.3	Ring-opening polymerisation.....	27
1.3.1	Polymerisability.....	29
1.3.1.1	Thermodynamic treatment of ΔG°	29
1.3.1.2	Flory-Huggins treatment of ΔG°	30
1.3.1.3	Equilibrium polymerisation.....	32
1.3.1.4	Chemical and physical factors affecting the polymerisability of cyclic monomers	34
1.3.1.4.1	Chemical factors affecting the polymerisability of monomers	34
1.3.1.4.2	Physical factors affecting ΔG	38
1.3.2	Cationic ring-opening polymerisation of cyclic ethers	38
1.3.2.1	Structure and reactivity of propagating species.....	38
1.3.2.1.1	Structure of the propagation species.....	38
1.3.2.1.2	Reactivity of the propagation species.....	39
1.3.2.2	Type of initiator and mode of initiation	43
1.3.2.2.1	Initiation by protonation	44
1.3.2.2.1.1	Using organic and inorganic protonic acids	44
1.3.2.2.1.2	Using complexes of Friedel-Craft reagents with protogens	46
1.3.2.2.2	Initiation by alkylation and acylation	49
1.3.2.2.2.1	Initiation by FC reagents in conjunction with cationogens	49
1.3.2.2.2.1.1	Trialkyloxonium salt	51
1.3.2.2.2.1.2	1,3-dioxolan-2-ylum salts.....	53
1.3.2.2.2.1.3	Using dialkyl methylum salt.....	54
1.3.2.2.2.1.4	Oxacarbenium salts	55
1.3.2.2.2.2	Initiation by super acid esters	55
1.3.2.2.3	Initiation by Lewis Acids	57
1.3.2.2.4	Initiation by hydride transfer	59
1.3.2.2.5	Initiation using photo-initiators	60
1.3.2.2.5.1	Photo-initiated cationic polymerisation using iodonium, sulphonium and selenium salt	60
1.3.2.2.6	Electrolytic initiation	64

1.3.2.3	Mode of formation and structure of cyclic oligomers.....	64
1.3.2.3.1	Mode of formation of cyclic oligomers.....	65
1.3.2.3.2	Structure of cyclic oligomers.....	67
1.3.2.3.2.1	Epoxide monomers.....	67
1.3.2.3.2.2	Oxetanes monomers	71
1.3.2.3.3	Ring chain equilibrium.....	75
1.3.2.4	“Living” polymers in the cationic polymerisation of cyclic ether	77
1.3.2.5	Cationic ring opening polymerisation of cyclic ethers with an Activated Monomer Mechanism (A.M.M).....	79
1.3.3	Anionic polymerisation of cyclic ethers.....	82
1.3.3.1	Alkali-metal based catalyst.....	82
1.3.3.2	Coordination polymerisation of cyclic ethers.....	85
2.1	Vacuum line techniques.....	91
2.2	Treatment of the glassware.....	92
2.3	Freeze-thaw degassing of solvent.....	92
2.4	Trap to trap distillation.....	93
2.5	Schlenk techniques.....	93
2.6	Argon dry-box	93
2.7	Preparation and purification of material	94
2.7.1	Monomers.....	94
2.7.1.1	Oxetane (Ox)	94
2.7.1.2	Tetrahydropyran (THP)	94
2.7.1.3	1,4-Dioxane (1,4-Dox)	94
2.7.2	Solvents	95
2.7.2.1	Dichloromethane	95
2.7.2.2	Ethanol.....	96
2.7.3	Catalysts and co-catalysts.....	97
2.7.3.1	Boron trifluoride diethyl ether complex (BF ₃ OEt ₂)	97
2.7.3.2	Boron trifluoride acetic acid complex (BF ₃ (CH ₃ COOH) ₂)	97
2.7.3.3	Boron trifluoride methanol complex (BF ₃ MeOH)	97
2.7.3.4	Silver hexafluoroantimonate salt (AgSbF ₆).....	97
2.7.3.5	Silver boron tetrafluoride salt (AgBF ₄)	97
2.7.4	Initiators.....	97
2.7.4.1	3-Phenoxypropyl bromide (C ₆ H ₅ O(CH ₂) ₃ Br)	97
2.7.4.2	Chloromethyl ethyl ether (CH ₃ CH ₂ OCH ₂ Cl).....	98

2.7.4.3	Bromomethyl ethyl ether ($\text{CH}_3\text{CH}_2\text{OCH}_2\text{Br}$).....	98
2.7.5	Additives.....	98
2.7.5.1	Dibenzo-18-crown-6-ether (db18c6e).....	98
2.7.5.2	Diphenyl ether (DPE).....	98
2.7.5.3	Veratrole (Vrol).....	98
2.7.5.4	2,6-Di-t-butyl-pyridine (DtBP).....	98
2.7.6	General reagents.....	99
2.7.6.1	Calcium hydride.....	99
2.7.6.2	Sodium hydroxide.....	99
2.7.6.3	Sodium metal.....	99
2.7.6.4	Benzophenone.....	99
2.7.6.5	Magnesium sulfate.....	99
2.7.6.6	3 Å molecular sieves.....	99
2.7.7	Preparation of solutions.....	99
2.7.7.1	Initiating system solution.....	99
2.7.7.1.1	Preparation of protonic initiator solution.....	100
2.7.7.1.1.1	$\text{BF}_3(\text{CH}_3\text{COOH})_2/\text{BF}_3\text{OEt}_2$ solution.....	100
2.7.7.1.1.2	$\text{BF}_3:\text{MeOH}$ solution.....	100
2.7.7.1.2	Preparation of alkylating initiator solution.....	100
2.7.7.1.3	Preparation of monomer solution.....	100
2.8	Polymerisation procedure.....	101
2.8.1	Calorimeter experiments.....	101
2.8.1.1	Homopolymerisation of oxetane experiments.....	101
2.8.1.2	Termination of the polymerisation.....	102
2.8.2	Kinetic study by calorimetric analysis.....	103
2.8.2.1	Theory.....	103
2.8.2.2	Kinetic measurement.....	104
2.8.3	Sampling reactions using Omnifit fittings.....	105
2.9	Size exclusion chromatography.....	105
2.9.1	Apparatus.....	106
2.9.2	Theory.....	107
2.9.3	The intrinsic viscosity of a polymer is related to its molecular weight by the equation	109
2.10	Nuclear magnetic resonance spectroscopy.....	109
3.1	Polymerisation initiated by protonic acids.....	114

3.1.1	Effect of the concentration of oxetane.....	114
3.1.2	Effect of the concentration of initiating system	123
3.1.3	Effect of the addition of monomer solution to an active polymer solution.....	130
3.1.4	Characterisation of cyclic oligomers.....	134
3.1.4.1	GLC and mass spectroscopy analysis.....	134
3.1.4.2	^1H and ^{13}C NMR analysis.....	135
3.1.4.3	Rate of formation of cyclic oligomers.....	136
3.1.5	Nature of the initiating species involved in the initiation process.....	139
3.1.5.1	Dependence between rate of initiation and rate of propagation	145
3.1.5.1.1	Using (1:1) $\text{BF}_3\text{OEt}_2/\text{BF}_3(\text{AcOH})_2$ as initiating system	145
3.1.5.1.1.1	Rate of initiation	145
3.1.5.1.1.2	Rate of propagation	146
3.1.5.1.1.3	Discussion.....	147
3.1.5.1.2	Polymerisation using an excess of BF_3OEt_2 at constant concentration of oxetane and $\text{BF}_3(\text{AcOH})_2$	148
3.1.5.1.2.1	Rate of initiation	148
3.1.5.1.2.2	Rate of propagation	150
3.1.5.1.2.3	Discussion.....	150
3.1.5.1.3	Using an excess of $\text{BF}_3(\text{AcOH})_2$ at constant concentration of oxetane and BF_3OEt_2	151
3.1.5.1.3.1	Rate of initiation	151
3.1.5.1.3.2	Rate of propagation	152
3.1.5.1.3.3	Discussion.....	152
3.2	Polymerisation initiated by oxacarbeniums salts.....	153
3.2.1	Effect of the time on the polymerisation	154
3.3	Conclusions.....	158
4.1	Effect of dibenzo-18-crown-6-ether and veratrole on the cationic ring opening polymerisation of oxetane	165
4.1.1	Use of dibenzo-18-crown-6-ether as additive	165
4.1.2	Use of veratrole as additive	170
4.1.3	Nature of the initiating species when additives are used as co-initiator...	172
4.1.3.1	Using dbce/ $\text{BF}_3(\text{AcOH})_2/\text{BF}_3\text{OEt}_2$ as initiating system	172
4.1.3.2	Using dbce/ BF_3MeOH as initiating system.....	179
4.1.3.3	Using veratrole	180
4.2	Effect of diphenylether (dpe) on the cationic ring opening polymerisation of oxetane	181

4.2.1	Discussion.....	184
4.3	Conclusions.....	186
5.1	Introduction.....	189
5.1.1	Concept of quasiliving and controlled polymerisation.....	190
5.1.1.1	Quasiliving polymerisation and its development	191
5.1.1.2	Controlled polymerisation as a non-living process	193
5.1.2	Idea of controlling the polymerisation of oxetane.....	194
5.1.2.1	Chemoselectivity of the CROP of oxetane in the presence of ether additive by ACE mechanism.....	195
5.1.2.1.1	Solvation-desolvation effect.....	195
5.1.2.1.2	Chemoselectivity of the cationic ring-opening reaction of oxetane	198
5.1.2.2	Prediction of the kinetic profile of the proposed “quasiliving” model.....	201
5.1.2.2.1	Rate of interconversion between “active” and “dormant” species	201
5.1.2.2.2	Kinetic profile of the proposed quasiliving polymerisation model	203
5.1.2.2.2.1	Fast initiation process	203
5.1.2.2.2.2	Slow initiation process	205
5.2	Development of the “quasiliving” CROP of oxetane using ether derivative as solvent	206
5.2.1	Effect of 1,4-dioxane on the CROP of oxetane at 35 °C	207
5.2.1.1	Polymerisation initiated by protonic reagents (BF ₃ :MeOH).....	207
5.2.1.1.1	Polymerisation in dichloromethane.....	208
5.2.1.1.2	Polymerisation in 1,4-dioxane.....	212
5.2.1.1.3	Discussions	221
5.2.1.1.3.1	Nature of the initiating species during the initiation process	221
(a)	Slow initiation process in 1,4-dioxane	225
(b)	“Fast initiation” process in 1,4-dioxane	227
(c)	Mathematical expression of the rate of initiation.....	229
5.2.1.1.3.2	Mechanism of propagation of oxetane in 1,4-dioxane	230
5.2.1.2	Polymerisation initiated by alkylating reagents	235
5.2.1.2.1	Effect of the initiator and counter-anion on the polymerisation.....	237
5.2.1.2.1.1	Polymerisation initiated by the active salt I1	237
5.2.1.2.1.2	Polymerisation initiated by oxacarbenium salt end-capped by 1,4-dioxane ...	240
5.2.1.2.1.2.1	Polymerisation initiated by the active salts I2.....	244
5.2.1.2.1.2.2	Polymerisation initiated by the active salt I3.	246
5.2.1.2.2	Effect of the ratio $[Dox]_0/[Ox]_0$ on control of the polymerisation.....	250

5.2.1.2.3	Effect of the size of the counter-ions on the reactivity of the propagating species in 1,4-dioxane	253
5.2.2	CROP of oxetane in tetrahydropyran at 35°C	258
5.2.2.1	Kinetic study.....	261
5.2.2.1.1	^1H and ^{13}C NMR analysis.....	261
5.2.2.1.2	SEC analysis.....	262
5.2.2.2	Mechanism of polymerisation tetrahydropyran.....	265
5.3	Conclusions.....	268
6.1	Uncontrolled polymerisation of oxetane in dichloromethane at 35°C	273
6.1.1	Kinetic and mechanism studies	274
6.1.2	Transfer to polymers.....	278
6.1.2.1	Molecular weight studies.....	278
6.1.2.2	Intra- and intermolecular transfer reactions	279
6.1.3	Mode of formation of cyclic oligomers.....	279
6.1.4	Termination reaction	282
6.1.4.1	Effect of the counter-ion on the reactivity of the propagating species.....	282
6.2	Development of the quasiliving polymerisation of oxetane at 35 °C	283
6.2.1	Controlling CROP of oxetane at 35 °C.....	283
6.2.2	CROP of oxetane in 1,4-dioxane at 35 °C	284
6.2.2.1	Study of the C.R.O.P of oxetane when initiated by $\text{R}(1,4\text{-dioxane})^+[\text{SbF}_6]^-$..	285
6.2.2.2	Mechanism of the quasiliving CROP of oxetane in 1,4-dioxane	285
6.2.2.2.1	Control over \overline{Mn} and $\overline{Mw}/\overline{Mn}$	287
6.2.2.2.2	Factors affecting the quasiliving character of the polymerisation process	288
6.2.2.3	Study of the CROP of oxetane initiated by $\text{CH}_3\text{CH}_2\text{O}^+(\text{C}_2\text{H}_4)_2\text{O};[\text{BF}_4]^-$..	289
6.2.2.4	Study of the CROP of oxetane initiated by $\text{H}^+;[\text{CH}_3\text{O}:\text{BF}_3]^-$	290
6.2.2.5	Effect of the counter-ion on the copolymerisation of 1,4-dioxane with oxetane.	292
6.2.3	CROP of oxetane in tetrahydropyran.	293
6.3	Further work	294

Table of figures

Figure 1. 1: Living anionic polymerisation of styrene initiated by sodium naphthalide.	27
Figure 1. 2: Cationic and anionic ring opening process of ethylene oxide treated as an S_N2 reaction.....	28
Figure 1.3: Equilibrium volume fraction of polymer ϕ_2 in the bulk polymerisation of tetrahydrofuran.....	31
Figure 1. 4: Variation of equilibrium monomer concentration $[M]_e$ with polymer concentration $[P]$ for the polymerisation of.....	33
Figure 1. 5: Cationic initiation via oxonium site.	38
Figure 1. 6: Propagation via oxonium ion by A.C.E. mechanism.	39
Figure 1. 7: Propagation reaction of oxetane through S_N2 process via cationic polymerisation.	40
Figure 1. 8: Propagation reaction of oxirane with various substituents through S_N1 (a) and S_N2 (b) in the cationic polymerisation.	41
Figure 1. 9: Mechanism of intramolecular (back-biting (a) and end-biting (b)) and intermolecular (c) transfer reactions.	42
Figure 1. 10: The use of protonic acid for the initiation of cyclic ethers.....	44
Figure 1. 11: Mechanism of annihilations of the growing oxonium by non-complex counter anion.	44
Figure 1. 13: Initiation reaction of oxetane involving Brönstead acid HA and Friedel-Crafts reagents MtX_n	47
Figure 1. 14: Termination reaction in presence of water.	47
Figure 1. 15: Mechanism of formation of monohydrate complex, $BF_3 : H_2O$, and dehydrate complex, $BF_3 : 2(H_2O)$	48
Figure 1. 16: Termination reactions by anion-splitting during the course of polymerisation of oxetane.	49
Figure 1. 17: Initiation reaction involving hydrogen halides as the Brönstead acid and Friedel-Crafts acid M_tX_n	49
Figure 1. 18: Initiation involving organic halide RX with Friedel-Crafts reagents, MtX_n , and silver salt, $AgMtX_{n+1}$	50
Figure 1. 19: Formation of tetrahydrofuranium salt by action of $SbCl_5$ on 4-chloro-4'-ethoxybutylether.	51
Figure 1. 20: Initiation by triethyloxonium tetrafluoroborate.....	52
Figure 1.21: Initiation by dialkyloxycarbenium salt.....	52
Figure 1. 22: Preparation of 1,3-dioxolane-2-ylum salt by hydride transfer.	53
Figure 1. 23: Initiation by 1,3-dioxolane-2-ylum salt.....	54
Figure 1. 24: Initiation by dialkyl methylum salt.	54
Figure 1. 25: Initiation by oxacarbenium salt.	55
Figure 1. 26: Polymerisation of EO initiated by BF_3	58

Figure 1. 27: The use of a promotor molecule for the initiation of BCMO.....	58
Figure 1. 28: Polymerisation of THF initiated by SbCl_5	59
Figure 1. 29: Initiating species in the polymerisation of THF initiate by trityl salt.	59
Figure 1. 31: Initiating species in the polymerisation of THF initiate by diazonium salt.	60
Figure 1. 32: Group of photo-initiators developed by Crivello et al., reference 167.	61
Figure 1. 33: Mechanism of photolysis of diaryliodonium salts at $\lambda < 360$ nm (first pattern)..	61
Figure 1. 34: Mechanism of photolysis of dialkyl-4-hydroxyphenylsulphonium salts at $\lambda < 360$ nm (second pattern).	62
Figure 1. 35: Mechanism of photolysis of diaryliodonium salts at $\lambda > 360$ nm (normal sunlight) using photosensitizer	62
Figure 1. 36: Production of perchlorate acid by electrolysis.	64
Figure 1. 37: formation of low strain macrocyclic tertiary oxonium ion.	65
Figure 1. 38: Mode of elimination of the macrocyclic from the polymer chain end.	65
Figure 1. 39: Mechanism of formation of non-strained dioxanium ion in the polymerisation of trans 2,3-butene oxide.	66
Figure 1. 40: Mechanism of redistribution of linear chain length by intermolecular transfer reactions.	67
Figure 1. 42: Mechanism of formation of isomerised side product through $\text{S}_{\text{N}}1$ mechanism.	69
Figure 1. 43: Direct ring opening expansion mechanism for the formation of cyclic oligomers larger than 1,4-dioxane. This scheme illustrates the formation of 12-crown-4-ether and 9-crown-3-ether.	70
Table 1. 9: Effect of the initiating system on the most abundant produced cyclic ethers. Solvent: (a) 1,2-dichloroethane or benzen, (b) dichloromethane, (c) methylchloride.	71
Figure 1. 44: Mode of formation of cyclic oligomers by end-biting transfer reaction.	72
Figure 1. 46: Mode of formation of cyclic dimer in the polymerisation of cyclopentene by metathesis polymerisation.	76
Figure 1. 47: Mechanism of acid alcoholysis of oxirane.	79
Figure 1. 48: Mechanism of propagation by Activation Monomer Mechanism A.M.M.	80
Figure 1. 49: Mode of formation of cyclic oligomers when polymerisation of oxirane proceeds mostly by AMM.	81
Figure 1. 51: Mechanism of anionic propagation of oxirane via free ions and ion-pairs.	83
Figure 1. 52: Mechanism of proton abstraction from the monomer by the growing alkoxyd anion.	84
Figure 1. 53: The coordinated anionic mechanism of the polymerisation of ethylene oxide.	85
Figure 1. 54: Coordinated metalloporphyrin based catalysts with isolated monuclear metal.	86
Figure 1. 55: Mechanism of polymerisation of ethylene oxide with (TPP)AlCl.	87
Figure 1. 56: Rapid exchange between the growing polymers attached to the catalyst and the dead ones possessing the OH end group.	88

Figure 2. 1: The vacuum line.....	91
Figure 2. 2: Storage flasks used.....	95
Figure 2. 3: Dichloromethane still.....	96
Figure 2. 4: Calorimeter.....	102
Figure 2. 6: Dependence of $\frac{1}{V} \cdot \frac{dT}{dt}$ on $-\frac{d[Ox]}{dt}$	105
Figure 2. 7: Size exclusion chromatograph.....	106
Figure 2. 8: Typical S.E.C. trace.....	107
Figure 2. 9: Calibration curve for S.E.C. using polystyrene standards.....	109
Figure 3. 1: Dependence of rate of polymerization on $[Ox]_0$	116
Figure 3. 2: Dependence of $\ln([Ox]_0/[Ox]_t)$ against time for the homopolymerisation of oxetane in dichloromethane at 35 °C.....	116
Figure 3. 3: Dependence of $\ln([Ox]_0/[Ox]_t)$ against time by calorimetric and gravimeter analysis.....	117
Figure 3. 4: Side reactions involved in the polymerisation of oxetane initiated by $BF_3(AcOH)_2/BF_3OEt_2$ in dichloromethane at 35 °C.....	118
Figure 3. 5: Dependence \overline{Mn} , Mp and $\overline{Mw}/\overline{Mn}$ on monomer conversion.....	121
$[Ox]_0 = 0.68$ M and $[I] = 0.0065$ M. $[I]_0 = [BF_3(AcOH)_2]_0 = [BF_3(AcOH)_2]_0$ (table 3.5 series S 3.13 and annex 3.5).	121
Figure 3. 6: : Dependence \overline{Mn} , Mp and $\overline{Mw}/\overline{Mn}$ on monomer conversion.....	121
Figure 3. 7: Dependence Mp over $[Ox]_0$ obtained at high monomer conversion.....	122
Figure 3. 8: Effect of the concentration of the initiating system $BF_3OEt_2/BF_3(AcOH)_2$ (1:1) on the rate of the monomer consumption	123
Figure 3. 9: Effect of the $[BF_3OEt_2]_0$ on the rate of monomer consumption in dichloromethane at 35 °C.	124
Figure 3. 11: Dependence of $\ln([M]_0/[M]_t)$ against time at various concentration of initiator. Polymerisation carried out in dichloromethane at 35 °C.....	126
Figure 3. 12: Dependence of $\ln([M]_0/[M]_t)$ against time at various concentration of $BF_3(AcOH)_2$. Polymerisation carried out in dichloromethane at 35 °C.	127
Figure 3. 13: Dependence of $\ln([M]_0/[M]_t)$ against time at various concentration of BF_3OEt_2 . Polymerisation carried out in dichloromethane at 35 °C.....	127
Figure 3. 14: Dependence of $\ln([M]_0/[M]_t)$ against time at various concentration of $BF_3(AcOH)_2$. Polymerisation carried out in dichloromethane at 35 °C.	128
Figure 3. 15: Dependence of $(1/Mp)$ against $[BF_3(AcOH)_2]_0$ for the homopolymerisation of oxetane in dichloromethane at 35 °C (table 3.2 series S 3.6).	129
Figure 3. 16: Dependence of $(1/Mp)$ against $[BF_3(AcOH)_2]_0$ for the homopolymerisation of oxetane in dichloromethane at 35 °C.....	129

Figure 3. 17: Dependence of $(1/M_p)$ against $[\text{BF}_3\text{OEt}_2]_0$ for the homopolymerisation of oxetane in dichloromethane at 35 °C. $[\text{Ox}]_0 = 1$ and $[\text{BF}_3(\text{AcOH})_2]_0 = 0.00435 \text{ M}$.	130
Figure 3. 18: Rate of the polymerisation after monomer addition.	131
Figure 3. 20: Proportions of cyclic oligomers produce throughout the polymerisation process.	136
Figure 3. 21: Proportions of cyclic oligomers produce through the polymerisation process.	138
Figure 3. 22: Proportions of cyclic oligomers produce through the polymerisation process.	138
Figure 3. 23: Proportions of cyclic oligomers produce throughout the polymerisation process.	139
Figure 3. 24: Mechanism of initiation of oxetane catalysed by BF_3 with H_2O .	139
Figure 3. 25: Nature of initiating species formed in dichloromethane in presence of $\text{BF}_3(\text{AcOH})_2$ and BF_3OEt_2 .	140
Figure 3. 26: Mechanism of esterification of carboxylic acid catalysed by BF_3 .	141
Figure 3. 27: State of equilibrium between initiating species in dichloromethane.	141
Figure 3. 28: Formation of boron trifluoride oxetane complex.	142
Figure 3. 29: Mechanism of initiation after addition of the initiating system solution into monomer solution.	143
Figure 3. 30: Mode of formation of 1:1 boron trifluoride acetic acid complex during the polymerisation process.	144
Figure 3. 31: Mechanism of transfer reaction to the co-catalyst.	144
Figure 3. 32: Concentration of initiating species when an equimolar solution of BF_3OEt_2 and $\text{BF}_3(\text{AcOH})_2$ is prepared in dichloromethane	145
Figure 3. 33: Dependence $(R_p)_{\text{max}}/[M]_0$ against $[\text{I}]_0 = [\text{BF}_3(\text{AcOH})_2]_0 = [\text{BF}_3\text{OEt}_2]_0$	147
Figure 3. 34: Concentration of initiating species in dichloromethane when an excess of BF_3OEt_2 is used in relation to the concentration of $\text{BF}_3(\text{AcOH})_2$.	149
Figure 3. 35: Concentration of initiating species when an excess of $\text{BF}_3(\text{AcOH})_2$ was used in relation to the concentration of BF_3OEt_2 .	151
Figure 3. 36: Mechanism of hydrolysis of oxacarbenium salts and formation of protonic initiator salts.	154
Figure 3. 37: Neutralisation of protonic initiator by 2,6-di- <i>t</i> -butyl-pyridine (DtBP).	154
Figure 3. 38: Basicity of the different nucleophilic reagents when the polymerisation is initiated by protonic initiator or oxacarbenium salts.	155
Figure 3. 39: Mechanism of polymerisation of oxetane in dichloromethane using $[\text{EtOCH}_2]^+[\text{BF}_4]^-$ as initiator at 35 °C.	156
Figure 3. 40: Dependence \overline{Mn} and $\overline{Mw}/\overline{Mn}$ over monomer conversion obtained using protonic and oxacarbenium salts as initiator.	157
Figure 3. 41: Effect of the initiator and counter-ion on the cyclic oligomers formation in dichloromethane at 35 °C.	157

Figure 4. 1: Evolution of \overline{Mn} and Q(SEC) with conversion.....	167
Figure 4. 2: Evolution of \overline{Mn} with conversion when the polymerisation is carried out without and with dbce according to the method 2	167
Figure 4. 3: Mechanism of cyclic oligomers (tetramer) formation by end-biting reactions in starving monomer solution.	168
Figure 4. 4: Mechanism of copolymerisation of oxetane with dbce when the polymerisation is carried out according to the method 1.	169
Figure 4. 5: Proportion of cyclic oligomers, Q(SEC), produced throughout the polymerisation using different initiators.....	173
Figure 4. 6: Mode of formation of boron trifluoride dibenzo-18-crown-6-ether complex....	173
Figure 4. 7: Chemical reactions involved when $\text{BF}_3(\text{AcOH})_2$, BF_3OEt_2 and dibenzo-18-crown-6-ether are mixed in dichloromethane at 35 °C.....	174
Figure 4. 8: Chemical reactions evolved when $\text{BF}_3(\text{AcOH})_2$, BF_3OEt_2 and dibenzo-18-crown-6-ether are mixed in dichloromethane at 35 °C.	175
Figure 4. 9: Mechanism of initiation after addition of the initiating system solution into monomer solution.	176
Figure 4. 10: Nature of initiating species when $\text{BF}_3(\text{AcOH})_2$, BF_3OEt_2 and dibenzo-18-crown-6-ether are mixed in dichloromethane at 35 °C (method 2). X = -OH or -Oac.....	177
Figure 4. 11: Mechanism of copolymerisation of dbce during the formation of cyclic oligomer by end-biting reactions when dbce is used as co-initiator (method 2)	178
Figure 4. 12: Mechanism of copolymerisation of dbce during the formation of cyclic oligomer by ring-opening expansion reactions when dbce is used as co-monomer (method 1).	178
Figure 4. 13: Mechanism of copolymerisation of dbce during the formation of cyclic oligomers by back-biting reactions when dbce is used as co-monomer (method 2).	179
Figure 4. 14: Mechanism of initiation of polymerisation of oxetane using $\text{BF}_3\text{:MeOH}$ as initiator and dibenzo-18-crown-6-ether as co-initiator.....	179
Figure 4. 15: Nature of initiating species when $\text{BF}_3(\text{AcOH})_2$, BF_3OEt_2 and veratrole are mixed in dichloromethane at 35 °C according to the method 2. X = -OH or -Oac.	180
Figure 4. 5: Evolution of Q and $(dT/dt)_{\text{max}}$ with the increase of concentration of dpe. Polymerisation carried out in DCM at 35 °C using an equimolar solution of $\text{BF}_3(\text{AcOH})_2/\text{BF}_3\text{OEt}_2$ as initiating system.....	182
Figure 4. 6: Evolution of \overline{Mn} and $\overline{Mw}/\overline{Mn}$ with the increase of the ratio $[\text{dpe}]_0/[\text{Ox}]_0$	183
Figure 4. 7: Basicity of different nucleophilic reagents in the polymerisation medium.	184
Figure 4. 8: Mechanism of polymerisation of oxetane in the presence of dpe in DCM at 35 °C. Polymerisation initiated by an equimolar solution of $\text{BF}_3(\text{AcOH})_2/\text{BF}_3\text{OEt}_2$	185
Figure 5. 1: Mechanism of the cationic polymerisation of oxetane.....	189
Figure 5. 2: Scheme of polymerisation process where “dormant” and “active” species are in dynamic equilibrium.	190
Figure 5. 3: Nature of the growing centres on the quasiliving polymerisation of vinylic monomers.....	191

Figure 5. 4: Formation of an oxonium ion in the polymerization of vinyl ethers initiated by $\text{Al}(\text{C}_2\text{H}_5)_3$ in the presence of 1,4-dioxane.	192
Figure 5. 5: Control radical polymerisation of vinylic monomer in the presence of nitroxide (persistent radical).....	193
Figure 5. 6: Formation of dormant species in quasiliving polymerisation of oxetane in the presence of additive T.....	194
Figure 5. 7: Nucleophilicity order of oxygen atom in the polymer and monomer.	195
Figure 5. 8: Reaction diagram of the second initiation stage of oxetane through $\text{S}_{\text{N}}2$ mechanism.	196
Figure 5. 9: Dependence of \overline{Mn} on conversion and $\text{Ln}([\text{Ox}]_0/[\text{Ox}]_t)$ on time for fast initiation process.	205
Figure 5. 10: Dependence of \overline{Mn} on conversion and $\text{Ln}([\text{Ox}]_0/[\text{Ox}]_t)$ on time for slow initiation.	206
Figure 5. 11: Basicity of cyclic ether measured by IR measurement referred to the literature. ...	207
Figure 5. 12: Evolution of $\text{Ln}([\text{Ox}]_0/[\text{Ox}]_t)$ against time when 1 M of oxetane is polymerised by 0.0077 M of BF_3MeOH in dichloromethane at 35 °C.	210
Figure 5. 13: Evolution \overline{Mn} against conversion when 1 M of oxetane is polymerised in dichloromethane.....	210
Figure 5. 14: Evolution \overline{Mn} after monomer addition.....	211
Figure 5.15: Reaction of redistribution of the growing polymer chains issues from intermolecular transfer reactions in dichloromethane.	212
Figure 5. 16: Mechanism of incorporation of 1,4-dioxane into polymer chains.	213
Figure 5. 17: Evolution of $\text{Ln}([\text{Ox}]_0/[\text{Ox}]_t)$ against time.....	218
Figure 5. 18: Evolution of \overline{Mn} and $\overline{Mw}/\overline{Mn}$ against % conversion.....	219
Figure 5. 19: Evolution of $\overline{Mn}_{(\text{SEC})}$ against $\overline{Mn}_{(\text{theory})}$	220
Figure 5. 20: Evolution \overline{Mn} and $\overline{Mw}/\overline{Mn}$ against conversion.	220
Figure 5. 21: Nature of initiating species when $\text{BF}_3\text{:MeOH}$ complex is in solution in dichloromethane.....	222
Figure 5. 22: Formation of trifloroborane oxetane complex.	223
Figure 5. 23: Mechanism of initiation after addition of $\text{BF}_3\text{:MeOH}$ solution into monomer solution.....	223
Figure 5. 24: Formation of boron trifluoride oxetane complex and boron trifluoride 1,4-dioxane complex.	225
Figure 5. 25: Mechanism of the “slow” initiation process when $\text{BF}_3\text{:MeOH}$ in solution dichloromethane is injected into monomer solution in 1,4-dioxane.....	226
Figure 5. 26: Mechanism of “fast” initiation after addition of $\text{BF}_3\text{:MeOH}$ solution into monomer solution in 1,4-dioxane.	228

Figure 5. 27: Termination reactions in cationic polymerisation.....	231
Figure 5. 28: Mechanism of polymerisation of oxetane in 1,4-dioxane.....	232
Figure 5. 29: Mechanism of reactivation of “dormant” species by oxetane via S _N 2 process.....	232
Figure 5. 30: Mechanism of end-biting reaction in 1,4-dioxane	233
Figure 5.31: Mechanism of the controlled polymerisation of oxetane in 1,4-dioxane initiated by BF ₃ ·MeOH at 35 °C.	234
Figure 5. 32: Interconversion between “active” and “dormant” species catalysed by BCl ₃	235
Figure 5. 33: Examples of active salts active in cationic polymerisation.....	236
Figure 5. 34: Active salts used in this study.	236
Figure 5. 35: Preparation of the active salts.....	237
Figure 5. 36: Evolution \overline{Mn} and $\overline{Mw}/\overline{Mn}$ against conversion.....	238
Figure 5. 37: Evolution of \overline{Mn} and $\overline{Mw}/\overline{Mn}$ after monomer addition	239
Figure 5. 38: Evolution of $\text{Ln}([Ox]_o/[Ox]_t)$ against time.....	239
Figure 5. 39: Mechanism of formation of active salts I2 and I3 in dry and freshly distilled 1,4-dioxane at room temperature.	241
Figure 5. 40: Mechanism of formation of “living monomeric polyoxetane” initiator I1 in dry and freshly distilled 1,4-dioxane at room temperature. Competition between S _N 2 and E2 reactions.	242
Figure 5. 41: Evolution of \overline{Mn} and $\overline{Mw}/\overline{Mn}$ after monomer addition.	244
Figure 5. 42: Evolution of $\text{Ln}([Ox]_o/[Ox]_t)$ against time.....	245
Figure 5.43: Evolution of \overline{Mn} and $\overline{Mw}/\overline{Mn}$ after monomer addition when 1 M of oxetane is polymerised in 1,4-dioxane using 0.0025 M of the active salt (I3) at 35°C.	246
Figure 5. 44: Evolution of $\text{Ln}([Ox]_o/[Ox]_t)$ against time when 1 M of oxetane is polymerised by 0.0077 M of the active salt (I3) at 35°C. Table 5.8 series S 5.10.	247
Figure 5.45: Evolution of \overline{Mn} and $\overline{Mw}/\overline{Mn}$ after monomer addition when 1 M of oxetane is polymerised in 1,4-dioxane using 0.0025 M of the active salt (I3) at 35°C.	249
Figure 5.46: Effect of the ratio $[Dox]_0/[Ox]_0$ on the slop of \overline{Mn} against conversion when the polymerisation is initiated by I1 at 35°C. [M] = 1 M and [I1] = 0.0025M.	251
Figure 5. 47: Effect of the ratio on the slop of \overline{Mn} against conversion when the polymerisation is initiated by I3 at 35 °C. [Ox] ₀ = 1 M and [I] ₀ = 0.0025M.....	252
Figure 5. 48: Instantaneous fraction of cyclic oligomers, Q, produced during the polymerisation initiated by CH ₃ CH ₂ OCH ₂ O ⁺ (C ₂ H ₄) ₂ O, ₂ [BF ₄] ⁻	253
Figure 5.49: Instantaneous mole fractions of 1,4-dioxane incorporated into the polymer, % _{mole} Dox , plotted against the conversion in oxetane.....	254
Figure 5. 50: Mechanism of quasiliving polymerisation of oxetane in 1,4-dioxane at 35 °C.	255

Figure 5.51: Mechanism of controlled polymerisation of oxetane in 1,4-dioxane initiated by $\text{CH}_3\text{CH}_2\text{O}^+(\text{C}_2\text{H}_4)_2\text{O};[\text{BF}_4]^-$.	257
Figure 5. 52: Initiator used for the polymerisation of oxetane in tetrahydropyran at 35°C.	258
Figure 5.53: Mole fraction in percent of additive incorporated into the polymer during the polymerisation process, $\%_{\text{mol}} A$, plotted against the conversion of oxetane.	262
Figure 5. 54: Evolution of \overline{Mn} and $\overline{Mw}/\overline{Mn}$ with \overline{Mn} (theory) in the cationic polymerisation of oxetane initiated by I4 in THP at 35 °C.	264
Figure 5.55: Evolution of \overline{Mn} and $\overline{Mw}/\overline{Mn}$ with $\overline{Mn}_{(\text{theory})}$ in the cationic polymerisation of oxetane in THP by BF_3MeOH .	265
Figure 5. 56: Mechanism of cationic ring-opening polymerisation of oxetane in tetrahydropyran at 35 °C.	266
Figure 5.57: Ion-pairs and free ions in equilibrium during the polymerisation of oxetane in tetrahydropyran at 35 °C.	267
Figure 6. 1: Mechanism of the cationic polymerisation of oxetane.	275
Figure 6. 2: Mechanism of formation of non-strained tertiary oxonium ions by back-biting reactions and ring opening expansion reaction.	281
Figure 6. 3: Formation of “dormant” species in quasiliving polymerisation of oxetane in the presence of additive T.	283
Figure 6. 4: Basicity of cyclic ether measured by IR measurement referred to the literature.	284
Figure 6. 5: Mechanism of polymerisation of oxetane in 1,4-dioxane.	286
Figure 6. 6: Mechanism of controlled polymerisation of oxetane in 1,4-dioxane initiated by $\text{CH}_3\text{CH}_2\text{O}^+(\text{C}_2\text{H}_4)_2\text{O};[\text{BF}_4]^-$.	290
Figure 6.7: Mechanism of controlled polymerisation of oxetane in 1,4-dioxane initiated by $\text{H}^+;[\text{CH}_3\text{O}:\text{BF}_3]^-$.	291
Figure 6. 8: Mechanism of reactivation of “dormant” species by oxetane via $\text{S}_{\text{N}}2$ process.	292

List of Annexes

Annex 3. 1: Typical S.E.C chromatogram of polyoxetane - Bimodal distribution.	297
Annex 3. 2: S.E.C chromatogram of polyoxetane materials obtained at high monomer conversion for different concentration of oxetane. Polymerisation carried out in dichloromethane at 35 °C. $[\text{BF}_3(\text{AcOH})_2]_0 = [\text{BF}_3(\text{AcOH})_2]_0 = 0.0065 \pm 0.005 \text{ M}$	298
Annex 3. 3: S.E.C chromatogram of polyoxetane materials obtained at High and low monomer conversion for a different concentration of oxetane. Polymerisation carried out in dichloromethane at 35 °C. $[\text{BF}_3(\text{AcOH})_2]_0 = [\text{BF}_3(\text{AcOH})_2]_0 = 0.0065 \pm 0.005 \text{ M}$	299
Annex 3. 4: S.E.C chromatogram of polymer obtained at different monomer conversion. Polymerisation carried in dichloromethane at 35°C. $[\text{Ox}]_0 = 1 \text{ M}$ and $[\text{BF}_3(\text{AcOH})_2]_0 = [\text{BF}_3(\text{AcOH})_2]_0 = 0.005 \text{ M}$ (table 3.5, series S 3.12).	299
Annex 3. 5: S.E.C chromatogram of polymer obtained at different monomer conversion. Polymerisation carried in dichloromethane at 35°C. $[\text{Ox}]_0 = 0.65 \text{ M}$ and $[\text{BF}_3(\text{AcOH})_2]_0 = [\text{BF}_3(\text{AcOH})_2]_0 = 0.0065 \text{ M}$ (table 3.5, series S 3.13).	300
Annex 3. 6: S.E.C chromatogram of polyoxetane materials obtained at high and low monomer conversion for a different concentration of $\text{BF}_3(\text{CH}_3\text{COOH})_2/\text{BF}_3\text{OEt}_2$ (1/1). Polymerisation carried out in dichloromethane at 35 °C. $[\text{Ox}]_0 = 1.07 \text{ M}$ and $0.00171 < [\text{I}]_0 < 0.00739 \text{ M}$ (table 3.2, series S 3.6).	301
Annex 3. 7: S.E.C chromatogram of polymer obtained at high monomer conversion for a different concentration of $\text{BF}_3(\text{CH}_3\text{COOH})_2/\text{BF}_3\text{OEt}_2$ (1/1). Polymerisation carried out in dichloromethane at 35 °C. $[\text{Ox}]_0 = 1.07 \text{ M}$ and $0.00171 < [\text{I}]_0 < 0.00739 \text{ M}$ (table 3.2, series S 3.6).	302
Annex 3. 8: S.E.C chromatogram of polymer obtained at high monomer conversion for a different concentration of BF_3OEt_2 . Polymerisation carried out in dichloromethane at 35 °C. $[\text{Ox}]_0 = 1.07 \text{ M}$, $[\text{BF}_3(\text{AcOH})_2]_0 = 0.00435 \text{ M}$ and $0.00171 < [\text{BF}_3\text{OEt}_2]_0 < 0.00739 \text{ M}$ (table 3.2, series S 3.7).	302
Annex 3. 9: S.E.C chromatogram of polymer obtained at high and low monomer conversion for a different concentration of BF_3OEt_2 . Polymerisation carried out in dichloromethane at 35 °C. $[\text{Ox}]_0 = 1.07 \text{ M}$, $[\text{BF}_3(\text{AcOH})_2]_0 = 0.00435 \text{ M}$ and $0.00171 < [\text{BF}_3\text{OEt}_2]_0 < 0.00739 \text{ M}$ (table 3.2, series S 3.7).	303
Annex 3. 10: S.E.C chromatogram of polyoxetane materials obtained at high monomer conversion for a different concentration of $\text{BF}_3(\text{AcOH})_2$. Polymerisation carried out in dichloromethane at 35 °C. $[\text{Ox}]_0 = 1.07 \text{ M}$, $[\text{BF}_3\text{OEt}_2]_0 = 0.00453 \text{ M}$ and $0.0043 < [\text{BF}_3(\text{AcOH})_2]_0 < 0.00179 \text{ M}$ (table 3.2, series S 3.8).	304
Annex 3. 12: S.E.C chromatogram of polyoxetane materials obtained at high monomer conversion for a different concentration of $\text{BF}_3(\text{AcOH})_2$. Polymerisation carried out in dichloromethane at 35 °C. $[\text{Ox}]_0 = 1.07 \text{ M}$, $[\text{BF}_3\text{OEt}_2]_0 = 0 \text{ M}$ and $0.0145 < [\text{BF}_3(\text{AcOH})_2]_0 < 0.00491 \text{ M}$ (table 3.2, series S 3.9).	305
Annex 3. 13: S.E.C chromatogram of polyoxetane materials obtained at high and low monomer conversion for a different concentration of $\text{BF}_3(\text{AcOH})_2$. Polymerisation carried out in dichloromethane at 35 °C. $[\text{Ox}]_0 = 1.07 \text{ M}$, $[\text{BF}_3\text{OEt}_2]_0 = 0 \text{ M}$ and $0.0145 < [\text{BF}_3(\text{AcOH})_2]_0 < 0.00491 \text{ M}$ (table 3.2, series S 3.9).	305

Annex 3. 14: SEC chromatogram of polyoxetane after a tentative of extension of polymer chain length by monomer addition on active polymer solution after full monomer conversion. Polymerisation carried out in dichloromethane at 35 °C (table 3.3, series S 3. 10 and S 3.11)..	306
Annex 3. 15: SEC chromatogram of the extracted cyclic oligomers with cyclohexane.....	306
Annex 3. 16: GLC chromatogram of cyclic oligomers extracted with cyclohexane.....	307
Annex 3. 18: TGA analysis of polyoxetane.....	309
Annex 3. 19: ^1H NMR spectrum of cyclic oligomers extracted with cyclohexane. Polymer prepared in dichloromethane at 35 °C. $[\text{Ox}]_0 = 1 \text{ M}$ and $[\text{BF}_3(\text{AcOH})_2]_0 = [\text{BF}_3(\text{AcOH})_2]_0 = 0.005 \text{ M}$ (table 3.5, series S 3.11.7).	310
Annex 3. 20: ^{13}C NMR spectrum of cyclic oligomers extracted with cyclohexane. Polymer prepared in dichloromethane at 35 °C. $[\text{Ox}]_0 = 1 \text{ M}$ and $[\text{BF}_3(\text{AcOH})_2]_0 = [\text{BF}_3(\text{AcOH})_2]_0 = 0.005 \text{ M}$ (table 3.5, series S 3.11.7).	311
Annex 3. 21: S.E.C chromatogram of polymer obtained at different monomer conversion. Polymerisation carried in dichloromethane at 35°C. $[\text{Ox}]_0 = 1 \text{ M}$ and $[\text{CH}_3\text{OCH}_2^+, [\text{BF}_4]^-]_0 = 0.003 \text{ M}$ (table 3.6, series S 3.14).	312
Annex 3. 22: S.E.C chromatogram of polymer obtained at different monomer conversion. Polymerisation carried in dichloromethane at 35°C. $[\text{Ox}]_0 = 1 \text{ M}$ and $[\text{CH}_3\text{OCH}_2^+, [\text{SbF}_6]^-]_0 = 0.003 \text{ M}$ (table 3.6, series S 3.15).	312
Annex 3. 23: SEC chromatograms of polyoxetane before and after degradation if pH is not neutralised when the polymerisation is terminated.....	313
Annex 4. 1: S.E.C chromatogram of polymer obtained at different monomer conversion when dbce is used as co-initiator. Polymerisation carried in dichloromethane at 35°C. $[\text{Ox}]_0 = 1 \text{ M}$ and $[\text{BF}_3(\text{AcOH})_2]_0 = [\text{BF}_3(\text{AcOH})_2]_0 = 0.0065 \text{ M}$ and $[\text{dbce}]_0 = 0.1235$ (table 4.1, series S 4.3).	313
Annex 4. 2: ^1H NMR spectra of polymer obtained at different monomer conversion using dbce as co-initiator. Polymerisation carried in dichloromethane at 35°C. $[\text{Ox}]_0 = 1 \text{ M}$ and $[\text{BF}_3(\text{AcOH})_2]_0 = [\text{BF}_3(\text{AcOH})_2]_0 = 0.0065 \text{ M}$ and $[\text{dbce}]_0 = 0.1235$ (table 4.1, series S 4.3)....	314
Annex 4. 3: ^{13}C NMR spectra of polymer obtained at different monomer conversion using dbce as co-initiator. Polymerisation carried in dichloromethane at 35°C. $[\text{Ox}]_0 = 1 \text{ M}$ and $[\text{BF}_3(\text{AcOH})_2]_0 = [\text{BF}_3(\text{AcOH})_2]_0 = 0.0065 \text{ M}$ and $[\text{dbce}]_0 = 0.1235$ (table 4.1, series S 4.3)....	315
Annex 4. 4: S.E.C chromatogram of poly(oxetane-co-dbce) using UV detector at $\lambda = 277 \text{ nm}$. Polymerisation carried in dichloromethane at 35°C using dbce as co-initiator. $[\text{Ox}]_0 = 1 \text{ M}$ and $[\text{BF}_3:\text{MeOH}]_0 = 0.008 \text{ M}$ and $[\text{dbce}]_0 = 0.0148 \text{ M}$ (table 4.2, series S 4.5).....	316
Annex 4. 5: S.E.C chromatogram of polymer obtained at different monomer conversion. Polymerisation carried in dichloromethane at 35°C. $[\text{Ox}]_0 = 1 \text{ M}$ and $[\text{BF}_3:\text{MeOH}]_0 = 0.008 \text{ M}$ (table 4.2, series S 4.4).	316
Annex 4. 6: S.E.C chromatogram of polymer obtained at different monomer conversion using dbce as co-initiator. Polymerisation carried in dichloromethane at 35°C. $[\text{Ox}]_0 = 1 \text{ M}$ and $[\text{BF}_3:\text{MeOH}]_0 = 0.008 \text{ M}$ and $[\text{dbce}]_0 = 0.0148 \text{ M}$ (table 4.2, series S 4.5).	317

Annex 4. 7: S.E.C chromatogram of polymer obtained at various concentration of dpe. Polymerisation carried in dichloromethane at 35°C. $[Ox]_0 = 1\text{ M}$ and $[BF_3:MeOH]_0 = 0.008\text{ M}$ and $0.05 < [dpe]_0 < 0.9\text{ M}$ (table 4.5, series S 4.8).....	318
Annex 4. 8: 1H NMR spectra of polymer obtained at various concentration of dpe. Polymerisation carried in dichloromethane at 35°C. Polymerisation carried in dichloromethane at 35°C. $[Ox]_0 = 1\text{ M}$ and $[BF_3:MeOH]_0 = 0.008\text{ M}$ and $0.05 < [dpe]_0 < 0.9\text{ M}$ (table 4.5, series S 4.8).....	319
Annex 4. 9: ^{13}C NMR spectra of polymer obtained at various concentration of dpe in dichloromethane at 35°C. $[Ox]_0 = 1\text{ M}$ and $[BF_3:MeOH]_0 = 0.008\text{ M}$ and $0.05 < [dpe]_0 < 0.9\text{ M}$ (table 4.5, series S 4.8).....	320
Annex 5. 1: ^{13}C NMR spectra of polymer obtained throughout the polymerisation in dichloromethane at 35°C. $[Ox]_0 = 1\text{ M}$ and $[BF_3:MeOH]_0 = 0.008\text{ M}$. Table 4.4 and 5.4, series S 4.4.	321
Annex 5. 2: 1H NMR spectra of polymer obtained throughout the polymerisation in dichloromethane at 35°C. $[Ox]_0 = 1\text{ M}$ and $[BF_3:MeOH]_0 = 0.008\text{ M}$. Table 4.4 and 5.4, series S 4.4.	322
Annex 5. 3: SEC chromatogram of polyoxetane after a tentative of extension of polymer chain length by monomer addition on active polymer solution after full monomer conversion. Polymerisation carried out in dichloromethane at 35 °C. (table 5.2, series S 5. 1).	323
Annex 5. 4: Calorimetric analysis. Trace of deflection temperature against time when the polymerisation of oxetane proceeds in dichloromethane at 35 °C. $[Ox] = 1\text{ M}$ and $[BF_3MeOH] = 0.0077\text{ M}$	323
Annex 5. 5: Calorimetric analysis. Trace of deflection temperature against time when the polymerisation of oxetane proceeds in 1,4-dioxane at 35 °C. $[Ox] = 1\text{ M}$, $[Dox]/[Ox] = 9.45$ and $[BF_3MeOH] = 0.0077\text{ M}$	324
Annex 5. 6: Calorimetric analysis. Trace of deflection temperature against time when the polymerisation of oxetane proceeds in 1,4-dioxane at 35 °C. $[Ox] = 0.66\text{ M}$, $[Dox]/[Ox] = 15.95$ and $[BF_3MeOH] = 0.0077\text{ M}$	324
Annex 5. 7: ^{13}C NMR spectra of polymer obtained throughout the polymerisation in 1,4-dioxane at 35°C. $[Ox]_0 = 1\text{ M}$, $[BF_3:MeOH]_0 = 0.0077\text{ M}$ and $[Dox]/[Ox] = 9.45$. Table 5.4 series S 5.2.	325
Annex 5. 8: ^{13}C NMR spectra of polymer obtained throughout the polymerisation in 1,4-dioxane at 35°C. $[Ox]_0 = 1\text{ M}$, $[BF_3:MeOH]_0 = 0.0077\text{ M}$ and $[Dox]/[Ox] = 9.45$. Table 5.4 series S 5.2.	326
Annex 5. 9: 1H NMR spectra of polymer obtained throughout the polymerisation in 1,4-dioxane at 35°C. $[Ox]_0 = 1\text{ M}$, $[BF_3:MeOH]_0 = 0.0077\text{ M}$ and $[Dox]/[Ox] = 9.45$. Table 5.4 series S 5.2.	327
Annex 5. 10: ^{13}C NMR spectrum of poly(ethylene oxide).	328
Annex 5. 11: 1H NMR spectrum of poly(ethylene oxide).	328
Annex 5. 12: SEC chromatogram of polyoxetane obtained throughout the polymerisation in 1,4-dioxane at 35°C. $[Ox]_0 = 1\text{ M}$, $[BF_3:MeOH]_0 = 0.0077\text{ M}$ and $[Dox]/[Ox] = 9.45$. Table 5.4 series S 5.2.	329

Annex 5. 13: SEC chromatogram of polyoxetane after a tentative of extension of polymer chain length by monomer addition on active polymer solution after full monomer conversion. Polymerisation carried out in 1,4-dioxane at 35 °C. Table 5.5 series S 5.4.	329
Annex 5. 14: SEC chromatogram of polyoxetane obtained throughout the polymerisation in 1,4-dioxane at 35°C. $[Ox]_0 = 0.66$ M, $[BF_3:MeOH]_0 = 0.0077$ M and $[Dox]/[Ox] = 15.95$. Table 5.4 series S 5.3.	330
Annex 5. 15: SEC chromatogram of polymer obtained throughout the polymerisation in 1,4-dioxane at 35°C. $[Ox]_0 = 1.124$ M, $[I1]_0 = 0.00114$ M and $[Dox]/[Ox] = 9.66$. Table 5.6 series S 5.5.	330
Annex 5. 16: ^{13}C NMR spectra of polymer obtained throughout the polymerisation in 1,4-dioxane at 35°C. $[Ox]_0 = 1.124$ M and $[I1]_0 = 0.00114$ M. Table 5.6 series S 5.5.	331
Annex 5. 17: 1H NMR spectra of polymer obtained throughout the polymerisation in 1,4-dioxane at 35°C. $[Ox]_0 = 1.124$ M and $[I1]_0 = 0.00114$ M. Table 5.6 series S 5.5.	332
Annex 5. 18: SEC chromatogram of polyoxetane after extension of polymer chain length by monomer addition on active polymer solution after full monomer conversion. Polymerisation carried out using "living monomeric polyoxetane" initiator I1 in 1,4-dioxane at 35 °C. Table 5.7 series S 5.9.	333
Annex 5. 20: SEC chromatogram of polyoxetane obtained throughout the polymerisation in 2:3 v/v 1,4-dioxane:dichloromethane at 35°C. $[Ox]_0 = 1.124$ M, $[I1]_0 = 0.00114$ M and $[Dox]/[Ox] = 3.86$. Table 5.6 series S 5.8.	334
Annex 5. 21: SEC chromatogram of polyoxetane obtained throughout the polymerisation in 1,4-dioxane at 35°C. $[Ox]_0 = 1.125$ M, $[I2]_0 = 0.00134$ M and $[Dox]/[Ox] = 9.66$. Table 5.6 series S 5.8.	334
Annex 5. 22: ^{13}C NMR spectra of polymer obtained throughout the polymerisation in 1,4-dioxane at 35°C. $[Ox]_0 = 1$ M, $[I3]_0 = 0.0025$ M and $[Dox]/[Ox] = 9.7$. Table 5.8 series S 5.10.	335
Annex 5. 23: SEC chromatogram of polyoxetane obtained throughout the polymerisation in 3/1 v/v 1,4-dioxane/dichloromethane at 35°C. $[Ox]_0 = 1$ M, $[I3]_0 = 0.0026$ M and $[Dox]/[Ox] = 8.22$. Table 5.8 series S 5.11.	336
Annex 5. 25: ^{13}C NMR spectra of polymer obtained throughout the polymerisation in tetrahydropyran at 35°C. $[Ox]_0 = 1$ M, $[BF_3:MeOH]_0 = 0.0077$ M and $[THP]/[Ox] = 8.73$. Table 5.10 series S 5.14.	337
Annex 5. 26: 1H NMR spectra of polymer obtained throughout the polymerisation in 1,4-dioxane at 35°C. $[Ox]_0 = 1$ M, $[BF_3:MeOH]_0 = 0.0077$ M and $[THP]/[Ox] = 8.73$. Table 5.10 series S 5.14.	338
Annex 5. 27: SEC chromatogram of polyoxetane obtained throughout the polymerisation in tetrahydropyran at 35°C. $[Ox]_0 = 1$ M, $[BF_3:MeOH]_0 = 0.0077$ M and $[THP]/[Ox] = 8.73$. Table 5.10 series S 5.14.	339
Annex 5. 28: SEC chromatogram of polyoxetane obtained throughout the polymerisation in tetrahydropyran at 35°C. $[Ox]_0 = 1.452$ M, $[I2]_0 = 0.00156$ M and $[THP]/[Ox] = 6$. Table 5.10 series S 5.15.	339
Annex 5. 29: ^{13}C NMR spectra of polymer obtained throughout the polymerisation in tetrahydropyran at 35°C. $[Ox]_0 = 1.452$ M, $[I2]_0 = 0.00156$ M and $[THP]/[Ox] = 6$. Table 5.10 series S 5.15.	340

Annex 5. 31: DSC trace of poly(oxetane-co-THP) (sample S 5.15.4, Table 5.10). Rate 5 °C/min.....	342
Annex 5. 32: DSC trace of poly(oxetane-co-1,4-dioxane) (series S 5.5.4, table 5.6). Rate 5 °C/min.....	342
Annex 5. 33: DSC trace of poly(oxetanene) (series S 4.4.4, table 4.4.8). Rate 5 °C/min.	343

1 CHAPTER 1

Introduction

1.1 Scope of the work

Oxetane based polymers are often used, in the form of thermoplastic elastomers (TPEs), for the manufacture of polymer-bonded explosives (PBXs) and show compatibility with nitroester plasticisers^[1]. The PBX casts are obtained by embedding granular explosives (HMX, RMX, NTO...but no TNT) in a plasticised polymeric material, which may have rubbery properties, such as hydroxy-terminated polybutadiene crosslinked with isocyanate, or plastic properties, e.g. polycaprolactone. The use of cast PBX brings significant advantages over traditional TNT-based explosives charges, which reduces vulnerability, burn uniformly and smoothly without detonation, the improvement of life duration (no limited), reliability and process reproducibility (no risks of cracking), high performance adapted for every type of application (missiles warheads, torpedoes, underwater mines, bombs, penetrators, shaped charges, shells...) and facilities logistics (storage, transportation, handling...). The development is continuing in this area to produce PBXs, which contain polymers that are energetic and will contribute to the explosive performance of the PBX. This application requires specific characteristics of the polymers, good control of its molecular weight, low molecular weight polydispersity, bifunctionality, amorphous and low glass transition temperature ($T_g < -40^\circ\text{C}$). For this purpose, homopolymers and multiblock copolymers and random copolymers based on oxetane and oxetane derivatives such as 3,3-bis(chloromethyl)oxetane (BCMO), 3,3-bis (azidomethyl)oxetane (BAMO), 3-Azidomethyl-3-methyloxetane (AMMO), 3-nitromethyl-3-methyloxetane (NIMMO) and/or cyclic ethers, particularly as tetrahydrofuran (THF), have been studied^[2-16]. Suitable energetic TPEs can also be prepared by coupling a telechelic low T_g prepolymers with monofunctional high T_g or crystalline prepolymer as terminal hard blocks. Linear ABA triblocks copolymers can also be synthesised by sequential polymerisation^[8]. Most of these polymers, however, prepared by cationic mechanism were reported to have broad molecular weight distribution. Moreover, synthesis of some block copolymers turned out to be a mixture of block copolymer and homopolymer, for which the length of block cannot be well regulated.

Living polymerisation is a powerful pathway to synthesis polymeric materials, whereby the topology can be controlled in a predictable way. The formation of polymers chains retaining their aptitude to growth during the all course of the polymerisation permit to develop well-

defined block and graft copolymers, as well as star, comb, ladder and macrocyclic polymers, and end functionalised polymers. In addition, polymers with predictable molecular weight and narrow molecular weight distribution are obtained. The potential importance, both academic and industrial, of such tailor-made polymers is well documented in the literature^[17-18].

This chapter aims to discuss the principles of ring opening polymerisation, and review some of the carried out in the area of the cyclic ethers, particularly with regards to oxetane and oxetane derivatives monomers. They are numerous problems encountered when generating *living growing polyethers*, which are tackled during the course of this investigation. In the following chapters, we will see how an understanding of the polymerisation of cyclic ethers at molecular weight level resulted in the ability to polymerise oxetane in a living manner using cationic initiator and permit to produce polyoxetane materials with narrow molecular weight distribution. This very promising polymerisation system could be an alternative to polymerise oxetane derivatives in living manner and to produce telechelic thermoplastic elastomers (TPEs) with narrow molecular distribution usable as binders for propellants.

1.2 General principles of polymerisation

For most practical purposes, a *polymer* may be defined as a large molecule built up by repetition of small, simple chemical units. The small molecules that combine with each other to form polymer molecules are termed *monomers* and the reaction, by which they combine, are termed *polymerisations*.

During the development of polymer science with the study of new polymerisation processes, classifications of polymers has come into use according to their method of preparation. There are basically two ways by which polymers may be produced synthetically from the simple starting material. Originally classified by Carothers^[19] into *addition and condensation polymers* on the basis of the compositional difference between the polymer and the monomer(s) from which it was synthesised, Flory^[20] in 1953 stressed the significant difference in the mechanism by which the polymers molecules are built up. These techniques are referred to as *step polymerisation* and *chain polymerisation*. The terms step growth and chain growth, are also used instead of step polymerisation and chain polymerisation, respectively.

Step polymerisations proceed by the stepwise reaction between functional groups of reactants, usually occurring with the elimination of a small molecule such as water, carbon dioxide or hydrogen chloride. The size of the polymer molecules increases slowly from monomer to dimer, trimer, tetramer, pentamer, hexamer, until eventually large polymer molecules containing large number of monomer molecules have been formed. Any two molecular species of not necessarily identical lengths can react with each other to produce one molecule. Examples of materials produced by this technique^[21] are polyesters (e.g. Dacron, Terylene, Melinex (ICI), Mylar (Du Pont)), polyurethane (e.g. Perlon U), polyamides (e.g. Nylon, Kevlar), phenyl-formaldehyde polymers (e.g. Novolaks) and poly(p-xylylene) (e.g. Parylene N).

Chain polymerisation proceeds by a propagation of the growing active centre by successive identical addition reactions of a large number of monomer molecule. Chain polymerisation, unlike step growth, involves at least three steps; initiation, where the active centre, acting as chain carrier, is created, propagation, in which the length of the chain increases and, termination, where the kinetic chain is brought to a halt by neutralisation or transfer of its activity. Chain growth can be classified according to the nature of the growing centre. These reactions have been documented and include free radical polymerisation^[22], ionic polymerisation^[23,24], both cationic and anionic, ring opening polymerisation^[25], and coordinative system, such as Ziegler-Natta^[26], ring opening metathesis^[27] and group transfer polymerisation^[28] where propagation involves both monomer and growing polymer chains being bonded to a catalyst centre.

1.2.1 Living polymerisation

The term *living* was first introduced in the 1950's by Szwarc et al. who reported anionic polymerisation of styrene free of *transfer* and *termination* reactions^[29], although the existence of such system had been postulated 20 years earlier by Ziegler^[30]. Since Szwarc's initial discovery, there has been great progress in the field of living anionic polymerisation^[31]. As well as anionic reactions, living polymerisation has been achieved in the area of cationic polymerisation^[32] in the 1980's and more recently, in 1990's, in the areas of group transfer polymerisation^[33]. In early 1990's, the development of the so-called chain-growth control in free radical polymerisation enabled also the preparation of polymer in a living-like manner^[40-44]. A number of review articles have been produced covering living anionic^[34],

cationic^[35], group-transfer^[33,36], coordination^[37,38], and chain-growth control in free radical polymerisation^[39-44].

1.2.1.1 Characteristics of living polymerisation

A *living polymerisation* is defined as a polymerisation in which propagation proceeds in the absence of termination or transfer reactions and the growing chain ends remain active once all monomer has been consumed. However, since most chain ends will eventually isomerise, react with their surroundings or otherwise decompose, this definition has been relaxed and a *polymer* is considered *living* if the growing centre remains active long enough for any further synthesis to be completed. One of the first living polymerisation reported by Szwarc^[29], was the anionic polymerization of styrene initiated by sodium naphthalide (figure 1.1). Sodium was added to a solution of naphthalene in THF to produce the green naphthyl radical-anion. Addition of styrene then led to transfer of an electron from the naphthyl radical-anion to the monomer producing a red styryl radical-anion. Two of these radical-anions combined to give a dianion that propagated from both ends. The living nature of this polymerisation was demonstrated by the persistence of the red colour from the styryl radical-anion when all the monomer had been consumed. Further evidence of the living nature was obtained by adding a second batch of monomer to the completed polymerisation upon where an increase in molecular weight was observed.

Living polymerisations have a number of certain characteristics, which distinguish them from more conventional polymerisations. If the rate of initiation is fast compared to the rate of propagation, so that all the polymer chains are initiated at approximately the same time and the reaction mixture is homogeneous, so that all the polymer chains grow at the same rate then polymers with narrow molecular weight distributions are obtained. The molecular weight distribution will then have a Poisson distribution^[45] give by;

$$\frac{\overline{M}_w}{\overline{M}_n} = 1 + \frac{\overline{M}_n}{(\overline{M}_n + 1)^2} \quad \text{E: 1.1}$$

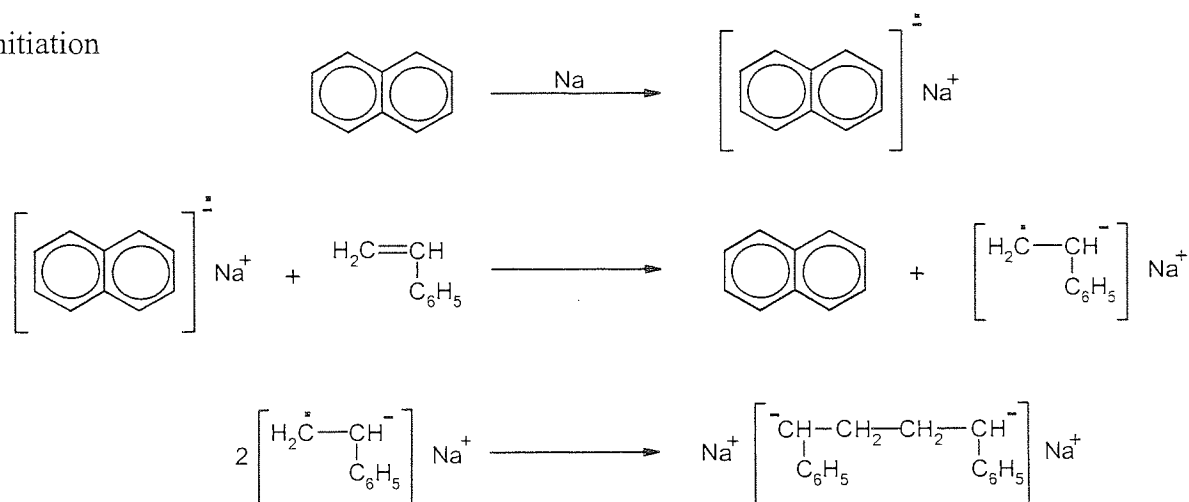
Under these conditions, if each initiating molecule gives rise to one discrete polymer chain, then the number average degree of polymerisation will be given by;

$$\overline{Dp}_n = \frac{[M]_0 - [M]}{[I]_0}$$

E: 1.2

However if the rate of initiation is slow then a broad molecular weight distribution will be obtained. For reactions with a high rate of initiation the molecular weight increases linearly with monomer conversion. Once all monomer has been consumed additional polymerisation will take place if more monomer is added to the reaction. Living polymerisation can be deliberately terminated by adding a reagent that will react with the propagating chain end, for example water, alcohols or protic acids depending on the nature of the active centre.

a) initiation



b) propagation

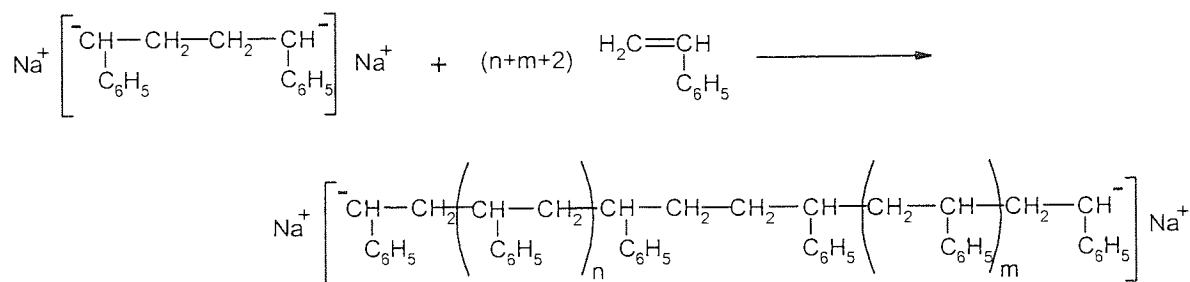


Figure 1. 1: Living anionic polymerisation of styrene initiated by sodium naphthalide.

1.3 Ring-opening polymerisation

Polymerisation and copolymerisation of non-hydrocarbon monomers, such as heterocyclic monomers, constitute a distinct group of synthetic polymers. Structurally classified as condensation polymers, since they contain a heteroatom or functional group in the polymer,

the ring opening polymerisation of most heterocyclic monomers is kinetically akin to a chain growth polymerisation.

Ring-opening polymerisation of cyclic monomers usually proceeds via ionic polymerisation. Some monomers, (cyclopropane^[46] and bicyclobutane^[47]), however, are known to be polymerised by a radical mechanism while the metathesis polymerisation of cycloalkenes^[48] and bicycloalkenes^[49] proceeds via a metallacarbene intermediate. Ionic polymerisations are divided into three types, cationic, anionic and coordinate anionic polymerisations, of which cationic is the most common. Monomers polymerise ionically include cycloalkanes^[50-53], bicyclobutane^[54,55], monomers containing endocyclic heteroatom(s), cyclic ethers^[56-58], cyclic formals^[59], bicyclic acetal^[60], sugar anhydrides^[61], cyclic sulfides^[62-64], cyclic disulfides, cyclic amines^[65-67], cyclic 1,3 oxaza compounds^[68-70], cyclic syloxanes^[71,72], and those containing both endocyclic and exocyclic heteroatoms, lactones^[73-76], carbonates, cyclic orthoesters, oxalanedione, thiolactone^[77], N-carboxyanhydrides^[78], lactam^[79-84] cyclic imides^[85,86], thiolactams^[86,87], phosphacyclic monomers^[87-89] in the monomer molecule.

The nature of the ether linkage imposes on the ring opening polymerisation of cyclic ethers, a cationic mechanism. Figure 1.2, shows the propagation steps of the cationic and the anionic ring opening polymerisation of ethylene oxide, both being treated as S_N2 reactions. As depicted in the scheme 1.2, the cationic process involve the rupture of the weak $C-O^+$ bond of the growing polymer with the formation of a new $C-O^+$ bond and transfer of charge, whereas in the anionic process the formation of the stronger strain-free bond takes place simultaneously with the rupture of strong $C-O$ bond of the monomer and again with the transfer of charge. Since a strong bond has to be ruptured in the anionic process but a weak one in the cationic, this difference in the strength of the ruptured bond accounts for the preference for the cationic mode of polymerisation of these monomers.

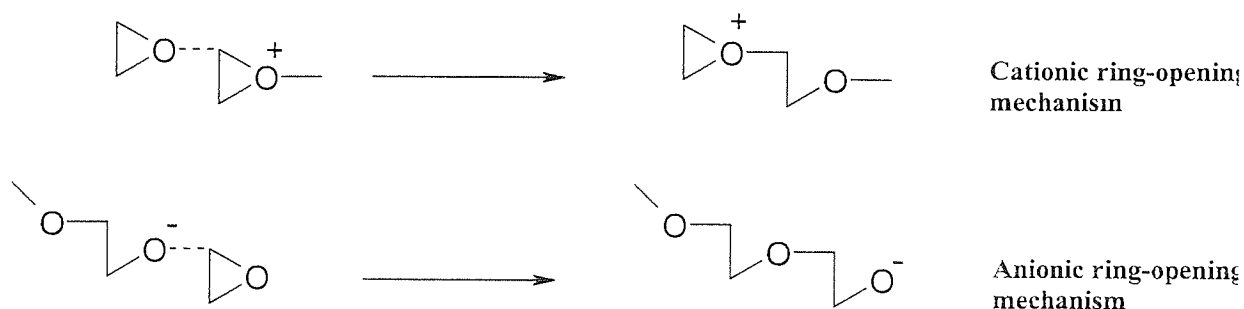


Figure 1. 2: Cationic and anionic ring opening process of ethylene oxide treated as an S_N2 reaction.

1.3.1 Polymerisability

The ability of a monomer to polymerise depends, in thermodynamic terms, on the polymerisation (ΔG°). This refers to the theoretical possibility of the monomer to undergo polymerisation regardless of the pathway of the reaction and the mechanism of the ring opening and does not take into account the actual feasibility of the interconversion.

1.3.1.1 Thermodynamic treatment of ΔG°

The polymerisation of a pure monomer to a high molecular mass amorphous polymer is thermodynamically allowed when the standard free energy change, ΔG° , accompanying the conversion is negative, $\Delta G^\circ < 0$. In an ideal system, the difference of the molar free energies of a monomer unit in an amorphous polymer G_P and the starting monomer, G_m , gives the standard free energy change,

$$\Delta G^\circ = G_P^\circ - G_m^\circ = \Delta H^\circ - T \cdot \Delta S^\circ \quad \text{E: 1.3}$$

The standard free energy change associated with any ring opening polymerisation is made up of an enthalpy term, ΔH° , and an entropy term, ΔS° . Most of the common polymerisations are exothermic, $\Delta H^\circ < 0$, and also lead to a reduction of the entropy of the system, $\Delta S^\circ < 0$. Hence, propagation is thermodynamically allowed only at temperature lower than the critical temperature, T_c , referred to as ceiling temperature, which can be defined as

$$T_c = \frac{\Delta H^\circ}{\Delta S^\circ} \quad \text{E: 1.4}$$

In special case of sulfur (S_8) the thermodynamic relationships are reversed and there is floor temperature, 159°C , below which no polymerisation occurs^[90,91]. The values of $3.17 \text{ kcal.mole}^{-1}$ and $4.63 \text{ cal.mole}^{-1}.\text{degree}^{-1}$ were obtained numerically for ΔH° , and ΔS° , respectively^[90].

The relation is more complex when living polymers soluble in solvent behaves ideally. The entropy of monomer, but not of high molecular mass polymer, increases on dilution. Hence, at every temperature below the ceiling temperature, the polymerisation becomes

thermodynamically prohibited at monomer concentration lower than the critical one, c_e , at which the living polymers reach the state of equilibrium with their monomer. This monomer equilibrium concentration, c_e , is given then by the relation:

$$\Delta G^\circ + RT \cdot \ln(c_e / c_o) = \Delta H^\circ - T \cdot \Delta S^\circ \quad \text{E: 1.5}$$

where c_o denotes the concentration of monomer in its pure liquid and ΔG° the change in the free energy on conversion of 1 mole of pure liquid monomer into monomeric segments of amorphous polymer.

1.3.1.2 Flory-Huggins treatment of ΔG°

In most cases, the interaction of the monomer with its polymer has to be taken into account as well as the interactions of the monomer and the polymeric segment with the solvent. For a system in which the polymer is soluble in its pure liquid monomer, the free energy of polymerisation in equilibrium mixture may be expressed as sum of three terms: $-\Delta \bar{G}_1$, the partial free energy change for the removal of one molecule of liquid monomer from the mixture; ΔG_{lc} , the free energy of polymerisation of one mole of liquid monomer to one base-mole of liquid amorphous polymer of infinite chain length and; $\Delta \bar{G}_2$, the partial free energy change for the addition of one base mole of polymer to the mixture. At equilibrium,

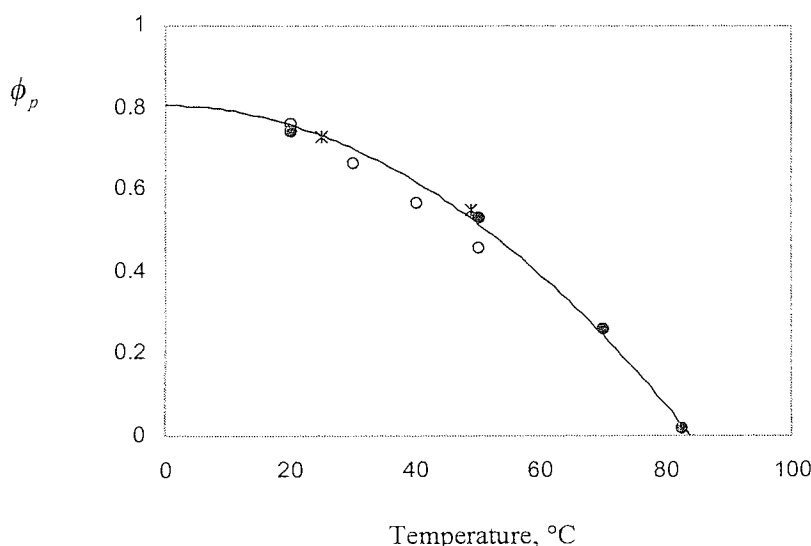
$$-\Delta \bar{G}_1 + \Delta G_{lc} + \Delta \bar{G}_2 = 0 \quad \text{E 1.6}$$

Inserting the appropriate expression for $\Delta \bar{G}_1$ and $\Delta \bar{G}_2$ from Flory-Huggins expression, a more exact thermodynamic treatment can be used leading to the following equation:

$$\Delta G_{lc} = RT \cdot (1 + \ln \phi_m + \chi_{mp} \cdot (\phi_p - \phi_m)) \quad \text{E 1.7}$$

where ϕ_m and ϕ_p are the equilibrium volume fractions of monomer and polymer respectively and χ_{mp} is the polymer/monomer interaction parameter in the Flory-Huggins^[92] equation for the free energy of mixing of polymer and solvent monomer. Figure 1.3, shows data for tetrahydrofuran plotted on this basis^[93]. The line drawn corresponds to the chosen value

$\chi_{mp}=0.3$, $\Delta H^\circ=-12.4 \text{ kJ.mol}^{-1}$ and $\Delta S^\circ= -40.8 \text{ J.K}^{-1}$, assumed to be independent of temperature. The values of the thermodynamic constants are in good agreement with the value reported by Dreyfuss and Dreyfuss^[94]. The ceiling temperature for polymerisation of pure tetrahydrofuran, giving soluble polymer, is 84°C . It should be noted that the ceiling temperature is not given by $\Delta H^\circ/\Delta S^\circ$ since this takes no account of the partial molar free energies of the monomer and polymers.



The line draw is theoretical and corresponds to the chosen value of χ , ΔH° , ΔS° . Results from (●) Sims, (*) Bawn et al, (○) Rosenberg et. al. Reproduced from the reference 93.

Figure 1.3: Equilibrium volume fraction of polymer ϕ_2 in the bulk polymerisation of tetrahydrofuran.

In the case of the living polymers soluble in solvent, the interactions of the monomer and polymeric segment with the solvent have to be taken into account. Using a similar thermodynamic treatment (than previously), Ivin and Leonard^[95], among others, have shown that in a non-ideal solution, the free energy of polymerisation can be expressed with the help of the monomer, polymer and solvent interaction parameters.

$$\Delta G_{lc} = RT \left(1 + \ln(\Phi_m) + \Phi_s \left(\chi_{ms} + \chi_{sp} \cdot \frac{V_m}{V_s} \right) + \chi_{mp} \cdot (\Phi_p - \Phi_s) \right) \quad \text{E: 1.8}$$

where the subscripts m, p, and s refer to monomer, polymer, and solvent, respectively, and the symbols ϕ and χ have their conventional meaning.

1.3.1.3 Equilibrium polymerisation

The magnitude of the equilibrium free monomer concentration may be used as a measure of polymerisability of a monomer. The polymerisation of monomers by addition, condensation and ring opening processes are normally characterised by a state of equilibrium in which the rate of the polymerisation is balanced by the rate of the depolymerisation.



Under such conditions, monomer cannot be quantitatively converted into polymer and living polymers reach a state of equilibrium with their monomer.

$$-\frac{d[M]}{dt} = k_p \cdot [P_{n-1}^*] \cdot [M]_e - k_{-p} \cdot [P_n^*] = 0 \quad \text{E: 1.9}$$

When n is large,

$$[P_{n-1}^*] = [P_n^*] \quad \text{E: 1.10}$$

and so

$$K = \frac{k_p}{k_{-p}} = \frac{1}{[M]_e} \quad \text{E: 1.11}$$

Given that the free energy of the system, ΔG , is equal to zero when the living polymer reach the state of equilibrium with its monomer, the equilibrium constant K is then related to the standard change in free energy ΔG° of polymerisation.

$$\Delta G^\circ = \Delta H^\circ - T \cdot \Delta S^\circ = -RT \cdot \ln K = RT \cdot \ln [M]_e \quad \text{E: 1.12}$$

Therefore the equilibrium concentration of monomer be established through the use of the Dainton-Ivin^[96] equation given by:

$$\ln[M]_e = \frac{\Delta H^\circ}{R} \cdot \frac{1}{T} - \frac{\Delta S^\circ}{R} \quad \text{E: 1.13}$$

The above relation was confirmed by Ofstead and Calderon^[97] who investigated the ring opening metathesis polymerisation of cyclopentene catalysed by $\text{WCl}_6/\text{EtOH}/\text{EtAlCl}_2$ system in benzene at different temperatures. The values of - 4.4 kcal/mol and - 14.8 cal/mol/degree were obtained for ΔH° , and ΔS° , respectively. When the equilibrium concentrations of monomer are plotted against temperature, a ceiling temperature of 150°C was calculated by extrapolation to zero conversion. It was further noted that the enthalpy of polymerisation calculated by Calderon is closed to the ring strain energy value of cyclopentene (4.9 kcal/mol) reported by Cox^[98].

The above relation holds for an ideal system, which implies that ΔG° and $[M]_e$ are unique for a given temperature. It has recently been shown that, at a given temperature, in the case of the anionic polymerisation of α -methyl-styrene^[99,100], cationic polymerisation of 1,3-dioxalane^[101] and cationic polymerisation of tetrahydrofuran^[102], the equilibrium concentration of monomers depends also on the initial concentration of living polymers. For a polymerisation in a pure monomer liquid or in solvent, the correct value of the equilibrium concentration is obtained by extrapolation of the observed values to a zero concentration of initiator.

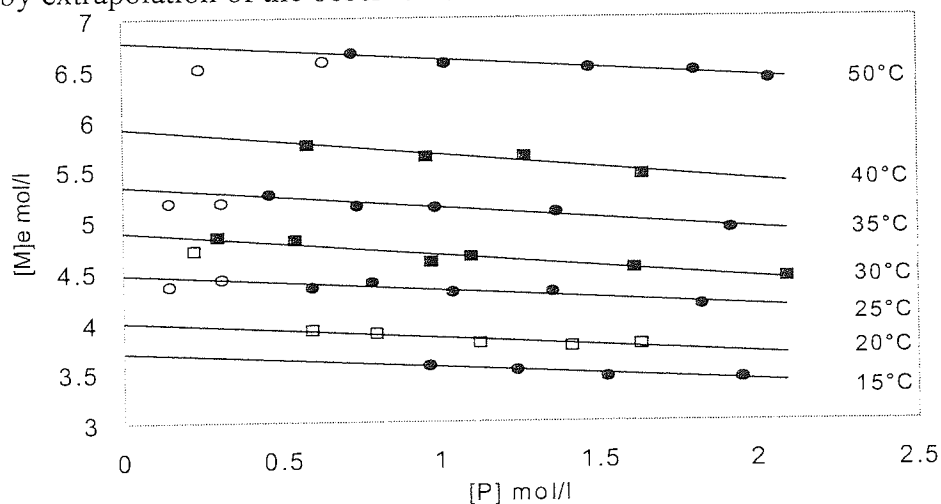


Figure 1. 4: Variation of equilibrium monomer concentration $[M]_e$ with polymer concentration $[P]$ for the polymerisation of

Similar observations have been made when the polymerisation is performed in various solvents at different initial concentrations of monomer, when concentration of living polymers was identical. In the case of the cationic ring opening polymerisation of tetrahydrofuran^[103], it was found that the correct value of the equilibrium concentration of monomer is obtained by extrapolation of the observed values to a starting concentration of tetrahydrofuran in its pure liquid monomer.

1.3.1.4 Chemical and physical factors affecting the polymerisability of cyclic monomers

As mentioned in the previous section, the magnitude of the equilibrium monomer concentration may be used as a measure of polymerisability. For a given homologous series of cyclic monomers, it appears that the polymerisability increases when the equilibrium free monomer concentration, $[M]_e$, decreases. Basically, value of $[M]_e$ for 3-, 4- and 8- to 11-membered ring compounds are usually very small and not easily measured. This is because ΔH° makes a large negative contribution to ΔG° . However for 5-, 6- and 7-membered rings ΔH° is rather small and $[M]_e$ values are in the range 0.01-5M, if indeed the compounds polymerise at all. The 7-membered rings are generally polymerisable but the sign of the free energy of polymerisation of 5- and 6-membered rings depends on the nature of the ring and on the steric effect of any substituents.

1.3.1.4.1 Chemical factors affecting the polymerisability of monomers

Dainton, Delvin and Small^[104], in describing their semi-empirical method of calculating free energies polymerisation for various ring compounds, commented that, within a homologous series of cyclic monomers, the most significant chemical factor that affects the polymerisability is the ring strain energy. Based on a comparison of theoretical enthalpies and entropies of polymerisation of series of cycloalkanes (table 1.1), it appears that, only for monomers of less than eight ring carbons, where negative entropies of polymerisation are encountered, is ring strain required for polymerisability. Examinations of carbocyclic rings, which do polymerise by ring-opening process, suggest that a favourable ΔG alone is not a sufficient condition for the homopolymerisation to occur. Cyclopentane, cycloheptane and cyclooctane are all characterised by negative Gibbs free energy of polymerisation but cannot be ring-opened at any temperature. Normally, the activation energy for carbon-carbon σ -

bond cleavage is high, because of the strength of the bond and its steric inaccessibility. In order for opening of carbocyclic ring to occur cleanly, the energy of activation must be reduced so that an accessible pathway is available as well. Only cyclopropane, cyclopropane derivative^[46,51-53] and bicyclobutane^[47,54,55], which are the most strained of the cycloalkane rings, polymerise. Ring strain not only provides a driving force, but also helps to reduce the activation energy by raising the ground state energy of the molecule ensuring that the overall process is energetically favourable.

Other factors of importance are the transition state stabilisation by resonance and/or inductive effects of the propagating centre and the minimisation of the steric interactions in the transition state. Consequently, cyclic monomers characterised by negative entropy of polymerisation must possess a minimum strain energy if polymerisation by ring opening polymerisation is to be thermodynamically possible. Moreover, a thermodynamically polymerisable monomer may be polymerisable if there is a mechanism capable of inducing its polymerisation. Only cyclohexane showed the combination of positive enthalpy and negative entropy of polymerisation, indicative of a monomer that is thermodynamically stable compared to the corresponding polymer.

Cycloalkane	ΔH° (kcal/mol)	ΔS° (cal/mol/degree)	ΔG° (kcal/mol)
Cyclopropane	-27	-16.5	-22.1
Cyclobutane	-25.1	-13.2	-21.2
Cyclopentane	-5.2	-10.2	-2.2
Cyclohexane	0.7	-2.5	1.4
Cycloheptane	-5.1	-0.7	-4.9
Cyclooctane	-8.3	+8.9	-11.0

Table 1. 1: Calculated heats, entropies and free energies for the hypothetical polymerisation of cycloalkanes.

In the polymerisation of cycloalkenes, a metallocarbene catalyst provides an easy route to the ring opening polymerisation of cyclo olefins by cleavage of the double bond, and the ability of cycloalkene for the ring opening polymerisation is exclusively dependent on the thermodynamic data. Examination of a series of cycloalkenes, where the ring size varies from 3 to 8, shows that cyclobutene^[104-107] and cyclooctene^[1008,109] proceed essentially to completion (ΔG large negative) whereas cyclopentene^[110] stops short at a measurable

equilibrium concentration (small negative ΔG). McCarthy et al.^[111] who investigated the ring opening metathesis polymerisation of cyclohexene catalysed by WCl_6/Me_4Sn system in toluene at various low temperature, observed that ΔG° for cyclohexene was close to zero from 0 to 25°C. Suspecting that ΔG° would be negative at low temperature, the addition of WCl_6/Me_4Sn catalyst to a 5 M solution of cyclohexene in toluene at -77°C resulted in polymerisation of cyclohexene to the equilibrium concentration of 88% of its initial value. Raising the temperature to room temperature regenerate the cyclohexene, demonstrating that the cyclohexene had polymerised and depolymerised reversibly by olefin metathesis. By destroying the catalyst at low temperature, they were able to isolate a poly (hexaenamer) as a series of oligomers (DP<20). The ceiling temperature was estimated to be about -23°C and values of -1 kJ/mol and -17 J/mol/degree were obtained for ΔH° , and ΔS° , respectively. Surprisingly, only the highly strained cyclopropene failed to polymerise in presence of metathesis catalyst. This is due to the fact that no catalyst capable of inducing its polymerisation is yet known. Table 1.6 shows the thermodynamic parameters calculated by Cherednichenko^[286] on polymerisation of cyclo olefins at 25°C.

Monomer	Polymer Geometry	ΔH (kJ/mol)	ΔS (J/mol/degree)	ΔG (kJ/mol)
Cyclopentene	Cis	-16	-46	-2.3
	Trans	-20	-46	-6.3
Cyclohexene	Cis	-3 to +1	-31	+6.2
	Trans	-1 to -3	-28	+7.3
Cycloheptene	Cis	-14 to -17	-20	-8
	Trans	-19 to -21	-17	-14
cis-cyclooctene	Cis	-20 to -21	-2	-19
	Trans	-21 to -23	-2	-20

Table 1. 2: Change of thermodynamic parameters on polymerisation of cyclo olefins at 25°C, reference 286. 1cal=4.18 J

Dainton and Ivin^[96], among others, pointed out for monomers possessing low ring strain energy, entropy factor can be the principal determinant of the free change energy of polymerisation. As shown in table 1.2, the entropy consideration predicts an increase in polymerisability (i.e., decrease in equilibrium monomer concentration) for cyclic monomers as ring size increases. This was confirmed by Calderon, Ofstead and Judy^[112] who readily

converted 1,9,17-cyclotetraeicosatriene (the 24-membered cyclic trimer of cyclooctene) to high polymer in good yield (80%) using a metathesis catalyst at 25°C.

The curious case of sulfur (S_8) must be mentioned by the fact that the polymerisation reaction is endothermic ($\Delta H^\circ = 3.17 \text{ kcal.mole}^{-1}$ and $\Delta S^\circ = 4.63 \text{ cal.mole}^{-1}.\text{degree}^{-1}$) and that the polymerisation occurs only above 159°C^[90,91].

In the case of the ring opening polymerisation of cyclic ethers, where the ring size varies from three to eight, the trend is similar that in cycloalkanes and cycloalkenes, where the 6-membered ring tetrahydropyran does not homopolymerise. The ^{13}C NMR spectrum (85-95 ppm region) of tetrahydropyran, when treated with $\text{CH}_3\text{OSO}_2\text{CF}_3$ gives a single peak corresponding to the formation of the methyloxonium ion, which is unable to react further. This shows clearly that the failure of tetrahydropyran to polymerise is due to failure to propagate rather than to inefficient initiation^[114].

Substituents have an adverse effect on the polymerisability of ring compounds in that they tend to stabilise monomers making, ΔG° less negative. For monomers where ΔG° is small, in the case of 5-, 6-, 7-membered compounds, substitution on the ring may render the monomer unpolymerisable under practical conditions. The sensitivity to substitution may be illustrated by the case of cyclopentene, tetrahydrofuran, 1,3-dioxolane and caprolactam, where the parents are all polymerisable. 3-Methylcyclopentene, 3-methyltetrahydrofuran, 4-methyl-1,3-dioxolane and 3-methylcaprolactam are all polymerisable, but 1-methylcyclopentene, 2-methyltetrahydrofuran, 2-methyl-1,3-dioxolane and N-methylcaprolactam are not, probably owing to steric hindrance. In the case of the 4-membered cyclic ethers, oxetane can be polymerised with the following substituents bischloromethyl, halomethyl, dimethyl, phenyl, sulfony, ester, cyano, nitratomethyl, bis-azidomethyl, azobenzene moiety in the 3-position and methyl in the 2-position.

Other chemical factors affecting the standard free energy change, ΔG° , are the geometric isomerism in the polymer (cis/trans) and the configurational isomerism in the polymer (tacticity) but they have a very small influence on ΔG° .

1.3.1.4.2 Physical factors affecting ΔG

The physical factors affecting ΔG include solvent, solubility, temperature, monomer and living polymer concentration in the reaction medium. All of these factors have already been discussed in the section 1.3.1. The other physical factor affecting significantly the polymerisability of monomers is the pressure of the system. It has been shown that the effect of the pressure P , on the ceiling temperature T_c can be expressed quantitatively by the Clapeyron equation,

$$\frac{d\ln T_c}{dP} = \frac{\Delta V_p}{\Delta H_p} \quad \text{E: 1.14}$$

where ΔV_p and ΔH_p are the volume and the heat changes on the polymerisation respectively. The linear dependence of $\ln T_c$ on pressure has been found experimentally in the case of the ring opening polymerisation of tetrahydrofuran^[114], where T_c is raised from 81 to 129 °C by increasing the pressure from 1 atm to 2500 atm. The slope $d\ln T_c/dP$ gives value of $\Delta V_p/\Delta H_p$ of 0.53 cm³.kJ⁻¹, in reasonable agreement with the known values of -9.5 cm³.mol⁻¹ and -18.0 kJ.mol⁻¹ for ΔV_p , and ΔH_p , respectively, which themselves will vary with the pressure. It should be noted that at given temperature, both values of ΔV_p and ΔH_p are negative and make ΔG more negative as the pressure is increased.

1.3.2 Cationic ring-opening polymerisation of cyclic ethers

1.3.2.1 Structure and reactivity of propagating species

1.3.2.1.1 Structure of the propagation species

In the cationic ring-opening polymerisation of cyclic ethers, the chain growth proceeds via *tertiary oxonium sites* that are formed upon alkylation, acylation or protonation of the monomer.

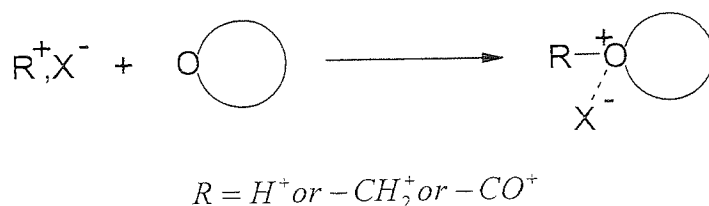


Figure 1. 5: Cationic initiation via oxonium site.

The mechanism of chain growth involves nucleophilic attack by the oxygen doublet of the incoming monomer at one of the two electron deficient carbon atoms in the α -position with respect to the oxonium site, whereby the cycle opens and the newly oxonium site is reformed on the attacking units:

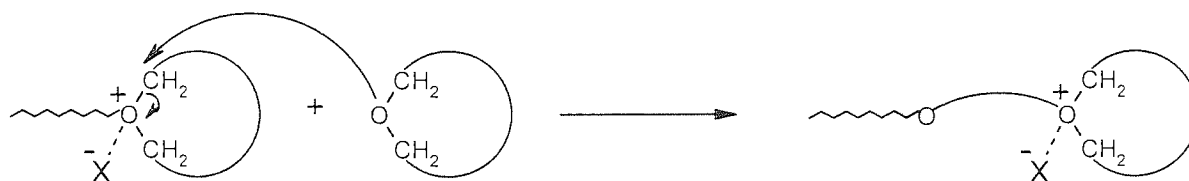


Figure 1. 6: Propagation via oxonium ion by A.C.E. mechanism.


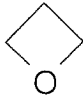
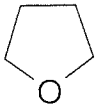
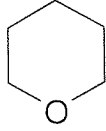
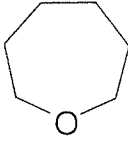
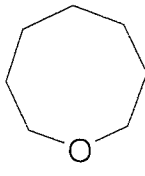
Because the active site appears at the end of the polymer chains and the attacking nucleophile is the uncharged monomer, the mechanism of propagation is known as Activation Chain-End Mechanism, A.C.E.^[115].

1.3.2.1.2 Reactivity of the propagation species

The main factors, governing the reactivity of the growing species are the ring strain of the cyclic ether and the nucleophilicity of the ether group of the attacking monomer; both depend on the ring size of the monomer.

In the monocyclic ethers, the more strained cyclic ethers produce, in general, a less stable and therefore a more reactive, tertiary oxonium ion. This is the case of 3- and 4-membered monomers for which the ring-opening polymerisation is an exothermic process. The values of $-22.6 \text{ kcal.mole}^{-1}$ and $-19.3 \text{ kcal.mole}^{-1}$ were determined for the enthalpy of polymerisation of oxirane^[116] and oxetane^[115], respectively. From the calculated values shown in the table 1.3, the most stable oxonium ion is derived from tetrahydropyran, but the polymerisation does not in fact take place owing to the thermodynamic stability of this monomer (see section 1.3.1.4.1)^[113]. The 5-members ring tetrahydrofuran, *THF*, which is the most stable of the homopolymerisable cyclic ether monomers, proceeds without any appreciable transfer reactions, indicating that the propagation proceeds via a stable tertiary oxonium species. This stability means that there is only a small free energy of polymerisation, and consequently a low ceiling temperature is observed ($85 \pm 2 \text{ }^{\circ}\text{C}$)^[25]. As a consequence, the depropagation reaction cannot be neglected and complete conversion is not obtained. This is also the case of 7- and 8-membered cyclic ethers for which similar states of equilibrium have been observed during the course of their polymerisations. Only 3- and 4-membered cyclic ethers polymerise

to completion owing to their high ring strain energy. Table 1.7 gives the values of the calculated ring strain energies, E , and the enthalpy of polymerisation, ΔH_p° , of some cyclic ethers^[117].

						
E	114	107	23	5	42	33
$-\Delta H_p^\circ$	94.5	81	15		33.5	

E : Ring strain ($\text{kJ}\cdot\text{mol}^{-1}$) energy of cyclic Ether.

ΔH_p° : Enthalpy of polymerisation ($\text{kJ}\cdot\text{mol}^{-1}$) of cyclic Ether.

Table 1. 3: Calculated ring strain energy and enthalpy of polymerisation of cyclic ether from three to eight members ring^[115,1177].

The ring strain of cyclic ether also affects the mode of opening of the oxonium site. In the figure 1.6, the mechanism of the cationic ring-opening polymerisation of cyclic ethers via tertiary oxonium ion is explained through an $\text{S}_{\text{N}}2$ process, in which the new etherate bond is formed and the old one is broken simultaneously. Whereas the existence of trialkyloxonium ion was observed directly by ^1H and ^{13}C NMR in the polymerisation of 5- and 7-membered cyclic ethers monomers^[118,119], the mechanism of polymerisation of oxirane and oxetane is still obscure and not as well documented as the polymerisation of tetrahydrofuran. In the case of the 4-membered ring monomers, an $\text{S}_{\text{N}}2$ mechanism involving a cyclic oxonium ion is generally accepted^[115,120-123].

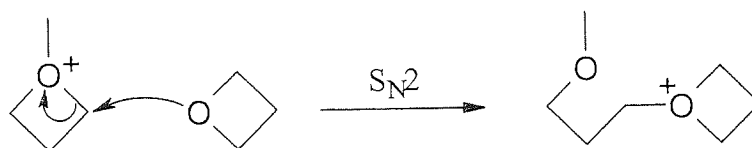
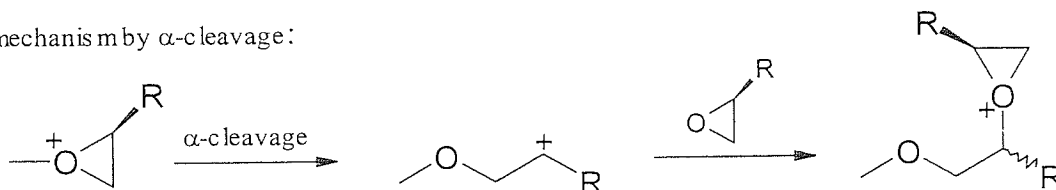


Figure 1. 7: Propagation reaction of oxetane through $\text{S}_{\text{N}}2$ process via cationic polymerisation.

For the highly strained 3-membered cyclic ether monomers, studies of the stereochemistry of the cationic polymerisation, as well as the analysis of isomerised cyclic oligomers (formation of cyclic oligomers with acetal linkage)^[123-130], seem to indicate that a carbenium ion may play a role in the polymerisation of those monomers, where the ring strain may facilitate the

unimolecular opening of the oxonium ion ring. Although no direct evidence has been shown for the participation of carbenium ions and/or tertiary oxonium ions in the propagation reaction of oxirane derivative monomers, a "borderline" S_N2 mechanism has been proposed, in which both S_N1 through α -cleavage, and S_N2 through β -cleavage, are implied (figure 1.8). Recently, Sasaki et al.^[131] who employed the semiempirical molecular orbital method (AM1) to investigate the pathway of the opening oxonium ion ring of oxetane and oxirane molecules possessing various substituent, showed that the computational results are in accordance with the proposed mechanisms.

(a) S_N1 mechanism by α -cleavage:



(b) S_N2 mechanism by β -cleavage:

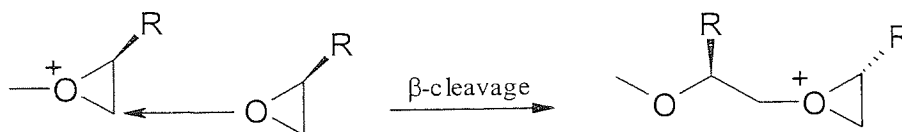
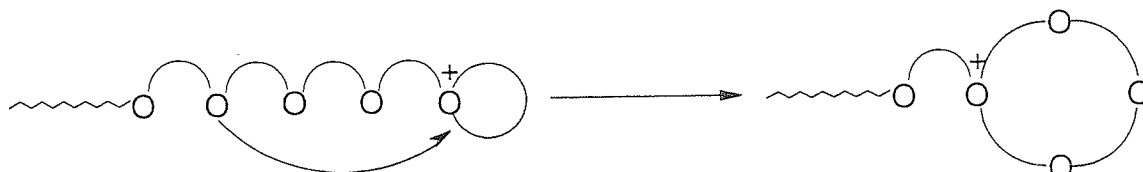


Figure 1. 8: Propagation reaction of oxirane with various substituents through S_N1 (a) and S_N2 (b) in the cationic polymerisation.

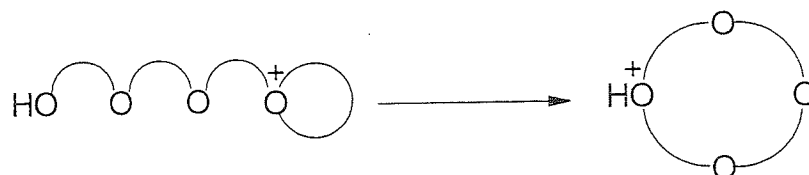
The basicity of the monomers also strongly affects the mode of the reaction of growing species. Various nucleophiles others than the monomer, such as linear ether groups in the polymer chain units and/or the functional end groups, are also present in the reaction system. Therefore chain growth competes with side reactions through intramolecular (back-biting and end-biting) and intermolecular transfer reactions (figure 1.9). For this reason, it is interesting to compare the nucleophilicity for oxetane and oxirane. The ring strains of oxirane and oxetane have been calculated to be 27.3 and 25.5 kcal/mol, respectively, and their pK_b values are 7.55 and 3.6, respectively. Although the two monomers have similar steric requirement and ring strains, the basicity of oxetane is considerably greater than that of the oxirane. The basicity of diethyl ether, oxirane and oxetane, are compared knowing that the pK_b of diethyl ether is 7.2, it appears that oxygen atoms in the polymer chain are more nucleophilic than the oxygen atom of ethylene oxide but less nucleophilic than the oxygen atom of the oxetane. This latter parameter should, therefore, be dominant in making the oxetane more reactive than ethylene oxide through the chain growth. This has been demonstrated by the fact that the

polymerisation of oxetane^[115] produces linear polymer of high molecular weight together with cyclic oligomers, mainly cyclic tetramer, although cyclic oligomers, mainly 1,4-dioxane, can be the main product of the cationic ring-opening polymerisation of ethylene oxide^[115] together with linear polymer of very low molecular weight. The mode of formation of cyclic oligomers and their equilibrium concentration with polymer chains will be discussed later in the section 1.3.2.3. The basicity of some cyclic ether is listed in the table 1.4.

(a) Back-biting reactions:



(b) End-biting reactions:



(c) Intermolecular transfer reactions:

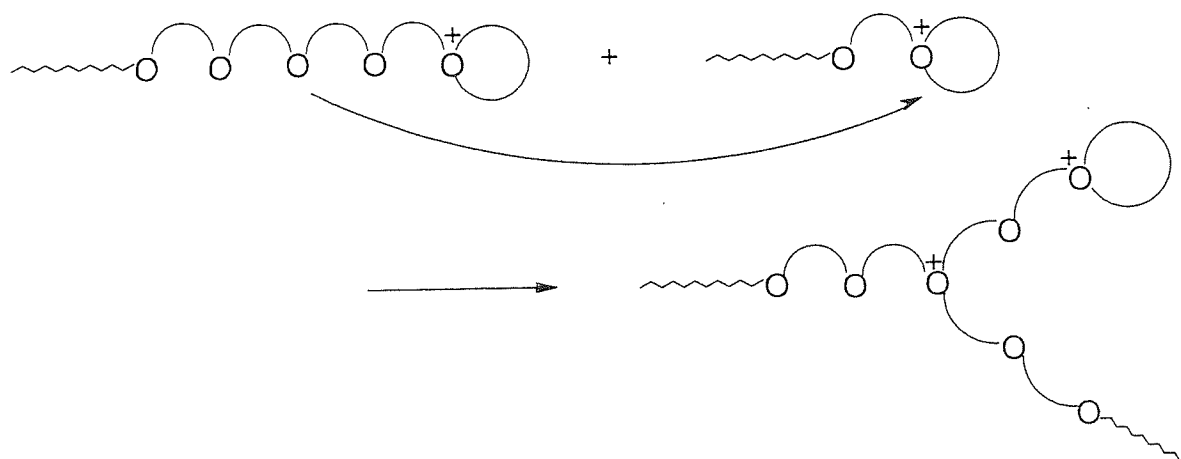
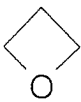
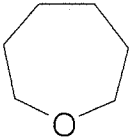
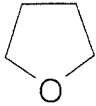
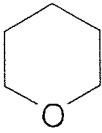
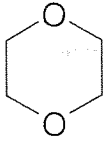
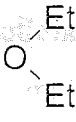



Figure 1. 9: Mechanism of intramolecular (back-biting (a) and end-biting (b)) and intermolecular (c) transfer reactions.

It must be noted that the probability of such side reactions increases with the amount of polymers formed, i.e. with conversion, as in all transfer reactions involving polymers. The reactivation of these oxonium salts one of the three equivalent C-O⁺ bonds has to be cleaved. Such a process leads to a redistribution of chain lengths by a random process, and it contributes to an increase in the polydispersity index.

						
3.60	4.01	4.22	4.83	5.85	7.2	7.55

pK_b values of some cyclic ethers. Nucleophilicity increases with the decrease of pK_b . As a reference, the values of 1,4-dioxane and diethyl ether as showed in the table.

Table 1. 4: Order of basicity of some cyclic ether.

The last factor that has to be considered is the stability and/or the nucleophilicity of the counter anion towards the growing tertiary oxonium ion. It is a great of importance that the counter-anion involved exhibits low nucleophilicity to prevent it from recombining with the growing centre. There are basically two groups of counter anion, complex anions such as $[SbF_6]^-$, and non-complex such as $CF_3SO_3^-$. Postulated to exist in the form of ion-pairs and free ions in the case of the cationic polymerisation of oxepane using $[SbF_6]^-$ as stable complex counter anion, it had been shown that the different form of the *living growing oxonium ions* have the same reactivities^[133]. The living character is lost when a less stable (more nucleophilic) complex anion is used. In fact, the polymerisation of THF with $AlCl_4^-$ as counter anion gives oligomer with a chlorine end group^[134]. In the case of non-complex counter anion such as $CF_3SO_3^-$, the destruction of the growing oxonium by non-complex counter anion is reversible and simultaneous existence of ion pairs (active growing species) and macroester (dormant species) can be observed^[135-138]. The stability of the counter-anion and the deactivation of the growing centre by anion splitting will be discussed, in the next section 1.3.2.2, for each type of initiator used.

1.3.2.2 Type of initiator and mode of initiation

The initiators used in cationic ring opening polymerisation of cyclic ethers are the same as in cationic polymerisation of vinylic monomers. Initiation occurs mainly by protonation, alkylation or acylation, though in some cases hydride ion transfer was found to occur. Here are few detailed examples.

1.3.2.2.1 Initiation by protonation

Protonic acids appear to be the most direct initiating agents of cationic polymerisation. However, they are not suitable for the production of polymers of high molecular weight and only 3 and 4 members ring cyclic ethers monomers can be successfully polymerised.

1.3.2.2.1.1 Using organic and inorganic protonic acids

Some inorganic and organic acids are able to cause the cationic ring-opening polymerisation of the cyclic ether monomers. The initiation results from transfer of a proton from an acid, AH , to the oxygen atom of a molecule of monomer. The equilibrium of protonation shifts to the right when a molecule of monomer reacts with the *secondary oxonium ion (II)* to be converted to a more reactive *tertiary oxonium ion (III)*. Thus a growing polymer with a hydroxyl end group is formed, according to:

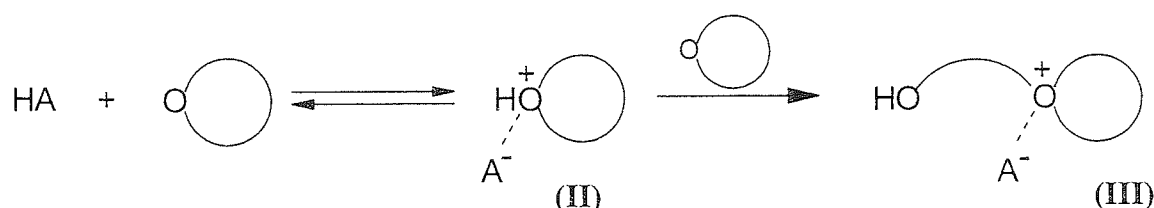


Figure 1. 10: The use of protonic acid for the initiation of cyclic ethers.

Only 3- and 4-membered cyclic ether monomers polymerise when initiated by protonic acids. THF fails to polymerise owing to the low ring strain associated with ring size. Indeed, the low basicity of the monomer does not permit the conversion of slightly a strained secondary oxonium ion to the reactive tertiary oxonium ion capable of cationic polymerisation.

Generally, the most reactive acids for initiation are those with the highest acidities (i.e. the lowest pK_a). This is because the counter-anion is less nucleophilic and consequently yields a much more stable oxonium ion able to propagate before collapsing irreversibly into dead polymers, according to:

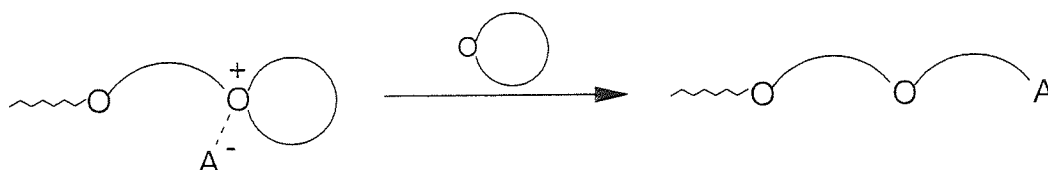


Figure 1. 11: Mechanism of annihilation of the growing oxonium by non-complex counter anion.

For these reasons, protonic acids are not suitable initiators for the production of polymers of high molecular weight. Only low molecular weight materials are obtained. The most effective

protonic initiators are perchloric acid and trifluorosulfonic acids (triflic acid) where irreversible annihilation of the growing oxonium ion with the counter-anion is less important than other strong acids.

The special case of triflic acid deserves some comments. This is the only superacid capable of initiating the polymerisation of tetrahydrofuran^[139]. Moreover, it has been reported that during the polymerisation, the active sites do not get lost upon recombination between the oxonium ion and its counter-anion, CF_3SO_3^- , and polymer of higher molecular weight can be obtained. This problem is described later (section 1.3.2.2.2.2). Table 1.5 gives the measurement of the pKa values of some strong acid in ethanoic acid and acetonitrile. Unfortunately pKa in the most commonly use solvents for cationic polymerisation, such as alkyl chlorides, are not available.

Brönstead acids	CH_3COOH Solvent	CH_3CN Solvent
$\text{CF}_3\text{SO}_3\text{H}$	4.7	2.6
HClO_4	4.9	1.6
FSO_3H	6.1	3.4
H_2SO_4	7.0	7.3
HCl	8.4	7.3
$\text{CH}_3\text{SO}_3\text{H}$	8.6	8.9
CF_3COOH	11.4	8.4
CCl_3COOH	12.2	10.6
CH_3COOH	12.8	12.7

Table 1. 5: pKa of some Brönstead acids in non-aqueous solvent.

Most of the studied protonation reactions seem to be more complex than shown in the simple scheme displayed above. In fact, proton affinities of the strong acids are far greater than the molecules of solvent employed in the cationic polymerisation. Consequently dimeric acid, trimeric acid and aggregations of acids molecules are often produce of reducing the effective concentration of initiating acid. Moreover, it was invoked in some mechanistic schemes dealing with the protonation of olefins that the interaction of acids with the monomer may result in two kind of ions pairs, the nonhomoconjugated $[\text{M}^+, \text{A}^-]$ and the more stable homoconjugated $[\text{M}^+, \text{A}_2\text{H}^-]$ pairs. The homoconjugated ion-pair $[\text{HM}^+, \text{A}_2\text{X}^-]$ is believed to be produced by the (slower) reaction of the non-aggregated but more abundant HA with the monomer, followed by diffusion-controlled association of the resulting $[\text{HM}^+, \text{A}^-]$ with HA, as

shown in the figure 1.12. The possible fast reaction of monomer with and $[H_2A^+, A^-]$ is thought to be improbable in view of the strong homoconjugation. For example, each molecule of triflic acid that initiates the polymerisation of alkene monomers yields a $CF_3SO_3^-$ that binds, due to the homoconjugation, to one or two acids molecules making the percentage of triflic acid available for the protonation of monomers between 33% to 50%, depending on the conditions prevailing in the reaction.

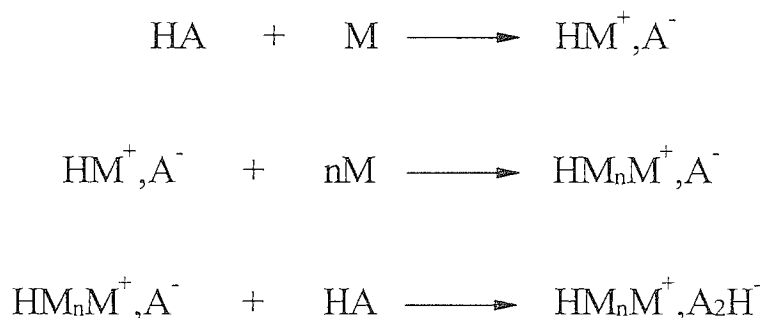
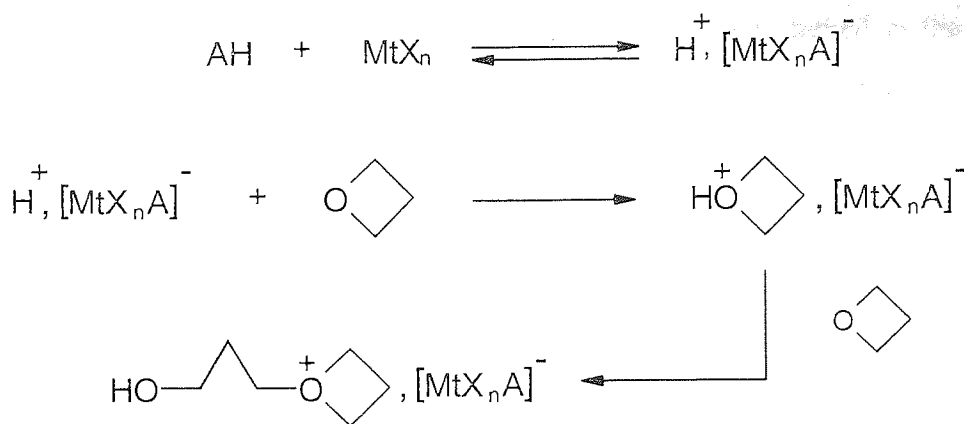


Figure 1. 12: Mechanism of formation of homoconjugated growing centre, HM_nM^+, A_2H^- .

If the formation of homoconjugated ions-pairs seems to be improbable when nucleophilic monomers such as cyclic ether are polymerised, the self-association of protonic acids still occurs when a solution of initiator is prepared prior to polymerisation.

1.3.2.2.1.2 Using complexes of Friedel-Craft reagents with protogens

Friedel-Craft reagents are complexes based on boron, aluminium or transition metal with a vacant orbital. The boron and aluminium FC reagents possess a vacant p-orbital whereas FC reagents based on transition metal have a vacant d-orbital. This property of FC reagents, M_nX_n , enables them to form, in a reversible way, a bond with a weak Brönstead acids (i.e. with high pKa), AH , yielding a proton coupled to an anion derived from FC reagents, $[M_nX_nA]^-$. By binding the residual negatively charge fragment, A^- , FC reagents facilitate the transfer of the proton to the monomer and produce a less nucleophilic counter-anion, $[M_nX_nA]^-$, than A^- . The equilibrium of the complex formation shifts to the right when the protonated monomer reacts with another molecule of cyclic ether to yield tertiary oxonium ion with a hydroxyl end group. In the figure 1.13, weak protonic acids act as the initiator, referred to as protogens, and the FC reagents are then the co-initiator. Like conventional protonic acids, only oxetane and oxetane derivatives can be polymerised by these initiator systems.



Where Mt= transition metal, boron or aluminium element, and X= halogen (usually)

Figure 1. 13: Initiation reaction of oxetane involving Brönstead acid HA and Friedel-Crafts reagents MtX_n.

The formation of complexes of FC reagents with weak protonic acids was conclusively proved in only a few cases, $\text{BF}_3 : \text{H}_2\text{O}$ complex^[140] becoming the classical initiating system employed for the polymerisation of 4-membered ring cyclic ether monomers. Indeed, the initial work carried out by Rose^[115] showed that the polymerisation of oxetane using BF_3 as initiator would not occur with BF_3 under absolutely anhydrous conditions and that the rate of the polymerisation was proportional to the amount of the water added. A small excess of water converts the inert BF_3 more efficiently into a powerful monohydrate complex, BF_3OH_2 , that initiate the polymerisation. This was also confirmed later by Farthing and Reynolds^[141] who observed that the polymerisation of 3,3-bis(chloromethyl)oxacyclobutane (BCMO) by BF_3 occurred only when a small amount of water was introduced into the reaction mixture.

In spite of its catalytic effect at low concentration, water inhibits polymerisation at higher concentrations. It reacts with the growing oxonium ion and destroys its activity, producing a telechelic polymer with lower molecular weight^[115].

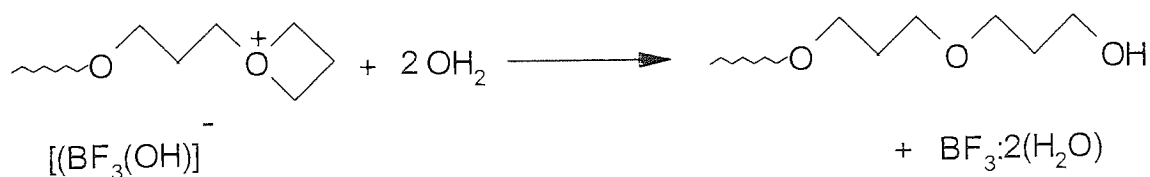


Figure 1. 14: Termination reaction in presence of water.

It converts the powerful monohydrate, $BF_3:H_2O$, initiating polymerisation into an inert dihydrated complex, $BF_3:2(H_2O)$. The maximum efficiency is achieved at the BF_3/H_2O ratio of about 3:2 (the equilibrium constant K_1 is larger than the equilibrium constant K_2 , figure 1.15)^[140], whereas for the $BCl_3:H_2O$ system^[142] the maximum is attained at a BCl_3/H_2O ratio of 1, whether determined at -75°C or -50°C .

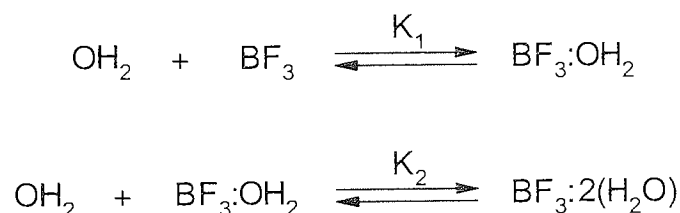


Figure 1. 15: Mechanism of formation of monohydrate complex, $BF_3:H_2O$, and dehydrate complex, $BF_3:2(H_2O)$.

Because water was used in extremely small quantities, some of the reported results were poorly reproducible. To improve this situation water was replaced by other protonic acids such as alcohol were used instead of water^[201]. Their utilisations led to similar results as those observed with water. Since then, oxetane and derivatives monomers such as BAMO, BCMO,...are commonly polymerised using alcohol as co-initiator of FC reagent^[201].

It must be noted that unlike conventional protonic acids AH , the use of complex of Friedel-Craft reagents with protogens to initiate the polymerisation of oxetane and oxetane derivative monomer generates a less nucleophilic counter-anion, $[M_nX_nA]^-$, than A^- . Nevertheless, because non-symmetrical anion complexes are not sufficiently stable to produce living polymers in carbocationic polymerisation, it is often reported that the A^- group and to lesser extent the X atoms, can be transferred to the oxonium ion in the course of the termination forming the integral part of the end-groups of the dead polymers^[115]. If the existence of termination reactions by anion-splitting were demonstrated in the case of the polymerisation of THF with $[AlCl_4]^-$ as counter anion^[134], in most cases, its existence was only based on the fact that polymeric materials of high molecular weight cannot be obtained. The figure 1.16 shows a schematic representation of termination reactions originate from anion splitting.

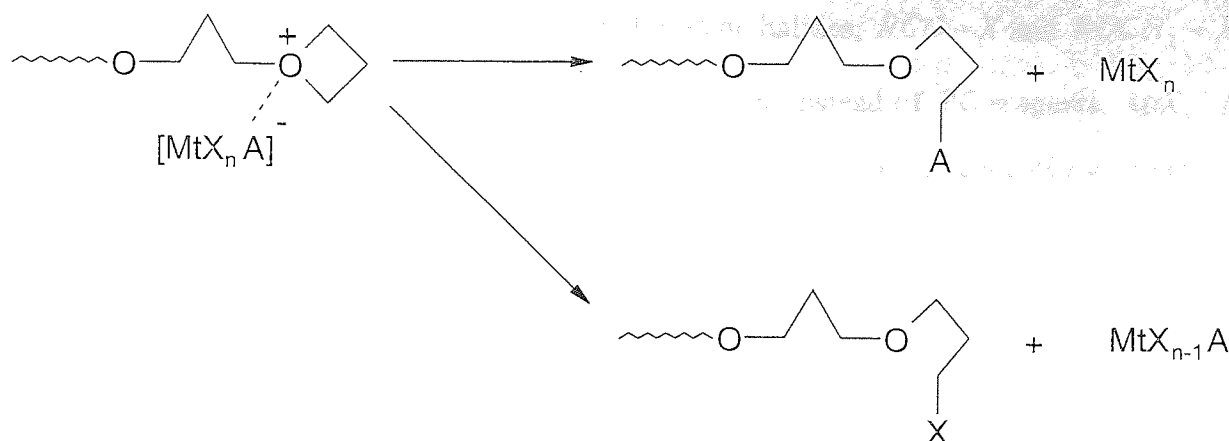


Figure 1. 16: Termination reactions by anion-splitting during the course of polymerisation of oxetane.

A second proposal for the mechanism of initiation was made because the existence of stable complexes such as $H^+, [M_t X_n A]^-$ are not formed with the hydrogen halides (e.g. TiBr and HBr). A modified mechanism is shown in figure 1.17.



Where M_t = metal, X = halogen (usually) and M = monomer

Figure 1. 17: Initiation reaction involving hydrogen halides as the Brönstead acid and Friedel-Crafts acid $M_t X_n$.

The most commonly used FC reagents in conjunction with protogens include BF_3 , $BF_3 \cdot OEt_2$, BCl_3 , $TiCl_4$, $SbCl_5$ and $AlCl_3$ and its alkyl derivatives, e.g., $AlEt_2Cl$. The protonic acids used are Cl_3COOH , $ClCH_2OOH$, CH_3COOH , $PhOH$, ROH , H_2O , HBr , HCl , etc. Water being usually, the most powerful initiator used conjunction to FC reagent to initiate the cationic polymerisation.

1.3.2.2.2 Initiation by alkylation and acylation

1.3.2.2.2.1 Initiation by FC reagents in conjunction with cationogens

If trivial HO end-groups are produced when polymer are formed by the initiation induced by protonic acids, a variety of functional groups can be attached to the polymer end when judiciously chosen cationogens are utilised as initiators in conjunction with FC reagents. For example, groups such as $RCO-$ and $ROCH_2-$ can be introduced into polymer by initiating

the polymerisation with a mixture of MtX_n and organic halides, $RCO-X$ and $ROCH_2-X$, respectively. Silver salt, $Ag^+, [MtX_{n+1}]^-$, can also be used instead of FC reagents, MtX_n . As shown in the scheme 1.23, the initiation process is visualised as a sequence of two reactions. The formation of the carbocation complex $R^+, [MtX_{n+1}]^-$ is followed by simple alkylation or acylation of a molecule of monomer. The latter reaction being referred as alkylation and acylation when the cationic site, R^+ , is a carbenium group, $-CH_2^+$, and acylium group, $-CO^+$, respectively.

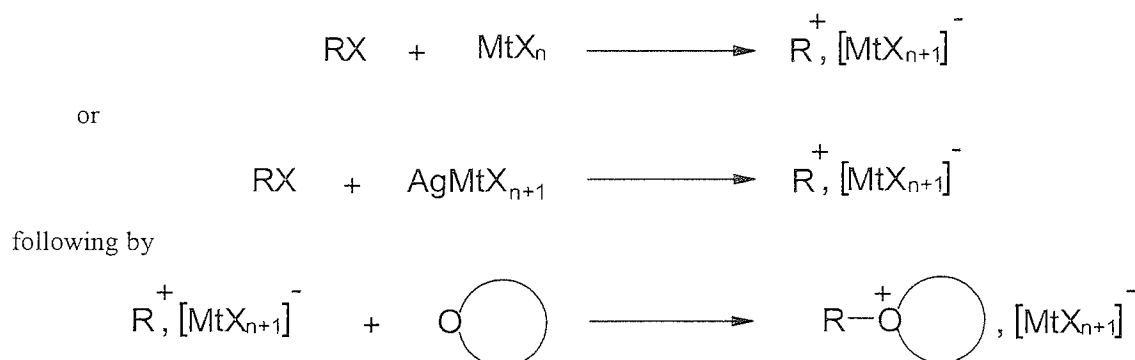


Figure 1. 18: Initiation involving organic halide RX with Friedel-Crafts reagents, MtX_n , and silver salt, $AgMtX_{n+1}$.

Unlike the initiation induced by protonation, all thermodynamically polymerisable cyclic ethers undergo cationic polymerisation when initiated by a mixture of MtX_n with RX . This is because no secondary oxonium ions are formed during the initiation process. Indeed, the nucleophilic attack of a molecule of monomer onto the cationic site of the carbocation complex, $R^+, [MtX_{n+1}]^-$, yields a straightforward tertiary oxonium ion. Moreover, the high electrophilicity of the carbocation, R^+ , and the high reactivity of the formed tertiary oxonium ion lead to a fast initiation with high initiating efficiency, sometimes almost quantitative.

Termination reaction by anion-splitting are less likely to occur with symmetrical anions such as $[SbF_6]^-$ and $[BF_4]^-$. Their charges are uniformly and spherically spread over their surface and there is only a weak interaction with the growing oxonium ion centre. In the table 1.6, representative complex anions have been classified with respect to their stability^[143].

group I	group II	group III
$[\text{AsF}_6]^- \sim [\text{SbF}_6]^- > [\text{PF}_6]^-$	$[\text{SbF}_6]^- > [\text{BF}_4]^-$	$[\text{AlCl}_4]^-$

Table 1. 6: Classification of complex anions with respect to their stability.

The anions of group I are the highest stability, and cause apparently no termination by anion splitting. Polymerisation and depolymerisation repolymerisation behaviour with changing temperature has been observed in the case of THF using $[\text{PF}_6]^-$ as counter anion^[144]. Among the anions listed above, $[\text{AlCl}_4]^-$ has the lowest stability. The polymerisation of THF with $\text{Et}_3\text{OAlCl}_4$ gives oligomers with a chlorine end group^[134]. However, the reversibility of the termination is taken in some case into account, since tetrahydrofuronium salt has been isolated in the following reaction^[145].

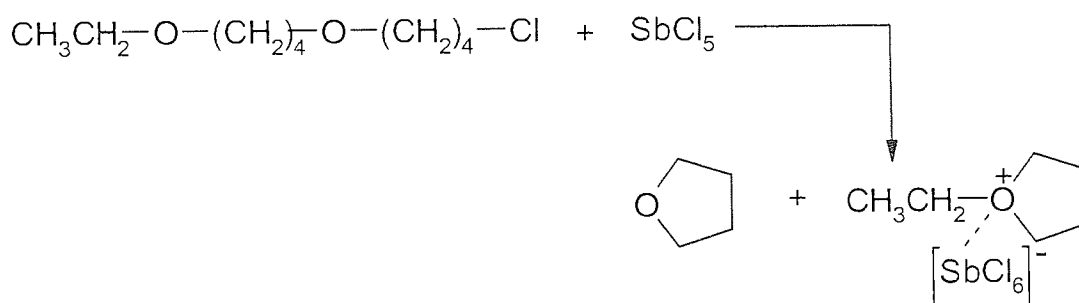


Figure 1. 19: Formation of tetrahydrofuranium salt by action of SbCl_5 on 4-chloro-4'-ethoxybutylether.

It must be noted that the anion-splitting competes with chain growth. In consequence, this type of termination is more important in the polymerisation of monomer of lower basicity such as 3-membered cyclic ether than for the monomer of higher basicity such as 4-membered cyclic ether. Anion splitting is supposed to be non-existent when an anion of group I and II are used.

This procedure can be adopted for a large variety of organic halide compounds. Here are listed few examples of mixtures of FC reagent or silver salt in conjunction with RC used in the polymerisation of cyclic ethers monomers.

1.3.2.2.2.1.1

Trialkyloxonium salt

Triethyloxonium tetrafluoroborate was first prepared by Meerwein^[146]. Since then, various trialkyl oxonium ion salts possessing complex anions, $[SbF_6]^-$, $[SbCl_6]^-$, $[FeCl_4]^-$ and $[AlCl_4]^-$ have been prepared^[147]. The initiation process is the simple alkylation of a molecule of monomers^[146]. The ring opening reaction of the cyclic tertiary oxonium ion constitutes the propagation reaction (figure 1.20).

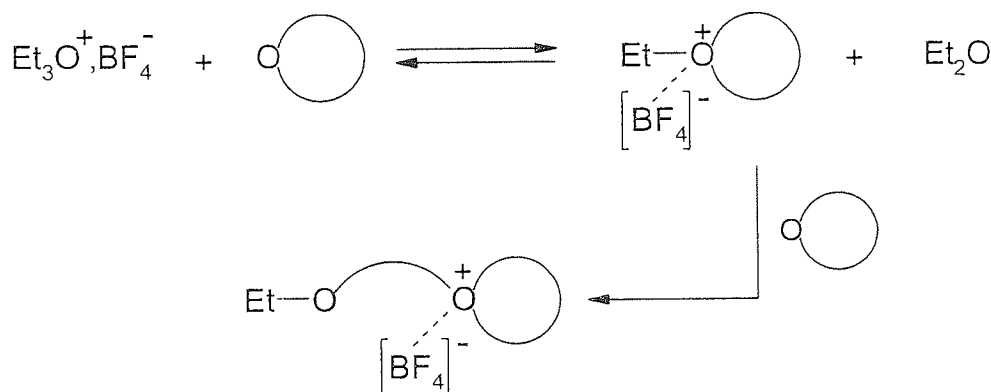


Figure 1. 20: Initiation by triethyloxonium tetrafluoroborate.

With monomer having high nucleophilic reactivity such as a 4-membered cyclic ether, the oxonium exchange reaction for the generation of the cyclic tertiary oxonium ion species is very efficient, sometimes almost quantitative. However, it has been mentioned that, during the polymerisation, the diethyl ether produced can react with the oxonium ion to yield an open chain tertiary oxonium-ion of a lesser reactivity. Upon deactivation of these oxonium salt, one of the three CH_2-O^+ bonds has to be cleaved by a molecule of monomer to regenerate the growing tertiary oxonium ion.

Another trialkyloxonium salt used for the initiation of cyclic ether monomers is the dialkyloxycarbenium salt (figure 1.21), which is prepared from an ortho-ester and a Lewis acid^[147]. The positive charge is stabilised by two alkoxy groups.

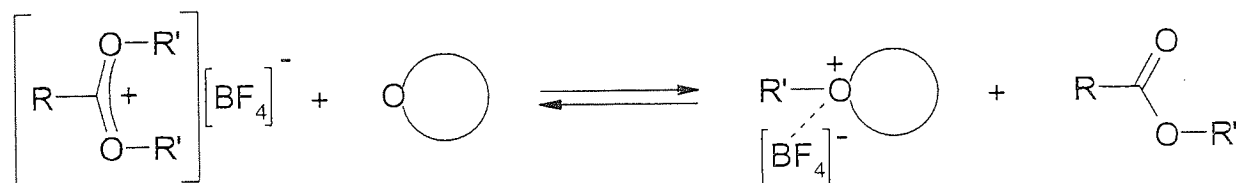


Figure 1.21: Initiation by dialkyloxycarbenium salt.

In this case, the oxonium exchange with cyclic ether is slow, and the, dialkyloxycarbenium salt is not consequently an efficient initiator for the cyclic ether polymerisation. Moreover, during the polymerisation reaction, the dialkyloxycarbenium salt can be reformed from the nucleophilic attack of the oxygen atom of the ester molecule onto a carbon atom in the α -position with respect to the oxonium site of the growing centre. The newly formed dialkyloxycarbenium salt bearing one or two polyalkoxy group, R' , can therefore reinitiate the polymerisation by nucleophilic attack of the oxygen atom of a molecule of monomer onto a carbon atom in α -position with respect to the oxonium site. In this scheme, the dialkyoxycarbenium salt involves equilibrium between *active* (propagating) and *dormant* (non-propagating) polymer chains.

1.3.2.2.2.1.2

1,3-dioxolan-2-ylum salts

1,3-Dioxolane-2-ylum salts can be prepared by the hydride transfer from dioxolane to triphenyl methyl cation^[148] or by Meerwein's procedure using a bromoethyl ester^[149].

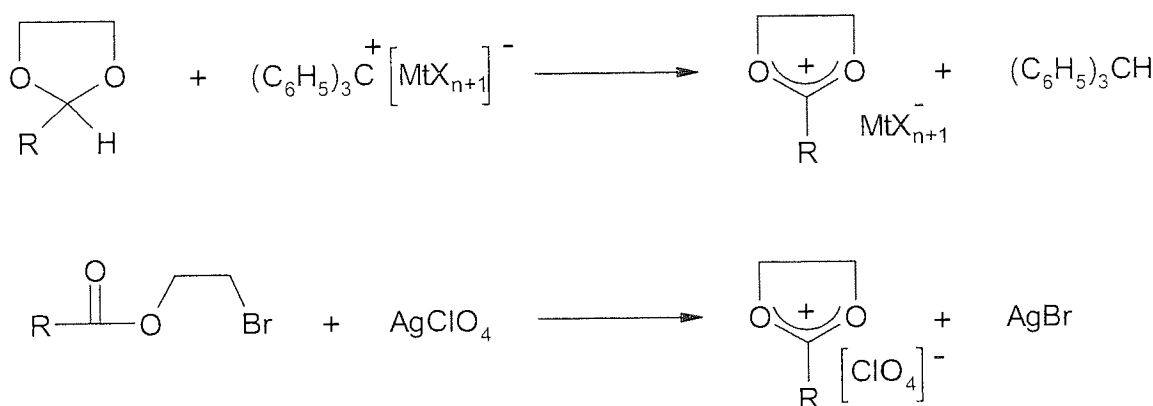


Figure 1. 22: Preparation of 1,3-dioxolane-2-ylum salt by hydride transfer.

Initiation proceeds according to the following scheme

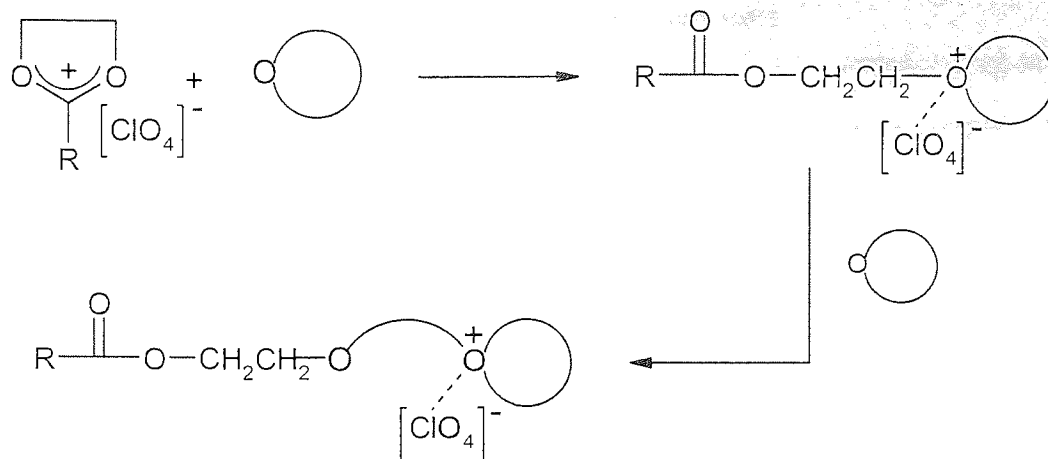


Figure 1. 23: Initiation by 1,3-dioxolane-2-ylum salt.

and an ester group is introduced to end the polymer. When a dioxoanylium ion with $R=H$ is used as catalyst, the formyl end group may be observed by NMR 1H ^[150] and the measured rate of initiation is comparable to that of propagation.

1.3.2.2.2.1.3

Using dialkyl methylium salt

Diphenyl methylium hexafluoroantimonate is an efficient initiator for the polymerisation of THF ^[151]. Initiation takes place quantitatively and is more rapid than propagation.

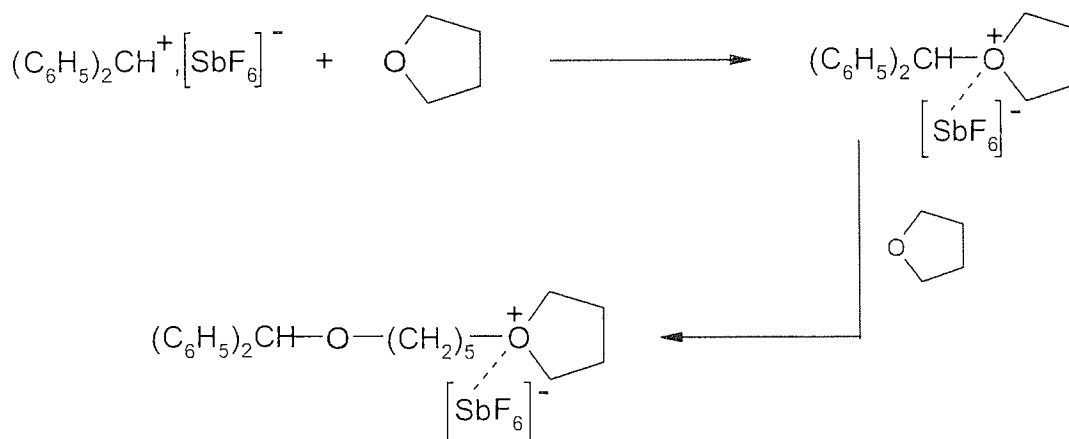


Figure 1. 24: Initiation by dialkyl methylium salt.

Similarly, the bifunctional dimethyl benzylium hexafluoroantimonate salt prepared from *p*-bis-(α,α -dimethylchloromethyl)benzene with hexafluoroantimony (AgSbF₆) was used to initiate the sequential polymerisation of NIMMO and BAMO ^[8].

Oxocarbenium ions are generally prepared by the reaction of the corresponding acid halide and a silver salt, Ag^+ , $[MtX_{n+1}]^-$,^[152]. Oxocarbenium salts react with the monomer to give also an ester end group to the polymer chain^[153].

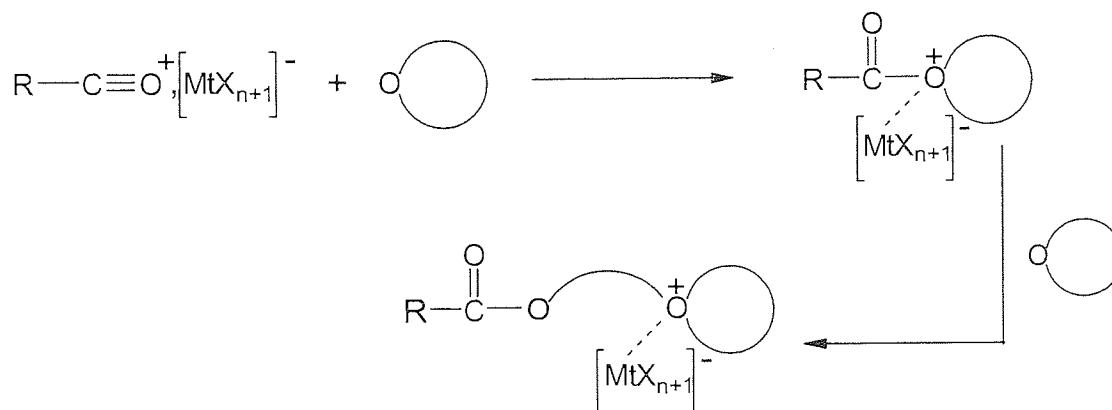
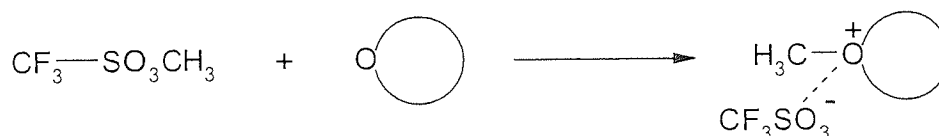


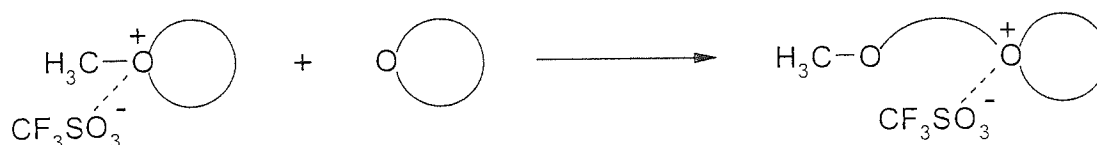
Figure 1. 25: Initiation by oxocarbenium salt.

1.3.2.2.2.2 Initiation by super acid esters

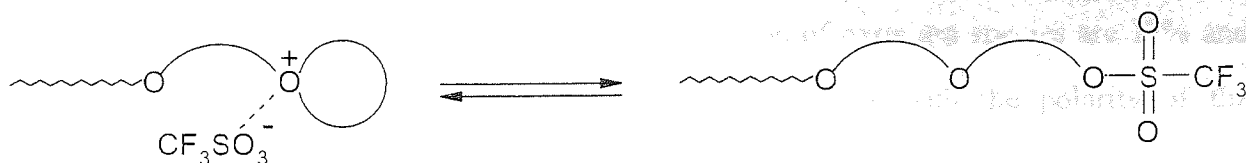
Super acid esters such as alkyl trifluoromethyl sulfonates, CF_3SO_3R , and fluoro sulfonates, FSO_3R , are strong (highly electrophilic) alkylating agents. Because, the coupling reaction between cation and anion to form an ester is reversible, the active site are not lost upon recombination between the oxonium ion and its counteranion. The most commonly used catalysts include CF_3SO_3H , CF_3SO_3R , FSO_3R , $ClSO_3R$, $(CF_3SO_2)_2O$, $(FSO_2)_2O$, and $(ClSO_2)_2O$. The initiation with a super acid derivative is in general characterised by a lower rate than with other initiators. As exemplified with methyl triflate as initiator, the initiation occurs by alkylation of molecule of monomer



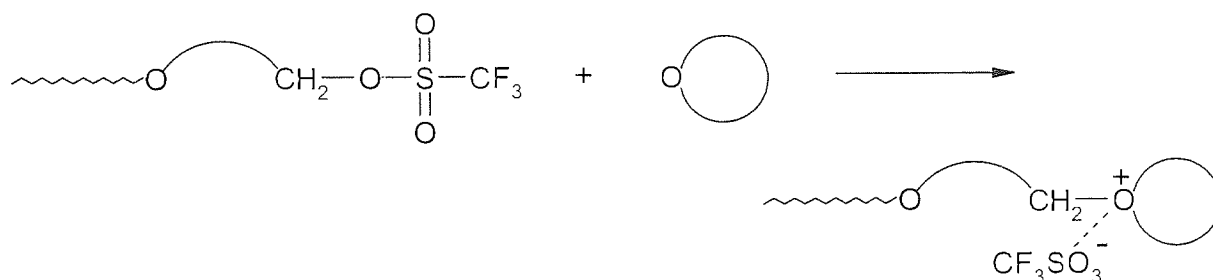
where upon chain growth can take place:



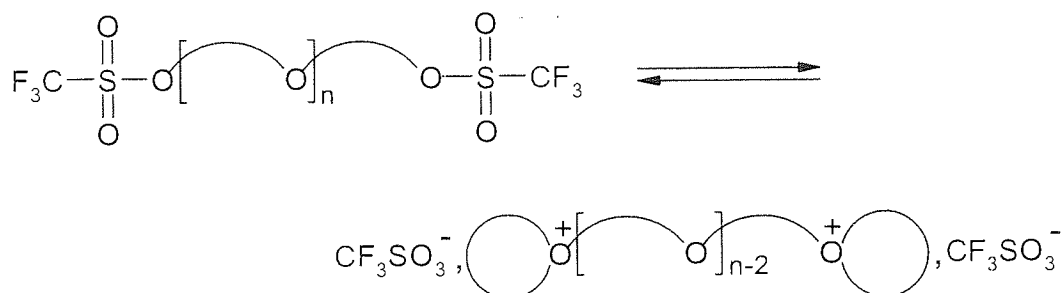
As indicated, the ion pair structure is in equilibrium with the ester form:



Whereas the nucleophilic attack of the monomer on the penultimate unit on the carbon α of the ester group, an oxonium species is produced on propagation:



If instead of the super acid ester, triflic anhydride is used as the initiator, the same initiation can occur at both chain ends, demonstrating that the anhydride behaves as a bifunctional initiator:



The simultaneous presence of the macroion together with the corresponding macroester has been directly observed by NMR^[135,136].

In the polymerisation of highly strained monomers (3- and 4-membered cyclic ethers), only macroester is observed, even in highly polar solvents^[137,138]. This is because the cyclic onium is highly strained and therefore collapses into an ester bond when a molecule of monomer has been incorporated into the polymer chain. In the case of 3-membered cyclic ethers, the monomer is quantitatively converted into dioxane by ethyle triflate^[138]. The basicity of the oxygen atom in the polymer chain favours back-biting to the chain growth. On the other end,

in the polymerisation of oxepane (7-membered ring) and tetrahydrofuran (5-membered ring) with $EtOSO_2CF_3$ in dichloromethane at 35°C, the fraction of oxonium species are 17% and 87%, respectively^[156]. The fraction of oxonium ion increases with the polarity of the polymerisation medium and with the increase of the temperature.

1.3.2.2.3 Initiation by Lewis Acids

In the previous section, we have seen the Lewis acids such as BF_3 , $AlCl_3$, $AlBr_3$, $SnCl_4$, SbF_5 , $FeCl_3$ and PF_5 are widely used as cationic initiators in the ring opening polymerisation of cyclic ethers. The necessity for a suitable co-catalyst depends on the nature of the monomer. The use of protonic acids in conjunction of Lewis acids has been found to polymerise the 3- and 4-membered cyclic ethers, whilst the use of organic halides as co-initiator promote the polymerisation of a large range of cyclic ethers such as 3-, 4-, 5-, 7-, 8-membered cyclic ethers monomers. There has been long debate as to whether or not a *pure* Lewis acid is capable of initiating polymerisation. The problem is not easy to settle as these species can react with so many impurities normally present, which may act as co-initiator of the polymerisation of the investigated monomer. For example, a trace of ubiquitous water in conjunction of with Lewis acid is a powerful initiator in cationic polymerisation, including a slow polymerisation. The experimental evidence in favour of direct initiation comes from the observation of high rates of polymerisation and quantitative conversions of monomer into polymer under the most rigorous exclusion of any impurities that could cooperate in the initiating process. The polymerisation of 3-membered cyclic ether monomers such as ethylene oxide, propylene oxide and epichlorhydrin have been claimed to fulfil these conditions. The action of the Lewis is considered to give rise to the formation of a zwitterion without the use of co-catalyst^[157]. The initiation of ethylene oxide by two molecules of boron trifluoride, BF_3 , is expressed as follows:

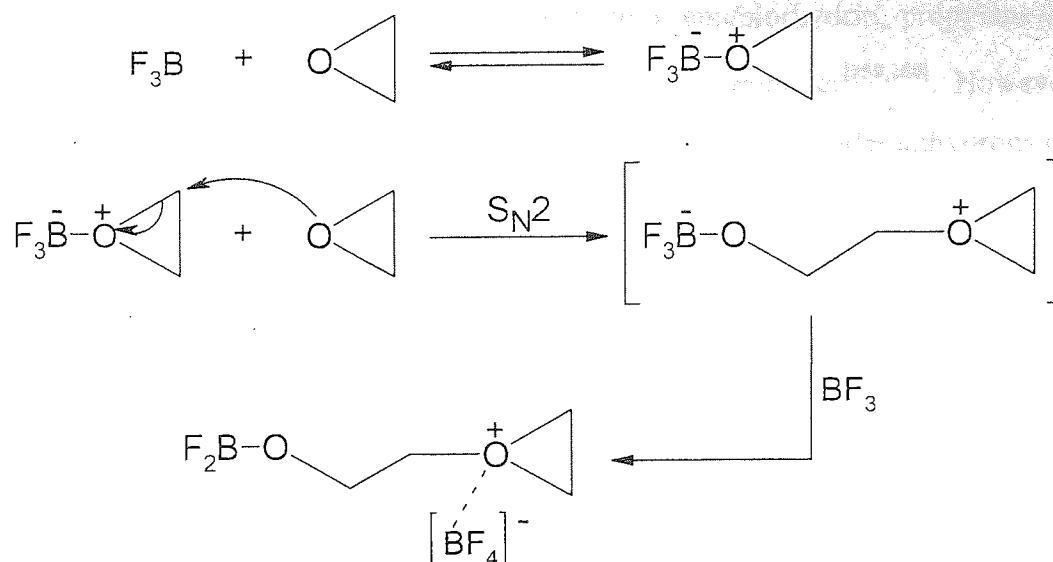


Figure 1. 26: Polymerisation of EO initiated by BF_3 .

The high reactivity of 3-membered cyclic ether towards Lewis acids in that such systems can be used as *promoter* in the initiation of other less strained monomers such as 4- and 5-membered cyclic ethers monomers. An example of this type of polymerisation includes the initiation of BCMO in the presence of either BF_3 , AlCl_3 or SnCl_4 with promoter molecules such as epichlorhydrin and propylene oxide^[168].

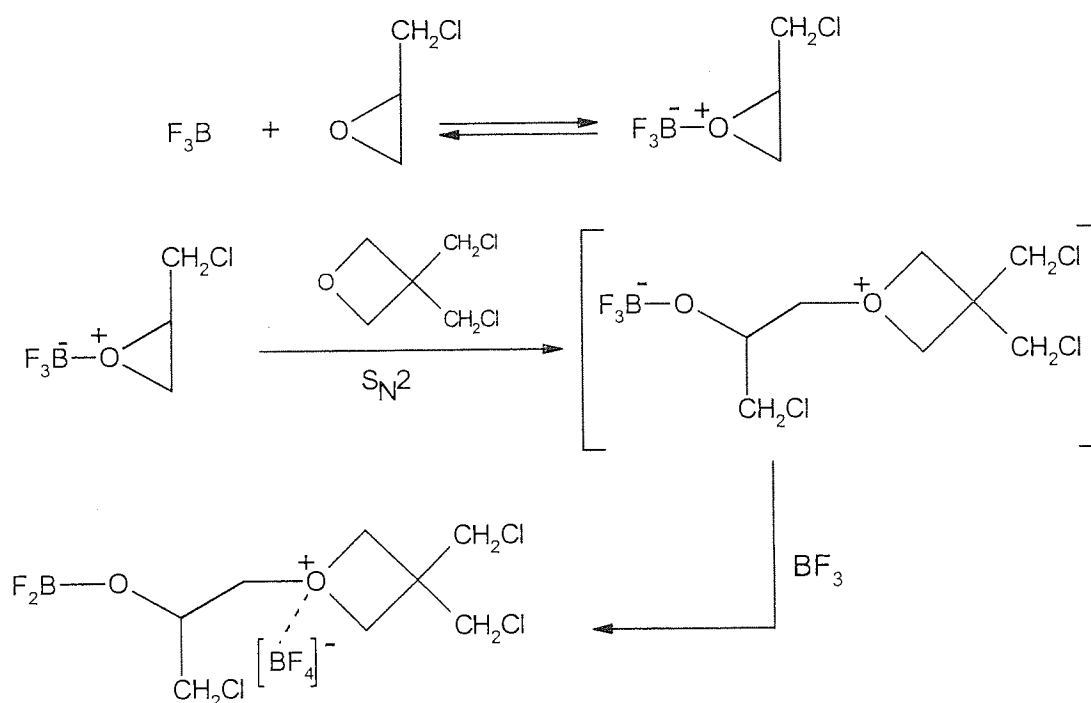


Figure 1. 27: The use of a promotor molecule for the initiation of BCMO.

In the polymerisation of THF by $AlEt_3/H_2O$ system, epichlorhydrin, propylene oxide, β -propiolactone and diketene were reported to function as promoter^[159,160]. However, when $SbCl_5$ is used as initiator, the polymerisation of THF^[161, 162] takes under anhydrous condition according to the figure 1.28:

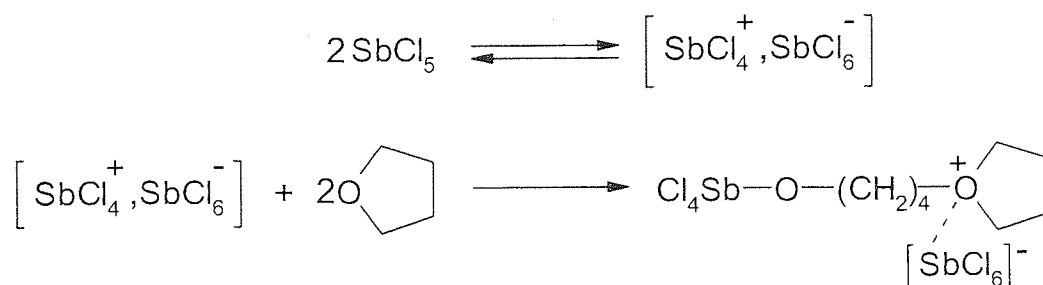


Figure 1. 28: Polymerisation of THF initiated by $SbCl_5$.

It must be noted that the promoter itself is a polymerisable compound. Therefore, it is liable to copolymerise, although its content in the polymer is very small.

1.3.2.2.4 Initiation by hydride transfer

Triphenylmethyl (trityl) salts may initiate the polymerisation of cyclic ethers by addition followed by hydride ion abstraction^[163,164]. The mechanism of initiation is shown in figure 1.29:

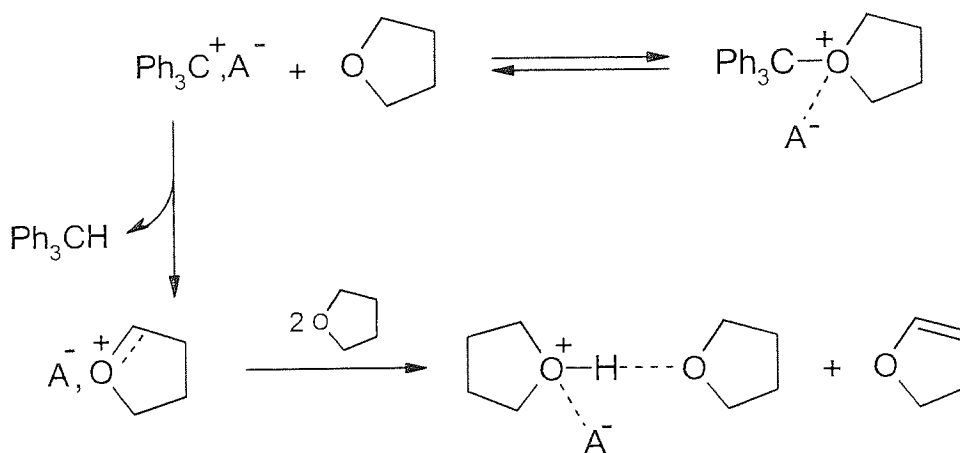


Figure 1. 29: Initiating species in the polymerisation of THF initiate by trityl salt.

The evidence for initiation involving hydride abstraction came from studies involving ^{14}C -labelled catalyst, which showed that the resulting polymer did not carry any end group

originating from the initiator^[164,165]. Initiation is thought to occur by direct attack of a molecule of monomer on the α carbon of the ether group of the protonated monomer stabilised by the interaction with non protonated monomer.

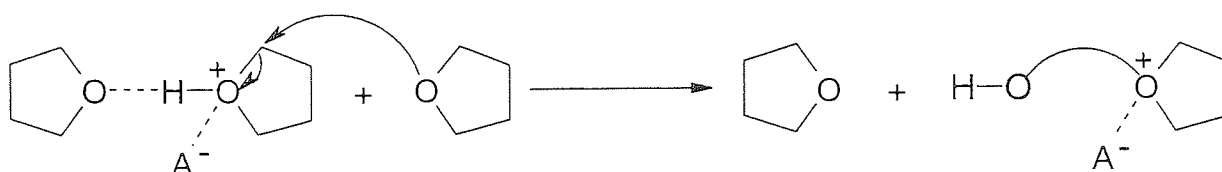


Figure 1.30: Initiation by hydride transfer via the formation protonated monomer stabilised by the interaction of with non protonated monomer.

The mode of initiation is still open because protonic acids do not initiate the polymerisation of tetrahydrofuran. The low basicity of the heterocyclic oxygen in tetrahydrofuran does not permit the conversion of slightly strain secondary oxonium ions to the reactive tertiary oxonium ion capable undergoing cationic polymerisation.

Another initiator which can induce initiation by hydride transfer is the diazonium salt shown in the figure 1.31^[166]. The initiation is similar to the trityl salt-catalysed polymerisation.

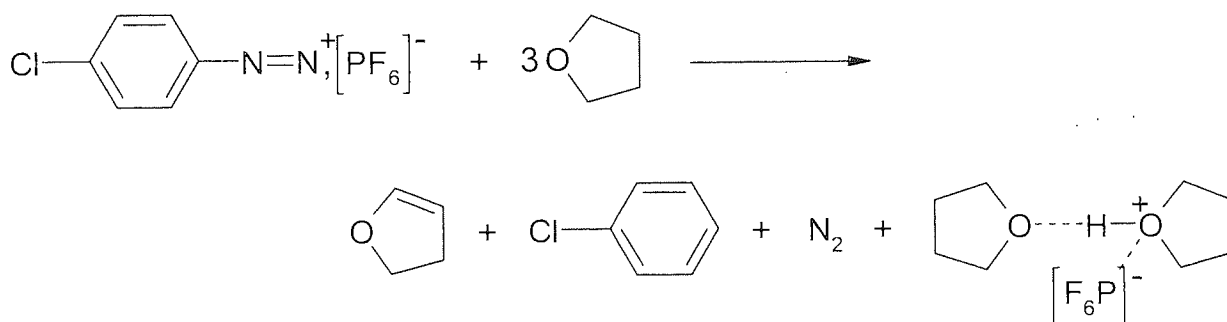
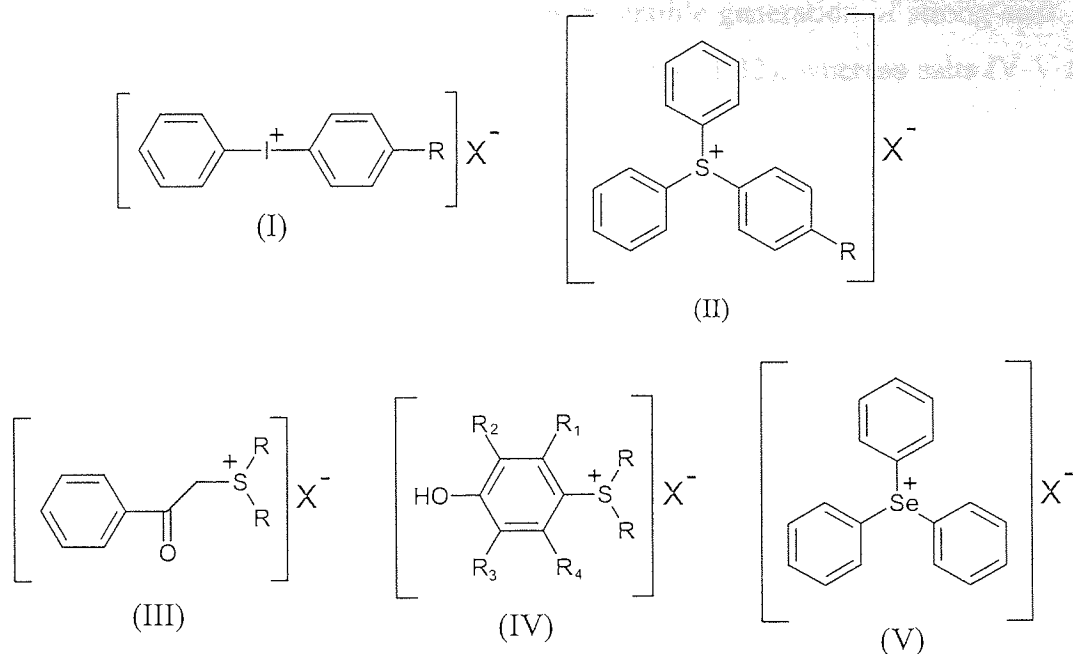


Figure 1. 31: Initiating species in the polymerisation of THF initiate by diazonium salt.

1.3.2.2.5 Initiation using photo-initiators

1.3.2.2.5.1 *Photo-initiated cationic polymerisation using iodonium, sulphonium and selenium salt*

A group of photo-initiators of cationic polymerisation has recently been developed by Crivello et al^[167]. These include the following salts; diaryliodonium (I), triarylsulphonium (II), dialkylphenacylsulphonium (III), dialkyl-4-hydroxyphenylsulphonium salts (IV) and triarylselenium salt (V).



where $X^- : [AsF_6]^-; [PF_6]^-; [SbF_6]^-; [BF_4]^-$

Figure 1.32: Group of photo-initiators developed by Crivello et al., reference 167.

Normally in the absence of light, these salts are quite stable towards the monomer even at high temperatures. On irradiation, usually at wavelengths less than 360nm, a photochemical process occurs producing a strong acids HX (i.e. HBF_4 , $HAsF_6$, HPF_6 or $HSbF_6$) capable to initiate at room temperature the polymerisation of large range of cyclic ethers monomers. There are two mechanistic patterns for the photodecomposition of the initiator. The first pattern (figure 1.33) involves the homolytic cleavage of a bond such as carbon-iodine bond in the case of diaryliodonium salt,

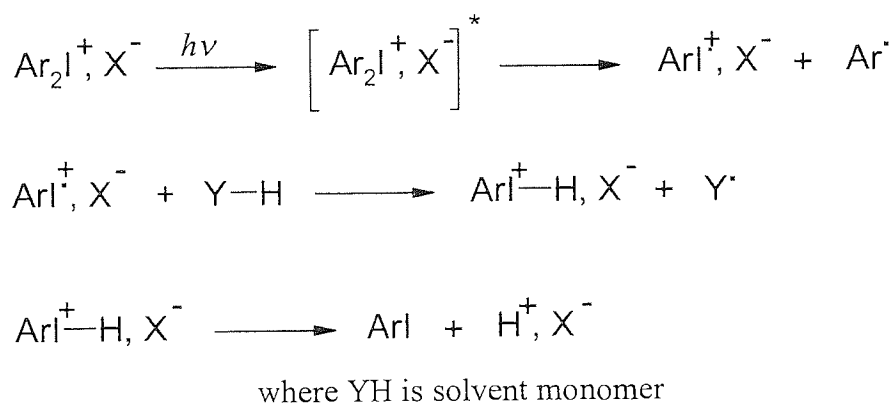


Figure 1.33: Mechanism of photolysis of diaryliodonium salts at $\lambda < 360$ nm (first pattern).

Whereas the second pattern, figure 1.34, involves reversible generation of strong acid. In the figure 1.32, the salt I-III follows the first pattern (see figure 1.33), whereas salts IV-V follow the second (see figure 1.34).

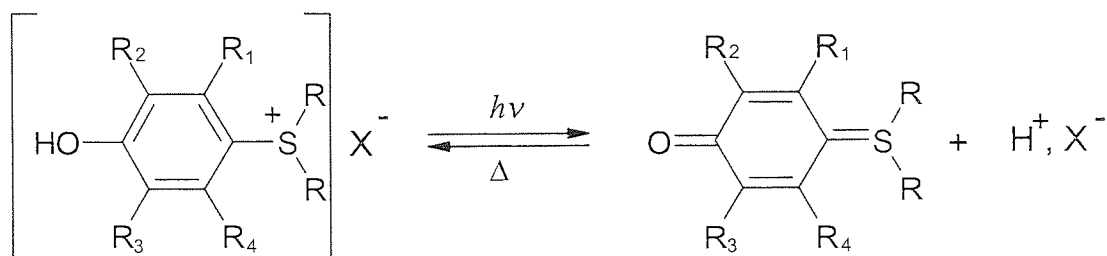
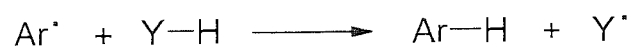
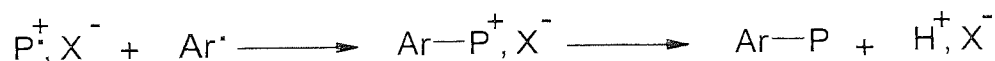
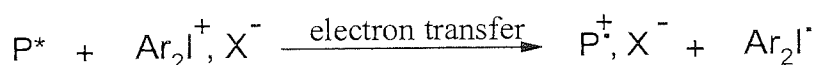
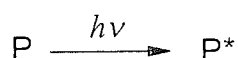


Figure 1. 34: Mechanism of photolysis of dialkyl-4-hydroxyphenylsulphonium salts at $\lambda < 360$ nm (second pattern).

Successful photopolymerisations of cyclic epoxides^[168] and oxetane derivatives^[168-170] have been reported using iodonium and sulphonium salt at a wavelength less than 360 nm. Photosensitizers such as acridine orange, acridene phosphine R, benzoflavine, setoflavine T and 2-isopropylthioxanthane can be used to induce photodecomposition of diaryliodonium salts by electron transfer at wavelengths longer than 360 nm^[169,171-173]. Triaryl sulfonium, dialkylphenacylsulfonium and dialkyl(4-hydroxyphenyl)sulphonium salts were sensitized by perylene and other polynuclear systems to produce hydrocarbons. Under these conditions polymerisation took place by normal sunlight^[174,175].



where YH is solvent monomer

Figure 1. 35: Mechanism of photolysis of diaryliodonium salts at $\lambda > 360$ nm (normal sunlight) using photosensitizer P.

Detailed studies carried out on photoinduced cationic polymerisations (of strain cyclic ethers) have shown that polymerisation not only depends on monomer structure but also on the nature of the counter anion. From the rate constant, it has been observed that the order of reactivity correlates well with the known relative nucleophilicities of counter anion, that is, $SbF_6^- > AsF_6^- > PF_6^- > BF_4^-$. In the case of the polymerisation of strained cyclic ether monomers, the reactivities are greater for oxetane monomers than for epoxides with closely related structure^[168]. This is ascribed to the higher basicity of the heterocyclic oxygen in oxetane than that for oxirane.

In addition to this general observation, it was also reported that the reactivities of cyclic ether monomers depend not only on their structure but also on the presence of others functional groups in the molecule. Oxetane monomers containing alkyl, aryl or propenyl ether groups are more reactive than those possessing ester, carbonate, or urethane. The presence of basic groups such as urethane, carbonate and ester moieties can easily interfere with the polymerisation by reacting with the growing centres^[170]. In the case of oxetane monomers containing propenyl ether groups, it was observed that the polymerisation of both functional groups take place simultaneously^[170]. In all likelihood, it seems that, in the presence of strong acids generated by photolysis of the photoinitiator (see figure 1.34), the vinyl ether groups can be protonated to give the resulting carbenium ions. During the course of polymerisation of the vinyl ether group, the attack of the carbenium ion on the oxetane monomer results in the rapid formation of the more stable oxetane oxonium cation which is consumed only by oxetane moieties. This was confirmed by infrared spectroscopy analysis which showed that polymerisation of the oxetane functional group proceeds at more rapid rate and to a higher degree of conversion than the propenyl ether functional group^[170].

It must be noted that during the photodecomposition of the initiator free radical species (Ar^\bullet and Y^\bullet) are also produced as transient intermediate. This means that both free radical and cationic polymerisation can take place simultaneously in some case. Irradiation of an equimolar mixture of 1,4-cyclohexene oxide and methyl methacrylate with Ar_3S^+, SbF_6^- yielded two homopolymers, polycyclohexene oxide (cationic) and poly(methylmethacrylate) (radical). The same system containing 2,6-di-terbutyl-4-methylphenol, which acts as an inhibitor of free radical polymerisation gave only polycyclohexene oxide. Conversely, the system with triethylamine which acts as poison for cationic polymerisation yielded only

polymethylmethacrylate. Using monomers, that contain functional groups susceptible to cationic and radical polymerisation to give a cross-linked insoluble polymer, could extend the multi-functional nature of sulphonium salts.

1.3.2.2.6 Electrolytic initiation

When a solution of tetrahydrofuran containing perchlorate salt is subject to electrolysis, poly-THF is produced in the anode cell^[176-178]. The polymerisation is due to the production of perchloride acid, $HClO_4$, according to the sequence:

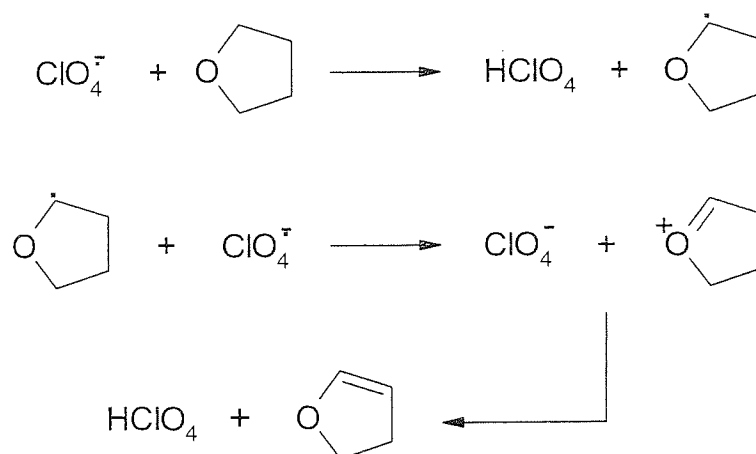


Figure 1. 36: Production of perchlorate acid by electrolysis.

Electrolytic initiation has also been observed with BCMO and trioxane^[179].

1.3.2.3 Mode of formation and structure of cyclic oligomers

In section 1.3.1.2, we have seen that cyclic oligomer formation depends on the ring strain contain in the tertiary oxonium ion and on the basicity of the oxygen atom in the polymer chain. In the case of the polymerisation of 3- and 4- membered rings, the polymerisation produces a large amount of cyclic oligomers, up to 50-100% and 4-50% for oxirane^[180] and oxetane^[115], respectively. However, the use of metal halide^[123,1127,181] or oxonium salt with stable counter anion ion^[159,165] is less favourable for cyclooligomerisation, and polymer formation is predominant; even if cyclic oligomers are formed, the polydispersity is not narrow. In the polymerisation of THF, only a small amount of cyclic oligomers is produced, 3%, indicating that the propagation proceeds via relatively stable tertiary oxonium species^[183]. The use of metal halide as counter-anion in the polymerisation of THF enables living polymer growth^[184-187]. In the case of the oxepane, Matyjaszewski et al. reported that

the polymerisation in the presence of stable counter-anion gives rise to living polymerisation^[133], which supposes a total exclusion of transfer reactions and therefore a total exclusion of formation of cyclic oligomers.

In this section, the mode of formation and the structure of the cyclic oligomers will be described only for 3- and 4-membered cyclic ether.

1.3.2.3.1 Mode of formation of cyclic oligomers

The cyclic oligomers are formed by back-biting (and/or tail-biting) reaction of the growing polymers, which produces a less strain macrocyclic tertiary oxonium ion.

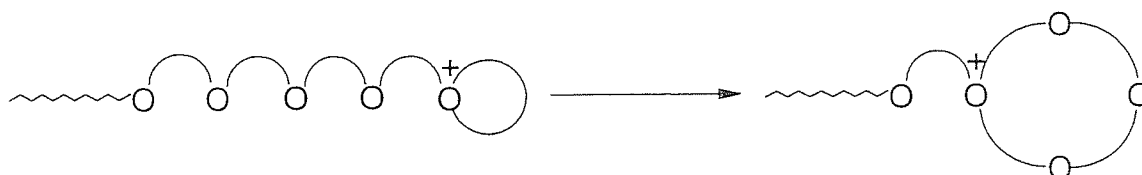


Figure 1. 37: formation of low strain macrocyclic tertiary oxonium ion.

As shown in the figure 1.38, the elimination of the macrocyclic from the polymer end, and the regeneration of the strained tertiary oxonium ion take place by nucleophilic attack of the monomer (pathway a) or the penultimate unit (pathway b) on the exocyclic carbon atom of the macrocyclic tertiary oxonium ion.

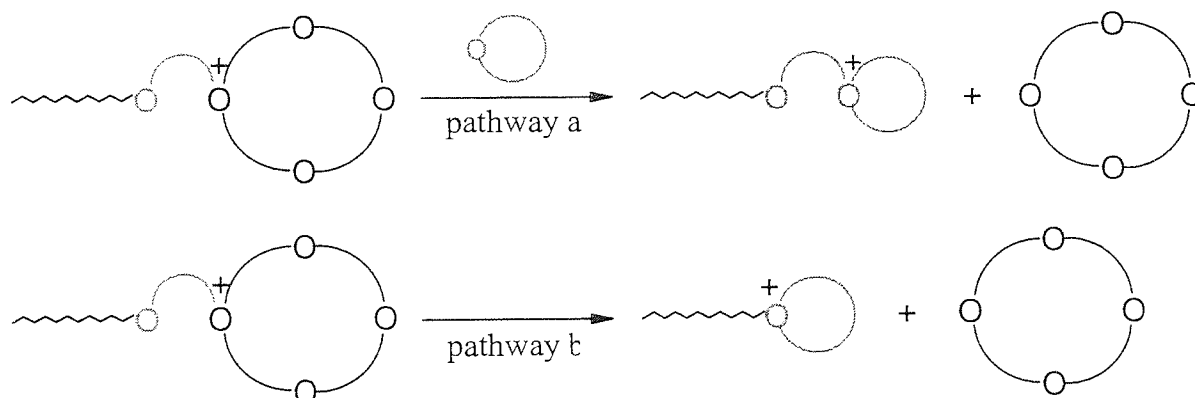


Figure 1. 38: Mode of elimination of the macrocyclic from the polymer chain end.

The *path b* takes place, in addition to the *path a*, only for the polymerisation of 3-membered cyclic ether monomers. This is ascribed to the higher basicity of the oxygen atoms in the polymer chain than the oxygen atom of ethylene oxide molecule. The direct proof for the

contribution of the pathway b in the cyclooligomerisation process is related to degradation of poly(ethylene glycol) into 1,4-dioxane in the presence of Et_3O^+ , BF_4^- either in the presence or absence of ethylene oxide^[123,189], indicating that formation of cyclic oligomers still occurs after completion of the polymerisation.

In the case of the polymerisation of *trans*-2,3-butene oxide, the absence of dioxane with two inverted carbon atoms strongly indicates that the formation of non-strained tertiary dioxanium ion (from dioxane) can also occur as follow^[129,130].

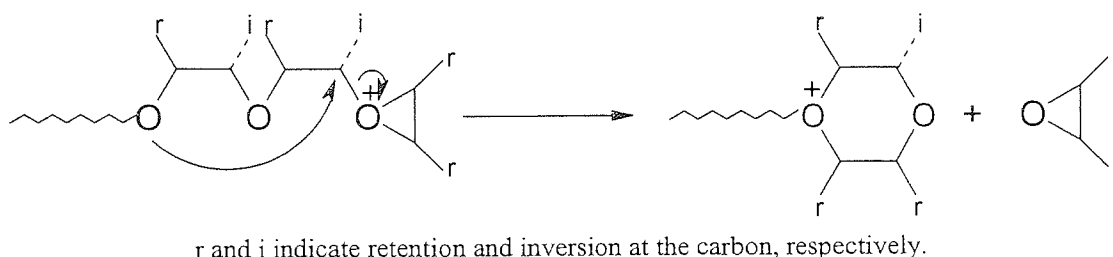


Figure 1. 39: Mechanism of formation of non-strained dioxanium ion in the polymerisation of *trans* 2,3-butene oxide.

It must be noted that intramolecular transfer reaction always occurs together with intermolecular transfer reactions. As shown in the figure 1.40, the intermolecular transfer reactions leads to a redistribution of linear chain length by random process, with eventually formation of linear polymers carrying tertiary oxonium ion at the both chain ends (pathway b in scheme 1.40).

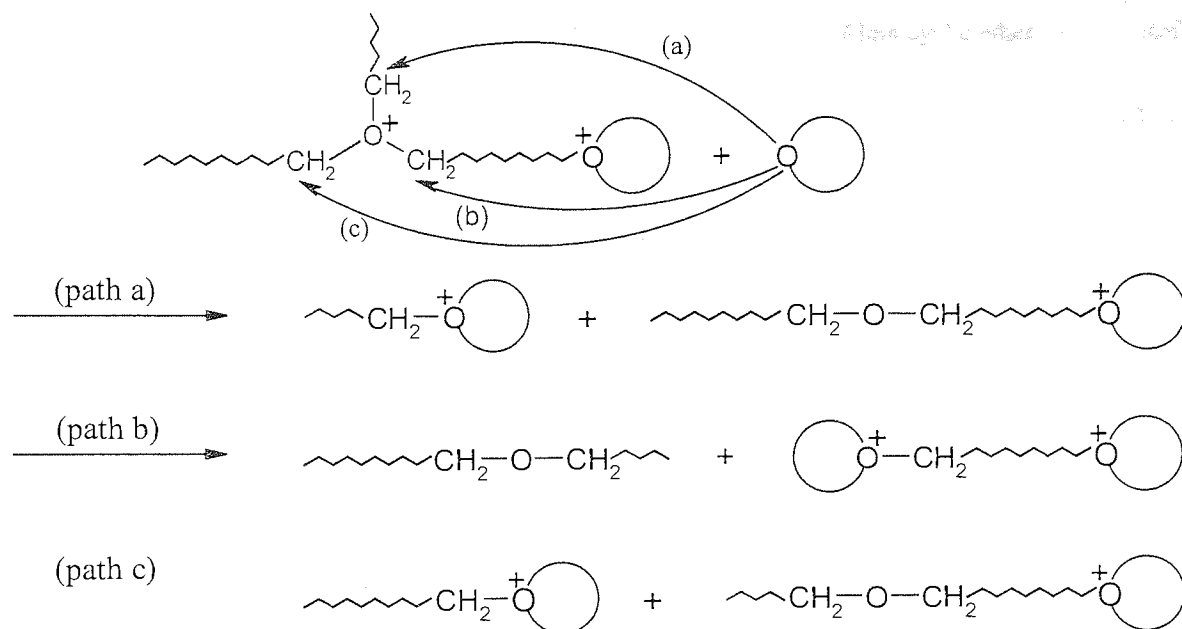


Figure 1. 40: Mechanism of redistribution of linear chain length by intermolecular transfer reactions.

As shown in the figure 1.40, the intermolecular transfer reactions leads to a redistribution of linear chain length by random process, with eventually formation of linear polymers carrying tertiary oxonium ion at the both chain ends (pathway b in figure 1.40).

1.3.2.3.2 Structure of cyclics oligomers

1.3.2.3.2.1 Epoxide monomers

In the polymerisation of epoxide monomers, the resulting cyclic oligomers are mainly 1,4-dioxane probably due to the low ring strain associated with the formation of dioxanium ion at the end of the polymer chain^[163]. However, depending on the nature of the substituent, initiator, solvent and temperature cyclic oligomers from dimer up to nonamer can be formed; a high temperature favours the cyclooligomerisation to chain growth. For example, the polymerisation of (R)-t-butylethylene oxide with BF_3OEt_2 as catalyst in hexane at 20°C formed mainly 12-crown-6-ether with R configuration at every asymmetric carbon^[188]. The specific formation of tetramer from (R)-t-butylethylene oxide is ascribed to the effect of the bulkiness of the t-butyl group, since isopropylethylene oxide^[188] gives at least seven major compounds of low molecular weight. Examples illustrated in the table 1.7 shows also that the ring size depends on the temperature as well as initiator and solvent.

Content has been removed for copyright reasons

^a some of the cyclic products contains acetal linkage in the molecule.
^b various solvent.

Table 1. 7: Formation of macrocyclic oligomers. Reproduced from the reference 197.

In addition, cyclic oligomers with acetal linkages are also formed in the polymerisation of oxirane monomers possessing electron-donating groups. For example, 2-methyl-1,3-dioxolane (C1) and 2-methyl-1,3,6-trioxocane (C2) are formed in the polymerisation of oxirane^[124-125]. In the polymerisation of styrene oxide, 2-benzyl-5-phenyl-1,3-dioxolane (C3), 2,4,6-tribenzyl-1,3,5-trioxolane (C4) and benzaldehyde are also formed^[126].

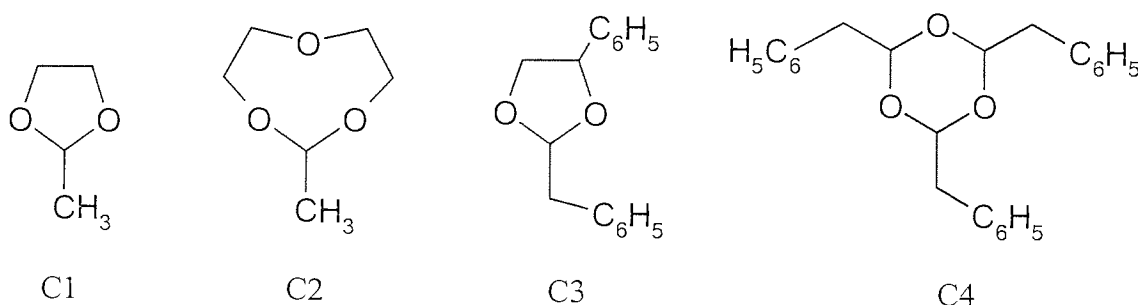


Figure 1. 41: Examples of isomerised cyclic oligomers.

The formation of isomerised side products can be explained only if the ring opening cycle occurs by an S_N1 process. In this case, the following mechanism has been proposed

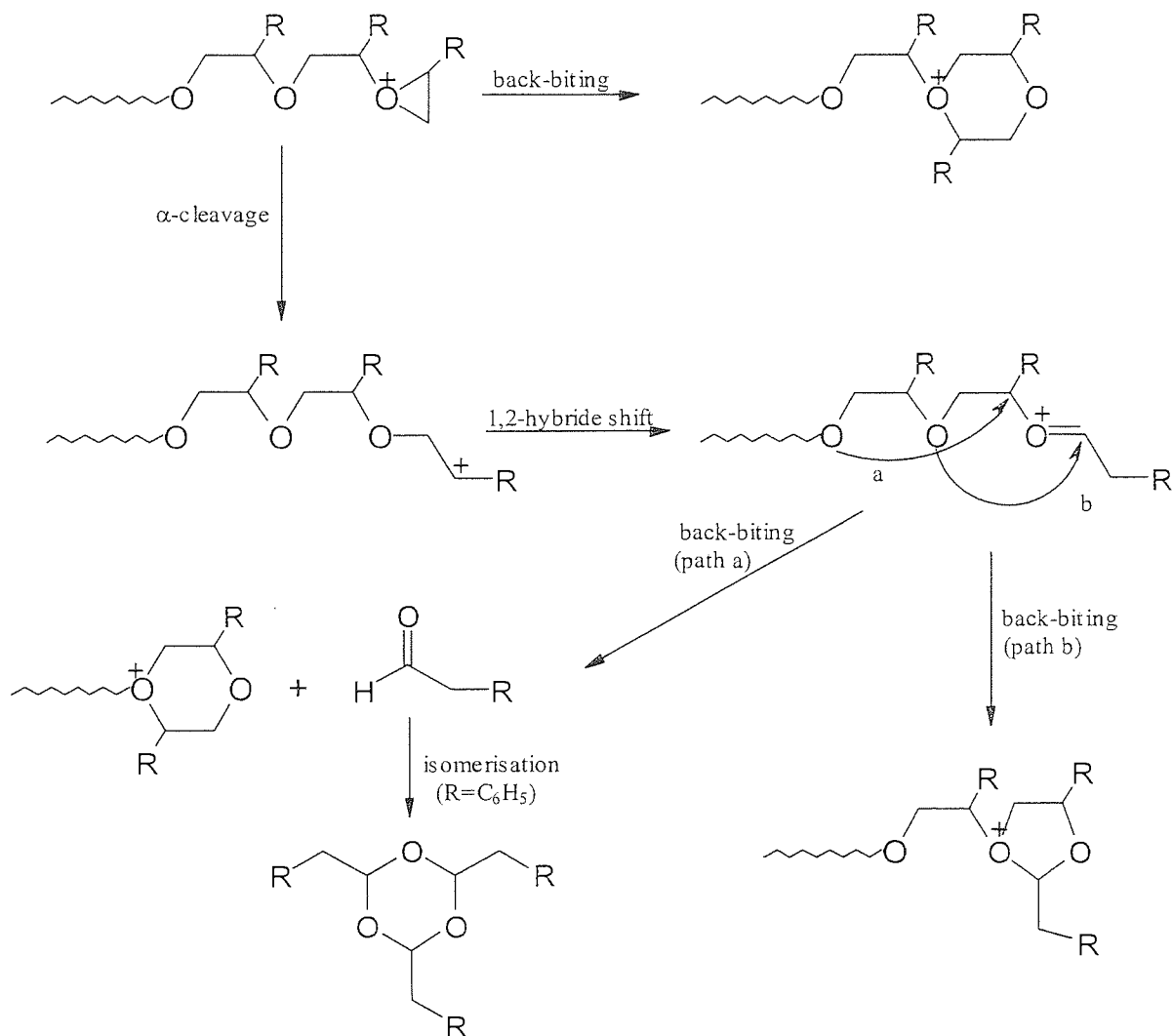


Figure 1. 42: Mechanism of formation of isomerised side product through S_N1 mechanism.

In accordance with this, the polymerisation of epichlorhydrin, which has an electron-withdrawing group on the epoxide ring, gives only normal cyclic products^[127].

Formation of macrocyclic oligomers by a ring expansion mechanism also occurs. This has been demonstrated by the fact that the polymerisation of non-deuteriated ethylene oxide in presence of deuteriated dioxane produces cyclic oligomers larger than dioxane (from trimer up to octamer) with at most two deuteriated units^[124]; the most abundant being cyclic tetramer. The two cyclic acetals 2-methyl-1,3-dioxolane (C1 in figure 1.41) and 2-methyl-1,3,6-trioxocane (C2 in figure 1.41) formed, are absolutely free of deuterium, indicating the ring opening process of dioxonium salt occurs by an S_N2 mechanism. Thus, the following

mechanism has to be considered for the formation of macrocyclic oligomers in the polymerisation of epoxide monomers:

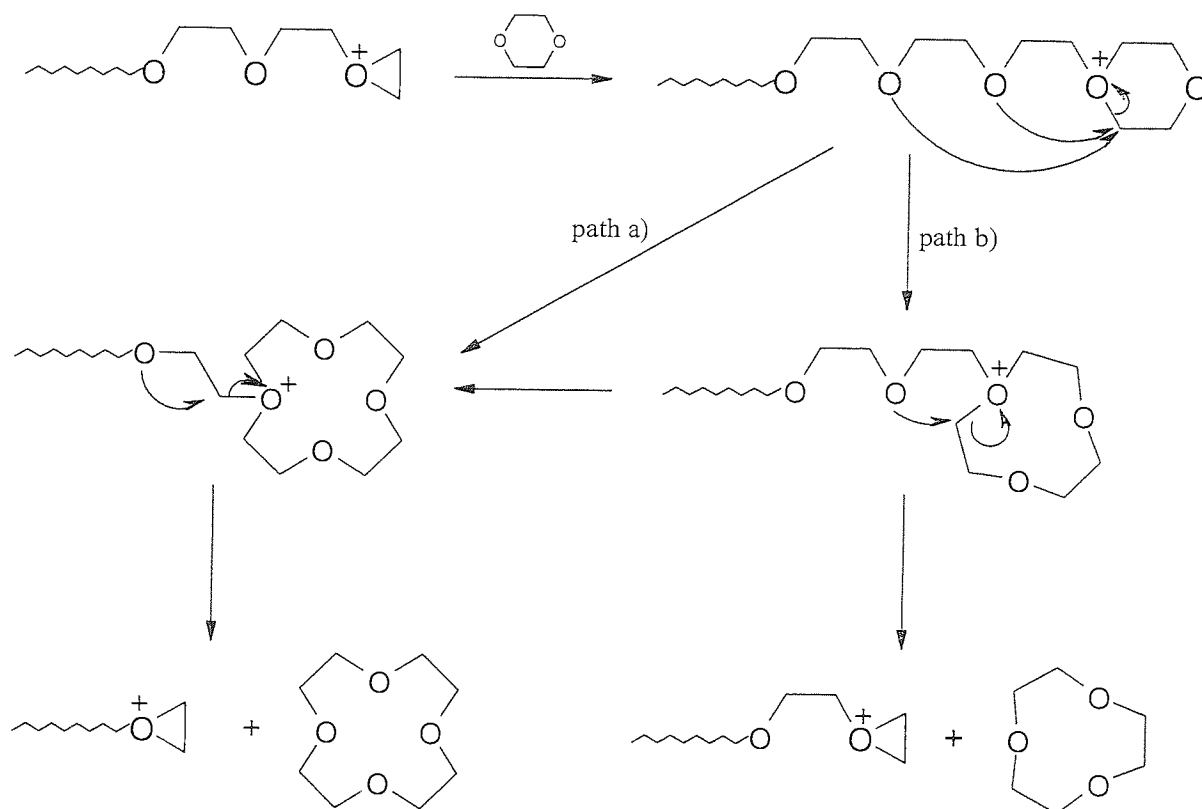


Figure 1. 43: Direct ring opening expansion mechanism for the formation of cyclic oligomers larger than 1,4-dioxane. This scheme illustrates the formation of 12-crown-4-ether and 9-crown-3-ether.

In the above scheme, Grønneborg et al. explained that the formation of cyclic tetramers is more favoured for its resistance to degradation than ease of formation^[124].

Crown ether are known to complex with metal cation in different way according to the size of the cavity and the cation. By taking advantage of this, cyclic oligomers with different ring sizes were synthesised with high selectivity when ethylene oxide is polymerisation in presence of various anhydrous salt^[180]. As shown in the table 1.8, the ring sizes of the resulting cyclic oligomers tend to increase with the size of the cation.

Salt	Tetramer (%)	Pentamer (%)	Hexamer (%)
Li BF ₄	30	70	0
Na BF ₄	25	50	25
K BF ₄	0	50	50
Rb BF ₄	0	0	100
Cs BF ₄	0	0	100
Ni (BF ₄) ₂	20	80	0
Cu (BF ₄) ₂	5	80	5
Zn (BF ₄) ₂	5	90	5
Hg (BF ₄) ₂	20	70	10

Table 1. 8: Distribution of cyclic oligoether obtained from the polymerisation of ethylene oxide using BF₃ as catalyst in presence of anhydrous Metal salt.

1.3.2.3.2.2 Oxetanes monomers

The formation of cyclic oligomers accompanying the polymerisation of 4-membered cyclic ether occurs only by an S_N2 mechanism as illustrated in the scheme 1.38 (pathway a). All possible cyclic oligomers from trimer up to nonamer are produce in decreasing concentration [198-200]. Table 1.9 shows that size of the most abundant cyclic oligomer depends on the natureof the initiator and on the nature of the solvent.

	Initiator	Trimer	Tetramer	Pentamer	Ref.
(a)	Et ₃ O ⁺ , X ⁻ X ⁻ : BF ₄ ⁻ , SbF ₆ ⁻ , SbCl ₆ ⁻	√	√		182
(b)	Et ₃ O ⁺ , BF ₄ ⁻		√	√	198
(a)	CF ₃ SO ₃ Me	√	√		182
(c)	BF ₃ /H ₂ O		√		115
(b)	BF ₃ /ROH ROH:EtOH, (CH ₂ OH) ₂ , ...		√		207

Table 1. 9: Effect of the initiating system on the most abundant produced cyclic ethers. Solvent: (a) 1,2-dichloroetane or benzen, (b) dichloromethane, (c) methylchloride.

As for the epoxide monomers, it is the temperature and the nature of the initiator which affect most the formation of cyclic oligomers. In general, cyclooligomerisation is insignificant below 50°C and increased with the temperature above 50°C. For example, in the polymerisation of oxetane initiated by BF₃/H₂O in methylchloride, the yield of cyclic

tetramers varies approximatively from 4 to 50% at -80°C and 100°C , respectively^[115]. Only 35% of cyclic oligomers are formed when triethyloxonium boron tetrafluoride salt is used at 100°C , while the use of other oxonium salts with stable counter-anions ($\text{Et}_3\text{O}^+, \text{PF}_6^-$ or $\text{Et}_3\text{O}^+, \text{SbCl}_6^-$ or $\text{Et}_3\text{O}^+, \text{SbF}_6^-$) produced insignificant conversion to cyclic oligomers even at high temperature^[182]. Polymerisation initiated by super acid derivative led to as much as 15% cyclic oligomers at 100°C , almost exclusively trimer^[182]. From these examples, it appears out that protonic acids with complex counter-anion produce more cyclic oligomers than other types of initiator. The formation of polymer chains with hydroxyl end groups generate a more nucleophilic oxygen atom than the etherate group in the backbone, and their participation in the possible chain transfer (end-biting and to a less extents the intermolecular transfer reaction according to the general dilution principle) can not be neglected. As depicted in the figure 1.44, the intramolecular reaction of the hydroxyl end group with the highly reactive strained growing centre may lead to “kinetic enhancement of macrorings”, in which the formation of macrocyclic ether is accompanied by regeneration of protonic acids^[182,202]. This assumption is in agreement with the fact that alkylating agent produce less cyclic oligomers than protonic initiator^[115,182,198].

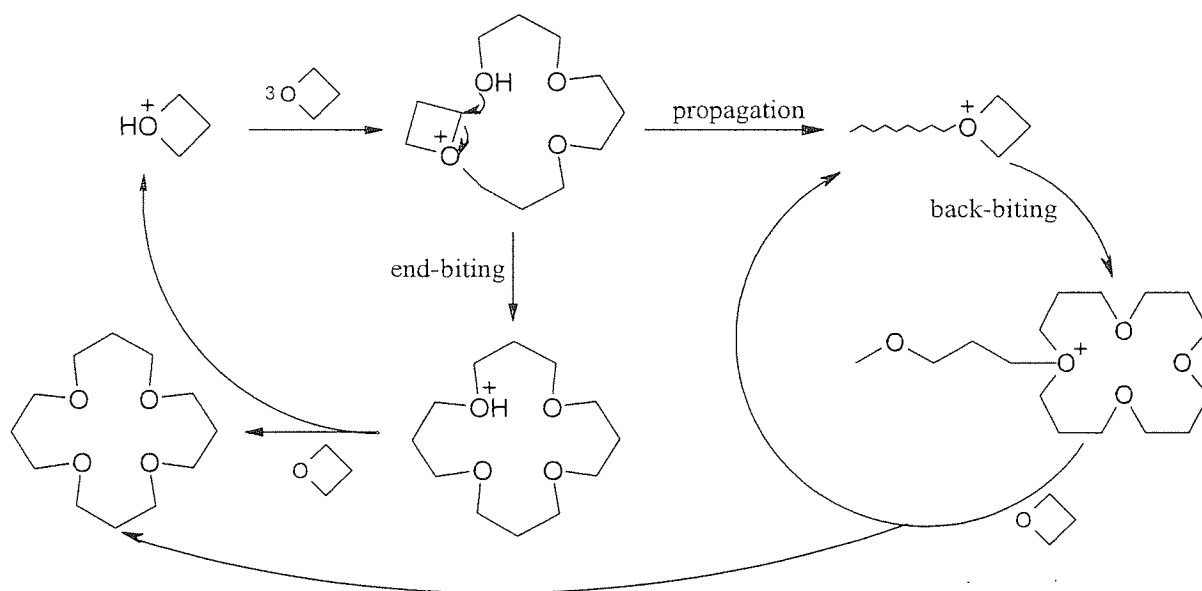


Figure 1. 44: Mode of formation of cyclic oligomers by end-biting transfer reaction.

The effect of the initiator on the oligomers formation is also a counter-anion effect. The polymerisation 3,3-dimethyloxetane initiated by triethyloxonium salt with different complex counter-anion, shows that the smaller the counter-anion, the higher is the amount of the produced cyclic oligomers^[198]. These results, summarised in table 1.10, reinforce the idea

that all reactions occur predominantly via ion-pairs but also suggest that the counter-anion exerts some steric hindrance on the oligomer formation. This was also observed in the polymerisation of oxetane^[182].



Aston University

Content has been removed for copyright reasons

Table 1.10: Effect of the counter-anion ion on the product distribution in the polymerisation of 3,3-dimethyloxetane initiated by oxacarbenium salt in methylene chloride at 20°C. Reference 198.

The size of the cyclic oligomers produced also varies with the nature of the counter-anion. The use triethyloxonium salts with metal halide as counter-anions and trifluoromethanesulfonate in the polymerisation of oxetane, shows that the tetramer/trimer ratio depends on nature of the counter-anion and solvent. For example, the complex counter-anions such as $[\text{BF}_4]^-$, $[\text{PF}_6]^-$, $[\text{SbCl}_6]^-$ and $[\text{SbF}_6]^-$ favour tetramer formation while trimer formation is preferred by the non-complex anion such as CF_3SO_3^- ^[182]. This tendency is enhanced by changing the nature of the solvent from 1,2-dichloroethane to benzene, as shown in the table 1.54, and by increasing the temperature of the polymerisation.

Counter-anion	Solvent	$\text{Ox}_3/\text{Ox}_4^{(a)}$
BF_4^-	$\text{ClCH}_2\text{CH}_2\text{Cl}$	0.5
	C_6H_6	0.18
CF_3SO_3^-	$\text{ClCH}_2\text{CH}_2\text{Cl}$	1.83
	C_6H_6	3.5

^(a) determined by Gas chromatographic analysis.

Table 1. 11: Formation of cyclic oligomers in the polymerisation of oxetane at 70°C.

The last factor that has a marked influence on the oligomer/polymer ratio is the initial concentration of monomer^[182,198]. Low monomer concentration favours the formation of

cyclic oligomers according to the general dilution principle. The initial initiator concentration has, however, no significant effect on this ratio.

The reasons for the preferential formation of cyclic tetramer is not easy to define as the effects of initiator, the counter-anion, the solvent and the reaction temperature on cyclic oligomers cannot be discussed separately from each others. The most convincing explanation was given by Bucquoye et al.^[198-200] who explain it in term of preferred polymer backbone conformation.

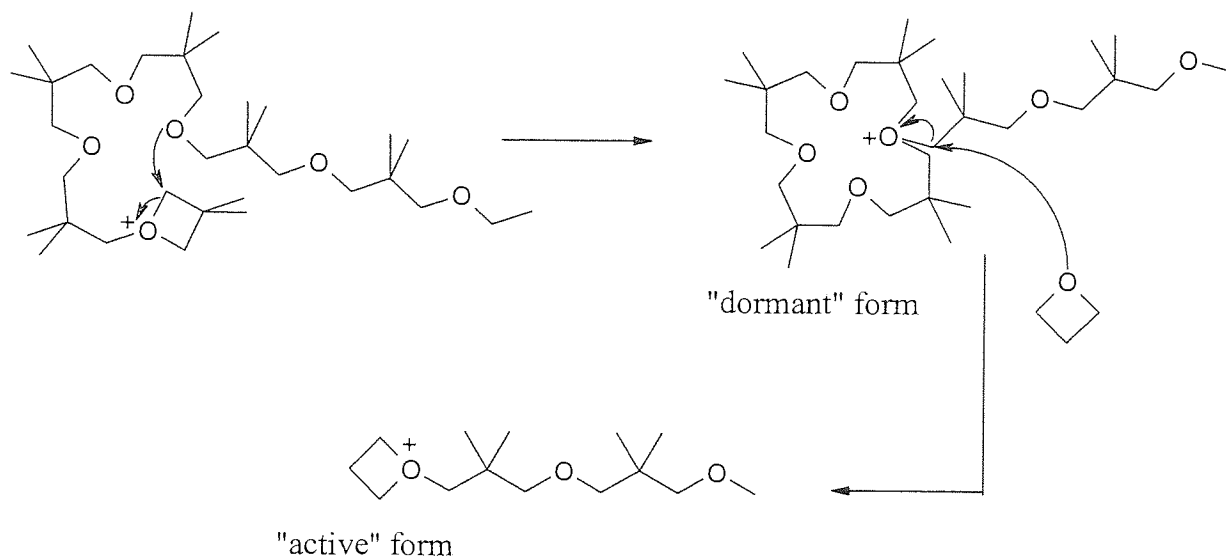


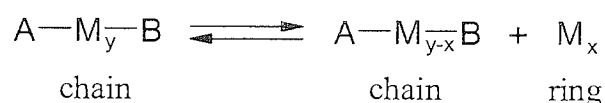
Figure 1. 45: Mode of formation of cyclic tetramers in the polymerisation of oxetane monomers.

As depicted in the above figure, they assume that the high cyclic tetramer formation is due to the fact that, in the most favourable conformation, the third oxygen atom is placed in an ideal position to react with the growing species in an S_N2 reaction; the presence of gem-substituent groups has no marked influence on the preferred conformation as they point out of the macrorings. The regeneration of the strained tertiary oxonium ion ("active" species) can then take place by nucleophilic attack of the monomer on the exocyclic carbon atom of the stable macrocyclic tertiary oxonium ion ("dormant" species), releasing cyclic tetramer from the polymer chain end. This explanation is generally accepted.

1.3.2.3.3 Ring chain equilibrium

Generally, when the monomer used in polymerisation is a cyclic molecule, depolymerisation phenomena lead to formation of cyclic oligomers together linear polymer. In the case of the cyclic ether molecules, we have seen that under certain conditions, oxetane^[115] and epoxides^[180] monomers produce a large amount of cyclic oligomers, up to 35% and 50%, respectively. Tetrahydrofuran may account for only 3%, indicating that the propagation proceeds via relatively stable tertiary oxonium species.

The thermodynamics of the ring chain equilibrium was quantitatively described by Jacobson and Stockmayer^[281] in 1950. This theory is based on the analysis of the conformational probability of the two units to meet and produce a cycle.



If the degree of polymerisation of linear polymer is high ($\overline{DP}_n \gg 1$) and if the fraction of the equivalent initial monomer converted at the equilibrium is closed to 1, the equilibrium constant for the formation of cyclic oligomers may be written as follow:

$$K_x = \frac{[A-M_{y-x}-B] \cdot [M_x]}{[A-M_y-B]} = [M_x] \quad \text{E: 1.15}$$

According to the authors, the equilibrium concentration of cyclic oligomers, with degree of polymerisation $\overline{DP}_n = x$, is given in the form of a simple relationship:

$$[M_x] = K_x = A \cdot x^{-5/2} \quad \text{E: 1.16}$$

where A is a constant characteristic for a given system and $(-5/2)$ is the gradient of the plot of $\log[M_x]_e$ against $\log(x)$ which can be slightly dependent on the solvent used^[282]. Equation E: 1.16 is usually valid only starting from a certain degree of polymerisation, below which the theory, neglecting the enthalpy factor, is not applicable. Under these conditions, if the ring-chain-equilibrium is thermodynamically controlled, the Jacobson Stockmayer equation

predicts that the equilibrium concentration of cyclic oligomer decreases as the size of the cyclic oligomer increases.

The Jacobson-Stockmayer (J-S) theory, first confirmed in 1965 for the polydimethylsiloxane^[203] equilibrates, has later been applied to a number of others system including, polyamides^[204], poly(1,3-dioxolane)^[205] and metathesis polymerisation^[206,283-285], whilst in the case of the polymerisation of epoxides (see table 1.8) and oxetane monomers^[115,208,198-200], the concentration of certain cyclic oligomers particularly tetramers, appears to deviate from predicted behaviours. Semlyen comprehensively reviewed in 1976 the ring-chain equilibria^[207].

It is also interesting to note that in the case of the anionic polymerisation of siloxane and methathesis polymerisation of cyclic olefins, the back-biting process give rise to direct formation of cyclic oligomers. As exemplified in the figure 1.46, the coordination of one double bond of the polymer chain on the metalacarbene catalyst by a random process is followed by the formation and simultaneous release of the formed cyclic oligomer. It appears therefore, that the model developed by Jacobson and Stockmayer is suitable to described the ring-chain equilibrate for the polydimethylsyloxane and methathesis polymerisation of cyclic olefins.

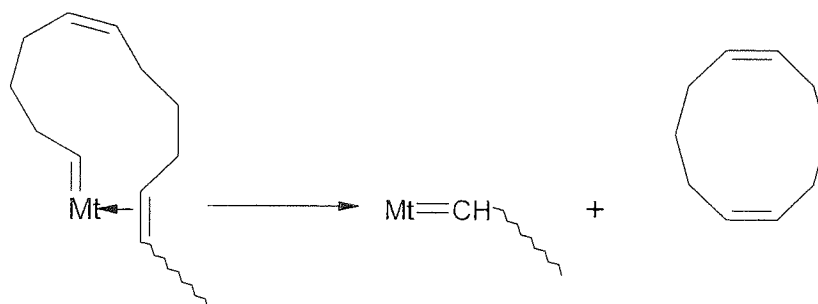


Figure 1. 46: Mode of formation of cyclic dimer in the polymerisation of cyclopentene by metathesis polymerisation.

In the case of the cationic polymerisation of epoxide and oxetane monomers, the formation of the cyclic oligomers always occurs in a two steps reactions. As described in the previous section (figures 1.37 and 1.38), the back-biting reactions firstly forms a macrocyclic oxonium salt at the polymer chain end. The macrocyclic oligomer is then released by action of an incoming monomer or by action of an oxygen atom in the backbone, depending on the basicity of the monomers. Knowing that the macrocyclic oxonium ion at the polymer chain

end can be enlarged to form cyclic tetramer in the case of epoxides monomers^[124], it is obvious that the model proposed by Jacobson-Stockmayer is not suitable because of this phenomenon. It is also interesting to note that the most abundant macrocyclic formed in the polymerisation of oxirane is the dimer (1,4-dioxane) which is undoubtedly the most stable of the produced macrocyclic ethers. In the case of the oxetane monomers, it will be interesting to study the relative stability of the macrocyclics formed during the polymerisation process to know if the phenomenon observed by Grønneborg et al. can also occur during the polymerisation of oxetane monomers.

1.3.2.4 “Living” polymers in the cationic polymerisation of cyclic ether

The nature of the initiator also affects the stability of the growing chain ends. When a tertiaryoxonium ion, fitted with stable counter-anion (that cannot undergo anion splitting), is used as initiator, oxetane monomers^[182,198,209], oxolane^[184-187,279,280] and oxepane^[133] can be polymerise without any appreciable termination reactions, providing the reaction medium does not contain any transfer agent such as amine, alcohols, water, etc. Under these conditions, the number of active sites remains constant during the whole propagation process. If transfer reactions are prevented as well, the mechanism of reaction then involves only two steps: initiation and propagation. In this respect, the polymerisation is truly “*living*”: The active sites are retained at the polymer chain end (polymers are *living*). Provided that initiation is rapid and quantitative with the monomer, the number average polymerisation degree of the polymer formed increases linearly with the conversion, $\overline{DP}_n = [M]_0 / [I]_0 \times conv$, and the resulting polymers are characterised by narrow polydispersities. Upon addition of further monomer, the existing polymer chains extend correspondingly.

In the case of polymerisation of *oxolane* (tetrahydrofuran)^[184] and oxepane^[133] initiated with 1,3-dioxolenium⁺, [SbF₆]⁻ salt (a very rapid and quantitative initiator), it is reported that the resulting polymers are “*living*”, and that the reactivities of ion pairs associated with large counter-anion (i.e. [AsF₆]⁻, [SbF₆]⁻, [SbCl₆]⁻, [PF₆]⁻) is comparable to the reactivity of the respective free ions. In this respect, if all the polymer chains are initiated at approximately the same time and if the reaction mixture is homogeneous, so that all the polymer chains, ion pairs and free ions, should grow at the same rate and therefore polymers with narrow molecular weight distributions should be obtained during the all course of the polymerisation.

However, polymerisation of THF and oxepane never goes to completion because of the existence of “*ceiling*” temperature and a corresponding significant concentration of monomer at equilibrium. Because of the progressive inactivation of the growing centre, chain transfer to the polymer takes place^[210]. The use of stable complex counter-anions only reduces the probability of transfer reactions but does not prevent them. Reversibility and chain redistribution, ensure the process is not *living* and contribute to a widening of molecular weight distribution, which is initially Poisson type and eventually reaches Flory’s most probable distribution at equilibrium ($\overline{M}_w/\overline{M}_n \cong 2$). If narrow molecular weight distributions are needed, polymerisation has to be limited to low conversions, provided reactivity of the respective free ions and ion pairs are equal. Similar observations have been reported for oxolane initiated by super acids ester initiators (i.e. $\text{CF}_3\text{SO}_3\text{C}_2\text{H}_5$). The rate of the interconversion between macroester and macron-pairs did not prevent transfer reactions to occur^[183].

It should be noted that the criteria of “*livingness*” is sometimes employed^[133,184] when the polymerisation of THF or oxepane is described. This assumption is based on the fact that the number of the tertiary oxonium ions is unchanged during the whole polymerisation process, that active sites are destroyed only by addition of nucleophile (i.e. tertiary amine, water, alkoxides, phenolate, or even lithium bromide) and that polymerisation depolymerisation processes occur by changing the temperature. If their studies provide indisputable evidence of the total absence of termination reactions (by anion-splitting), they establish the absence of transfer reactions. As depicted by the figures 1.37, 1.38 and 1.40, the characteristic feature of transfer reactions (intra- and intermolecular reactions) is to generate “dormant” species. “Dormant” species may regenerate the growing oxonium ion by reactions with monomer. Such processes only reduce temporarily the reactivity of the growing centre at the polymer chains end but do not destroyed them. In this respect, the growing polymer chain can be assumed to be *living* during the all course of the polymerisation. Besides, the increase in viscosity or gelation of the polymerisation system observed by Rosenberg as the conversion increases, and the decrease of viscosity after treatment with small amount of methanolic KOH, indicate that polymeric network materials are undoubtedly formed by intermolecular transfer reactions^[210]. Thus, polymerisation of THF and oxepane can be assume to be *living* since there is a large excess of monomer (with higher basicity than the open chain ether) to favour the propagation rather than transfer reactions. In consequence, polymerisations are

living only at low monomer conversion. Only SEC data should be considered to prove the absence of transfer reactions and this during the entire course of the polymerisation.

The chief characteristics of THF polymerisation is also found in oxetane^[182,198] polymerisations, though transfer reactions occur more significantly^[115]. Since oxetane and oxirane are more strained than THF, the polymerisations of these monomers are more favoured than that of THF. Equilibrium monomer concentrations are lower and conversion almost quantitative.

1.3.2.5 Cationic ring opening polymerisation of cyclic ethers with an Activated Monomer Mechanism (A.M.M)

Until 1984, it was thought that the *activated chain end* (A.C.E) mechanism, first proposed by Rose^[115], was the sole mechanism by which cationic ring opening polymerisation of cyclic ethers could be achieved. A second mechanism was then demonstrated by Penczek^[211-213] which was entitled *activated monomer mechanism* (A.M.M). This mechanism is based on the established mechanism of acid alcoholysis of oxirane.

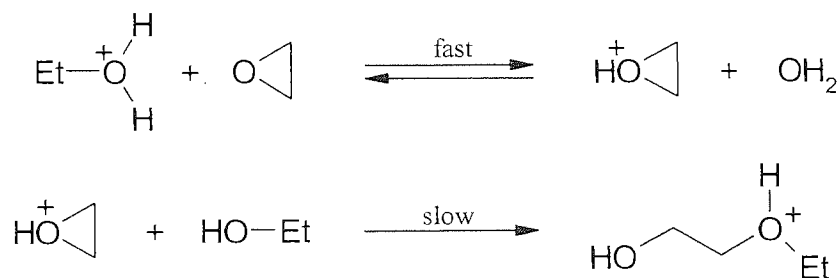


Figure 1. 47: Mechanism of acid alcoholysis of oxirane.

In the scheme shown above, proton serve as catalyst and 2-hydroxyl ethyl ether is ultimately formed. If an excess of ethylene oxide is present in the system, the proton at the end of the chain transfer to the monomer and chain growth proceeds on the hydroxyl chain ends by addition of the protonated monomer (activated monomers). After each addition, a new hydroxyl group is formed. Thus, the overall scheme of propagation can be presented in the following way.



Figure 1. 48: Mechanism of propagation by Activation Monomer Mechanism A.M.M.

This polymerisation belongs, therefore, to *chain polymerisation* with initiation that can be described by figure 1.47 if ethanol is an initiator.

The relative contribution of A.M.M and A.C.E mechanism has been studied for the polymerisation of oxirane^[214], propylene oxide and epichlorhydrine^[215-218]. The conventional A.C.E mechanism would apply if the protonic catalyst is added to the oxirane solution. In this case the added alcohol acts as transfer agent during the course of the polymerisation producing linear oligomers of low average molecular weight. To polymerise oxirane monomers by an AMM, the polymerisation has to proceed under monomer starved conditions. In this case a solution of alcohol has to be produced in the solvent for polymerisation and the protonic acid catalyst is added to this solution. The monomer is then added slowly into the solution so that at any instant its concentration is only of the order of the initiator (i.e. alcohol initiator and subsequently the terminal hydroxyl group of the produced polymer chains). The proton, initially from the protonic acid catalyst, slowly protonates the monomer, as would be the case in the initiation step of the ACE mechanism. However, because the concentration of the monomer is of the order of that of the initiator, the only nucleophile present capable of attacking the hydroxonium compound is the alcohol (i.e. hydroxyl end groups are more nucleophilic than oxygen atoms in the polymer chain that are more nucleophilic than the oxygen atom of oxirane monomers).

The main advantage Penczek deduced is that with the ACE mechanism up to 50% of the propylene oxide used is converted into cyclic tetramers, whilst the proportions of tetramers drops to 0.95% when the polymerisation mechanism switched mostly to AMM by slowly adding monomers^[219]. Side reactions that do not appear are the direct result of some ACE propagation which is an inherent property of AMM. As the polymerisation proceeds, polymer units start to compete in the chain growth with the terminal hydroxyl group. The following process has been proposed in the polymerisation of ethylene oxide^[212,213].

When oxetane monomers contain and hydroxyl group such as 3-hydroxy-oxetane^[225], 3-methyl-3-hydroxymethyloxetane^[226], 3-ethyl-3-hydroxymethyloxetane^[227,228], 3,3-bis(hydroxymethyl) oxetane^[229], activation monomer polymerisation turned out to be a route to hyperbranched or star-like polyethers.

1.3.3 Anionic polymerisation of cyclic ethers

As described in the previous section, if the use of a super acid ester or alkylating agent fitted with stable complex counter-anion permit to generate *living* growing polymer chains by ACE mechanism, it is almost impossible to achieve truly *living* polymerisation by cationic technique. This observation is also applied when the polymerisation occurs by A.M.M. Various side reactions (intra- and intermolecular transfer reactions) tend to occur by ACE mechanism because of the presence of oxygen atom in the polymer chains. For a large variety of monomers, anionic polymerisations and/or anionic coordination polymerisation often constitutes a method of choice to prevent chain breaking reactions to occur. This supposes that the monomer under investigation undergoes anionic and/or anionic coordination polymerisation.

1.3.3.1 Alkali-metal based catalyst

In the anionic polymerisation of oxirane with potassium t-butoxide (t-BuOK) in DMSO, it was found that the molecular weight of the polymer increased linearly with the molar ratio of the monomer consumed to the initiator^[230]. This is one of the characteristic features of *living* polymerisation.

The mutual attraction of the oppositely charge ions ,eans that the living growing polymer chains exist as contact ions pairs in equilibrium with aggregates of ions pairs. As shown in figure 1.50, the tight ions pairs dissociate into free ions, with which they are in equilibrium, and then all species, the ion-pairs and free ions, contribute to the propagation, each in its specific and distinct fashion. The aggregated ion pairs being the dormant inactive species.

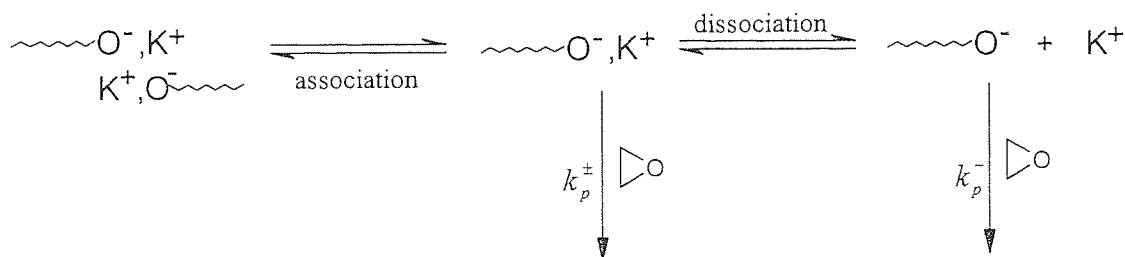


Figure 1. 50: Nature of the growing species in the anionic ring opening polymerisation of oxirane.

As shown in the figure 1.50, the growth of the free polymeric anion occurs by direct attack of the carbon atom adjacent to the heteroatom. The splitting of the carbon-heteroatom bond opens the monomer ring and regenerates the alkoxide anion at the polymer chain end. In the case of tight ion-pairs, the mechanism is more complex. The polarisation of the incoming monomer by the tight ion-pair polymeric anion proceeds simultaneously with the splitting of the carbon-oxygen bond of the monomer and the regeneration of the alkoxide ion-pairs at the polymer chain ends without transfer of the K^+ cation from the previously active centre to the newly formed one. This phenomenon only observed when K^+ , Rb^+ and Cs^+ are used as cation, is called *push-pull mechanism* [231-234,238] and is responsible of the enhancement of reactivities of the tight ion pairs. Its effect becomes dominant and makes the tight ion-pairs more reactive than free ions when the charge of the attacking molecules is greatly delocalised. This has been observed during the initiation process, when oxirane polymerisation is initiated by dibenzocarbazyl salt [232].

a) propagation via free ions (k_p^-)



b) propagation via paired-ions (k_p^+)

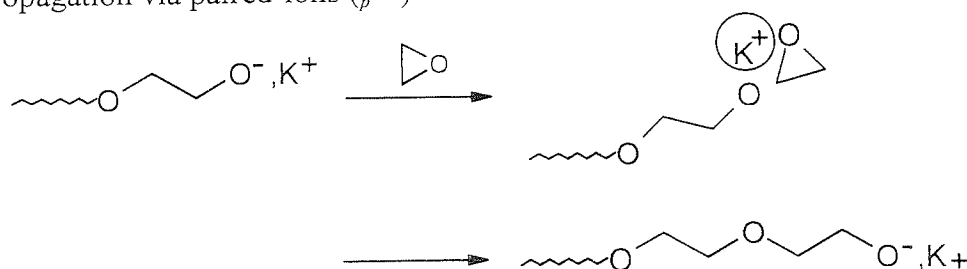


Figure 1. 51: Mechanism of anionic propagation of oxirane via free ions and ion-pairs.

The following relation then gives the apparent rate constant of propagation of ionic polymerisation:

$$k_{p_{app}} = (1 - \alpha) \cdot k_p^+ + \alpha \cdot k_p^- \quad \text{E: 1.17}$$

Where α denote the fraction of free ion, $k_{p_{app}}$ the apparent rate constant of propagation, k_p^+ the rate constant of propagation via ion-pairs and k_p^- the rate constant of propagation via free ions. The rate constant of propagation has been calculated and found to be equal to $0.05 \text{ M}^{-1} \text{ s}^{-1}$ and $1.7 \text{ M}^{-1} \text{ s}^{-1}$ for k_p^- and k_p^+ , respectively^[231]. This observation is in contrast with the cationic polymerisation of oxepane and THF, where the reactivities of ion-pairs associated to with large anions (SbCl_6^- , AsF_6^- , and PF_6^-) is comparable to the reactivities of the respective free ions^[133,184-187].

Different types of initiators have also been used in the living polymerisation of oxirane. This includes: potassium t-butoxide^[230], carbazyl and dibenzocarbazyl salts of potassium^[232,233,239], 9-methylfluorenyl salt of potassium^[232], fluorenyl salt of potassium, naphtyl and anthracenyl salt of sodium^[233,235,236]. The first four are monofunctional initiators, while the last three behave as bifunctional initiators.

In the polymerisation of propylene oxide under similar conditions, the molecular weight of the polymer reaches a maximum which is much lower than that calculated^[230,237]. This is ascribed to proton abstraction from the methyl group of the monomer by the growing alkoxide anion. The above chain breaking reaction has also been observed in the case of the polymerisation of tri- and tetramethylene oxide^[230].

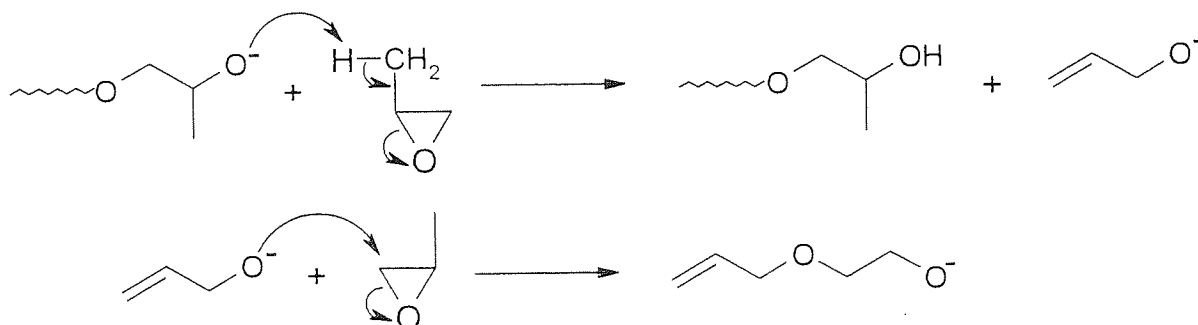


Figure 1. 52: Mechanism of proton abstraction from the monomer by the growing alkoxide anion.

If anionic ring opening polymerisation constitutes a method of choice to polymerise ethylene oxide in a living manner, the use of anionic initiator turned out to be ineffective for the polymerisation of 4-member cyclic ethers. This is ascribed to the higher polymerisability of epoxides than oxetane monomers.

1.3.3.2 Coordination polymerisation of cyclic ethers

The first report on the coordination polymerisation of cyclic ethers is ascribed to Pruitt and Bragett who polymerised propylene oxide with ferric chloride propylene oxide as catalyst^[240]. An interesting feature of these coordinated systems is that polymerisation proceeds without transfer (inter- and intramolecular transfer reactions) and termination reactions and that stereoregular (isotactic) polymers are obtained. Later Price^[241] proposed the “coordinate anionic mechanism”, in which the monomer is coordinate to the catalyst and activated towards nucleophilic attack, providing orientation of reacting molecules, leading to stereospecific polymerisation.

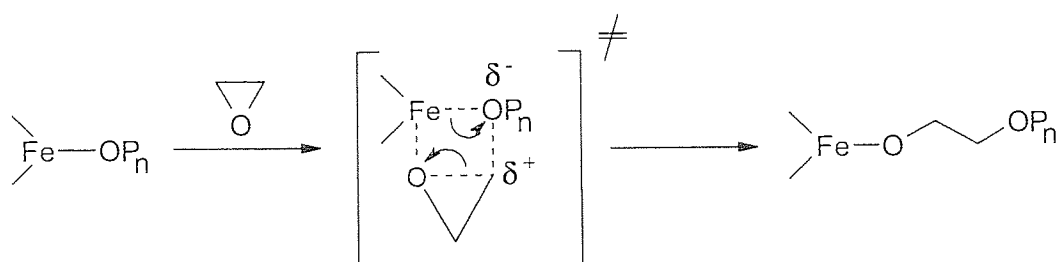


Figure 1. 53: The coordinated anionic mechanism of the polymerisation of ethylene oxide.

A few years later, various types of catalyst were found to be effective for the stereoselective polymerisation of epoxide: aluminium isopropoxide/zinc chloride^[242], dialkylzinc/water^[243], dialkylzinc/alcohol^[243], trialkylaluminium/water^[244] and trialkylaluminium/water/acetylacetone^[245]. These organometallic catalysts were later found to be good catalyst for many others monomers, particularly for the homopolymerisation of oxetane^[246-250], and copolymerisation of tetrahydrofuran and oxepane with epoxide and oxetane monomers^[251]. Optically active catalysts such as diethylzinc/(R)-(-)-borneol^[252,253] and diethylzinc/(R)-(-)-3,3-dimethyl-1,2-dimethyl-butanediol^[254] were reported to be effective in the enantiosymmetric polymerisation of (R,S)-propylene oxide. Special interest has also been devoted to the development of well-defined catalyst that can be isolated in the form of single crystal and characterised by RX. The first reported:

$[Zn(OCH(Me)CH_2OMe)_2]_2 \cdot [EtZnOCH(Me)CH_2OMe]_2$, $[Zn(OMe)_2] \cdot [EtZnOMe]_6$ and $[Zn(OCH_2CH_2OMe)_2] \cdot [EtZnOCH_2CH_2OMe]_6$ were isolated from the reaction between diethylzinc/1-methoxy-2-propanol (7:8)^[255], diethylzinc/methanol (7:8)^[256-258] and diethylzinc/2-methoxyethanol (7:8)^[259], respectively. However, all of these coordination catalyst systems turned out to be unfavourable for the synthesis of polyether with controlled chain length, since these catalysts tend to be highly aggregated in solution and different catalyst sites may have different reactivities when initiating and propagating species are formed. This is considered to be responsible for the high molecular weight and broad polydispersity of these polymers.

Coordinated metalloporphyrin based catalysts with isolated mononuclear metal species have been developed. Such catalysts include: (5,10,15,20-tetraphenylporphyrinato) aluminium chloride [(TPP)AlCl], methoxide [(TPP)AlOMe], 1-propanethiolate [(TPP)AlSPr] and (5,10,15,20-tetraphenyl-21-methylporphyrinato)zinc methoxide [(MTTP)ZnOMe]^[260-263].

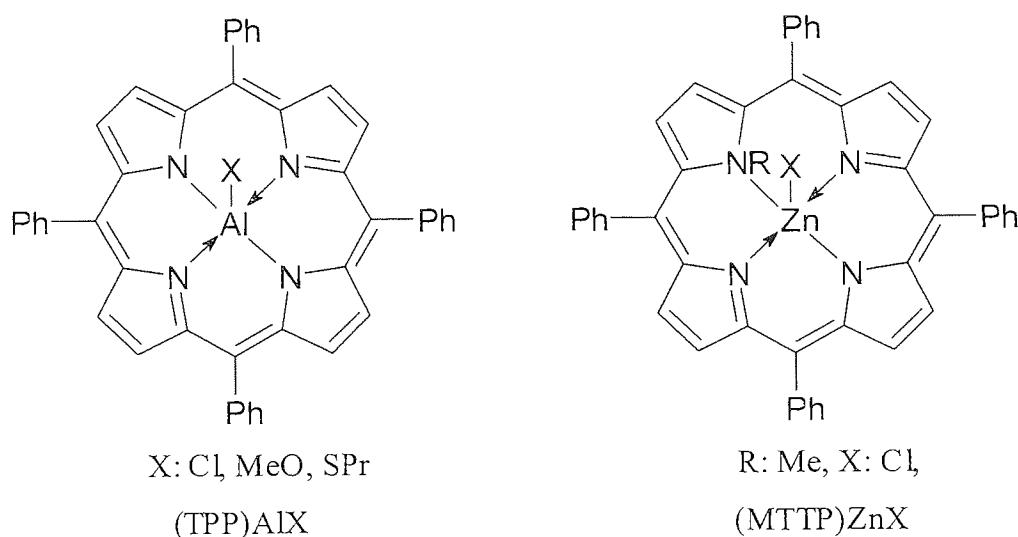


Figure 1. 54: Coordinated metalloporphyrin based catalysts with isolated mononuclear metal.

Porphinatoaluminium catalysts were derived from the reaction of diethylaluminium chloride with 5,10,15,20-tetraphenylporphyrin (TPPH) and from the reaction of triethylaluminium with TPPH, followed by treatment with methanol or 1-propanol. The porphinatozinc catalysts were obtained analogously from the reaction of diethylzinc with 5,10,15,20-tetraphenyl-21-methylporphyrine (MTPPH), followed by treatment with methanol.

In comparison with the highly associated catalyst containing multinuclear species (i.e. $\rightarrow Mt-X \rightarrow Mt-X \rightarrow$ and $\rightarrow Mt-X-Mt-X \rightarrow$), metalloporphyrin catalysts form monomeric species. By taking advantage of the above, polymerisation of epoxides^[264,265] and oxetane^[207,266-268] showed all the signs of the *living polymerisation*. This includes: linear dependency of \overline{Mn} with % conversion and by changing the epoxide-to-catalyst mol ratio, very narrow molecular weight distribution through the polymerisation ($\overline{Mw}/\overline{Mn} < 1.1$) and synthesis of block copolymers with narrow average molecular weight distribution. Among these catalysts, (TPP)AlCl is of the highest activity. The mechanism of these polymerisations proposed by Inoue et al.^[264], involve a simultaneous participation of two metalloporphyrin molecules; an illustration of this mechanism is shown in scheme 1.64.

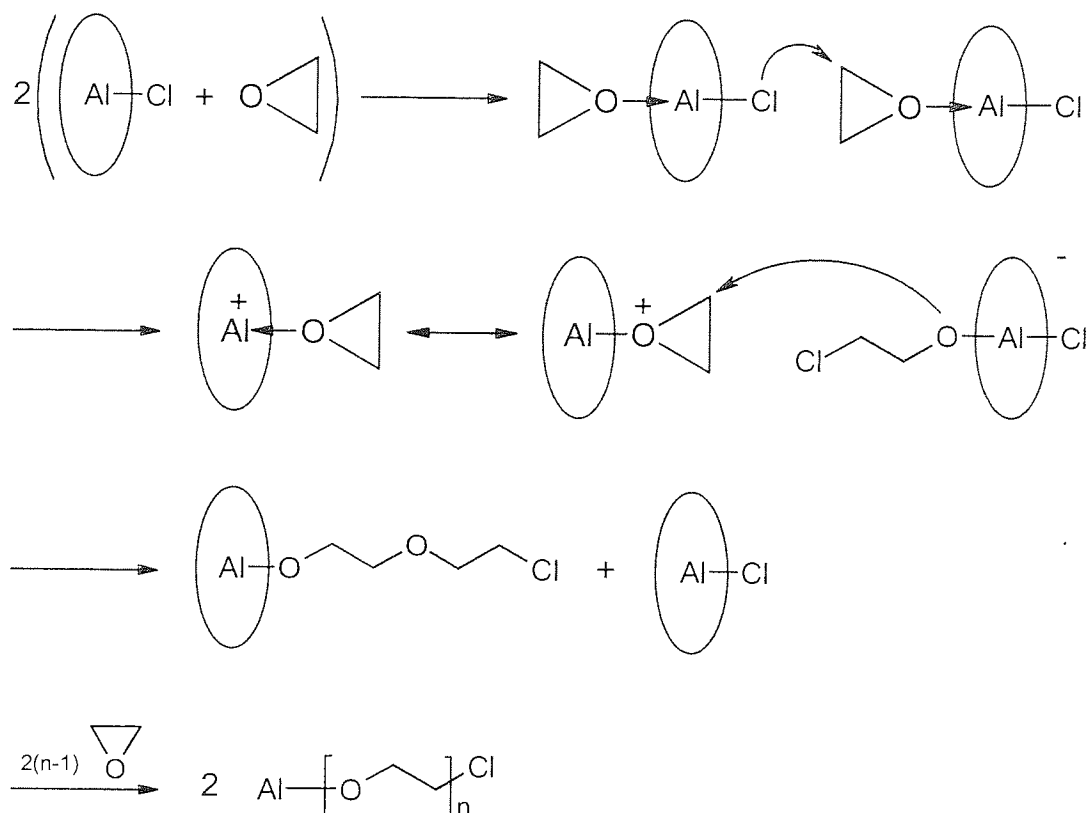


Figure 1. 55: Mechanism of polymerisation of ethylene oxide with (TPP)AlCl.

The simultaneous participation of two metalloporphyrin molecules in the mechanism was later proved by Inoue et al. who observed that the presence of monomeric organo-aluminium compound with bulky substituents (e.g. methylaluminium di(2,6-di-*t*-butylphenoxyde) or methylaluminium di(2,6-di-*t*-butyl-4-methylphenoxyde) which sterically prevent the polymerisation, accelerate the Al-porphynito initiated polymerisation of epoxide by a factor of about 500. The activation of monomer by the chosen Lewis acid is believe to enhance its

reaction with porpheryn catalyst^[1,275-278] yielding polymers with narrow molecular weight distribution.

This mechanism becomes more complex if protonic reagents are present in the polymerisation medium. Indeed, Inoue et al.^[269] discovered that the number of the polymer molecules is not limited by the amount of initiator (AlX) but can be increased if required by addition of protonic reagents such as H₂O or ROH. This observation causes this polymerisation system to be named “*Immortal polymerisation*” because protonic agents are unable to terminate the polymerisation. As shown in the figure 1.56, the concept of *immortal polymerisation* is accounted for by the unusual reactivity of the aluminium atom-axial ligand bond (Al-X).

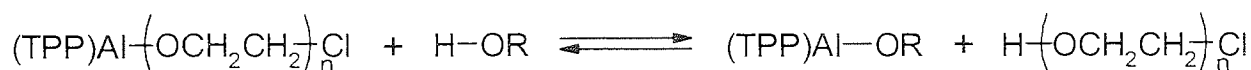
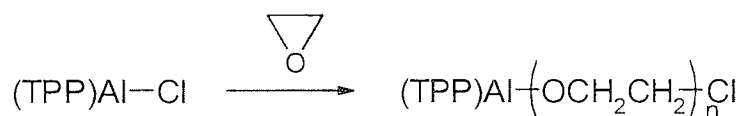
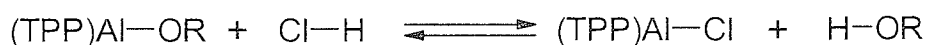


Figure 1. 56: Rapid exchange between the growing polymers attached to the catalyst and the dead ones possessing the OH end group.

The chain transfer reactions shown above are reversible and occur much more rapidly than chain growth; approximately 8 times faster. The consequence of this is that narrow molecular weight distribution of polymers are obtained.

(5,10,15,20-tetraphenylporpherinato) aluminium chloride [(TPP)AlCl] was also used in the attempted living polymerisation of oxetane derivative monomers such as 3,3-dimethyl-oxetane, 3-hydroxymethyl-oxetane and 3-methyl-3-nitratomethyl-oxetane (NIMMO) but all were unsuccessful^[207]. The main reason for the failure of polymerisation of the substituted oxetanes is accounted for by the steric factor and possibly by competition between the cyclic ether group and the functional group (i.e. -OH and -ON₂O) present in the side chain of the same molecule of monomer, which is trying to compete with the active site centre on the metal. On the other hand, trialkylaluminium/water/acetylacetone catalysts (Vandenberg

chelate catalyst) turn off to be effective for the polymerisation of 2-methyloxetane^[249], as well as for the copolymerisation of 3-(trimethylsilyloxy)oxetane, 3,3-bis(trimethylsilyloxy)oxetane and 3,3-bis(chloromethyl) with epoxide or THF^[251], however, the produced polymer exhibit a broad molecular weight distribution. These results strongly indicate that oxetane derivative monomers can undergo coordination polymerisation.

The concept of using metalloporphyrin in a combination with an appropriate Lewis acid for promoting coordination polymerisation led to the development of new coordinated catalyst with isolated mononuclear metal species. For instance, the chiral {2,2'-[(1R,2R)-1,2-cyclohexylenebis(nitrilomethylidene)]diphenylato}aluminium chloride [(Sal)AlCl] appeared to produce low molecular weight poly(propyleneoxide), characterised by narrow distribution of molecular weight^[263,270,271]. The achiral (25,27-dimethoxy-p-t-butylcalix[4]aren-26,28-dilato)aluminium chloride [(dma)AlCl] has been successfully applied for the polymerisation of propylene oxide and cyclohexene oxide, leading to an interesting bifunctional, low-molecular weight polyether of relatively narrow molecular weight distribution^[272-274]. It will be interesting to use this newly developed catalyst in the attempt to polymerise oxetane derivative monomers in a *living* manner.

2 CHAPTER 2

Experimental

Controlling the experimental environment is essential in the cationic ring opening polymerisation of cyclic ethers. The intermediates involved during the polymerisation (oxonium ions) are known to be very sensitive toward moisture. Water can act as a co-catalyst and also modify the mechanism of polymerisation by acting as a transfer agent. For this reason the purification and preparation of monomers, solvent and catalyst solutions, as well as the polymerisation reactions, were carried out using either high vacuum techniques or in an atmosphere of argon to exclude disadvantageous impurities. These experimental requirements are vital particularly when living polymerisation is required.

2.1 Vacuum line techniques

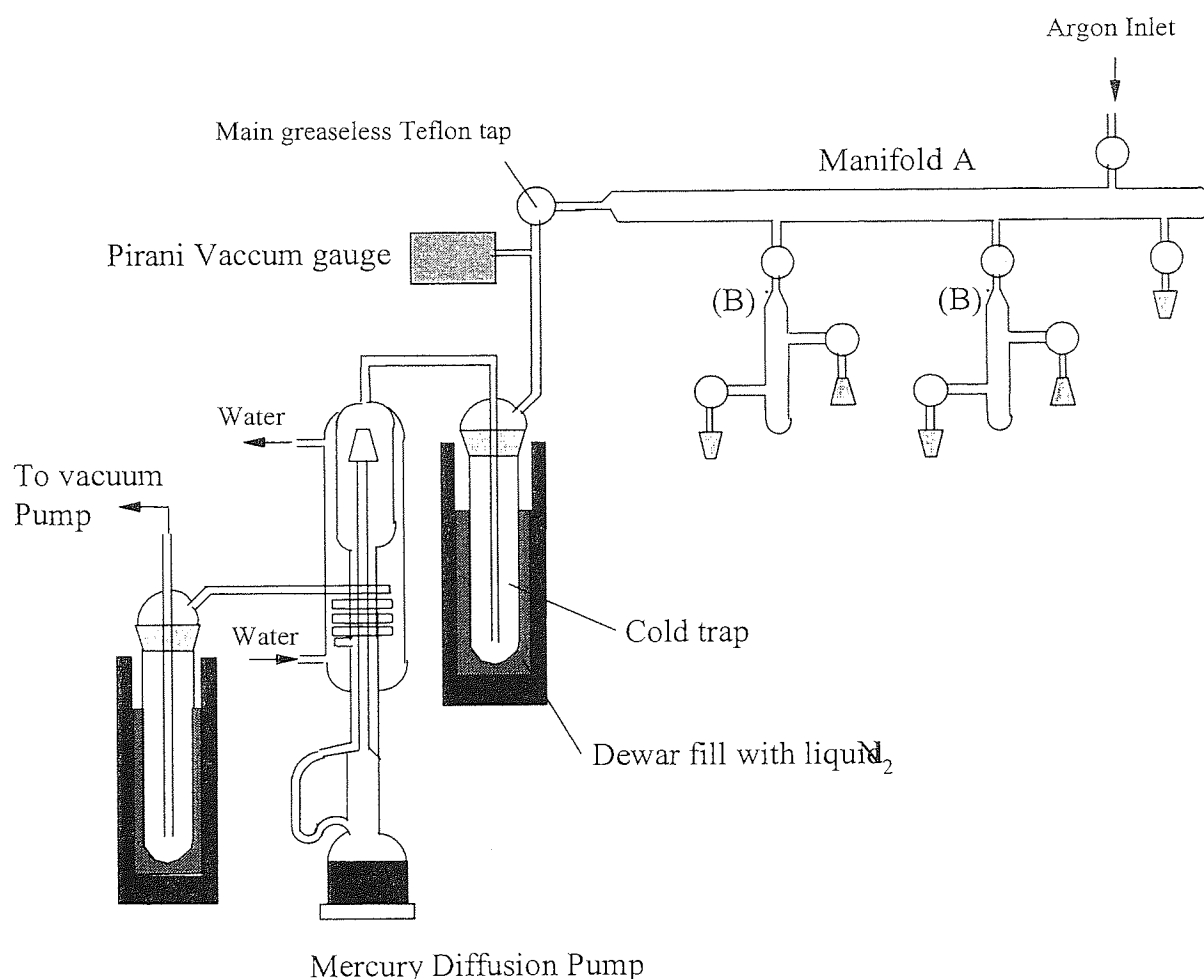


Figure 2. 1: The vacuum line.

The vacuum line, shown in Figure 2.1, was constructed of glass and consisted of a main manifold (A) and two sub-manifolds (B) connected via PTFE greaseless taps. A series of B19

ground glass joints were connected to the manifold by means of PTFE taps. The manifolds were connected to a Metrovac rotary vacuum pump. The vacuum pump used generates a pressure of approximately 10^{-2} mm Hg, and the whole system is capable of achieving a vapour pressure of 10^{-5} mm Hg. Two liquid nitrogen cold traps were present to protect the vacuum pump from any vapour coming from the manifold. The pressure inside the system was measured by the use of a pirani gauge. An argon supply was connected to the manifold to allow manipulation of materials under an inert atmosphere rather than a vacuum. Prior to use, the glassware was flamed with a Bunsen while under vacuum, to remove any moisture that may be absorbed onto the inside surface.

2.2 Treatment of the glassware

All glass vessels were cleaned prior to use with a suitable solvent then soaked in Decon 90 wash thoroughly with water and finally by rinsed with acetone. The apparatus were dried in an oven at 240°C for at least 4 hours. To minimise the readsorption of moisture onto the glass, vessels were evacuated while still hot, flamed with the Bunsen and then put into argon atmosphere if required.

2.3 Freeze-thaw degassing of solvent

In order to remove dissolved gases and facilitate the distillation of materials under high vacuum, liquids were degassed using a freeze-thaw procedure. The flask containing the material to be degassed was attached to the vacuum line with its tap closed and the manifold evacuated. The contents of the flask were then frozen by immersing the flask in liquid nitrogen (b.p -195.8°C). Once the material was frozen the relevant taps were opened and the flask evacuated. When the pressure in the flask was minimised, the main tap or sub-manifold tap, was closed and the frozen liquid melted, releasing any gases trapped by the freezing process into the manifold. The tap on the flask was closed, and the main tap opened to evacuate the manifold. The contents of the flask were frozen and the degassing procedure repeated until no further difference between freezing stages and the freeze-thaw process could be observed.

2.4 Trap to trap distillation

Once degassed, it was possible to transfer the liquids to a second vessel using the vacuum line by a trap-to-trap distillation procedure. The flask containing the degassed material was attached to one of the sub-manifolds and the vacuum line was evacuated. The receiver flask was then attached to the same sub-manifold and, if empty, evacuated before immersion in liquid nitrogen. The sub-manifold was isolated from the vacuum pump by closing the relevant tap, after which the taps on the appropriate ground glass joints and flasks were opened to allow the material to distil.

2.5 Schlenk techniques

To enable the handling of sensitive materials under an inert atmosphere an argon supply was connected to the vacuum line. So that the Schlenk technique could be used, the appropriate apparatus was attached to the manifold, evacuated and then the main tap was closed. Argon was introduced into the manifold and flask and a slight positive pressure was maintained. This was monitored by an oil bubbler connected in parallel to the argon supply. The tap on the apparatus was then removed, enabling materials to be introduced into the apparatus using dry syringes under a contra flow of argon. Similar methods were also used to remove liquids from a flask using a syringe or to place solid material into a flask.

2.6 Argon dry-box

A dry-box supplied by Halco Engineering Ltd was used to enable materials to be stored and manipulated under an inert atmosphere. This maintained an argon atmosphere, which was constantly re-circulated through absorber columns to remove oxygen and water from the atmosphere. Typically, a BASF R311 catalyst was used to remove oxygen and 3Å molecular sieve to absorb moisture to below 1 ppm and 5 ppm respectively. To prevent air from entering the system, access to the dry box was via a double door posting port. The inner door of the port was sealed, the outer door opened and the apparatus then placed into the port. Once the outer door was closed, the port was evacuated and filled with argon. The evacuation/filling process was repeated three times before opening the inner door to bring the apparatus into the main part of the dry-box.

2.7 Preparation and purification of material

2.7.1 Monomers

2.7.1.1 Oxetane (Ox)

Oxetane of 99% purity, obtained from Lancaster Chemicals, was dried over calcium hydride for 48 hours in a stoppered flask fitted with a Teflon rotaflo tap kept open to allow hydrogen to escape (Scheme 2.2 (a)). The oxetane was then degassed using the freeze-thaw (see section 2.3) methodology and stored under argon.

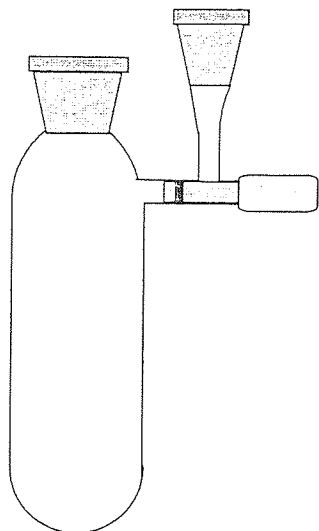
Prior to use, the oxetane was degassed as previously described and then distilled, using the trap-to-trap method, into a stopper flask fitted with a Teflon rotaflo tap containing benzophenone and sodium. Once degassed, the oxetane was left to stand for 10-15 minutes. This acted as a check for dryness, as the sodium/benzophenone radical anion formed has a characteristic blue colour, but is extremely sensitive to moisture and oxygen. The oxetane was then distilled into a weighed monomer solution storage flask (figure 2 (b)) by trap-to-trap distillation method. This was carried out because reaction between sodium and oxetane has been found to take place if the mixture is allowed to stand for sometime at room temperature.

2.7.1.2 Tetrahydropyran (THP)

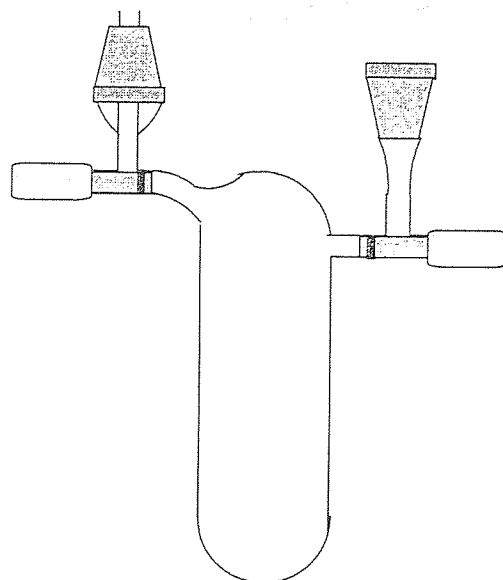
Tetrahydropyran, 99% purity, was obtained from Aldrich Chemicals. Procedure described as in section 2.7.1.1.

2.7.1.3 1,4-Dioxane (1,4-Dox)

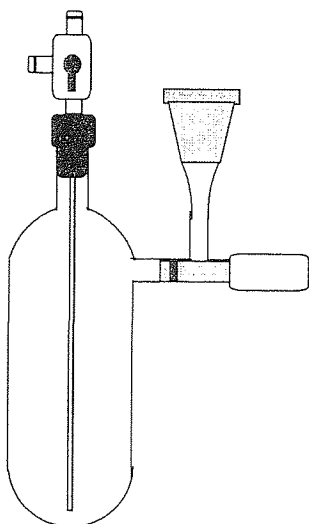
HPLC grade 1,4-dioxane, 99% purity, was obtained from Aldrich Chemicals. Procedure described as in section 2.7.1.1.



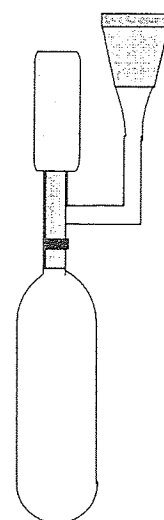
(a) solvent and monomer drying flask



(b) Monomer solution storage flask



(c) Catalyst solution storage flask.



(d) Schlenk

Figure 2. 2: Storage flasks used.

2.7.2 Solvents

2.7.2.1 Dichloromethane

SPS grade dichloromethane (DCM) 99.9% purity, unstabilised, was obtained from Romil Chemicals and stored in the dry box. As dichloromethane forms an azeotrope with water, rigorous drying precautions were necessary. Prior to use DCM was dried over calcium hydride (CaH_2) for at least 24 hours and then refluxed for several hours under an inert atmosphere using the distillation apparatus shown in figure 2.3. DCM was then distilled into

a solvent flask discarding the first 10%, degassed on the vacuum line and distilled using the trap-to-trap method as required.

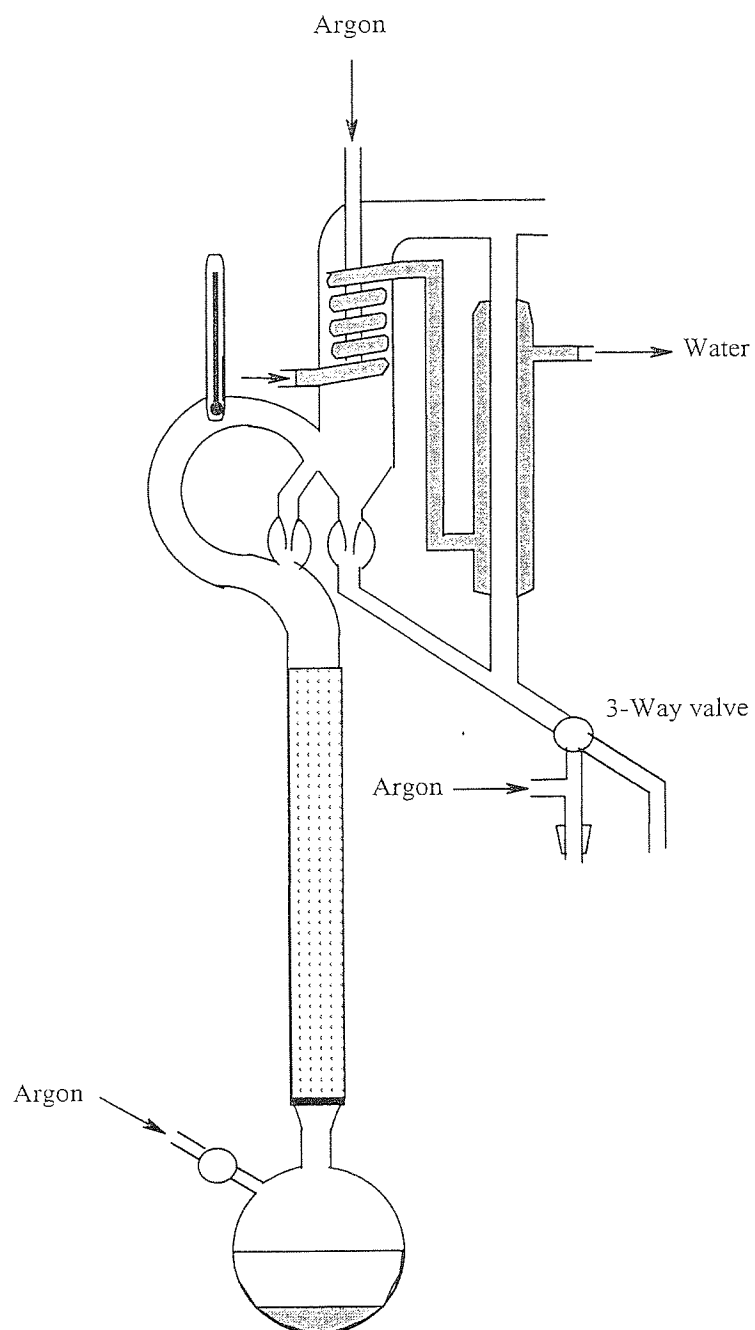


Figure 2. 3: Dichloromethane still.

2.7.2.2 Ethanol

S.L.R grade ethanol was obtained from Fisons and used as supplied.

2.7.3 Catalysts and co-catalysts

2.7.3.1 Boron trifluoride diethyl ether complex (BF_3OEt_2)

Boron trifluoride diethyl ether 99% purity, obtained from Lancaster Chemicals, is a self-drying agent. It gives off toxic fumes on hydrolysis and has to be handled at all times in the glove box.

2.7.3.2 Boron trifluoride acetic acid complex ($\text{BF}_3(\text{CH}_3\text{COOH})_2$)

Boron trifluoride acetic acid complex was obtained from Lancaster Chemicals. It was stored at all times in the dry box and used without further purification.

2.7.3.3 Boron trifluoride methanol complex (BF_3MeOH)

Boron trifluoride methanol complex was obtained from Lancaster Chemicals. It was stored at all times in the dry box and used without further purification.

2.7.3.4 Silver hexafluoroantimonate salt (AgSbF_6)

Silver hexafluoroantimonate salt 97% purity, obtained from Lancaster Chemicals, was stored in the glove box and used without further purification.

2.7.3.5 Silver boron tetrafluoride salt (AgBF_4)

Silver boron tetrafluoride salt 98% purity, obtained from Lancaster Chemicals, was stored in the glove box without further purification.

2.7.4 Initiators

2.7.4.1 3-Phenoxypropyl bromide ($\text{C}_6\text{H}_5\text{O}(\text{CH}_2)_3\text{Br}$)

3-Phenoxypropyl bromide, 96% purity, obtained from Aldrich Chemicals, was dried over 3 Å molecular sieve for 48 hours in a stoppered flask fitted with Teflon rotaflo tap (figure 2.2 (a)). Prior to its use, it was degassed by freeze-thaw methodology and then vacuum distilled, using the trap-to-trap method, into a Schlenk vessel fitted with Teflon rotaflo (figure 2.2 (d)). The solution was then stored in the dry box and used without further purification.

2.7.4.2 Chloromethyl ethyl ether ($\text{CH}_3\text{CH}_2\text{OCH}_2\text{Cl}$)

Chloromethyl ethyl ether was obtained from Aldrich Chemicals. Procedure described as in section 2.7.4.1.

2.7.4.3 Bromomethyl ethyl ether ($\text{CH}_3\text{CH}_2\text{OCH}_2\text{Br}$)

Bromomethyl ethyl ether was obtained from Aldrich Chemicals. Exactly the same procedures were carried out as in section 2.7.4.1 for the preparation of Bromomethyl ethyl ether.

2.7.5 Additives

2.7.5.1 Dibenzo-18-crown-6-ether (db18c6e)

Dibenzo-18-crown-6-ether, 98% purity, obtained from Aldrich Chemicals was dried in a vacuum oven at 25 °C for 48 hours, stored under argon into a stoppered flask fitted with rotaflo tap and used without further purification. It was dissolved in distilled DCM using Schlenk apparatus (figure 2.2 (d)), and the resultant solution was degassed using freeze-thaw techniques.

2.7.5.2 Diphenyl ether (DPE)

Diphenyl ether 99% purity, obtained from Aldrich Chemicals, was dried in vacuum oven at 20°C for 1 hour, stored in the dry box and used without further purification. It was dissolved in DCM using Schlenk apparatus (figure 2.2 (d)), and the resultant solution degassed using freeze-thaw techniques.

2.7.5.3 Veratrole (Vrol)

Veratrole 97% purity was obtained from Aldrich Chemicals. Prior to use it was dried over 3Å molecular sieves and vacuum distilled at 80°C, using conventional distillation apparatus. It was dissolved in DCM using Schlenk apparatus (figure 2.2 (d)), and the resultant solution was degassed using freeze-thaw techniques.

2.7.5.4 2,6-Di-*t*-butyl-pyridine (DtBP).

Di-*tert*-butylpyridine, 99% purity was supplied by Aldrich Chemicals. Prior to use it was vacuum distilled at 90°C, using a conventional distillation apparatus, to remove any monosubstitued pyridine. The distillate was stored in the glove box.

2.7.6 General reagents

2.7.6.1 Calcium hydride

Powdered anhydrous calcium hydride, 90-95% purity, 40 mesh, was obtained from Aldrich Chemical Company and used as supplied.

2.7.6.2 Sodium hydroxide

A.C.S. grade sodium hydroxide (97+% purity) in pellet form was supplied by Aldrich Chemical Company and used as supplied.

2.7.6.3 Sodium metal

Sodium metal was supplied in paraffin oil by B.D.H. Chemicals. The paraffin oil was removed by washing with hexane. Any tarnished pieces of metal were removed prior to use.

2.7.6.4 Benzophenone

Benzophenone, 99% purity, was obtained from Janssen Chemicals and used as supplied.

2.7.6.5 Magnesium sulfate

A.C.S. grade (97%) magnesium sulfate was obtained from Aldrich Chemicals. Prior to use the magnesium sulfate was dried in an oven at 200 °C for at least 48 hours.

2.7.6.6 3 Å molecular sieves

3Å molecular sieves were obtained from Lancaster synthesis. Prior to use 3Å molecular sieves were dried in an oven at 200°C for at least 48 hours.

2.7.7 Preparation of solutions

2.7.7.1 Initiating system solution

The original vessel shown in Scheme 2.2 (c) was developed in our laboratory to enable the injection of a required volume of initiator solution into a polymerisation reaction vessel without contamination. The components of this vessel were purchased from Omnifit, and half of a 10-mm glass chromatography column was attached to the top of the vessel. The column

was connected to a 3-way column bleed valve equipped with a Luerlock syringe adaptor. This valve originally designed to stand up to high pressure, turned out to be efficient also at low pressure (high vacuum).

2.7.7.1.1 Preparation of protonic initiator solution

2.7.7.1.1.1 $BF_3(CH_3COOH)_2/BF_3OEt_2$ solution

The required concentration of $BF_3OEt_2/BF_3(CH_3COOH)_2$ solution was made in dried and distilled dichloromethane (see section 2.7.2.1). The preparation was carried out in a dry box and the amount of BF_3OEt_2 and $BF_3(CH_3COOH)_2$ was extracted using a glass syringe. It was then added to a catalyst flask which already contained a known volume of dichloromethane. The solution was then degassed using freeze-thaw techniques, put into argon atmosphere and stored in the glove box.

2.7.7.1.1.2 $BF_3:MeOH$ solution.

The initiating system solution was prepared as described above (see section 2.7.7.1.1.1).

2.7.7.1.2 Preparation of alkylating initiator solution

The required quantity of silver salt with stable complex anion was transferred to a dried clean catalyst flask (figure 2.2 (c)) in a dry box. The flask was then taken out from the dry box, attached to the vacuum line and evacuated before a certain volume of solvent (DCM, THP or 1,4-dioxane) was distilled into the catalyst flask using trap-to-trap method (section 2.4). Next, the flask was put back into the dry box and the required amounts of di-tert-butylpyridine followed by initiator were drowned out into the catalyst vessel using a clean, dried glass syringe. The solution was then degassed on the vacuum line using freeze-thaw techniques, put into an argon atmosphere and stirred for at least 3 hours. Because silver salts are photosensitive, aluminium foil was used to protect the solution against the ambient sunlight.

2.7.7.1.3 Preparation of monomer solution

The monomer was prepared as described in the section 2.7.1.1. The required volume of dried solvent was distilled into the monomer solution storage flask using the trap-to-trap method. The preparation of the dichloromethane, tetrahydropyran and 1,4-dioxane are described in sections 2.7.2.1, 2.7.1.2 and 2.7.1.3, respectively.

2.8 Polymerisation procedure

The cationic polymerisation of oxetane was studied in solution at 35°C under an inert atmosphere using different initiating systems and different solvents. Because the ring opening of oxetane is an exothermic process ($\Delta H^\circ = -19.3 \text{ kcal.mol}^{-1}$ at -9°C in methyl chloride^[115]), the reaction was monitored by means of a calorimeter. A modification of the technique described by Biddulph and Plesch^[287] was used. The calorimeter is shown in Scheme 2.5. The increase of temperature was measured using Gl23 Thermocouple (2k Ω , supplied by RS Composant Ltd). The change in resistance as a function of temperature was measured by Knauer auto-potentiometer linked to a chart recorder.

2.8.1 Calorimeter experiments

2.8.1.1 Homopolymerisation of oxetane experiments

In a typical experiment, the calorimeter (figure 2.5) was attached to a vacuum line through (A) and the monomer flask to (C), with the taps B, D, E, F, G opened and H and I closed. To minimise the reabsorption of moisture onto the glass, the calorimeter was evacuated, flamed with Bunsen burner and left to cool down. At this stage, the pressure inside the calorimeter was evaluated by closing the tap (B) for 5 minutes and then measuring the pressure when the tap (B) was reopened. No difference in pressure is characteristic of a good vacuum. When the whole system was evacuated, the tap (B) was closed and the required amount of monomer solution was poured into the flask. The flask was then placed under an argon atmosphere by opening (B). Subsequently, the taps (B) and (D) were closed, the calorimeter was placed on a magnetic stirrer and the thermistor was connected to Knauer auto-potentiometer Bridge. To insure that the reaction proceeds under adiabatic conditions, the water from the thermostat bath at 35 °C was continually passed through the double jacket. When the system is balanced to 35 °C, the required amount of catalyst was injected into the calorimeter by means of the bleed valve system after, which Teflon tubing, bleed valve and Hamilton gas tight syringe were cleaned several times with the catalyst solution. Prior to their use, the Hamilton syringes, Teflon tubing and bleed valves were cleaned with adequate solvent, dried at 100°C for 4 hours and then allowed to cool under argon in the desiccators. Zero time was taken after the catalyst had been added.

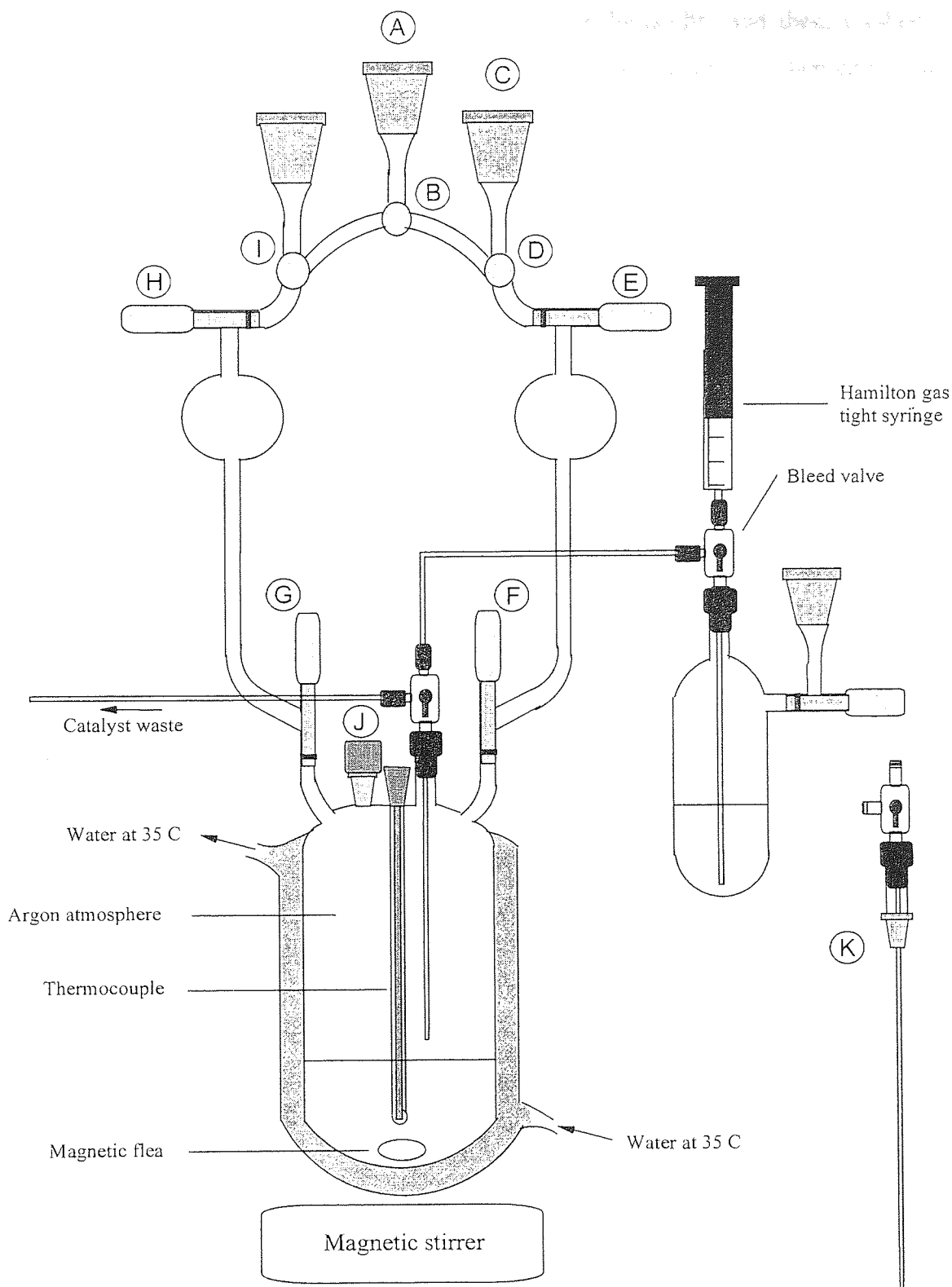


Figure 2. 4: Calorimeter.

2.8.1.2 Termination of the polymerisation

The reaction mixture was terminated by adding a large excess of ethanol (20ml of ethanol in 25ml of polymerisation solution) through (E), while stirring. The resultant solution was

washed twice with a 10% NaOH solution to neutralise the acidity and then, washed again twice with distilled water to remove the salts. The aqueous fraction was then extracted with dichloromethane, and dried over MgSO_4 . The drying agent was filtered off and washed with dry dichloromethane. The polymer was recovered by removal of the solvent to constant weight.

2.8.2 Kinetic study by calorimetric analysis

2.8.2.1 Theory

Under adiabatic conditions, the rate at which the reaction evolves, $\frac{dQ}{dt}$ (J.s^{-1}), may be written as the function of the rate of polymerisation, R_p ($\text{mol.L}^{-1}.\text{s}^{-1}$), shown by the equation E: 2.1.

$$\frac{dQ}{dt} = \Delta H_p \cdot V \cdot R_p \quad \text{E: 2.1}$$

Because the first law of thermodynamics predicts that heat release at constant volume is proportional to the change of the temperature (see equation E: 2.2),

$$\begin{aligned} dU &= \delta Q + \delta W \\ dU &= \delta Q - PdV \\ dU &= dQ \\ dU &= C_p \cdot dT \end{aligned} \quad \text{E: 2.2}$$

the initial rate at which the temperature increases, $(dT/dt)_i$ (K.s^{-1}), can be used to estimate the initial rate of the propagation reaction, R_p ($\text{mol.l}^{-1}.\text{s}^{-1}$). Because,

$$C_p - C_v \approx 0 \quad \text{E: 2.3}$$

for most of the solide and liquid, $(dT/dt)_i$ can then be expressed by the following equation,

$$\left(\frac{dT}{dt} \right)_i \cdot \frac{1}{V} = - \frac{\Delta H_p}{C_p} \cdot R_p \quad \text{E: 2.4}$$

where ΔH_p (J.mol^{-1}) is the enthalpy of the reaction, V (L) is the total volume of the polymerisation solution and, C_p (J.K^{-1}) is constant-pressure heat capacity of the whole

system. Similarly, C_v ($J.K^{-1}$) is constant-volume heat capacity of the whole system. In practice, the above equation is only valid for a small and fast increase of temperature (less than $5^\circ C$ within one minute).

2.8.2.2 Kinetic measurement

In a typical experiment, the polymerisation was terminated while the polymerisation reaction was proceeding under adiabatic conditions (see figure 2.5).

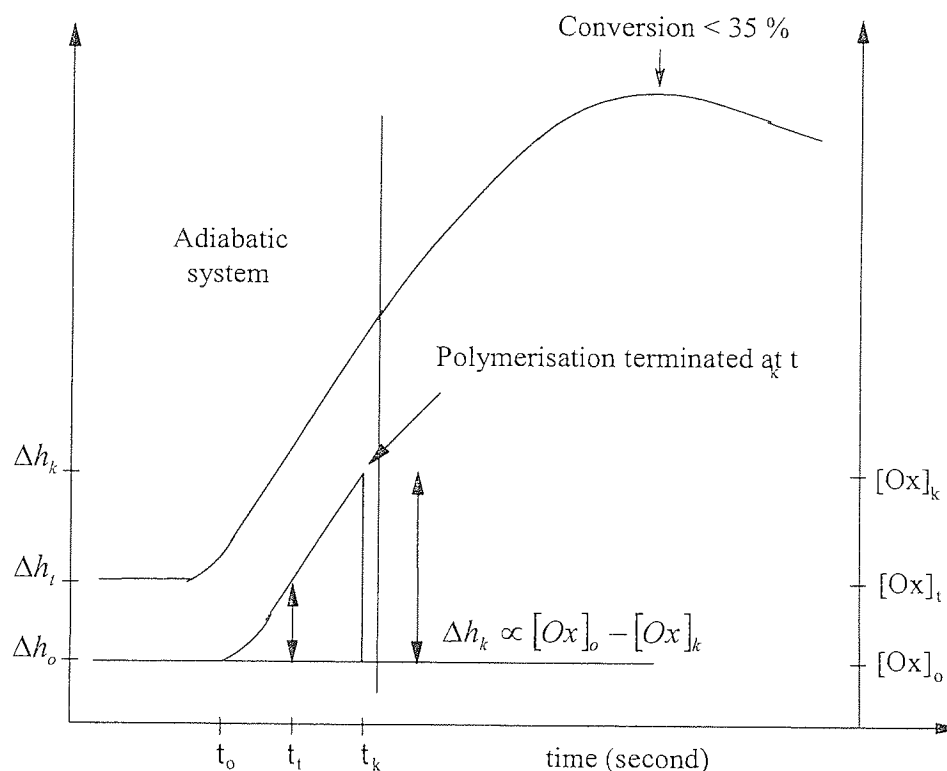


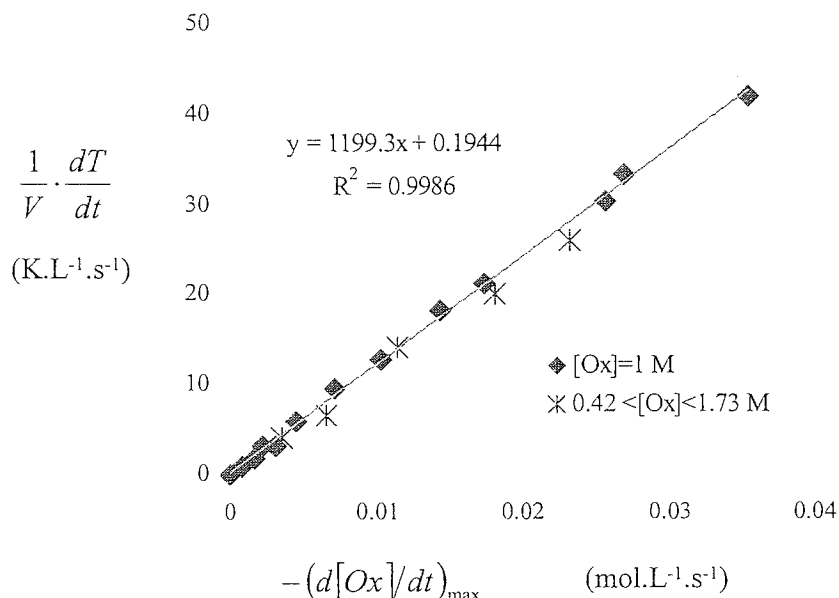
Figure 2. 5: Trace of deflection against time of polymerisation.

When the bridge was calibrated, it was found that the change in temperature associated with one full-scale deflection is equivalent to $5^\circ C$. Thus, the rate of temperature change during the polymerisation could be measured in units of $^\circ C.s^{-1}$, since the chart recorder was set to a constant speed ($mm.s^{-1}$). The deflection in mm was also converted to change in concentration of oxetane (mol/L) using the equation E: 2.5.

$$[Ox]_t = [Ox]_o \cdot \left(1 - \frac{\Delta h_t}{\Delta h_k} \cdot conversion_k \right)$$

E: 2.5

Here $[Ox]_o$ ($mol.L^{-1}$) is the initial concentration of oxetane, t (s) is the time of the reaction, $conversion_k$ is the yield of the produced polymers determined by gravimetric analysis at t_k . Δh_t (mm) is proportional to the concentration of oxetane converted into polymer at given time t . The initial rate at which the monomer is consumed, $-(d[Ox]/dt)_t$, was then given by the slope of the plot of $[Ox]_t$ against the time. Figure 2.6 shows the observed linear dependence of $\frac{1}{V} \cdot \left(\frac{dT}{dt} \right)$ against $-\frac{d[Ox]}{dt}$ with an intercept close to the origin strongly, indicating that the kinetic measurements were performed under adiabatic conditions.



(Data from chapter 3).

Figure 2. 6: Dependence of $\frac{1}{V} \cdot \frac{dT}{dt}$ on $-\frac{d[Ox]}{dt}$

2.8.3 Sampling reactions using Omnifit fittings

The procedure for carrying out the polymerisation remained the same as described in Section 2.8.1.1 with the sampling system (K) attached to the position (J). Once the polymerisation was initiated, the reaction vessel was maintained under a blanket of argon. A sample could be taken by opening the three-way valve (F) to the vessel and drawing out a quantity of the polymerisation into a dry Hamilton gas tight syringe. The valve was then closed and the sample injected directly into ethanol or water. The syringe and Teflon tubing leaving the vessel were then washed and dried with dichloromethane in preparation for the next sample. In this way, samples of polymer could be taken without contamination of the remaining polymerisation. This procedure was also used to inject a second charge of monomer solution to active polymer solution free of monomer.

2.9 Size exclusion chromatography

Size exclusion chromatography (S.E.C.), otherwise known as gel permeation chromatography (G.P.C.) is a technique for determining the molecular weight and molecular weight distribution of a polymer sample. The polymer sample is separated into fractions by a sieving action according to the hydrodynamic volume of the molecules. This is achieved by

passing a solution of the sample through a series of columns containing a stationary phase of cross linked polystyrene swollen by solvent. The swollen stationary phase contains pores whose size distribution is controlled. Polymer molecules with large hydrodynamic volume can enter a smaller fraction of the pores and hence are eluted more rapidly than smaller molecules to which a larger volume of pore solvent is accessible.

2.9.1 Apparatus

Figure 2.7 shows a schematic diagram for the size exclusion chromatograph used in these studies. The mobile phase, HPLC grade THF, was pumped at $1 \text{ cm}^3/\text{min}$ by a Knauer HPLC pump. Solutions of the polymer sample, $\sim 0.05\%$ w/v, were prepared in a sample of THF used as solvent and introduced to the system by means of a Rheodyne injector equipped with a $100 \mu\text{L}$ loop. The sample was pumped through a $5 \mu\text{m}$ in-line filter and then Polymer Laboratories $5 \mu\text{m}$ guard column, to remove any undissolved material. Two gel columns supplied by Polymer Laboratories were used in series, a $5 \mu\text{-PL}$ gel column with an exclusion limit of 10^3 \AA and a mixed B column. The eluted solution was then passed through a Knauer differential refractometer and variable wavelength UV detector connected in series, the outputs from these were passed to a Polymer Laboratories DCU and analysed using PL Caliber[®] software.

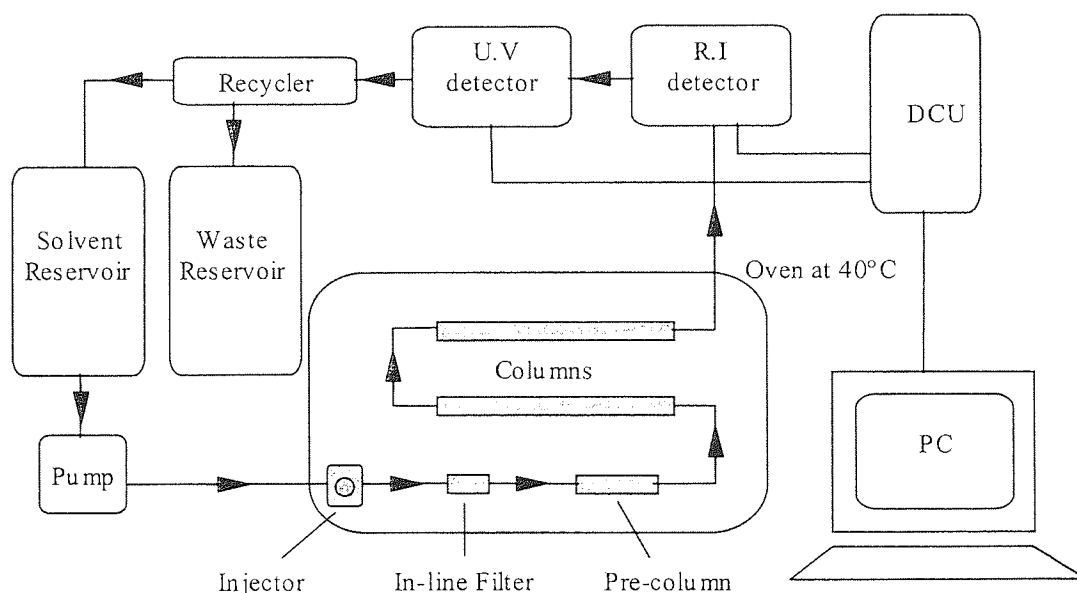


Figure 2. 7: Size exclusion chromatograph.

2.9.2 Theory

Figure 2.8 shows a typical S.E.C. trace. If a differential refractometer is used as a detector then the difference in refractive index (Δn) at any elution volume is proportional to the height, h , at that point. The difference in refractive index will depend on the concentration of polymer in the eluent and hence the weight fraction of polymer at that elution volume.

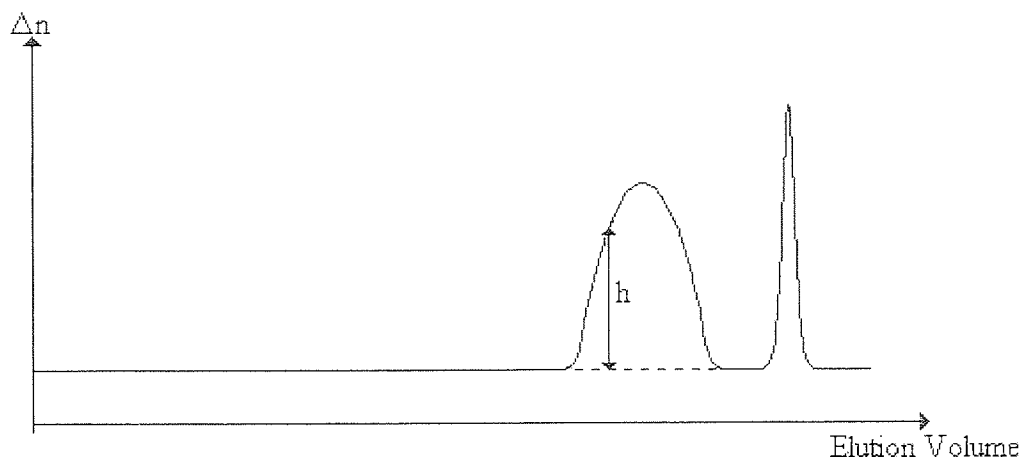


Figure 2. 8: Typical S.E.C. trace.

The number average (\overline{M}_n) and weight average (\overline{M}_w) molecular weights of a polymer can be calculated from:

$$\overline{M}_n = \frac{\sum N_i M_i}{\sum N_i} \quad \text{and} \quad \overline{M}_w = \frac{\sum N_i M_i^2}{\sum N_i M_i} \quad \text{E: 2.6}$$

where N_i = number of molecules of molecular weight M_i .

If W_i is the weight fraction of polymer at molecular weight M_i then;

$$W_i \propto N_i M_i \quad \text{and} \quad N_i \propto \frac{W_i}{M_i} \quad \text{E: 2.7}$$

And;

$$\overline{M}_n = \frac{\sum W_i}{\sum W_i / M_i} \quad \text{and} \quad \overline{M}_w = \frac{\sum W_i M_i}{\sum W_i} \quad \text{E: 2.8}$$

Given the above relationships the molecular weights can be calculated from the SEC trace by:

$$\overline{M}_n = \frac{\sum h_i}{\sum h_i/M_i} \text{ and } \overline{M}_w = \frac{\sum h_i M_i}{\sum h_i}. \quad \text{E: 2.9}$$

In order to obtain values for M_i it was necessary to determine how the molecular weight of eluted polymer varied with elution volume. This was achieved by calibrating the columns using polystyrene standards of known molecular weight and molecular weight distribution ($\overline{M}_w/\overline{M}_n$) less than 1.1. The logarithm of the molecular weight was plotted against elution volume and a 3rd order polynomial equation obtained. Figure 2.9 shows the calibration curve obtained.

Since the hydrodynamic volume of a given molecular weight varies with polymer type, this calibration only provides absolute molecular weights for samples of polystyrene. However it is possible to obtain absolute molecular weights for polymers other than the calibrant by using the universal calibration method. The hydrodynamic volume of a polymer molecule in solution can be shown to be proportional to its intrinsic viscosity and molecular weight. Two polymers eluting at the same elution volume must have the same hydrodynamic volume therefore:

$$[\eta]_1 M_1 = [\eta]_2 M_2 \quad \text{E: 2.10}$$

where $[\eta]_1$ and $[\eta]_2$ are the intrinsic viscosities of the two polymers and M_1 and M_2 their molecular weights.

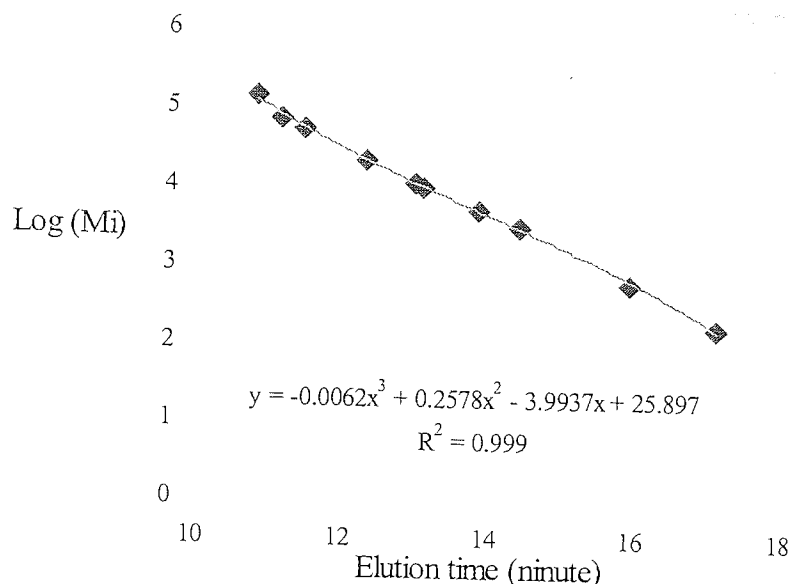


Figure 2. 9: Calibration curve for S.E.C. using polystyrene standards.

2.9.3 The intrinsic viscosity of a polymer is related to its molecular weight by the equation

$$[\eta] = Km^\alpha \quad \text{E: 2.11}$$

where K and α are the Mark Houwink constants for polymers in different solvents.

Therefore for co-eluting polymers:

$$K_1 M_1^{\alpha_1} M_1 = K_2 M_2^{\alpha_2} M_2. \quad \text{E: 2.12}$$

Rearranging equation E: 2.12 gives:

$$\log M_2 = \frac{(1 + \alpha_1)}{(1 + \alpha_2)} \log M_1 + \frac{1}{(1 + \alpha_2)} \log \left(\frac{K_1}{K_2} \right). \quad \text{E: 2.13}$$

Therefore if the Mark Houwink constants are known for both the calibrant standard and the polymer then absolute molecular weights may be determined.

2.10 Nuclear magnetic resonance spectroscopy

Fourier transform high resolution ^1H and ^{13}C N.M.R. were carried out using a Bruker AC 300 spectrometer. Solutions of the samples were prepared in deuterated chloroform with a small quantity of tetramethyl silane (TMS) as reference.

For ^{13}C analysis the P.E.N.D.A.N.T pulse technique was used, with methyl and methine carbons appearing as positive peaks and methylene and quaternary carbons as negative peaks.

The S.P.E.E.D technique is another pulsing technique that was used for ^{13}C analysis. During the analysis, the signals corresponding to carbonyl and quaternary carbons were enhanced, and signals from methine, methylene and methyl carbons were decoupled.

The spectra were analysed using WinNMR and mestec software supplied by Bruker.

CHAPTER 2

Experimental

Controlling the experimental environment is essential in the cationic ring opening polymerisation of cyclic ethers. The intermediates involved during the polymerisation (oxonium ions) are known to be very sensitive toward moisture. Water can act as a co-catalyst and also modify the mechanism of polymerisation by acting as a transfer agent. For this reason the purification and preparation of monomers, solvent and catalyst solutions, as well as the polymerisation reactions, were carried out using either high vacuum techniques or in an atmosphere of argon to exclude disadvantageous impurities. These experimental requirements are vital particularly when living polymerisation is required.

3 CHAPTER 3

Studies of the *cationic ring-opening polymerisation (C.R.O.P)* of oxetane initiated by protonic acid and oxacarbenium salts in dichloromethane at 35 °C

In an initial investigation, we were interested in the studies of the cationic ring opening polymerisation of oxetane in dichloromethane at 35 °C using different sources of initiating species. For this purpose, protonic acids ($\text{BF}_3(\text{CH}_3\text{COOH})_2$ and BF_3OEt_2) and oxacarbenium salts ($[\text{CH}_3\text{CH}_2\text{OCH}_2]^+[\text{BF}_4]^-$ and $[\text{CH}_3\text{CH}_2\text{OCH}_2]^+[\text{SbF}_6]^-$) were used as initiating system.

3.1 Polymerisation initiated by protonic acids

The initiating solution was prepared in dichloromethane as described in the section 2.7.7.1.1.1 and stored in the dry box for at least one week. The polymerisation reaction was carried out as shown in the section 2.8.1.1. In all experiments, the polymerisation reaction was terminated by addition of a large volume of ethanol. The inactive polymer solution was then treated as described in the section 2.8.1 and the volatile materials were removed by evaporation for several days at room temperature in the fume cupboard. The yield of the polyoxetane was determined by weight and the products were analysed by Size Exclusion Chromatography (S.E.C) using polystyrene as standard, and ^1H and ^{13}C NMR.

3.1.1 Effect of the concentration of oxetane

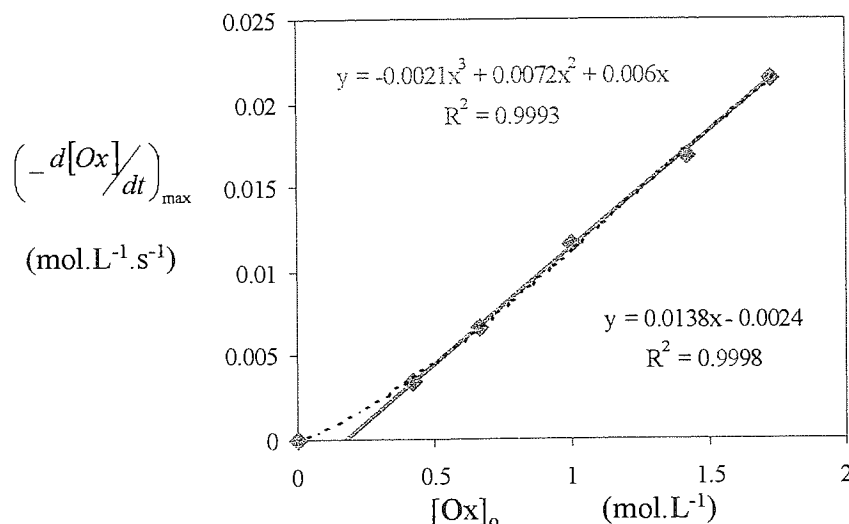
A series of experiments was carried out in dichloromethane using $0.0065 \pm 0.005\text{M}$ of $\text{BF}_3(\text{CH}_3\text{COOH})_2$, $0.0065 \pm 0.005\text{M}$ of BF_3OEt_2 and various concentrations of oxetane. The total volume of polymerisation solution was kept constant. The excess of acetic acid in relation to boron trifluoride has been estimated at 0.3 %. Table 3.1 summarises this study.

As shown in the figure 3.1, the linear dependence of the plot of initial rate of monomer consumption on the initial concentration of monomer seems to indicate that the polymerisation reaction is first order with respect to the monomer concentration. The rate of the consumption of oxetane can therefore be written as shown by equation E: 3.1.

$$-\frac{d[\text{Ox}]}{dt} = k_{P_{app}} \times [\text{Ox}]_o \quad \text{E: 3.1}$$

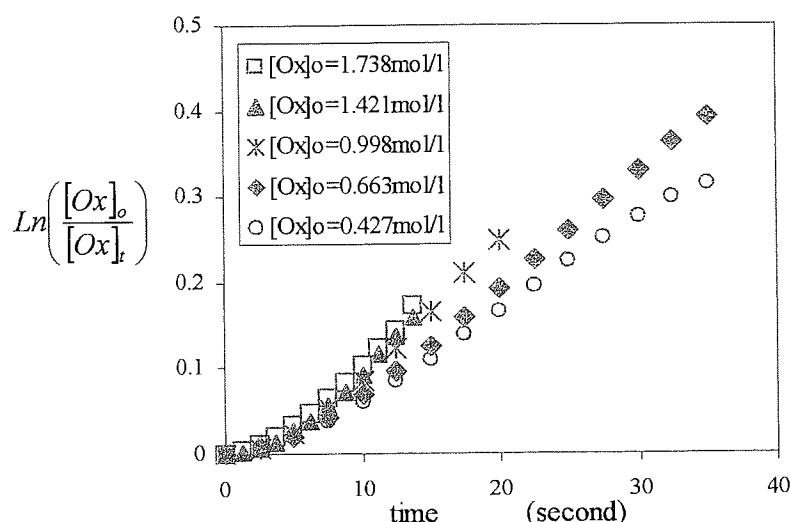
Entry	$[\text{BF}_3\text{OEt}_2]_0$ mol/l	$[\text{BF}_3(\text{AcOH})_2]_0$ mol/l	$[\text{Ox}]_0$ mol/l	$-(d[\text{Ox}]/dt)_i$ mol.l^{-1}	$(dT/dt)_{\text{max}}$ $^{\circ}\text{C.s}^{-1}$	conversion %	time t_k second	Mp
S 3.1.1	0.0066	0.0066	1.738	0.5809	0.0214	18.3	17.1	44,000
S 3.1.2	0.0064	0.0065	1.731	0.5905		85.2	540	22,000
S 3.2.1	0.0065	0.0064	1.421	0.4524	0.017	13.9	17.5	25,800
S 3.2.2	0.0064	0.0065	1.419	0.4381		83.4	600	17,900
S 3.3.1	0.0061	0.0064	0.998	0.3270	0.0112	21.1	23.7	14,600
S 3.3.2	0.0065	0.0065	1.003	0.3190		79.2	510	14,300
S 3.4.1	0.0065	0.0065	0.663	0.1524	0.0064	41.5	55	6,700
S 3.4.2	0.0065	0.0065	0.663	0.1619		92.2	558	7,200
S 3.5.1	0.0066	0.0066	0.423	0.0954	0.0034	23.9	40.8	6,100
S 3.5.2	0.0064	0.0065	0.423	0.0988		95.2	538	4,600

Table 3. 1: Effect of oxetane concentration on the rate of polymerisation.



$[\text{BF}_3(\text{AcOH})_2]_0 = [\text{BF}_3(\text{AcOH})_2]_0 = 0.0065 \pm 0.005 \text{ M}$ (table 3.1).

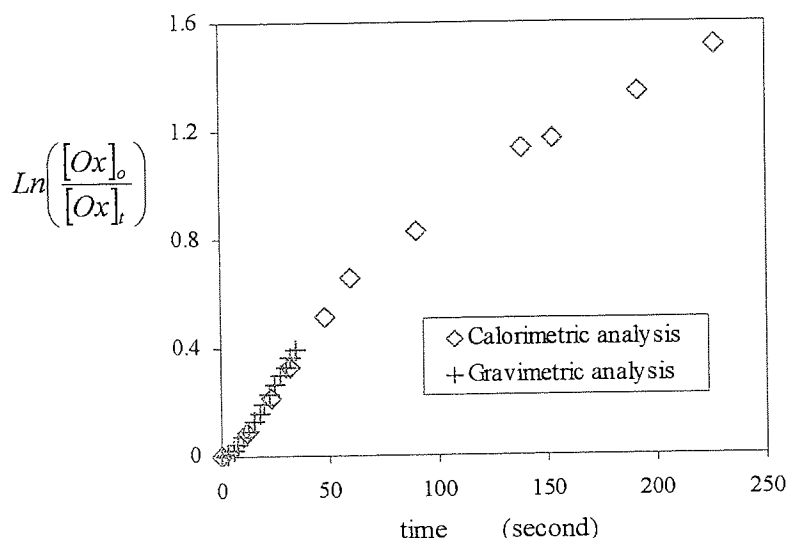
Figure 3. 1: Dependence of $-(d[\text{Ox}]/dt)_{\text{max}}$ on $[\text{Ox}]_0$.



$[\text{BF}_3(\text{AcOH})_2]_0 = [\text{BF}_3(\text{AcOH})_2]_0 = 0.0065 \text{ M}$ and $0.42 < [\text{Ox}]_0 < 1.72 \text{ M}$ (table 3.1).

Figure 3. 2: Dependence of $\text{Ln}([[\text{Ox}]_0]/[\text{Ox}]_t)$ against time for the homopolymerisation of oxetane in dichloromethane at 35°C

Equation E: 3.1 predicts the rate dependence for reaction of oxetane in the feed. The plot of $\text{Ln}([[\text{Ox}]_0]/[\text{Ox}]_t)$ against time of the reaction describes a family of sigmoid curves, each of which is determined by a concentration of oxetane (figure 3.2). A gravimetric analysis carried out until high conversion in monomer confirmed the sigmoid form plot of $\text{Ln}([[\text{M}]_0]/[\text{M}]_t)$ against time (figure 3.3).



$[Ox] = 0.68 \text{ M}$ and $[BF_3(AcOH)_2]_0 = [BF_3(AcOH)_2]_0 = 0.0065 \text{ M}$ (table 3.5 series S 3.13).

Figure 3. 3: Dependence of $\ln\left(\frac{[Ox]_0}{[Ox]_t}\right)$ against time by calorimetric and gravimeter analysis.

The analysis of these curves showed that the initiation step is slow in relation to the propagation step and that the polymerisation reaction does not appear to be living. Indeed, in the early stages of the reaction, the increase of the apparent rate constant of monomer consumption, $k_{p_{app}}$, could indicate that the concentration of active species increases while the chains grow. In the later stages, the decrease of $k_{p_{app}}$ during the polymerisation reaction seems to indicate that the decrease of monomer concentration favours the termination reactions if they occur and the transfer reactions over the propagation step. As shown by figure 3.4, the effects of these two side reactions are respectively to decrease the stationary concentration of growing chains end and to change the molar ratio of each active species in favour of the non strained oxonium ions (A2, A3 and A4), which exhibit a smaller apparent rate constant of reaction towards oxetane than the strained oxonium ion A1. Consequently, the apparent rate constant of monomer consumption, $k_{p_{app}}$, decreases during the course of the reaction. Besides, the surprising increase of the initial $k_{p_{app}}$ with the initial concentration of oxetane, figure 3.1, is an even stronger indication that the formation of tertiary oxonium ions is a slow process and that the increase of the initial monomer concentration accelerates the rate of the initiation step in relation to the rate of propagation. It must be noted however that the change of the temperature during the polymerisation process could also affect the value of $k_{p_{app}}$.

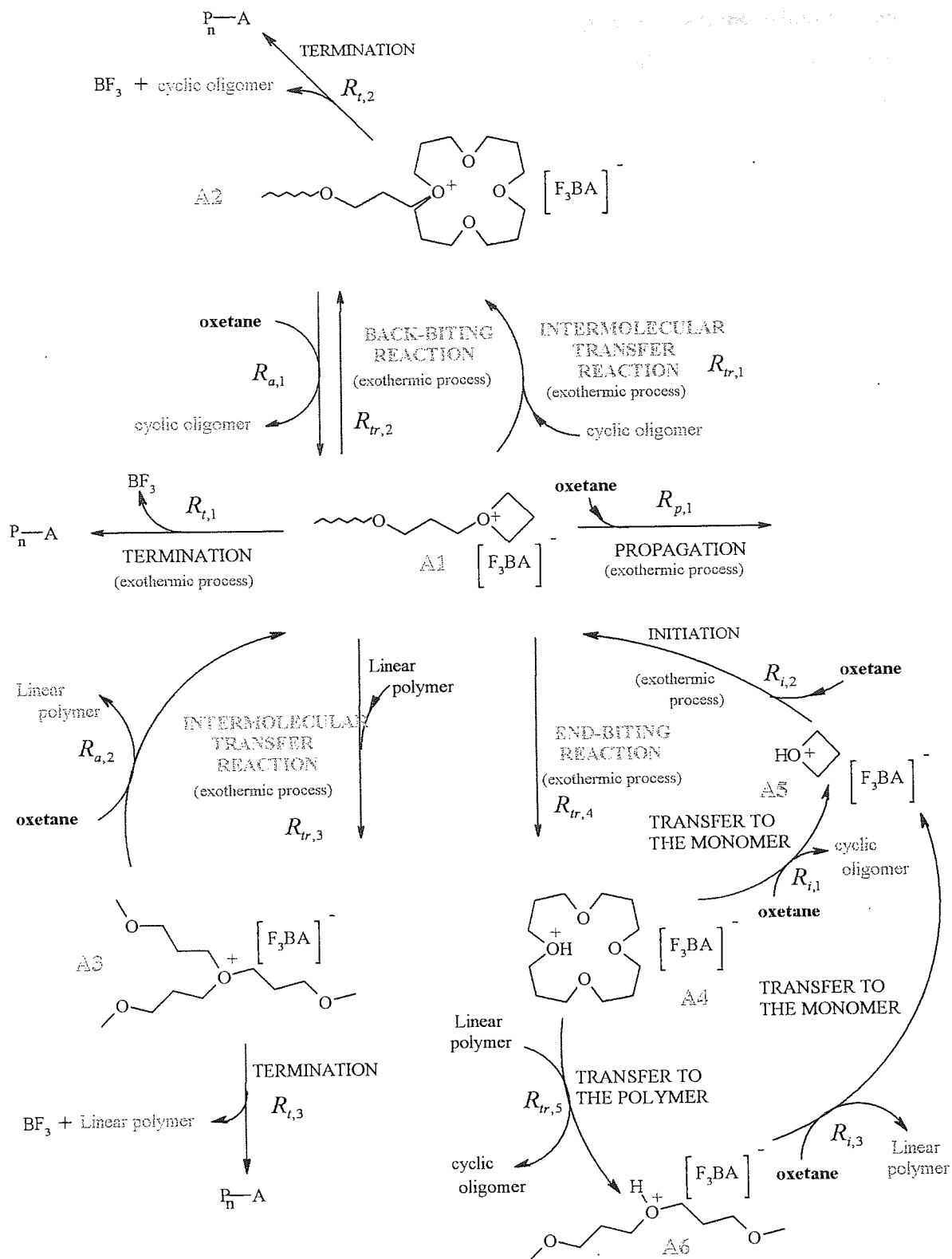


Figure 3. 4: Side reactions involved in the polymerisation of oxetane initiated by $\text{BF}_3(\text{AcOH})_2/\text{BF}_3\text{OEt}_2$ in dichloromethane at 35 °C.

It is interesting also to note that calorimetric analysis only measures the rate at which the strain contained in the oxonium ion is released by ring opening reactions, while the rate of polymerisation determined by gravimetric analysis corresponds to the rate at which the monomer is converted into polymer. Thus, if the mode of the ring-opening process is visualised as described by the figure 3.4, the quantity $-d[Ox]/dt$ should be dependent on the method used to monitor the rate of the monomer consumption. Equations E: 3.2 and E: 3.3 represent the mathematical expression of the rate of the monomer consumption monitored by calorimetric and by gravimetric analysis, respectively.

$$\text{Calorimetric analysis: } -\frac{d[Ox]}{dt} = k_{p,1} \cdot [A1] \cdot [Ox] + \sum_{j=1}^4 R_{tr,j} + R_{i,1} + R_{i,2} \quad \text{E: 3.2}$$

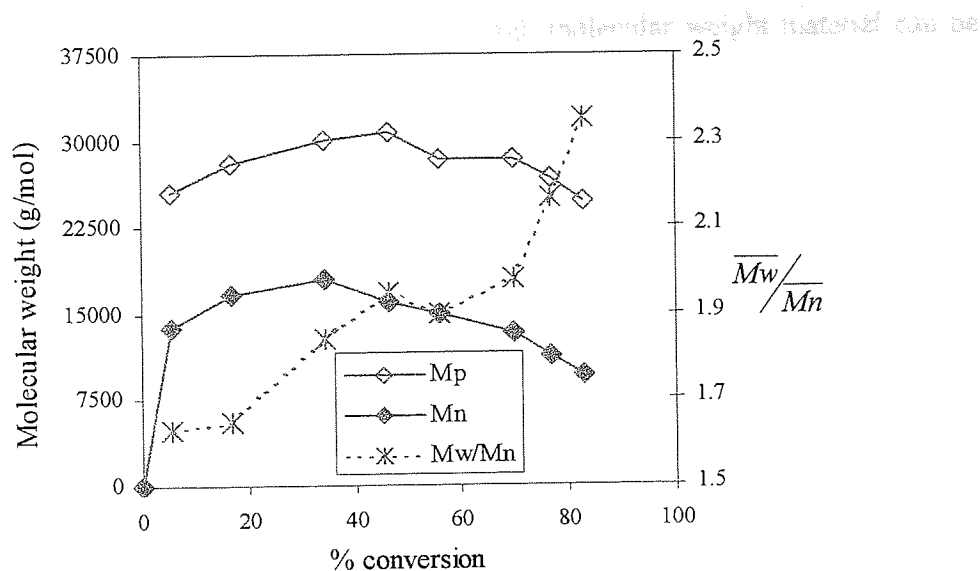
$$\text{Gravimetric analysis: } -\frac{d[Ox]}{dt} = k_{p,1} \cdot [A1] \cdot [Ox] + \sum_{j=1}^2 R_{a,j} + \sum_{j=1}^3 R_{i,j} \quad \text{E: 3.3}$$

The similarity on the slopes of $\ln([M]_0/[M]_t)$ against time obtained by calorimetric and gravimetric analysis (see figure 3.3) seems to indicate that early in the reaction (conversion lower than 15-20%) the growing oxonium ions are mainly in the form of strained tertiary oxonium ions (A1). The subsequent decrease and loss of adiabatic conditions as early as 25-30% of monomer is consumed is probably due to the subsequent decrease in concentration of strained oxonium ion (A1) in favour of the non-strained oxonium ions (A2, A3, A4 and A6). As already mentioned (figure 3.4 and equation E 3.2), this is the endocyclic nucleophilic attack of the strained oxonium ions by an oxygen atom from the monomer or from the polymer that produce the heat of the polymerisation.

The molecular weight and the molecular weight distribution were analysed by Size Exclusion Chromatography (S.E.C) against polystyrene standards. A typical chromatogram of polymer prepared in this experiment is shown in annex 3.1. The polymer has a broad molecular weight distribution and illustrates the presence of low molecular weight oligomer together with higher molecular weight materials. In all experiments, SEC traces of the polyoxetane shows that the high molecular weight materials peak extends to the low molecular weight materials. Previous work on the polymerisation of oxetane suggests that the oligomers peak is cyclic oligomers and principally cyclic tetramers ^[115,234].

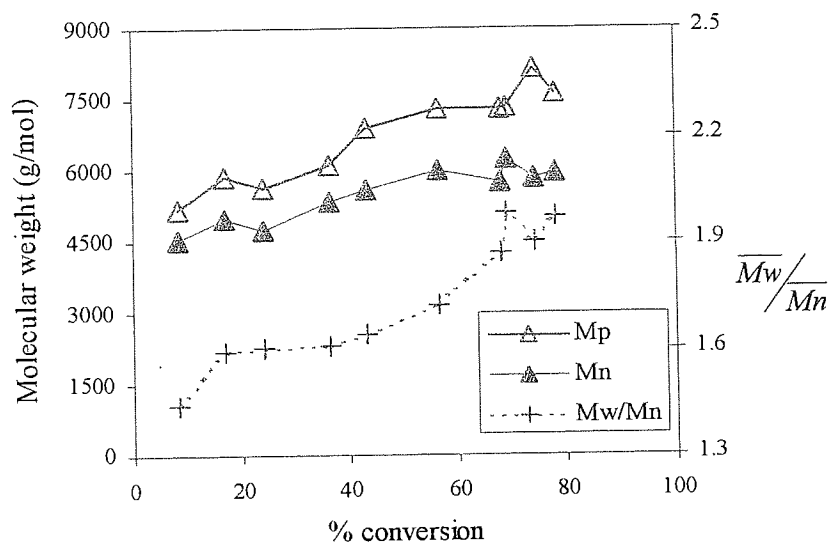
In some experiments where the polymerisation occurred, the S.E.C analysis has shown that the S.E.C traces go beyond the calibration borderlines. The consequence of this is that the number average weight molecular weight \overline{Mn} and the weight average weight molecular weight \overline{Mw} data are increased or reduced depending on whether the traces reaches the upper or the lower calibration borderlines. We have then followed the effect of time on the reaction and the effect of the initial concentration of oxetane on the chains length by means of the peak weight molecular weight M_p of the high molecular weight material and by means of "Overlay analysis" of the S.E.C traces of the polymers.

In all experiments, the S.E.C analysis proved to be in agreement with the kinetics analysis, that of a polymerisation reaction characterised by the presence of transfer reactions. In annex 3.3, the S.E.C traces of polymers at different initial concentrations of oxetane seem to indicate that at low monomer conversion, the polymer is formed more rapidly than cyclic oligomers and subsequently the decrease of monomer concentration favours side reactions involving a slight decrease in the molecular weight of the high molecular weight material with, a broadening of its molecular weight distribution ($1.5 < \overline{Mw}/\overline{Mn} < 2.5$), and formation of cyclic oligomers (annex 3.3 and 3.4). Several reports ascribe the decrease of the molecular weight to the intramolecular transfer reactions, while the broadening of the molecular weight distribution is mainly due to intermolecular transfer reaction. This can be visualised in the figures 3.5 and 3.6, where the increase of the initial concentration of monomer enhances the formation of cyclic oligomers (see annex 3.2, 3.4 and 3.5) and the decrease of the molecular weight of the molecular weight of the high molecular weight materials. At constant concentration of initiator, the enhancement of cyclic oligomers formation with the increase of the initial concentration of monomer (see annex 3.2, 3.4 and 3.5) suggests that transfer reactions are not irreversible process of termination and that once formed, the non-strained tertiary oxonium ions (A2, A3 and A4) can be reactivated, by molecule of monomer, into strain tertiary oxonium ions (A1) capable of propagation. In the figure 3.5, the linear increase of \overline{Mn} with % conversion shows that the reactions of redistribution of the polymers chain length induced by the interconversion (see figure 3.4) between strained tertiary oxonium ions (A1) and non-strained oxoniums ions A2, A3 and A4) affect more significantly long polymer chains when high Dp are targeted than short polymer chains when low Dp are targeted. The intercept of the (Y) axis shows clearly that transfer reactions still proceed.



$[Ox]_0 = 1M$ and $[I]_0 = 0.005 M$. $[I]_0 = [BF_3(AcOH)_2]_0 = [BF_3(AcOH)_2]_0$ (table 3.5 series S 3.12 and annex 3.4)

Figure 3. 5: Dependence \overline{Mn} , Mp and $\overline{Mw}/\overline{Mn}$ on monomer conversion



$[Ox]_0 = 0.68 M$ and $[I] = 0.0065 M$. $[I]_0 = [BF_3(AcOH)_2]_0 = [BF_3(AcOH)_2]_0$ (table 3.5 series S 3.13 and annex 3.5).

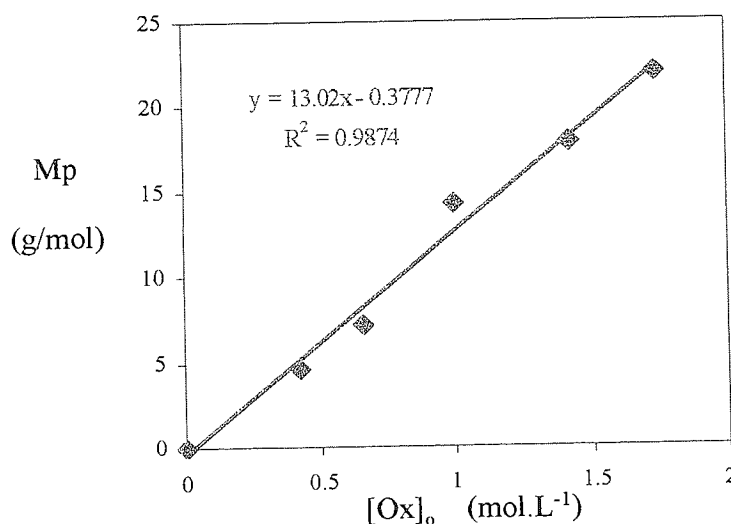
Figure 3. 6: : Dependence \overline{Mn} , Mp and $\overline{Mw}/\overline{Mn}$ on monomer conversion.

The redistribution of the polymer chains length during the polymerisation process suggests that \overline{DPn} is kinetically controlled by the transfer reactions, termination reactions if they occur and also by the rate at which tertiary oxonium ions are produced. Therefore, the

number average degree of polymerisation, \overline{DP}_n , of high molecular weight material can be written as shown by the equation (E: 3.4):

$$\overline{DP}_n = \frac{R_{p,1} + \sum_{j=1}^2 R_{a,j}}{\sum_{j=1}^3 R_{t,j} + \sum_{j=1}^5 R_{tr,j} + R_i} \quad \text{E: 3.4}$$

where $R_{p,1}$ ($\text{mol.L}^{-1}.\text{s}^{-1}$) is the rate of propagation of the active species (A1), $R_{a,j}$ ($\text{mol.L}^{-1}.\text{s}^{-1}$) is the rate at which A2 ($j=1$) and A3 ($j=2$) are converted into active strained oxonium ions (A1), $R_{t,j}$ ($\text{mol.L}^{-1}.\text{s}^{-1}$) is the rate at which each active (A1, A2 and A3) species are irreversibly terminated by anion splitting, $R_{tr,j}$ ($\text{mol.L}^{-1}.\text{s}^{-1}$) is the rate of transfer reactions (intra- ($j=2$ and 4) and intermolecular ($j=1, 3$ and 5) transfer reactions) and R_i ($\text{mol.L}^{-1}.\text{s}^{-1}$) is the rate at which tertiary oxonium ions are formed during the initiation process as well as by transfer to the monomer (see figure 3.5).



$[I]_0 = [\text{BF}_3(\text{AcOH})_2]_0 = [\text{BF}_3(\text{AcOH})_2]_0 = 0.0065 \text{ M}$ (table 3.1 and annex 3.2).

Figure 3. 7: Dependence Mp over $[\text{Ox}]_0$ obtained at high monomer conversion.

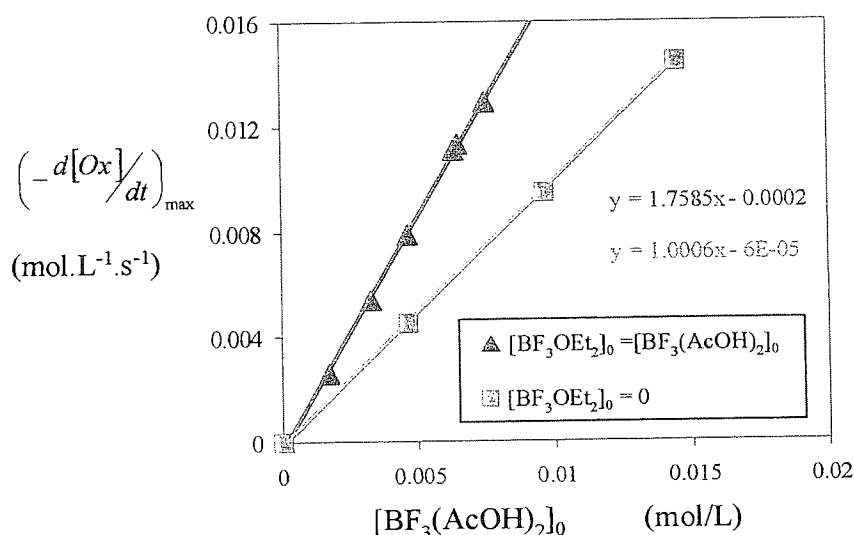
In the figure 3.7, the linear dependence of M_p of the high molecular weight material on the initial concentration of oxetane also indicate that at constant concentration of $\text{BF}_3(\text{CH}_3\text{COOH})_2$ and constant concentration of BF_3OEt_2 , the number average degree of polymerisation \overline{DP}_n depends on the initial concentration of oxetane. The see above \overline{DP}_n can therefore be written as shown by the equation E: 3.5 where K is constant.

$$\overline{DP}_n = K \times [Ox]_0$$

E: 3.5

3.1.2 Effect of the concentration of initiating system

We have investigated the effect of the concentration of boron trifluoride acetic acid complex and boron trifluoride diethyl ether complex on the rate of propagation and on molecular weight. A series of experiments was carried out using oxetane (1.07 M), and a range of concentrations of $BF_3(AcOH)_2$ and/or BF_3OEt_2 . The total volume of polymerisation solution was kept constant by adjusting the amount of dichloromethane used. In the table 3.2, the series S 3.6 corresponds to the experiments carried out at concentration of BF_3OEt_2 equal to the concentration of $BF_3(AcOH)_2$, while in the series S 3.7 and S 3.8, only the concentration of only one co-catalyst was varied, BF_3OEt_2 and $BF_3(AcOH)_2$, respectively. In the series S 3.9 S 3.7.9 and S 3.7.10, only $BF_3(AcOH)_2$ was used as catalyst. This study is summarised in the table 3.2.



(See table 3.2 series S 3.6 and S 3.9).

Figure 3. 8: Effect of the concentration of the initiating system BF_3OEt_2 / $BF_3(AcOH)_2$ (1:1) on the rate of the monomer consumption

Figure 3.8 shows the plot of the rate of monomer consumption against the initial concentration of $BF_3(AcOH)_2$ when the polymerisation of oxetane was initiated by (▲) an equimolar solution of $BF_3(AcOH)_2$ / BF_3OEt_2 (table 3.2, S 3.7) and by (◻) $BF_3(AcOH)_2$ (table 3.2, S 3.9). In both cases, the initial rate of monomer consumption exhibited a linear dependence on catalyst concentration, and gave an intercept close to the origin. From the

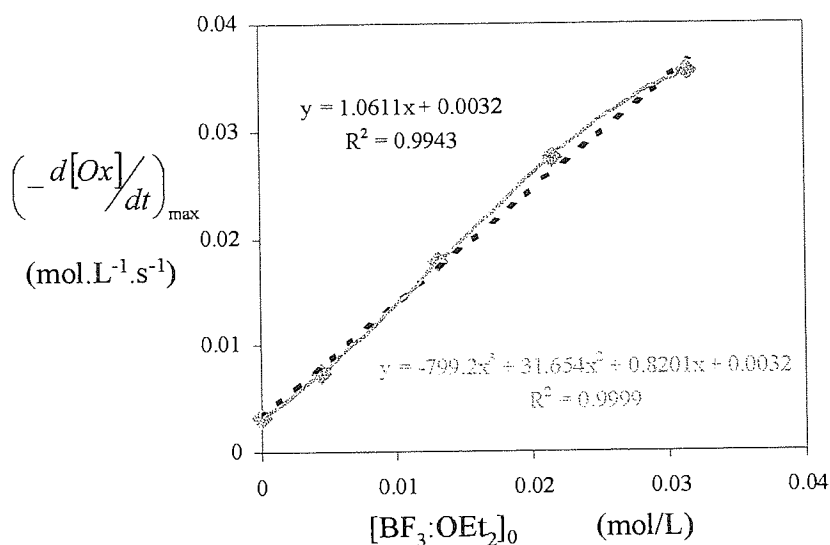
value of the gradient, it appears therefore that the addition of one molar equivalent of BF_3OEt_2 does not accelerate significantly the initial rate of monomer consumption. From this kinetic data it appears that the initial rate of monomer consumption can be written as follow:

$$-\frac{d[M]}{dt} = k \cdot [\text{Cat}] \cdot [M] \quad \text{E: 3.6}$$

with

$k = 1.06 \text{ L} \cdot \text{mol}^{-1} \cdot \text{s}^{-1}$ at $[\text{Cat}]_0 = [\text{BF}_3(\text{AcOH})_2]_0$ and $[\text{BF}_3\text{OEt}_2]_0 = 0 \text{ M}$ and,

$k = 1.72 \text{ L} \cdot \text{mol}^{-1} \cdot \text{s}^{-1}$ at $[\text{Cat}]_0 = [\text{BF}_3\text{OEt}_2]_0 = [\text{BF}_3(\text{AcOH})_2]_0$.



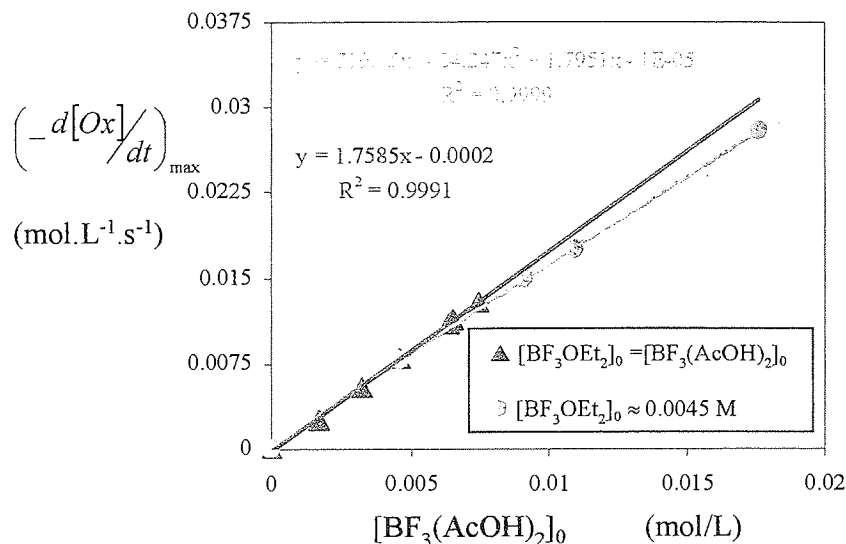
$[\text{BF}_3\text{OEt}_2]_0 = 0.0044 \text{ M}$ (table 3.2 series S 3.7).

Figure 3. 9: Effect of the $[\text{BF}_3\text{OEt}_2]_0$ on the rate of monomer consumption in dichloromethane at 35°C .

In the figure 3.9, where the concentration of $\text{BF}_3(\text{AcOH})_2$ was kept equal to $0.00435 \pm 0.0002 \text{ mol/l}$, the plot of $-d[\text{Ox}]/dt$ against $[\text{BF}_3\text{OEt}_2]_0$, showed that BF_3OEt_2 accelerate significantly the rate of polymerisation only at $[\text{BF}_3\text{OEt}_2]/[\text{BF}_3(\text{AcOH})_2] > 1$. However, as the concentration of BF_3OEt_2 increases, the slope starts to curve. The sigmoid dependence of $-d[\text{Ox}]/dt$ against $[\text{BF}_3\text{OEt}_2]_0$, suggests that BF_3OEt_2 acts more likely as co-catalyst in presence of $\text{BF}_3(\text{AcOH})_2$ than as catalyst of the initiation process. In the figure 3.10, the non linear dependence of $-d[\text{Ox}]/dt$ against $[\text{BF}_3(\text{AcOH})_2]_0$, at concentration of BF_3OEt_2 equal to $0.00453 \pm 0.0006 \text{ mol/l}$, reinforce this idea.

Entry	[BF ₃ OEt ₂] mol.l ⁻¹	[BF ₃ (AcOH) ₂] mol.l ⁻¹	(dT/dt) _{max} °C.s ⁻¹	-(dM/dt) _i mol.l ⁻¹	time t _k second	Mp g/mol	conversion %
S 3.6.1	0.00747	0.00747	0.411	0.0129	26	14,200	18
S 3.6.2	0.00739	0.00747	0.409		700	11,220	89.6
S 3.6.3	0.00651	0.00651	0.351	0.0113	27	15,700	22
S 3.6.4	0.00662	0.00651	0.349		792	13,200	87.8
S 3.6.5	0.00638	0.00638	0.331	0.0111	25.8	16,800	17.9
S 3.6.6	0.00635	0.00635	0.337		731	13,700	81.6
S 3.6.7	0.00463	0.00463	0.247	0.0079	33	22,600	16.2
S 3.6.8	0.00479	0.00479	0.238		1000	17,200	80.9
S 3.6.9	0.00328	0.00328	0.152	0.0054	59	31,600	17.5
S 3.6.10	0.00309	0.00309	0.157		953	21,800	72
S 3.6.11	0.00171	0.00171	0.081	0.0026	73	32,300	11.4
S 3.6.12	0.00172	0.00172	0.079		1239	26,800	60
S 3.7.1	0.03148	0.00435	1.094	0.0355	15	14,950	30.49
S 3.7.2	0.03075	0.00425	1.083		348	7,430	79
S 3.7.3	0.02154	0.00415	0.836	0.0275	18	13,500	26.73
S 3.7.4	0.02178	0.00422	0.845		474.4	9,370	92.77
S 3.7.5	0.01279	0.00447	0.548	0.0178	26.4	16,560	26.54
S 3.7.6	0.01251	0.00427	0.539		554	13,090	85.22
S 3.7.7	0.00452	0.00449	0.236	0.0073	43.8	16,730	21.3
S 3.7.8	0.00465	0.00455	0.241		810	16,290	76.61
S 3.7.9	0	0.00483	0.0134	0.0045	48	25,210	10.90
S 3.7.10	0	0.00491	0.0128		828	18,720	70.64
S 3.8.1	0.00453	0.0176	0.872	0.025	23	4,900	35.15
S 3.8.2	0.00453	0.0179	0.869		332	6,570	85
S 3.8.3	0.00453	0.0109	0.552	0.0175	22.2	11,420	26.26
S 3.8.4	0.00453	0.0101	0.521		504	9,870	78.24
S 3.8.5	0.00453	0.0045	0.472	0.0158	27	17,420	26.43
S 3.8.6	0.00453	0.0043	0.469		805	16,370	73.24
S 3.9.1	0	0.00961	0.328	0.0106	32	16,500	13.99
S 3.9.2	0	0.00959	0.324		495	13,000	69.04
S 3.9.3	0	0.0145	0.477	0.0152	25.8	13,970	15.1
S 3.9.4	0	0.0148	0.472		332	9,450	73.12

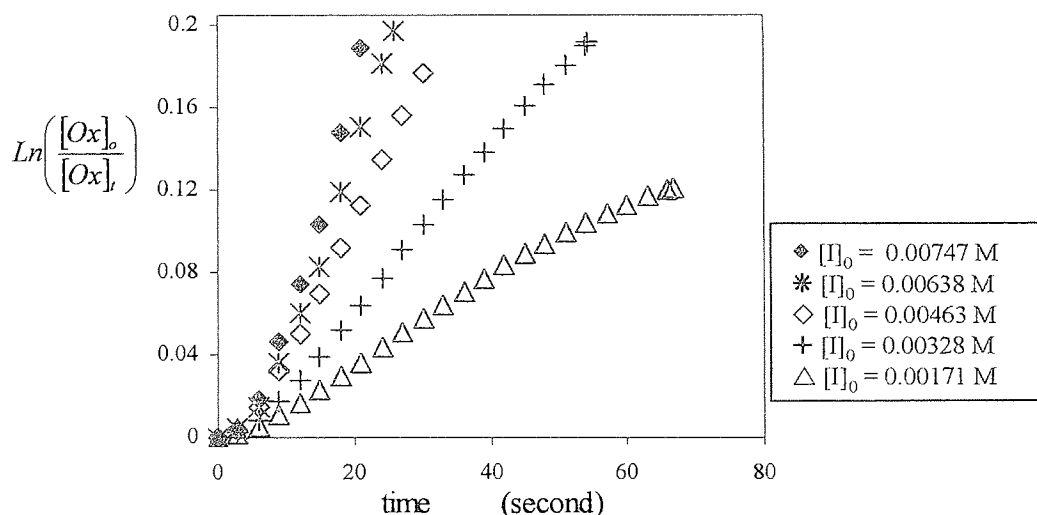
Table 3. 2: Effect of the catalyst concentration on the polymerisation of oxetane (1.07 M) in dichloromethane at 35 °C.



$[\text{BF}_3\text{OEt}_2]_0 \approx 0.0045 \text{ M}$ (table 3. 2 series S 3.6 and S 3.8).

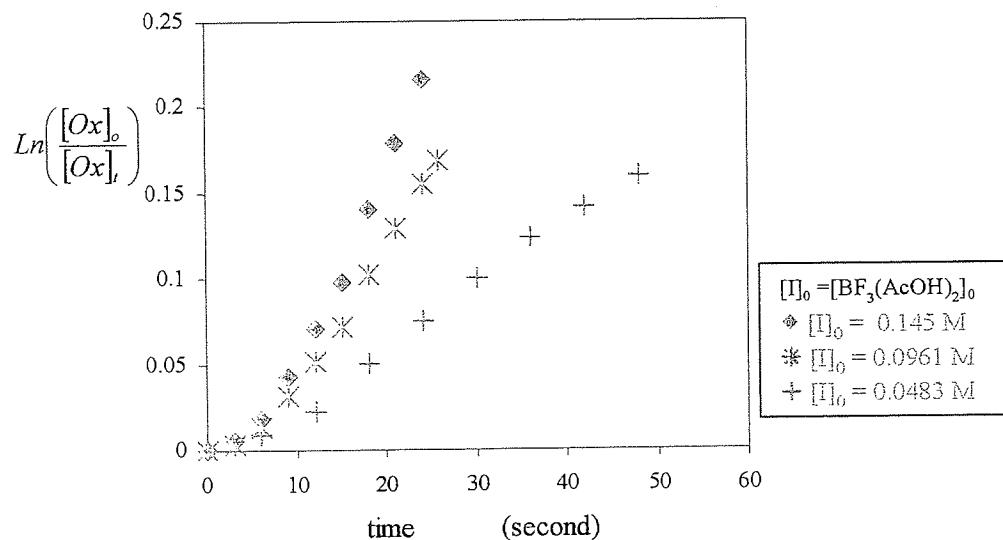
Figure 3. 10: Effect of the $[\text{BF}_3(\text{AcOH})_2]_0$ on the rate of monomer consumption in dichloromethane at 35 °C.

As expected, the kinetic analysis of oxetane consumption (figures 3.11, 3.12, 3.13 and 3.14) exhibits the characteristic sigmoid form of the plot $\text{Ln}([M]_0/[M]_t)$ of against time. It is interesting to note that at constant concentration of $\text{BF}_3(\text{AcOH})_2$, the increase of the concentration of BF_3OEt_2 increases the rate of initiation in relation to the rate of propagation (figure 3.13).



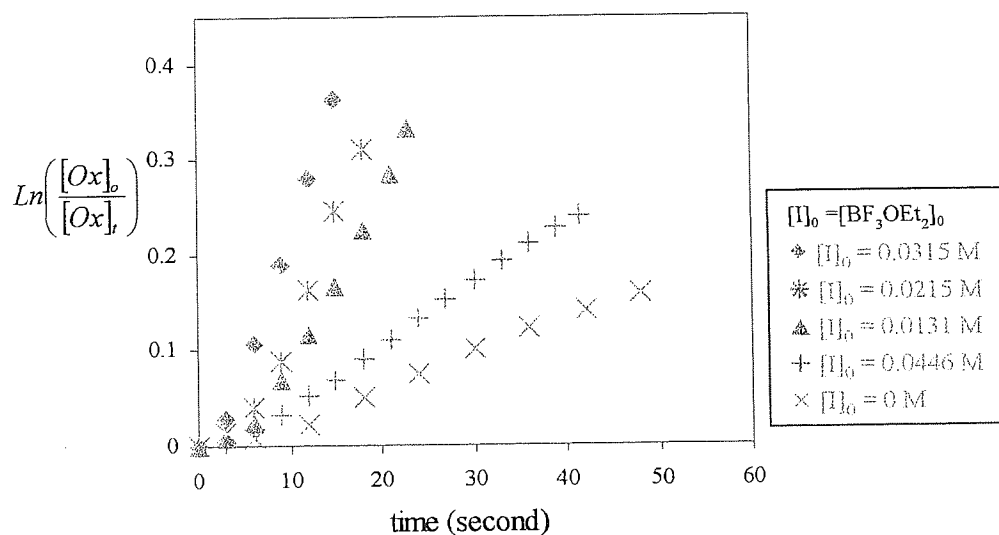
$[\text{Ox}]_0 = 1 \text{ M}$ and $[\text{I}]_0 = [\text{BF}_3(\text{AcOH})_2]_0 = [\text{BF}_3(\text{AcOH})_2]_0$ (table 3.2 series S 3.6).

Figure 3. 11: Dependence of $\text{Ln}([M]_0/[M]_t)$ against time at various concentration of initiator. Polymerisation carried out in dichloromethane at 35 °C



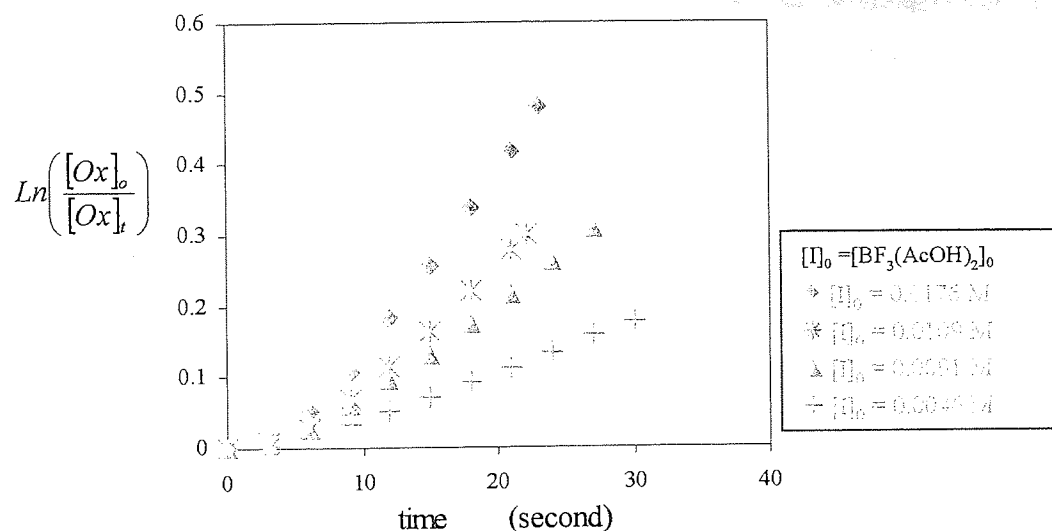
$[\text{Ox}]_0 = 1 \text{ M}$ and $[\text{BF}_3\text{OEt}_2]_0 = 0.0045 \text{ M}$ (table 3.2 series S 3.9).

Figure 3. 12: Dependence of $\text{Ln}\left(\frac{[\text{M}]_0}{[\text{M}]_t}\right)$ against time at various concentration of $\text{BF}_3(\text{AcOH})_2$. Polymerisation carried out in dichloromethane at 35°C .



$[\text{Ox}]_0 = 1 \text{ M}$ and $[\text{BF}_3(\text{AcOH})_2] = 0.00435 \text{ M}$ (table 3.2 series S 3.7).

Figure 3. 13: Dependence of $\text{Ln}\left(\frac{[\text{M}]_0}{[\text{M}]_t}\right)$ against time at various concentration of BF_3OEt_2 . Polymerisation carried out in dichloromethane at 35°C .



$[Ox]_0 = 1M$ and $[BF_3OEt_2] = 0.00453 M$ (table 3.2 series S 3.8).

Figure 3. 14: Dependence of $\ln([M]_0/[M]_t)$ against time at various concentration of $BF_3(AcOH)_2$. Polymerisation carried out in dichloromethane at 35 °C.

Once more, the molecular weight data turn out to be in agreement with the kinetic data. In figure 3.10, 3.11, 3.12 and 3.14, while the increase of initial concentration of $BF_3(AcOH)_2$ increases the concentration of growing oxonium ions, the overlay analysis of the polymer at high monomer conversion (annex 3.7, 3.8, 3.10 and 3.12) show that low concentration of $BF_3(AcOH)_2$ favours the formation cyclic oligomers whilst still producing linear polymer of higher molecular weight. The enhancement of formation of cyclic oligomers with the decrease of catalyst concentration is in agreement with the principle of dilution which state that the dilution favours the intramolecular over intermolecular reactions. This can only be explained if transfer reactions generate a temporarily inactive species. As shown in the figure 3.4, the formation of non-strained tertiary oxonium ions (A2, A3 and A4) by intra- and intermolecular transfer reactions can be followed by nucleophilic attack of the lone pair electrons of oxygen of the incoming monomer onto one of the three electron deficient carbons in α -position with respect to the oxonium site, reforming a strained tertiary oxonium ions (A1) capable of propagating. In the case of formation of macrocyclic tertiary oxonium ions (A2) by intramolecular transfer reactions, the attack of the exocyclic deficient carbon in the α -position with respect to the oxonium site by the incoming monomer will regenerate the active tertiary oxonium ion, with formation of a cyclic oligomers.

In the figures 3.16 and 3.17, the plot of the inverse of the peak weight molecular weight ($1/M_p$) against concentration of BF_3OEt_2 and $BF_3(CH_3COOH)_2$ intersect (Y) axis at constant

value. In the figure 3.15, the curvature of the slope as the concentration of initiator decreases, notably at $[I]_0 < 0.005$ M, reinforces the idea that transfer reactions affect more significantly long polymer chains than short one.

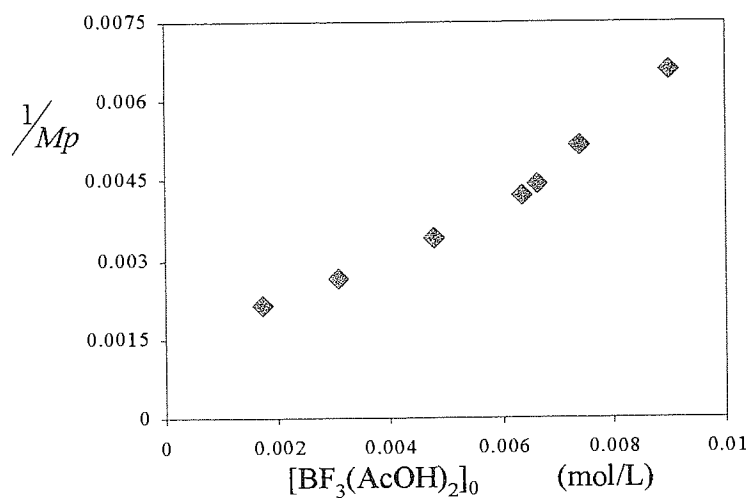


Figure 3. 15: Dependence of $(1/M_p)$ against $[BF_3(AcOH)_2]_0$ for the homopolymerisation of oxetane in dichloromethane at 35 °C (table 3.2 series S 3.6).

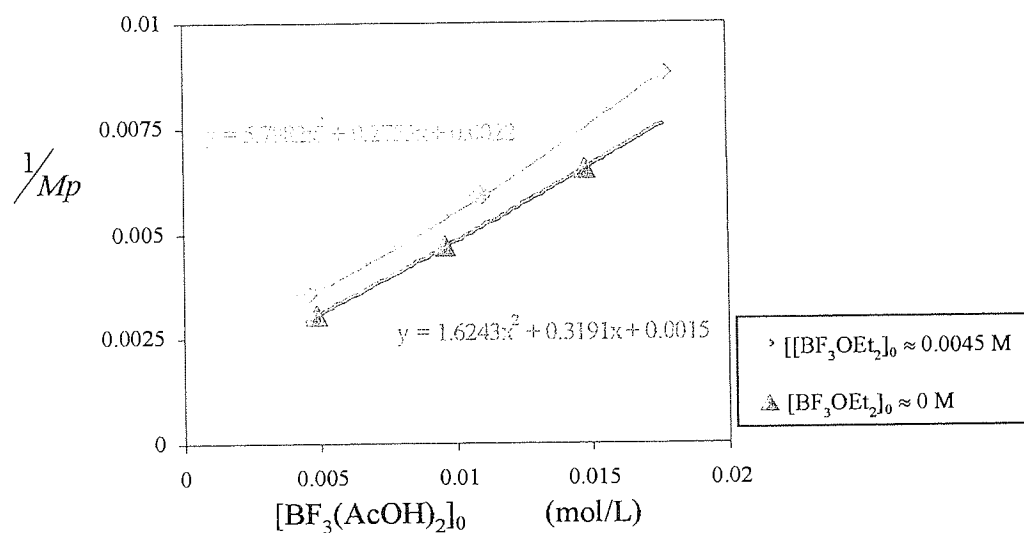


Figure 3. 16: Dependence of $(1/M_p)$ against $[BF_3(AcOH)_2]_0$ for the homopolymerisation of oxetane in dichloromethane at 35 °C.

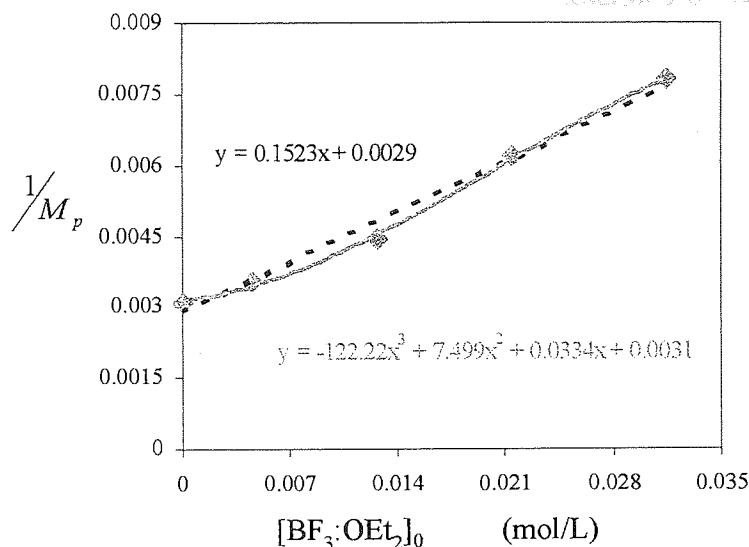


Figure 3. 17: Dependence of $(1/M_p)$ against $[\text{BF}_3\text{OEt}_2]_0$ for the homopolymerisation of oxetane in dichloromethane at 35 °C. $[\text{Ox}]_0 = 1$ and $[\text{BF}_3(\text{AcOH})_2]_0 = 0.00435 \text{ M}$.

3.1.3 Effect of the addition of monomer solution to an active polymer solution

From the studies carried out in the section 3.1.1 and 3.1.2, it seemed to us interesting to establish if the addition of a given amount of a monomer to an active polymer solution free in monomer will restart the polymerisation because of the absence of the terminations reactions. A series of experiments was then carried out in which the concentration of oxetane was 0.92 M and the concentration of BF_3OEt_2 and $\text{BF}_3(\text{AcOH})_2$ were respectively 0.00433 M and 0.00439 M. The total volume of the solution was equal to 22 ml. After a given time, respectively 1 hour and 3 days, 5 ml of solution of oxetane (4.98 M) in dichloromethane was added to the active polymer solution to produce a concentration of oxetane approximately equal to the original. The monomer solution was added using the sampling system as described in the section 2.8.3. Similarly, a second charge of monomer was added 30 minutes after the first monomer addition, using approximately 5 ml of solution of oxetane (6.8 M) in DCM. Considering the dilution factor and knowing yield of the polymerisation just before the monomer solution was added (samples S 3.10.1, S 3.10.2, S 3.11.1 and S 3.11.2), the concentration of monomer, BF_3OEt_2 and $\text{BF}_3(\text{AcOH})_2$ were calculated using the equation E: 3.52. The initial rates of the monomer consumption before and after monomer addition were also measured by calorimetric analysis. The polymerisation reaction was then terminated by addition of a large volume of ethanol ($\approx 30 \text{ ml}$), 30 minutes after that the monomer solution

was added, and the polymer solution was treated as described in the section 2.8.1.2. This study is summarised in the table 3.3.

In the table 3.3, the entry S 3.10.2 and S 3.11.2 correspond to the experiments in which the first monomer addition was performed after 2 hours and 3 days, respectively. The examination of the calorimetric analysis data before and after the monomer addition showed that the monomer addition restarted the polymerisation faster (figure 3.18). The enhancement of the rate of propagation after monomer addition can only be explained if the rate of initiation is slow in relation to the rate of propagation in the first case. This observation is in good agreement with the fact that at constant concentration of initiating system, the increase of monomer concentration accelerates the initial rate of polymerisation (section 3.1.1, figure 3.2). In the figure 3.4, the unchanged value of the rate of monomer consumption after monomer was added (table 3.3 series S 3.10.2 and S 3.11.2), strongly indicates that termination reactions do not seem to occur significantly when the growing centres are mostly in the form of non strained tertiary oxonium ions. In the experiment S 3.10.1 and S 3.11.1 where the polymerisation reaction was terminated respectively after 2 hours and 3 days, the decrease of \overline{Mn} with the time of polymerisation, indicates that transfer reactions still occur even in starving monomer conditions (annex 3.14 and figure 3.19).

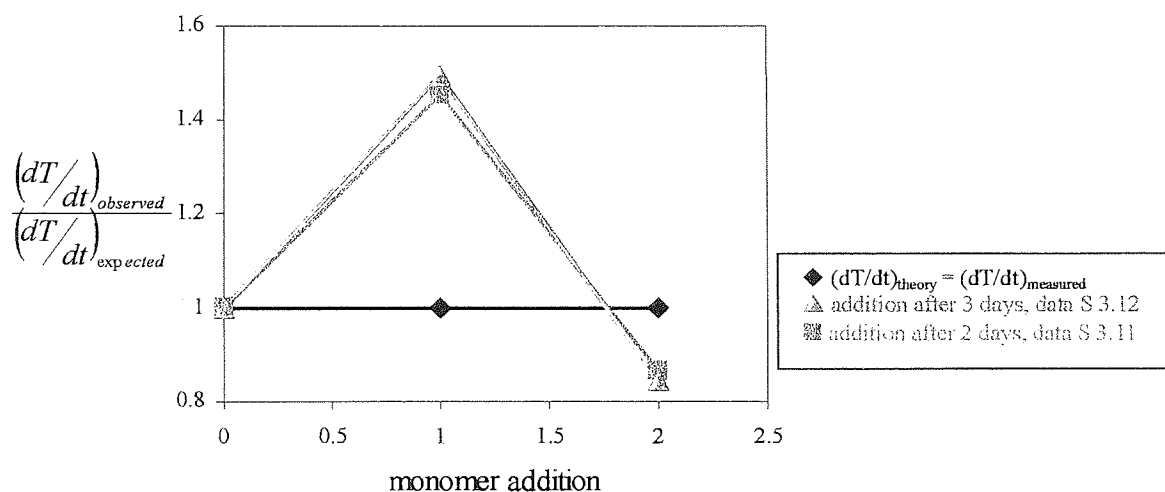


Figure 3. 18: Rate of the polymerisation after monomer addition.

	Before monomer addition					After monomer addition					SEC analysis						
Entry	[I] ₀ mol/l	[Ox] ₀ mol/l	(dT/dt) measured °C.s ⁻¹	conv. %	time t _k	time t _{add}	[Cat] ₀ mol/l	[Ox] ₀ mol/l	(dT/dt) expected °C.s ⁻¹	(dT/dt) measured °C.s ⁻¹	conv. %	Mn (theory) g/mol	Mn (SEC) g/mol	Mp g/mol			
S 3.10.1	0.0044	1	0.205	89	2 h										11,030	7,000	10,000
S 3.10.2	0.0044	1	0.208	-	-	Before monomer addition					79	22,800	9,460	11,500			
						2 h	0.0036	0.94	0.157	0.228							
S 3.103	0.0043	1	0.197	-	-	Before monomer addition					-	33,840	10,450	18,600			
						2 h	0.0035	0.94	0.152	0.225							
						After monomer addition											
S 3.11.1	0.0044	1	0.205	97	3 days	30 min	0.003	0.9	0.184	0.149	64	12,020	4,200	8,000			
						Before monomer addition					85	23,210	5,890	6,380			
S 3.11.2	0.0043	1	0.197	-	-	3 days	0.0036	0.91	0.147	0.225							
S 3.11.3	0.0043	1	0.2	-	-	Before monomer addition					15,100	6,380	32,930				
						Before monomer addition											
						3 days	0.0036	0.91	0.148	0.221							
						After monomer addition											
						3 days	0.0031	0.89	0.186	0.147	58						

$$\left(\frac{dT}{dt}\right)_{\text{expected}j} = \frac{[BF_3MeOH]_{0,j}}{[BF_3MeOH]_{0,j-1}} \cdot \frac{[Ox]_{0,j}}{[Ox]_{0,j-1}} \cdot \left(\frac{dT}{dt}\right)_{\text{measured}j-1} \quad E: 3.52$$

$$\overline{Mn}_{theory,j} = \sum_{j=0}^i \left(\frac{[Ox]_{0,j}}{[I]_{0,j}} \cdot conv_j \right) \quad E: 3.53$$

Table 3. 3: Effect of the monomer addition on the rate of polymerisation.

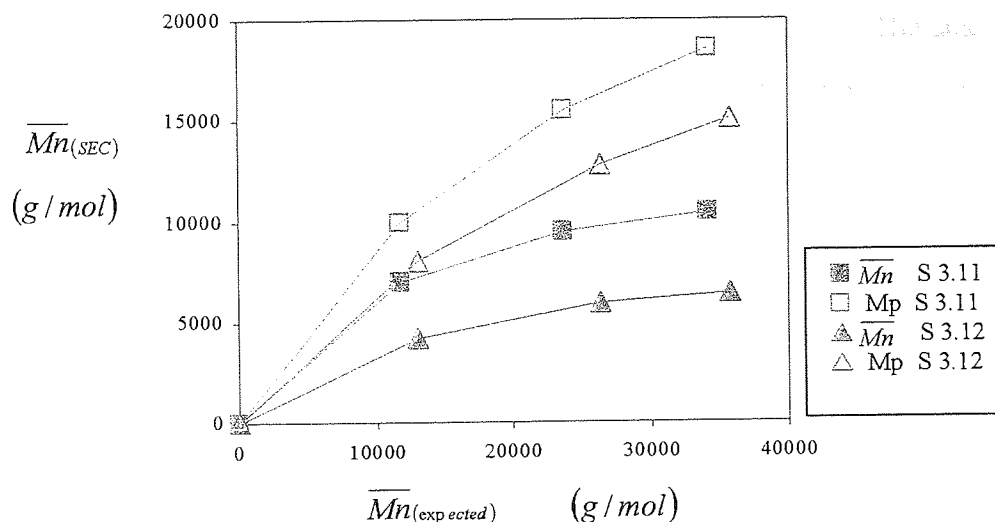


Figure 3. 19: Dependence \overline{Mn} , \overline{Mp} after monomer addition.

In the experiment S 3.10.3 and S 3.11.3 (table 3.3), the second monomer solution was added 30 minutes after the first monomer addition. The calorimetric analysis showed that a second monomer addition would restart the polymerisation with a rate of polymerisation independent of the time of the first monomer addition. These data are an even stronger indication that terminations reactions do not seem to occur significantly during the polymerisation process. The decrease of the rate of monomer consumption is slightly smaller than the expected rate of polymerisation considering the dilution factor (equation E: 3.52). This could be ascribed to the enhancement of transfer reactions due to the initial presence of polymeric materials (polymer chain and cyclic oligomers) when the polymerisation restart. In the figure 3.19, the non linear increases \overline{Mn} after monomer additions suggests that transfer reactions do not destroy the growing centres but induce redistributions of the molecular weight distribution of the growing polymer chains. The apparent increase of the oligomers peak is certainly due to an enhancement of transfer reactions (annex 3.14).

The gel permeation chromatographic studies revealed that during the storage of the polymer materials, chain breaking reactions occurs if the acidity of the inactive polymer solution is not neutralised (annex 3.23). Because of this, a large excess of ethanol was employed to terminate the polymerisation, the inactive polymer solution was washed twice with a 10% NaOH solution and then, washed again twice, with distilled water to remove the salts (see section 2.8.1.2). Consequently, if annihilation of growing centre by anion splitting occurs during the polymerisation process, the resulting polyoxetane materials, $\text{CH}_3\text{-COO-Pn}$, might

be hydrolysed and the $\text{CH}_3\text{-COO}^-\text{Na}^+$ extracted by distilled water. This could explain the absence of signal relative to $\text{CH}_3\text{-COO-P}_n$ by ^1H and ^{13}C NMR analysis. The analysis of the polymer materials by ^{19}F NMR showed that the polyoxetane do not contain fluorine.

3.1.4 Characterisation of cyclic oligomers

Since the early work carried out by Rose in 1954 on the cationic ring opening polymerisation of oxetane and oxetane derivatives^[115], the formation of cyclic oligomers was intensively study by several research groups^[182,198-200]. Dreyfuss et al., Goethals et al. among others, found that oxetane formed not only cyclic tetramers but also cyclic trimer and cyclic pentamers^[182,198-200,209,279]. In early 1970, Buckcoyed et al. reported that cyclic oligomers up to nonamer and possibly higher could be formed during the polymerisation process^[198-200]. In all reports, cyclic tetramer was found to be most abundant.

In the light of these results, it seemed therefore interesting to characterise the nature of the produced cyclic oligomers. For this, 1 M of a solution of oxetane in dichloromethane was polymerised at 35°C using $0.0065 \pm 0.005\text{M}$ of $\text{BF}_3(\text{CH}_3\text{COOH})_2$, $0.0065 \pm 0.005\text{M}$ of BF_3OEt_2 . After complete monomer consumption, the polymerisation was terminated by addition of ethanol and the polymerisation solution was treated as described in the section 2.8.1.2. The isolated semi crystalline polymeric material was then treated by cyclohexane that was found to extract the low molecular weight materials (see annex 3:15). The extracted materials was analysed by MS spectrometer, GLC analysis and ^1H and ^{13}C NMR spectroscopy. The polymer residue as well as the non treated polyoxetane materials were analysed by S.E.C and ^1H and ^{13}C NMR analysis.

3.1.4.1 GLC and mass spectroscopy analysis

Gas liquid chromatographic analysis of the extracted materials was performed using a Varian Aerograph 1200 apparatus equipped with a 3 m column packed with OV-1 (2%) on Gaschrom Q, temperature programmed from 60 to 280 °C at 8 °C/min. The peak areas were determined with a Varian CDS-101 integrator. The structure of the low molecular materials contained in the extracted materials was analysed by a chemical ionisation mass spectrograph. The mass spectrum shown in the annex 3.17, revealed that extracted oligomeric materials are exclusively cyclic oligomers. By coupling the GLC (annex 3.16) and MS data, it was found that cyclic oligomers from tetramer up to cyclic oligomers containing 15

oxetane units were formed in decreasing concentration, cyclic tetramers being the most abundant (98%). In 1965, Bucquoye et al.^[182] reported that cyclic oligomers higher than nonamers could not be observed by GLC probably because of the limitations of the techniques. It appears therefore that for the large cyclic oligomers, the signal observed by GLC might correspond to side compounds, knowing that in the injector the cyclic oligomers can be decomposed at 300 °C. Analysis of polyoxetane materials by TGA showed that the degradation starts at 300°C (annex 3.18). Gas Liquid Chromatography coupled to mass spectroscopy or MALDI TOF spectroscopy or HPLC chromatography could be a more accurate technique to identify and to determine the concentration of each cyclic oligomer.

3.1.4.2 ¹H and ¹³C NMR analysis

The non treated polyoxetane materials, cyclic oligomers and polymer residues were analysed using 350 MHz NMR spectroscopy. The ¹H and ¹³C NMR spectroscopy are represented in the annex 3.19 and 3.20, respectively. Examination of these spectrums revealed that corresponding ¹H and ¹³C signals of cyclic oligomers and linear polymer do not have the same chemical shift. Table 3.4 summarise this study.

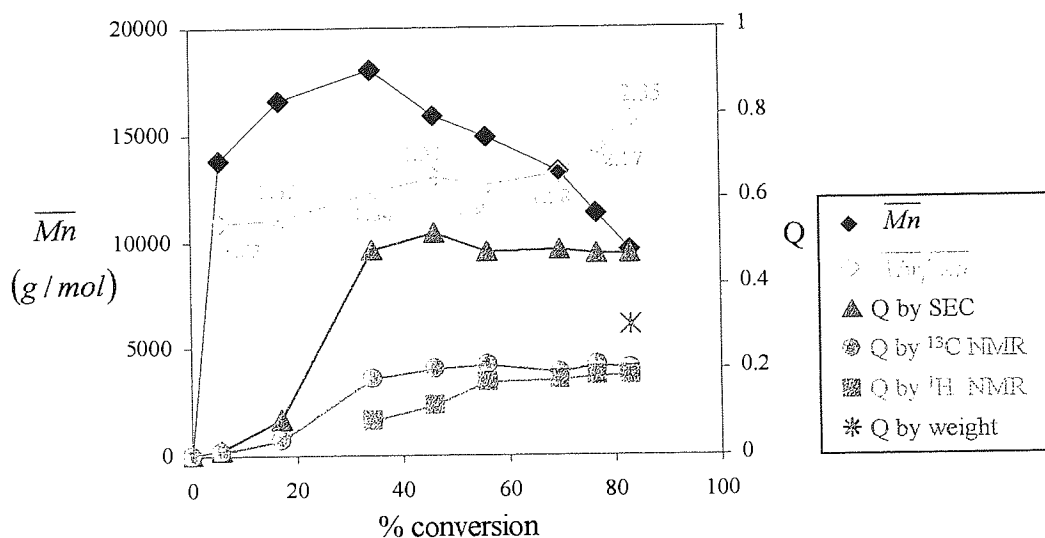
	Structure	¹ H* ppm	¹³ C* ppm
Oxetane	OCH ₂ CH ₂ CH ₂ O	t: 4.29; 4.27; 4.24	70.83
	OCH ₂ CH ₂ CH ₂ O	q: 2.31; 2.28; 2.26; 2.23; 2.10	21.12
Linear polymer chains	-OCH ₂ CH ₂ CH ₂ O-	t: 3.50; 3.48; 3.46	67.49
	-OCH ₂ CH ₂ CH ₂ O-	q: 1.866; 1.845; 1.823; 1.80; 1.782	29.76
Small cyclic oligomers (almost tetramer)	-OCH ₂ CH ₂ CH ₂ O-	t: 3.563; 3.545; 3.527	66.07
	-OCH ₂ CH ₂ CH ₂ O-	q: : 1.837; 1.819; 1.802; 1.783; 1.765	30.15
Large cyclic oligomers	-OCH ₂ CH ₂ CH ₂ O-	t: 3.50; 3.48; 3.46	67.49; 67.19; 67.09
	-OCH ₂ CH ₂ CH ₂ O-	q: 1.866; 1.845; 1.823; 1.80; 1.782	29.76

* CDCl₃ was used as solvent.

Table 3. 4: Comparison of ¹H and ¹³C chemical shifts for linear polymers and cyclic oligomers.

3.1.4.3 Rate of formation of cyclic oligomers

Although different methods were used to characterise and identify cyclic oligomers, none of them turned out to be an accurate method for the determination of the proportions of cyclic oligomers formed during the polymerisation process (see figure 3.20). Indeed, the SEC analysis showed that there is not a good separation between small cyclic oligomers peak and higher molecular weight materials (see annex 3.15). Moreover, the variation of $(dn/dc)_{c \rightarrow 0}$ as the molecular weight of the materials increases could be an additional problem when a refractometer is used as the detector. Peak overlapping was also encountered by ^1H NMR analysis when triplets corresponding to CH_2 in α position of the oxygen atom were integrated (see annex 3.19 and table 3.4). Only the ^{13}C NMR analysis gives well defined and well separated signals (see annex 3.20 and table 3.4) but unfortunately this technique is not a quantitative method for this purpose. This is illustrated in the figure 3.20 and 3.21 where the proportions of small cyclic oligomers ($Q = \text{Area (small cyclic oligomers)}/\text{Area (cyclic + linear polymer)}$) produce throughout the polymerisation was studied for two targeted degree of polymerisation (D_p), 200 and 105, respectively. In the both cases, it is interesting to note that when the process of polymerisation tend to produce as much cyclic oligomers than linear polymers, the \overline{Mn} of the high molecular weight materials decreases inducing a broadening of the molecular weight distributions. The decreases of \overline{Mn} is less significant when less cyclic oligomers are formed, that is for low degree of polymerisation (D_p). This study is summarised in the Table 3.5.



Series	[I] ₀ mol/l	[Ox] ₀ mol/l	time s	conv. %	\overline{Mn} g/mol	Mp	$\frac{\overline{Mw}}{\overline{Mn}}$	Q		
								¹ H NMR ^a $\delta(-OCH_2-)$	¹³ C NMR ^a $\delta(-OCH_2-)$	SEC ^b
			*							
S 3.12.1	0.005	1	19.2	5.63	13,800	25,600	1.63	Overlap	0.015	0.015
S 3.12.2	0.005	1	52.8	16.85	16,600	28,100	1.65	Overlap	0.05	0.085
S 3.12.3	0.005	1	120	34.3	18,000	30,120	1.84	Overlap	0.197	0.515
S 3.12.4	0.005	1	240	46.3	15,900	30,700	1.95	Overlap	0.21	0.52
S 3.12.5	0.005	1	440	56	14,900	28,400	1.9	0.17	0.205	0.477
S 3.12.6	0.005	1	660	69.7	13,280	28,400	1.98	0.176	0.19	0.48
S 3.12.7	0.005	1	880	76.8	11,320	26,700	2.17	0.185	0.21	0.47
S 3.12.8	0.005	1	2,200	82.9	9,620	24,800	2.35	0.18	0.2	0.44
S 3.13.1	0.0065	0.68	12	8.14	4540	5185	1.44			0.117
S 3.13.2	0.0065	0.68	23.4	16.81	5000	6220	1.59			0.157
S 3.13.3	0.0065	0.68	31.8	24.0	4730	5190	1.6			0.132
S 3.13.4	0.0065	0.68	48.6	36.25	5360	5900	1.61			0.167
S 3.13.5	0.0065	0.68	60.0	43.13	5610	6880	1.64			0.221
S 3.13.6	0.0065	0.68	90.0	56.33	5890	7630	1.72			0.271
S 3.13.7	0.0065	0.68	138	67.83	5740	7300	1.87			0.227
S 3.13.8	0.0065	0.68	153	69.05	6250	7340	1.98			0.255
S 3.13.9	0.0065	0.68	192	73.96	5840	8630	1.9			0.297
S 3.13.10	0.0065	0.68	227	78	5940	7620	1.97			0.25
S 3.13.11	0.0065	0.68	540	91.2	5620	7200	1.95			4.21

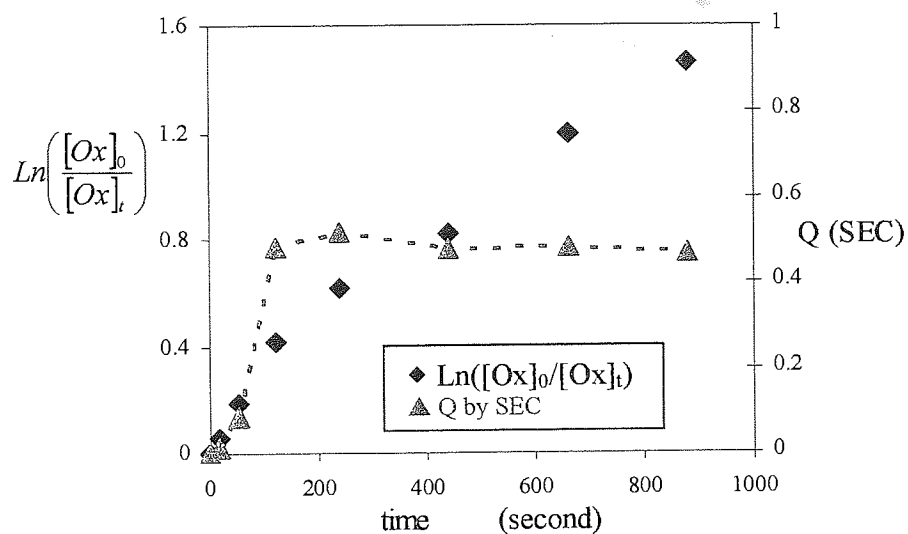
^a Q = Area($\delta(-OCH_2-)$ from cyclic material)/Area($\delta(-OCH_2-)$ from cyclic and linear materials)

^b Q = Area(cyclic oligomer peak)/Area(cyclic oligomers + linear polymer)

^c Q = weight(extracted materials)/{weight(extracted materials + residual material)}.

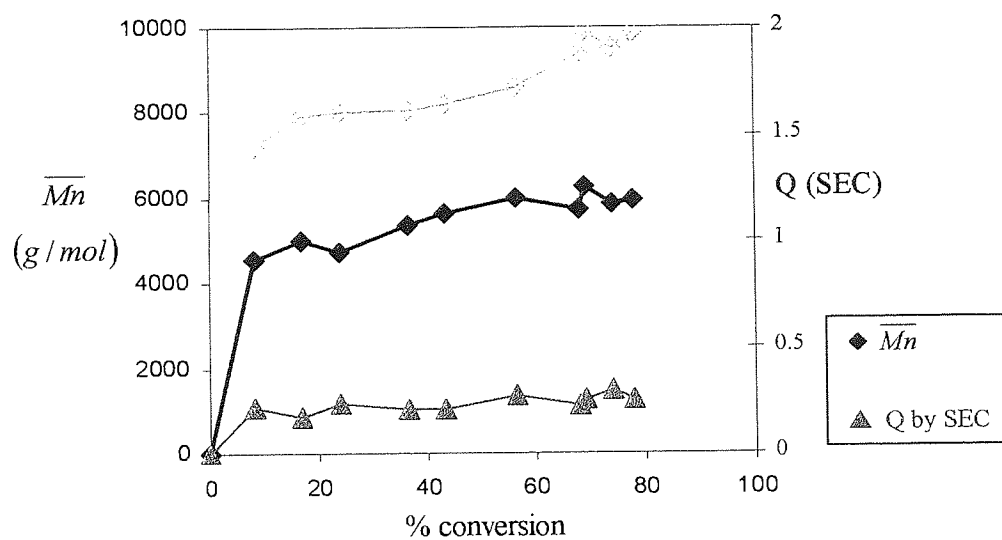
[I]₀ = [BF₃OEt₂]₀ = [BF₃(AcOH)₂]₀

Table 3. 5: Proportions of cyclic oligomers produce through the polymerisation process for Dp = 105 (Series S 3.13) and Dp = 200 (Serie S 3.12).



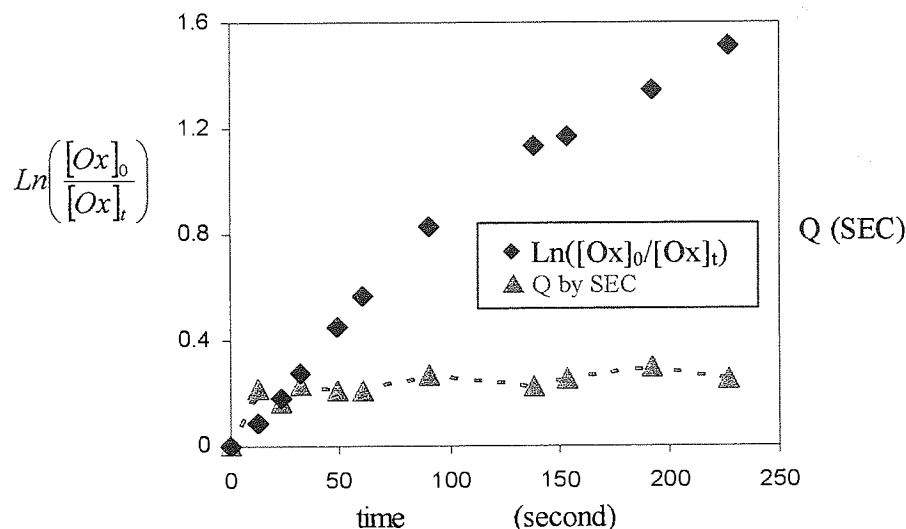
$D_p = 200$. [Oxetane] = 1 M and $[BF_3OEt_2] = [BF_3(AcOH)_2] = 0.005$ M.

Figure 3. 21: Proportions of cyclic oligomers produce through the polymerisation process.



$D_p = 105$. [Oxetane] = 0.68 M and $[BF_3OEt_2] = [BF_3(AcOH)_2] = 0.0065$ M.

Figure 3. 22: Proportions of cyclic oligomers produce through the polymerisation process.



$D_p = 105$. [Oxetane] = 0.68 M and $[\text{BF}_3\text{OEt}_2] = [\text{BF}_3(\text{AcOH})_2] = 0.0065$ M.

Figure 3. 23: Proportions of cyclic oligomers produce throughout the polymerisation process.

3.1.5 Nature of the initiating species involved in the initiation process

In 1954, when Rose^[115] investigated the mechanism of polymerisation of oxetane catalysed by BF_3 with H_2O or EtOH as co-catalyst, it was reported that as soon as the monomer are protonated, the formed secondary oxonium are converted into tertiary oxonium ions faster than secondary oxonium ions are formed. This was ascribed to the high strain contained in the ring of the secondary oxonium ions. Because the reactants were simultaneously added to the monomer solution, the rate of initiation was postulated to be kinetically controlled by the rate at which boron trifluoride oxetane complex reacts with H_2O .

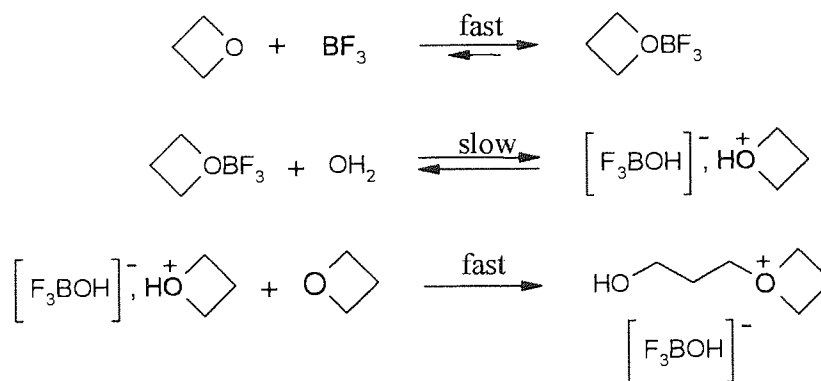


Figure 3. 24: Mechanism of initiation of oxetane catalysed by BF_3 with H_2O .

Because the concentration of catalyst and co-catalyst are low, the rate of initiation was considered to be slow and not dependent on the monomer concentration.

$$R_i = k_i \cdot [BF_3Ox] \cdot [OH_2]$$

E: 3.8

Our kinetic investigations on the cationic polymerisation of oxetane initiated by a mixture of $BF_3(AcOH)_2$ and BF_3OEt_2 , showed that at constant catalyst concentration and various concentration of oxetane, the initial apparent rate constant of monomer consumption, $(k_{p,app})_{max}$, depends on the concentration of oxetane. Because transfer reactions do not occur significantly during the initiation process, this phenomenon was ascribed to a slow initiation process, which is believed to be kinetically controlled by the rate at which the initiating species react with the monomer. In all experiments, the rate constant of the monomer consumption was found to be a maximum between 10 and 25% monomer conversion, indicating that the concentration of growing centres increases with the growth of polymer chains. When the rate of monomer consumption was measured at various concentration of catalyst (section 3.1.2), the analysis of the kinetic data showed that BF_3OEt_2 acts more likely as co-catalyst in presence of $BF_3(AcOH)_2$ than as catalyst of the initiation process. This suggests that during the preparation of the initiating system solution in dichloromethane (see section 2.7.7.1.1.2), the addition of boron trifluoride diethyl ether complex on boron trifluoride acetic acid complex could evolve the following chemical reactions.

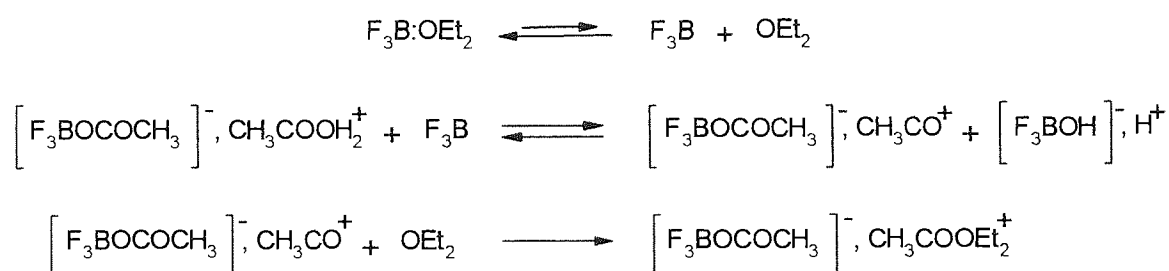
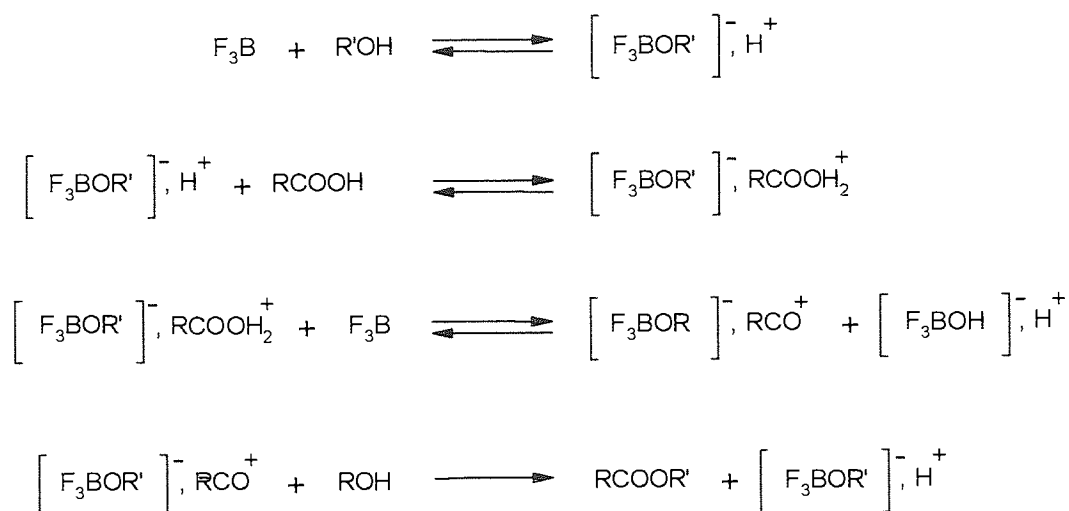


Figure 3. 25: Nature of initiating species formed in dichloromethane in presence of $BF_3(AcOH)_2$ and BF_3OEt_2 .

Because dichloromethane is not a complexing solvent, boron trifluoride exists mostly in the form of boron trifluoride diethyl ether complex. However, as shown in the above figure, $\{CH_3COOH_2^+\}$ can be dehydrated by BF_3 , forming boron trifluoride monohydrate complex, $H^+, [F_3BOH]^-$ and an acylium ion complex $\{CH_3CO^+\}$. The highly reactive acylium ion then react with a molecule of etherate, which is the only nucleophilic reagent in solution, to form

the more stable alkylating agent, $[F_3BOCOCH_3]^-, CH_3COOEt_2^+$. A similar mechanism has been proposed for the esterification of carboxylic acids catalysed by BF_3 (figure 3.26), in which ROH is the nucleophilic reagent^[288,289].



Reference 288.

Figure 3. 26: Mechanism of esterification of carboxylic acid catalysed by BF_3 .

In the figure 3.26, because the two first steps of the reaction are reversible, $[F_3BOCOCH_3]^-, [CH_3COOH_2]^+$ cannot be quantitatively converted into $[F_3BOCOCH_3]^-, [CH_3COOEt_2]^+$ and $[F_3BOH]^-, H^+$ in the presence of F_3BOEt_2 . Under such conditions, the system undoubtedly reaches a state of equilibrium in which the concentration of each initiating species does not vary. At equilibrium, the reaction can be represented by the following equation:



Figure 3. 27: State of equilibrium between initiating species in dichloromethane.

where the concentration of F_3BOEt_2 , $[F_3BOCOCH_3]^-, [CH_3COOEt_2]^+$, $[F_3BOH]^-, H^+$ and $[F_3BOCOCH_3]^-, [CH_3COOH_2]^+$ are determined by the "equilibrium constant" K.

The existence of the above pseudo equilibrium (figure 3.27) is in agreement with kinetic data. The enhancement of the initial rate of monomer consumption (see figure 3.9) in presence of an excess of BF_3OEt_2 suggest that initiating species issue of the chemical reaction between

$[\text{F}_3\text{BOCOCH}_3]^-, \text{CH}_3\text{COOH}_2^+$ and BF_3OEt_2 are more reactive towards the monomer than $[\text{F}_3\text{BOCOCH}_3]^-, \text{CH}_3\text{COOH}_2^+$. Indeed, the 1:2 complex with H_2O , ROH or RCOOH is always more stable than the corresponding 1:1 complex^[289] indicating that $[\text{BF}_3\text{OH}]^-, \text{H}^+$ is presumably more reactive than $[\text{F}_3\text{BOCOCH}_3]^-, [\text{CH}_3\text{COOH}_2]^+$. Moreover, the alkylating complex reagent is also more reactive toward the monomer than the protonating complex reagent. Besides, the quasi identical rate of polymerisation when the polymerisation of oxetane is initiated by $\text{BF}_3(\text{AcOH})_2/\text{BF}_3\text{OEt}_2$ (1/1) or with an excess $\text{BF}_3(\text{AcOH})_2$ (see figure 3.10) suggests that the reaction of $\text{BF}_3(\text{AcOH})_2$ with BF_3OEt_2 involves an equilibrium between the initiating species which favour the reactant ($K \ll 1$). This is in agreement with the fact that BF_3OEt_2 and $\text{BF}_3(\text{AcOH})_2$ are very stable complex. The stability of the initiating solution (at least 7 days at room temperature) is an even stronger indication that the initiating species are in equilibrium and that the equilibrium favours the more stable initiating species form.

It must be noted that the pseudo equilibrium described in the figure 3.27 exist only in the absence of other nucleophilic reagents than diethyl ether. When the initiating solution is added to the monomer solution, the high nucleophilicity of oxetane disrupt the equilibrium by converting the (1:1) boron trifluoride diethyl ether complex into (1:1) boron trifluoride oxetane complex.



Figure 3. 28: Formation of boron trifluoride oxetane complex.

The direct consequence of this is that during the initiation process, the three initiating species initiate the polymerisation without being affected by any equilibrium that might balance their concentrations considering their different reactivity towards the monomer ($k_{i2} > k_{i3} > k_{i1}$). Therefore, the mode of initiation can be visualised as shown in the figure 3.29:

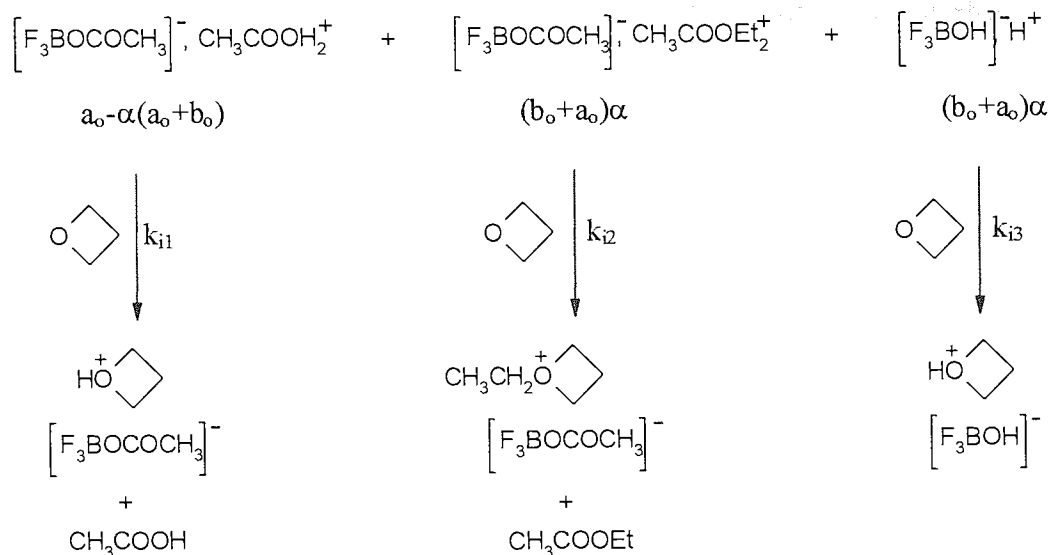


Figure 3. 29: Mechanism of initiation after addition of the initiating system solution into monomer solution.

where a_o and b_o represent the initial concentration of $\text{BF}_3(\text{AcOH})_2$ and BF_3OEt_2 , ($a_o - c_{eq}$) the concentration of $\text{BF}_3(\text{AcOH})_2$ at the equilibrium with $\alpha = c_{eq}/(a_o + b_o) \ll 1$, and k_{i1} , k_{i2} , k_{i3} the constant rate of reaction of oxetane with $[\text{F}_3\text{BOCOCH}_3]^{-}, \text{CH}_3\text{COOH}_2^{+}$, $[\text{F}_3\text{BOCOCH}_3]^{-}, \text{CH}_3\text{COOEt}_2^{+}$ and $[\text{F}_3\text{BOH}]^{-}, \text{H}^{+}$, respectively. Because oxonium salts and protonating complex reagents are highly reactive towards nucleophilic reagents, in the presence of high concentrations of oxetane, the rate at which each initiating species react with a molecule of monomer can be assumed to be fast and efficient in high yield. Therefore, the rate of initiation can be written as follow:

$$R_i = -\frac{d[\text{BF}_3(\text{AcOH})_2]}{dt} - \frac{d[[\text{BF}_3\text{OAc}], \text{AcOH}_2^{+}]}{dt} - \frac{d[[\text{BF}_3\text{OH}], \text{H}^{+}]}{dt} \quad \text{E: 3.9,}$$

$$R_i = (k_{i1} \cdot [\text{BF}_3(\text{AcOH})_2] + k_{i2} \cdot [[\text{BF}_3\text{OAc}], \text{AcOH}_2^{+}] + k_{i3} \cdot [[\text{BF}_3\text{OH}], \text{H}^{+}]) \cdot [\text{M}] \quad \text{E: 3.10}$$

and

$$R_i = (k_{i1} \cdot (a_o - \alpha \cdot (a_o + b_o)) + \alpha \cdot (k_{i2} + k_{i3}) \cdot (a_o + b_o)) \cdot [\text{M}]_o \quad \text{E: 3.11}$$

with

$$k_{i2} > k_{i3} > k_{i1} \quad \text{E: 3.12.}$$

The initial concentration of $[\text{F}_3\text{BOCOCH}_3]^-$, $[\text{CH}_3\text{COOH}_2]^+$, $[\text{F}_3\text{BOCOCH}_3]^-$, $[\text{CH}_3\text{COOEt}_2]^+$ and $[\text{BF}_3\text{OH}]^-$, H^+ , being respectively equal to $a_0 - c_{\text{eq}}$, c_{eq} and c_{eq} , with $\alpha = c_{\text{eq}}/(a_0 + b_0)$.

It is interesting to note that during the initiation process, AcOH is formed, which can act as co-catalyst. As shown in the figure 3.30, a molecule of 1:1 boron trifluoride ether complex can react with a molecule of acetic acid to produce a secondary oxonium ion based on oxetane or on the polymeric material depending on the nature of the complexing agent. Because of the low concentration of the reactants, this could lead to slow late initiation that could be responsible of the enhancement of the rate of polymerisation observed after the first monomer addition (see section 3.1.3)

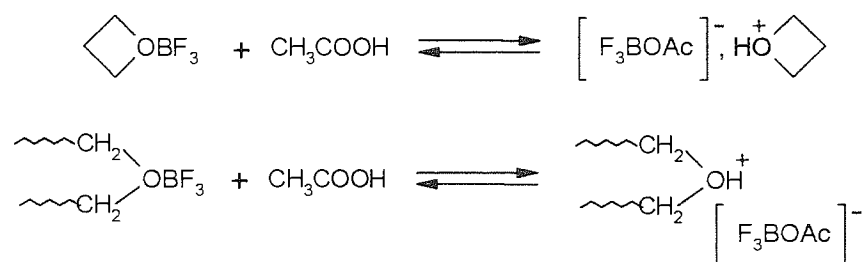


Figure 3. 30: Mode of formation of 1:1 boron trifluoride acetic acid complex during the polymerisation process.

In addition to the slow initiation, the formation of AcOH, AcOEt and OEt₂ can also act as transfer agents. As shown in the figure 3.31, the termination of the growing centre by AcOH or AcOEt will regenerate a new growing species, a secondary and tertiary oxonium ions, depending on the nature of the transfer agent. If these reactions are kinetically unfavourable at high concentrations of oxetane because of the high reactivity of the monomer towards the growing centre, these reactions could then happen at high conversion (low monomer concentration) when most of the polymer chains are in the formed of non strained tertiary oxonium ions.

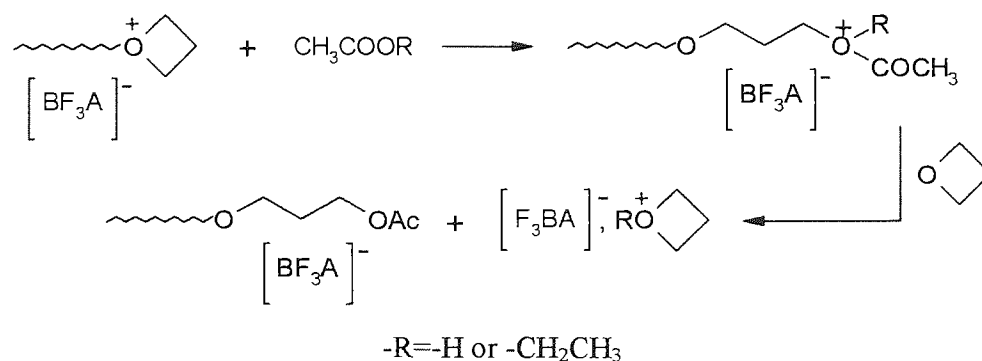


Figure 3. 31: Mechanism of transfer reaction to the co-catalyst.

3.1.5.1 Dependence between rate of initiation and rate of propagation

In view of these observations, it appears that, if BF_3OEt_2 acts as co-catalyst of $\text{BF}_3(\text{AcOH})_2$, the total concentration of initiating species $(a_0 + \alpha \cdot (a_0 + b_0))$ initially introduced in the monomer solution must be thermodynamically controlled by the constant K . Therefore, if the mode of initiation showed in the figure 3.29 is quantitative when the polymerisation reaches the maximum rate of monomer consumption, at constant concentration of oxetane, the rate of initiation and the rate of polymerisation should exhibit the same dependence with the change of concentration of the catalyst and co-catalyst.

3.1.5.1.1 Using (1:1) $\text{BF}_3\text{OEt}_2/\text{BF}_3(\text{AcOH})_2$ as initiating system

When an equimolar solution of BF_3OEt_2 and $\text{BF}_3(\text{AcOH})_2$ is prepared in dichloromethane, at the equilibrium (figure 3.32), the concentration of each active species are determined by the equilibrium constant K :

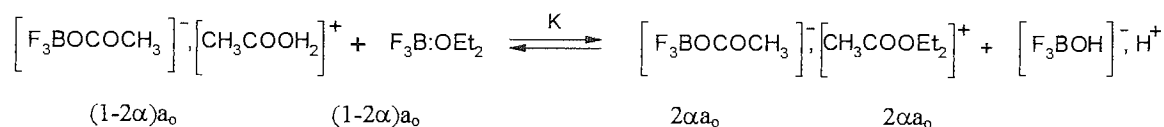


Figure 3. 32: Concentration of initiating species when an equimolar solution of BF_3OEt_2 and $\text{BF}_3(\text{AcOH})_2$ is prepared in dichloromethane

where (a_0) represent the initial concentration of $\text{BF}_3(\text{AcOH})_2$ and BF_3OEt_2 , and $(a_0 - a_t)$ and $(1 - 2\alpha)$ the concentration and the mol fraction of $\text{BF}_3(\text{AcOH})_2$ at the equilibrium with $\alpha = a_t/2a_0$.

3.1.5.1.1.1 Rate of initiation

After addition of a given amount of initiating solution (1 ml) on monomer solution (21 ml), the initial rate of initiation can be written as follow:

$$R_i = (k_{i1} \cdot (1 - 2\alpha) + 2 \cdot (k_{i2} + k_{i3}) \cdot \alpha) \cdot a_0 \cdot [\text{Ox}]_0 \quad \text{E: 3.13.}$$

Knowing that

$$a_0 = [\text{Cat}] = [\text{BF}_3(\text{AcOH})_2]_0 = [\text{BF}_3\text{OEt}_2]_0 \quad \text{E: 3.14,}$$

and that

$$\alpha = \frac{\sqrt{K}}{2 \cdot (\sqrt{K} + 1)} \quad \text{E: 3.15,}$$

with

$$K = \frac{[BF_3OAc]^-, AcOEt_2^+ \times [BF_3OH]^-, H^+]}{[BF_3OAc]^-, AcOH_2^+ \times [BF_3OEt_2]} = \left(\frac{2\alpha}{(1-2\alpha)} \right)^2 \quad \text{E:}$$

3.16,

the initial rate of initiation is then equal to:

$$R_i = \left(k_{i1} + \frac{\sqrt{K}}{\sqrt{K} + 1} \cdot (k_{i2} + k_{i3} - k_{i1}) \right) \cdot [BF_3(AcOH)_2]_0 \cdot [Ox]_0 \quad \text{E: 3.17.}$$

3.1.5.1.1.2 Rate of propagation

Assuming that the initiation shown in the figures 3.29 and 3.32 is quantitative when the polymerisation reaches the maximum rate of monomer consumption, the concentration of growing centres can be written as follow:

$$[R^+, X^-] = (1 + 2\alpha) \cdot a_0 \quad \text{E: 3.18.}$$

By combining the equations E: 3.15 and E: 3.18, the above equation becomes:

$$[R^+, X^-] = \left(\frac{2\sqrt{K} + 1}{\sqrt{K} + 1} \right) \cdot a_0 \quad \text{E: 3.19.}$$

If k_p is the rate constant of propagation when the growing center are mostly in the form of strain growing oxonium ions, the rate of propagation is equal to:

$$\left(-\frac{d[Ox]}{dt} \right)_{\max} = k_p \cdot \left(\frac{2\sqrt{K} + 1}{\sqrt{K} + 1} \right) \cdot [I]_0 \cdot [Ox]_0 \quad \text{E: 3.20}$$

with

$$[I]_0 = [BF_3(AcOH)_2]_0 = [BF_3OEt_2]_0$$

3.21.

3.1.5.1.1.3 Discussion

From the equation E: 3.17, it appears that the rate of initiations depends only on the initial concentration of monomer and on the initial concentration of catalyst. Moreover, the number fraction of each initiating species does not seem to be affected by the initial concentration of the reactants (see Equation E: 3.15). In the Figure 3.33., the linear dependence of $(R_p)_{\max}/[Ox]_0$ on the $[BF_3(AcOH)_2]$ (Δ), with $[BF_3(AcOH)_2]=[BF_3OEt_2]$, intersects the (X) axis close to the origin.

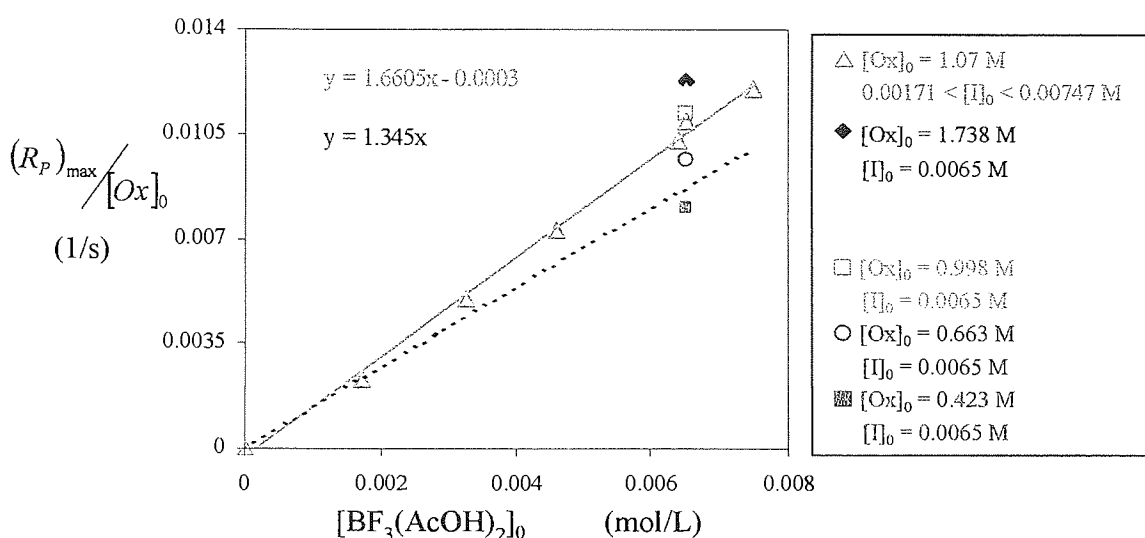


Figure 3. 33: Dependence $(R_p)_{\max}/[M]_0$ against $[I]_0 = [BF_3(AcOH)_2]_0 = [BF_3OEt_2]_0$

This similarity of the evolution of the apparent rate of initiation with the change of the initial catalyst concentration strongly indicates that at the same initial concentration of oxetane (1.07 M), the concentration of growing centre (R^+) increase linearly with the concentration of catalyst (a_0). This is in agreement with the equation E: 3.19. In the figure 3.33, the slightly deflection from the slope (---) strongly indicates that an increase of (a_0) slightly increases the mole fraction of catalyst converted into growing centre. Because the increase of the catalyst concentration increases the probability of the occurring intermolecular transfer reactions, this phenomenon can only be explained by the increase of the rate at which the boron trifluoride oxetane complex reacts with the produced acetic acid (see figure 3.29) and/or by an increase

of the mole fraction of initiating species converted into growing centre. Because the increase of concentration of $\text{BF}_3(\text{AcOH})_2$ (with $[\text{BF}_3(\text{AcOH})_2] = [\text{BF}_3\text{OEt}_2]$) does not increase significantly the fraction of initiating species converted into growing centres when the polymerisation occurs at constant concentration of oxetane, the gradient of the slope (x) gives the rate constant of propagation of strained oxonium ions, k_p , factor of the average mole fraction of catalyst converted into growing centre, $\langle f \rangle$.

$$k_p \cdot \langle f \rangle = 1.72 \text{ l.mol}^{-1} \cdot \text{s}^{-1}$$

with

$$\langle f \rangle = \frac{[R^+]}{2 \cdot [I]_0}$$

Similar behaviour was also observed when the polymerisation was carried out at various concentrations of oxetane and constant concentration of catalyst, $[I]_0 = 0.0065 \text{ M}$. As shown in the figure 3.33, the increase of concentration of oxetane from 0.42 M to 1.78 M leads to an increase in $(k_{p,app})_{\max}$ from 0.008 M to 0.0124 M at constant concentration of $[I]_0 = 0.0065 \text{ M}$.

This can be explained by an increase of the concentration of growing centres and therefore by an increase of the initiator efficiency (f), as the concentration of oxetane increases (see equation E: 3.13). However as the concentration of oxetane is higher 1.41 M, the apparent rate constant of propagation does not seem to increase significantly with the increase of $[\text{Ox}]_0$, indicating that the mode of initiation showed in the figure 3.29 tends to be quantitative as concentration of oxetane is higher than 1.41 M. This strongly indicates that the rate of initiation is kinetically controlled by the rate at which the initiating species react with oxetane. It must be noted that the rate at which the boron trifluoride oxetane complex would react with a molecule of acetic acid does not depend on the concentration of oxetane.

3.1.5.1.2 Polymerisation using an excess of BF_3OEt_2 at constant concentration of oxetane and $\text{BF}_3(\text{AcOH})_2$

3.1.5.1.2.1 Rate of initiation

When an excess of BF_3OEt_2 is used in relation to the concentration of $\text{BF}_3(\text{AcOH})_2$, at the equilibrium the concentration of each initiating species can be visualised as follow:

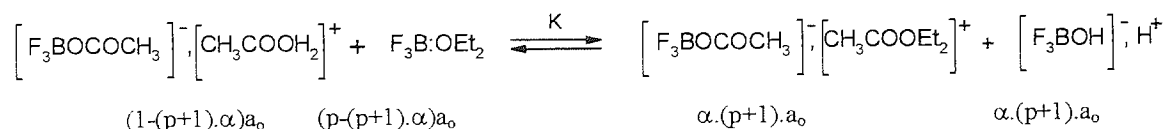


Figure 3. 34: Concentration of initiating species in dichloromethane when an excess of BF_3OEt_2 is used in relation to the concentration of $\text{BF}_3(\text{AcOH})_2$.

where a_o and $p \cdot a_o$ are respectively the concentration of $\text{BF}_3(\text{AcOH})_2$ and BF_3OEt_2 , a_t and $(1 - \alpha(p+1))$ are the concentration and the mole fraction of the remaining $\text{BF}_3(\text{AcOH})_2$ when the system reaches a state of equilibrium with $((1 - \alpha) = a_t / ((p+1)a_o))$. Under such conditions, the rate of initiation can be expressed as follow:

$$R_i = (k_{i1} \cdot (1 - (p+1) \cdot \alpha) + (k_{i2} + k_{i3}) \cdot (p+1) \cdot \alpha) \cdot a_o \cdot [\text{Ox}]_o \quad \text{E: 3.22.}$$

After rearrangement of the above equation, E: 3.18, the relation becomes:

$$R_i = (k_{i1} + (k_{i2} + k_{i3} - k_{i1}) \cdot (p+1) \cdot \alpha) \cdot a_o \cdot [\text{Ox}]_o \quad \text{E: 3.23.}$$

Knowing that

$$K = \frac{\alpha^2 \cdot (p+1)^2}{(1 - \alpha \cdot (p+1)) \cdot (p - \alpha \cdot (p+1))} \quad \text{E: 3.23,}$$

and assuming that $p \gg \alpha(p+1)$ at $p > 1$ since $\alpha \ll 1$, the above equations becomes:

$$K = \frac{\alpha^2 \cdot (p+1)^2}{(1 - \alpha \cdot (p+1)) \cdot p} \quad \text{E: 3.24}$$

after rearrangement the above equation becomes:

$$\alpha^2 \cdot (p+1)^2 + K \cdot p \cdot (p+1) \cdot \alpha - K \cdot p = 0 \quad \text{E: 3.25.}$$

Because $\alpha > 0$, the unique solution of the above equation is:

$$\alpha = \frac{K \cdot p}{2 \cdot (p+1)} \cdot \left(\sqrt{1 + \frac{4}{K \cdot p}} - 1 \right) \quad \text{E: 3.26.}$$

By combining the Equation E: 3.22 and E: 3.26, the initial rate of initiation can be represented by the following equation:

$$R_i = k_{i1} \cdot [BF_3(AcOH)_2]_0 \cdot [Ox]_0 + k_2 \cdot (k_{i2} + k_{i3} - k_{i3}) \cdot [BF_3OEt_2]_0 \cdot [Ox]_0 \quad \text{E: 3.27,}$$

with

$$k_2 = \frac{K}{2} \cdot \left(\sqrt{1 + \frac{4}{K} \cdot \frac{[BF_3(AcOH)_2]_0}{[BF_3OEt_2]_0}} - 1 \right) \quad \text{E: 3.28.}$$

3.1.5.1.2.2 Rate of propagation

Similarly, if the initiation shown in the figures 3.29 and 3.34 is quantitative when the polymerisation reaches the maximum rate of monomer consumption, the concentration of growing centre can be written as follow:

$$[R^+, X^-] = (1 + (p+1)\alpha) \cdot a_0 \quad \text{E: 3.29}$$

By combining the equation E: 3.29 and E: 3.26, the concentration of growing centres generated at $(R_p)_{\max}$ is equal to:

$$[R^+] = \left(1 + \frac{K \cdot p}{2} \cdot \left(\sqrt{1 + \frac{4}{K} \cdot \frac{[BF_3(AcOH)_2]_0}{[BF_3OEt_2]_0}} - 1 \right) \right) \cdot a_0 \quad \text{E: 3.30}$$

or

$$[R^+] = [BF_3OEt_2]_0 + \frac{K}{2} \cdot \left(\sqrt{1 + \frac{4}{K} \cdot \frac{[BF_3(AcOH)_2]_0}{[BF_3OEt_2]_0}} - 1 \right) \cdot [BF_3(AcOH)_2]_0 \quad \text{E: 3.31.}$$

Therefore, the rate of polymer consumption can be equal to:

$$\left(-\frac{d[Ox]}{dt} \right)_{\max} = k_p \cdot [BF_3(AcOH)_2]_0 \cdot [Ox]_0 + k_p \cdot k_2 \cdot [BF_3OEt_2]_0 \cdot [Ox]_0 \quad \text{E: 3.32.}$$

3.1.5.1.2.3 Discussion

From the equations, E: 3.27 and E: 3.28, it appears that at constant concentration of oxetane and $\text{BF}_3(\text{AcOH})_2$ and at $p > 1$, the initial rate of initiation does not exhibit a linear increase with the concentration of BF_3OEt_2 . This is due to the fact that k_2 (see equation E: 3.28) decreases as the concentration of BF_3OEt_2 increases. The similarity in the evolution of the apparent rate of propagation with the change of the initial concentration of BF_3OEt_2 (see figure 3.9), is an even stronger indication that BF_3OEt_2 acts more likely as a co-catalyst than as an initiating species. This is illustrated also by the form of the Equation E: 3.31. A linear increase of R_p with the increase of concentration of BF_3OEt_2 would indicate that BF_3OEt_2 act as catalyst.

3.1.5.1.3 Using an excess of $\text{BF}_3(\text{AcOH})_2$ at constant concentration of oxetane and BF_3OEt_2

3.1.5.1.3.1 Rate of initiation

When an excess of $\text{BF}_3(\text{AcOH})_2$ was used in relation to the concentration of BF_3OEt_2 , at the equilibrium, the concentration of each initiating species can be visualised as follow:

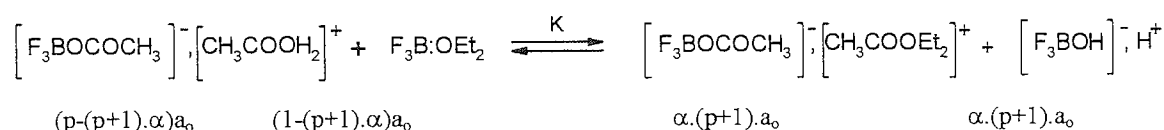


Figure 3. 35: Concentration of initiating species when an excess of $\text{BF}_3(\text{AcOH})_2$ was used in relation to the concentration of BF_3OEt_2 .

where a_0 and $p.a_0$ are respectively the concentrations of BF_3OEt_2 and $\text{BF}_3(\text{AcOH})_2$, α and $(1-\alpha(p+1))$ are the concentration and the mole fraction of the remaining $\text{BF}_3(\text{AcOH})_2$ when the system reach the state of equilibrium with $((1-\alpha) = a_0/((p+1)a_0))$. Under such conditions, the rate of initiation can be expressed as follow:

$$R_i = (k_{i1} \cdot p + (k_{i2} + k_{i3} - k_{i1}) \cdot (p+1) \cdot \alpha) \cdot a_0 \cdot [\text{Ox}]_0 \quad \text{E: 3.33}$$

with

$$K = \frac{\alpha^2 \cdot (p+1)^2}{(p - \alpha \cdot (p+1)) \cdot (1 - \alpha \cdot (p+1))} \quad \text{E: 3.34.}$$

Assuming that $p \gg \alpha(p+1)$ at $p > 1$, working out the above the equation E: 3.34 gives the equation E: 3.26. By combining the equations E: 3.26 and E: 3.33, the initial rate of initiation can be written as:

$$R_i = (k_{i1} + k_3 \cdot (k_{i2} + k_{i3} - k_{i1})) \cdot [BF_3(AcOH)_2]_0 \cdot [Ox]_0 \quad \text{E: 3.35,}$$

with

$$k_3 = \frac{K}{2} \left(\sqrt{1 + \frac{4}{K} \cdot \frac{[BF_3OEt_2]_0}{[BF_3(AcOH)_2]_0}} - 1 \right) \quad \text{E: 3.36.}$$

3.1.5.1.3.2 Rate of propagation

If the initiation show in the figures 3.29 and 3.35 is quantitative when the polymerisation reaches the maximum rate of monomer consumption, the concentration of growing centre can be written as follow:

$$[R^+, X^-] = (p + (p+1)\alpha) \cdot a_0 \quad \text{E: 3.37}$$

By combining the equations E: 3.18 and 3.26, the concentration of growing generated at $(R_{p,app})_{\max}$ is equal to:

$$[R^+] = \left(1 + \frac{K}{2} \cdot \left(\sqrt{1 + \frac{4}{K} \cdot \frac{[BF_3OEt_2]_0}{[BF_3(AcOH)_2]_0}} - 1 \right) \right) \cdot p \cdot a_0 \quad \text{E: 3.38}$$

or

$$[R^+] = \left(1 + \frac{K}{2} \cdot \left(\sqrt{1 + \frac{4}{K} \cdot \frac{[BF_3OEt_2]_0}{[BF_3(AcOH)_2]_0}} - 1 \right) \right) \cdot [BF_3(AcOH)_2]_0 \quad \text{E: 3.39.}$$

Therefore, the rate of polymer consumption can be equal to:

$$\left(-\frac{d[M]}{dt} \right)_{\max} = k_p \cdot (1 + k_3) \cdot [BF_3(AcOH)_2]_0 \cdot [Ox]_0 \quad \text{E: 3.40.}$$

3.1.5.1.3.3 Discussion

From the equations, E: 3.35 and E: 3.36, it appears that at constant concentration of oxetane and BF_3OEt_2 and at $p > 1$, the initial rate of initiation does not exhibit a linear increase with the concentration of $\text{BF}_3(\text{AcOH})_2$. This is due to the fact that k_3 (see equation E: 3.36) decreases as the concentration of $\text{BF}_3(\text{AcOH})_2$ increases. The dependence of evolution of the apparent rate of propagation (E: 3.40) with the change of the initial concentration of $\text{BF}_3(\text{AcOH})_2$, is an even stronger indication that BF_3OEt_2 acts more likely as co-catalyst than as an initiating species (see figure 3.10). This is also illustrated by the form of the equations E: 3.38 and E: 3.39.

3.2 Polymerisation initiated by oxacarbeniums salts

The cationic ring opening polymerisation of oxetane was carried out in dichloromethane at 35°C using $[\text{EtOCH}_2]^+[\text{MtX}_n]^-$ ($[\text{MtX}_n]^- = [\text{BF}_4]^-$ and $[\text{SbF}_6]^-$) as initiating species. The initiating solution was also prepared in dichloromethane as described in the section 3.2.2 using $\text{EtOCH}_2\text{Cl}/\text{AgMtX}_n$ in a molar ratio of 1/1.1. Because the oxacarbenium salts cannot be prepared with rigorous exclusion of moisture contamination, trace molecules of water ($\epsilon \ll 1$) can hydrolyse oxacarbenium salts and form protonating reagents (see figure 3.36) capable of initiating the polymerisation.

To prevent the formation of protonic initiator, 1 mol equivalent of 2,6-di-*t*-butyl-pyridine (DtBP)^[290] was added to an equimolar solution of $\text{EtOCH}_2\text{Cl}/\text{AgMtX}_n$ prepared in dry dichloromethane (see section 2.7.7.1.2). Because the nucleophilic site of the DtBP is sterically hindered by two *t*-butyl groups, this strong Brönstead base behaves as a very weak Lewis base. Consequently, molecules of DtBP are unreactive towards oxacarbenium salts and protonation of this strong Brönstead base forms a very stable ammonium salt incapable initiating the polymerisation even in a presence of highly nucleophilic monomers such as oxetane (see figure 3.37).

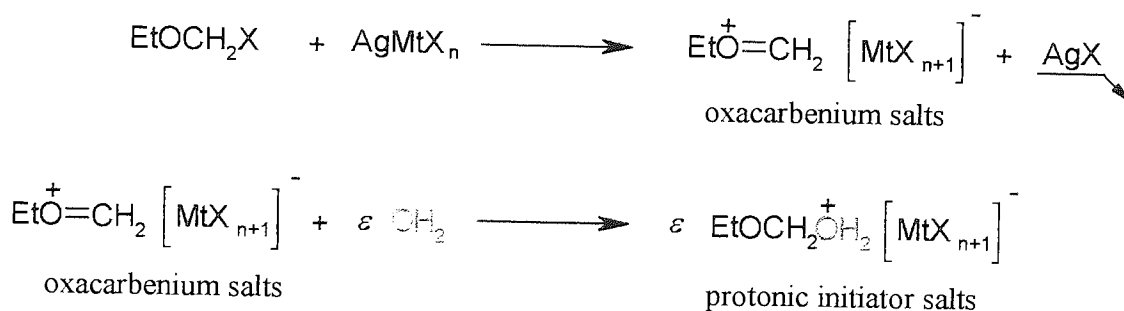


Figure 3. 36: Mechanism of hydrolysis of oxacarbenium salts and formation of protonic initiator salts.

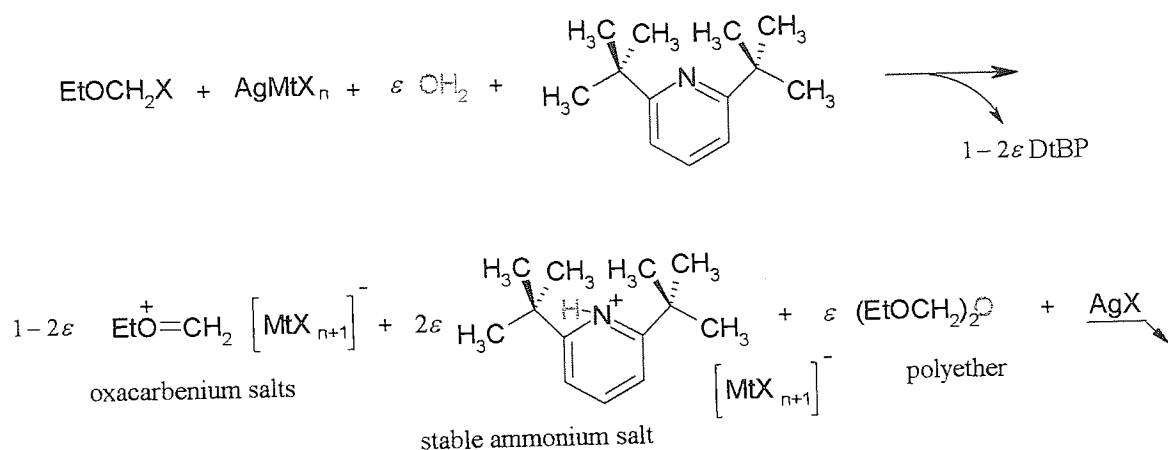


Figure 3. 37: Neutralisation of protonic initiator by 2,6-di-t-butyl-pyridine (DtBP).

However, it is interesting to note that the formation of $(\text{EtOCH}_2)_2\text{O}$ can eventually act as transfer reagent during the polymerisation process.

3.2.1 Effect of the time on the polymerisation

In the present work, we focussed our investigations only on the effect of the initiator and size of the counter-anion on the transfer reactions occurring. For this purpose, a solution of 1 M of oxetane in dichloromethane was polymerised at 35 °C using 0.003 M of $[\text{EtOCH}_2]^+[\text{MtX}_n]^-$ ($[\text{MtX}_n]^- = [\text{BF}_4]^-$ and $[\text{SbF}_6]^-$) as initiating system. The total volume of polymerisation solution was kept constant and equal to 25 ml. The polymerisation a reaction was followed by withdrawing active polymer samples using sampling technique as described in the section 2.8.3. The active polymer solutions were deactivated in a large excess volume of ethanol and the inactive polymer solution was treated as described in the section 2.8.1.2. The rate of polymerisation was monitored by gravimetric analysis and the resulting polymers were analysed SEC and NMR analysis. This study is summarised in the table 3.6, where S 3.14 and S 3.15 corresponds to the experiments carried out using respectively $[\text{BF}_4]^-$ and $[\text{SbF}_6]^-$ as counter ion.

In the section 3.1 (table 3.5 series S 3.12, figure 3.5 and annex 3.4) where 0.005 M of an equimolar solution of $\text{BF}_3(\text{ACOH})_2/\text{BF}_3\text{OEt}_2$ was used to polymerise 1 M solution of oxetane, it was found that as soon as a few percent of monomer was consumed (10 %), side reactions started to occur significantly to produce cyclic oligomers by intramolecular transfer reactions (figure 3.4). This involved a decrease of \overline{Mn} and a broadening of the molecular weight due to the intermolecular transfer reactions. Later, it was also found that the intramolecular transfer reactions are much more favoured than intermolecular transfer reactions as the concentration of protonic initiator decreases (table 3.5 series S 3.13, figure 3.6 and annex 3.5). In this present study, where the concentration of initiating species is lower (0.003 M), the SEC and NMR analysis revealed that oxacarbenium salts affect differently the occurring transfer reactions depending on the size of the counter ion. Indeed, when $[\text{EtOCH}_2]^+[\text{BF}_4]^-$ was used as initiator, the cyclic oligomers start to be form after 40 % of monomers was consumed (see figure 3.41 and annex 3.21). The enhancement of cyclic oligomers formation when protonic initiator was used (figure 3.41 and annex 3.4), is certainly due to the existence of hydroxyl tail groups that favour intramolecular transfer reactions by end-biting reactions. Indeed, if with compare the nucleophilicity of different components present in the solution during the polymerisation, it appears that the tail group, $\text{CH}_3\text{CH}_2\text{-O-}$, formed during the initiation by oxacarbenium salts is less nucleophilic than the oxygen atom in the oxetane, which in turn is both less nucleophilic than the hydroxyl tail group, -OH , when protonic reagents are used as initiator (figure 3.38).

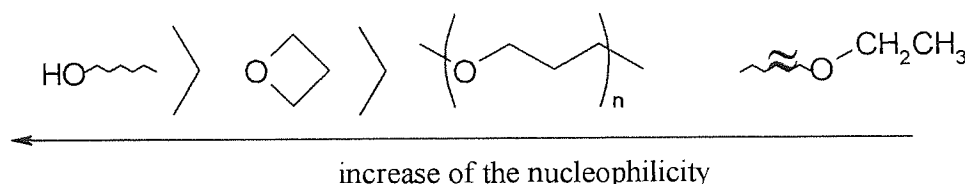


Figure 3. 38: Basicity of the different nucleophilic reagents when the polymerisation is initiated by protonic initiator or oxacarbenium salts.

Therefore, the low proportion of cyclic oligomers formed during the first 60 % of monomer conversion suggests that the process of back-biting reactions is slow in comparison to the process of propagation ($k_p > k_{tr,1}$). At conversion > 60 %, the decrease of monomer concentration increases the probability of transfer reactions (back-biting and intermolecular transfer reactions). This is believe to be responsible of the redistribution of the polymer chains length and therefore to decrease of \overline{Mn} . (see figure 3.40 and table 3.6 series 3.14). As the polymerisation proceeds, the enhancement of cyclic oligomers formation is certainly due

to the fact that the concentration of oxetane is too low to compete efficiently with transfer reactions. As depicted in the figure 3.39, it is likely that in starving monomer condition, oxetane ensure only the interconversion between strained (A2 and A3) and non-strained (A1) tertiary oxonium ions.

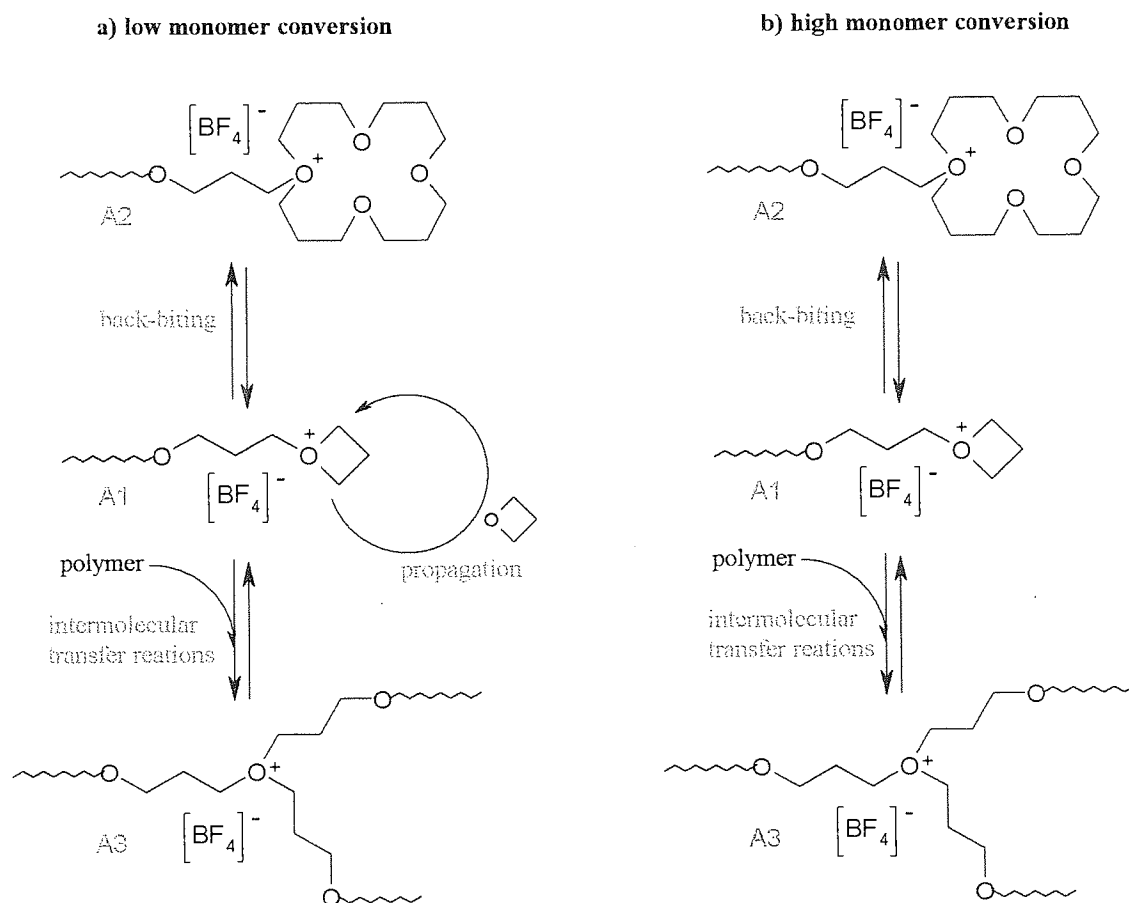


Figure 3. 39: Mechanism of polymerisation of oxetane in dichloromethane using $[\text{EtOCH}_2]^+[\text{BF}_4]^-$ as initiator at 35 °C.

In the case of $[\text{EtOCH}_2]^+[\text{SbF}_6]^-$, the proportion of cyclic oligomers produced during the polymerisation is very little, even after 98% of monomer was consumed (see figure 3.41 and annex 3.22). The decrease of \overline{Mn} after 60 % of monomer is consumed strongly indicates that transfer reactions are not prevented but only reduced. This phenomenon can only be explained if the growing centre and counter-ion are in the form of ion-pairs. This supposes that the growing centre may have different reactivity depending on the size of the counter ion. Unfortunately, the kinetic study did not permit an comparison of the reactivity of the propagating centre with different counter-ions. Indeed, at low monomer conversion (when

\overline{Mn} increases with the conversion), the higher molecular weight obtained with $[\text{EtOCH}_2]^+[\text{BF}_4]^-$ than with $[\text{EtOCH}_2]^+[\text{SbF}_6]^-$, strongly indicate that the initiator efficiencies are different.

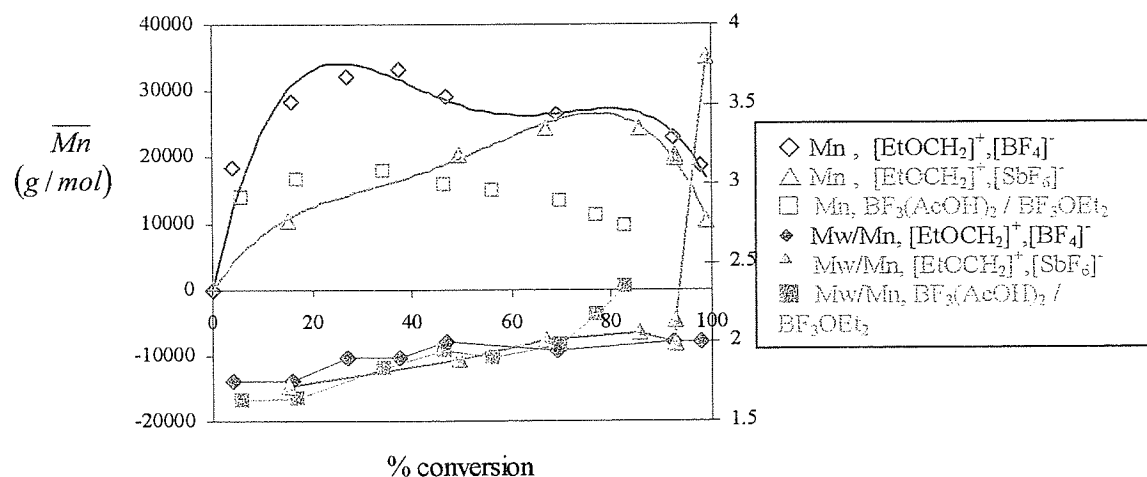


Figure 3. 40: Dependence \overline{Mn} and $\overline{Mw}/\overline{Mn}$ over monomer conversion obtained using protonic and oxocarbenium salts as initiator.

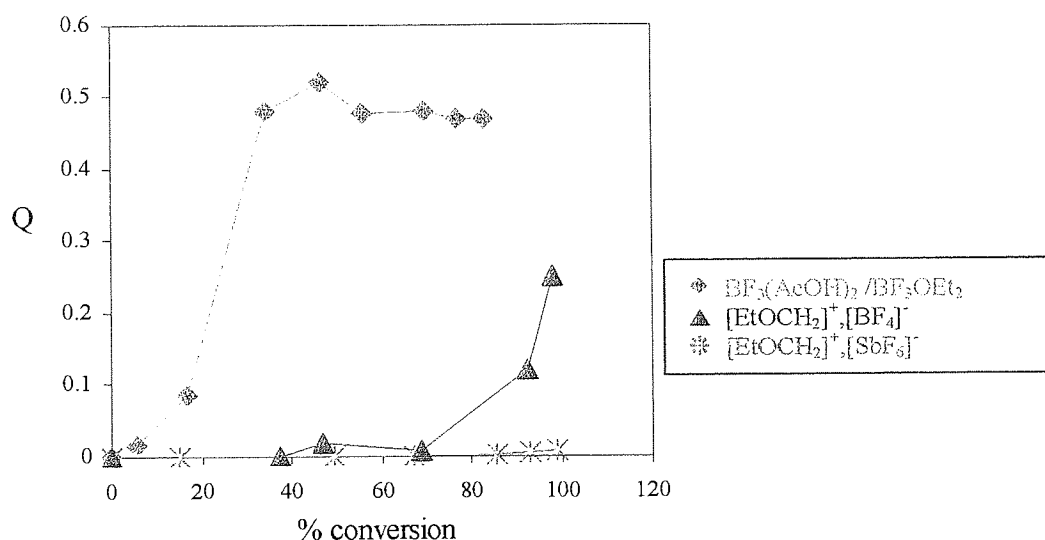


Figure 3. 41: Effect of the initiator and counter-ion on the cyclic oligomers formation in dichloromethane at 35 °C.

The cyclic oligomers produced when $[\text{EtOCH}_2]^+[\text{BF}_4]^-$ was used as catalyst were extracted by cyclohexane and was analysed by MS. The chromatograms presented in annex 3.23 shows that large cyclic oligomers are still produced. The most abundant of them is cyclic tetramers.

Entry	time t_k	conversion %	\overline{Mn} g/mol	Mp g/mol	$\frac{\overline{Mw}}{\overline{Mn}}$	Q SEC*
S 3.14.1	2 min	04.3	14250	19350	1.72	0
S 3.14.2	6 min	15.7	31370	49550	1.76	0
S 3.14.3	11 min	26.9	32300	63800	1.9	0
S 3.14.4	23 min	37.4	33230	68000	1.9	0
S 3.14.5	43 min	46.7	29120	55200	2	0.002
S 3.14.6	120 min	69.1	26500	43200	2	0.007
S 3.14.7	26 h	92.6	22950	40620	2.05	0.12
S 3.14.8	96 h	>98	18690	32360	2.1	0.28
S 3.15.1	3 min	15	10500	18000	1.72	0
S 3.15.2	13 min	49.3	20420	38700	1.89	0
S 3.15.3	30 min	66.9	24450	44260	2.02	0
S 3.15.4	68 min	85.7	24450	35480	2.06	0
S 3.15.5	106 min	92.7	20370	39400	2.1	0.005
S 3.15.6	153 min	92.8	19700	36500	2.14	0.006
S 3.15.7	17 h	>98	10360	39430	3.8	0.007

* Q = Area(cyclic oligomer peak)/Area(cyclic oligomers + linear polymer)

Table 3. 6: homopolymerisation of oxetane in dichloromethane using $[\text{EtOCH}_2]^+[\text{M}^-\text{X}_n]^-$ as initiator at 35 °C. $[\text{Ox}]_0 = 1 \text{ M}$ and $[\text{I}]_0 = 0.003 \text{ M}$.

3.3 Conclusions

The cationic ring-opening polymerisation of oxetane in dichloromethane using boron trifluoride acetic acid complex ($\text{BF}_3(\text{CH}_3\text{COOH})_2$) together with boron trifluoride diethyl ether complex (BF_3OEt_2) was studied at 35 °C. Analysis of the kinetic data showed that BF_3OEt_2 acts as co-initiator. Based on the mechanism of esterification of carboxylic acid catalysed by BF_3 ^[288,289], a mechanism of initiation was proposed in which $[\text{F}_3\text{BOCOCH}_3]^+; \text{CH}_3\text{COOH}_2^+$, $[\text{F}_3\text{BOCOCH}_3]^+; \text{CH}_3\text{COOEt}_2^+$ and $[\text{BF}_3\text{OH}]^+; \text{H}^+$ are the initiating species. The concentration of these are determined by the initial concentration of $\text{BF}_3(\text{CH}_3\text{COOH})_2$ and BF_3OEt_2 . Because the rate of formation of the growing centre is kinetically controlled by the rate at which the initiating species reacts with the monomer^[115], the analytical equation of the initial rate of propagation $(-d[M]/dt)_{\text{initial}}$, was calculated and found to be in agreement with

the observed rate of monomer consumption, $(-d[M]/dt)_{\max}$, when monitored at various concentrations of $\text{BF}_3(\text{CH}_3\text{COOH})_2$, BF_3OEt_2 and monomer. From these studies, it appeared that at $[\text{BF}_3(\text{AcOH})_2]_0 \geq [\text{BF}_3\text{OEt}_2]_0$, the rate of initiation and the initial rate of monomer consumption can be represented as follows:

$$\left(\frac{d[R^+]}{dt} \right)_{\text{initial}} = (k_{i1} + k_2 \cdot (k_{i2} + k_{i3} - k_{i1})) \cdot [\text{BF}_3(\text{AcOH})_2]_0 \cdot [\text{Ox}]_0 \quad \text{E: 3.41}$$

$$-\left(\frac{d[\text{Ox}]}{dt} \right)_{\text{initial}} = k_p \cdot k \cdot [\text{BF}_3(\text{AcOH})_2]_0 \cdot [\text{Ox}]_0 \quad \text{E: 3.42}$$

where

$$k = k_2 - 1 = \frac{2\sqrt{K} + 1}{\sqrt{K} + 1} \text{ at } [\text{BF}_3(\text{AcOH})_2]_0 = [\text{BF}_3\text{OEt}_2]_0 \quad \text{E: 3.43}$$

and

$$k = k_2 + 1 \text{ with } k_2 = \frac{K}{2} \cdot \left(\sqrt{1 + \frac{4}{K} \cdot \frac{[\text{BF}_3\text{OEt}_2]_0}{[\text{BF}_3(\text{AcOH})_2]_0}} - 1 \right) \text{ at } [\text{BF}_3(\text{AcOH})_2]_0 > [\text{BF}_3\text{OEt}_2]_0, \quad \text{E: 3.44}$$

while at $[\text{BF}_3\text{OEt}_2]_0 > [\text{BF}_3(\text{AcOH})_2]_0$, the rate of initiation and propagations becomes:

$$\left(\frac{d[R^+]}{dt} \right)_{\text{initial}} = k_i \cdot [\text{BF}_3\text{OEt}_2]_0 \cdot [M]_0 + k_2 \cdot (k_{i2} + k_{i3} - k_{i1}) \cdot [\text{BF}_3(\text{AcOH})_2]_0 \cdot [M]_0 \quad \text{E: 3.45}$$

$$-\left(\frac{d[M]}{dt} \right)_{\text{initial}} = k_p \cdot [\text{BF}_3(\text{AcOH})_2]_0 \cdot [M]_0 + k_p \cdot k_2 \cdot [\text{BF}_3\text{OEt}_2]_0 \cdot [M]_0 \quad \text{E: 3.46}$$

with

$$k_2 = \frac{K}{2} \cdot \left(\sqrt{1 + \frac{4}{K} \cdot \frac{[BF_3(AcOH)_2]_o}{[BF_3OEt_2]_o}} - 1 \right) \quad \text{E: 3.47.}$$

Because the protonation of a molecule of monomer by $[F_3BOCOCH_3]^+; CH_3COOH_2^+$ produces a molecule of acetic acid, this can then react with a molecule of 1:1 boron trifluoride diethyl ether complex to produce a secondary oxonium ion based on oxetane or on the polymeric material depending on the nature of the complexing reagent (see figure 3.30). Because the concentration of the reactants is low, this initiation process is believed to be very slow and therefore responsible for the observed enhancement of the rate of polymerisation in the first monomer addition experiments. In this case, it is interesting to note that the rate of formation of secondary oxonium ions does not depend on the concentration of oxetane:

$$\frac{d[R^+]}{dt} = k_{i4} \cdot [BF_3M] \cdot [AcOH] + k_{i5} \cdot [BF_3Polymer] \cdot [AcOH] \quad \text{E: 3.48.}$$

The Gel Permeation Chromatography as well as 1H and ^{13}C NMR, Gas Liquid Chromatography and Mass Spectroscopy studies showed that linear polymers are produced together with cyclic oligomers. Previous work in polyoxetane showed that cyclic oligomers from trimer up to octamer are formed^[115,182,198-200,209,279]. The most abundant of these is cyclic tetramer. From our investigation, it was found by GLC that large cyclic oligomers of up to 15 monomer units are also formed during the polymerisation process.

The analysis of the molecular weight data showed that the polymerisation reaction seems to be characterised by two stages. A first stage in which linear polymers of high molecular weight are formed is followed by a second stage, in which side reactions occur dominantly to form a large extent of cyclic and linear oligomers after 15 % to 25 % of monomer has been consumed. Besides, monomer addition experiments showed that irreversible termination reactions do not occur enough to be noticeable. The model developed by Rose explained the formation of cyclic oligomers in terms of "back-biting" and "end-biting" reactions^[115]. The formation of the linear polymers of high molecular weight distribution was attributed mainly to the intermolecular transfer reactions. From our investigation, it was found that intra- and intermolecular transfer reactions compete during the polymerisation process. Indeed, at constant concentration of monomer, the proportions of cyclic oligomers produced during the

polymerisation was found to increase as the targeted Dp was increased, inducing a decrease of \overline{Mn} during the course of the polymerisation. While at low targeted Dp, less cyclic oligomers are formed but \overline{Mn} increases throughout the polymerisation. Considering the large proportions of cyclic oligomers formed during the polymerisation process (33% of monomer is converted into cyclic oligomers when 1 M of oxetane is polymerised by 0.005 M of an equimolar solution of $\text{BF}_3(\text{CH}_3\text{COOH})_2/\text{BF}_3\text{OEt}_2$), the transfer reactions do not irreversibly terminate the active growing centre (strain tertiary oxonium ions) but only generate a less reactive growing centre (non strain tertiary oxonium). Because oxetane is the stronger nucleophilic reagent in the polymerisation medium, this can later regenerate the active growing centre (strain tertiary oxonium ions) by nucleophilic attack of the monomer onto one of the three electron deficient carbon atoms in α -position with respect to the oxonium ion site (see figure 3.4), inducing a redistribution of the molecular weight distribution. This can be visualised by the fact that the formation of cyclic oligomers induces a curvature of the slope $\ln([M]_0/[M]_t)$ against time. Because termination reactions do not seem to occur significantly during the course of the polymerisation, this slope curvature reinforces the idea that strain and non-strain tertiary oxonium ions are in equilibrium together throughout the polymerisation and that, as the monomer is consumed, the mole fraction of non-strain tertiary oxonium (dormant species) formed increases. In addition, the non-linear increase of the polymer chain length after the addition of monomer is an even stronger indication that polymer chains are not terminated. Consequently, the rate of propagation can be expressed as follows:

$$-\frac{d[M]}{dt} = \left(k_{p,1} \cdot f_{A1} + \sum_{i=2}^4 k_{a,i} \cdot f_{Ai} \right) \cdot [R^+, X^-] \cdot [Ox] \quad \text{E: 3.49}$$

with

$$k_{p,1} \gg k_{Ai} \quad \text{E: 3.50}$$

where $k_{p,1}$ represents the rate constant of propagation of strain oxonium ions (A1) and $k_{a,2}$, $k_{a,3}$ and $k_{a,4}$ represent the rate at which the non-strain cyclic tertiary oxonium ions, respectively A2, A3 and A4, are converted into strain tertiary oxonium ions (A1). Because

transfer reactions induce a redistribution of the molecular weight, \overline{DP}_n is undoubtedly kinetically controlled by all non-stationary reactions initiated by $\text{BF}_3(\text{AcOH})_2/\text{BF}_3\text{OEt}_2$ which involves the rate at which the tertiary oxonium ions (R_i) are produced, a fast propagation ($-d[\text{Ox}]/dt$), chain breaking reactions $\left(\sum_{i=1}^4 R_{tr}\right)$, and termination reactions $\left(\sum_{i=1}^{i=3} R_{t,i}\right)$ if they occur. Therefore, the average molecular weight distribution \overline{DP}_n of the produced high molecular weight materials can be written as follows:

$$\overline{DP}_n = \frac{-d[\text{Ox}]/dt}{\sum_{i=1}^{i=3} R_{t,i} + \sum_{i=1}^4 R_{tr} + R_{\text{initiation}}} \quad \text{E: 3.51}$$

Although the polymerisation does not appear to be living, the plot of $1/\overline{DP}_p$ against $[\text{BF}_3\text{OEt}_2]_0$ or $[\text{BF}_3(\text{AcOH})_2]_0$ as well as the plot of \overline{DP}_p against $[\text{Ox}]_0$ showed that polymer of given molecular weight can be targeted depending on the mole ratio of $[\text{Ox}]_0/[\text{Cat}]_0$.

Because $\text{BF}_3(\text{AcOH})_2/\text{BF}_3\text{OEt}_2$ induce a complex initiation process, the cationic ring-opening polymerisation of oxetane was investigated using synthetically prepared oxacarbenium salt associated with anions ($[\text{EtOCH}_2]^+, \text{X}^-$ with $\text{X} = \text{BF}_4^-$ or SbF_6^-) which induces a fast initiation process by alkylation. In comparison to $\text{BF}_3(\text{AcOH})_2/\text{BF}_3\text{OEt}_2$, the use of $[\text{EtOCH}_2]^+; [\text{BF}_4]^-$ (alkyl reagent) as cationic initiator was found to slow down the cyclic oligomer. This is explained by the fact the protonic initiator produce a hydroxyl tail group that might enhance the formation of cyclic oligomers by end-biting reactions. Surprisingly, when $[\text{EtOCH}_2]^+; [\text{SbF}_6]^-$ was used as initiator, the cyclic oligomers formation was significantly reduced (low cyclic oligomer formation even after that 90 % of monomer was consumed) but did not permit to control the polymerisation over \overline{M}_n and $\overline{M}_w/\overline{M}_n$. This counter-ion effect can only be explained if in dichloromethane the growing polymer chain ends are in the form of ions pairs. In the form of tight ion pairs, the very large counter-ion $[\text{SbF}_6]^-$ could sterically disfavour the cyclic oligomer formation, what does not $[\text{BF}_4]^-$. Several report in cationic polymerisation affirmed that the growing centre can only exist in the form of ion pairs and

free ions and that free ions and ion pairs exhibit the same reactivity^[133,184,291,292]. This was explained by the fact that the counter-ions involved in cationic polymerisation are very large ($[\text{BF}_4]^-$, $[\text{PF}_6]^-$, $[\text{SbF}_6]^-$, $[\text{SbCl}_6]^-$), and therefore interact only weakly with the cations. In addition, a survey of published data shows only a small variation in the value of dissociation constants of large number of ion-pairs composed of various organic cations and bulky counter-ions, such as $[\text{BCl}_4]^-$, $[\text{SbCl}_6]^-$ and $[\text{PF}_6]^-$. In this present, it is obvious that the size of the counter-ions affect the reactivity of the growing centre.

4 CHAPTER 4

**Studies of the effect of ether additives on
the cationic *ring-opening polymerisation*
(C.R.O.P) of oxetane in dichloromethane
using protonic initiator at 35 °C**

4 CHAPTER 4

Studies of the effect of ether additives on the *cationic ring-opening polymerisation* (C.R.O.P) of oxetane in dichloromethane using protonic initiator at 35 °C

Recently, Gouardere et al. reported that the polymerisation of oxetane in presence of dibenzo-18-crown-6-ether can reduce the formation of cyclic compounds but does not produce polymer with controlled molecular weight and narrow polydispersity. Similar effects were also observed when veratrole was used instead of dibenzo-18-crown-6-ether (dbce). In both case, the polymerisation of oxetane was carried out at 35 °C in dichloromethane using $\text{BF}_3\text{:EtOH}$ as initiating system^[293]. Because only two equivalents of additive were used in relation to the concentration of initiation system, the authors wanted to find out whether the additives, particularly dbce, could affect the reactivity of the growing centre by producing a more stable propagating centre. In order to obtain a better understanding on the effect of the ether additive on the cationic ring opening polymerisation of oxetane, a series of experiments was carried out in which 1 M of oxetane was polymerised at 35 °C in dichloromethane by 0.004 M of an equimolar solution of $\text{BF}_3(\text{AcOH})_2/\text{BF}_3\text{OEt}_2$ in the presence of different kinds of additives such as dibenzo-18-crown-6-ether (macrocyclic ether), veratrole (chelate reagent) and diphenyl ether (monoetherate derivative). Because $\text{BF}_3(\text{AcOH})_2/\text{BF}_3\text{OEt}_2$ mixture induces a complex mode of initiation (see chapter 3), BF_3MeOH was also used as initiating system. The polymerisation reactions were carried out as shown in the section 2.8.1. In all experiments, the polymerisation reaction was terminated by addition of a large excess volume of ethanol. The inactive polymer solution was then treated as described in the section 2.8.1 and the volatile materials were removed by evaporation over several days at room temperature. The yield of the polyoxetane material was determined by gravimetric analysis and the products were analysed by Size Exclusion Chromatography (S.E.C), using polystyrene as standard, and ^1H and ^{13}C NMR.

4.1 Effect of dibenzo-18-crown-6-ether and veratrole on the cationic ring opening polymerisation of oxetane

4.1.1 Use of dibenzo-18-crown-6-ether as additive

When these investigations were carried out using dibenzo-18-crown-6-ether as additive, it appeared that the way the additive was added to the monomer solution was crucial. Indeed, when the polymerisation was carried out by adding the initiating system solution into the monomer solution containing already the additive (*method 1*), the presence of dibenzo-18-

crown-6-ether did not reduce the formation of cyclic oligomers (table 4.1 series S 4.1), even if a large excess of additive (table 4.1, series S 4.2) was employed. The SEC analysis showed that there is no difference between the polymer made with and without dibenzo-19-crown-6-ether.

Series	P	time t_k second	Rate °C/s/l	\overline{Mn} g/mol	M_p g/mol	$\frac{\overline{Mw}}{\overline{Mn}}$	conversion %	Q(SEC)
S 3.1	0	19.2	-	13,800	25,600	1.63	5.63	0.015
S 3.2	0	52.8	2.84	16,600	28,100	1.65	16.85	0.085
S 3.3	0	120	2.87	18,000	30,120	1.84	34.3	0.515
S 3.7	0	880	2.82	11,320	26,700	2.17	76.8	0.47
S 3.8	0	7,200	2.84	9,620	24,800	2.35	82.9	0.440
S 4.1 ⁽¹⁾	1	120	2.72	14,800	27,820	1.85	32.5	0.48
S 4.2 ⁽¹⁾	5	120	2.35	15,500	30,220	1.84	33.4	0.52
S 4.3.1 ⁽²⁾	0.95	23.5	-	17,780	28,640	1.38	10.9	0.025
S 4.3.2 ⁽²⁾	0.95	45	3.32	16,130	26,500	1.63	15	0.067
S 4.3.3 ⁽²⁾	0.95	120	3.26	15,740	23,400	1.66	26.5	0.112
S 4.3.4 ⁽²⁾	0.95	865	3.3	9,530	17,700	1.9	82	0.122
S 4.3.5 ⁽²⁾	0.95	6,900	3.29	8,850	14,120	2.07	89	0.482

(1) addition of dbce according to the *method 1*, (2) addition of dbce according to the *method 2*.

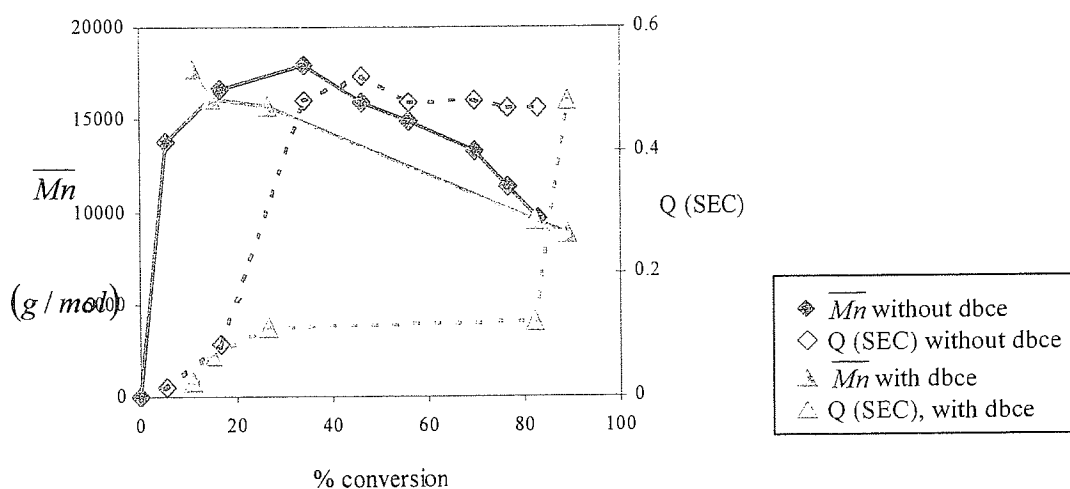
$$P = [\text{dbce}] / ([\text{BF}_3(\text{AcOH})_2] + [\text{BF}_3\text{:OEt}_2])$$

$$Q = \text{Area}(\text{cyclic oligomer peak}) / \text{Area}(\text{cyclic oligomers} + \text{linear polymer})$$

Table 4. 1: Effect of dibenzo-18-crown-6-ether on the cationic polymerisation of oxetane in dichloromethane at 35 °C. $[\text{Ox}]_0 = 1 \text{ M}$ and $[\text{BF}_3(\text{AcOH})_2]_0 = [\text{BF}_3\text{OEt}_2]_0 = 0.0065 \text{ M}$.

The reduction of the formation of cyclic oligomer was observed only when $\text{BF}_3(\text{AcOH})_2/\text{BF}_3\text{OEt}_2$ and dibenzo-18-crown-6-ether was mixed in dichloromethane and then injected into the monomer solution (method 2). The SEC chromatogram and ^1H and ^{13}C NMR spectrum of the produced polyoxetane materials are shown in annex 4.1, 4.2 and 4.3, respectively. As mentioned by Gouarderes at al.[293], the reduction of cyclic oligomer

formation was not able to control the polymerisation in term of molecular weight and the molecular weight distribution ($1.3 < \overline{M}_w/\overline{M}_n < 1.9$). This is illustrated in figure 4.1, where the plot (-◆-) of \overline{M}_n against monomer conversion showed that high molecular weight material is rapidly formed during the first 10 % of monomer consumption and then, the molecular weight decreases to reach, at high monomer conversion, approximately the same \overline{M}_n than in absence of additives (see annex 3.4).



$[\text{Ox}]_0 = 1 \text{ M}$ and $[\text{I}]_0 = [\text{BF}_3(\text{AcOH})_2]_0 = [\text{BF}_3\text{OEt}_2]_0 = 0.0065 \text{ M}$.

Figure 4. 1: Evolution of \overline{M}_n and Q(SEC) with conversion

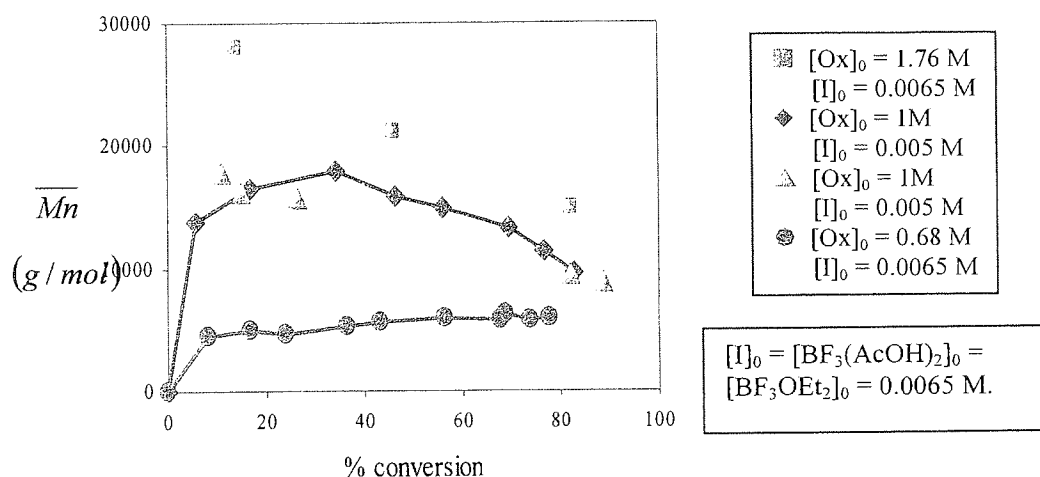


Figure 4. 2: Evolution of \overline{M}_n with conversion when the polymerisation is carried out without (■, ◆ and ▲) and with dbce according to the method 2

In the chapter 2, we showed that the evolution of \overline{Mn} with conversion was strongly dependent on the targeted Dp (see figure 4.2) due to the fact that the reactions of redistribution of the polymer chain length by transfer reactions (intra- and intermolecular transfer reactions) affect more significantly long polymer chain length than short one (see figure 4.2). In this present study, the decrease of \overline{Mn} , while cyclic oligomers formation is reduced, shows that the reactions of redistribution of the polymer chain length are not suppressed but only reduced when dbce is used as co-initiator.

Contrary to Gouarderes et al.^[293], it was observed that as soon as 82 % of monomer was consumed, cyclic oligomer formation was drastically enhanced (table 4.1 series S 4.3.5 and figure 4.1) and this without inducing a significant decrease of \overline{Mn} . The proportion of cyclic oligomers (Q (SEC)) produced between 82 % and 89 % of monomer consumption was calculated by SEC analysis and found to increase from 0.112 to 0.48. Knowing that back-biting and intermolecular transfer reactions induce a redistribution of polymer chains length, the enhancement of cyclic oligomer while \overline{Mn} did not decrease significantly can only be possible if the cyclic oligomers are mainly formed by end-biting reactions (see figure 4.3). This implies that $\text{BF}_3(\text{AcOH})_2/\text{BF}_3\text{OEt}_2/\text{dbce}$ (1/1/1.8) like $\text{BF}_3(\text{AcOH})_2/\text{BF}_3\text{OEt}_2$ (1/1) mixture induce a slow process of initiation by protonation.

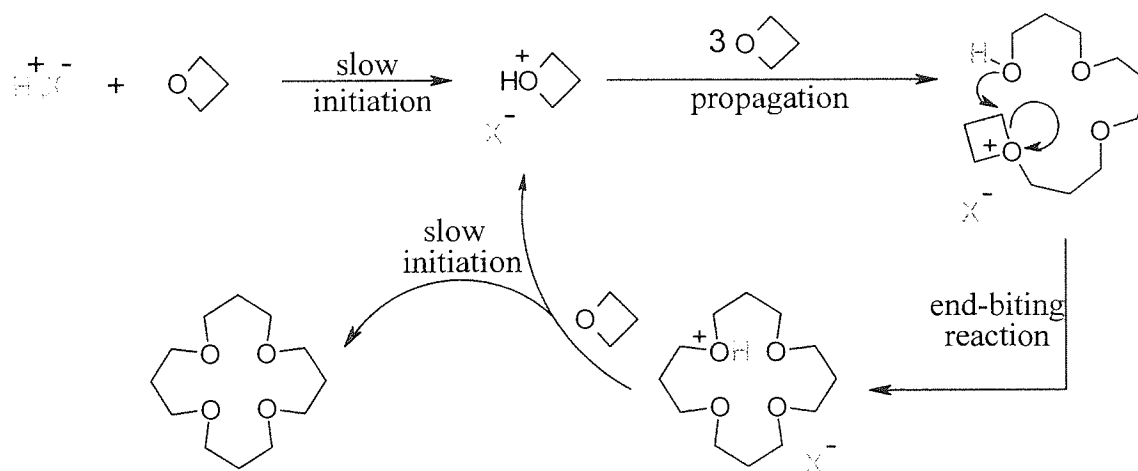


Figure 4. 3: Mechanism of cyclic oligomers (tetramer) formation by end-biting reactions in starving monomer solution.

Indeed, as illustrated in the figure 4.3, in starving monomer conditions, the growing centre generated by protonation of a molecule of oxetane can only incorporate few molecules of monomer before undergoing end-biting reactions. This is due to the fact that the hydroxyl

end group is the stronger nucleophilic reagent in the polymerisation medium and that intramolecular transfer reactions are generally more favourable than intermolecular transfer reactions.

Further investigations showed that the strain free dibenzo-18-crown-6-ether can be incorporated into the polymer, and this independently on the method used to add the additive into the reaction flask. This was observed when the polymeric materials were analysed by SEC using the UV detector at $\lambda = 254$ nm (annex 4.4). If one considers the way the additive was added into the polymerisation mixture, for example when $\text{BF}_3(\text{AcOH})_2/\text{BF}_3\text{OEt}_2$ (1/1) mixture is added into monomer solution containing dbce (*method 1*), the incorporation of dbce can only occur via a copolymerisation type mechanism:

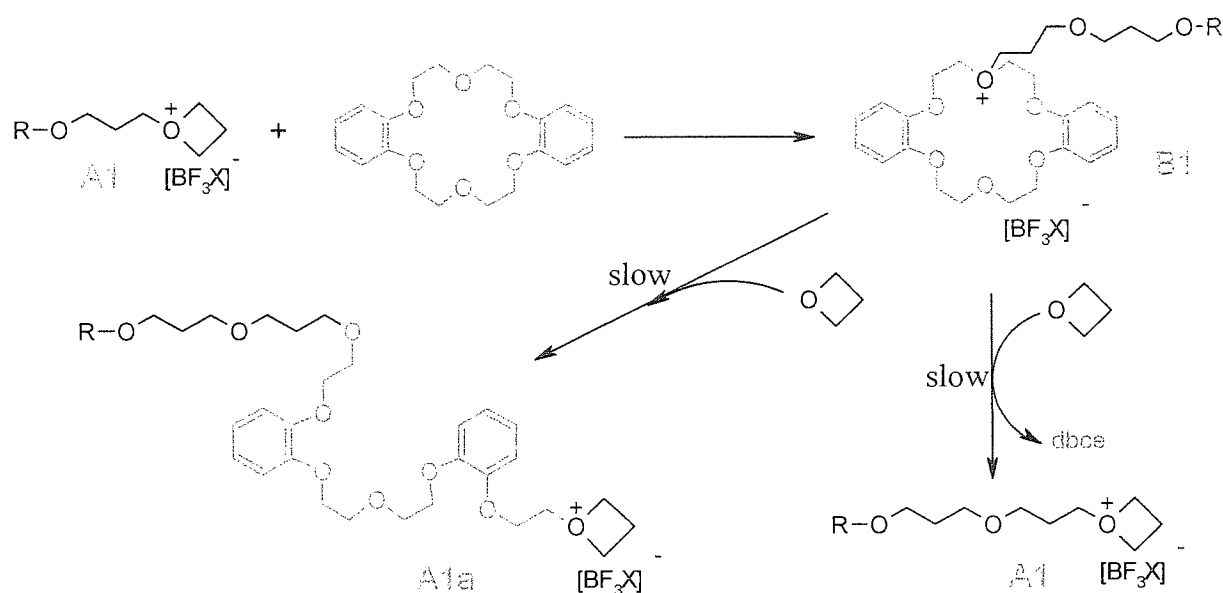


Figure 4. 4: Mechanism of copolymerisation of oxetane with dbce when the polymerisation is carried out according to the method 1.

As shown in the figure 4.4, the mechanism of chain growth can be momentarily disrupted by the nucleophilic attack of one of the oxygen atoms of the dbce molecule onto one of the two electron deficient carbon atoms in the α -position with respect to the oxonium site A1. Because the oxygen atom of oxetane is much more nucleophilic than the oxygen atoms from dbce, it appears now obvious that the main factors governing the formation of B1 are the reactivity of the growing centre (A1) and the concentration of the reactants (oxetane and dbce) rather than their respective basicities. This is probably because of the high ring strain contained by the oxonium site A1. Because oxygen atoms of molecules of oxetane are also much more nucleophilic than the oxygen atoms in the back-bone, the incorporation of dbce

into the polymer chain is believed to occur principally by nucleophilic attack of the oxygen atom of the oncoming oxetane onto one of the two endocyclic electron deficient carbon atoms in α -position with respect to the oxonium site (B1). The nucleophilic attack by the monomer onto the exocyclic electron deficient carbon atoms will displace the molecule of dbce and will regenerate A1. Similar results were reported by Furukawa^[294] and others^[295-298] when they attempted to polymerise 3,3-bis(chloromethyloxy)oxetane in the presence of 6-membered cyclic ether monomer that do not homopolymerise. Using elemental analysis, Furukawa showed that the copolymerisation in chloroform of an equimolar solution of BCMO with THP by 5 mole % of BF_3OEt_2 produce a copolymer containing 33.5 % THP mole units after that 80 % of BCMO was consumed whereas with an equimolar solution of BCMO with 1,4-dioxane, the resulting copolymer contained 19 % of 1,4-dioxane units after that 60 % of BCMO were consumed. Similarly, when Grønneberg^[124] et al. studied the polymerisation of non-deuteriated ethylene oxide in the presence of deuteriated 1,4-dioxane, they showed that strain free 1,4-dioxane can be enlarged by a back-biting reaction when the growing centre carries a 1,4-dioxonium salt. In that case, it is interesting to note that the oxygen atom in the back-bone is more nucleophilic than the oxygen atom of the ethylene oxide.

The reduction of cyclic oligomer formation was also observed when 0.008 M of BF_3MeOH was used as initiator. The SEC traces of polymer showed that the cyclic oligomer are formed after 80 % monomer conversion (annex 4.6) and that dbce is also incorporated into the polymer. This study is summarised in the table 4.2.

4.1.2 Use of veratrole as additive

When the polymerisation of oxetane was carried out using veratrole as additive, both method 1 and method 2 did not permit to reduce the cyclic oligomer formation even if 10 molar equivalents of additive were employed. Moreover, the SEC traces of the produced polyoxetane materials showed that veratrole was not incorporated into the polymer chains. This study is summarised in the table 4.3.

Series	P	time t_k second	Rate °C/s/l	\overline{Mn} g/mol	Mp g/mol	$\frac{\overline{Mw}}{\overline{Mn}}$	conversion %	Q SEC
S 4.4.1	0	14.4	5.83	7,020	11,820	1.77	8.9	0.15
S 4.4.2	0	34.8	5.79	7,890	12,820	1.71	28.6	0.18
S 4.4.3	0	83.4	5.8	7,160	12,900	1.89	53.4	0.24
S 4.4.4	0	129.6	5.82	6,000	11,150	2.01	67	0.24
S 4.4.5	0	245	5.87	5,840	11,500	2.08	75.4	0.28
S 4.4.6	0	594	5.78	4,920	11,550	2.24	79.4	0.29
S 4.4.7	0	955	5.81	4,820	11,370	2.32	80	0.31
S 4.4.8	0	1134	5.85	4,500	10,990	2.39	80.8	0.32
S 4.5.1	1.85	55.2	3.42	13,320	25,700	1.38	18	0.025
(1)	1.85	732	3.45	16,240	26,500	1.63	73	0.067
S 4.5.2	1.85	953	3.45	10,530	16,240	1.68	80	0.073
(1)	1.85	7200	3.47	10,240	16,320	1.69	89	0.38
S 4.5.3								
(1)								
S 4.5.4								
(1)								

$P = [\text{dbce}]/[\text{BF}_3\text{MeOH}]$,

(1) addition of dbce according to the method 2,

$Q = \text{Area}(\text{cyclic oligomer peak})/\text{Area}(\text{cyclic oligomers} + \text{linear polymer})$,

Table 4. 2: Effect of dibenzo-18-crown-6-ether on the cationic polymerisation of oxetane in dichloromethane at 35 °C using BF_3MeOH as initiating system. [Oxetane] = 1 M and $[\text{BF}_3\text{MeOH}] = 0.008$ M

Series	P	time t_k second	Rate °C/s/l	\overline{M}_n g/mol	M_p g/mol	$\frac{\overline{M}_w}{\overline{M}_n}$	conversion %	Q SEC
S 4.6.1 ⁽¹⁾	2	37.2	3.01	11,670	24,320	1.83	6.1	0.035
S 4.6.2 ⁽¹⁾	2	53.4	2.97	17,600	31,100	1.85	15.2	0.14
S 4.6.3 ⁽¹⁾	2	873	2.97	12,290	25,120	2.15	53.7	0.43
S 4.7.1 ⁽¹⁾	9.6	49.2	3.12	16,780	29,300	1.63	16.9	0.12
S 4.7.2 ⁽¹⁾	9.6	88	3.09	22,500	37,380	1.65	29.7	0.454
S 4.7.3 ⁽¹⁾	9.6	170.4	3.05	19,400	31,940	1.84	42.5	0.49

$P = [\text{veratrole}]/[\text{BF}_3\text{MeOH}]$,

(1) addition of dbce according to the method 2,

$Q = \text{Area}(\text{cyclic oligomer peak})/\text{Area}(\text{cyclic oligomers} + \text{linear polymer})$,

Table 4. 3: Effect of veratrole on the cationic polymerisation of oxetane in dichloromethane at 35 °C. [Oxetane] = 1 M and $[\text{BF}_3(\text{AcOH})_2] = [\text{BF}_3\text{OEt}_2] = 0.0065 \text{ M}$.

4.1.3 Nature of the initiating species when additives are used as co-initiator

4.1.3.1 Using dbce/ $\text{BF}_3(\text{AcOH})_2/\text{BF}_3\text{OEt}_2$ as initiating system

In the chapter 3, it was seen that the probability of transfer reactions (intra- and intermolecular transfer reactions) occurring depends on the nature of the species involved in the initiation process. Indeed, when the alkylating reagent ($[\text{EtOCH}_2]^+$, $[\text{BF}_4]^-$) was used instead of protonic initiator ($\text{BF}_3(\text{AcOH})_2/\text{BF}_3\text{OEt}_2$ mixture), the cyclic oligomer was formed only after that 50 % of monomer was consumed. This was explained by the fact that protonic initiator produces a hydroxyl end group that enhance the formation of cyclic oligomers by end-biting reactions during the entire course of the polymerisation, while the cyclic oligomers can only be formed with alkylating reagents by a back-biting process. The reduction of cyclic oligomer formation was achieved only when the oxacarbenium salt was associated with a large counter-anion, such as $[\text{SbF}_6]^-$. With large counter-anions, the propagating species are believed to exist in the form of tight ion-pairs rather than free ions. In the form of tight ion pairs, the very large counter-anion $[\text{SbF}_6]^-$ is believed to sterically disfavour the transfer reactions. This is shown in the figure 4.4.

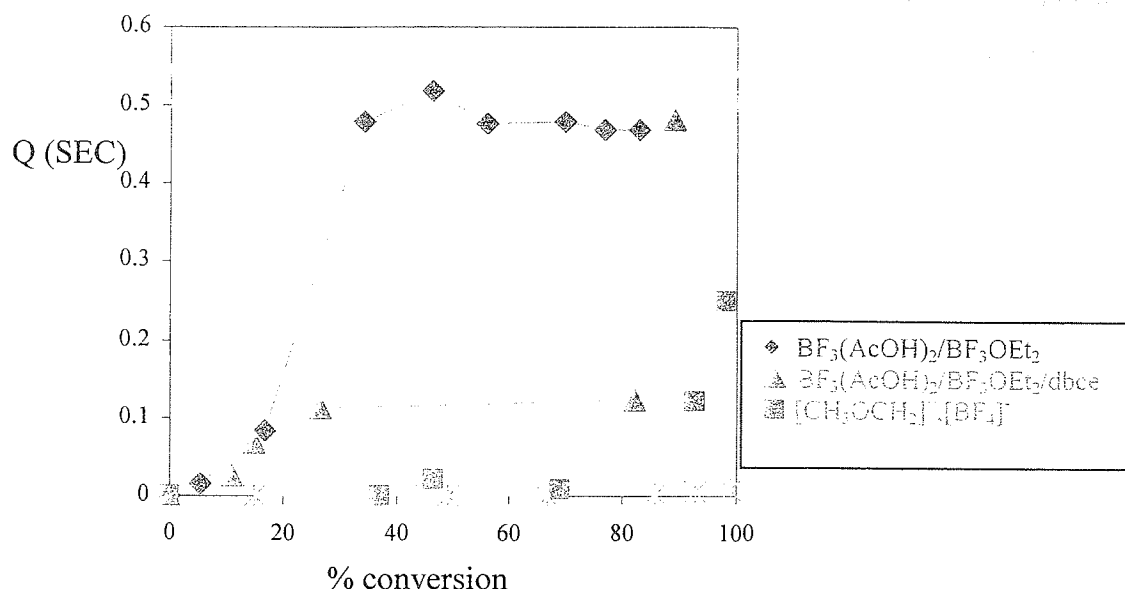


Figure 4. 5: Proportion of cyclic oligomers, Q(SEC), produced throughout the polymerisation using different initiators.

In the present work, where oxetane was polymerised in presence of dibenzo-18-crown-6-ether or veratrole, the cyclic oligomer formation was reduced only when BF₃(AcOH)₂, BF₃OEt₂ and dbce were mixed according to the method 2 and then injected into the monomer solution. The formation of cyclic oligomers observed after that 82 % of monomer was consumed can only be explained if dibenzo-18-crown-6-ether in conjunction with BF₃(AcOH)₂/BF₃OEt₂ (1/1) mixture generates an initiating species that slows down the initiation by protonation. Indeed, if we take into consideration the way the initiating system was prepared, the mixture in dichloromethane of 1 molar equivalent of BF₃OEt₂ with 1.8 molar equivalent of dibenzo-18-crown-6-ether can only lead to the formation of boron trifluoride dibenzo-18-crown-6-ether complex by ligand exchange reaction:

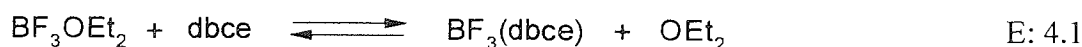
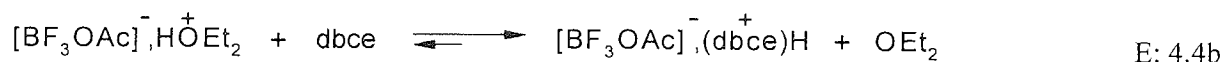
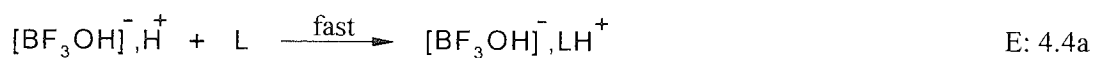
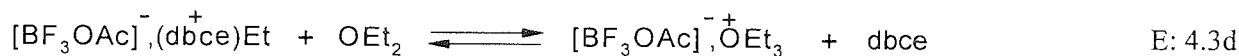
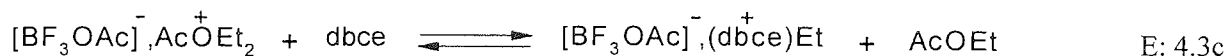
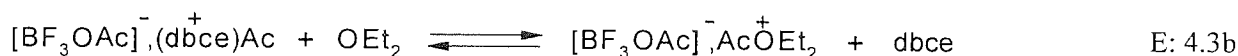
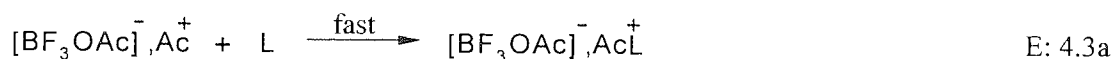
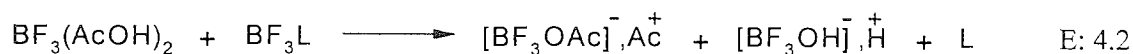


Figure 4. 6: Mode of formation of boron trifluoride dibenzo-18-crown-6-ether complex.

Therefore, when 1 molar equivalent of BF₃(AcOH)₂ is added into the solution, BF₃OEt₂ and BF₃(dbce) can act as co-catalyst (see figure 4.6, equation E: 4.2). Because dibenzo-18-crown-6-ether and OEt₂ are the unique nucleophilic reagent present in the solution, the acylium ion, [BF₃OAc]⁻,Ac⁺, and the proton, [BF₃OH]⁻,H⁺, can then be quantitatively converted into a more stable acylating reagent, [BF₃OAc]⁻,AcL⁺, (equation E: 4.3a), and a

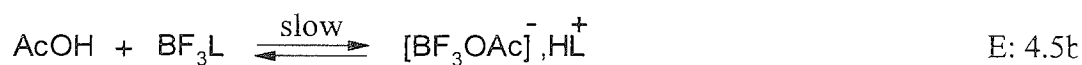
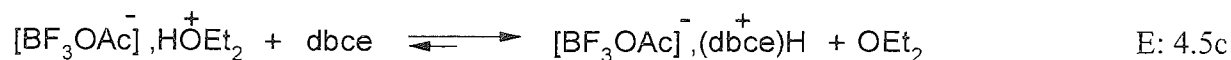
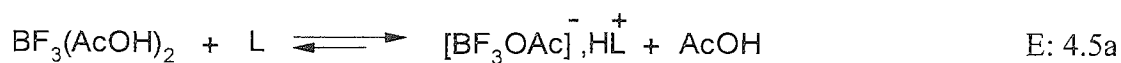
more stable protonic reagent, $[\text{BF}_3\text{OH}]^-, \text{HL}^+$, (equation E: 4.4a). Because the concentration of nucleophilic reagent is higher than the concentration of initiating species ($[\text{dbce}]_0 + [\text{OEt}_2]_0 - ([\text{BF}_3\text{OEt}_2]_0 + [\text{BF}_3(\text{AcOH})_2]_0) = 0.52 \text{ mol}$), the produced acylating species, $[\text{BF}_3\text{OAc}]^-, \text{Ac}(\text{dbce})^+$, can then be reversibly converted into alkylating species, $[\text{BF}_3\text{OAc}]^-, \text{EtL}^+$ (see E: 4.3b, E: 4.3c and E: 4.3d, figure 4.6). Similarly, protonic reagents can also exist in the form of $[\text{BF}_3\text{OH}]^-, \text{HOEt}_2^+$ and $[\text{BF}_3\text{OH}]^-, \text{H}(\text{dbce})^+$. However, because the electronegative oxygen atoms of the crown ether can complex the proton, H^+ , within the macrocycle, the encapsulate proton, $[\text{BF}_3\text{OH}]^-, \text{H}(\text{dbce})^+$, is believed to be less favourable for the deprotonation than $[\text{BF}_3\text{OH}]^-, \text{HOEt}_2^+$. This macrocyclic effect is believed to pull the equilibrium E: 4.4b to the formation of $[\text{BF}_3\text{OH}]^-, \text{H}(\text{dbce})^+$. This implies that the equilibria E: 4.3b, E: 4.3c and E: 4.3d favour the formation of $[\text{BF}_3\text{OAc}]^-, \text{AcOE}_2^+$ and $[\text{BF}_3\text{OAc}]^-, \text{OEt}_3^+$ rather than the formation of $[\text{BF}_3\text{OAc}]^-, \text{Ac}(\text{dbce})^+$ and $[\text{BF}_3\text{OAc}]^-, \text{Et}(\text{dbce})^+$.



$\text{L} = \text{dbce}$ or OEt_2

Figure 4. 7: Chemical reactions involved when $\text{BF}_3(\text{AcOH})_2$, BF_3OEt_2 and dibenzo-18-crown-6-ether are mixed in dichloromethane at 35 °C.

Similar reactions can also occur when dibenzo-18-crown-6-ether (dbce) and OEt₂ act as co-catalyst of BF₃(AcOH)₂:



L = dbce or OEt₂

Figure 4. 8: Chemical reactions evolved when BF₃(AcOH)₂, BF₃OEt₂ and dibenzo-18-crown-6-ether are mixed in dichloromethane at 35 °C.

Under such conditions, the nature of the initiating species involved in the initiation process can be represented as shown in the figure 4.8. Therefore, when the initiating mixture containing dbce is injected into the monomer solution, the initiation can then occur as follows:

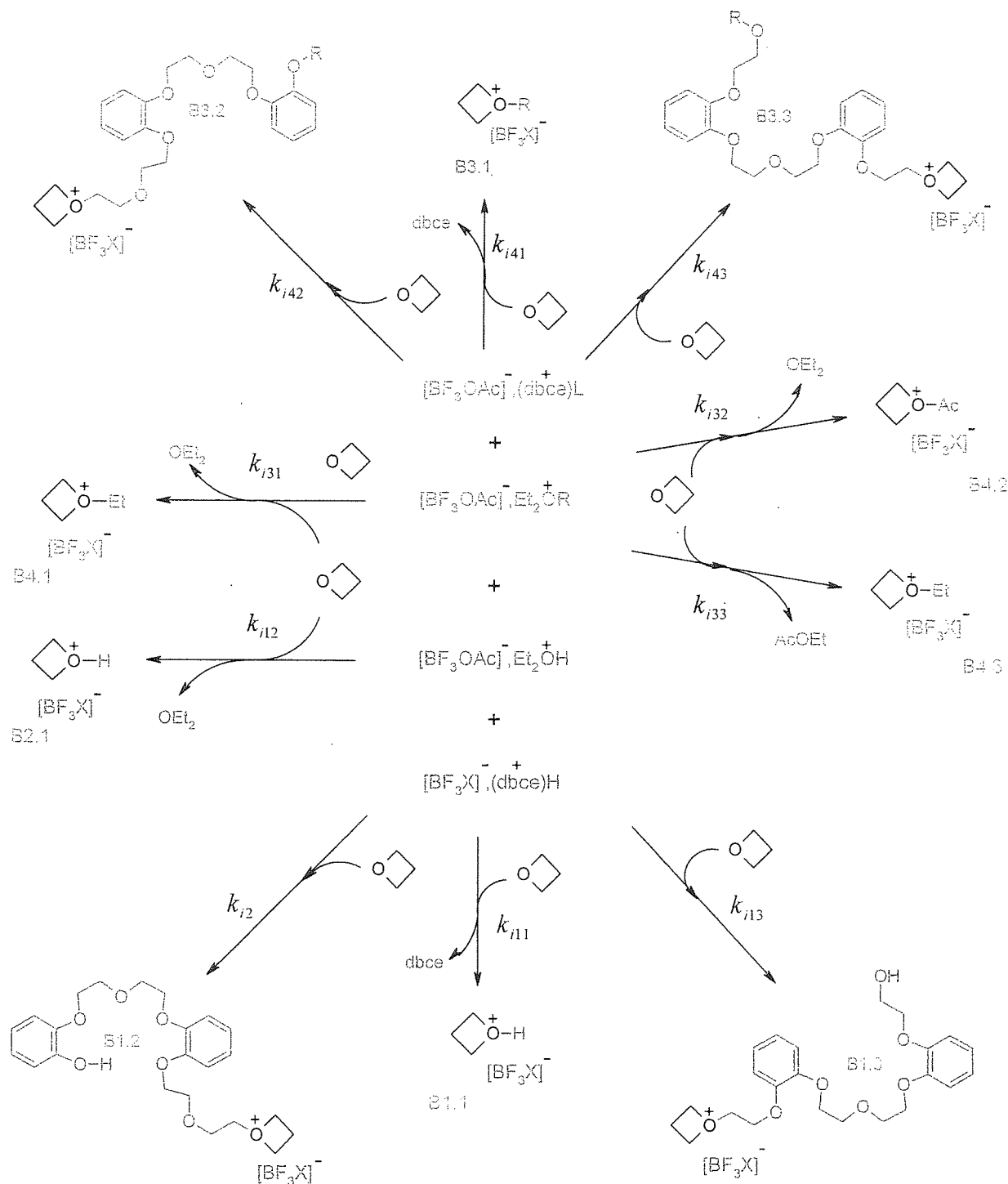
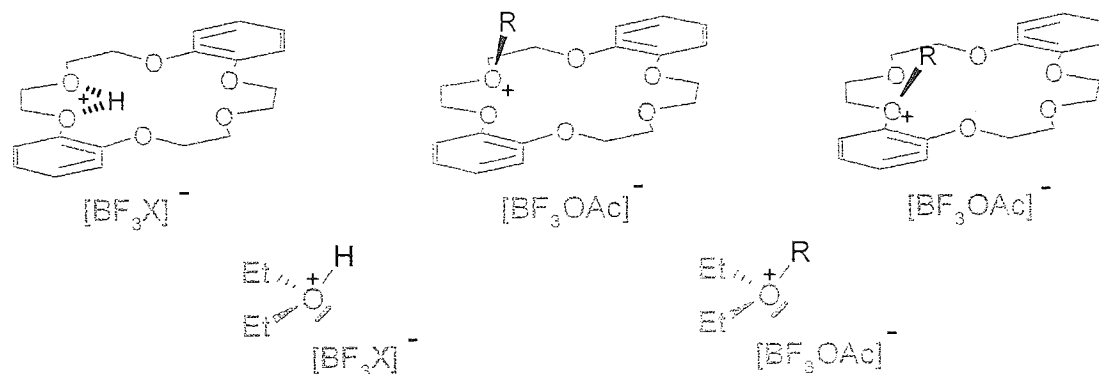


Figure 4. 9: Mechanism of initiation after addition of the initiating system solution into monomer solution.



with X = HO- or CH₃COO- and R = C₂H₅- or CH₃CO-

Figure 4. 10: Nature of initiating species when BF₃(AcOH)₂, BF₃OEt₂ and dibenzo-18-crown-6-ether are mixed in dichloromethane at 35 °C (method 2). X = -OH or -Oac.

As previously mentioned, the complexation of H⁺ within the crown-ether does not only weaken the acidity of H⁺ but can also sterically hinder the protonation of reacting monomer. In the case of alkylating and acylating reagents (see figure 4.8), the formation of an oxonium ion based on the oxygen atom of the crown-ether seats the exocyclic carbon above the ring and therefore does not sterically hinder the alkylation or the acylation of the monomer. For this reason, [BF₃OAc]⁻,(dbce)R⁺ and [BF₃OAc]⁻,Et₂OR⁺ are believe to have approximately the same reactivity towards alkylation and toward acylation of the monomer:

$$k_{ij1} \geq k_{i2} > k_{ik} \text{ (with } j = 3 \text{ or } 4 \text{ and } k = 1, 2 \text{ or } 3) \quad \text{E: 4.6}$$

$$k_{i41} \approx k_{i43} \approx k_{i31} \text{ and } k_{i42} \approx k_{i21} \quad \text{E : 4.7}$$

Because only a fraction of dbce is incorporated into the polymer, it can be assumed that:

$$k_{ij1} > k_{ij2} \text{ and } k_{ij1} > k_{ij3} \text{ (for } j = 1, 3 \text{ or } 4) \quad \text{E: 4.8}$$

The high molecular weight, \overline{Mn} , obtained at low monomer conversion (conversion < 10 %) when dbce is used as co-initiator reinforce the idea that only a small fraction of initiating species is initially involved in the initiation process (see figure 4.1). Moreover, the enhancement of the initial rate of monomer consumption, while the initiator efficiency is initially lower, is in agreement with the fact that the formation of cyclic oligomers is reduced (see table 4.1).

When the polymers were analysed by SEC using UV detector at 277 nm, it was observed at high monomer conversion that a small fraction of low molecular weight material, presumably cyclic oligomers, also contain dbce units (see annex 4.4). This was observed by overlapping the SEC traces of polymeric materials obtained using the UV and RI detector. Because this fraction seems to be more significant when dbce is used as co-initiator (method 2) than as co-monomer (method 1), this suggests that the low molecular weight material containing dbce unit could have been produced by end-biting reactions of B1.2 and B1.3:

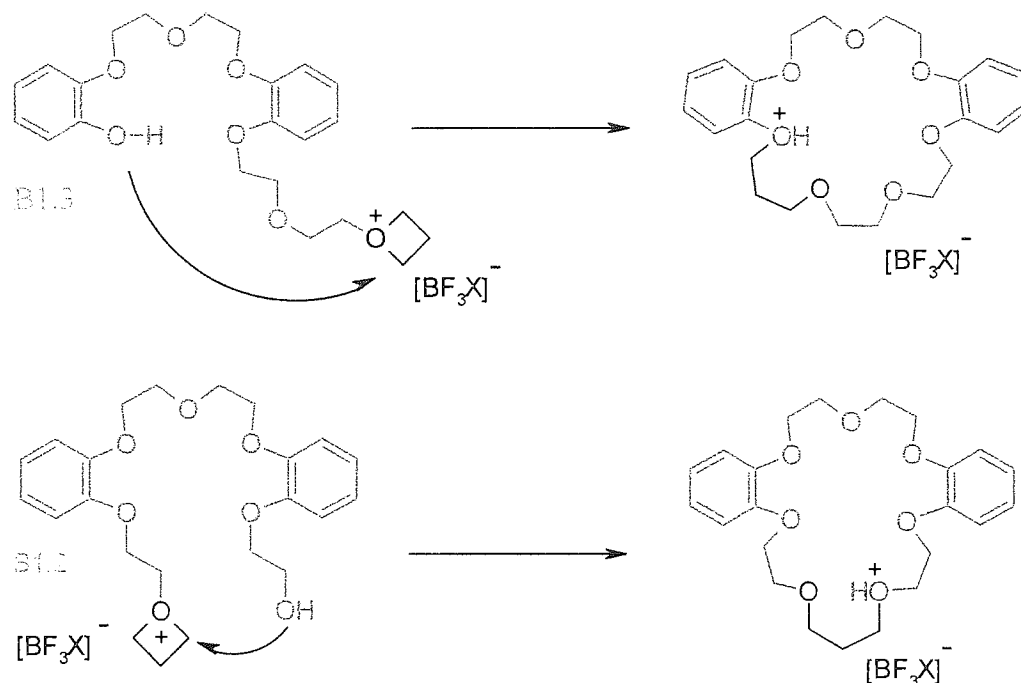


Figure 4. 11: Mechanism of copolymerisation of dbce during the formation of cyclic oligomer by end-biting reactions when dbce is used as co-initiator (method 2)

Because low molecular weight material containing dbce are also formed when dbce is used as co-monomer (method 1), this could also been formed by a ring-opening expansion reaction mechanism:

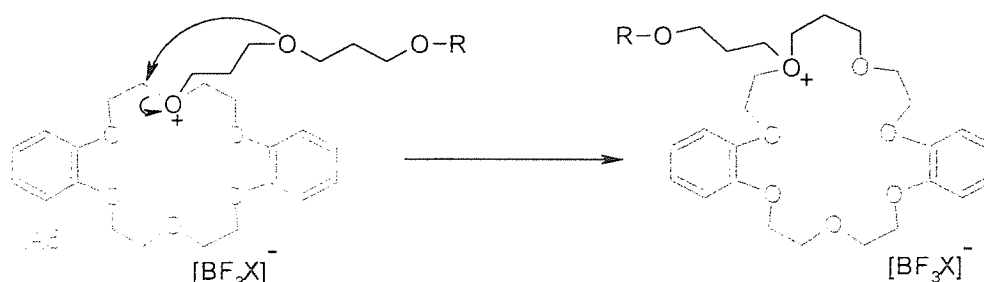


Figure 4. 12: Mechanism of copolymerisation of dbce during the formation of cyclic oligomer by ring-opening expansion reactions when dbce is used as co-monomer (method 1).

and/or by a back-biting reactions:

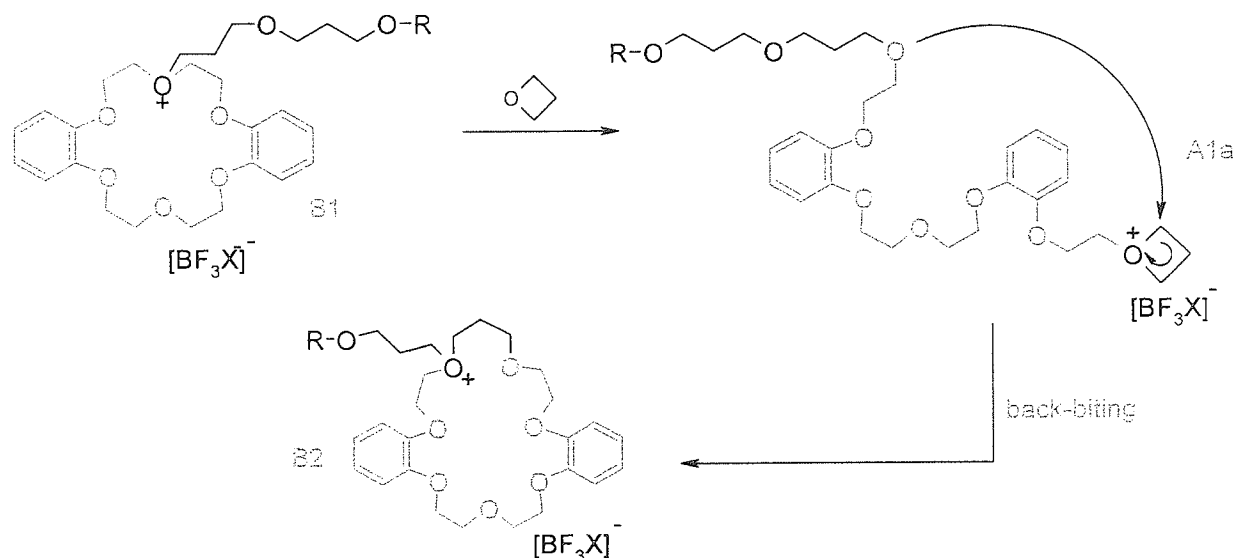


Figure 4.13: Mechanism of copolymerisation of dbce during the formation of cyclic oligomers by back-biting reactions when dbce is used as co-monomer (method 2).

Because dbce interacts with stationary phase of the SEC column (elution volume of dbce is higher than the elution volume of the toluene), it cannot be excluded that cyclic oligomers contain several oxetane monomer units.

4.1.3.2 Using dbce/ BF_3MeOH as initiating system

In comparison to $\text{BF}_3(\text{AcOH})_2/\text{BF}_3\text{OEt}_2$, when the polymerisation was conducted using 1 molar equivalent of $\text{BF}_3\text{:MeOH}$ with 1 molar equivalent of dbce, the reduction of cyclic oligomer was accompanied by a decrease of the rate at which the monomer was consumed.

The polymer formed showed higher \overline{Mn} than in the absence of additives. As illustrated in the figure 4.13, this is probably due to the fact that, initially, only a fraction of $\text{BF}_3\text{:MeOH}$ initiates the polymerisation. If $k_{i1} \gg k_{i2}$

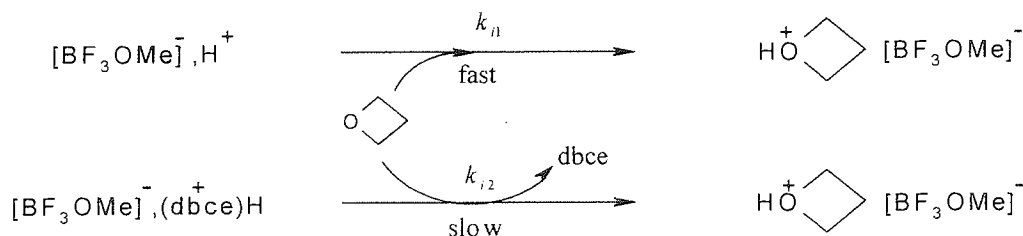


Figure 4.14: Mechanism of initiation of polymerisation of oxetane using $\text{BF}_3\text{:MeOH}$ as initiator and dibenzo-18-crown-6-ether as co-initiator.

Because protonating reagents produce cyclic oligomer principally by end-biting reactions (see chapter 3) and this during the all course of the polymerisation, the reduction of cyclic oligomer formation during the first 89 % monomer conversion suggests that a ratio $[Oxetane]_t/[(Oxetane),H^+]_t$ exists above which the probability of the end-biting reactions, p_{tr3} , is reduced. This can be represented by the following equation;

$$p_{tr3} = \frac{R_{tr3}}{R_{tr3} + R_{tr2} + R_{tr1} + R_{p,1}} = f\left(\frac{[Oxetane]_t}{[(Oxetane),H^+,X^-]_t}\right) \quad \text{E: 4.7}$$

where $R_{p,1}$ (mol.l⁻¹.s⁻¹) is the rate of propagation of the active species (A1), R_{trj} (mol.l⁻¹.s⁻¹) is the rate at which each active species (A1) undergo (j = 1) end-biting reaction, (j = 2) back-biting reaction, (j = 3) intermolecular transfer reaction (see figure 3.4). $[(Oxetane),H^+]_t$ represents the concentration of secondary oxonium ions produced at any given, remaining, concentration of oxetane, $[Oxetane]_t$. The enhancement of cyclic oligomers after 80 % monomer conversion is certainly due to the fact that the newly generated growing centres undergo end-biting reactions because of the low concentration of oxetane. The low molecular weight obtained at high monomer conversion suggests that redistribution of molecular weight by transfer reactions occurs during the entire course of the polymerisation process.

4.1.3.3 Using veratrole

In contradiction to Gouarderes[293], when veratrole was used as an additive, the cyclic oligomer formation was not reduced even if 10 mol equivalent of veratrole were used as co-initiator.

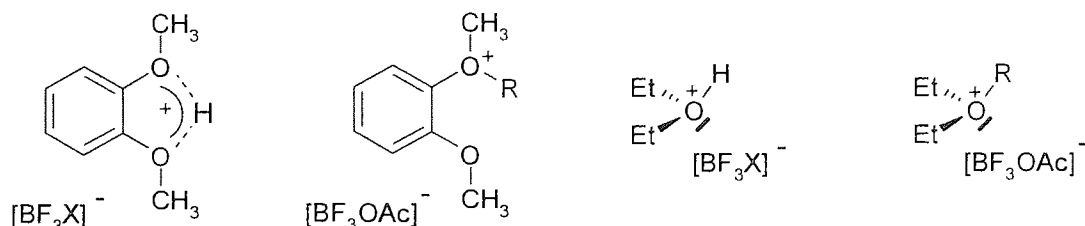


Figure 4. 15: Nature of initiating species when $BF_3(AcOH)_2$, BF_3OEt_2 and veratrole are mixed in dichloromethane at 35 °C according to the method 2. X = -OH or -Oac.

As illustrated in figure 4.14, the complexation of H^+ by veratrole can only weaken the acidity of the protonating species but does not sterically hinder the protonation of the monomer. This reinforces the idea that the macrocycle can bind the H^+ inside the crown-ether and therefore slow down the initiation by protonation.

4.2 Effect of diphenylether (dpe) on the cationic ring opening polymerisation of oxetane

In the previous chapter, we showed that transfer reactions do not terminate irreversibly the active growing centre (strained tertiary oxonium ion) but only generate temporarily a less reactive species (non-strained tertiary oxonium ion). Because oxetane is the stronger nucleophilic reagent in the polymerisation medium, the active growing centre (strained tertiary oxonium ion) can be regenerated by nucleophilic attack of the monomer onto one of the three electron deficient carbon atoms in α -position with respect to the oxonium site (see figure 3.4), inducing a redistribution of the molecular weight distribution with formation of cyclic oligomers if the "dormant" species are in the form of non-strained cyclic tertiary oxonium ions (A2, figure 3.4). This was partially proved by the fact that the second monomer addition restarts the polymerisation reaction with the expected initial rate of monomer consumption once all of the growing centres are in the form of dormant species (section 3.1.3).

In the present work, we were interesting to find out whether dpe can affect the polymerisation process by end-capping the growing centre. For this purpose a series of experiments was carried out in which oxetane (1 M) was polymerised by an equimolar solution of $BF_3(AcOH)_2/BF_3OEt_2$ (0.005 M) in the presence a various concentration of diphenyl ether. The polymerisation was prepared according to the method 1 (see section 4.1.1.) and the concentration of diphenyl ether was varied from 0.05 M ($P = 10$ and $R = 0.004$) to 0.9 M ($P = 180$ and $R = 0.72$). The total volume of the solution was kept constant and equal to 21 ml. In all experiments, the polymerisation was terminated after 300 seconds and the polymer was analysed by SEC and NMR analysis. This study is summarised in the table 4.5.

When this investigation was carried out, it was found that dpe affects the polymerisation depending on the ratio P and/or R . Indeed, at low concentration of dpe ($P < 20$) the presence of dpe did not affect the polymerisation of oxetane. This is in agreement with the results

obtained with veratrole. The reduction of cyclic oligomer formation was observed only at $P = 40$. However, as soon as $Q \geq 80$, the cyclic oligomer formation was enhanced and this until $Q = 180$. The proportion of cyclic oligomers produced during the polymerisation was followed by ^1H and ^{13}C NMR (see annex 4.8. and 4.9). SEC analysis could not be used to observe the increase of cyclic oligomers peak when $Q \geq 80$. This is because the peak related to the free dpe present in the polymer material overlapped the cyclic oligomer peak (see annex 4.7). Because of this, the proportion of monomer incorporated into cyclic oligomer, Q , was calculated by ^{13}C NMR using the well defined and the well separated signals due to CH_2 in α position of the oxygen atom ($-\text{OCH}_2-\text{CH}_2-\text{CH}_2-\text{O}-$). The SEC analysis using UV detector at $\lambda = 277$ nm showed that dpe is not incorporated into the polymer.

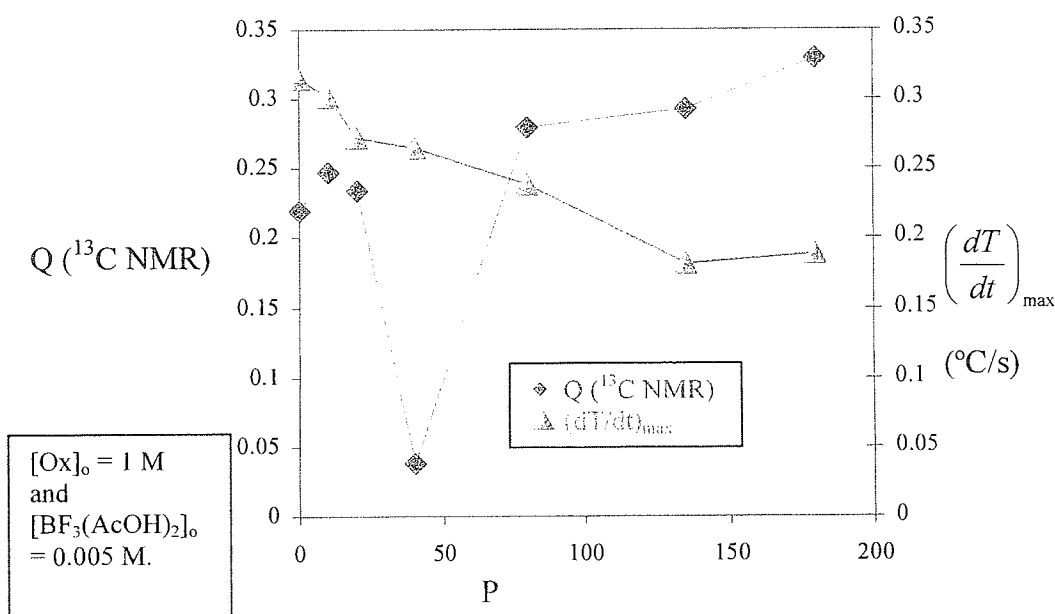


Figure 4. 5: Evolution of Q and $(dT/dt)_{\text{max}}$ with the increase of concentration of dpe. Polymerisation carried out in DCM at 35°C using an equimolar solution of $\text{BF}_3(\text{AcOH})_2/\text{BF}_3\text{OEt}_2$ as initiating system.

In all experiments, the presence of dpe did not affect the polymerisation in term of \overline{Mn} and $\overline{Mw}/\overline{Mn}$ even when the formation of cyclic oligomers was enhanced at $P \geq 80$ (see figure 4.16). This can only be explained if the growing centres are in the form of stable “dormant” species and that the cyclic oligomer formation occurs mostly by end-biting reactions. The decrease of the rate at which the monomer is initially incorporated into the polymer chain suggests even more strongly that dpe end-caps the growing centre during the course of the polymerisation.

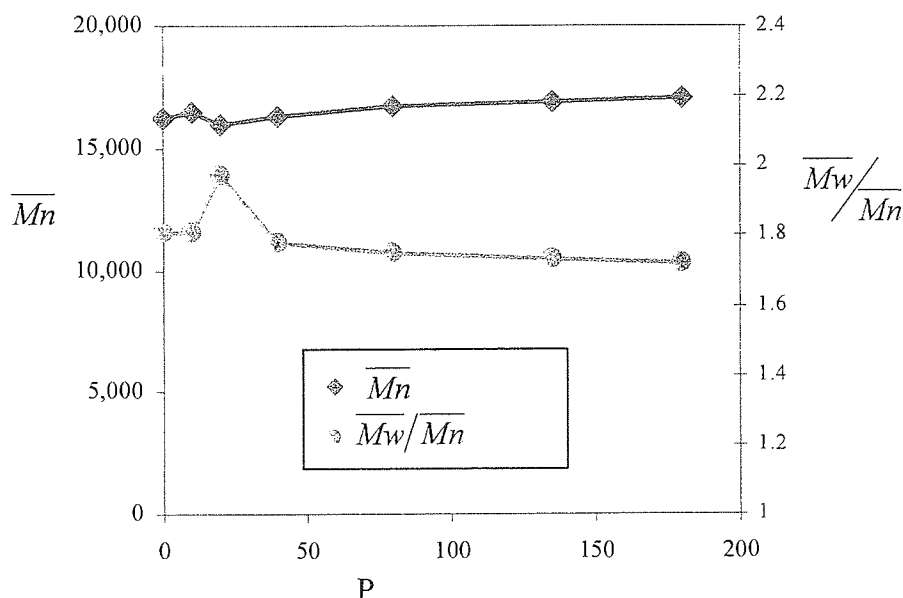


Figure 4. 6: Evolution of \overline{Mn} and $\overline{Mw}/\overline{Mn}$ with the increase of the ratio $[dpe]_0/[Ox]_0$. Polymerisation carried out in dichloromethane at 35 °C using an equimolar solution of $BF_3(AcOH)_2/BF_3OEt_2$ as initiating system. $[Ox]_0 = 1$ M and $[BF_3(AcOH)_2]_0 = 0.005$ M.

Series	P	R	Rate °C/s	\overline{Mn} g/mol	Mp g/mol	$\overline{Mw}/\overline{Mn}$	Conversion %	Q ¹³ C NMR
S 6.9	0	0	0.315	16,250	28,600	1.81	53.3	0.22
S 14.1 ⁽¹⁾	10	0.04	0.301	16,450	30,400	1.81	52.5	0.248
S 14.2 ⁽¹⁾	20	0.08	0.273	16,000	32,000	1.97	48.4	0.225
S 14.3 ⁽¹⁾	40	0.16	0.265	16,300	28,900	1.78	43.8	0.038
S 14.4 ⁽¹⁾	80	0.32	0.238	16,750	29,300	1.75	(2)	0.28
S 14.5 ⁽¹⁾	135	0.54	0.181	16,900	30,200	1.73	(2)	0.293
S 14.6 ⁽¹⁾	180	0.72	0.189	17,100	29,800	1.72	(2)	0.329

(1) method 1.

(2) remaining dpe on the polyoxetane materials.

$P = [dpe]/([BF_3(AcOH)_2] + [BF_3:OEt_2])$ and $R = [dpe]/[oxetane]$.

$Q_{13C\ NMR} = \text{Area}\{\text{cyclic}(-C-O-)\}/\text{Area}(\text{cyclic}(-C-O-) + \text{linear}(-C-O-))$.

Table 4. 4: Effect of diphenyl ether on the cationic polymerisation of oxetane in dichloromethane at 35 °C using an equimolar solution of $BF_3(AcOH)_2/BF_3OEt_2$ as initiating system. $[Ox]_0 = 1$ M and $[BF_3(AcOH)_2]_0 = 0.005$ M.

4.2.1 Discussion

From comparison of the nucleophilicity of the different components present in the solution during the polymerisation, it appears that the hydroxyl end group formed during the initiation process, -OH, is more nucleophilic than the oxygen atom of the oxetane molecule which in turn is both more nucleophilic than the oxygen atom present in the back-bone of the polymer chain and that in the macrocyclic oligomers. Because the non-bonding electron of the oxygen atom can be delocalised in the phenyl group, dpe is believed to be the weakest nucleophilic reagent:

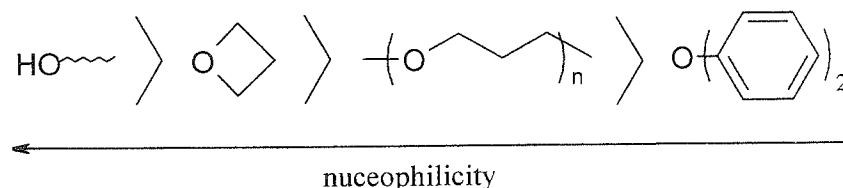
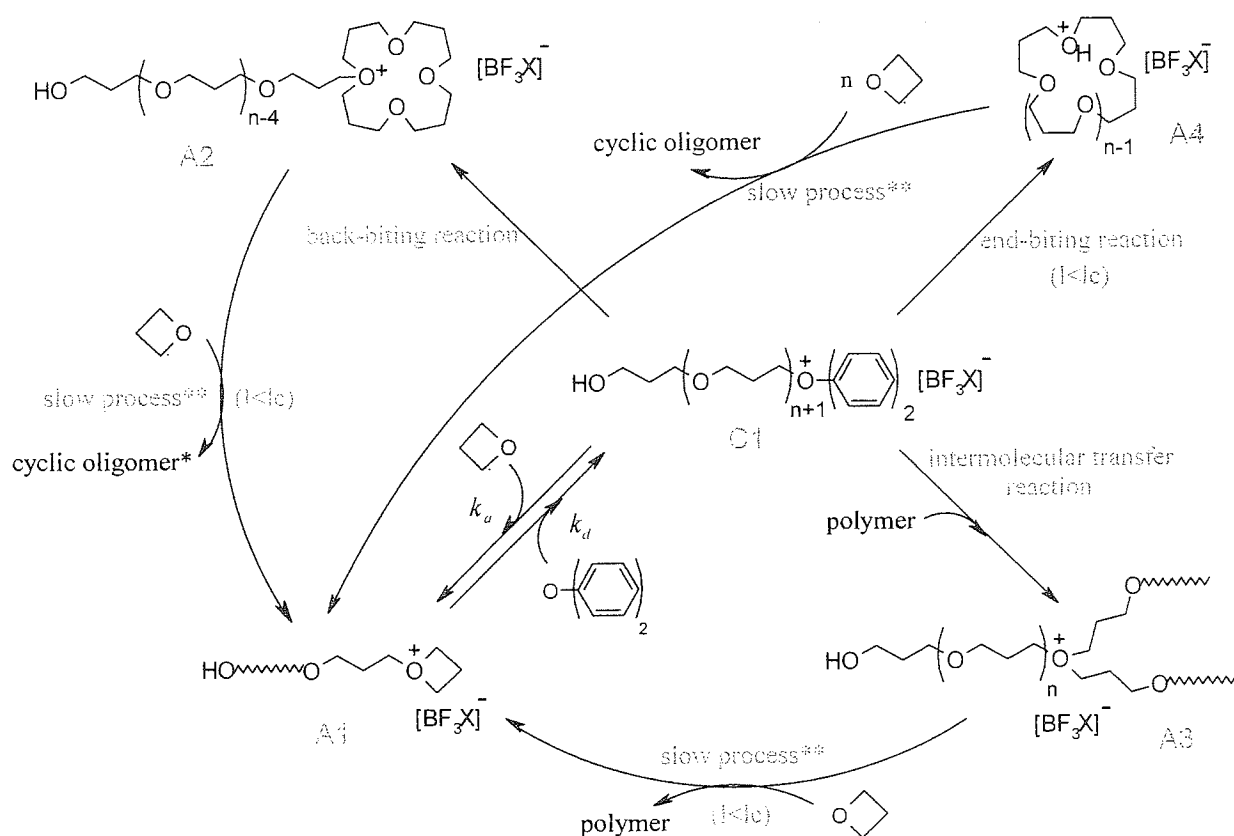


Figure 4. 7: Basicity of different nucleophilic reagents in the polymerisation medium.

Therefore, at $P = 40$ or $R = 0.16$, the reduction in cyclic oligomer formation observed when 50 % of monomer was consumed, suggests that the concentration of dpe is sufficiently high to end-cap the growing centre before that the reactions of cyclic oligomer formation starts to occur. At higher concentration ($P > 80$ or $R > 0.32$), the enhancement of cyclic oligomer formation can only be explained if the “dormant” polymer chain, C1, bearing a hydroxyl end group, undergoes an end-biting reaction rather than to undergo propagation, back-biting and/or intermolecular transfer reactions. Indeed, the life time of the growing centre before to be end-capped by dpe, τ , becomes shorter as the concentration of dpe increases (see equation E: 4.8),

$$\tau = \frac{[R^+, X^-]}{R_d} = \frac{1}{k_d \cdot [dpe]_0} \quad \text{E: 4.8}$$

This makes the length (noted l) of the resulting “dormant” polymer chains shorter once end-capped by dpe. As the chain length increases, the entropy factors disfavour the end-biting reaction in favour of back-biting and intermolecular transfer reactions.



X = -OH, -OOCCH₃.

R = -H, COCH₃, -C₂H₅.

* If oxetane attack the endocyclic electron deficient carbon.

** The oxonium sites are sterically hinder.

Figure 4. 8: Mechanism of polymerisation of oxetane in the presence of dpe in DCM at 35 °C. Polymerisation initiated by an equimolar solution of $\text{BF}_3(\text{AcOH})_2/\text{BF}_3\text{OEt}_2$.

Because the back-biting reaction produces linear polymer chains with a macro cyclic oxonium ion site, A2, we believe that the proportion of cyclic oligomers issue from back-biting reactions increases as the length of the lateral chains decreases. Indeed, the lateral chain can sterically hinder the attack of the exocyclic electron deficient α -carbon with respect to the oxonium site. This steric hindrance is believed to be significantly reduced as the length of the lateral chain decreases. Therefore, the proportion of cyclic oligomer produced by back-biting or end-biting reaction is then dependent on the ratios $[\text{Ox}]/t/[(\text{oxetane})\text{H}^+]/t$ and $[\text{Ox}]/t/[\text{dpe}]/t$. The end-biting reaction is more favour as the above both ratio decreases. This supposes that for a given concentration of dpe, the formation cyclic oligomers is firstly enhanced by a back-biting reaction and then by an end-biting reaction as the concentration of

oxetane decreases in the polymerisation medium. These suppose also that there is a critical chain length below which the formation of cyclic oligomer is enhanced.

It is interesting to note that the reactivation of the dormant species (C1) by a molecule of oxetane does not induce a redistribution of molecular weight of the produced active growing centre (A1).

4.3 Conclusions

The effect of ether additive on the cationic ring-opening polymerisation of oxetane was studied at 35 °C in dichloromethane using 1 M of oxetane and 0.008 M of initiator ($\text{BF}_3(\text{CH}_3\text{COOH})_2/\text{BF}_3\text{OEt}_2$ or BF_3MeOH). This study showed that the addition of ether additives can affect differently the polymerisation depending on the nature of the additives and depending on the method used to add the additive.

When diphenyl ether was used as additives (according to the method 2), the cyclic oligomer formation was reduced only for $[\text{Ox}]_0/[\text{Dpe}]_0 = 40$. Because the rate of monomer consumption decreased as the concentration of dpe was increased, the addition of dpe is believed to end-cap the growing centre. The enhancement of cyclic oligomer formation observed when $40 < [\text{Ox}]_0/[\text{Dpe}]_0 < 180$, indicates that it exists a critical chain length below which the “dormant” polymer chain (end-capped by dpe) produces a large proportion of cyclic oligomers by intramolecular transfer reactions. Because the hydroxyl end group is the stronger nucleophilic reagent in the polymerisation medium, the end-biting reactions is believed to be the main source of formation of cyclic oligomers. Back-biting reactions are also believed to produce cyclic oligomers if, Dp of the lateral chain is not too high to sterically hinder the accessibility of the oxonium site by a molecule of monomer. For this reasons, high molecular weight polymer chains that undergo transfer reactions are believed to have a longer life time than the shorter one. This could explain why \overline{Mn} and $\overline{Mw}/\overline{Mn}$ of the produced high molecular weight do not change as the concentration of dpe increases in the polymerisation medium. Because of the steric hindrance, it cannot be excluded that the high molecular weight polymer in the formed of “dormant” species undergo forward on intramolecular chains rearrangements.

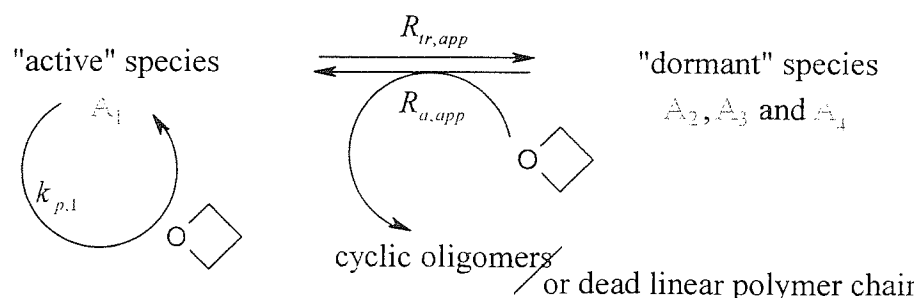
When dbce was used as additive, the cyclic oligomer formation was slowed down only when dbce and protonic reagents ($\text{BF}_3(\text{AcOH})_2/\text{BF}_3\text{OEt}_2$ (1/1) or BF_3MeOH) were mixed in dichloromethane and then injected into the monomer solution (method 2). For this respect, dbce is believed to act as co-initiator. Because the use of dbce/ BF_3MeOH slows down the initial rate of monomer consumption, the complexation of H^+ within the crown-ether is believed to sterically hinder the protonation of molecules of monomer. The direct consequence of this is that only a fraction of initiating species, BF_3MeOH , initially initiates the polymerisation. This is believed to be responsible of the reduction of cyclic oligomers formation during the first 82 % monomer conversion due to the formation of high molecular weight materials before transfer reactions occur. Because the rate of initiation is slow in relation to the rate of monomer consumption, this is believed to be responsible for the enhancement of the formation of cyclic oligomers. Indeed, in starving monomer conditions, the protonation of the monomer by $[\text{F}_3\text{BX}]^+;(\text{dbce})\text{H}^+$ produces growing polymer chain with hydroxyl end group that undergoes end-biting rather than to propagation. This can be visualised by the fact that the enhancement of cyclic oligomers does not significantly decrease the M_n of the high molecular weight. The slightly decrease of \overline{M}_n shows that back-biting reactions only produce a small proportion of cyclic oligomers. In the case of $\text{BF}_3(\text{AcOH})_2/\text{BF}_3\text{OEt}_2$ (1/1) was used as initiating system, the reduction of cyclic oligomers did not induce a significant change in the initial rate of monomer consumption. This is believed to be due to the existence of alkylating and acylating reactive species. Because veratrole did not affect the polymerisation of oxetane when used as co-initiator, this reinforces the idea that dbce binds the proton inside the crown-ether. Further investigation showed that dbce can be incorporated into the polymer when used as co-monomer.

5 CHAPTER 5

**From uncontrolled to control and then
“quasiliving” cationic *ring-opening*
polymerisation (C.R.O.P) of oxetane by
activation chain-end (A.C.E) mechanism**

5.1 Introduction

In the chapter 3, we saw that when oxetane is polymerised at 35 °C in dichloromethane by cationic initiation, the growing centres coexist in the form of “active” and “dormant” species. Indeed, as the polymerisation proceeds, the oxygen atom in the backbone can attack the growing centres via an S_N2 mechanism converting the strained tertiary oxonium ions (“active” species, A1) into less reactive growing centres (“dormant” species), respectively acyclic (A4) and non-strained cyclic (A2 and A3) oxonium ions as the side reactions occur by inter- or intramolecular transfer reactions (see figure 3.4). The polymerisation is then a non-living reaction. Because the second addition of a monomer solution to an active polymer solution restarts the polymerisation with the expected initial rate of monomer consumption (see section 3.1.3), termination reactions are believed to don’t occur significantly during the polymerisation process. Consequently, the curvature of the slope when $\ln([Ox]_0/[Ox]_t)$ was plotted against time can only be explained if the fraction of “dormant” species increases as the monomer is consumed. Knowing that oxetane and the hydroxyl tail group are the stronger nucleophilic reagents in the polymerisation medium, the activation of the “dormant” species is believed to occur by nucleophilic attack of the oxonium site by the oxygen atom of oxetane via an S_N2 mechanism. In this respect, “active” (strained tertiary oxonium ions) and “dormant” (acyclic and non-strained oxonium monomer ions) species are believed to be in equilibrium throughout the polymerisation. Therefore, the cationic ring-opening polymerisation of oxetane in dichloromethane at 35 °C can then be schematised as follow:



A1: mono- and/or α,ω -functionalised “active” species.

Figure 5. 1: Mechanism of the cationic polymerisation of oxetane.

where $k_{p,1}$, is the rate constant at which the monomer is consumed by the “active” species (A1), $R_{tr,app}$ is the apparent rate at which transfer reactions occur and $R_{a,app}$ is the apparent rate which “dormant” species (A2, A3 and A4) are converted into “active” species (A1). As illustrated in the figure 5.1, cyclic oligomers are formed during the reactivation of the “dormant” species when the oxygen atom of an oxetane molecule attacks the endocyclic electron deficient carbon atoms in the α -position with respect to the oxonium site (A2 and A3, see figure 3.5). Similarly, dead polymer chains can also be produced if the reactivation of the acyclic tertiary oxonium ions produces an α - γ growing polymer chains.

5.1.1 Concept of quasiliving and controlled polymerisation

Polymerisation reactions with formation of “dormant” and “active” species are often used in non-living polymerisation to suppress or to reduce side reactions from occurring.

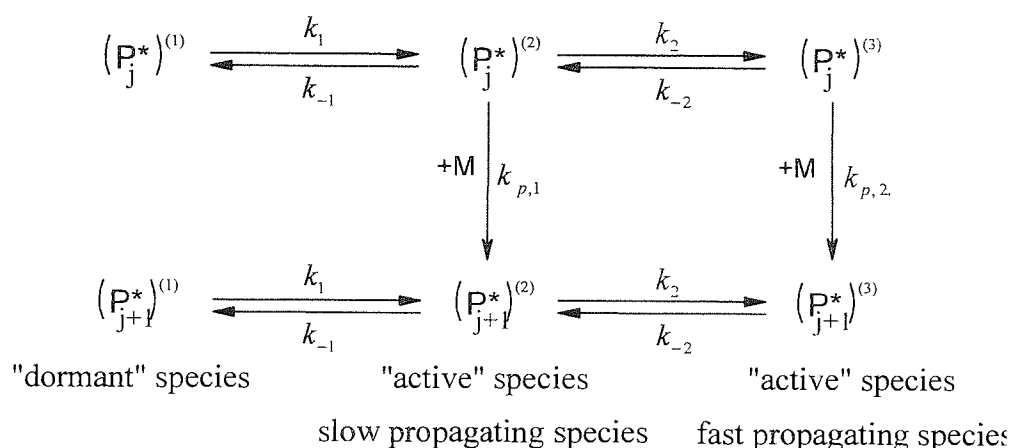


Figure 5. 2: Scheme of polymerisation process where “dormant” and “active” species are in dynamic equilibrium.

This concept of polymerisation predicts that in system where a dynamic equilibrium exists between “active” and “dormant” species control over \overline{Mn} and $\overline{Mw}/\overline{Mn}$ can be achieved throughout the polymerisation if the rate constant of interconversion, k_i and k_{-i} are much larger than the rate $k_{p,i} \times [M]$. Under such conditions the effect on the MWD is negligible and the ratio P_w/P_n is almost identical to a Poisson distribution [45, 299-305].

$$U_{app} \approx U_{pois} = \frac{P_w}{P_n} - 1 = \frac{P_n - 1}{P_n^2} \quad \text{E: 5.1}$$

The polymerisation is called “quasiliving” if irreversible terminations and transfer to the monomer, polymer, solvent and initiator are suppressed during the entire course of the polymerisation. If the rate of interconversion is comparable to those of propagation, the polymerisation leads to a broadening of MWD and the apparent distribution or the experimental non-uniformity parameter is then composed of Poisson distribution, U_{app} , and an excess value stemming from interconversion^[302,305]:

$$U_{app} = U_{pois} + \sum_{i=1}^n U_{i,i+1} \quad \text{E: 5.2}$$

5.1.1.1 Quasiliving polymerisation and its development

The concept of the so-called quasiliving polymerisation was approached by Kennedy, Faust, Fehervary, Kelen and Tudos in the early 1980's in the case of the cationic polymerisation of vinylic monomers[306-308]. They showed that in a system where a dynamic equilibrium exists between “active” and “dormant” species, irreversible termination and transfer to the monomer can be avoided by keeping the monomer concentration low

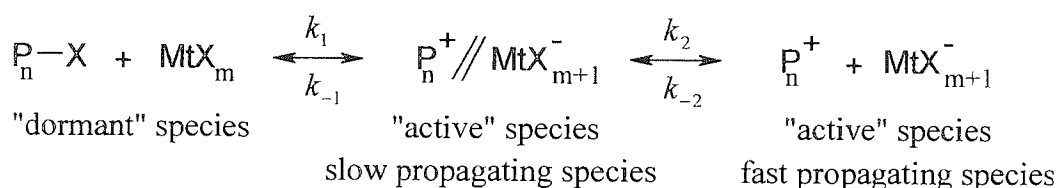


Figure 5. 3: Nature of the growing centres on the quasiliving polymerisation of vinylic monomers.

Using a continuous addition of monomer, Puskas and Kovas were able to control at low temperature the polymerisation of styrene, para-t-butylstyrene^[309] and isobutylene^[310,311] over \overline{Mn} and $\overline{Mw}/\overline{Mn}$. Sawamoto^[312,313] reported the quasiliving polymerisation of vinyl ether and methyl vinyl ether by 1,4-di(2-chloro-isopropyl) benzene (dicumylchloride)/AgSbF₆ at -70 °C. \overline{Mn} increases linearly, and molecular weight polydispersity of 1.4-1.7 were obtained. Sawamoto explained the broad molecular weight distributions in these polymerisations by the coexistence of various active species such as ion pairs and free ions, which were believed to have very different reactivities. If the “truly” living character of the so-called quasiliving polymerisation is still debated in some cases, the development of this concept turned out to

be a powerful method to control or to improve the control of polymerisation of various monomers by ionic and radical polymerisations. For example the cationic polymerisation of vinyl ethers initiated by $(C_2H_5)_3AlCl_2$ and a cationogen, e.g. water, is a non-living reaction. The polymerisation is claimed to exhibit a "living" character on the addition of an excess of an ester, such as ethyl acetate^[314,315] or ethyl benzoate^[316], or an ether, for example diethyl ether, THF, THP, oxepane or dioxane^[315,317-319]. The ester or ether combines with the active centre to produce an unreactive oxonium ion which is in rapid equilibrium with the propagating carbocation, as shown in figure 5.4. The rapid interconversion between the different ions is believed to be responsible of the "living character" of the polymerisation.

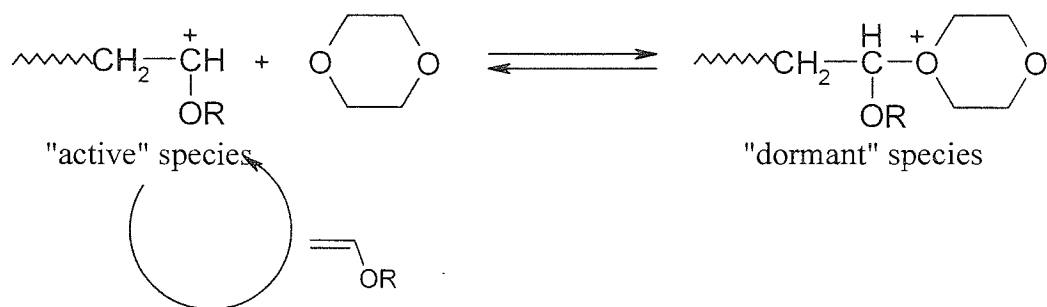


Figure 5. 4: Formation of an oxonium ion in the polymerization of vinyl ethers initiated by $Al(C_2H_5)_3$ in the presence of 1,4-dioxane.

Similarly, the radical polymerisation of vinylic monomers[39] can also be controlled when performed in the presence of an additive such as iniferter[40], persistent radical[41], xanthate[44] and organometallic[42,43]. The general principle of the controlled radical polymerisation is based on the idea of decreasing the probability that two radicals have to disproportionate or to undergo coupling reactions by reversibly converting the largest proportion of the growing radicals into "dormant" species. The rapid interconversion between "dormant" and "active" species gives rise to the propagating species of a very short lifetime reducing the probability of chain breaking reactions occurring.

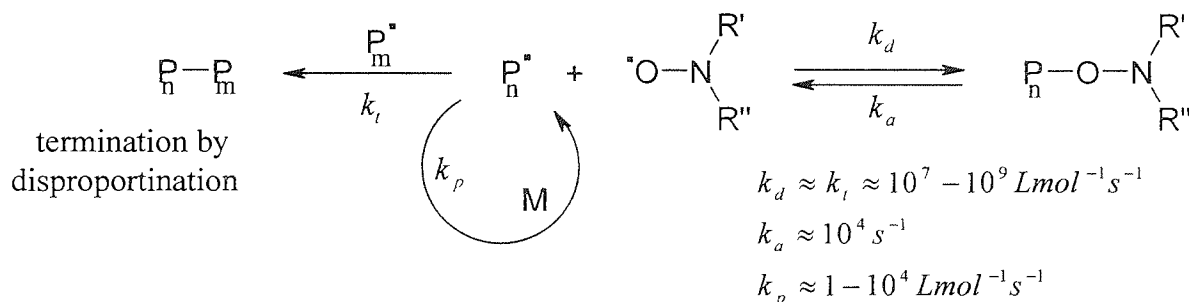


Figure 5. 5: Control radical polymerisation of vinylic monomer in the presence of nitroxide (persistent radical).

5.1.1.2 Controlled polymerisation as a non-living process

In comparison with living polymerisation, a “quasiliving” polymerisation can be defined as a process characterised by the absence of transfer and irreversible termination reactions. Therefore, if one of these two conditions does not apply, the polymerisation process can then be classified as “uncontrolled” polymerisation. However, under certain circumstances, when the initiation is fast in comparison to propagation, when the rate of interconversion of the coexisting species are much larger than rate of propagation and when short D_p are targeted, a “non quasiliving” system can still appear to be “quasiliving” if side reactions are sufficiently reduced to observe a linear increase of \overline{Mn} with conversion and the formation of polymer with a narrow average molecular weight distribution. These “non-quasiliving” polymerisations are then called “controlled” or “pseudoliving” polymerisations. This is the case of the so-called “controlled radical polymerisation” (see figure 5.5) for which irreversible terminations reactions cannot be suppressed but only reduced. This is due to the fact that reversible and irreversible terminations reactions are both diffusion controlled ($k_t \approx k_d \approx 10^7 - 10^9 M^{-1}s^{-1}$ see figure 5.5) and therefore compete during the entire course of the polymerisation. In this respect, if p_t represents the probability that radicals undergo chain breaking reactions

$$p_t = \frac{R_t}{R_t + R_d} = \frac{1}{1 + \frac{k_d}{k_t} \cdot \frac{[T]}{[R^\bullet]}} \approx \frac{1}{1 + \frac{[T]}{[R^\bullet]}} \quad \text{E: 5.3}$$

the equation E: 5.3 shows that irreversible termination reactions can be suppressed by adding a large excess of additive, T. Unfortunately, the chemoselectivity of the free radical polymerisation ($k_p \approx 1 - 10^4 M^{-1}s^{-1}$ and $k_t \approx k_d \approx 10^7 - 10^9 M^{-1}s^{-1}$) obliges us to favour the propagation over termination ($R_p > R_t$) which exclude the term of “living radical polymerisation” and imposes the term of “controlled radical polymerisation”. Here k_d and k_t represent the rate constant at which the growing radical, R^\bullet , are respectively reversibly and irreversibly terminated. $[T]$ represents the concentration of the deactivating reagents (here nitroxide).

5.1.2 Idea of controlling the polymerisation of oxetane

In the chapter 3, we show that if the use of $[\text{SbF}_6]^-$ as counter-anion reduced significantly transfer reactions (back-biting reactions) from occurring, it did not permit control over \overline{M}_n and $\overline{M}_w/\overline{M}_n$. Because terminations reactions do not seem to occur during the polymerisation process, the use of an additive that can end-cap reversibly the growing centres seem to us to be an alternative to prevent transfer reactions from occurring and consequently to control the polymerisation during the entire course of the polymerisation.

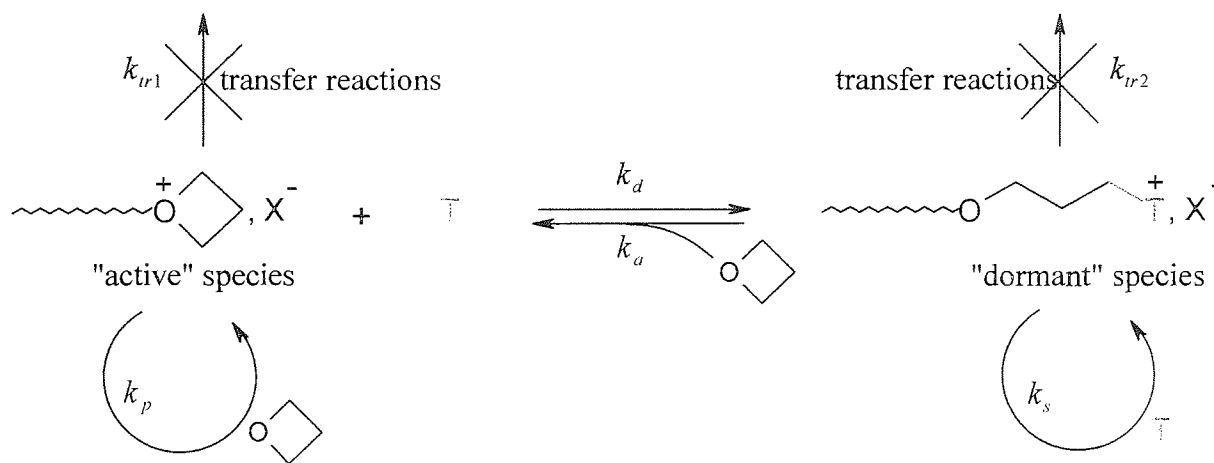


Figure 5. 6: Formation of dormant species in quasiliving polymerisation of oxetane in the presence of additive T

As illustrated in the figure 5.6, the principle of the control of the polymerisation is based on the idea of decreasing the probability that the oxygen atoms in the polymer have to attack the growing species by converting the “active” species into “dormant” species. To achieve such equilibrium in which the “dormant” species is activated by a molecule of monomer, the additive has to fulfil three requirements. Firstly, the monomer has to be more basic than the additive otherwise the growing polymers chains will be irreversibly terminated by the additive when $R_s > R_a$. Secondly, to compete efficiently with transfer reactions ($R_d \gg R_{tr1}$ and $R_s \gg R_{tr2}$), the additive has to be more nucleophilic than the oxygen atom in the backbone of the polymer chains. Moreover, because the rate of transfer reactions increases as the polymerisation progress, the additive will probably have to be used as solvent. This third requirement implies that the additive must have a low boiling point to enable the purification

using trap-to-trap method. Indeed, rigorous drying precautions are necessary in cationic polymerisation and therefore the stability of the solvent over calcium hydride (CaH₂) and/or sodium benzophenone mixture are crucial for the achievement of “living” polymerisation.

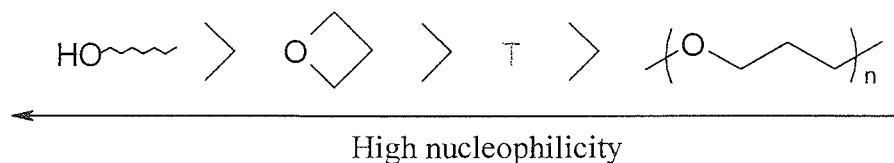


Figure 5. 7: Nucleophilicity order of oxygen atom in the polymer and monomer.

However, as for *controlled radical polymerisation*, this is the chemoselectivity of the cationic ring-opening polymerisation of oxetane by A.C.E mechanism that will be the determinant factor to classify the system as *quasiliving* or *controlled* polymerisation process.

5.1.2.1 Chemoselectivity of the CROP of oxetane in the presence of ether additive by ACE mechanism

5.1.2.1.1 Solvation-desolvation effect

In 1971, Saegusa et al.^[320] later showed that at low temperature ($T < -20\text{ }^{\circ}\text{C}$) where transfer reactions are significantly reduced, the transition-state theory could be used to calculate the activation parameter that kinetically controls ring-opening process involved in the cationic polymerisation of oxetane and oxetane derivative monomers. This theory predicts^[321] that k_p can be expressed by

$$k_p = \frac{k^* T}{h} \exp\left(-\frac{\Delta F^\ddagger}{RT}\right) \quad \text{E: 5.4}$$

where k^* is the Boltzmann constant, h is the Plank constant and

$$\Delta F^\ddagger = \Delta H^\ddagger - T\Delta S^\ddagger \quad \text{E: 5.5}$$

The combination of these two equations after rearrangement leads to the Arrhenius equation

$$k_p = A^\ddagger \exp\left(-\frac{\Delta E^\ddagger}{RT}\right) \quad \text{E: 5.6}$$

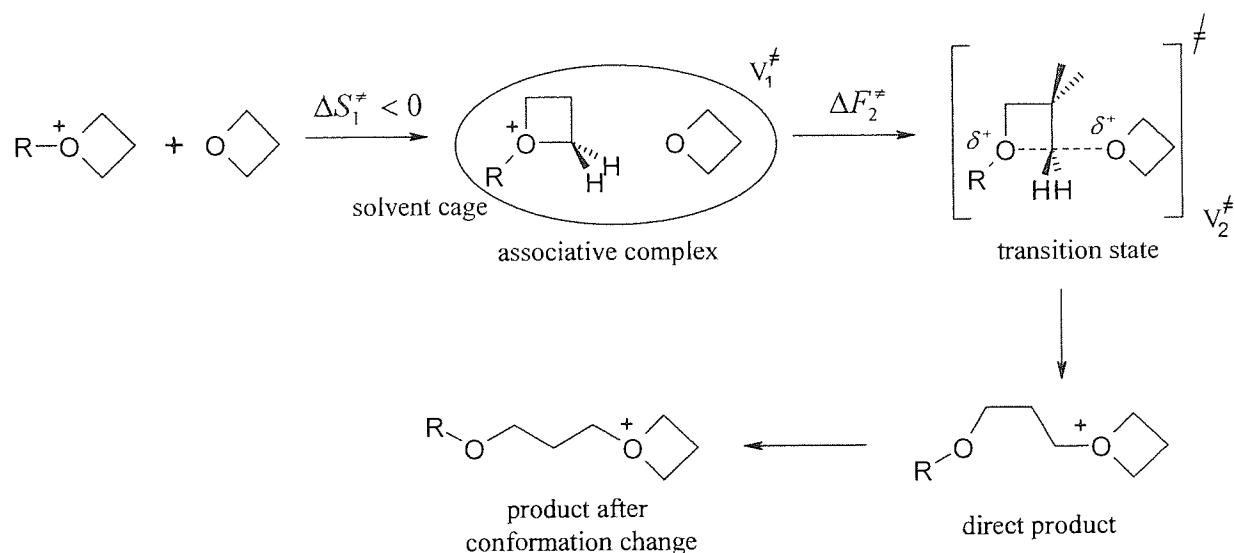
from which the frequency factor

$$A^\ddagger = \frac{k^* T}{h} \cdot e \cdot \exp\left(\frac{\Delta S^\ddagger}{R}\right) \quad \text{E: 5.7}$$

and the activation energy

$$\Delta E^\ddagger = \Delta H^\ddagger - RT \quad \text{E: 5.8}$$

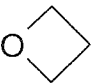
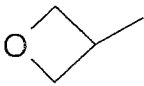
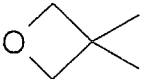
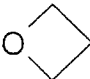
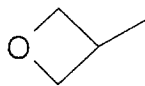
can be obtained if the plot of $\log(kp)$ against $1/T$ exhibits a linear dependence. As schematised in the figure 5.8, ΔE^\ddagger (or enthalpy activation energy, ΔH^\ddagger) is believed to represent the energy required for the system to enable the reactions to occur once the reactants formed an associative complex while, entropy, ΔS^\ddagger , is understood as the energy required for the two solvated reactants (oxonium ions and nucleophilic reactant) separated by an infinite distance to form an associative complex within the variation of the activation volume of the solvent cage during the transition state ($V_2^\ddagger - V_1^\ddagger$) is also taken into account. In the case of the ring-opening reactions, it is generally accepted that ΔE^\ddagger depends only on the ring strain of the oxonium site and on the nucleophilicity of the attacking group^[322-324].



This diagram is based on the computational study (AM1) performed by Sasaki et al. on the photoinitiated cationic ring-opening polymerisation of oxetane derivative monomers [325].

Figure 5. 8: Reaction diagram of the second initiation stage of oxetane through S_N2 mechanism.

Saegusa et al.^[322] studied the ring-opening homopolymerisation of unsubstituted, 3-methyl, and 3,3-dimethyloxetane and showed that the introduction of methyl into the oxetane ring increased the rate of polymerisation. According to the authors this result cannot be explained in terms of ring strain (ΔF^*) and basicity ($\Delta\nu_{OD}$). Indeed, the examination of the activation parameter showed that the substitution of the methyl group decreased the negative value of the activation entropy (favourable for the k_p increases) whereas it increased the activation enthalpy (unfavourable for the k_p). Though the ring strain and the basicity of the monomer are important factors determining the reactivity ratios of the cationic ring-opening copolymerisation of cyclic ether^[326,327], this kinetic studies strongly indicated that the activation entropy is the more influential parameter in the cationic ring-opening homopolymerisation of oxetane and oxetane derivatives monomers. Among the various kinds of factors that can be considered to interpret this finding, the solvation-desolvation effect seems, according to the authors, the most plausible explanation.

Solvent	Methylcyclohexane			Dichloromethane	
Monomer					
ΔF (kcal/mol) ^a	21.5	17.7	14.0	21.5	17.7
$\Delta\nu_{OD}$ (cm ⁻¹) ^b	103	106	99	103	106
k_p at -20 °C (L/(mol.sec))	0.18	0.92	3.4	0.019	0.11
ΔE^* (kcal/mol)	11.2	11.8	12.6	14.2	16.1
A_p (L/(mol.sec))	1.3×10^9	1.5×10^{10}	2.3×10^{11}	5.3×10^{10}	8.3×10^{10}
ΔF^* (kcal/mol)	15.4	14.7	14.2	17.0	15.7
ΔH^* (kcal/mol)	10.7	11.3	12.1	13.7	15.6
ΔS^* (e.u)	-18.6	-14.6	-8.5	-12.1	-1.3

a) Measure of the ring strain, ΔF , taken from the reference 328. The value of cyclobutane, methycyclobutane and 1,1-dimethylcyclobutane was used for oxetane, 3-methyloxetane and 3,3-dimethyloxetane.

b) Basicity determined by FTIR spectroscopy based on the variation of ν_{OD} of methanol-o-d in benzene and ν_{OD} of methanol-o-d and monomer in benzene. $\Delta\nu_{OD} = \Delta\nu_{OD}(\text{benzene}) - \Delta\nu_{OD}(\text{monomer})$. The basicity increases with the increase of $\Delta\nu_{OD}$.

Table 5. 1: Kinetic parameters of polymerisation in methylcyclohexane and dichloromethane solution taken from the reference 322.

Saegusa et al.^[322] studied the ring-opening homopolymerisation of unsubstituted, 3-methyl, and 3,3-dimethyloxetane and showed that the introduction of methyl into the oxetane ring increased the rate of polymerisation. According to the authors this result cannot be explained in terms of ring strain (ΔF^\ddagger) and basicity ($\Delta \nu_{OD}$). Indeed, the examination of the activation parameter showed that the substitution of the methyl group decreased the negative value of the activation entropy (favourable for the k_p increases) whereas it increased the activation enthalpy (unfavourable for the k_p). Though the ring strain and the basicity of the monomer are important factors determining the reactivity ratios of the cationic ring-opening copolymerisation of cyclic ether^[326,327], this kinetic studies strongly indicated that the activation entropy is the more influential parameter in the cationic ring-opening homopolymerisation of oxetane and oxetane derivatives monomers. Among the various kinds of factors that can be considered to interpret this finding, the solvation-desolvation effect seems, according to the authors, the most plausible explanation.

thane



Aston University

Content has been removed for copyright reasons

Table 5. 1: Kinetic parameters of polymerisation in methylcyclohexane and dichloromethane solution taken from the reference 322.

It is interesting to note that the decrease of k_p with the increase of the polarity of the solvent is compatible with an S_N2 mechanism of propagation.

5.1.2.1.2 Chemoselectivity of the cationic ring-opening reaction of oxetane

In chapter 4, we showed that in dichloromethane at 35 °C, the reactivity of the strained oxonium ions towards the ring-opening reaction depends more on the strain contained in the ring than on the nucleophilicity of the attacking group, while the reactivity towards S_N2 reactions of “dormant” species originating from transfer reactions depend exclusively on the nucleophilicity of the attacking group. Therefore for the quasiliving system described in the scheme 5.6, if we consider the nucleophilicity of the reactants (oxetane, cyclic ether additive and acyclic ether) it appears then that

$$k_p > k_d > k_{tr1(int\ er)} \quad \text{E: 5.9}$$

and

$$k_p > k_a > k_s > k_{tr2(int\ er)} \quad \text{E: 5.10}$$

In the case of back-biting reactions, the comparison of $k_{tr(int\ ra)}$ with $k_{tr(int\ er)}$ is a bit tricky knowing that the entropy factor can contribute to the enhancement of $k_{tr(int\ ra)}$. This implies that

$$k_{tr1(int\ ra)} \geq k_{tr1(int\ er)} \quad \text{E: 5.11}$$

and

$$k_{tr2(int\ ra)} \geq k_{tr2(int\ er)} \quad \text{E: 5.12}$$

Considering the findings of Saegusa et al, it seems to us that the achievement of quasiliving polymerisation could be possible if the additive is used as solvent. The idea here is to surround the growing centres (“active” and “dormant” species) with molecules of additive in order to compete more efficiently with transfer reactions, particularly back-biting reactions.

Indeed, if the ring-opening reaction is kinetically controlled by solvation-desolvation effects, the used of the additives as solvent should strongly affect the reactivity of the reactions occurring, particularly back-biting reactions. Knowing that basicity and ring strain of a cyclic ether play a significant role in the copolymerisation reactivity ratio, it can be expected that if the additive is use as solvent

$$k_d > k_{tr1(int\ er)} \approx k_{tr1(int\ ra)} \quad \text{E: 5.13}$$

and

$$k_p > k_a > k_s > k_{tr2(int\ er)} \approx k_{tr2(int\ ra)} \quad \text{E: 5.14}$$

Therefore, if R_{tr1} ($\text{L.mol}^{-1}.\text{s}^{-1}$) and R_{tr2} ($\text{L.mol}^{-1}.\text{s}^{-1}$) denote respectively the rate at which “active” (R^+, X^-), and “dormant” (RT^+, X^-) species undergo transfer reactions, the rate at which living i-mer undergo transfer reactions, R_{tr} ($\text{L.mol}^{-1}.\text{s}^{-1}$), can be expresses as follow

$$R_{tr} = R_{tr1} + R_{tr2} \quad \text{E: 5.15}$$

where

$$R_{tr1} = k_{tr1} \cdot [R^+, X^-] \cdot \{[Ox]_0 - [Ox]_t\} \quad \text{E: 5.16}$$

and

$$R_{tr2} = k_{tr2} \cdot [RT^+, X^-] \cdot \{[Ox]_0 - [Ox]_t\} \quad \text{E: 5.17}$$

with

$$k_{tr1} \approx k_{tr1(int\ ra)} \approx k_{tr1(int\ er)} \quad \text{E: 5.18}$$

and

$$k_{tr2} \approx k_{tr2(\text{int } ra)} \approx k_{tr2(\text{int } er)} \quad \text{E: 5.19}$$

Here k_{tr1} ($\text{L.mol}^{-1}.\text{s}^{-1}$) and k_{tr2} ($\text{L.mol}^{-1}.\text{s}^{-1}$) are the rate constants at which the oxygen in the polymer attack R^+, X^- and RT^+, X^- respectively. $\{[Ox]_0 - [Ox]_t\}$ represents the concentration of monomer consumed during the polymerisation. Knowing that

$$\text{conversion} = \frac{[Ox]_0 - [Ox]_t}{[Ox]_0} \quad \text{E: 5.20}$$

the combination of E: 5.15, E: 5.16, E: 5.17 and E: 5.20 leads to

$$R_{tr} = (k_{tr1} \cdot [R^+, X^-] + k_{tr2} \cdot [RT]_t) \cdot [Ox]_0 \cdot \text{conversion} \quad \text{E: 5.21}$$

Similarly, if R_d ($\text{mol.L}^{-1}.\text{s}^{-1}$) and R_s ($\text{mol.L}^{-1}.\text{s}^{-1}$) represent the rate at which the additive T reacts with R^+, X^- and RT^+, X^- , respectively

$$R_d = k_d \cdot [R^+, X^-] \cdot [T]_0 \quad \text{E: 5.22}$$

and

$$R_s = k_s \cdot [RT^+, X^-] \cdot [T]_0 \quad \text{E: 5.23}$$

Here k_d ($\text{L.mol}^{-1}.\text{s}^{-1}$) is the rate constant at which R^+, X^- is deactivated by a molecule of monomer while k_s ($\text{L.mol}^{-1}.\text{s}^{-1}$) denotes the rate constant at which the additive that end-capped the growing centre is displaced by another molecule of additive. Knowing that R_a ($\text{L.mol}^{-1}.\text{s}^{-1}$) is the rate at which RT^+, X^- is converted to R^+, X^- , we have then

$$R_a = k_a \cdot [RT^+, X^-] \cdot [Ox]_t \quad \text{E: 5.24}$$

or

$$R_a = k_a \cdot [RT^+, X^-] \cdot [Ox]_0 \cdot (1 - \text{conversion}) \quad \text{E: 5.25}$$

The probability that the living i-mer undergoes transfer reactions is then given by the following two equations

$$p_{tr1} = \frac{R_{tr1}}{R_{tr1} + R_d} = \frac{1}{1 + \frac{R_d}{R_{tr1}}} = \frac{1}{1 + \frac{k_d}{k_{tr1}} \cdot \frac{[T]_0}{[Ox]_0} \cdot \frac{1}{\text{conversion}}} \quad \text{E: 5.26}$$

and

$$p_{tr2} = \frac{R_{tr2}}{R_{tr2} + R_a + R_s} = \frac{1}{1 + \frac{R_a}{R_{tr2}} + \frac{R_s}{R_{tr2}}} = \frac{1}{1 + \frac{k_s}{k_{tr2}} + \left(\frac{k_a}{k_{tr2}} \cdot \frac{[T]_0}{[Ox]_0} - \frac{k_s}{k_{tr2}} \right) \cdot \frac{1}{\text{conversion}}} \quad \text{E: 5.27}$$

As expected, the equations E: 5.26 and E: 5.27 show that the probability of the occurring transfer reactions increases throughout the polymerisation. However p_{tr} can be reduced by increasing the ratio $[T]_0/[Ox]_0$ when the additive is used as solvent. As previously explained, the “living” character of this quasiliving system strongly depends on the chemoselectivity of the polymerisation which is in favour of the propagation and reversible termination since

$$k_d > k_a > k_{tr1} \quad \text{E: 5.28}$$

and

$$k_p > k_a > k_s > k_{tr2} \quad \text{E: 5.29}$$

5.1.2.2 Prediction of the kinetic profile of the proposed “quasiliving” model

5.1.2.2.1 Rate of interconversion between “active” and “dormant” species

If R^+, X^- and RT^+, X^- denote respectively the living i-mer in the form of active and dormant species, the rate of interconversion between “dormant” and “active” species is then given by

$$-\frac{d[R^+, X^-]}{dt} = k_d \cdot [R^+, X^-] \cdot [T] - k_a \cdot [RT^+, X^-] \cdot [Ox] \quad \text{E: 5.30}$$

and

$$-\frac{d[R^+, X^-]}{dt} = \frac{d[RT^+, X^-]}{dt} \quad \text{E: 5.31}$$

Here, k_d ($\text{L.mol}^{-1}.\text{s}^{-1}$) denotes the rate constant of deactivation of R^+, X^- by the additive and k_a ($\text{L.mol}^{-1}.\text{s}^{-1}$) the rate constant at which RT^+, X^- is activated by a molecule of monomer. For such an ideal type of quasiliving system, the life time of the living i-mer in the form of dormant species, τ_{RT^+, X^-} , appears then to increase with a decrease of the concentration of monomer

$$\tau_{RT^+, X^-} = \frac{[RT^+, X^-]}{R_a} = \frac{1}{k_a \cdot [Ox]_0} \cdot \frac{1}{(1 - \text{conversion})} \quad \text{E: 5.32}$$

while the life time of the active growing centres before being deactivated by the additive is constant during the entire course of the polymerisation

$$\tau_{R^+, X^-} = \frac{[R^+, X^-]}{R_d} = \frac{1}{k_d \cdot [T]_0} \quad \text{E: 5.33}$$

The direct consequence of this is that the fraction of living i-mer in the form of dormant species increases as the polymerisation progress. This implies that

$$-\frac{d[R^+, X^-]}{dt} = \frac{d[R^+, X^-]}{dt} \neq 0 \quad \text{E: 5.34}$$

Thus, if K is a parameter representing the “equilibrium” between “active” and “dormant” species

$$K = \frac{[RT^+, X^-] \cdot [Ox]}{[R^+, X^-] \cdot [T]_0} \quad \text{E: 5.35}$$

the combination of the equations E: 5.30, E: 5.34 and E: 5.35 follows by the rearrangement of the resulting equations gives

$$K = \frac{k_a}{k_d} \cdot \left(1 + \frac{1}{k_d \cdot [R^+, X^-] \cdot [T]_0} \cdot \left(- \frac{d[R^+, X^-]}{dt} \right) \right) \quad \text{E: 5.36}$$

If we consider the equations 5.34 and 5.36, it appears then that the equilibrium between “active” and “dormant” species does not reach a steady state of their concentrations. Consequently K varies during the entire course of the polymerisation.

5.1.2.2.2 Kinetic profile of the proposed quasiliving polymerisation model

5.1.2.2.2.1 Fast initiation process

In a quasiliving system where the reactivation of “dormant” species occurs by incorporation of a molecule of monomer, the rate of monomer consumption is given by

$$- \frac{d[Ox]}{dt} = k_p \cdot [R^+, X^-] \cdot [Ox] + k_a \cdot [RT^+, X^-] \cdot [Ox] \quad \text{E: 5.37}$$

Therefore, in absence of termination (as well as transfer) reactions, the total concentration of living i-mer, c_0 , complete initiation ($f = 1$), remains constant during the polymerisation process. Thus in a system where active and dormant species are in a dynamic equilibrium

$$c_0 = [R^+, X^-] + [RT^+, X^-] = [I]_0 \quad \text{E: 5.38}$$

Here, $[I]_0$ represent the initial concentration of initiating species initially introduced in the polymerisation medium. If α_i denotes the fraction of living i-mer in the form of active species,

$$[R^+, X^-]_t = \alpha_i \cdot c_0 \quad \text{E: 5.39}$$

and

$$[RT^+, X^-]_t = (1 - \alpha_i) \cdot c_0 \quad \text{E: 5.40}$$

The combination of the equations E: 5.37, E: 5.38, E: 5.39 and E: 5.40 gives

$$-\frac{d[Ox]}{dt} = (k_a + (k_p - k_a) \cdot \alpha_i) \cdot c_0 \cdot [Ox] \quad \text{E: 5.41}$$

which, upon integration of the equation E: 5.41 leads to

$$\text{Ln} \left(\frac{[Ox]_0}{[Ox]_t} \right) = k_{p,app} \cdot t \quad \text{E: 5.42}$$

with

$$k_{p,app} = k_a + (k_p - k_a) \cdot \alpha_i \quad \text{E: 5.43}$$

Here, $k_{p,app}$ ($\text{L} \cdot \text{mol}^{-1} \cdot \text{s}^{-1}$) represents the apparent rate constant of monomer consumption.

Because α_i decreases as the polymerisation progresses the slope of $\text{Ln} \left(\frac{[Ox]_0}{[Ox]_t} \right)$ against time is not linear dependence. As illustrated in the figure 5.9, a first estimate of k_p and k_a can be obtain from the slope for the maximum and the minimum value of $k_{p,app}$. Consequently, if the rates of interconversion between coexisting species are much larger than the rate of propagation, the linear dependence \overline{Mn} conversion should intercept the origin and

the produced polymer should be characterised by a very narrow molecular weight distribution ($\overline{M}_w/\overline{M}_n < 1.2$) that will decrease throughout the polymerisation process.

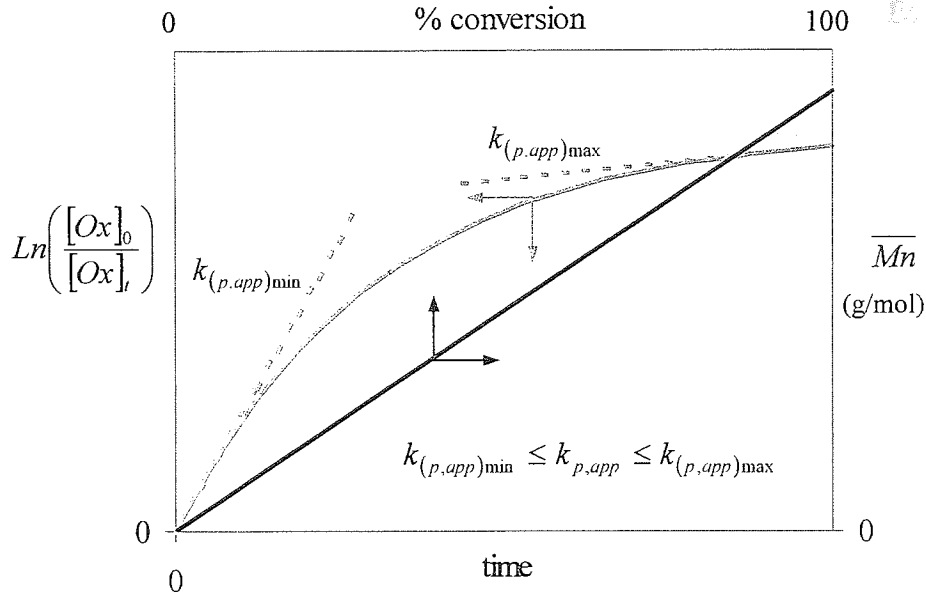


Figure 5. 9: Dependence of \overline{M}_n on conversion and $\ln([Ox]_0/[Ox]_t)$ on time for fast initiation process.

$$k_a \leq k_{p,app} \leq k_p \quad \text{E: 5.44}$$

with

$$k_{(p,app)max} \leq k_p \quad \text{E: 5.45}$$

and

$$k_{(p,app)min} \geq k_a \quad \text{E: 5.46}$$

5.1.2.2.2.2 Slow initiation process

It must be noted that even for full monomer conversion, the initiator is not always completely converted to living polymer chains. This is because the initiation is slow in relation to the rate of propagation. Therefore, if f_t denotes the fraction of initiator converted to polymer at a

given monomer conversion, in absence of termination reactions the total concentration of living i-mer is given by the following relation

$$c_0 = [R^+, X^-]_i + [RT]_i = f_i \cdot [I]_0$$

E: 5.47

This supposes that initially, the plot of $\ln([Ox]_0/[Ox]_i)$ against time should exhibit retardation and \overline{Mn} against conversion will lead to the formation of polymer characterised by a broad average molecular weight distribution and non linear dependence of \overline{Mn} against conversion.

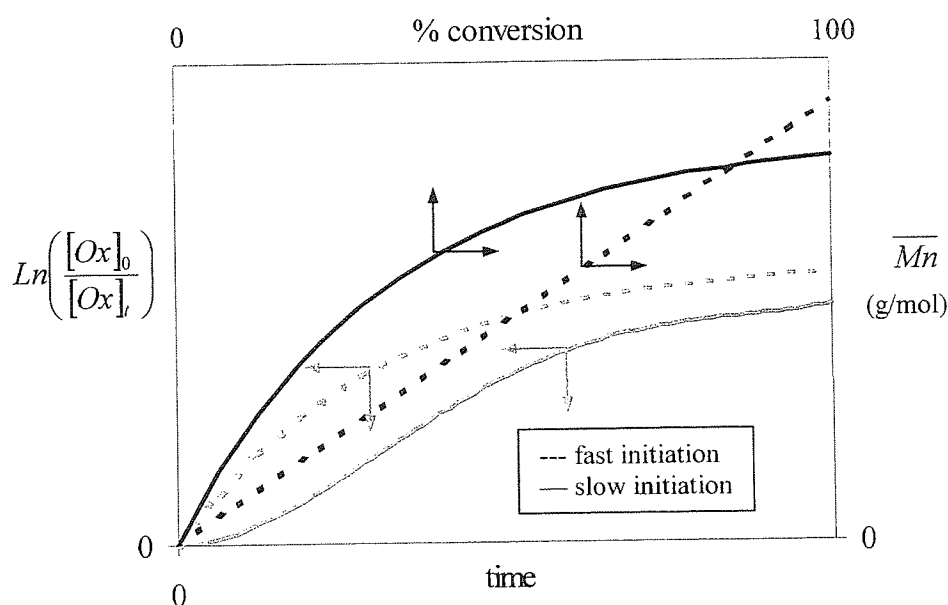


Figure 5. 10: Dependence of Mn on conversion and $\ln([Ox]_0/[Ox]_i)$ on time for slow initiation.

5.2 Development of the “quasiliving” CROP of oxetane using ether derivative as solvent

The use of cyclic ether as additive that does not homopolymerise (very low ring strain) seems to us to be the alternative to polymerise oxetane in a “living” manner. Indeed, as shown in the figure 5.11, 1,4-dioxane ($pK_b = 5.85$) and tetrahydropyran ($pK_b = 4.83$) are more basic than diethyl ether ($pK_b = 7.20$) but less nucleophilic than oxetane ($pK_b = 3.60$). Moreover, both can be used as solvent and can easily be dried and purified over CaH_2 and over Na/Benzophenone using trap-to-trap method (see section 2.7.1).

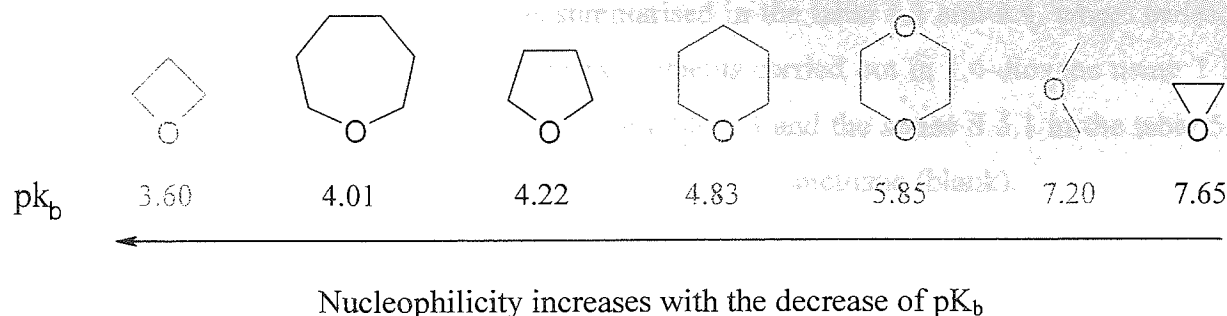


Figure 5. 11: Basicity of cyclic ether measured by IR measurement referred to the literature.

In the previous chapters we showed that the probability of the transfer reaction occurring in dichloromethane was strongly dependent on the nature of the initiator but also on the nature of the counter-anions. Because of this, protonic reagents and alkylating reagents bearing different counter-anion were utilised to initiate the cationic polymerisation of oxetane.

5.2.1 Effect of 1,4-dioxane on the CROP of oxetane at 35 °C

In the present work, we focussed our investigations on the effect on the ratio $[1,4-dioxane]_0/[Ox]_0$ of the initiator and size of the counter-anion on the control of the polymerisation of oxetane. For this purpose, a solution of 1 M of oxetane in 1,4-dioxane or in mixed solvent (1,4-dioxane/dichloromethane) was polymerised at 35 °C using protonic or alkylating reagents as initiating system. The total volume of polymerisation solution was kept constant and equal to 25 ml. The polymerisation reactions were followed by withdrawing active polymer samples the using sampling technique described in the section 2.8.3. The active polymer solutions were deactivated in a large excess volume of ethanol or 10% NaOH solution depending on whether the polymerisation was performed in mixed solvent or 1,4-dioxane. The inactive polymer solution was treated as described in the section 2.8.1. The rate of polymerisation was monitored by gravimetric analysis and the resulting polymers were analysed by Size Exclusion Chromatography (S.E.C) against polystyrene standards and by 1H and ^{13}C NMR analysis.

5.2.1.1 Polymerisation initiated by protonic reagents ($BF_3:MeOH$)

Because $BF_3(AcOH)_2/BF_3OEt_2$ induces a very complex mode of initiation, $BF_3/MeOH$ was used as the protonic reagent. The initiator solution was then prepared in dichloromethane as described in the section 2.7.7.1.1.2 and the polymerisation reaction carried out as described

above in the section 5.2.1. This study is summarised in the table 5.3 and 5.4, where series S 5.2 and S 5.3 and S 5.4 correspond to the experiments carried out in 1,4-dioxane using 1 M and 0.66 M of oxetane. The series S 4.4 in the table 5.3 and the series S 5.1 in the table 5.2 correspond to the series experiments carried out in dichloromethane (blank).

5.2.1.1.1 Polymerisation in dichloromethane

Because the stability of the counter-anion, $[\text{BF}_3\text{OMe}]^-$, towards anion-splitting reactions is crucial for the achievement of quasiliving polymerisation of oxetane in 1,4-dioxane, we were interested to know if the addition of monomer solution to an active polymer solution could restart the polymerisation with the expected rate of monomer consumption. For this purpose, series of experiments was then carried out in which the concentration of oxetane was 1 M and the concentration of BF_3MeOH was 0.0077 M. The total volume of the solution was equal to 22 ml. After 90 minutes, 5 ml of freshly prepared solution of oxetane (4.98 M) in dichloromethane was added to the active polymer solution to produce a concentration of oxetane approximately equal to the original. The monomer solution was added using the sampling system as described in the section 2.8.3. Similarly, a second monomer addition was injected 90 minutes after the first monomer addition, using approximately 5 ml of a solution of 5.6 M oxetane in dichloromethane. Considering the dilution factor and knowing the yield of the polymerisation just before the monomer solution was added, the concentration of monomer, the concentration of BF_3MeOH and the expected rate of monomer consumption were calculated. Here, the expected rate of monomer consumption, as measured by $(dT/dt)_{\text{expected}}$, was calculated on the basis that the mole number of growing centres is constant (see E 5. 48). This study is summarised in the table 5.2.

	Before monomer addition					After monomer addition					SEC analysis				
	[I] ₀ mol/l	[Ox] ₀ mol/l	(dT/dt) measured °C.s ⁻¹	conv. %	time t _k min	time t _{add} min	[Cat] ₀ mol/l	[Ox] ₀ mol/l	(dT/dt) expected °C.s ⁻¹	(dT/dt) measured °C.s ⁻¹	conv. %	Mn (theory) g/mol	Mn (SEC) g/mol	M _w /M _n	
Entry															
S 5.1.1	0.0077	1	5.85	92	90							6,780	4,500	2.4	
S 5.1.2	0.0077	1	5.83	-	-		Before monomer addition						14,170	6,800	2.3
						90	0.0062	1	5.01	5.3	79				
							Before monomer addition								
						90	0.0062	1	5.01	5.3	-				
S 5.1.3	0.0077	1	5.84	-	-		After monomer addition						21,200	7,200	2.4
						200	0.0052	0.985	4.18	0.149	64				

Table 5. 2: Effect of the monomer addition on the rate of polymerisation, \overline{Mn} and $\overline{Mw}/\overline{Mn}$ when the polymerisation is initiated by BF₃:MeOH in dichloromethane at 35 °C.

$$\left(\frac{dT}{dt}\right)_{\text{expected}j} = \frac{[BF_3MeOH]_{0,j}}{[BF_3MeOH]_{0,j-1}} \cdot [Ox]_{0,j} \cdot \left(\frac{dT}{dt}\right)_{\text{measured}j-1} \quad E: 5.48$$

$$\overline{Mn} = \sum_{j=0}^j \left(\frac{[Ox]_{0,j}}{[BF_3MeOH]_{0,j}} \cdot conv_j \right) \quad E: 5.49$$

As expected, the initial rate of polymerisation, $(dT/dt)_{\text{measured}}$, measured after the second monomer addition (see table 5.2, series S 5.1.3) showed that termination reactions do not occur significantly to be kinetically observed by **calorimetric** analysis. Assuming the absence of termination reactions, the rate at which the monomer was consumed was then investigated (see table 5.3, series S 4.4).

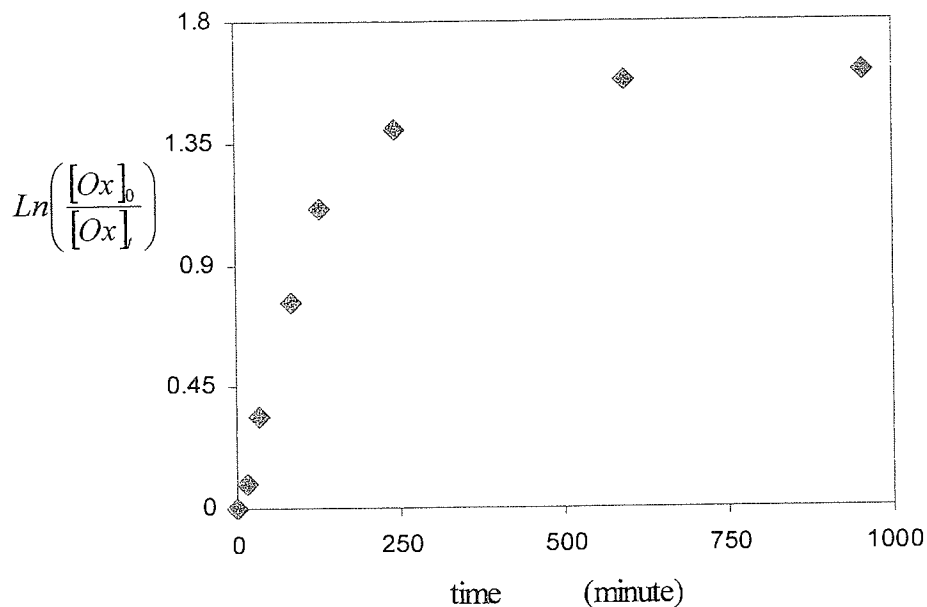


Figure 5. 12: Evolution of $\ln([Ox]_0/[Ox]_t)$ against time when 1 M of oxetane is polymerised by 0.0077 M of BF_3MeOH in dichloromethane at 35 °C. Table 5.3 series S 4.4, annex 4.5.

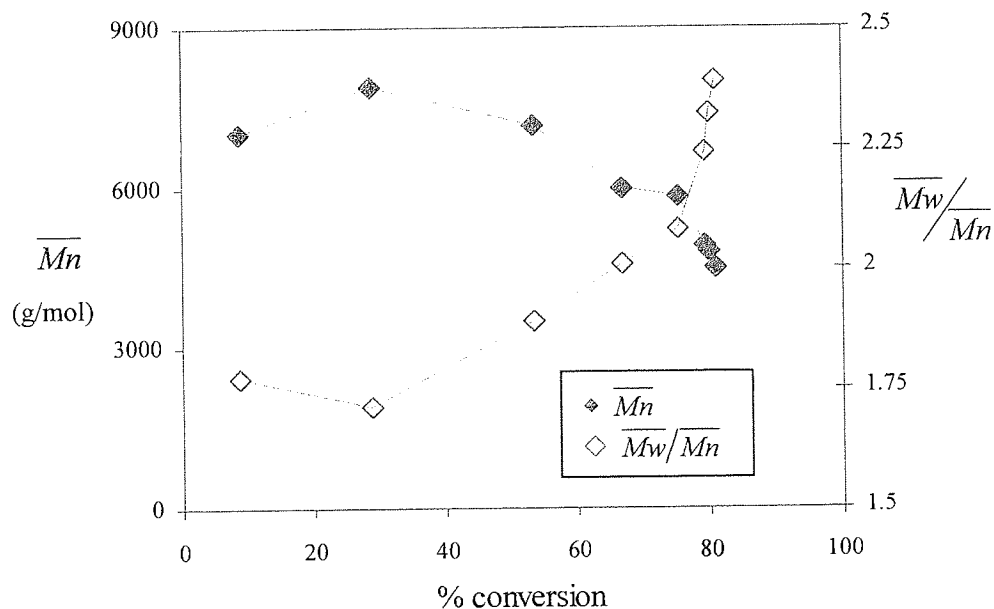
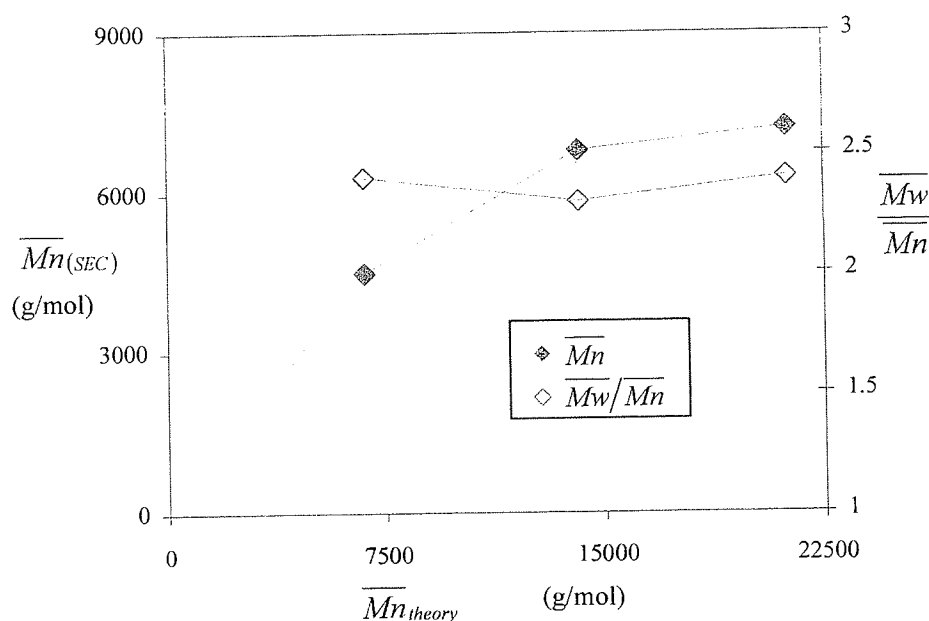


Figure 5. 13: Evolution \overline{Mn} against conversion when 1 M of oxetane is polymerised in dichloromethane using 0.0077 M of BF_3MeOH at 35 °C. Table 5.3 series S 4.4, annex 4.5.

As shown in the figure 5.12, the curvature of the slop when $\ln([Ox]_0/[Ox]_t)$ was plotted against time can only be explained by the increase of the mole fraction of “dormant” species due to the occurrence of transfer reactions (intra- and intermolecular transfer reactions). The formation of cyclic oligomers together with linear polymers (see SEC traces in annex 4.5 and ^1H and ^{13}C NMR spectr in annex 5.1 and 5.2, respectively) as well as the evolution of \overline{Mn} against conversion show clearly that the polymerisation of oxetane in dichloromethane is an uncontrolled polymerisation process (see figure 5.13). Because the mole fraction of “active” growing species decreases throughout the polymerisation, the enhancement of $k_{p,app}$ after monomer addition can only be explain if “dormant” and “active” species are in some sort of equilibrium as long as there is enough monomer in the polymerisation media to reactivate “dormant” species. Therefore, the non linear increases of \overline{Mn} after monomer addition (see figure 5.14) are certainly due to the occurring transfer reactions that induce a redistribution of the polymer chains during the reactivation of the “dormant” species.



$[Ox]_i = 1.0\text{M}$ is polymerised in CH_2Cl_2 using 0.0077 M of BF_3MeOH at 35°C . Table 5.2 series S 5.1.

Figure 5. 14: Evolution \overline{Mn} after monomer addition.

Consequently, if termination reactions are prevented, the cationic ring-opening polymerisation of oxetane in dichloromethane appears as an uncontrolled polymerisation process (see figure 5.12) during which the total concentration of growing centres can only increase. Because the reactivation of the dormant species issue from intermolecular transfer

reactions can generate dead polymer chains and α - γ growing polymer chains (see figure 5.15), in this respect the growing polymer chains are not living.

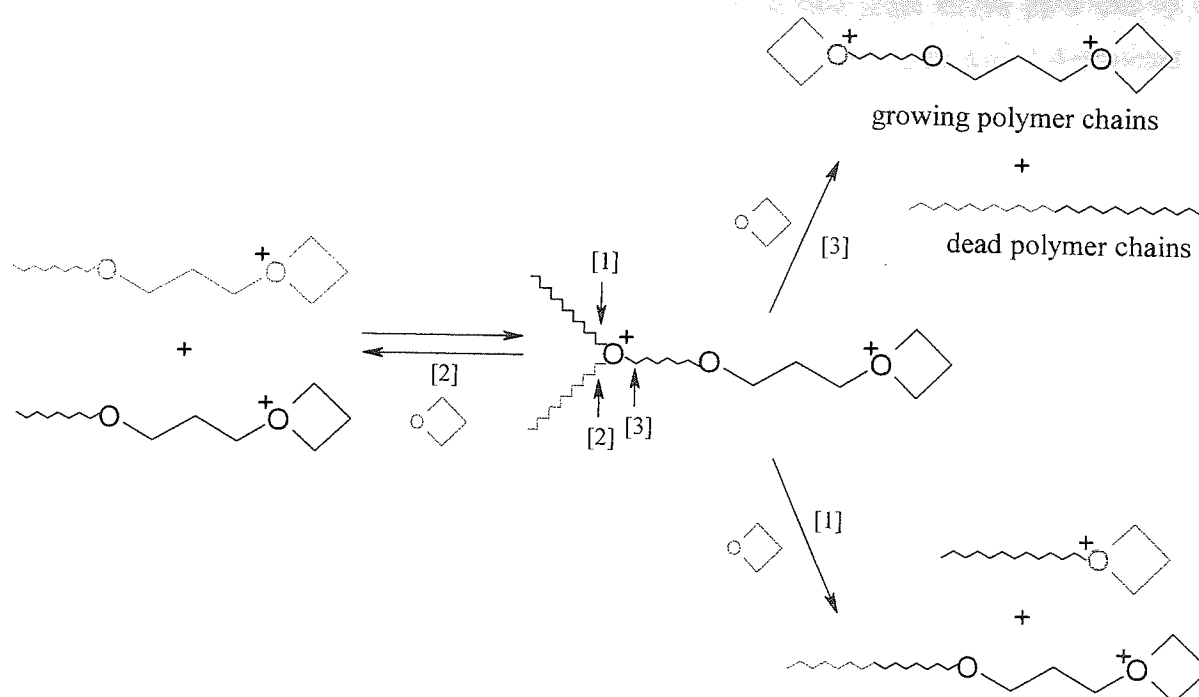


Figure 5.15: Reaction of redistribution of the growing polymer chains issues from intermolecular transfer reactions in dichloromethane.

5.2.1.1.2 Polymerisation in 1,4-dioxane

In 1968, Furukawa^[329] reported that tetrahydropyran and 1,4-dioxane which both lacks the ability to homopolymerise can easily be copolymerise with 3,3-bis(chloromethyloxy)tetrahydrofuran in the presence of BF_3OEt_2 . Using element analysis, the authors found that the mole fraction of 6-membered cyclic ether monomer incorporated in the poly(3,3-bis(chloromethyloxy)tetrahydrofuran) was found to be 33.5 % and 19 % for tetrahydropyran and 1,4-dioxane, respectively. Because of this, each polymers synthesised in the presence of 1,4-dioxane were then analysed by ^1H and ^{13}C NMR spectroscopy. Similarly, the ^{13}C NMR revealed the presence of 1,4-dioxane monomer units into the polyoxetane. A typical ^{13}C NMR spectrum (annex 5.7 and 5.9) of polymer synthesised in 1,4-dioxane with BF_3MeOH show that each 1,4-dioxane units incorporated into the polymer were surrounded by two oxetane units. Indeed, in addition to the main in-chain carbon resonances observed at 67.49 and 29.76 ppm, assigned to $-\text{OCH}_2\text{CH}_2\text{CH}_2\text{O}-$ and $-\text{OCH}_2\text{CH}_2\text{CH}_2\text{O}-$ groups, respectively, three additional peaks of similar intensity at the level of 2-8 % of the main ones were also observed. The first two peaks at 69.89 and 69.76 ppm, found in the region of resonance of the in-chain carbon of poly(ethylene oxide) (annex 5.9), were assigned to $-\text{OCH}_2\text{CH}_2\text{OCH}_2\text{CH}_2\text{O}-$ and $-\text{OCH}_2\text{CH}_2\text{OCH}_2\text{CH}_2\text{O}-$ groups, respectively.

$\text{OCH}_2\text{CH}_2\text{OCH}_2\text{CH}_2\text{O}$ - groups, respectively. The third peak at 68 ppm of similar intensity of the peaks at 69.89 and 29.76 ppm was assigned to $\text{OCH}_2\text{CH}_2\text{CH}_2\text{OCH}_2\text{CH}_2\text{OCH}_2\text{CH}_2\text{OCH}_2\text{CH}_2\text{CH}_2\text{O}$ - carbon shifted from 67.49 ppm due to the ethylene oxide fragment. Therefore we conclude that there is only one way 1,4-dioxane can be incorporated into the polymer chains (see figure 5.16).

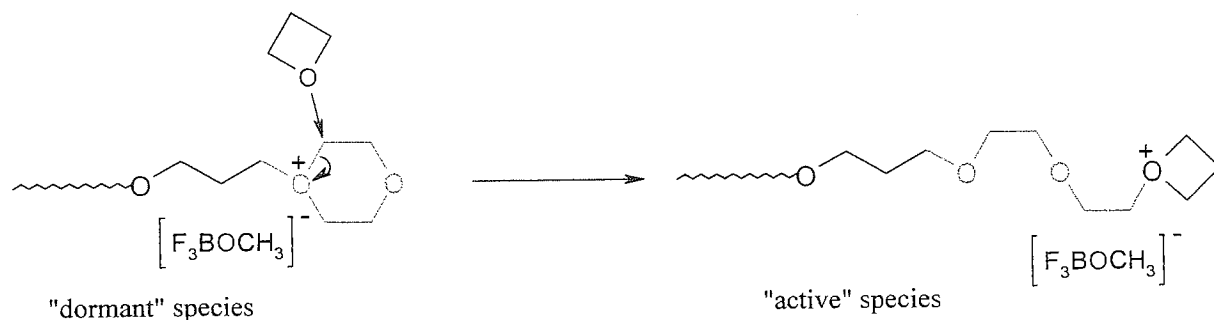


Figure 5. 16: Mechanism of incorporation of 1,4-dioxane into polymer chains.

At conversion of 72 %, the peak at 66.06 and 30.15 ppm that we found to be the carbon resonance of $\text{-OCH}_2\text{CH}_2\text{CH}_2\text{O-}$ fragment of small cyclic oligomers (cyclic tetramers) reached a the range of intensity of 2 to 5 % of intensity of the main peaks. In starving monomer condition (conversion > 84.2 %), additional peaks appeared with the enhancement of the peak at 66.06 ppm. The peaks at 66.56 and 65.78 ppm were then assigned to oxetane fragments shifted from 60.06 ppm due to the presence of 1,4-dioxane fragment in the cyclic oligomers. Similarly, the signals at 68 and 67.85 ppm found also in the region of resonance of the poly(ethylene oxide) were assigned to the resonance of 1,4-dioxane fragment in cyclic and/or linear oligomers. Because ^1H NMR spectroscopy (annex 5.9 and 5.11) could not distinguish the 1,4-dioxane peaks units from oxetane units, the copolymer composition was calculated using ^{13}C NMR using the equation E: 5.50 and it was found that even low conversions of oxetane, the proportion of 1,4-dioxane incorporated in the polymer (ring and chains) was constant and approximately equal to 5 % of the monomer units. This study is summarised in the table 5.4 and 5.5. From 72 % to 90 % monomer conversion, the fraction of cyclic oligomers was estimated to be equal to 5 % monomer conversion. The ^1H and ^{13}C chemical shift are summarised in the table 5.3. From ^1H NMR analysis, in addition to the main chain resonance observed at 3.48 and 1.82 ppm, assigned to $\text{-OCH}_2\text{CH}_2\text{CH}_2\text{O-}$ and $\text{-OCH}_2\text{CH}_2\text{CH}_2\text{O-}$ groups, respectively, six multiplets were also observed, three triplets at 4.25, 3.73 and 3.59 ppm and three multiplets at 2.65, 2.56 and 1.92 pm. These peaks that are sometimes observed when the polymerisation is performed in dichloromethane were assigned

to $-\text{CH}_2-$ groups of oxetane fragments of the small oligomer chains ($\text{Dp} < 4\text{-}5$); $\text{OCH}_2\text{CH}_2\text{CH}_2\text{O}-$ for the triplets and $-\text{OCH}_2\text{CH}_2\text{CH}_2\text{O}-$ for the multiplets.

	Structure	Chemical shift*				Peak formation
		¹³ C NMR		¹ H NMR		
		δ (ppm)	Intensity	δ (ppm)	Intensity	
Polymer chains	-OCH ₂ CH ₂ CH ₂ O-	67.49 (a)	I ₁	t: 3.48	I ₁	Since
	-OCH ₂ CH ₂ CH ₂ O-	29.76 (a)	2.I ₂ ≈ I ₁	q: 1.823	2.I ₂ ≈ I ₁	beginning
	-	70.23 (a)	I ₃	(a)	(a)	Since
	OCH ₂ CH ₂ CH ₂ OCH ₂ CH ₂ OCH ₂ CH ₂ OC	69.85 (a)	I ₄ ≈ I ₃	(a)	(a)	beginning
	H ₂ CH ₂ CH ₂ O-	68 (a)	I ₅ ≈ I ₃	(a)	(a)	After 14 %
Cyclic oligomers	-	67.49 (a)	I ₁	(a)	(a)	conv
	-OCH ₂ CH ₂ CH ₂ O-	66.07 (b)	I ₈	t: 3.545	I ₈	After 14 %
	-OCH ₂ CH ₂ CH ₂ O-	30.15 (b)	2.I ₉ ≈ I ₈	q: 1.802	2.I ₉ ≈ I ₈	conv
	-	(c)	I ₁₀	(a)	(a)	After 14 %
	OCH ₂ CH ₂ CH ₂ OCH ₂ CH ₂ OCH ₂ CH ₂ OC	(c)	I ₁₁ ≈ I ₁₀	(a)	(a)	conv
	H ₂ CH ₂ CH ₂ O-	66.56	I ₁₂ ≈ I ₁₀	(a)	(a)	After 84 %
	-	65.78	I ₁₃ ≈ I ₁₀	(a)	(a)	conv

* CDCl_3 was used as solvent.

(a): peaks overlap.

Table 5. 3: chemical shift δ (ppm) of $-\text{CH}_2-$ in the polyoxetane produced in the presence 1,4-dioxane.

Series	[Ox] ₀	[I] ₀	[Dox] ₀ /[I] ₀	P (E: 5.49)	% mole Dox ¹³ C NMR	% weight Dox (E: 5.50)	Conversion (E: 5.51)	Mn (theory)	Mn (SEC)	Mp (SEC)	Mw/Mn (SEC)	Time Second	Q NMR
S 4.4.1	1	0.008	0	8.9	-	-	8.9	670	7,020	11,820	1.77	14.4	0
S 4.4.2	1	0.008	0	28.6	-	-	28.6	2154	7,890	12,820	1.71	34.8	0.15
S 4.4.3	1	0.008	0	53.4	-	-	53.4	4022	7,160	12,900	1.89	83.4	0.18
S 4.4.4	1	0.008	0	67	-	-	67	5047	6,000	11,150	2.01	129.6	0.24
S 4.4.5	1	0.008	0	75.4	-	-	75.4	5680	5,840	11,500	2.08	244.8	0.24
S 4.4.6	1	0.008	0	79.4	-	-	79.4	5981	4,920	11,550	2.24	594	0.28
S 4.4.7	1	0.008	0	80	-	-	80	6026	4,820	11,370	2.32	955.2	0.31
S 4.4.8	1	0.008	0	80.8	-	-	80.8	6087	4,500	10,990	2.39	1134	0.32
S 5.2.1	1	0.0077	9.45	5.8	2.5	3.8	5.6	438	1,400	2,680	1.82	39	0
S 5.2.2	1	0.0077	9.45	15.5	5.8	8.5	14.2	1,164	2,665	4,340	1.56	85	0.03
S 5.2.3	1	0.0077	9.45	30.9	3.9	6.1	29.1	2,322	3,645	6,300	1.75	163	0.03
S 5.2.4	1	0.0077	9.45	40.5	4.1	6.1	38	3,040	3,945	6,930	1.77	239	0.026

(a) SEC traces of polymers go beyond the borderline of the calibration curve.

(b) Formation of additional ¹³C NMR peaks that are not been well identified.

Table 5. 4: Effect of 1,4-dioxane on \overline{Mn} and $\overline{Mw}/\overline{Mn}$ when the polymerisation of oxetane is initiated by BF₃:MeOH at 35 °C. Beyond

Entry	Before monomer addition					After monomer addition					NMR ¹³ C	SEC analysis		
	[I] ₀ mol/l	[Ox] ₀ mol/l	(dT/dt) measured °C.s ⁻¹	Conv. %	time t _k min	time t _{add} min	[Cat] ₀ mol/l	[Ox] ₀ mol/l	(dT/dt) expected °C.s ⁻¹	(dT/dt) measured °C.s ⁻¹	conv. %	Mn (theory) g/mol	Mn (SEC) g/mol	Mw/Mn
S 5.4.1	0.00771		5.85 4.6	96.2	150						5.2	7,802	4,560	2.05
S 5.4.2	0.00771		-	-	-	Before monomer addition					5.6	14,438	9,200	1.87
						150	0.0063	0.98	5.95	5.95	80			

Table 5.5: Effect of the monomer addition when the polymerisation initiated by BF₃:MeOH is performed in 1,4-dioxane at 35 °C.

Knowing the composition of the copolymer %_{mole}Dox and the yield P, the fraction of oxetane converted into polymer during the first 80 % monomer conversion was then calculated using the equation E: 5.53:

$$\%_{mole}Dox = \frac{((I_3 + I_4)/4 + I_5/2)/2}{((I_3 + I_4)/4 + I_5/2)/2 + ((I_1/2 + I_3)/2 + (I_8/2 + I_9)/2)/2} \cdot 100 \quad \text{E: 5.50}$$

$$P = \frac{\text{weight}(\text{polymer})}{\text{weight}(\text{oxetane})} \cdot 100 \quad \text{E: 5.51}$$

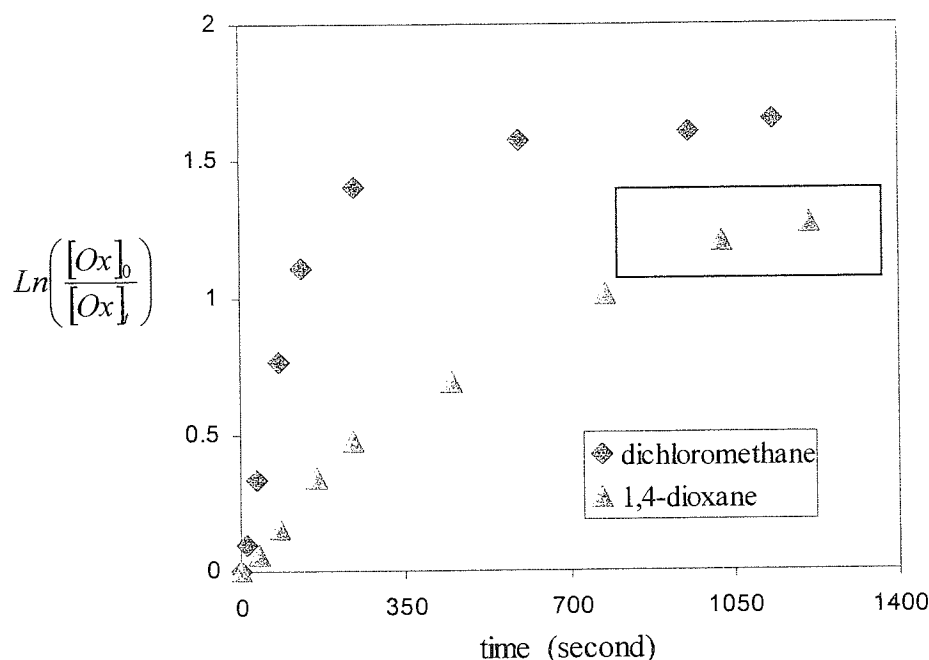
$$\%_{weight}DO = \frac{\%_{mole}Dox \cdot M_{dioxane}}{\%_{mole}Dox \cdot M_{dioxane} + (100 - \%_{mole}Dox) \cdot M_{Oxetane}} \cdot 100 \quad \text{E: 5.52}$$

$$\text{Conversion} = P \cdot \frac{(100 - \%_{weight}Dox)}{100} \quad \text{E: 5.53}$$

Here %_{mole}Dox and %_{weight}Dox denote respectively the mole fractions and the weight fraction of 1,4-dioxane in the polymer while $M_{oxetane}$ and $M_{dioxane}$ are the molecular weight of oxetane and 1,4-dioxane, respectively.

Knowing the conversion, the rate at which oxetane was consumed during the polymerisation was then investigated. As expected, the kinetic analysis showed that the use of 1,4-dioxane as solvent reduces significantly the rate at which the oxetane is consumed. Indeed, as shown in the table 5.4, 35 minutes are required in 1,4-dioxane to convert 77.6 % of oxetane into polymer while in dichloromethane 75.4 % of monomer is consumed within 4 minutes. Similarly, the calorimetric analysis showed spontaneous decrease of the rate at which the temperature evolved during the first 10 seconds of the polymerisation process indicating that the growing centres are almost spontaneously end-capped by the 1,4-dioxane (see annex 5.4, 5.5 and 5.6). Because terminations by anion-splitting do not seem to occur significantly during the polymerisation, the curvature of the slop plot of $\ln([Ox]_0/[Ox])$ against time can only be explained if the mole fraction of "dormant" species increases with the decrease of the

concentration of oxetane (see figure 5.17). The sigmoid form plot of $\ln([Ox]_0/[Ox]_t)$ against time strongly indicates that the initiation is slow in relation to the rate of propagation.

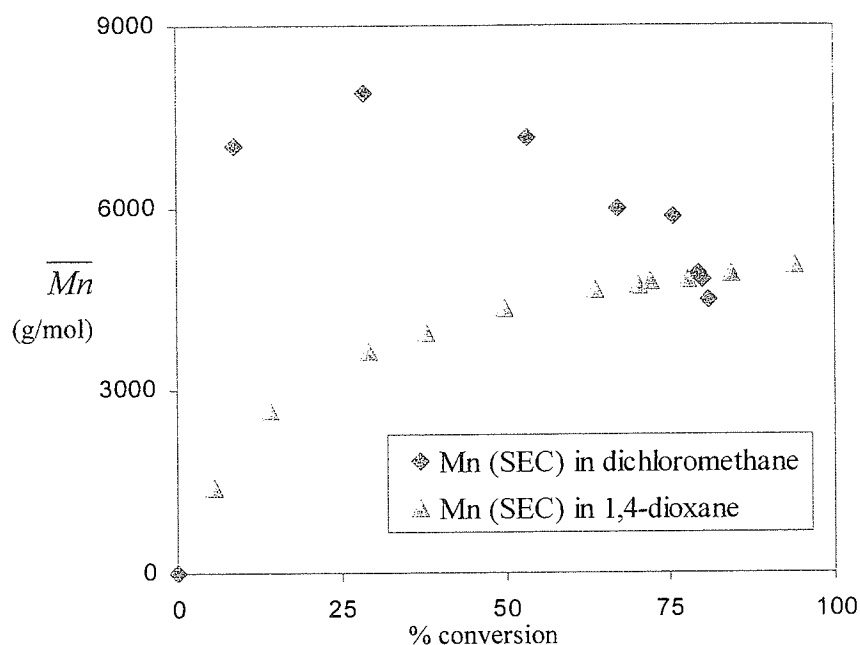


1 M of oxetane is polymerised by 0.0077 M of BF_3MeOH at 35 °C in (♦) dichloromethane (series S 4.4, table 5.4) and (◐) 1,4-dioxane (series S 5.2, table 5.4).

Figure 5. 17: Evolution of $\ln([Ox]_0/[Ox]_t)$ against time.

The reversible deactivation of the “actives” species by 1,4-dioxane was demonstrated when \overline{Mn} was plotted against conversion (see figures 5.18) or $\overline{Mn}_{(theory)}$ (see figures 5.19). Indeed, for the first time we observed a non-linear increase of the molecular weight which could be characteristic of “quasiliving” or controlled polymerisation induced by a slow initiation process. The SEC traces of the produced polymers are shown in the annex 5.12. The living character of the growing polymer chains was demonstrated by the fact that the monomer addition extends the length of polymer chains (SEC traces in annex 5.13). However, because the initiation is slow in relation to the propagation, it cannot be excluded that growing polymers chains are still generated when the monomer solution is added onto the active polymer solution. This is believed to be responsible of the formation of polymer with a broad polydispersity ($1.5 < \overline{Mw}/\overline{Mn} < 2.5$). Therefore, the linear dependence of \overline{Mn} with $\overline{Mn}_{(theory)}$

(see figure 5.20) cannot be used as criteria of “livingness” because we cannot predict the dependence of \overline{Mn} against $\overline{Mn}_{(theory)}$ after monomer addition.



1 M of oxetane is polymerised by 0.0077 M of BF_3MeOH at 35 °C in (♦) dichloromethane (table 5.4 series 5.2 and annex 5.8) and (Δ) 1,4-dioxane (table 5.4 series S 4.4 and annex 4.5).

Figure 5. 18: Evolution of \overline{Mn} and $\overline{Mw}/\overline{Mn}$ against % conversion.

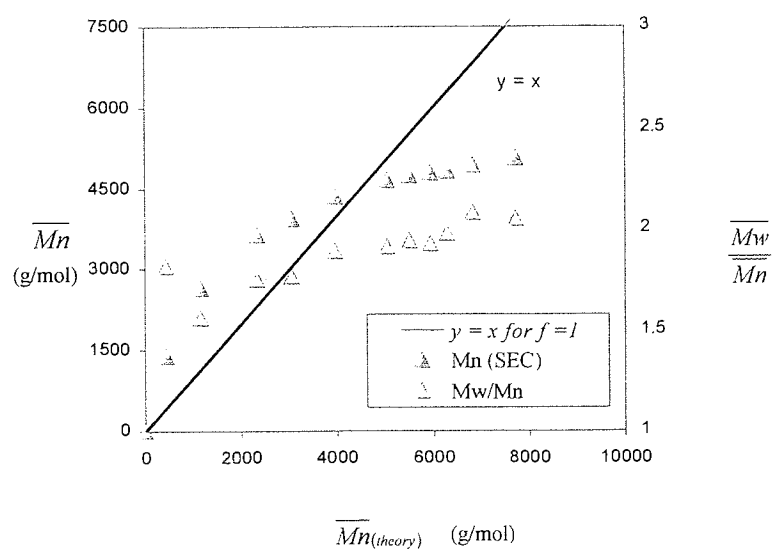
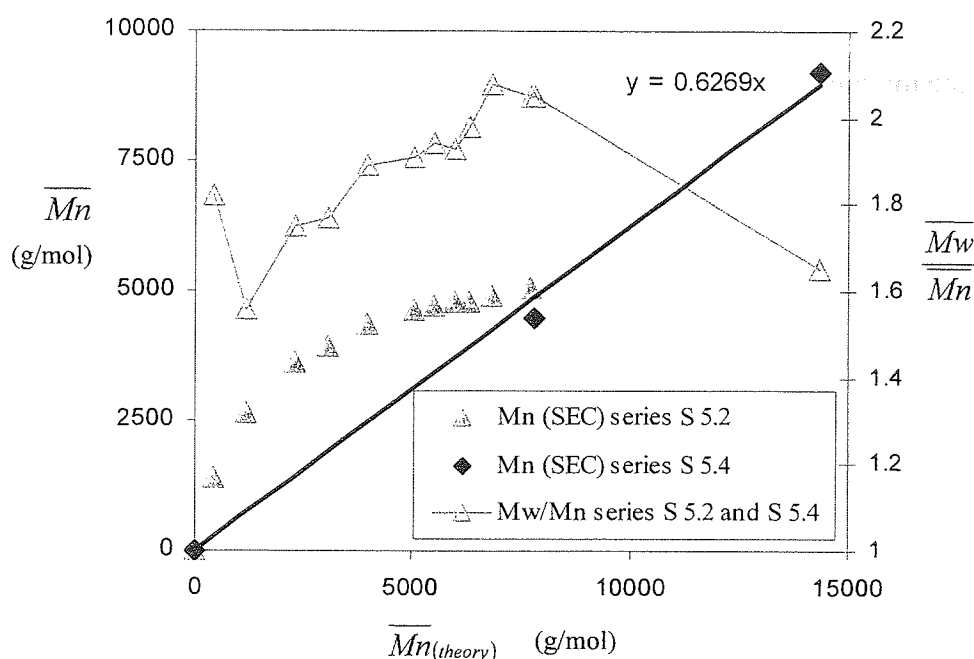


Figure 5. 19: Evolution of $\overline{Mn}_{(SEC)}$ against $\overline{Mn}_{(theory)}$ when 1 M of oxetane is polymerised by 0.0077 M of BF_3MeOH at 35 °C in 1,4-dioxane (table 5.4 series S 5.2 annex 5.8).



Results taken before (table 5.4 series S 5.2 annex 5.8) and after (table 5.5 series S 5.4 annex 5.9) monomer addition.

Figure 5. 20: Evolution \overline{Mn} and $\overline{Mw}/\overline{Mn}$ against conversion.

$\overline{Mn}_{(theory)}$ was calculated as followed,

$$\overline{Mn}_{(theory)} = M_{ox} \cdot \frac{[Ox]_0}{[I]_0} \cdot conv_{(Ox)} + M_{dioxane} \cdot \frac{[Dox]_0}{[I]_0} \cdot conv_{(Dox)} \quad \text{E: 5.54}$$

Knowing the composition in mole fraction of 1,4-dioxane incorporated into the polymer, the contribution of 1,4-dioxane to the increase of \overline{Mn} can then be calculated based on the oxetane conversion,

$$M_{dioxane} \cdot \left(\frac{[Dox]_0}{[I]_0} \cdot conv_{(Dox)} \right) = M_{dioxane} \cdot \left(\frac{[Ox]_0}{[I]_0} \cdot (\%_{mol} Dox) \cdot conv_{(Ox)} \right) \quad \text{E: 5.55}$$

By combining the equations E: 5.54 and E: 5.55,

$$\overline{Mn}_{(theory)} = \frac{[Ox]_0}{[I]_0} \cdot (M_{Ox} + M_{Dox} \cdot (\%_{mol} Dox)) \cdot conv_{(Ox)} \quad \text{E: 5.56}$$

M_{Ox} and M_{Dox} are the molecular weights of the respective co-monomers, oxetane and 1,4-dioxane. The $conv_{(Ox)}$ and $conv_{(Dox)}$ denote the mole fraction of oxetane and 1,4-dioxane that was incorporated into the polymer during the polymerisation.

The slow character of the initiation process induced by the presence of 1,4-dioxane was demonstrated when different Dp were targeted at concentrations of $BF_3:MeOH$ equal to 0.0077 M. Indeed, if we compare the SEC traces of the polymer produced when Dp of 80 ($[1,4\text{-dioxane}]_0/[Ox]_0 = 15.95$, annex 5.14) and Dp of 125 ($[1,4\text{-dioxane}]_0/[Ox]_0 = 9.45$, annex 5.12) were targeted, it appears in the both cases that \overline{Mn} increases during the entire course of the polymerisation. This is an indication that “living” growing polymer can be produced independently of the ratio $[Ox]_0/[BF_3:MeOH]_0$. However, as the monomer is consumed we can observe the formation of different fractions of polymer of different molecular weight. Because these fractions appear at retention times shorter than the retention time of cyclic tetramers, we strongly believe that different generation of living polymers are produced during the polymerisation process. Here, only a MALDI ToF analysis of the polymer could confirm the structure of the different polymer fractions. Because the different fractions of polymers appear more clearly as the ratio $[1,4\text{-dioxane}]/[\text{oxetane}]$ increases, we strongly believed that 1,4-dioxane affects the rate of initiation by slowing down the rate at which oxetane is protonated. This study is summarised in the table 5.4 where the series S 5.2 and S 5.3 correspond to experiments carried out for Dp of 125 ($[\text{oxetane}] = 1 \text{ M}$) and Dp of 80 ($[\text{oxetane}] = 0.68 \text{ M}$). In the both case the concentration of $BF_3:MeOH$ was constant and equal to 0.0077 M.

5.2.1.1.3 Discussions

5.2.1.1.3.1 *Nature of the initiating species during the initiation process*

The chemical reactions in which complexes are formed lead always to a dynamic chemical equilibrium in which complexes and reactants coexist in solution. In such system, the equilibrium constant is called a “complexation constant” and is noted K_c . Similarly, when a complex is put into solution, the spontaneous decomposition of the complex leads also to a reversible equilibrium for which the decomposition constant noted K_d is equal to $1/K_c$. Generally, K_c is very high ($K_c = 1.7 \times 10^6$ for $[Ag(NH_3)_2]^+$) and the corresponding reaction are

often considered as quasi total. This implies that during the preparation of the solution of $\text{BF}_3\cdot\text{MeOH}$ in dichloromethane (see Chapter 2), $\text{BF}_3\cdot\text{MeOH}$, BF_3 and MeOH coexist in solution as described in the figure 5.21.

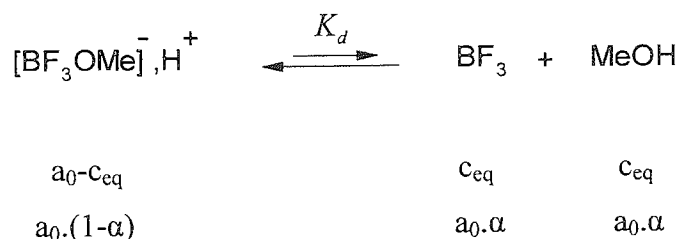


Figure 5. 21: Nature of initiating species when $\text{BF}_3\cdot\text{MeOH}$ complex is in solution in dichloromethane.

Therefore, concentrations of $[\text{F}_3\text{BOMe}]^-, \text{H}^+$, BF_3 and MeOH at the equilibrium are given by

$$K_d = \frac{[\text{BF}_3] \cdot [\text{MeOH}]}{[[\text{F}_3\text{BOMe}]^-, \text{H}^+]} = \frac{\alpha^2}{1 - \alpha} \cdot a_0 \quad \text{E: 5.57}$$

where $K_d \ll 1$ due to fact that dichloromethane is not a complexing solvent. The resolution of the equation E: 5.57 for $\alpha > 0$, gives then a unique solution

$$\alpha = \frac{K_d}{2a_0} \left(\sqrt{1 + \frac{4a_0}{K_d}} - 1 \right) \quad \text{E: 5.58}$$

where, (a_0) represents the concentration of $\text{BF}_3\cdot\text{MeOH}$ before dissociation and $(a_0 - c_{\text{eq}})$ and $(1 - \alpha)$ the concentration and the mole fraction of $\text{BF}_3\cdot\text{MeOH}$ at the equilibrium with $\alpha = c_{\text{eq}}/a_0$. It is interesting to note that α is a constant depending only on K_d and a_0 . Because α is very low due to general high value of K_c , the equation E: 5.58 can be approximated to the following relationship,

$$\alpha = \sqrt{\frac{K_d}{a_0}} \quad \text{E: 5.59}$$

5.2.1.1.3.1.1 Mechanism of initiation in dichloromethane

When the initiating solution is added to the monomer solution, the high nucleophilicity of oxetane is believed to disrupt the equilibrium by converting trifloroborane into (1:1) trifloroborane oxetane complex.



Figure 5. 22: Formation of trifloroborane oxetane complex.

The mechanism of initiation can then be visualised as shown in the figure 5.23.

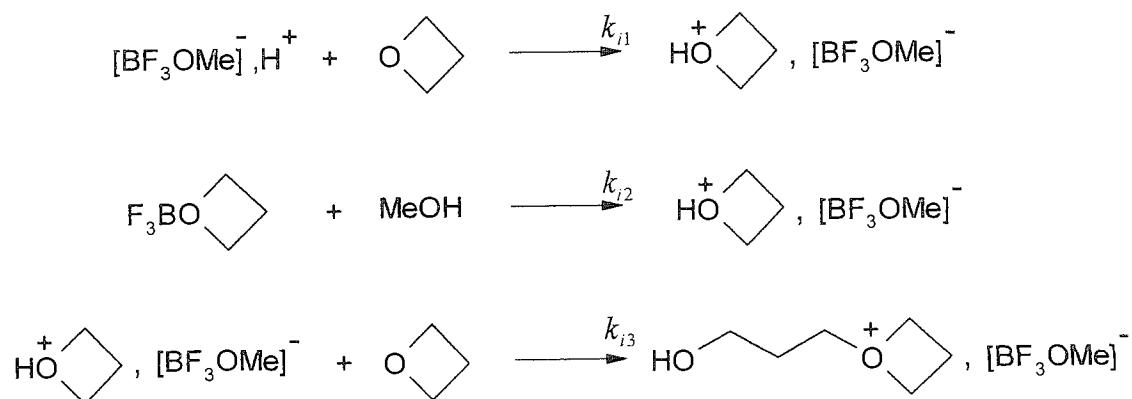


Figure 5. 23: Mechanism of initiation after addition of $\text{BF}_3\text{:MeOH}$ solution into monomer solution.

Because the rate of initiation is kinetically controlled by the rate at which the monomer is protonated^[115], the initial rate of initiation, $(R_i)_0$, can then expressed as follow

$$(R_i)_0 = R_{i1} + R_{i2} \quad \text{E: 5.60}$$

where

$$R_{i1} = k_{i1} \cdot \left[[\text{F}_3\text{BOMe}]^-, \text{H}^+ \right]_{eq} \cdot [\text{Ox}]_0 \quad \text{E: 5.61}$$

and

$$R_{i2} = k_{i2} \cdot [\text{F}_3\text{BOMe}]_{eq} \cdot [\text{MeOH}]_{eq} \quad \text{E: 5.62}$$

Knowing that

$$a_0 = \left[[F_3BOMe]^-, H^+ \right]_{eq} + [F_3BOx]_{eq} \quad \text{E: 5.63}$$

and

$$\left[[F_3BOMe]^-, H^+ \right]_{eq} = a_0 \cdot (1 - \alpha) \quad \text{E: 5.64}$$

By combining the equations E: 5.60, E: 5.619, E: 5.62, E: 5.63 and E: 5.64, and after rearrangement, the initial rate of initiation can be written as follow:

$$(R_i)_0 = k_{i1} \cdot (1 - \alpha) \cdot a_{01} \cdot [Ox]_0 + k_{i2} \cdot (\alpha a_{01})^2 \quad \text{E: 5.65}$$

or

$$(R_i)_0 = k_{i1} \cdot \left(1 - \sqrt{\frac{K}{a_{01}}} \right) \cdot a_{01} \cdot [Ox]_0 + k_{i2} \cdot K_d \cdot a_{01} \quad \text{E: 5.66}$$

Here a_{01} (Mol/l) represents the total concentration of initiator in the polymerisation medium. Because $K_d \ll 1$, $a_{01} \ll [Ox]_0$ and $k_{i1} > k_{i2}$, the initiation process described by the equation E: 5.62, is believed to be very slow in comparison to the process of initiation described by the equation E: 5.61. This is in agreement with our observation when we plotted $\ln([Ox]_0/[Ox]_t)$ against time. The slightly increase of $k_{p,app}$ in the early stage of the polymerisation, suggests that $[F_3BOMe]^-, H^+$ is fully converted into secondary oxonium as soon as few percent of monomers are consumed (from 20 % to 30 %). Besides the small increase of $R_{p,app}$ after monomer addition shows that the fraction of boron trifluoride in the form of BF_3 :Oxetane (1/1) complex is very low ($\alpha < 1$). Consequently, as the polymerisation progresses the rate of initiation denoted R_i is believed to be kinetically controlled by R_{i2} (see Equation E: 5.67)

$$R_i = k_{i2} \cdot [BF_3 : Ox] \cdot [MeOH] \quad \text{E: 5.67}$$

5.2.1.1.3.1.2 Mechanism of initiation in 1,4-dioxane

Because the rate of initiation is kinetically controlled by the rate at which oxetane is protonated, the use of 1,4-dioxane as solvent will affect the mechanism of initiation. Indeed, when the solution of BF_3MeOH in dichloromethane is added into the monomer solution, BF_3 is spontaneously and fully converted into boron trifluoride oxetane complex and boron trifluoride 1,4-dioxane complex (see figure 5.24).

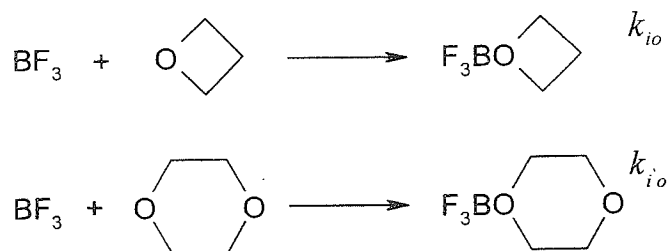


Figure 5. 24: Formation of boron trifluoride oxetane complex and boron trifluoride 1,4-dioxane complex.

At this stage of the process, the rate of initiation is then kinetically controlled by the rate at which oxetane is protonated. In the section 5.2.1.1.3.1, we showed that the initiation process in dichloromethane is characterised by two mechanisms of protonation of monomer. One fast and dependent on the concentration of oxetane (R_{i1}), and the other slow and kinetically controlled by concentrations of methanol and BF_3 (R_{i2}). These two modes of initiation can now be considered separately.

(a) Slow initiation process in 1,4-dioxane

One can consider first of the "slow initiation process" from reaction between boron trifluoride cyclic ether complex and methanol, illustrated in the figure 5.25. If $c_{\text{F}_3\text{B}:1,4\text{-dioxane}}$ and γ (with $\gamma = c_{\text{F}_3\text{B}:1,4\text{-dioxane}} / (a_{01} \cdot \alpha)$) represent respectively the concentration and the mole fraction of BF_3 :1,4-dioxane complex, the mole fraction of BF_3 :oxetane complex is then equal to $(1-\gamma)$.

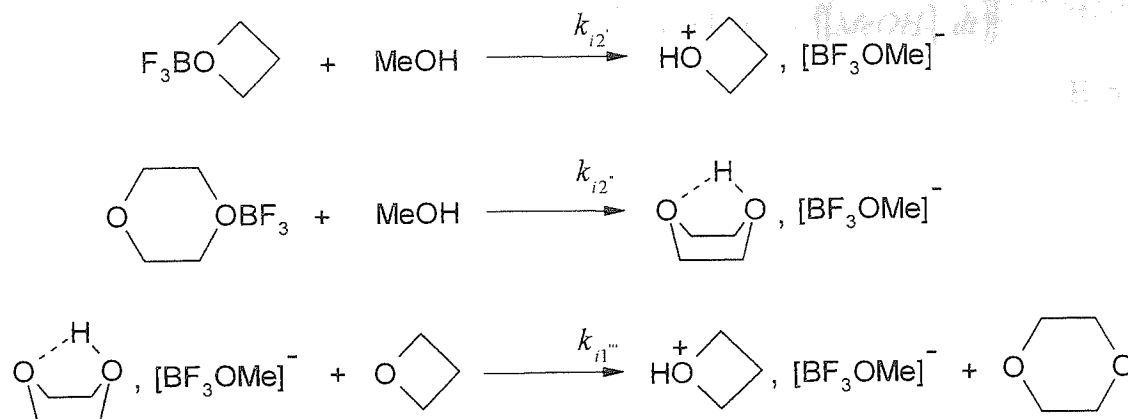


Figure 5. 25: Mechanism of the “slow” initiation process when $\text{BF}_3\text{:MeOH}$ in solution dichloromethane is injected into monomer solution in 1,4-dioxane.

Regardless of the basicity of oxetane and 1,4-dioxane, γ is believed to increase as the ratio $[1,4 - \text{Do}]_0 / [\text{Ox}]_0$ increases.

$$\gamma = f\left(\frac{[1,4 - \text{Do}]}{[\text{Ox}]}\right) \quad \text{E: 5.68}$$

Because the rate of formation of $(\text{dioxane})\text{H}^+ , [\text{F}_3\text{BOMe}]^-$ from the reaction between $\text{BF}_3\text{:1,4-dioxane}$ and MeOH is kinetically controlled by the concentration of methanol,

$$-\frac{d[\text{BF}_3 : 1,4 - \text{dioxane}]}{dt} = k_{i2} \cdot [\text{BF}_3 : 1,4 - \text{dioxane}] \cdot [\text{MeOH}] \quad \text{E: 5.69}$$

the integration of the equation E: 5.69 after rearrangement enables the determination of concentration (see the equation E: 5.72) and the mole fractions (see the equation E: 5.73) of $(\text{dioxane})\text{H}^+ , [\text{F}_3\text{BOMe}]^-$ once the solution of the equation E: 5.69 (see equation E: 5.70) is combined with the equation E: 5.71.

$$[\text{BF}_3 : 1,4 - \text{dioxane}]_t = \alpha \cdot \gamma \cdot a_{01} \cdot \exp(-k_{i2} \cdot \int [\text{MeOH}] \cdot dt) \quad \text{E: 5.70}$$

$$[(\text{dioxane})\text{H}^+ , [\text{BF}_3\text{OMe}]^-]_{02} = \alpha \cdot \gamma \cdot a_{01} - [\text{BF}_3 : 1,4 - \text{dioxane}]_t \quad \text{E: 5.71}$$

$$\left[(1,4\text{-dioxane})H^+, [BF_3OMe]^-\right]_{02} = \alpha \cdot \gamma \cdot a_{01} \cdot \left(1 - \exp\left(-k_{i2} \cdot \int [MeOH] \cdot dt\right)\right)$$

E: 5.72

with

$$\delta_i = \exp\left(-k_{i2} \cdot \int [MeOH] \cdot dt\right)$$

E:

5.73

Here, δ_i represents the fraction of $BF_3:1,4\text{-dioxane}$ remaining during the polymerisation process. If R_{i2} represents the rate of protonation of boron trifluoride cyclic ether complex by methanol, then

$$R_{i2} = k_{i2} \cdot [BF_3 : Oxe \tan e] \cdot [MeOH] + k_{i1} \cdot \left[(1,4\text{-dioxane})H^+, [BF_3OMe]^-\right]_{02} \cdot [Ox]$$

E: 5.74

After combination of the equations E: 5.72, E: 5.73 and E: 5.74,

$$R_{i2} = k_{i2} \cdot [BF_3 : Oxe \tan e] \cdot [MeOH] + k_{i1} \cdot a_{01} \cdot \alpha \cdot (1 - \delta_i) \cdot [Ox]$$

E: 5.75

with

$$[Ox] = [Ox]_0 \cdot \exp(-k_{p,app} \cdot t)$$

E: 5.76

Because the protonation reaction always generate a weaker acid, the presence of 1,4-dioxane is believed to slow down the rate of the slow initiation process knowing that once protonated, 1,4-dioxane has to transfer the proton to oxetane. However, because only a small fraction of $[F_3BOMe]^+H^+$ is dissociated ($\alpha \ll 1$) in dichloromethane, it is believe that the decrease of the rate of initiation from dichloromethane to 1,4-dioxane is essentially due to the decrease of rate of the "fast initiation" process.

(b) "Fast initiation" process in 1,4-dioxane

The fast initiation process can be represented as follow,

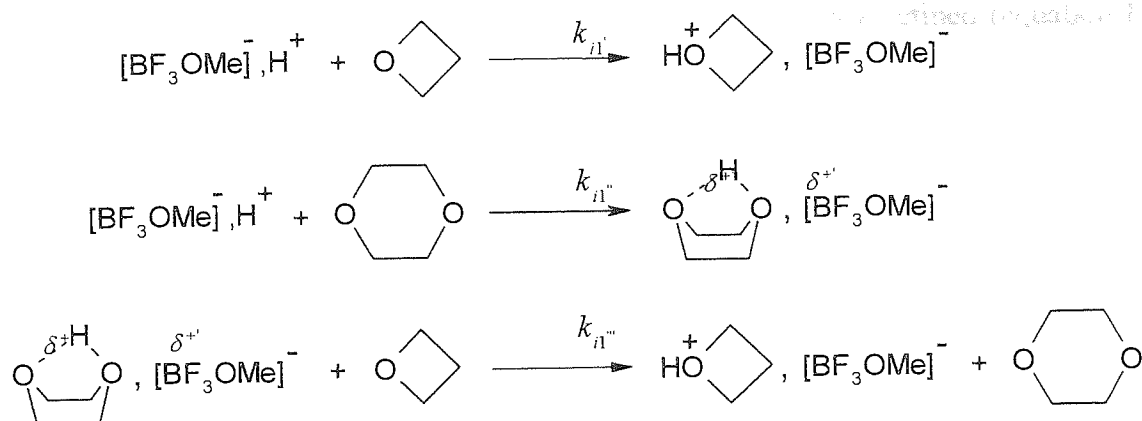


Figure 5. 26: Mechanism of “fast” initiation after addition of $\text{BF}_3\text{:MeOH}$ solution into monomer solution in 1,4-dioxane.

Because the rate of initiation is kinetically controlled by the rate at which oxetane is protonated, the initial rate of the fast initiation process, $(R_{il})_0$, can be written as follows,

$$(R_{il})_0 = k_{il'} \cdot \left[[\text{F}_3\text{BOMe}]^-, \text{H}^+ \right]_0 \cdot [\text{Ox}]_0 + k_{il'''} \cdot \left[[\text{F}_3\text{BOMe}]^-, (\text{dioxane})\text{H}^+ \right]_0 \cdot [\text{Ox}]_0 \quad \text{E: 5.77}$$

If c_{ox} and β (with $\beta = c_{ox} / (a_{01} \cdot (1 - \alpha))$) represent respectively the concentration and the fraction (in mole) of $[\text{F}_3\text{BOMe}]^-, \text{H}^+$ involved in the protonation of oxetane, while the concentration and the mole fraction of $[\text{F}_3\text{BOMe}]^-, \text{H}^+$ that undergo protonation of 1,4-dioxane are equal to $a_0 \cdot (1 - \alpha) \cdot c_{ox}$ and $(1 - \beta)$, respectively. Here, $a_0 \cdot (1 - \alpha)$ represents the concentration of non dissociated $\text{BF}_3\text{:MeOH}$. Here β is dependent on the basicity of cyclic ethers but also on the ratio $[1,4 - \text{Do}]_0 / [\text{Ox}]_0$.

$$\beta = f\left(\frac{[1,4 - \text{Do}]}{[\text{Ox}]}\right) \quad \text{E: 5.78}$$

Because the protonation of cyclic ether by $[\text{F}_3\text{BOMe}]^-, \text{H}^+$ is a fast process, it can then be assumed that the concentration of protonated 1,4-dioxane, $\left[(\text{dioxane})\text{H}^+, [\text{F}_3\text{BOMe}]^- \right]_{01}$, initially involved in the protonation of oxetane is equal to the initial concentration of $[\text{F}_3\text{BOMe}]^-, \text{H}^+$ involved in the protonation of 1,4-dioxane.

$$\left[(\text{dioxane})\text{H}^+, [\text{F}_3\text{BOMe}]^- \right]_{01} = (1 - \beta) \cdot (1 - \alpha) \cdot a_{01} \quad \text{E: 5.79}$$

Therefore, the initial rate of initiation reaction R_{i1} as previously defined (equation E: 5.77) can be express as follow,

$$(R_{i1})_0 = k_{i1'} \cdot \beta \cdot (1 - \alpha) \cdot a_{01} \cdot [Ox]_0 + k_{i1''} \cdot (1 - \beta) \cdot (1 - \alpha) \cdot a_{01} \cdot [Ox]_0 \quad \text{E: 5.80}$$

After rearrangement of the above equation,

$$(R_{i1})_0 = (k_{i1''} + (k_{i1'} - k_{i1''}) \cdot \beta) \cdot (1 - \alpha) \cdot a_{01} \cdot [Ox]_0 \quad \text{E: 5.81}$$

Because $[F_3BOMe]^-H^+$ is stronger acid than $[F_3BOMe]^-(1,4\text{-dioxane})H^+$,

$$k_{i1'} > k_{i1''} \quad \text{E: 5.82}$$

Therefore, with

$$0 < \beta < 1, \quad \text{E: 5.83}$$

the $k_{i1,app}$ appears to decrease from $k_{i1'}$ to $k_{i1''}$ as the ratio $[1,4\text{-Do}]/[Ox]$ increases

$$k_{i1''} < k_{i1,app} < k_{i1'} \quad \text{E: 5.84}$$

This is in perfect agreement with our kinetic investigations that show that at equal concentration of $BF_3:MeOH$, $(k_{p,app})_i$ decreases as the targeted Dp decreases. This suggests that the transfer of proton from 1,4-dioxane to the monomer is a slow process.

(c) Mathematical expression of the rate of initiation

Because the rate of initiation is a linear combination of R_{i1} (see equation E: 5.80) and R_{i2} (see equation E: 5.75), the initial rate of initiation, $(R_i)_0$, can then be written as follow

$$(R_i)_0 = k_{i1,app} \cdot [Ox]_0 + k_{i2,app} \cdot [MeOH]_0 \quad \text{E: 5.85}$$

with

$$k_{i1,app} = \left\{ \left\{ k_{i1}^{\infty} + (k_{i1}^{\cdot} - k_{i1}^{\infty}) \cdot \beta \right\} - \left\{ k_{i1}^{\infty} \cdot (1 - \alpha \cdot \gamma_t \cdot \exp(-k_{p,app} \cdot t)) + (k_{i1}^{\cdot} - k_{i1}^{\infty}) \cdot \beta \right\} \cdot \alpha \right\} \cdot a_{01}$$

E: 5.86

and

$$k_{i2,app} = k_{i2}^{\cdot} \cdot [BF_3 : Oxe \tan e]_0$$

E: 5.87

Because the direct protonation of oxetane by $[F_3BOMe]^{-}, H^{+}$ is a fast process, as the polymerisation progresses, only $[F_3BOMe]^{-}, (1,4\text{-dioxane})H^{+}$, $BF_3:Oxetane$ and $BF_3:1,4\text{-dioxane}$ will initiate the polymerisation. Therefore,

$$k_{i1,app} = k_{i1}^{\infty} \cdot \left([(dioxane)H^{+}, [F_3BOMe]^{-}]_{01} + a_{01} \cdot \alpha \cdot (1 - \delta_t) \right)$$

E: 5.88

and

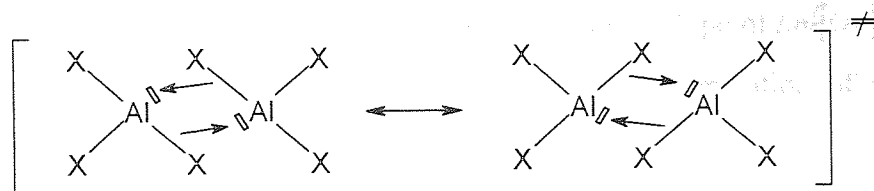
$$k_{i2,app} = k_{i2}^{\cdot} \cdot [BF_3 : Oxe \tan e]$$

E: 5.89

5.2.1.1.3.2 Mechanism of propagation of oxetane in 1,4-dioxane

As expected, our investigation of the polymerisation of oxetane in 1,4-dioxane showed that the reversible deactivation of the "active" growing centre by 1,4-dioxane slows down the polymerisation process but also reduces transfer reactions from occurring. The control character of the polymerisation was demonstrated by the fact that \overline{Mn} increases during the entire course of the polymerisation and that upon addition of monomer the "living" polymer chains are extended. The stability of the "active" species towards anion splitting reactions is believed to be due to the nature of the growing centres. Indeed, unlike carbocationic polymerisation (see figure 5.27), oxonium ions do not have an empty orbital that we believe is the driving force in the process of the anion splitting reaction.

Formation of ligand LX



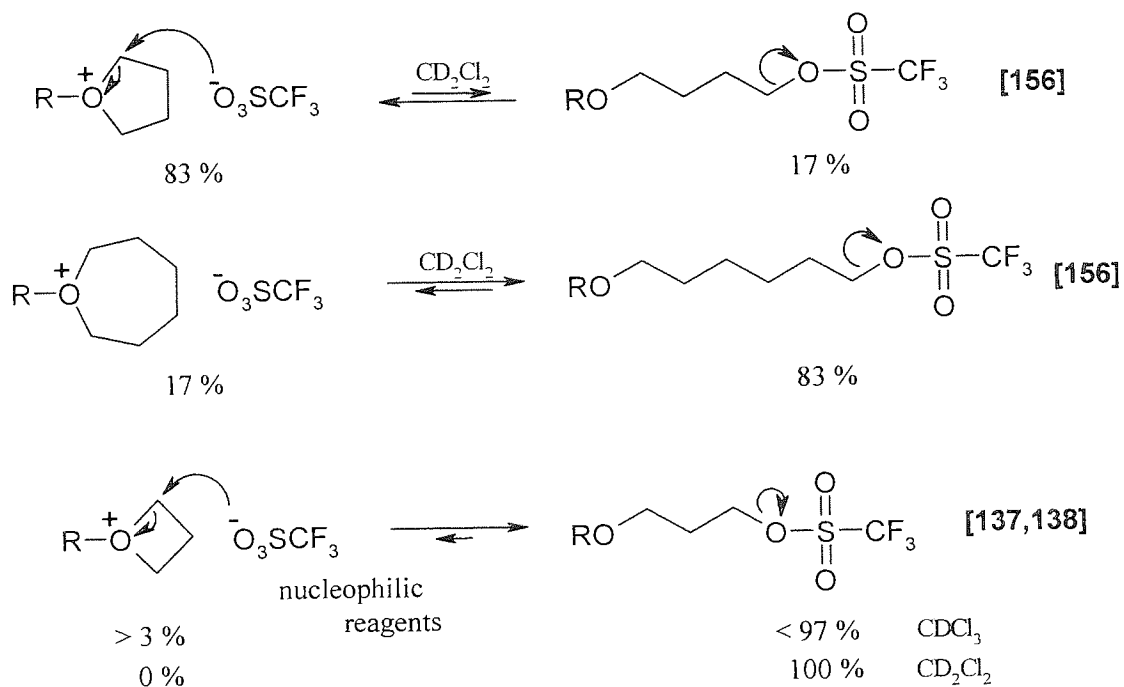
Dynamic equilibrium between "active" and "dormant" species in carbocationic polymerisation



Anion-splitting reaction in carbocationic polymerisation in carbocationic polymerisation



Dynamic equilibrium between "active" and "dormant" species in CROP of cyclic ether by super acid ester



Anion-splitting reaction in CROP of oxetane

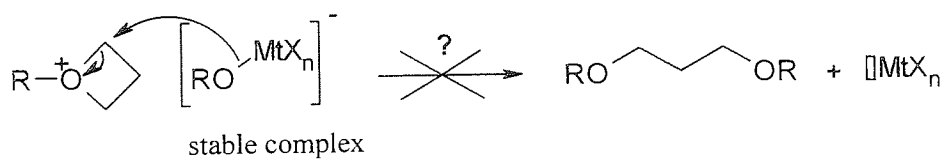


Figure 5. 27: Termination reactions in cationic polymerisation.

Because termination reactions are prevented, the reactivation of "dormant" species by a molecule of monomer was demonstrated by the curvature of slope of $\ln([Ox]_0/[Ox]_t)$ against time. Based on the kinetic studies, the mechanism of polymerisation of oxetane in 1,4-dioxane can be represented as follow,

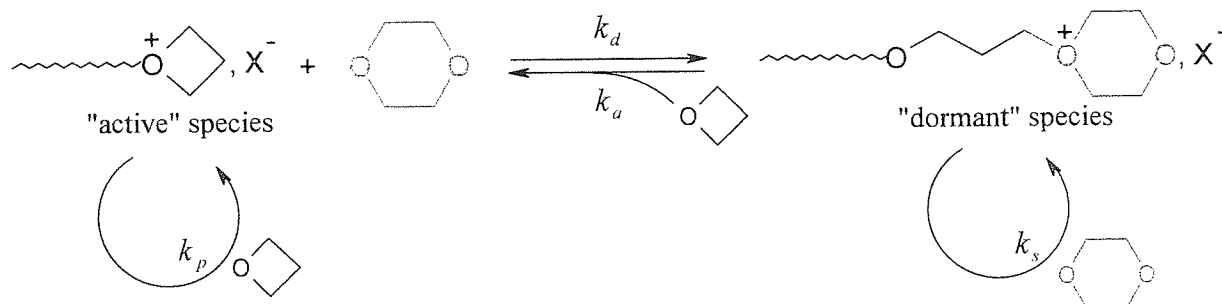
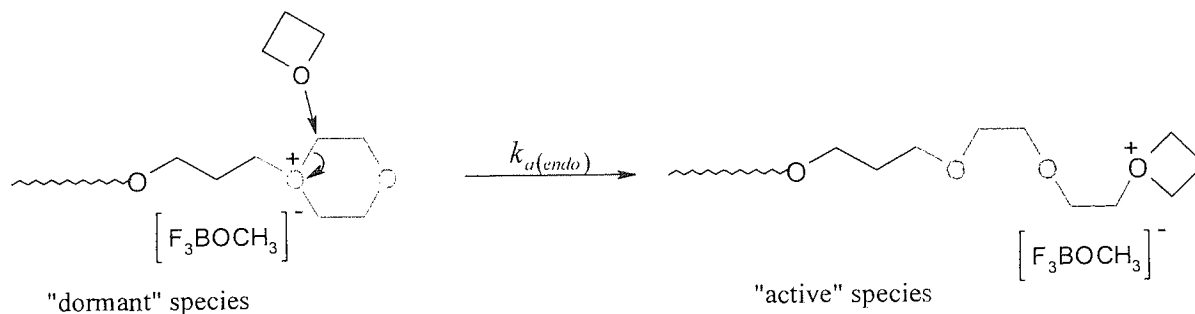


Figure 5. 28: Mechanism of polymerisation of oxetane in 1,4-dioxane.

Further investigation showed that the reactivation of "dormant" species by oxetane can also occur by nucleophilic attack of the endo-cyclic electron deficient carbon atom in the α -position of the dioxanium site (see figure 5.29).

Copolymerisation of 1,4-dioxane by oxetane



Substitution Nucleophile 2 of 1,4-dioxane by oxetane

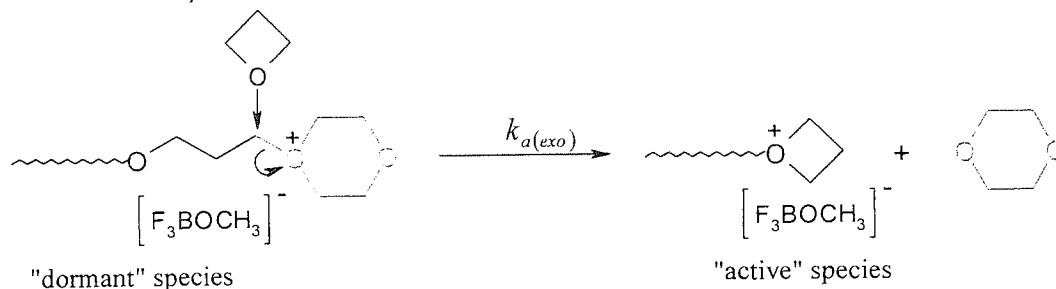


Figure 5. 29: Mechanism of reactivation of "dormant" species by oxetane via S_N2 process.

Indeed, the ^{13}C NMR analysis revealed that 1,4-dioxane can be copolymerised and that each 1,4-dioxane units is surrounded by two oxetane monomer units. This clearly shows that 1,4-dioxane is not sufficiently nucleophilic to ring-open the 1,4-dioxanium ions once the “active” growing centre is deactivated by a molecule of 1,4-dioxane. Here, the incorporation of 1,4-dioxane reinforces the idea that the reactivation of “dormant” species by oxetane occurs by a bimolecular process, most probably $\text{S}_{\text{N}}2$ considering the nature of the polymerisation of oxetane^[114,120-123]. The ^{13}C NMR, showed that the copolymer contains less than 6 % of 1,4-dioxane monomer units. Therefore, if $p_{a(\text{endo})}$ and $p_{a(\text{exo})}$ represent respectively the probability that oxetane attack the endo-cyclic and exo-cyclic electron deficient carbon atom in the α -position of the oxonium site, the apparent rate constant of activation can then be expressed as follows,

$$k_a = k_{a(\text{endo})} + (k_{a(\text{exo})} - k_{a(\text{endo})}) \cdot p_{a(\text{exo})} \quad \text{E: 5.90}$$

with

$$p_{a(\text{endo})} + p_{a(\text{exo})} = 1 \quad \text{E: 5.91}$$

It must be noted that $p_{a(\text{endo})}$ and $p_{a(\text{exo})}$ are constant during the entire course of the polymerisation. ^{13}C NMR analysis has also revealed that cyclic oligomer formation was not prevented but only reduced. Because cyclic oligomers are formed at the end of the polymerisation process, we believed that the process cyclic oligomers formation occurs mainly by end-biting reactions due to fact that the initiation process is incomplete.

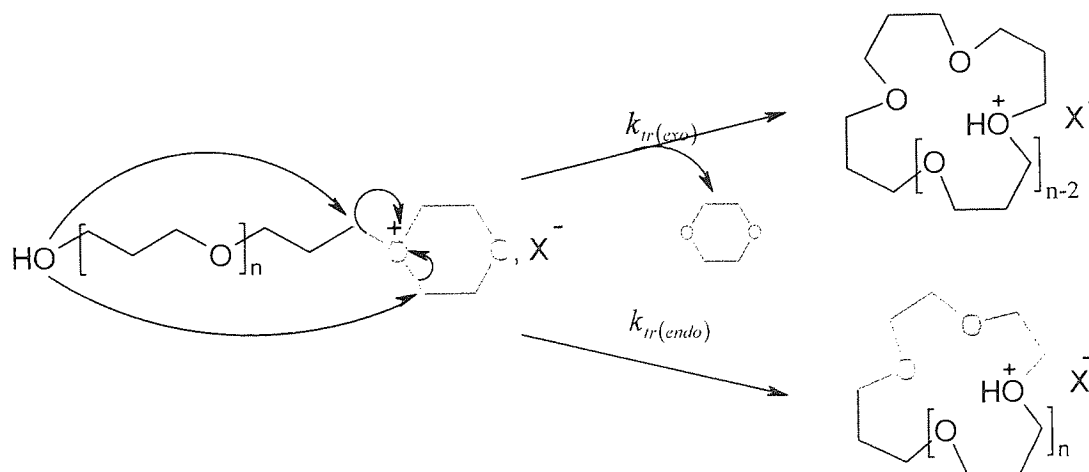


Figure 5. 30: Mechanism of end-biting reaction in 1,4-dioxane

Because, hydroxyl tail group is the stronger nucleophilic reagent in the polymerisation medium, the ring-opening expansion of dioxanium salts by end-biting reaction could explain the formation of cyclic oligomers containing 1,4-dioxane fragment for the growing species that do not reach a sufficiently high chain length to entropically disfavour the end to end polymer chains reactions. This could explain the formation of the peaks at 66.18 and 66.78 ppm that we assigned to the $\text{-OCH}_2\text{CH}_2\text{CH}_2\text{OCH}_2\text{CH}_2\text{OCH}_2\text{CH}_2\text{OCH}_2\text{CH}_2\text{CH}_2\text{O-}$ fragment in cyclic oligomers. According to the ^{13}C NMR, the CH_2 groups of 1,4-dioxane fragment appear to have identical chemical shift in linear and cyclic polymeric material. For this reason, the polymerisation cannot be classified as a quasiliving process but as a "controlled" polymerisation process even if we strongly believe that all the polymer chains involved initially in the polymerisation process are living (see figure 5.31).

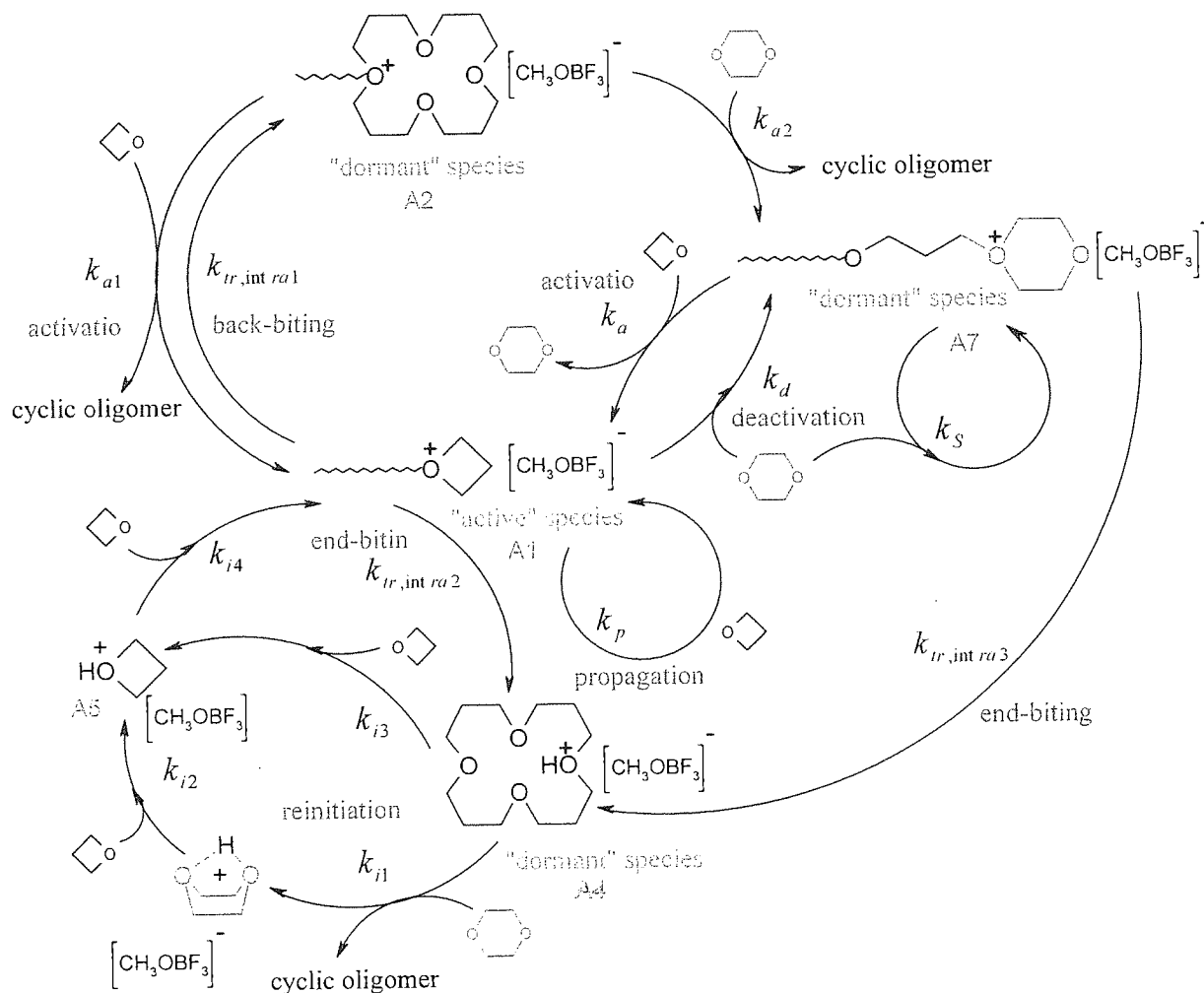


Figure 5.31: Mechanism of the controlled polymerisation of oxetane in 1,4-dioxane initiated by $\text{BF}_3 \cdot \text{MeOH}$ at 35°C .

The broad polydispersity of the polymers formed is ascribed to a slow initiation process rather than the intermolecular transfer reactions. This was demonstrated by the fact that the \overline{Mn} increases continuously during the polymerisation process, that the curvature of the slope of \overline{Mn} against conversion intercept the origin and that the monomer addition experiments extend the living polymer chains.

5.2.1.2 Polymerisation initiated by alkylating reagents

“Living monomeric polymer” initiators are often used in “quasiliving” cationic polymerisation to provide the satisfactory evidence for the absence of transfer and terminations reactions. The idea here is to prepare in situ an “active monomeric” species identical to the “living” growing polymer chains. For example, the reaction of cumyl chloride with boron trichloride leads in millisecond to the following equilibrium

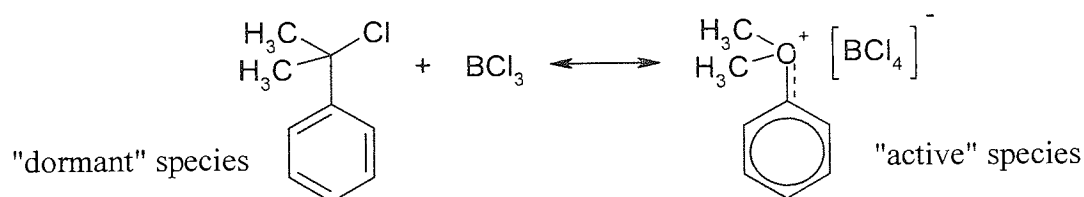


Figure 5. 32: Interconversion between “active” and “dormant” species catalysed by BCl₃.

which in the presence of styrene yields monodisperse end-functionalised polystyrene chloride. Under such conditions, the initiation process is not slower than the propagation and the truly living character of the polymerisation can be demonstrated if the number average degree of polymerisation is given by the following relations

$$\overline{DPn} = \frac{[M]_0}{[I]_0} \times \text{conversion} \quad \text{E: 5.92}$$

provided that all the initiator was utilised effectively ($f = 1$). To satisfy the criteria of livingness, the resulting polymer should have a Poisson molecular mass distribution provided that the propagation is irreversible and upon monomer addition the *living polymer chains* have to be extended correspondingly. According to Szwarc, the truly living character of the polymerisation is preferred to the criteria of controlled polymerisation only if high molecular weight materials can be produced while the polymerisation proceeds under living conditions.

Since the development of the quasiliving cationic polymerisation, different types of stable salts have been used by many researchers in their attempts to satisfy the criteria for living polymerisation. From the most common used active salts, diphenylmethylium Ar_2CH^+ (S1), derivatives of oxacarbenium $\text{RC}=\text{O}^+$ (S2), alkoxy-carbenium ROCH_2^+ (S3), oxonium R_3O^+ (S4), sulfonium R_3S^+ (S5) and various ions participating in the numerous cationic ring-opening polymerisation turned out to be active initiators in cationic polymerisation when associated with large and non-nucleophilic anions derived from Friedel and Craft reagents such as $[\text{SbX}_6]^-$ (with $\text{X} = \text{Cl}, \text{F}$). This class of initiator has been classified by Ledwith and Sherrington^[330].

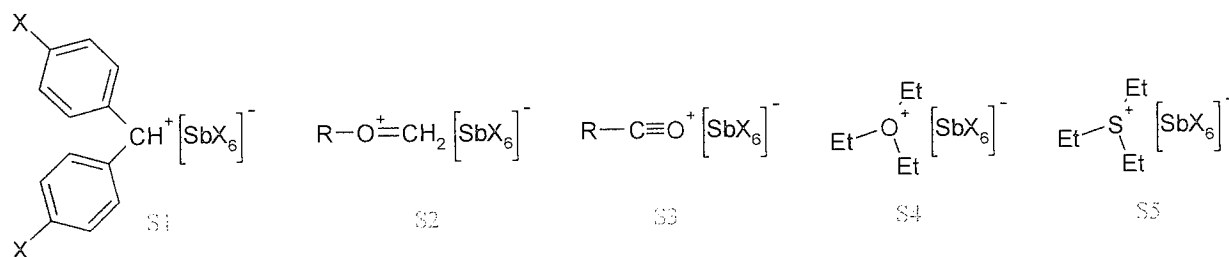


Figure 5. 33: Examples of active salts active in cationic polymerisation.

Because protonic reagents induce a slow initiation, the use of synthetically prepared “living monomeric polyoxetane” initiator associated with a large counter-anion seemed to us to be the alternative to develop the “quasiliving” cationic ring-opening polymerisation of oxetane in 1,4-dioxane. The synthetically prepared initiators used in this present study are represented in the figure 5.34.

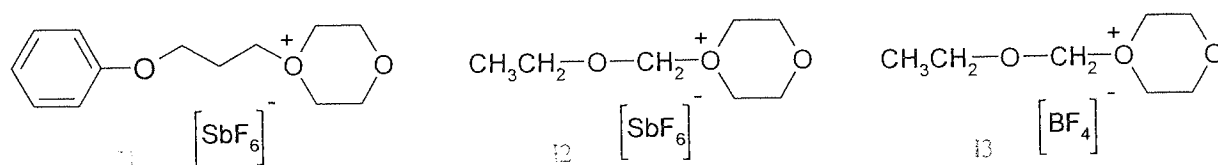


Figure 5. 34: Active salts used in this study.

Each initiator was synthesised at room temperature in dried and freshly distilled 1,4-dioxane as described in the section 2.1.1. Because the oxoniums salts cannot be prepared with rigorous exclusion of moisture contamination, traces of water (ppm) can hydrolyse oxacarbenium salts and form protonating reagents capable of initiating the polymerisation.

Because of this 1 mol equivalent of 2,6-di-*t*-butyl-pyridine (DtBP) was added to the equimolar solution of $\text{RCH}_2\text{Cl}/\text{AgMtX}_n$ to prevent the formation of protonic initiator.

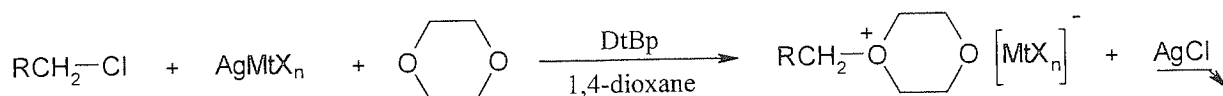


Figure 5. 35: Preparation of the active salts.

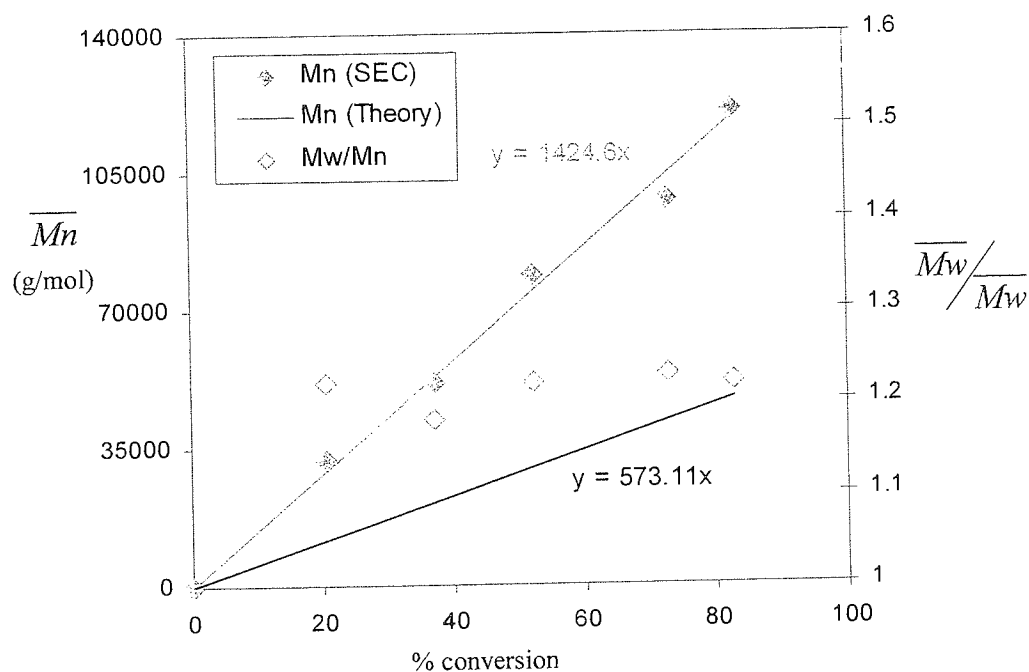
The polymerisation reaction was then carried out by injecting the initiating system mixture in the calorimeter already containing the solution of monomer in 1,4-dioxane or mixture of dichloromethane and 1,4-dioxane. In all experiments, the initiating system was injected into the reaction vessel already containing the monomer solution using sampling technique as described in the chapter 2.8.1. The total volume of polymerisation solution was kept constant and equal to 25 ml. The polymerisation reactions were followed by withdrawing active polymer samples using sampling technique as described in the section 2.8.3. The active polymer solutions were deactivated in a large excess volume of ethanol and the inactive polymer solution was treated as described in the section 2.8.1.2. The rate of polymerisation was monitored by gravimetric analysis and the resulting polymers were analysed SEC and NMR analysis.

5.2.1.2.1 Effect of the initiator and counter-anion on the polymerisation

5.2.1.2.1.1 Polymerisation initiated by the active salt II

As expected, when **II** was used as “living monomeric polyoxetane” initiator (fast initiator), polymers with narrow molecular weight distribution ($1.18 < \overline{Mw}/\overline{Mn} < 1.24$) were produced with no cyclic oligomers formation. The absence of cyclic oligomers was showed both by SEC analysis (annex 5.15) and by ^{13}C NMR (annex 5.16). The living nature of the polymerisation was demonstrated by the fact that the linear increase of \overline{Mn} with the conversion intercepts the origin (figure 5.36) and upon addition of further monomer, the existing polymer chains were extended correspondingly (figure 5.37). The production of high molecular weight material with narrow molecular weight distribution ($\overline{Mn} = 160,000 \text{ g/mol}$ and $\overline{Mw}/\overline{Mn} = 1.2$) showed clearly that transfer (intra- and intermolecular transfer reactions) and termination reactions are both prevented. Here the

constant but small value of $\overline{Mw}/\overline{Mn}$ is ascribed to slow exchange between “active” and “dormant” species in comparison to the propagation. The SEC traces of the product are represented in the annex 5.15 and 5.18.



Oxetane polymerised in 1,4-dioxane using 0.00114 M of “living monomeric polyoxetane” initiator (11) at 35°C. Table 5.6 series S 5.5.

Figure 5.36: Evolution \overline{Mn} and $\overline{Mw}/\overline{Mn}$ against conversion

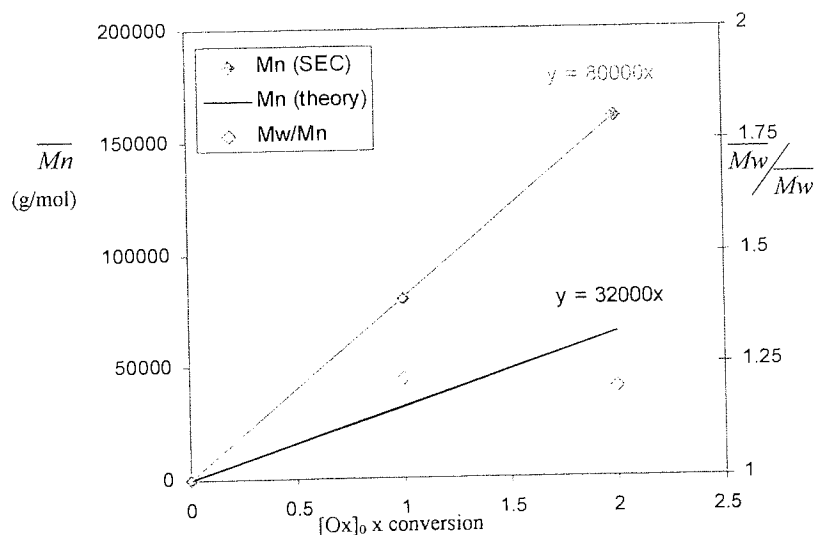
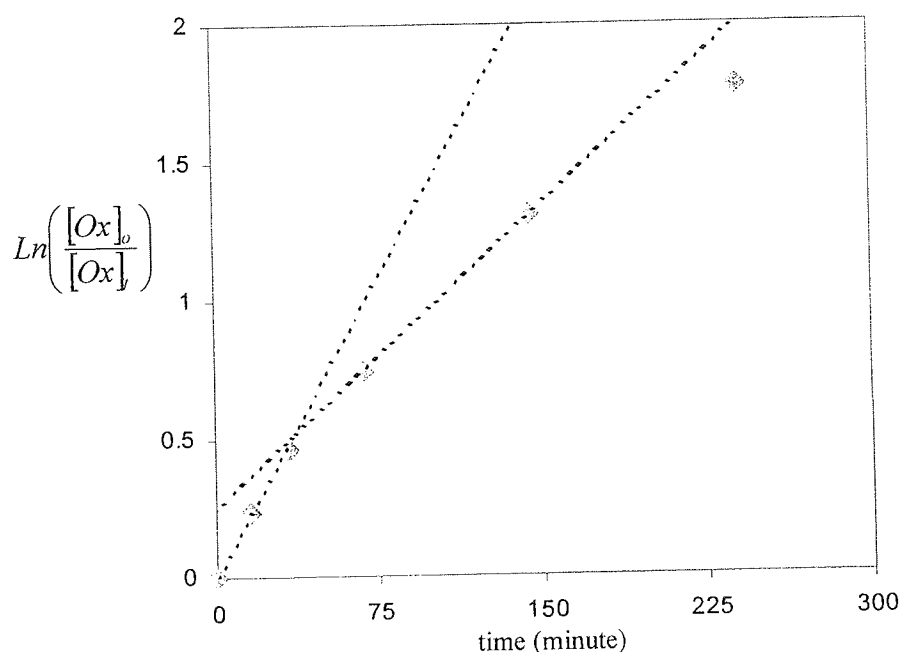


Figure 5.37: Evolution of \overline{Mn} and $\overline{Mw}/\overline{Mn}$ after monomer addition when 1 M of oxetane is polymerised in 1,4-dioxane using “living monomeric polyoxetane” initiator (11) at 35°C. Table 5.7 series S 5.9.

Knowing the composition of the polymer in 1,4-dioxane, the rate at which oxetane was consumed was then investigated. As expected the slope of $\text{Ln}([Ox]_0/[Ox]_t)$ against time showed that "active" and "dormant" species are in some sort of dynamic equilibrium which favours the formation of "dormant" species as the monomer concentration decreases in the polymerisation feed. This clearly showed that the reactivation of the "dormant" is a bimolecular process that involves a molecule of monomer. The continuous decrease of $k_{p,app}$ is one more indication that the initiation by **II** is a fast process in comparison with the step of propagation. In this respect, the polymerisation process can then be classified as a "quasiliving" polymerisation process.



Oxetane (1M) polymerised by 0.00114 M "living monomeric polyoxetane" initiator (**II**) at 35°C. Table 5.6 series S 5.5.

Figure 5. 38: Evolution of $\text{Ln}([Ox]_0/[Ox]_t)$ against time

Because of the living nature of the polymerisation of oxetane in 1,4-dioxane, the low initiator efficiency revealed by SEC analysis ($f = 0.4$) can only be explained by the existence of reaction of elimination (probably E2) during the preparation of the initiator at room temperature. Indeed, in organic chemistry, S_N2 reactions on primary carbon are generally allowed to proceed at low temperature ($T < -50^\circ\text{C}$) in order to favour S_N2 over E2, particularly in the presence of a good leaving group such Br catalysed by silver salt. This is what Burgess et al.^[333] did when they attempted to polymerised THF by PSty with end-

terminal bromine (Br-PSt-Br). Indeed, when Br-PSt-Br was combined with silver perchlorate, AgOCl₄, to initiate the polymerisation of THF, the initiation efficiency (or block copolymerisation efficiency) turned out to be greatly dependent on the reaction temperature because of the β -hydrogen elimination reaction which results in the formation of dead polymer (macromonomer of PStyr) and HOCl₄ capable to initiate the polymerisation of THF. A model polymerisation using 1-bromoethylbenzene showed that β -proton elimination was reduced from 63 % to 33% and < 5% when the initiation of THF were performed at room temperature, 0 °C and -78 °C, respectively^[331-335]. In our present investigation, the low initiator efficiency (\approx 40 %) observed by SEC analysis against PS standards is in agreement with general observation. In the next page, the figure 5.40 represents different possible chemical reactions that could be involved at room temperature during the preparation of the initiator. The ¹H and ¹³C NMR analysis in deuteriated 1,4-dioxane C₄D₈O₂ in sealed tube should be able to reveal the presence of the side compounds. This implies that in the future, the initiator **II** will have to be prepared at low temperature in dichloromethane in the presence of 1 or 2 mole equivalent of 1,4-dioxane in respect to the concentration of RBr.

5.2.1.2.1.2 Polymerisation initiated by oxacarbenium salt end-capped by 1,4-dioxane

In order to enable the preparation of fast initiator at room temperature, bromomethyl methyl ether was then used instead of phenoxypropyl bromide. As shown in the figure 5.39, the action of silver salt on CH₃CH₂OCH₂Br generates a stable oxacarbenium ion by S_N1 that is rapidly and reversibly end-capped by 1,4-dioxane. Similar equilibrium where also reported in the living cationic polymerisation of vinyl ether in presence of 1,4-dioxane^[315,317-319] and on the cationic polymerisation of 1,3-dioxepane^[336]. Here the non nucleophilic proton trap (DtBP) was used only to prevent the hypothetical formation of protonic initiator in the case of the presence of moisture.

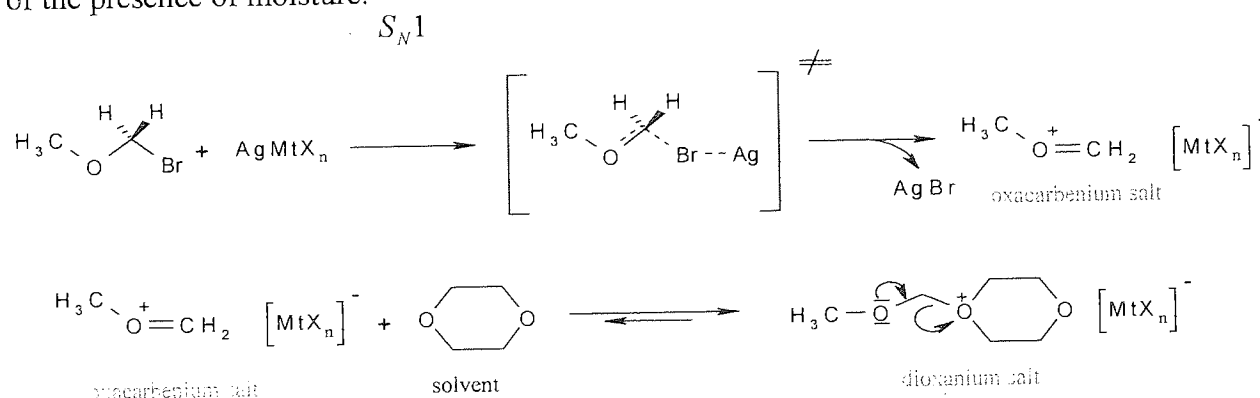


Figure 5. 39: Mechanism of formation of active salts **II** and **III** in dry and freshly distilled 1,4-dioxane at room temperature.

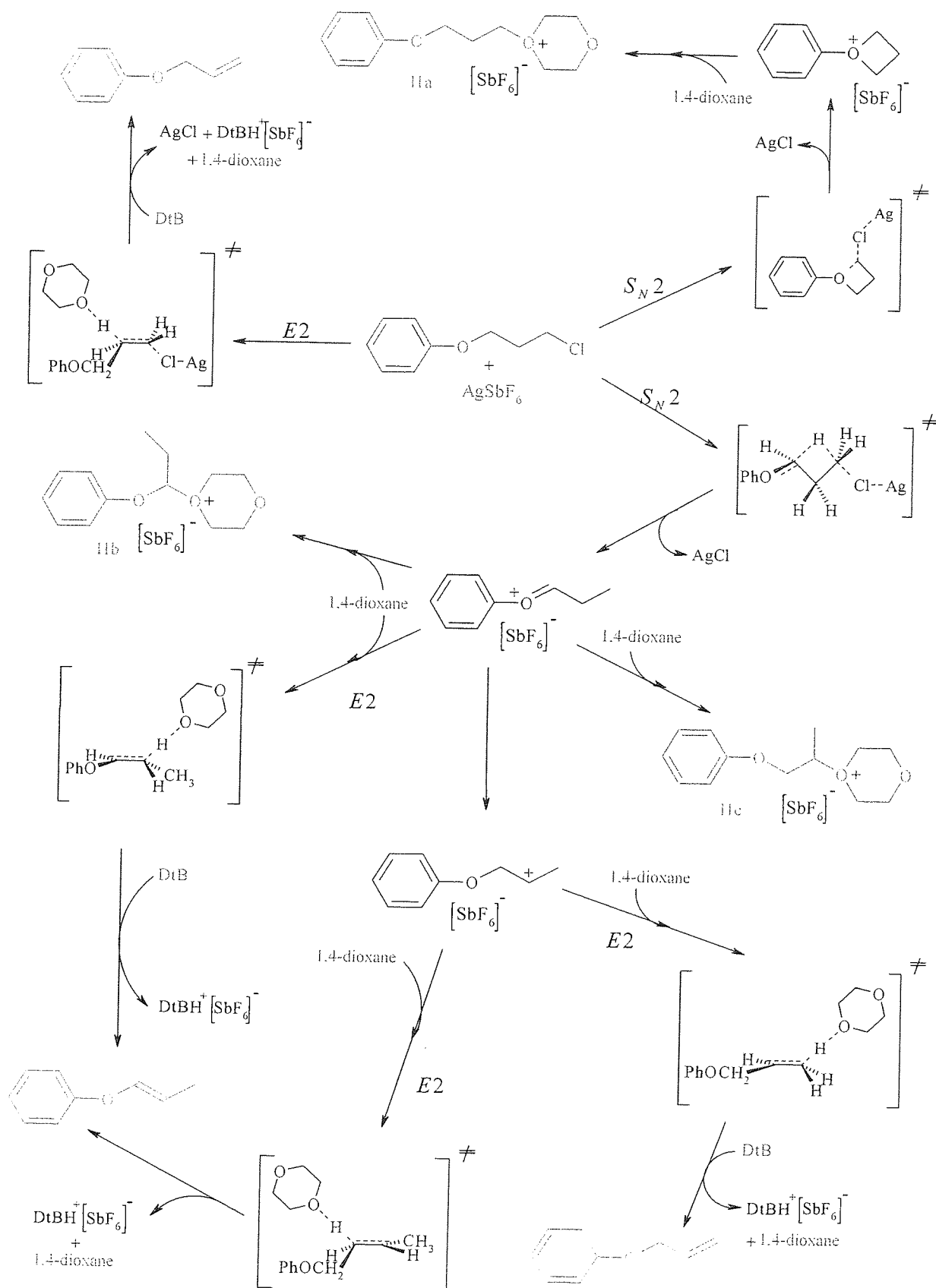


Figure 5. 40: Mechanism of formation of "living monomeric polyoxetane" initiator II in dry and freshly distilled 1,4-dioxane at room temperature. Competition between S_N2 and $E2$ reactions.

Series	[Ox] ₀	[I] ₀	[Dox] ₀ /[Ox] ₀	% dioxane in dcm	P (E: 5.49)	% mole ¹³ C NMR	Conversion (E: 5.51)	Mn (theory)	Mn (SEC)	Mp (SEC)	Mw/Mn (SEC)	Time minute
S 5.5.1 ^a	1.124	0.00114	9.66	100	20.7	0	20.7	11,850	31,920	37,780	1.22	16
S 5.5.2 ^a	1.124	0.00114	9.66	100	37	0	37	21,190	51,700	64,130	1.18	34
S 5.5.3 ^a	1.124	0.00114	9.66	100	52.5	0	52.5	30,050	79,000	98,430	1.22	68
S 5.5.4 ^a	1.124	0.00114	9.66	100	73.45	0.4	73	41,840	98,000	123,700	1.26	145
S 5.5.5 ^a	1.124	0.00114	9.66	100	84.15	0.9	83	47,570	120,61	151,200	1.23	240
S 5.6.1 ^a	1.124	0.00114	7.25	75	19.9	0	19.9	11,405	0	45,410	1.93	2
S 5.6.2 ^a	1.124	0.00114	7.25	75	45.8	0	45.8	26,265	31,040	105,800	1.72	6
S 5.6.3 ^a	1.124	0.00114	7.25	75	69.5	0.4	69.1	40,043	61,220	159,140	1.79	21
S 5.6.4 ^a	1.124	0.00114	7.25	75	74.4	0.5	74.4	42,628	88,700	164,000	1.73	30
S 5.6.5 ^a	1.124	0.00114	7.25	75	96.5	0.7	95.4	54,697	94,820	231,130	1.96	300
S 5.7.1 ^a	1.124	0.00114	3.86	40	38.1	0	38.1	21,778	0	72,400	1.92	3

(a) polymerisation initiated by $C_6H_5O(CH_2)_3O^+(C_2H_4)_2O, [SbF_6]^-$

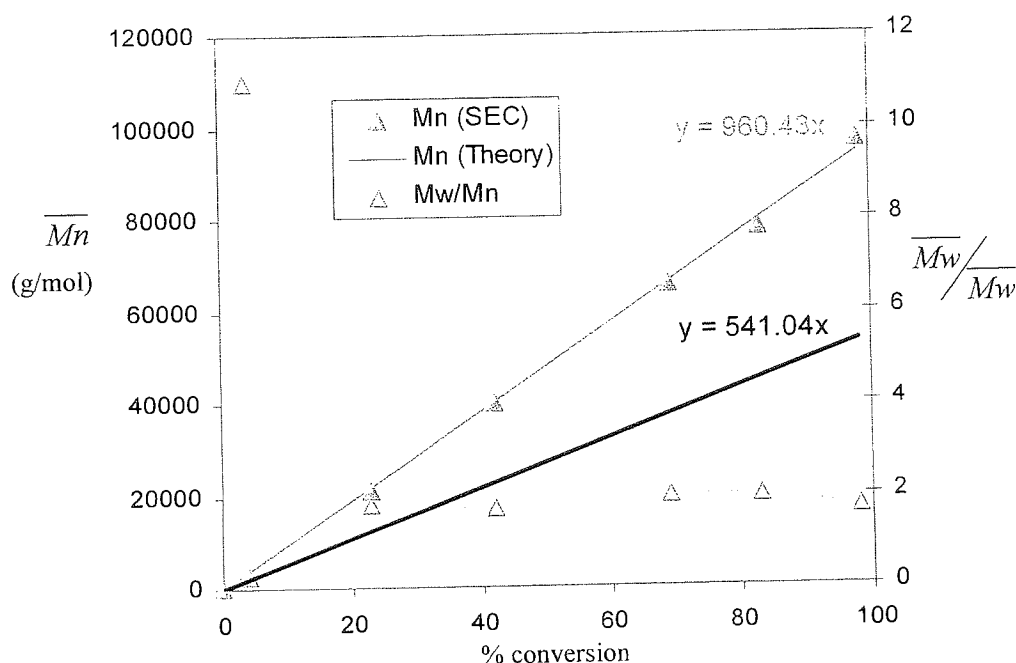
(b) polymerisation initiated by $CH_3CH_2OCH_2O^+(C_2H_4)_2O, [SbF_6]^-$

Table 5. 6: Effect of 1,4-dioxane on \overline{Mn} and $\overline{Mw}/\overline{Mn}$ when the polymerisation of oxetane is initiated at 35 °C by "living monomeric polyoxetane" associated with $[SbF_6]^-$ as counter-ion.

Entry	Before monomer addition					After monomer addition					NMR ^{13}C	SEC analysis		
	$[\text{I}]_0$	$[\text{Ox}]_0$	P	$\% \text{ mole } ^{13}\text{C NMR}$	time t_k min	time t_{add}	$[\text{Cat}]_0$	$[\text{Ox}]_0$	P	$\% \text{ mole } ^{13}\text{C NMR}$	time t_k min	Mn (theory) g/mol	Mn (SEC) g/mol	Mw/Mn g/mol
S 5.9.1	0.002	1.125	97.83	1.1	300							31,845	79,500	1.24
S 5.9.2	0.002	1.125				After monomer addition					96.3	67,115	160,100	1.2
						300	0.0187	1.18	97.5	0.95	900			

Table 5.7: Effect of monomer addition on \overline{Mn} and $\overline{Mw}/\overline{Mn}$ when the polymerisation is initiated by $\text{C}_6\text{H}_5\text{O}(\text{CH}_2)_3\text{O}^+(\text{C}_2\text{H}_4)_2\text{O}, [\text{SbF}_6]^-$ in 1,4-dioxane at 35 °C.

5.2.1.2.1.2.1 Polymerisation initiated by the active salts **12**. When $\text{CH}_3\text{CH}_2\text{OCH}_2\text{O}^+(\text{C}_2\text{H}_4)_2\text{O}, [\text{SbF}_6]^-$ was used instead of $\text{C}_6\text{H}_5\text{O}(\text{CH}_2)_3\text{O}^+(\text{C}_2\text{H}_4)_2\text{O}, [\text{SbF}_6]^-$, the change of $\text{PhO}(\text{C}_2\text{H}_4)_3$ group by EtOCH_2 group did not give the expected control over $\overline{M}_w/\overline{M}_n$ ($1.7 < \overline{M}_w/\overline{M}_n < 2$). The polymerisation, however, showed the other attributes of living polymerisation which include linear increases of \overline{M}_n with the conversion and decrease of the polydispersity as the polymerisation goes from low to high conversion (figure 5.41). This study is summarised in the table 5.6, series S 5.8. The SEC traces of the produced polymer are showed in the annex 5.21.

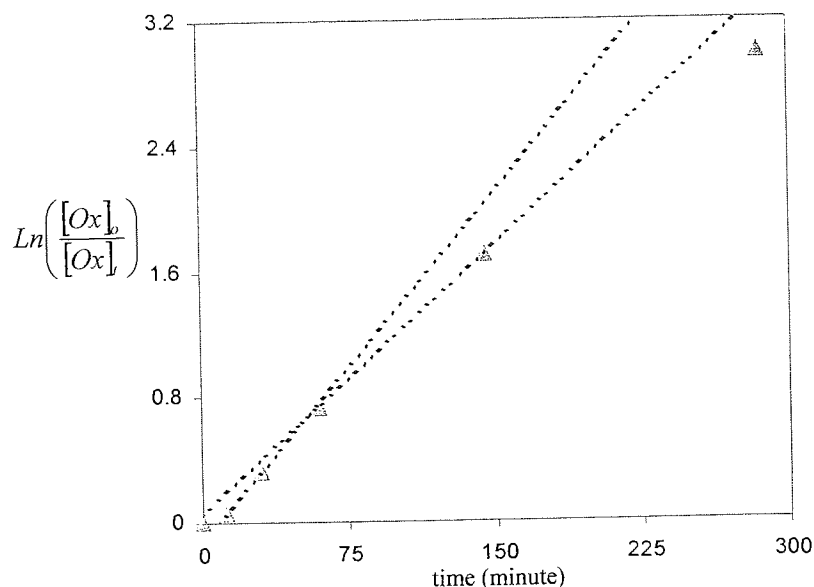


Oxetane (1.125 M) polymerised in 1,4-dioxane using 0.00134 M of the active salt (**12**) at 35°C. Table 5.6 series S 5.8.

Figure 5. 41: Evolution of \overline{M}_n and $\overline{M}_w/\overline{M}_n$ after monomer addition.

Because **11** yields living growing polymers with narrow average molecular weight distribution, the decrease of $\overline{M}_w/\overline{M}_n$ from 12 to 1.7 can only be explained by a non spontaneous initiation process ascribed most probably to a lack of solubility of **12** in 1,4-dioxane. Indeed, in poorly solvating media, such as 1,4-dioxane, the use of $\text{CH}_3\text{CH}_2\text{OCH}_2-$ group instead of $\text{C}_6\text{H}_5\text{OCH}_2\text{CH}_2\text{CH}_2-$ group might reduce the solubility of the active salts **12** favouring the association of ion-pairs into aggregate. The formation of small and soluble aggregates could then be responsible for the formation of polymer of broad polydispersity in the early stage of the polymerisation. The slope of $\text{Ln}([Ox]_0/[Ox]_t)$ against time shows an

induction period during the first 12 minutes of the polymerisation process. The linear dependence of \overline{Mn} against conversion strongly indicates that living i-mers are not associated into aggregates.



1 M of oxetane polymerised by 0.00134 M of the active salt (12) at 35°C. Table 5.6 series S 5.8.

Figure 5.42: Evolution of $\text{Ln}([Ox]_0/[Ox]_t)$ against time.

Because the dissociation of ion-pairs in 1,4-dioxane is most probably an endothermic process, the association of small aggregates into higher insoluble aggregates might also occur during the preparation of 12. The precipitation of such insoluble aggregates could then explain the low initiator efficiency observed by SEC analysis. To find out whether insoluble aggregates can be form during the preparation of I2, the insoluble material resulting from the reaction of $\text{CH}_3\text{CH}_2\text{OCH}_2\text{-Cl}$ with AgSbF_6 and DtBP was then extracted by filtration using a suction pump. The resulting solid, mostly composed of silver salt was then washed several times with dry and freshly distilled 1,4-dioxane in order to remove any material soluble in 1,4-dioxane. The solid was then dried in a vacuum oven at room temperature for at least 20 minutes. When the resulting solid was added into a solution of 80 % v/v of oxetane in dichloromethane, an intense exothermic polymerisation occurred and polymer with a broad polydispersity was formed.

5.2.1.2.1.2.2 Polymerisation initiated by the active salt I3.

When $\text{CH}_3\text{CH}_2\text{OCH}_2\text{O}^+(\text{C}_2\text{H}_4)_2\text{O}, [\text{BF}_4]^-$ was used instead of $\text{CH}_3\text{CH}_2\text{OCH}_2\text{O}^+(\text{C}_2\text{H}_4)_2\text{O}, [\text{SbF}_6]^-$, the loss of the control over $\overline{Mw}/\overline{Mn}$ was more significant

($1.8 < \overline{Mw}/\overline{Mn} < 2.2$) and the evolution of \overline{Mn} against conversion (figure 5.48) showed a initial curvature characteristic of a slow initiation process, that was confirmed by the sigmoid form plot of $\ln([Ox]_0/[Ox]_t)$ against time (figure 5.49). The SEC traces of the produced polymers are shown in the annex 5.22 and 5.23.

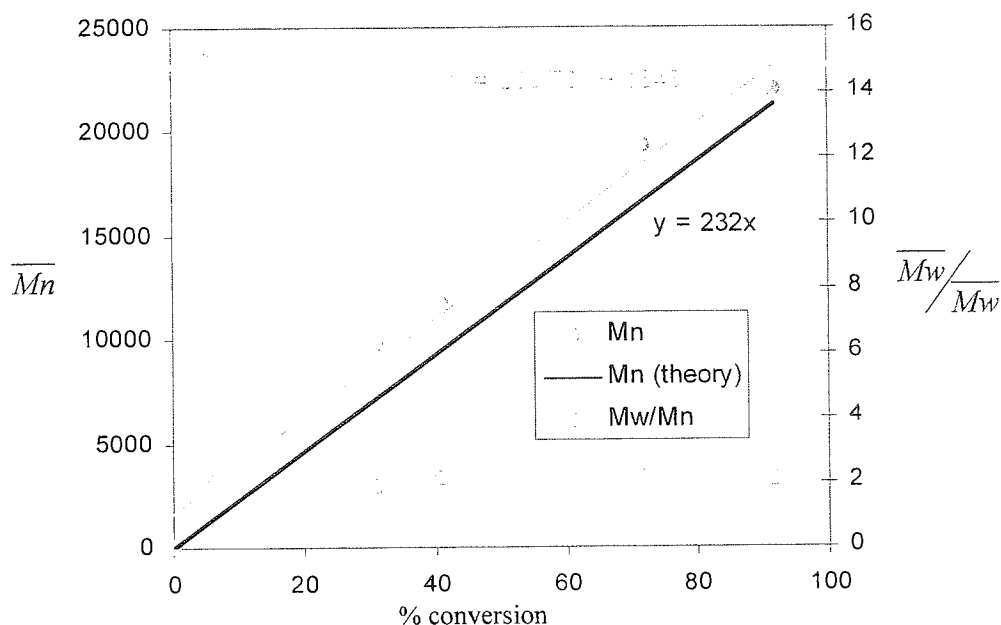


Figure 5.43: Evolution of \overline{Mn} and $\overline{Mw}/\overline{Mn}$ after monomer addition when 1 M of oxetane is polymerised in 1,4-dioxane using 0.0025 M of the active salt (I3) at 35°C. Table 5.8 series S 5.10 annex 5.16.

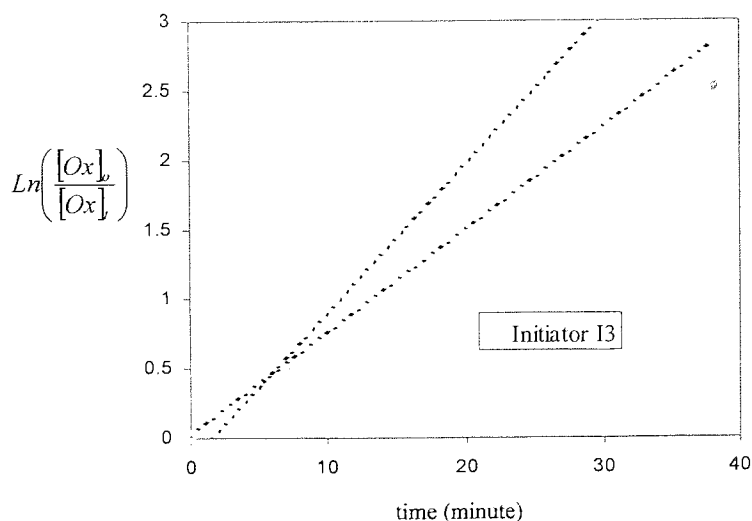


Figure 5.44: Evolution of $\ln([Ox]_0/[Ox]_t)$ against time when 1 M of oxetane is polymerised by 0.0077 M of the active salt (I3) at 35°C. Table 5.8 series S 5.10.

Series	[Ox] ₀ mol/l	[I2] ₀ mol/l	[Dox] ₀ /[I] ₀	P (E: 5.49) %	% dioxane in dem	% ^{mole} ₁₃ C NMR Dox	Conversion (E: 5.51) %	Mn (theory) g/mol	Mn (SEC) g/mol	Mp (SEC) g/mol	Mw/Mn (SEC) g/mol	Time Second	Q
S 5.10.1	1	0.0025	9.7	5.15	100	1.5	5	1,160	3,500		15	120	0
S 5.10.2	1	0.0025	9.7	32.45	100	3.01	31	7,190	9,770		1.87	300	0
S 5.10.3	1	0.0025	9.7	42.63	100	2.54	41	9,510	11,670		2.09	300	0
S 5.10.3	1	0.0025	9.7	75.67	100	3.25	72	16,700	14,280		2.12	420	0
S 5.10.4	1	0.0025	9.7	98.12	100	4.2	92	21,350	22,030		2.05	420	0
S 5.10.4	1	0.0026	8.22	24.22	75	1.98		5,440	51,240	98,430	1.98	1,020	0.003
S 5.10.5	1	0.0026	8.22	51.14	75	2.4	23.5	11,435	58,030	107,620	1.95	2,180	0.004
S 5.10.5	1	0.0026	8.22	61.84	75	2.75	49.3	13,762	61,680	136,260	1.96	95	0
S 5.11.1	1	0.0026	8.22	73.31	75	3.16	59.3	15,585	60,370	123,280	2.09	545	0
S 5.11.1	1	0.0026	8.22	84.28	75	3.32	68.9	18,585	45,670	109,230	2.26	960	0
S 5.11.2	1	0.0026	8.22	88.4	75	3.98	80.1	19,256	39,660	88,670	2.06	1,800	0
S 5.11.2	1	0.0025	5.48	24.7	50	1.75	83.2	5,568	19,320		2.02	3,000	0.001
S 5.11.3	1	0.0025	5.48	52.5	50	1.9		11,832	27,540		1.98	3,060	0.004
S 5.11.4	1	0.0025	5.48	66.18	50	2.2	24	14,848	31,000		2.05	60	0
S 5.11.5	1	0.0025	5.48	88.3	50	2.48	51	19,720	36,870		2.07	420	0
S 5.11.6	1	0.0025	5.48	94.5	50	3.15	64	20,880	32,470		2.09	1,115	0
S 5.11.6	1	0.0025	5.48	97.28	50	3.28	85	21,844	19,520		2.10	1,920	0.007

Table 5. 8: Effect of 1,4-dioxane on \overline{Mn} and $\overline{Mw}/\overline{Mn}$ when the polymerisation of oxetane is initiated by $\text{CH}_3\text{CH}_2\text{OCH}_2\text{O}^+(\text{C}_2\text{H}_4)_2\text{O}, [\text{BF}_4]^-$ at 35 °C.

Entry	Before monomer addition						After monomer addition				NMR ^{13}C	SEC analysis		
	$[\text{I}]_0$	$[\text{Ox}]_0$	P	$\% \text{ mole } ^{13}\text{C NMR}$	time t_k min	time t_{add}	$[\text{Cat}]_0$	$[\text{Ox}]_0$	P	$\% \text{ mole } ^{13}\text{C NMR}$	time t_k min	Mn (theory) g/mol	Mn (SEC) g/mol	Mw/Mn g/mol
S 5.13.1	0.0025	1	98.25	4.29	300							23,200	23,430	2.35
S 5.13.2	0.0025	1										48,550	47,120	2

Table 5. 9: Effect of monomer addition on \overline{Mn} and $\overline{Mw}/\overline{Mn}$ when the polymerisation oxetane is initiated by $\text{CH}_3\text{CH}_2\text{OCH}_2\text{O}^+(\text{C}_2\text{H}_4)_2\text{O}, [\text{BF}_4]^-$ in 1,4-dioxane at 35 °C.

The living character of the existing growing polymer was confirmed by the fact that the monomer addition extends correspondingly the polymer chain length. The polymerisation however did not permit the production of narrower $\overline{M}_w/\overline{M}_n$ after monomer addition.

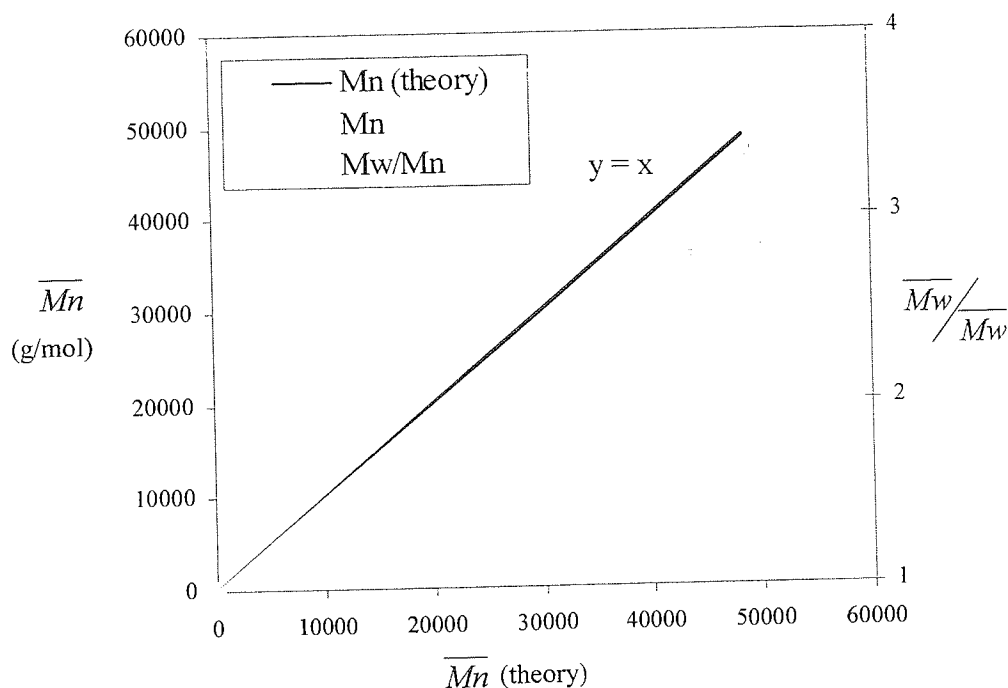


Figure 5.45: Evolution of \overline{M}_n and $\overline{M}_w/\overline{M}_n$ after monomer addition when 1 M of oxetane is polymerised in 1,4-dioxane using 0.0025 M of the active salt (13) at 35°C. Table 5.9 series S 5.13 annex 5.19.

Surprisingly, the use of $[\text{BF}_4]^-$ instead of $[\text{SbF}_6]^-$ led to an increase of initiator efficiency which is in accord to the SEC data almost quantitative. This result seems to indicate that the decrease of the size of the counter-ion can modify the solubility of the initiator and therefore the state of aggregation in 1,4-dioxane. Unlike 11 and 12, the ^{13}C NMR analysis showed that a small proportion of cyclic oligomers were formed at high monomer conversion (see annex 5.24). In this respect, the cationic ring-opening polymerisation of oxetane in 1,4-dioxane initiated by $\text{CH}_3\text{CH}_2\text{OCH}_2\text{O}^+(\text{C}_2\text{H}_4)_2\text{O}, [\text{BF}_4]^-$ at 35 °C cannot be classified as quasiling polymerisation process but as controlled polymerisation process in the sense that transfer reactions are not suppressed but only reduced and that \overline{M}_n increases linearly throughout the polymerisation process and after monomer addition.

5.2.1.2.2 Effect of the ratio $[\text{Dox}]_0/[\text{Ox}]_0$ on control of the polymerisation

A series of experiments was then carried out in which ≈ 1 M of oxetane was polymerised in 1,4-dioxane or in mixed solvent (1,4-dioxane/dichloromethane) at 35 °C using either 11 or 13

as initiating system. The total volume of polymerisation solution was kept constant and equal to 25 ml. The ratio $[Dox]_0/[Ox]_0$ was adjusted by fixing the composition of the mixed solvent. The initiator solution was prepared in pure 1,4-dioxane. This study is summarised in the Table 5.6 and 3.6 where the series S 5.5, S 5.6, S 5.7 and S 3.15 represent respectively the experiments carried out with 0.0015 M of **II** in pure 1,4-dioxane (annex 5.15), in 3:1 v/v 1,4-dioxane:dichloromethane (annex 5.19), in 2:3 v/v 1,4-dioxane: dichloromethane (annex 5.20) and in pure dichloromethane (annex 3.22) when ≈ 1 M of oxetane is polymerised by 0.0015 M of **II**. The series S 5.10, S 5.11, S 5.12 in the table 5.8 and the series S 3.14 in the table 3.6 represent respectively the experiments carried out in pure 1,4-dioxane (annex 5.23), in 3:1 v/v 1,4-dioxane:dichloromethane (annex 5.25), in 1:1 v/v 1,4-dioxane:dichloromethane (annex 5.26) and in pure dichloromethane (annex 3.21) using 0.0015 M of **II** to polymerise 1 M of oxetane.

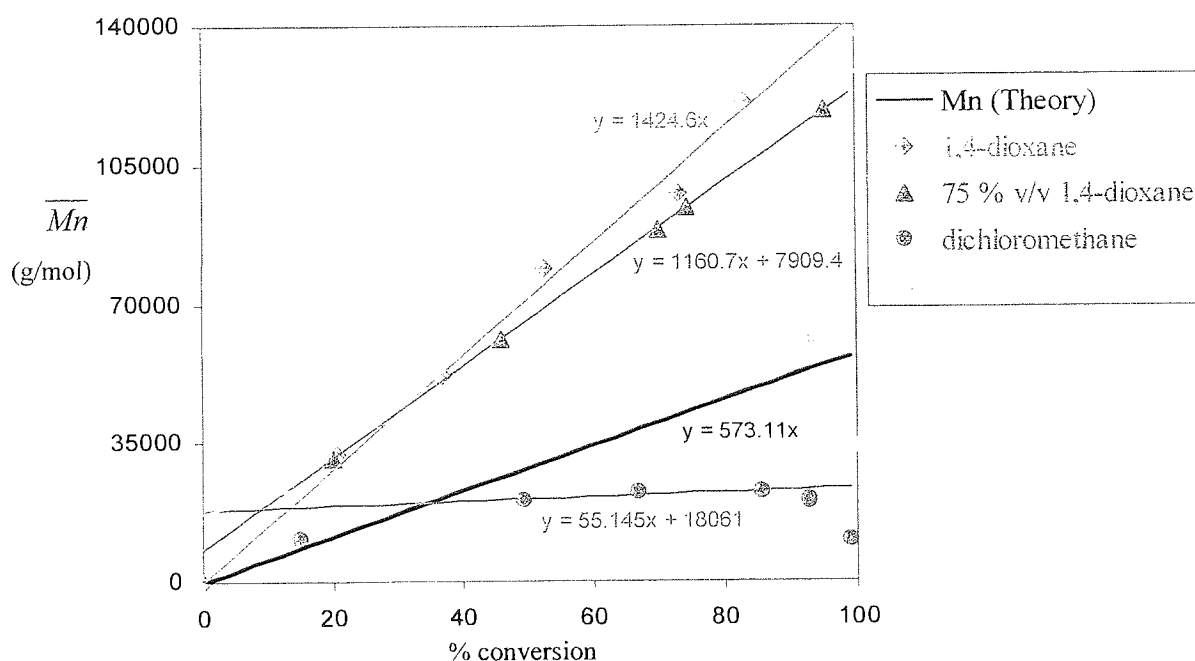


Figure 5.46: Effect of the ratio $[Dox]_0/[Ox]_0$ on the slope of \overline{Mn} against conversion when the polymerisation is initiated by **II** at 35°C. $[M] = 1$ M and $[I] = 0.0025$ M.

As expected, mixed solvent did not give the same control than as pure 1,4-dioxane. Indeed, as shown in the figure 5.46, when the polymerisation was initiated by **II** in 3:1 v/v 1,4-dioxane:dichloromethane, high molecular weight material was produced but the linear dependence \overline{Mn} conversion intercepted the Y axis and the polymer obtained had broader polydispersity than in pure 1,4-dioxane. In 2:3 v/v 1,4-dioxane:dichloromethane, the control

of the polymerisation was lost throughout the polymerisation process. The polymer produced was characterised by lower \overline{Mn} , broader $\overline{Mw}/\overline{Mn}$ and \overline{Mn} decreases with conversion as soon as 92 % of monomer are consumed. In comparison with $[\text{SbF}_6]^+$, $[\text{BF}_4]^+$ in mixed solvent had a tremendous effect on the control of the polymerisation. As shown in the figure 5.47, in 3:1 v:v 1,4-dioxane:dichloromethane the linear dependence \overline{Mn} against conversion intercepted the Y axis but, as soon as 80 % of monomer was consumed, \overline{Mn} decreased leading to the formation of cyclic oligomers that was observed by NMR spectroscopy. In 1:1 v:v 1,4-dioxane:dichloromethane the linear dependence \overline{Mn} conversion get shorter, the Y axis intercept becomes higher and the cyclic oligomers start to be formed at 50 % monomer conversion.

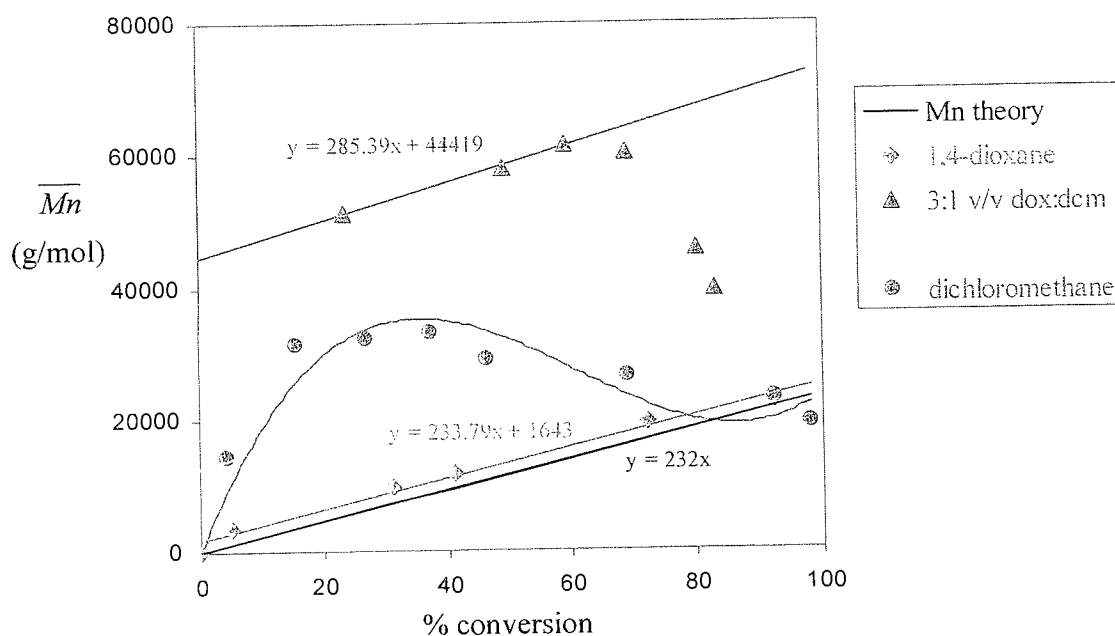


Figure 5. 47: Effect of the ratio on the slop of \overline{Mn} against conversion when the polymerisation is initiated by 13 at 35 °C. $[\text{Ox}]_0 = 1 \text{ M}$ and $[\text{I}]_0 = 0.0025 \text{ M}$.

Besides, the kinetic study showed that the rate of polymerisation gets faster as the ratio $[\text{Dox}]_0/[\text{Ox}]_0$ decreased. This shows clearly that the control of the polymerisation depends on the rate at which the growing centres are end-capped by 1,4-dioxane. Indeed, by decreasing the ratio $[\text{Dox}]_0/[\text{Ox}]_0$, the life-time of the active growing centre is increased and therefore the rate at which the monomer is initially consumed increases in relation to the rate of initiation. This is believed to be responsible to the increase of the intercept of the Y axis with the decreases of the ratio $[\text{Dox}]_0/[\text{Ox}]_0$. In the later stage of the polymerisation, if the process

of the polymerisation in 1,4-dioxane appears “quasiliving” when $\text{C}_6\text{H}_5\text{O}(\text{CH}_2)_3\text{O}^+(\text{C}_2\text{H}_4)_2\text{O}, [\text{SbF}_6]^-$ is used as “living monomeric oxetane” initiator, the loss of control over \overline{Mn} appears obvious when 3:2 v/v dichloromethane:1,4-dioxane is used as polymerisation medium (see figure 5.46). This is because the initial concentration of 1,4-dioxane is too low to prevent transfer reactions from occurring ($R_{tr} > R_d$). In the case of $\text{CH}_3\text{CH}_2\text{OCH}_2\text{O}^+(\text{C}_2\text{H}_4)_2\text{O}, [\text{BF}_4]^-$, it is interesting to note that the control over \overline{Mn} is lost since 1:3 v/v dichloromethane:1,4-dioxane is used as polymerisation medium whereas with $\text{C}_6\text{H}_5\text{O}(\text{CH}_2)_3\text{O}^+(\text{C}_2\text{H}_4)_2\text{O}, [\text{SbF}_6]^-$ \overline{Mn} still increases linearly with the conversion. The figure 5.48 shows the instantaneous fraction of cyclic oligomers formed in different solvent during the polymerisation process when initiated by $\text{CH}_3\text{CH}_2\text{OCH}_2\text{O}^+(\text{C}_2\text{H}_4)_2\text{O}, [\text{BF}_4]^-$ at 35 °C.

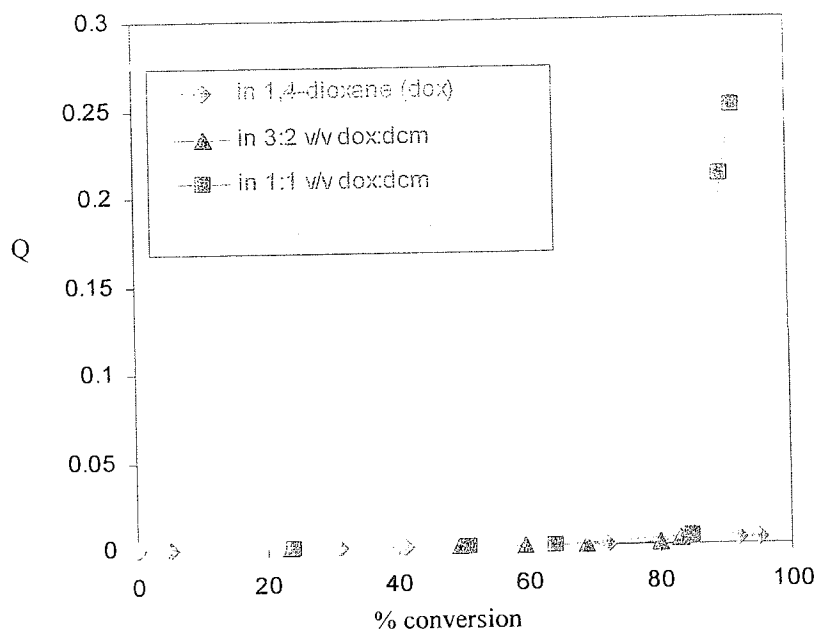


Figure 5. 48: Instantaneous fraction of cyclic oligomers, Q , produced during the polymerisation initiated by $\text{CH}_3\text{CH}_2\text{OCH}_2\text{O}^+(\text{C}_2\text{H}_4)_2\text{O}, [\text{BF}_4]^-$. $Q = \text{Area}(\delta_{(-\text{OCH}_2-)} \text{ from cyclic material}) / \text{Area}(\delta_{(-\text{OCH}_2-)} \text{ from cyclic and linear materials})$.

5.2.1.2.3 Effect of the size of the counter-ions on the reactivity of the propagating species in 1,4-dioxane

In the Chapter 3, we showed that the use of alkoxycarbenium salts ($\text{CH}_3\text{CH}_2\text{OCH}_2^+, \text{X}^-$ with $\text{X} = [\text{BF}_4]$ and $[\text{SbF}_6]$) instead of protonic reagents reduce the cyclic oligomer formation by preventing end-biting reactions from occurring. This is because the oxygen atom in open chain is less nucleophilic than the oxygen atom of the monomer whereas the hydroxyl tail

group is more nucleophilic than the monomer. Further investigation showed that size of the counter-ion affects the reactivity of the growing centre towards propagation and side reactions (back-biting and intermolecular transfer reactions). Indeed, when $\text{EtOCH}_2^+[\text{BF}_4]^-$ was used as initiator instead of protonic reagents, the cyclic oligomers formation was reduced only during the first 50 % monomer conversion whereas the use of $\text{CH}_3\text{CH}_2\text{OCH}_2^+[\text{SbF}_6]^-$ reduces the formation of cyclic oligomers during the entire course of the polymerisation. Because $\text{CH}_3\text{CH}_2\text{OCH}_2^+[\text{SbF}_6]^-$ did not permit the control over \overline{Mn} and $\overline{Mw}/\overline{Mn}$, the size of the counter-ion is believed to affect more significantly the intra- than the intermolecular transfer reactions. This unexpected result was explained by the fact that, in dichloromethane, all the growing centres are in the form of ion-pairs and that the counter-anion can modify the reactivity of the growing centre depending on the size of the counter-ion.

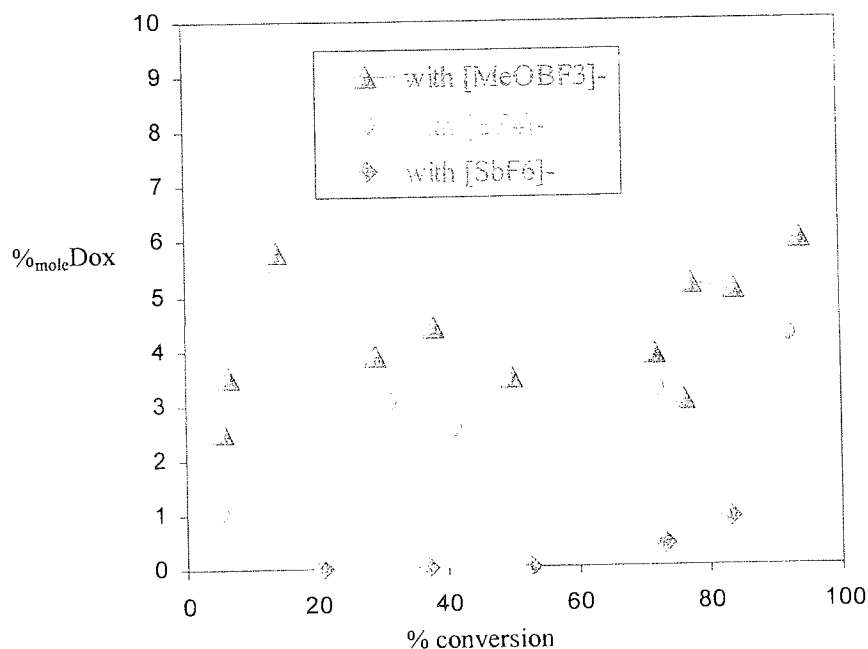


Figure 5.49: Instantaneous mole fractions of 1,4-dioxane incorporated into the polymer, $\%_{mole} \text{Dox}$, plotted against the conversion in oxetane.

In 1,4-dioxane, the ^{13}C NMR also showed that the mechanism of reactivation of “dormant” species by the monomer depends also on the size of the counter-ion. Indeed, when $[\text{SbF}_6]^-$ was used as counter-ion, the incorporation of 1,4-dioxane occurred only at high monomer conversion when the process of polymer chain extension tends to occur principally by reactivation of the “dormant” species, whereas with $[\text{BF}_4]^-$ and $[\text{MeOBF}_3]^-$, 1,4-dioxane was incorporated into the polymer from the beginning of the polymerisation (see figure 5.49). This shows clearly that in 1,4-dioxane most of the growing centres and counter-ions are

associated into ion-pairs and that the size of the counter-ion can sterically disfavour the reactivation of "dormant" species by copolymerisation. This indicates that p_{endo} and therefore p_{exo} depends strongly on the size of the counter-ion when the reaction occurs in poorly solvating media. Therefore,

$$p_{a(\text{endo}),[\text{SbF}_6]^-} < p_{a(\text{endo}),[\text{BF}_4]^-} \leq p_{a(\text{endo}),[\text{F}_3\text{BOCH}_3]^-}$$

E:

5.93

Further investigation showed that the "quasiliving" character of the polymerisation of oxetane in 1,4-dioxane was dependent on the size of the counter-ion associated with the growing centres. Indeed, all the characteristics of living growing polymer chains generated spontaneously during the initiation process were achieved when $[\text{SbF}_6]^-$ was used as counter-ion. These include linear dependence \overline{Mn} with conversion, decrease of $\overline{Mw}/\overline{Mn}$ with the conversion, production of polymer of narrow polydispersity, polymer chains extension after monomer addition and no cyclic oligomers formations. Therefore, the mechanism of CROP of oxetane initiated by $\text{RO}^+(\text{C}_2\text{H}_4)_2\text{O}, [\text{SbF}_6]^-$ ($\text{R} = \text{CH}_3\text{CH}_2\text{OCH}_2-$ or $\text{C}_6\text{H}_5\text{O}(\text{CH}_2)_3-$) in 1,4-dioxane at 35 °C can be classified as a quasiliving polymerisation process and the mechanism of polymerisation schematised as follows

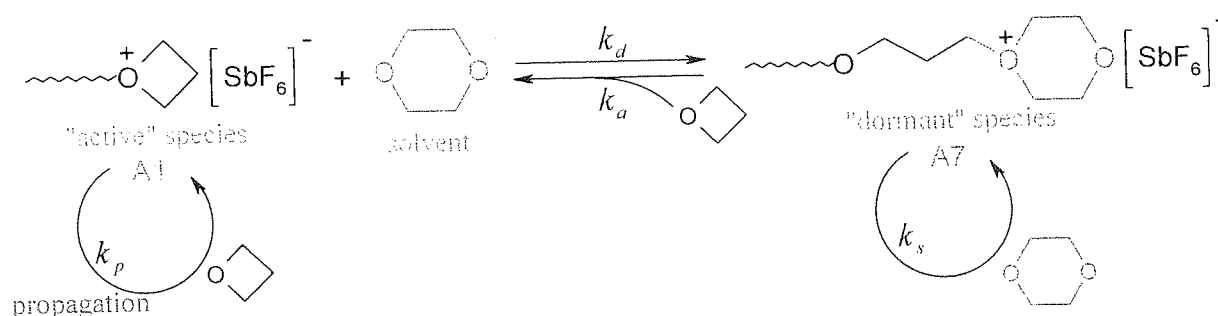


Figure 5. 50: Mechanism of quasiliving polymerisation of oxetane in 1,4-dioxane at 35 °C.

Thus, the analytical expression of the rate of monomer consumption can be expressed as follow:

$$-\frac{d[\text{Ox}]}{dt} = (k_a + (k_p - k_a) \cdot \alpha_i) \cdot c_0 \cdot [\text{Ox}]$$

E : 5.94

where k_p ($\text{L}\cdot\text{mol}^{-1}\text{s}^{-1}$) represents the rate constant at which the "active" species (A1) propagates and k_a is the apparent rate constant of activation of "dormant" species (A7). $[\text{Ox}]$ represents the concentration of oxetane and c_0 denotes the total concentration of growing centres ($c_0 = [\text{A1}] + [\text{A7}]$). Here, α_t denotes the instantaneous mole fraction of propagating species in the form of "active" species (A1). Because the equilibrium between "active" and "dormant" species does not reach a steady state of their concentrations, the analytical expression of the equilibrium constant $K_{(t)}$ (E: 5.97) can be expressed from the equations E: 5.95 and E: 5.96:

$$-\frac{d[\text{A1}]}{dt} = k_d \cdot [\text{A1}] \cdot [\text{T}] - k_a \cdot [\text{A7}] \cdot [\text{Ox}] \neq 0 \quad \text{E: 5.95}$$

and

$$K_{(t)} = \frac{k_d}{k_a} \cdot \left(1 - \frac{1}{k_d \cdot [\text{A1}] \cdot [\text{T}]_0} \cdot \left(-\frac{d[\text{A1}]}{dt} \right) \right) = f(t) \quad \text{E: 5.96}$$

with

$$K_{(t)} = \frac{[\text{A7}]_t \cdot [\text{Ox}]_t}{[\text{A1}]_t \cdot [\text{T}]_0} \quad \text{E: 5.97}$$

Here, the determination of α_t ($\alpha_t = [\text{A1}]/c_0$) implies the resolution of the equation E: 5.96 for which no solution has been found so far.

Further investigations also showed that the association of active salt into aggregates is not beneficial for the initiation and therefore for control over $\overline{Mw}/\overline{Mn}$. This is because the $[\text{SbF}_6]^-$ is a very large counter-ion and that the dissociation of the ions pairs, and therefore the dissociation of the aggregates, depends only on the polarity of the solvent. However, in poorly solvating solvents such as 1,4-dioxane, the dissociation of soluble aggregates, responsible of the non-spontaneous initiation, becomes more facile with more soluble alkylating reagents. This was demonstrated by the loss of control over $\overline{Mw}/\overline{Mn}$ when $\text{EtOCH}_2\text{O}^+(\text{C}_2\text{H}_4)_2\text{O} \cdot [\text{SbF}_6]^-$ was used instead of $\text{C}_6\text{H}_5\text{OCH}_2\text{CH}_2\text{CH}_2\text{O}^+(\text{C}_2\text{H}_4)_2\text{O} \cdot [\text{SbF}_6]^-$.

In the case of $[\text{BF}_4]^-$ (13) the ^{13}C NMR analysis showed that cyclic oligomers (1-2 % of monomer are converted into cyclic oligomers) were formed at high monomer conversion. Because \overline{M}_n increases linearly with conversion and that, upon monomer addition, the polymer chains length are extended correspondingly, the polymerisation can then be classified as a controlled polymerisation process even if cyclic oligomers formation is not suppressed and that polymers of large polydispersity ($\overline{M}_w/\overline{M}_n \approx 2$) are produced. This suppose that intermolecular transfer reactions are suppressed in the presence of 1,4-dioxane. Therefore, the mechanism of the polymerisation process initiated by $\text{CH}_3\text{CH}_2\text{OCH}_2\text{O}^+(\text{C}_2\text{H}_4)_2\text{O}, [\text{BF}_4]^-$ in 1,4-dioxane at 35 °C can be represented as follow.

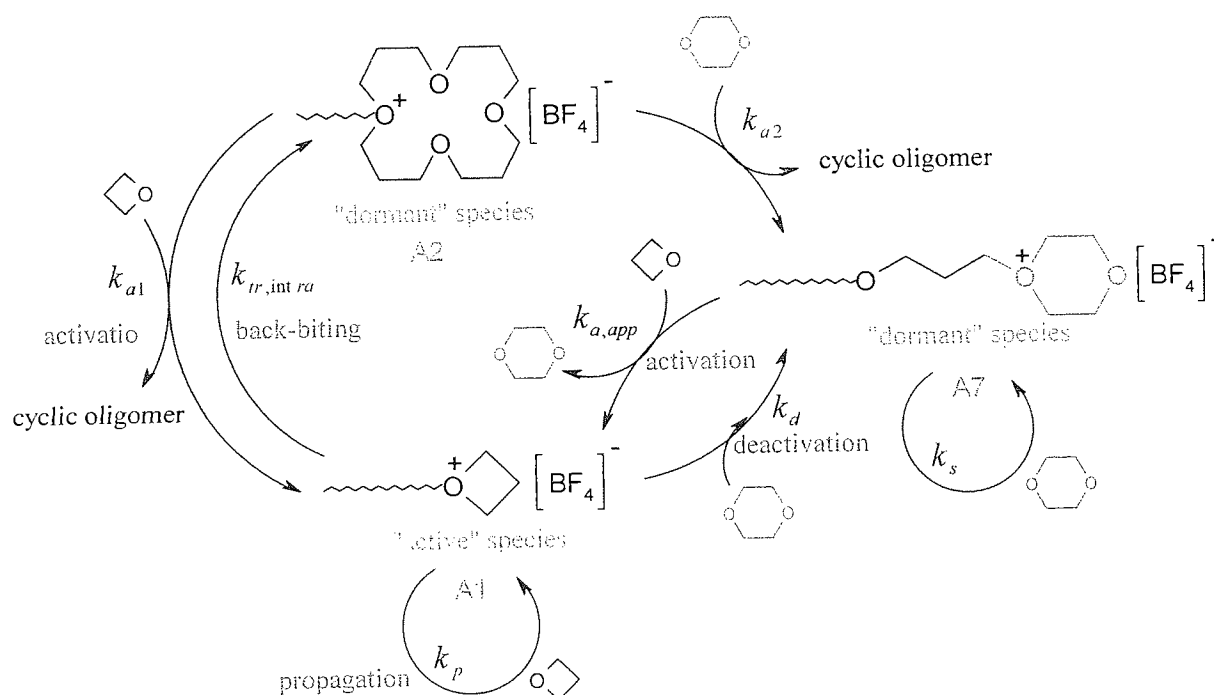


Figure 5.51: Mechanism of controlled polymerisation of oxetane in 1,4-dioxane initiated by $\text{CH}_3\text{CH}_2\text{OCH}_2\text{O}^+(\text{C}_2\text{H}_4)_2\text{O}, [\text{BF}_4]^-$.

The high initiator efficiency when $\text{CH}_3\text{CH}_2\text{OCH}_2\text{O}^+(\text{C}_2\text{H}_4)_2\text{O}, [\text{BF}_4]^-$ was used instead of $\text{CH}_3\text{CH}_2\text{OCH}_2\text{O}^+(\text{C}_2\text{H}_4)_2\text{O}, [\text{SbF}_6]^-$ is ascribed to the size of the counter-ions. Because $[\text{BF}_4]^-$ is smaller than $[\text{SbF}_6]^-$, this factor is believe to be beneficial for solvation of the ion-pairs initiator in 1,4-dioxane. Because the monomer addition experiments extend the growing polymer chains when initiated with $\text{BF}_3:\text{MeOH}$, the polymerisation can then be classified as a controlled polymerisation process even if cyclic oligomers are formed more significantly.

The non-linear dependence of \overline{Mn} on conversion throughout the polymerisation process is due to the fact that the initiation is slow in comparison to the rate propagation.

The effect of the counter-ions on the "quasiliving" and control character of the polymerisation appears clearly in mixed solvents. Indeed, in 3:1 v/v 1,4-dioxane:dichloromethane the polymerisation was not controlled with $[\text{BF}_4]^-$ whereas with $[\text{SbF}_6]^-$ \overline{Mn} still increases linearly with conversion. Figure 5.48 shows the evolution of cyclic oligomer formation with the conversion as the composition of solvent in dichloromethane varied from 0 to 100%.

5.2.2 CROP of oxetane in tetrahydropyran at 35°C

As for 1,4-dioxane, the effect of the initiator on the cationic ring-opening polymerisation of oxetane in THP at 35 °C was investigated. The initiators used in this study are represented in the figure 5.52.

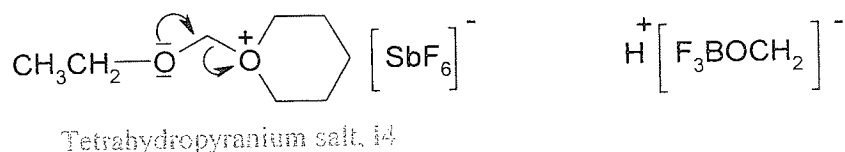



Figure 5. 52: Initiator used for the polymerisation of oxetane in tetrahydropyran at 35°C.

The tetrahydropyranium salt, $\text{CH}_3\text{CH}_2\text{OCH}_2\text{O}^+(\text{CH}_2)_5[\text{SbF}_6]^-$, was prepared according to the procedure described in the section 2.7.7.1.2 using 1:1:1:1.1 of $\text{CH}_3\text{CH}_2\text{OCH}_2\text{Cl}:\text{AgSbF}_6:\text{DtBP}$ in dry and freshly distilled THP. The solution of $\text{BF}_3:\text{MeOH}$ in dichloromethane was prepared as described in the section 2.7.7.1.1.2. The polymerisation was then carried out as described in the section 2.8.1. In all experiments, the polymerisation reaction was terminated by addition of a large excess of 10% NaOH solution. The inactive polymer solution was then treated as described in section 2.8.1 and the volatile materials were removed by evaporation in the fume cupboard over several days at room temperature. The yield of the polyoxetane was determined by weight and the products were analysed by Size Exclusion Chromatography (S.E.C) against polystyrene standards, and ^1H and ^{13}C NMR. This study is summarised in the table 5.10, where series S 5.14 and S 5.15 correspond to the experiments carried out in tetrahydropyran using respectively $\text{BF}_3:\text{MeOH}$ and $\text{CH}_3\text{CH}_2\text{OCH}_2\text{O}^+(\text{CH}_2)_5[\text{SbF}_6]^-$, as initiating system.

Series	[Ox] ₀	[I2] ₀	[THP] ₀ /[I] ₀ ^P	% mole THP ¹ H NMR	% weight THP ¹ H NMR	Conv.	Mn (theory)	Mn (SEC)	Mp (SEC)	Mw/Mn (SEC)	Time Second	Q ¹³ C NMR
S 5.14.1 ^a	1	0.0077	8.73	19.27	26.14	14.7	670	2,000	3,250	1.49	610.8 s	0
S 5.14.2 ^a	1	0.0077	8.73	22.81	30.47	25.4	2154	2,570	4,945	1.68	1,206 s	0
S 5.14.3 ^a	1	0.0077	8.73	21.34	28.69	42.5	4022	3,260	6,260	1.7	2,314 s	0.2
S 5.14.3 ^a	1	0.0077	8.73	27.93	36.5	93	5047	6,620	11,020	1.78	1day	0.7
S 5.14.4 ^a	1.452	0.00156	6	19.96	27	4.68	3,187	1,600	2,710	1.51	4 min	0
S 5.14.5 ^a	1.452	0.00156	6	15.98	22	15.29	10,069	8,260	9,980	1.18	17 min	0
S 5.14.6 ^a	1.452	0.00156	6	19.14	25.98	30.62	20,829	22,260	25,730	1.31	53 min	0
S 5.15.1 ^b	1.452	0.00156	6	21.25	28.58	57.47	39,896	38,800	52,280	1.38	1 h	580
S 5.15.2 ^b	1.452	0.00156	6	22.06	29.57	71	49,670	43,500	56,880	1.56	min	0
S 5.15.3 ^b	1.452	0.00156	6	25.36	33.51	87.39	63,000	73,000	118,92	1.6	2 h	450
S 5.15.4 ^b								0			min	
S 5.15.5 ^b											19 h	
S 5.15.6 ^b												

Table 5.10: Effect of tetrahydropyran on \overline{Mn} and $\overline{Mw}/\overline{Mn}$ when the polymerisation of oxetane is initiated by $\text{CH}_3\text{CH}_2\text{OCH}_2(\text{OC}_5\text{H}_{10})^+[\text{SbF}_6]^-$ and $[\text{BF}_3:\text{MeOH}]$ at 35 °C.

Structure	Chemical shift*			
	¹³ C NMR		¹ H NMR	
	δ (ppm)	Intensity	δ (ppm)	Intensity
Polymer Chains	-OCH ₂ CH ₂ CH ₂ O-	I ₁	q: 1.4389, 1.4120, 1.3894, 1.3605, 1.3018	I _{1,3018}
	-OCH ₂ CH ₂ CH ₂ O-	2*I ₂ ≈ I ₁	1.3422	2* I _{1,3018}
	-	I ₃	q: 1.6285, 1.6054, 1.5823, 1.5587, 2* I _{1,3018}	2* I _{1,3018}
	OCH ₂ CH ₂ CH ₂ OCH ₂ CH ₂ CH ₂ OCH ₂ CH ₂ OCH ₂ CH ₂ O-	2*I ₄ ≈ I ₃	1.5367	2* I _{1,3018}
	CH ₂ CH ₂ O-	2*I ₅ ≈ I ₃	t: 3.4005, 3.3820, 3.3235	2* I _{1,3018}
	-	I ₆ ≈ I ₃	t: 3.50, 3.48 and 3.46	2* I _{1,3018}
THP	OCH ₂ CH ₂ CH ₂ OCH ₂ CH ₂ CH ₂ CH ₂ OCH ₂ CH ₂ OCH ₂ CH ₂ O-	I ₁	q: 1.866, 1.845, 1.823, 1.80, 1.782	2* I _{1,3018}
		2*I ₁ ≈ I ₃	m: 3.65	2*I _{1,59}
		2*I ₂ ≈ I ₃	m: 1.59	2*I _{1,59}
		I ₃	m: 1.59	I _{1,59}

* CDCl₃ was used as solvent.

Table 5. 11: Chemical shift δ (ppm) of -CH₂- in the polyoxetane produced in the presence tetrahydropyran.

5.2.2.1 Kinetic study

5.2.2.1.1 ^1H and ^{13}C NMR analysis

As for 1,4-dioxane, the ^{13}C and ^1H NMR analysis (annex 5.27, 5.28, 5.31 and 5.32) showed that THP can easily be copolymerised with oxetane at 35°C . Studies by ^{13}C NMR analysis of the monomer sequence distribution showed that each unit of THP incorporated into the polymer is flanked by two oxetane monomer units. The chemical shifts of each CH_2 group (carbon and proton) are represented in the table 5.11.

Using the integral values of the CH_2 peaks centred at 1.5823 $\text{CH}_2(\beta)$, 1.3894 $\text{CH}_2(\gamma)$ and 1.823, the composition of the copolymer in THP, $\%_{\text{mole}}\text{THP}$, and the conversion of oxetane were calculated using the equation E: 5.98 and E: 5.101 respectively.

$$\%_{\text{mole}}\text{THP} = \frac{(I_1/4 + I_2/2)}{(I_1/4 + I_2/2) + I_3} \quad \text{E: 5.98}$$

$$P = \frac{\text{weight}(\text{polymer})}{\text{weight}(\text{oxetane})} \cdot 100 \quad \text{E: 5.99}$$

$$\%_{\text{weight}}\text{THP} = \frac{\%_{\text{mole}}\text{THP} \cdot M_{\text{THP}}}{\%_{\text{mole}}\text{THP} \cdot M_{\text{THP}} + (100 - \%_{\text{mole}}\text{THP}) \cdot M_{\text{Oxetane}}} \cdot 100 \quad \text{E: 5.100}$$

$$\text{Conversion} = P \cdot \frac{(100 - \%_{\text{weight}}\text{DO})}{100} \quad \text{E: 5.101}$$

Here $\%_{\text{mole}}\text{THP}$ and $\%_{\text{weight}}\text{THP}$ denote respectively the mole fractions and the weight fraction of tetrahydropyran units in the polymer while M_{oxetane} and M_{THP} are the molecular weights of oxetane and THP, respectively. I_δ is the integral value of the peak centred at δ ppm.

From figure 5.53, it appears clearly that the reactivity of THP towards copolymerisation with oxetane is unaffected by the size of the counter-ion and is superior to the reactivity of 1,4-dioxane towards copolymerisation with oxetane. The slight difference in %_{mol}THP, when [SbF₆]⁻ and [BF₃OMe]⁻ were used as counter-ion, is probably due to the fact that the ratio [THP]₀/[Ox]₀ was higher when the polymerisation was initiated by BF₃:MeOH than by I4 (see table 5.11).

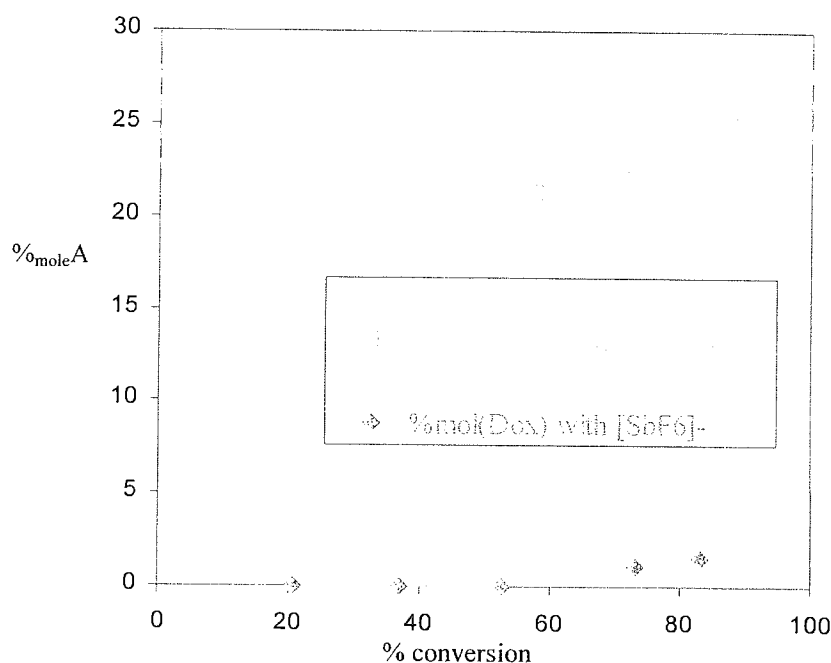


Figure 5.53: Mole fraction in percent of additive incorporated into the polymer during the polymerisation process, %_{mol} A, plotted against the conversion of oxetane.

The study of cyclic oligomer formation by ¹³C NMR showed that cyclic oligomers were prevented only when CH₃CH₂OCH₂O⁺(CH₂)₅[SbF₆]⁻ was used as initiator. Many report suggest that the cyclic oligomers formation can be reduced/or prevented by copolymerisation. In this study, the copolymerisation process shows clearly that cyclic oligomers can be prevented only if the initiator used generates a tail group less nucleophilic than the oxygen in the monomer. Because cyclic oligomers are still formed when BF₃O:MeOH was employed as initiator, the copolymerisation process is believed to prevent only the back-biting process. With BF₃O:MeOH, the cyclic oligomers are probably formed by end-biting reactions.

5.2.2.1.2 SEC analysis

Because the plot of \overline{Mn} against monomer conversion is very hard to interpret when a copolymerisation process is involved, we have then plotted \overline{Mn} (SEC) against \overline{Mn} (theory). Here \overline{Mn} (theory) was calculated based on ^1H NMR analysis and on the equation E: 5.104. Because,

$$\overline{Mn}_{(theory)} = M_{ox} \cdot \frac{[Ox]_0}{[I]_0} \cdot conv_{(Ox)} + M_{THP} \cdot \frac{[THP]_0}{[I]_0} \cdot conv_{(THP)} \quad \text{E: 5.102}$$

From knowledge of the composition in mole fraction of THP incorporated into the polymer, the contribution of THP to the increase of \overline{Mn} can then be calculated based on the oxetane conversion,

$$M_{THP} \cdot \left(\frac{[THP]_0}{[I]_0} \cdot conv_{(THP)} \right) = M_{THP} \cdot \left(\frac{[Ox]_0}{[I]_0} \cdot (\%_{mol} THP) \cdot conv_{(Ox)} \right) \quad \text{E: 5.103}$$

By combining the equations E: 5.102 and E: 5.103,

$$\overline{Mn}_{(theory)} = \frac{[Ox]_0}{[I]_0} \cdot (M_{Ox} + M_{THP} \cdot (\%_{mol} THP)) \cdot conv_{(Ox)} \quad \text{E: 5.104}$$

Here, M_{Ox} and M_{THP} are the molecular weight of the respective co-monomer, oxetane and tetrahydropyran, respectively. The $conv_{(Ox)}$ and $conv_{(THP)}$ denote the mole fraction of oxetane and THP that was incorporated into the polymer during the polymerisation.

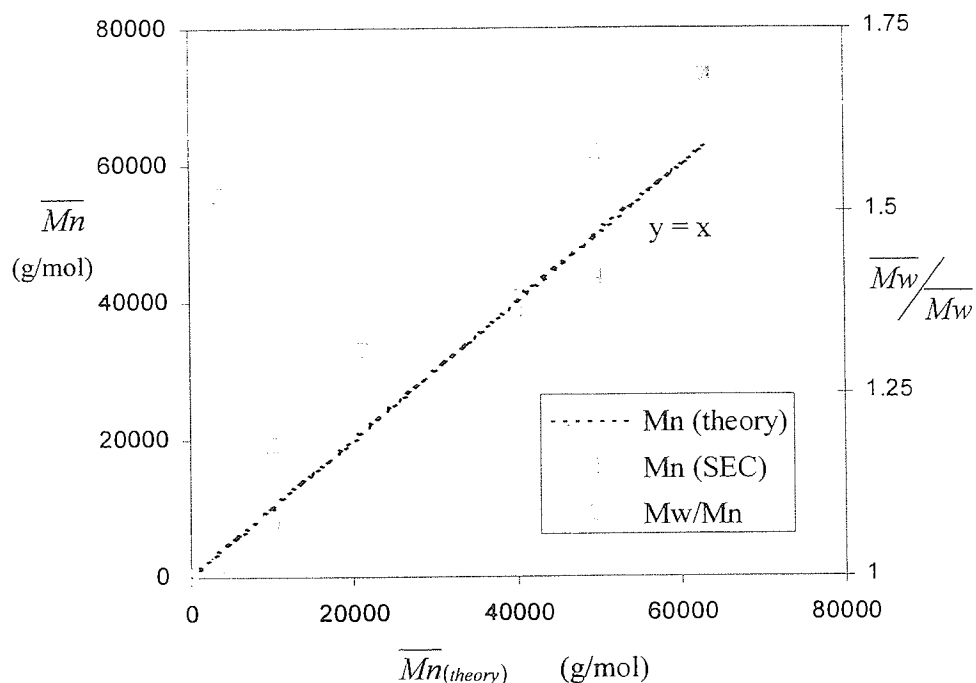


Figure 5.54: Evolution of \overline{Mn} and $\overline{Mw}/\overline{Mn}$ with \overline{Mn} (theory) in the cationic polymerisation of oxetane initiated by I4 in THP at 35 °C. Table 5.10 series S 5.15 and annex 5.30.

When I4 was used as initiator, the plot of \overline{Mn} against $\overline{Mn}_{(theory)}$ shows a linear dependence that intercepts the origin. This shows that the initiation process is not slower than the propagation and that the growing polymers chains are living. Because the molecular weight of the polymer was determined against PSty standards, the value of the gradient of the slope of \overline{Mn} against $\overline{Mn}_{(theory)}$ cannot be used to determine the initiator efficiency. The increase of $\overline{Mw}/\overline{Mn}$ as the polymerisation progresses could be due to the incorporation of THP that disrupts the control of the polymerisation over $\overline{Mw}/\overline{Mn}$.

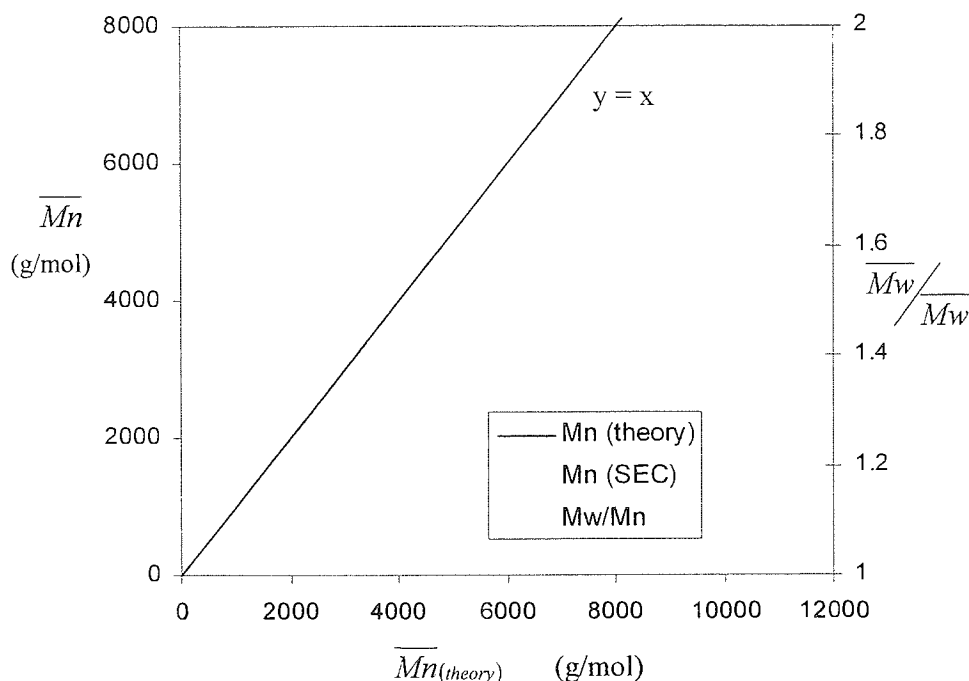


Figure 5.55: Evolution of \overline{Mn} and $\overline{Mw}/\overline{Mn}$ with $\overline{Mn}_{(theory)}$ in the cationic polymerisation of oxetane in THP by BF_3MeOH . Table 5.10 series S 5.14 and annex 5. 29.

When BF_3MeOH was used as initiator, the linear dependence of \overline{Mn} against $\overline{Mn}_{(theory)}$ intercepts the Y axis. This is believed to be due to the slow character of the initiation process in comparison with the propagation. Because tetrahydropyran is a polar solvent, the initiator is believed not to associate into aggregates.

5.2.2.2 Mechanism of polymerisation tetrahydropyran

Our investigation of the polymerisation of oxetane in tetrahydropyran showed that deactivation of the growing centre, Al , by tetrahydropyran generate living growing polymers when initiated by alkylating reagents. With protonic reagents cyclic oligomers are still formed most probably by end-biting reaction. The living character of the growing centre was demonstrated by the fact that \overline{Mn} increases during the entire course of the polymerisation. In comparison to 1,4-dioxane the reactivation of “dormant” species is believe to occur by copolymerisation rather than nucleophilic attack of exo-cyclic electron deficient carbon atom in the α -position of the oxonium site.

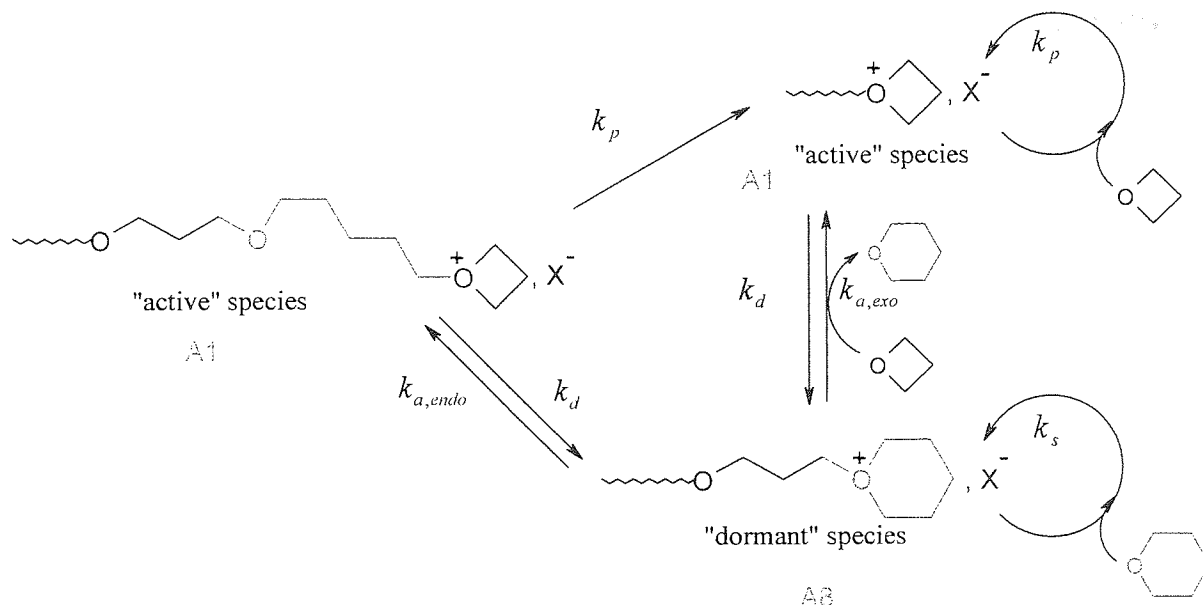


Figure 5.56: Mechanism of cationic ring-opening polymerisation of oxetane in tetrahydropyran at 35 °C.

Because THP is incorporated into the polymer and this independently of the size of the counter-ions, it cannot be excluded that ion-pairs and free ions coexist in equilibrium in tetrahydropyran (see figure 5.57). The incorporation of THP during the polymerisation process could be ascribed to free ions. Therefore, if α_i represents the instantaneous fraction of "active" species in equilibrium with dormant species and β and γ the fraction of "active" and "dormant" species in the form of free ions, then

$$k_{p,app} = (k_{p\pm} + \beta \cdot (k_{p\pm} - k_{p+})) \cdot \alpha_i \cdot a_0 \quad \text{E: 5.105}$$

$$k_{d,app} = (k_{d\pm} + \beta \cdot (k_{d\pm} - k_{d+})) \cdot \alpha_i \cdot a_0 \quad \text{E: 5.106}$$

$$k_{a,app} = (k_{a\pm} + \beta \cdot (k_{a\pm} - k_{a+})) \cdot (1 - \alpha_i) \cdot a_0 \quad \text{E: 5.107}$$

here,

$$k_{a\pm} = k_{a(endo)\pm} + (k_{a(exo)\pm} - k_{a(endo)\pm}) \cdot p_{a(exo)\pm} \quad \text{E: 5.108}$$

with

$$p_{a(exo)\pm} + p_{a(endo)\pm} = 1$$

E: 5.109

and

$$k_{a+} = k_{a(endo)+} + (k_{a(exo)+} - k_{a(endo)+}) p_{a(exo)+}$$

E: 5.110

with

$$p_{a(exo)+} + p_{a(endo)+} = 1$$

E: 5.111

a_o represents the concentration of initiator, $f \cdot [I]_0$, converted into growing species.

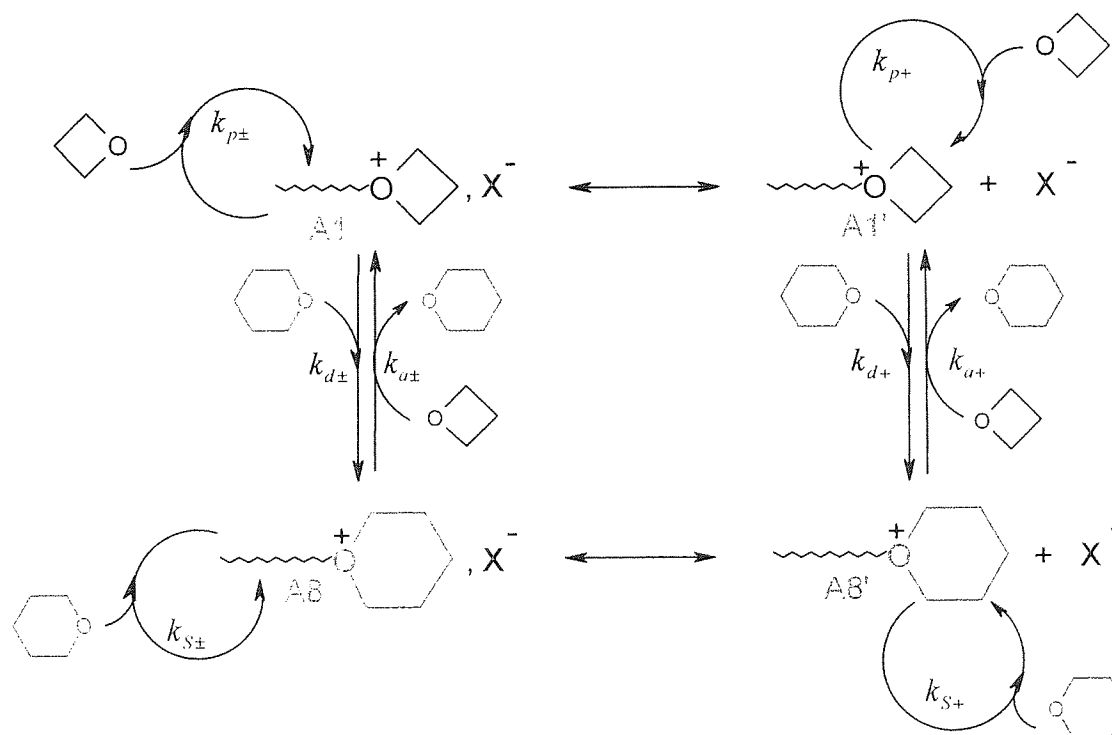


Figure 5.57: Ion-pairs and free ions in equilibrium during the polymerisation of oxetane in tetrahydropyran at 35 °C.

β and γ can be expressed by their respective constant of dissociation noted $K_{d,dof}$ and $K_{d,act}$, respectively.

$$K_{d,dor} = \frac{[RT^+] \cdot [X^-]}{[RT^+, X^-]} = \frac{[A8'] \cdot [X^-]}{[A8]} = \frac{\beta^2}{1-\beta} \cdot \alpha \cdot a_0 \quad \text{E: 5.112}$$

$$K_{d,act} = \frac{[R^+] \cdot [X^-]}{[R^+, X^-]} = \frac{[A1'] \cdot [X^-]}{[A1]} = \frac{\gamma^2}{1-\gamma} \cdot (1-\alpha) \cdot a_0 \quad \text{E: 5.113}$$

The resolution of the above equation for $\alpha > 0$ and $\beta > 0$ gives respectively,

$$\beta = \frac{K_{d,dor}}{2 \cdot \alpha_i \cdot a_0} \cdot \left(\sqrt{1 + \frac{4 \cdot \alpha_i \cdot a_0}{K_{d,dor}}} - 1 \right) \quad \text{E: 5.114}$$

$$\gamma = \frac{K_{d,act}}{2 \cdot (1-\alpha) \cdot a_0} \cdot \left(\sqrt{1 + \frac{4 \cdot (1-\alpha) \cdot a_0}{K_{d,dor}}} - 1 \right) \quad \text{E: 5.115}$$

5.3 Conclusions

Polymerisations with reversible equilibria between “active” and “dormant” species are often used in polymerisation to suppress^[307,308,314-319] or to reduce^[39-44] side reactions from occurring. Our investigation of the cationic ring-opening polymerisation of oxetane, showed that the formation of such an equilibrium in which the “dormant” species are activated by a molecule of monomer can be achieved if the reversible deactivating reagents used as solvent are more nucleophilic than the oxygen atom in the backbone of the polymer chain and less nucleophilic than the oxygen atom of the monomer. Under such conditions and according to the chemoselectivity of the CROP of oxetane, the additive can compete efficiently with transfer reactions and the end-capped growing polymers chains will not be irreversibly terminate by the additive. Based on this concept, our investigation of the cationic ring-opening polymerisation of oxetane in *1,4-dioxane* (cyclic ether monomer that does not homopolymerise) at 35 °C showed that the molecular weight of the produced polymers increases with conversion and with monomer addition after that 95% of monomer was consumed. Because conventional initiators (Friedel and Craft reagents with protogens) induce a slow initiation, polymers with broad molecular weight distribution were produced. Using well soluble “living polyoxetane monomeric” initiator as fast initiator (II), polymers with narrow molecular weight distribution were produced without cyclic oligomers. The \overline{Mn}

increases linearly with the conversion and upon monomer addition the existing polymers chains were extended correspondingly. High molecular weight with narrow number average molecular distribution ($\overline{Mn} = 160,000 \text{ g/mol}$ and $\overline{Mw}/\overline{Mn} = 1.2$) were produced successfully. On the basis of the kinetic data, a mechanism of polymerisation was proposed in which "dormant" species is reactivated by molecule of monomer via S_N2 reaction whereas the bimolecular process of deactivation of the "active" species (most probably a S_N2 mechanism process) involved one molecule of 1,4-dioxane. At constant concentration of 1,4-dioxane, the reversible equilibrium between "active" growing centres and "dormant" species makes the concentration of "active" and "dormant" species both dependent on the remaining concentration of oxetane; the mole fraction of "dormant" species increases as the concentration of oxetane decreases during the process of polymerisation. Because the use of fast initiator (II) produced throughout the polymerisation polymers of identical polydispersity ($\overline{Mw}/\overline{Mn} \approx 1.2$), the rate of interconversion between "active" and "dormant" species is believed to be slow or at least comparable of that of propagation. The validity of this original mechanism was shown by the fact that the use of dichloromethane as co-solvent was not beneficial for the control over \overline{Mn} and $\overline{Mw}/\overline{Mn}$ since by decreasing the initial concentration of 1,4-dioxane gradually increase the probability of the occurring transfer reaction unfavourable of the control of the polymerisation.

Further investigation showed that the choice of the initiator and corresponding counter-ion were decisive for the quasiliving character of the polymerisation process. Indeed, because protonic initiator generate nucleophilic hydroxyl tails groups, a process of cyclic oligomers formation by end-biting reactions occurs in parallel to the polymerisation process for the growing species that do not reach a sufficiently high chain length to entropically disfavour end to end polymer chains reactions. This assumption was based on the fact that the existing growing polymer chains were extended throughout the polymerisation process and after monomer addition. In this respect the polymerisation process initiated by protonic reagents (here $\text{BF}_3:\text{MeOH}$) can be classified as *controlled polymerisation process* even if the polymerisation is characterised by slow initiation process and by the formation of cyclic oligomers. With "living monomeric polyoxetane" initiator, the quasiliving character of the polymerisation was found to be dependent on the size of the counter-ions. Indeed, cyclic oligomers formation was prevented only with large counter-ions such as $[\text{SbF}_6]^-$. When $[\text{BF}_4]^-$ was used as counter-ions cyclic oligomers formation was only reduced. Unfortunately,

the ^{13}C NMR did not permit to quantify accurately the fraction of cyclic oligomers produced that we approximated to be 1-2 % of the produced materials. Because 1,4-dioxane is poor ionising solvent, the solubility of the initiator turned out to be decisive to prevent the formation of big insoluble aggregates and small insoluble aggregates responsible of slow initiation process. In this respect, the polymerisation process initiated alkylating reagent associated with $[\text{SbF}_6]^-$ can then be classified as *quasiliving polymerisation* leading to the formation of narrow ($\overline{Mw}/\overline{Mn} \approx 1.2$) or large ($1.6 < \overline{Mw}/\overline{Mn} < 2$) polydispersity depending on the solubility of the initiator. With alkylating associated with $[\text{BF}_4]^-$, the polymerisation process can only be classified as *controlled polymerisation process* leading to linear increases of \overline{Mn} with conversion, large polydispersity ($\overline{Mw}/\overline{Mn} \approx 2$) and formation of approximately 5 % of cyclic oligomers at high monomer conversion.

Surprisingly, the analysis by ^{13}C NMR of the polymers showed that the strain free 1,4-dioxane that do not homopolymerise can be copolymerised and this dependently of the size of the counter-ions. Indeed, with small and/or asymmetric counter-ion ($[\text{BF}_4]^-$, $[\text{MeOBF}_3]^-$), the composition of polymer in 1,4-dioxane reaches a maximum value around 4-5 % as soon as 5 to 10 % of monomer was consumed while with $[\text{SbF}_6]^-$ the copolymerisation starts at high oxetane conversion (conversion > 70 %), and then reaches maximum value of 1-2% at about 80% oxetane conversion. This unexpected result is believed to be due to nature of the associated ions pairs. Indeed, with $[\text{SbF}_6]^-$, the counter-ion is believed to sterically disfavours the reactivation of the “dormant” species by copolymerisation. With smaller and/or asymmetrical counter-ions, the steric hindrance on the process of reactivation of the “dormant” species appears then to be reduced. Because the dissociation of tight ions pairs is favoured by the increases of the polarity of the medium and with the decreases of the size of the counter-ions, it cannot be exclude that the decrease of the size of the counter-ions or the use of asymmetric counter-ions could favour the dissociation of ion-pairs into less stereoselective loose ion-pairs. This could explain the lack of control as we go for large to smaller or asymmetric counter-ions. So far in cationic polymerisation, there is no clear evidence in the literature on rather the growing centre exist in the form of tight or/and loose ion-pairs when the polymerisation is performed in poor solvating medium.

The use of *tetrahydropyran* instead of 1,4-dioxane also led to the development of control polymerisation process over \overline{Mn} and $\overline{Mw}/\overline{Mn}$. As for 1,4-dioxane the reduction of cyclic

oligomers formation was improved by using alkylating reagents instead of protonic reagents. However, because tetrahydropyran is highly polar solvent, the reactivity of the “active” and “dormant” species were found to be unaffected by the size of the counter-ions and the reactivity of THP towards the copolymerisation with oxetane was found to be superior to the reactivity of 1,4-dioxane. It must be noted that the use of alkylating reagents associated $[\text{SbF}_6]^-$ did not permit to prevent cyclic oligomers formation from occurring. Besides, the plot of $\overline{Mn}_{(SEC)}$ against expected $\overline{Mn}({}^{13}\text{H}, \text{NMR})$ showed that the initiation was quantitative and that the initiator do not associate into aggregates. Here, this is the copolymerisation process that is believe to responsible of the continuous increases of the polydispersity ($1.18 < \overline{Mw}/\overline{Mn} < 1.56$) when “living monomeric polyoxetane” initiator (**14**) is used as fast initiator.

The DSC analysis of poly(oxetane-co-tetrahydropyran), poly(oxetane-co-1,4-dioxane) and poly(oxetane) are shown in the annex 5.33, 5.34 and 5.35.

6 CHAPTER 6

Conclusions and further work

Since the early 1980's, the development of the so-called quasiliving polymerisation process where propagating (living or/and "non-living") species are in dynamic equilibrium with "dormant" species turned out to be a powerful method of controlling or improving the control of monomers that fail to polymerise in living manner by ionic and radical polymerisation. Our investigation of the conventional uncontrolled C.R.O.P of oxetane showed that, in the apparent absence of termination reactions, the concept of reversible deactivation of propagating species into a "dormant" form could be used to prevent or reduce the probability of occurring transfer reactions which were unfavourable to the control of the polymerisation over \overline{Mn} and $\overline{Mw}/\overline{Mn}$.

6.1 Uncontrolled polymerisation of oxetane in dichloromethane at 35°C

The first part of this work focused on the investigation of the kinetics and mechanism of the cationic ring-opening polymerisation of oxetane by an A.C.E mechanism in dichloromethane at 35 °C using four different cationic systems, $\text{BF}_3(\text{CH}_3\text{COOH})_2/\text{BF}_3\text{OEt}_2$, $\text{BF}_3:\text{CH}_3\text{OH}$ and $\text{CH}_3\text{CH}_2\text{OCH}_2^+, \text{X}^-$ (with $\text{X} = \text{SbF}_6$ and BF_4). Because the polymerisation of oxetane is an exothermic process ($\Delta H^\circ = 19.3$ kcal/mol), calorimetric analysis was employed to measure the rate of monomer consumption under adiabatic conditions during the first 10-15 % of monomer conversion. Gravimetric analysis was also used to follow the overall evolution of the % of monomer converted into polymer. Because the polymerisation produced linear polymer together with cyclic oligomers, the number average molecular weight (\overline{Mn}), the peak molecular weight (Mp) and the polydispersity ($\overline{Mw}/\overline{Mn}$) of the linear polymer was determined by SEC analysis in THF using polystyrene standard. The cyclic oligomers were

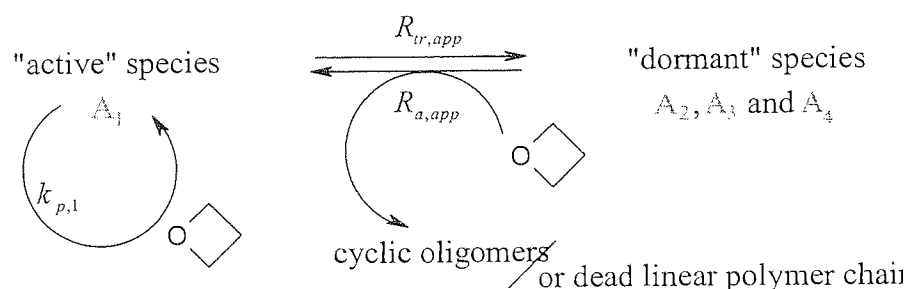
extracted with hexane and the extracted materials were analysed by ^1H & ^{13}C NMR, MS and GLC.

6.1.1 Kinetic and mechanism studies

The mechanism of polymerisation of oxetane was first proposed by Rose in 1954^[115]. The overall process involved 3 steps: *initiation*, where a strained tertiary oxonium ions acting as chain carrier is created, *propagation*, where the chain growth is explained through an $\text{S}_{\text{N}}2$ process^[115,131] and *transfer*, where the kinetic chains are thought to be brought to a halt by the formation of strain-free tertiary oxonium ions via intra and intermolecular transfer reactions. Regarding the existence of *irreversible termination* reactions by anion-splitting, no work so far provides the conclusive evidence of its existence^[320,322]. Because the active site appears at the end of the polymer chains and the attacking nucleophile is the uncharged monomer, the mechanism of propagation is known as Activation Chain End (A.C.E) mechanism, ^[115]. All reactions involved in the ring-opening process are believed to proceed via $\text{S}_{\text{N}}2$ type ^[115,131].

Our investigation of the *C.R.O.P* of oxetane showed that the *irreversible termination* reactions caused by anion-splitting are not significantly kinetically observed by calorimetric analysis. This was demonstrated by the fact that two successive monomer additions into active polymer solution almost free of monomer restarts the polymerisation with approximately the expected rate of monomer consumption (see sections 3.1.3 and 5.2.1.1.1). Consequently, *transfer reactions* exist implying that growing centres coexisting in various forms (A_i), each of each have different reactivity towards the monomer. Indeed, as the polymerisation proceeds, the oxygen atom in the backbone can attack the growing centre via an $\text{S}_{\text{N}}2$ mechanism converting the strained tertiary oxonium ions ("active" or propagating species, A_1) into less reactive growing centres ("dormant" species), respectively acyclic (A_4) and non-strained cyclic (A_2 and A_3) oxonium ions as the side reactions occur by inter- or intramolecular transfer reactions (see figure 3.4). Because the polymerisation proceeds without appreciable irreversible termination reactions, the curvature of the slope when $\text{Ln}([Ox]_0/[Ox])$ was plotted against time, can only be explained if the fraction of "dormant" species increases as the monomer is consumed. Because the oxygen atom in oxetane is much more nucleophilic than that of open-chain ethers (see figure 1.13), oxetane is believe to regenerate the active growing centre ("active" species) by nucleophilic attack of the monomer onto one of the three electron deficient carbons in the α -position with respect to the

oxonium ion site of the dormant species (see scheme 3.5). This was demonstrated by the fact that the addition of monomer onto active polymer solution almost frees of monomer restart the polymerisation as expected if we consider that all growing centre in the form of "dormant" form are spontaneously converted into strain tertiary oxonium ions in a large excess of monomer. In this respect "active" (strained tertiary oxonium ions) and "dormant" (acyclic and non-strained tertiary oxonium ions) species are believe to be in some sort of equilibrium in which the mole fraction of "active" and "dormant" species, respectively f_{A1} and $\left(\sum_{i=2}^4 f_{Ai}\right)$ are monomer concentration dependent and vary in opposite way $\left(f_{A1} + \sum_{i=2}^4 f_{Ai} = 1\right)$. Therefore, the cationic ring-opening polymerisation of oxetane in dichloromethane at 35 °C can be schematised as follow:



A1: mono- and/or α,ω -functionalised "active" species.

Figure 6. 1: Mechanism of the cationic polymerisation of oxetane.

The analytical expression of the rate of monomer consumption can then be approached by the following equations:

$$-\frac{d[Ox]}{dt} = \left(k_{p,1} \cdot f_{A1} + \sum_{i=2}^4 k_{a,i} \cdot f_{Ai} \right) \cdot [R^+, X^-] \cdot [Ox] \quad \text{E: 6.1}$$

with $k_{p,1} \gg k_{a,i}$

Here $k_{p,1}$ represents the rate constant of propagation involving strained oxonium ions (A1) and k_{a2} , k_{a3} and k_{a4} represent the rate at which the strainfree tertiary oxonium ions, respectively A2, A3 and A4, are converted into strain tertiary oxonium ions (A1). $[R^+, X^-]$

denotes the overall concentration of tertiary oxonium ions. The figure 6.1 shows that the cyclic oligomers are formed during the reactivation of the "dormant" species when the oxygen atom of an oxetane molecule attacks the endocyclic electron deficient carbon atoms in α -position with respect to the oxonium site (A2 and A3, see figure 3.5). Similarly, dead polymer chains can also be produced if the reactivation of the acyclic tertiary oxoniums ion produces α - γ growing polymer chains (see figure 5.15).

The overall kinetic order of rate of monomer consumption was examined using $\text{BF}_3(\text{CH}_3\text{COOH})_2/\text{BF}_3\text{OEt}_2$ as initiating system. The analysis of the kinetic data showed that BF_3OEt_2 acts as co-initiator of $\text{BF}_3(\text{CH}_3\text{COOH})_2$ when mixed together before being added into monomer solution. Based on the mechanism of esterification of carboxylic acids catalysed by BF_3 ^[288], a mechanism of initiation was proposed in which $[\text{F}_3\text{BOCOCH}_3]^-; \text{CH}_3\text{COOH}_2^+$, $[\text{F}_3\text{BOCOCH}_3]^-; \text{CH}_3\text{COOEt}_2^+$ and $[\text{BF}_3\text{OH}]^-; \text{H}^+$ are believed to be the initiating species. The concentration of these are determined by the initial concentration of $\text{BF}_3(\text{CH}_3\text{COOH})_2$ and BF_3OEt_2 . Because the rate of formation of the growing centre is kinetically controlled by the rate at which the initiating species reacts with the monomer^[115], the analytical equation of the initial rate of propagation, $(-d[\text{Ox}]/dt)_{\text{initial}}$, was calculated and was found to be in agreement with the observed rate of monomer consumption, $(-d[\text{Ox}]/dt)_{\text{max}}$, when monitored at various concentrations of $\text{BF}_3(\text{CH}_3\text{COOH})_2$, BF_3OEt_2 and monomer. From these studies, it appeared that at $[\text{BF}_3(\text{AcOH})_2]_0 \geq [\text{BF}_3\text{OEt}_2]_0$, the rate of initiation and the initial rate of monomer consumption can be represented as follows:

$$\left(\frac{d[R^+, X^-]}{dt} \right)_{\text{initial}} = (k_{i1} + k_2 \cdot (k_{i2} + k_{i3} - k_{i1})) \cdot [\text{BF}_3(\text{AcOH})_2]_0 \cdot [\text{Ox}]_0 \quad \text{E: 6.2}$$

$$-\left(\frac{d[\text{Ox}]}{dt} \right)_{\text{initial}} = k_p \cdot k \cdot [\text{BF}_3(\text{AcOH})_2]_0 \cdot [\text{Ox}]_0 \quad \text{E: 6.3}$$

where

$$k = k_2 = \frac{2\sqrt{K} + 1}{\sqrt{K} + 1} \text{ at } [\text{BF}_3(\text{AcOH})_2]_0 = [\text{BF}_3\text{OEt}_2]_0 \quad \text{E: 6.4}$$

and

$$k = 1 + k_2 \quad \text{with} \quad k_2 = \frac{K}{2} \cdot \left(\sqrt{1 + \frac{4}{K} \cdot \frac{[BF_3OEt_2]_0}{[BF_3(AcOH)_2]_0}} - 1 \right) \quad \text{at} \quad [BF_3(AcOH)_2]_0 > [BF_3OEt_2]_0,$$

E: 6.5

while at $[BF_3OEt_2]_0 > [BF_3(AcOH)_2]_0$, the rate of initiation and propagations becomes:

$$\left(\frac{d[R^+]}{dt} \right)_{\text{initial}} = k_i \cdot [BF_3OEt_2]_0 \cdot [Ox]_0 + k_2 \cdot (k_{i2} + k_{i2} - k_{i2}) \cdot [BF_3(AcOH)_2]_0 \cdot [Ox]_0$$

E: 6.6

$$-\left(\frac{d[Ox]}{dt} \right)_{\text{initial}} = k_p \cdot [BF_3(AcOH)_2]_0 \cdot [Ox]_0 + k_p \cdot k_2 \cdot [BF_3OEt_2]_0 \cdot [Ox]_0 \quad \text{E: 6.7}$$

with

$$k_2 = \frac{K}{2} \cdot \left(\sqrt{1 + \frac{4}{K} \cdot \frac{[BF_3(AcOH)_2]_0}{[BF_3OEt_2]_0}} - 1 \right). \quad \text{E: 6.8}$$

Because the protonation of a molecule of monomer by $[F_3BOCOCH_3]^-; [CH_3COOH_2]^+$ produces a molecule of acetic acid, this can then react with a molecule of 1:1 boron trifluoride ether complex to produce a secondary oxonium ion based on oxetane or on the polymeric material depending on the nature of the complexing reagent (see figure 3.30). Because the concentration of the reactants is low, this initiation process is believed to be very slow and therefore responsible for the enhancement of the rate of polymerisation in the first monomer addition experiments. In this case, it is interesting to note that the rate of formation of secondary oxonium ions does not depend on the concentration of oxetane:

$$\frac{d[R^+, X^-]}{dt} = k_{i4} \cdot [BF_3Ox] \cdot [AcOH] + k_{i5} \cdot [BF_3Poly(oxetane)] \cdot [AcOH] \quad \text{E: 6.9}$$

It must be noted that kinetic analysis does not provide any evidence of the existence of $[\text{F}_3\text{BOCOCH}_3]^-;\text{CH}_3\text{COOH}_2^+$, $[\text{F}_3\text{BOCOCH}_3]^-;\text{CH}_3\text{COOEt}_2^+$ and $[\text{BF}_3\text{OH}]^-;\text{H}^+$ that we believe to be the initiating species involved in the mechanism of initiation. However, it can be concluded that the mechanism of initiation based on the mechanism of esterification of carboxylic acids catalysed by BF_3 ^[288] are consistent with our kinetic data. ^1H NMR analysis studies at different temperature should provide the evidence of the existence of $[\text{F}_3\text{BOCOCH}_3]^-;\text{CH}_3\text{COOH}_2^+$, $[\text{F}_3\text{BOCOCH}_3]^-;\text{CH}_3\text{COOEt}_2^+$ and $[\text{BF}_3\text{OH}]^-;\text{H}^+$.

6.1.2 Transfer to polymers

6.1.2.1 Molecular weight studies

The molecular weight analysis of the polymers showed that the evolution of \overline{Mn} with conversion in oxetane is strongly dependent on the ratio $[\text{Ox}]_0/[\text{I}]_0$. Indeed, a targeted Dp of 52 showed a constant increases of \overline{Mn} with the conversion whereas a targeted Dp of 135 showed a continuous decrease of \overline{Mn} throughout the polymerisation process. In between (Dp = 100), \overline{Mn} was found to initially increase and then decrease as soon as transfer reactions start to compete with propagation (see figure 4.2). This phenomenon is believed to be due to the fact that the redistribution of the molecular weight distribution induced by chain breaking reactions and by reactivation of "dormant" species affects long polymer chains more significantly than short ones. In all cases, the polydispersity was found to increase throughout the polymerisation process.

Although the polymerisation does not appear to be living, further investigation showed that the plot of $1/DP_p$ against $[\text{BF}_3\text{OEt}_2]_0$ or $[\text{BF}_3(\text{AcOH})_2]_0$ as well as the plot of DP_p against $[\text{Ox}]_0$ exhibits a linear dependence (see chapter 1). In these circumstances, it cannot be excluded that \overline{DPn} is kinetically controlled by all non-stationary state reactions which involve the rate at which the tertiary oxonium ions (R_i) are produced, the rate at which the monomer is consumed ($-d[\text{Ox}]/dt$), chain breaking reactions $\left(\sum_{i=1}^4 R_{tr}\right)$ and termination

reactions $\left(\sum_{i=1}^3 R_{t,i}\right)$ if they occur. Therefore, the average number molecular weight \overline{DP}_n of the high molecular weight material can be written as follows:

$$\overline{DP}_n = \frac{-d[Ox]/dt}{\sum_{i=1}^3 R_{t,i} + \sum_{i=1}^4 R_{tr} + R_i} \quad \text{E: 6.10}$$

6.1.2.2 Intra- and intermolecular transfer reactions

Further investigation showed that intra- and intermolecular transfer reactions compete during the polymerisation process (section 3.1.2). Indeed, at constant concentration of monomer the SEC analysis, as well as ^1H and ^{13}C NMR analysis showed that the fraction of cyclic oligomers formed during the polymerisation process increases with the decrease of the concentration of initiator ($\text{BF}_3(\text{CH}_3\text{COOH})_2/\text{BF}_3\text{OEt}_2$) concentration. This strongly indicates that “dormant” species are effectively reactivated during the polymerisation and that the dilution favours intra-molecular over intermolecular transfer reactions. However, because the formation of cyclic oligomers was found to slow down and be slightly reduced when alkylating initiators ($[\text{CH}_3\text{CH}_2\text{OCH}_2]^+[\text{BF}_4]^-$) was used instead of protonic reagents, end-biting reactions appear then to be a faster process of cyclic oligomer formation than back-biting reactions. Consequently, a series of experiments in which the concentration of $[\text{CH}_3\text{CH}_2\text{OCH}_2]^+[\text{BF}_4]^-$ is reduced, whereas the concentration of monomer is constant, should provide more conclusive evidence that acyclic and non-strained tertiary oxonium ions issue from intermolecular and back-biting transfer reactions are reactivated once formed and after monomer addition.

6.1.3 Mode of formation of cyclic oligomers

In the case of the cationic polymerisation of cyclic ether monomers, the formation of the cyclic oligomers always occurs in two step reactions. First intramolecular transfer reactions form a macrocyclic oxonium salt at the polymer chain end and then the macrocyclic oligomer is released by the action of an incoming monomer and/or by the action of an oxygen atom in the backbone of the polymer chain. In the case of the polymerisation of oxirane, Grønneborg^[124] showed by using dioxane-d8 that the macrocyclic oxonium ion at the polymer chain end can be enlarged by a direct ring opening expansion mechanism from dimer to tetramers and then released during the process of reactivation of the “dormant”

species. Because 1,4-dioxane is the more abundant cyclic oligomer formed, the authors explained the enhancement of cyclic tetramers in terms of its resistance to degradation rather than its ease of formation. In the case of the polymerisation of THF, it is reported that the stability of the growing centres towards ring-opening expansion reaction favours the depolymerisation process and intermolecular transfer reactions^[210] over the back-biting reactions for which the cyclic oligomers represent only 3 % of the produced materials. In the case of the polymerisation of oxetane, the high ring strain contained in the monomers enhances the reactivity of the growing centre towards transfer reactions (intra- and intermolecular transfer reactions)^[115]. Based on these observations, it is possible that the direct ring-opening expansion mechanism reported by Grønneborg et al. also occurs during the process of polymerisation of oxetane (see figure 6.2) leading to the predominant formation of cyclic tetramers. This phenomenon of ring-opening expansion mechanism could explain why the Jacobson-Stockmayer equation^[203] is not a suitable model to predict the concentration of cyclic oligomers in equilibrium with straight chain molecules when oxetane is polymerised using a cationic initiator^[115, 198-200]. This is also valid for the cationic polymerisation of epoxide monomers for which large cyclic oligomers are produced together with cyclic dimer^[124, 127, 128, 188, 190, 192-195].

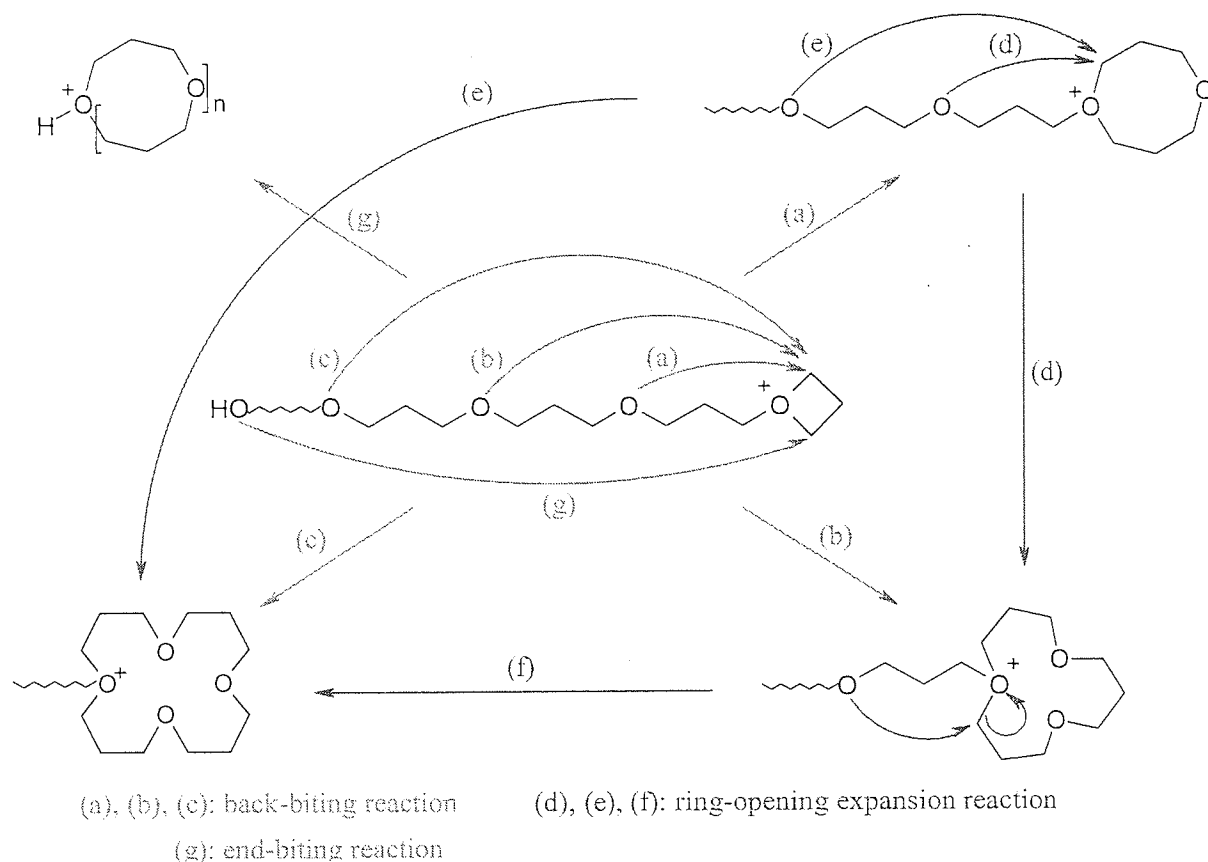


Figure 6. 2: Mechanism of formation of non-strained tertiary oxonium ions by back-biting reactions and ring opening expansion reaction.

Previous work in polyoxetane showed that all other possible cyclic oligomers from trimer up to nonamer are also produced in decreasing concentration^[198-200]. From our investigation, it was found by mass spectroscopy that large cyclic oligomers of up to 15 monomer units are also formed during the polymerisation process. Because GLC chromatography did not enable the observation of the presence of large cyclic oligomers (see section 3.1.4.1), MS coupled with GLC does not seem to be a good technique of fractionating and to quantifying each fraction of cyclic oligomer, soluble in hexane. During the last ten years, MALDI TOF analysis has turned out to be a powerful spectroscopic technique for the determination of the absolute \overline{Mn} and $\overline{Mw}/\overline{Mn}$ of a non-uniform polymer provided that the macromolecules do not have absolute molecular weight higher than 10,000 g/mol. Because the cyclic oligomers are small macrocyclics ($m/z < 1,000$ g/mol) this spectroscopic technique should then be used to quantify each fraction of oligomers of identical absolute molecular weight (m/z).

6.1.4 Termination reaction

The stability of the "active" and "dormant" species towards anion splitting reactions is believed to be a feature of the nature of the growing centres. Unlike carbocationic polymerisation (see figure 5.27), oxonium ions do not have an empty orbital, believed to be the driving force in the process of the anion-splitting reaction. This assumption, based only on the calorimetric analysis of data before and after successive monomer addition, does not provide all the satisfactory evidence of the absence of irreversible termination reactions. Moreover, the uncontrolled character of the polymerisation process in the redistribution of the polymer chain length makes the SEC data inappropriate for such investigation. Therefore, the direct measure of the number of the tertiary oxonium ions remaining unchanged during the whole polymerisation process should provide more conclusive evidence for this possibility. Saegusa et al. who investigated the kinetic polymerisation of oxetane by BF_3THF below 0°C showed by the phenoxide end-capped method that the concentration of propagating species reaches rapidly approximately 80% of the initial catalyst concentration^[320-322]. The slight increase of $[\text{R}^*]$ throughout the polymerisation process could then be due to the slow character of the initiation process.

6.1.4.1 Effect of the counter-ion on the reactivity of the propagating species

Several reports of cationic polymerisation affirmed that the growing centre can only exist in the form of ion pairs and free ions and that free ions and ion pairs exhibit the same reactivity^[115,133,185,337,338]. This was explained by the fact that the counter-ions involved in cationic polymerisation are very large (BF_4^- , PF_6^- , SbF_6^- , SbCl_6^-), and therefore interact only weakly with the cations. In addition, a survey of published data shows only a small variation in the value of dissociation constants of a large number of ion-pairs composed of various organic cations and bulky counter-ions, such as BCl_4^- , SbCl_6^- and PF_6^- . Our investigation showed that, when the polymerisation of oxetane was initiated by $\text{CH}_3\text{CH}_2\text{OCH}_2^+;\text{X}^-$, the use of $[\text{SbF}_6]^-$ instead of $[\text{BF}_4]^-$ resulted in the ability to reduce significantly the cyclic oligomers formation (low cyclic oligomer formation even after 90 % of monomer being consumed) but did not allow the \overline{Mn} and $\overline{Mw}/\overline{Mn}$ to be controlled (section 3.2.1). This counter-ion effect can only be explained if, in dichloromethane, the growing polymer chain ends (strained tertiary oxonium ions) and counter-ions are associated in the form of ion-pairs and/or loose ion-pairs and that the size of the counter-ions affects the chemoselectivity of the strained tertiary oxonium ions towards propagation and transfer to polymer.

6.2 Development of the quasiliving polymerisation of oxetane at 35 °C

The second part of this work was focused on the development of a polymerisation process that enabled the preparation of polymers with predictable molecular weight and narrow molecular weight distribution. In this study $\text{BF}_3:\text{CH}_3\text{OH}$, $\text{C}_6\text{H}_5\text{O}(\text{CH}_2)_3\text{O}^+(\text{C}_2\text{H}_4)_2\text{O}, [\text{SbF}_6]^-$ (II), and $\text{CH}_3\text{CH}_2\text{OCH}_2\text{T}^+, \text{X}^-$ (with $\text{T} = \text{O}(\text{C}_2\text{H}_4)_2\text{O}$ or OC_5H_{10} and $\text{X} = \text{SbF}_6$ or BF_4) were used as initiating system.

6.2.1 Controlling CROP of oxetane at 35 °C

Because irreversible termination reactions do not seem to occur during the polymerisation process, the idea of using an ether additive that can end-cap the propagating growing centre seemed to us to be one method to temporarily generating a strainless tertiary oxonium ("dormant" species) that can be reversibly reactivated by a molecule of oxetane and this without inducing redistribution $\overline{M}_w/\overline{M}_n$ by chain breaking reactions and without formation of cyclic oligomers or dead polymer chains (see figure 6.3).

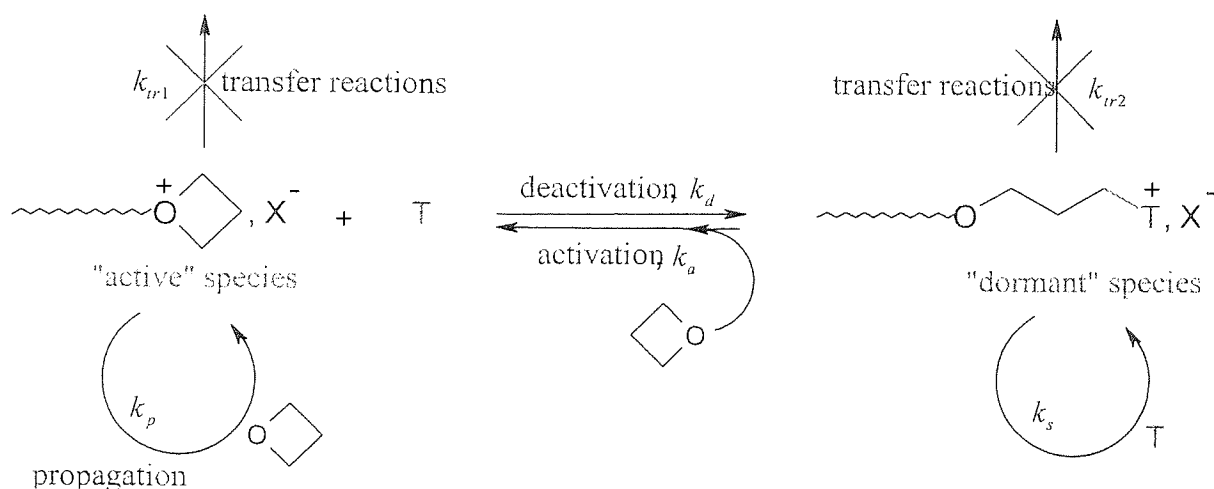


Figure 6. 3: Formation of "dormant" species in quasiliving polymerisation of oxetane in the presence of additive T.

Assuming that such a quasiliving system could prevent transfer reactions from occurring, the mechanism of polymerisation was discussed and it was shown that the determinant factors for the control of the polymerisation over \overline{M}_n and $\overline{M}_w/\overline{M}_n$ are the rate of initiation, the rate

of propagation and the rates of interconversion between “active” and “dormant” species. Because diphenyl ether ($pK_b > 7.2$) was found to enhance the formation of cyclic oligomers (see section 4.2), the use of an ether additive as a solvent which is more nucleophilic than the oxygen atom in the backbone of the polymer chains (i.e. $pK_b < 7.2$) but less nucleophilic than the oxygen atom of the monomer (i.e. $pK_b > 3.6$) seemed to us to be the avenue to explore in order to compete efficiently with transfer reactions, prevent the irreversible termination of the growing centre by the additive and therefore control polymerisation over \overline{Mn} and $\overline{Mw}/\overline{Mn}$. For this purpose, the use of 1,4-dioxane ($pK_b = 4.83$) and tetrahydropyran ($pK_b = 5.85$) as solvent were examined.

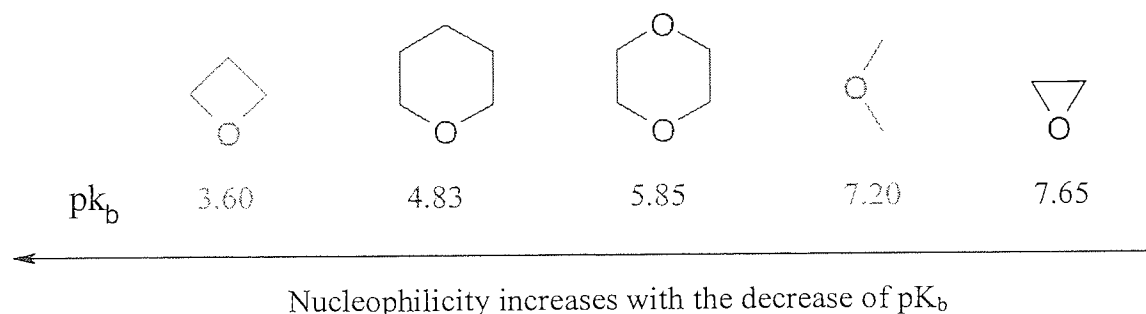


Figure 6. 4: Basicity of cyclic ether measured by IR measurement referred to the literature.

6.2.2 CROP of oxetane in 1,4-dioxane at 35 °C

As expected, the studies of the CROP of oxetane in 1,4-dioxane, a cyclic ether monomer that does not homopolymerise, showed that, independent of the nature the initiating system, the molecular weight of the produced polymers always increased with conversion and with a second monomer addition after the consumption of almost 95% of monomer. Because conventional initiators (Friedel and Craft reagents with protogens, here $BF_3:MeOH$) induce a slow initiation, \overline{Mn} did not increase linearly with conversion and the polymers produced were characterised by broad molecular weight distributions. Using “living polyoxetane monomeric” initiator as a fast initiator, \overline{Mn} was found to increase linearly with the conversion and after a second monomer addition. However, the choice of the initiator and corresponding counter-ion turned out to play a significant role in the chemoselectivity of the polymerisation towards propagation and transfer reactions and therefore in the control of polymerisation over \overline{Mn} and $\overline{Mw}/\overline{Mn}$.

6.2.2.1 Study of the C.R.O.P of oxetane when initiated by $R(1,4\text{-dioxane})^+; [\text{SbF}_6]^-$

The living character of the CROP of oxetane in 1,4-dioxane was achieved and demonstrated when $\text{C}_6\text{H}_5\text{O}(\text{CH}_2)(1,4\text{-dioxane})^+; [\text{SbF}_6]^-$ was used as "living polyoxetane monomeric" initiator. Indeed, molecular weight studies by SEC analysis showed that polymers with narrow molecular weight distribution were produced ($\overline{M}_w/\overline{M}_n \approx 1.2$) without cyclic oligomers, that \overline{M}_n increases linearly with the conversion and, upon second monomer addition, the existing polymers chains were extended correspondingly. High molecular weight with narrow number average molecular distribution ($\overline{M}_n = 160,000 \text{ g/mol}$ and $\overline{M}_w/\overline{M}_n = 1.2$) were produced successfully with no formation of cyclic oligomers.

6.2.2.2 Mechanism of the quasiliving CROP of oxetane in 1,4-dioxane

The kinetics of the polymerisation of oxetane was investigated and discussed. It was found, as expected, that both "active" and "dormant" species take part in the process of chain growth in their own ways. Indeed, in the apparent absence of irreversible termination reactions, the significant curvature of the slope of $\text{Ln}([Ox]_0/[Ox]_t)$ against time could only be explained if "dormant" species are reactivated by molecules of monomer whereas the "active" species grows by the successive addition of monomer before being end-capped by one molecule of 1,4-dioxane. At constant concentration of 1,4-dioxane, the reversible equilibrium between "active" growing centres and "dormant" species makes both the concentration of "active" and "dormant" species dependent on the remaining concentration of oxetane; the mole fraction of "dormant" species increases as the concentration of oxetane decrease during the process of polymerisation. Because of the chemoselectivity of the ring-opening reaction of oxetane, all bimolecular reactions involved in the polymerisation proceed more likely via $\text{S}_\text{N}2$ reaction. Therefore, the mechanism of CROP of oxetane in 1,4-dioxane can be schematised as follows

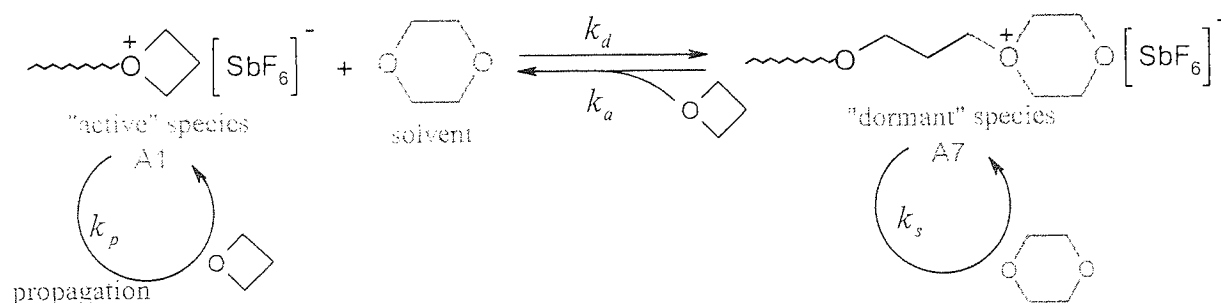


Figure 6. 5: Mechanism of polymerisation of oxetane in 1,4-dioxane.

and the analytical expression of the rate of monomer consumption can be expressed as follows:

$$-\frac{d[Ox]}{dt} = (k_a + (k_p - k_a) \cdot \alpha_t) \cdot c_0 \cdot [Ox] \quad \text{E: 6.11}$$

where k_p ($\text{L} \cdot \text{mol}^{-1} \cdot \text{s}^{-1}$) represents the rate constant at which the “active” species (A1) propagate and k_a is the apparent rate constant of activation of “dormant” species (A7). $[Ox]$ represents the concentration of oxetane and c_0 denotes the total concentration of growing centres ($c_0 = [A1] + [A7]$). Here, α_t denotes the instantaneous mole fraction of propagating species in the form of “active” species (A1). Because the equilibrium between “active” and “dormant” species does not reach a steady state of their concentrations, the analytical expression of the equilibrium constant $K_{(t)}$ (E: 6.14) can be expressed from the equations E: 6.12 and E: 6.13:

$$-\frac{d[A1]}{dt} = k_a \cdot [A1] \cdot [T] - k_a \cdot [A7] \cdot [Ox] \neq 0 \quad \text{E: 6.12}$$

and

$$K_{(t)} = \frac{k_d}{k_a} \cdot \left(1 - \frac{1}{k_a \cdot [A1] \cdot [T]_0} \cdot \left(-\frac{d[A1]}{dt} \right) \right) = f(t) \quad \text{E: 6.13}$$

with

$$K_{(t)} = \frac{[A7]_t \cdot [Ox]_t}{[A1]_t \cdot [T]_0} \quad \text{E: 6.14}$$

Here, the determination of α_t ($\alpha_t = [A1]/c_0$) implies the resolution of the equation E: 6.13 for which no solution has been found so far.

6.2.2.2.1 Control over \overline{Mn} and $\overline{Mw}/\overline{Mn}$

Because the formation of cyclic oligomers was prevented during the entire course of the polymerisation and after monomer addition, throughout the polymerisation process produced polymers of almost identical polydispersity ($\overline{Mw}/\overline{Mn} \approx 1.2$), suggest that the rate of interconversion between “active” and “dormant” species is slow or at least comparable to that of propagation. This assumption is in agreement with the curvature of the slope $\ln([Ox]_0/[Ox]_t)$ against time which is an indication that the rate constant of propagation (k_p , L/mol/s) is much larger than the rate constant of reactivation ($k_{a,app}$ L/mol/s) of “dormant” species by the monomer ($k_p \gg k_a$). Because the reactivity of the “active” species (strained tertiary oxonium ions) depends more on the ring-strain of the oxonium site ($\Delta H_p = 19$ kcal/mol) than on the nucleophilicity of the attacking group, it appears then according to the nucleophilicity attacking group (see figure 6.4) that

$$k_p \geq k_d \gg k_a > k_s \quad \text{E: 6.15}$$

The above relationship (see E: 6.15) shows that at an early stage of the polymerisation the rate of activation of “dormant” species is probably too slow in relation to the rate of propagation to give good control over $\overline{Mw}/\overline{Mn}$ knowing that the rate of deactivation is slightly faster or comparable to the rate of propagation ($[Dox]/[Ox] = 9$ and $k_p \geq k_d$).

$$\frac{R_p}{R_d} = \frac{k_p}{k_d} \cdot \frac{[Ox]_0}{[Dox]_0} \cdot \left(\frac{100 - \text{conversion}}{100} \right) \quad \text{E: 6.16}$$

Because number of molecules of monomer incorporated by the “active” species A1 just before deactivation can be approximated by the equation E: 6.16, the control over $\overline{Mw}/\overline{Mn}$ should then be improved throughout the polymerisation since the decrease of the concentration of oxetane decrease R_d/R_p . This could explain why $\overline{Mw}/\overline{Mn}$ tends to decrease slightly throughout the polymerisation. The slight decrease of $\overline{Mw}/\overline{Mn}$ after monomer addition experiments is certainly due as well to the expansion of the polymer chains that always tend to narrower the polydispersity in polymer synthesis. Therefore, it will be interesting to investigate the effect of the increase of the ratio $[Dox]/[Ox]$ on the control of

polymerisation over $\overline{Mw}/\overline{Mn}$. Moreover, the sequential monomer addition experiments should also be performed.

6.2.2.2.2 Factors affecting the quasiliving character of the polymerisation process

Because 1,4-dioxane is a poor ionising solvent, the solubility of the initiator turned out to be decisive to prevent the formation of large insoluble aggregates and small insoluble aggregates responsible of a slow initiation process. When $\text{CH}_3\text{CH}_2\text{O}^+(\text{C}_2\text{H}_4)_2\text{O};[\text{SbF}_6]^-$ (12) was used as initiator, the polymers produced showed broad polydispersity ($1.6 < \overline{Mw}/\overline{Mn} < 2$) but no cyclic oligomers were formed. In this respect, the polymerisation process initiated by “living monomeric polyoxetane” initiator associated with $[\text{SbF}_6]^-$ as counter-ion can then be classified as a *quasiliving polymerisation* leading to the formation of narrow ($\overline{Mw}/\overline{Mn} \approx 1.2$) or large ($1.6 < \overline{Mw}/\overline{Mn} < 2$) polydispersity depending on the solubility of the initiator in 1,4-dioxane.

Further investigations showed that at constant concentration of oxetane and II, the use of dichloromethane as co-solvent was not beneficial to the quasiliving character of the polymerisation and therefore for the control over \overline{Mn} and $\overline{Mw}/\overline{Mn}$. Table 6.1 shows how the decrease of the ratio $[\text{dox}]/[\text{ox}]$ enhances the rate of the polymerisation and produces polymers with lower \overline{Mn} and broader polydispersity. This is because the decrease of the initial concentration of 1,4-dioxane gradually increases the probability of the transfer reaction unfavourable for the control of the polymerisation occurring (see equations E: 5.26 and E: 5.27) since intra and intermolecular transfer reactions are responsible for the process of chain breaking reactions when the formed “dormant” species are reactivated by a molecule of monomer.

Initiator	$\overline{Mw}/\overline{Mn}$	\overline{Mn}	$\frac{[Dox]_0}{[Ox]_0}$	Targeted Dp	Solvent	Conversion %	Time minute
II	1.92	35,000	3.86	986	dox/dcm	38	3
	1.94	45,800				92	28
	2	36,740				95	260
	1.72	61,220	7.25	986	dox/dcm	45.8	6
	1.73	88,700				74.4	30
	1.96	118,860				95.4	300
	1.22	31,220	9.66	986	Dox	20.7	16
	1.26	98,000				73	145
	1.2	120,000				83	240

Table 6. 1: Effect of the ratio $[Dox]/[Ox]$ on \overline{Mn} , $\overline{Mw}/\overline{Mn}$ and rate of monomer consumption when 1.125 M of oxetane is initiated at 35 °C by 0.00114 M of $C_6H_5O(CH_2)_3O^+(C_2H_4)_2O; [SbF_6]^-$.

6.2.2.3 Study of the CROP of oxetane initiated by $CH_3CH_2O^+(C_2H_4)_2O; [BF_4]^-$.

Further investigation showed that when "living monomeric polyoxetane" was used as a fast initiator, the quasiling character of the polymerisation was strongly dependent on the size of the counter-ions. Indeed, the cyclic oligomer formation was prevented only when $[SbF_6]^-$ was used as counter-ions. When a smaller counter-ion was used, such as $[BF_4]^-$, the cyclic oligomer formations was significantly reduced but not prevented. Unfortunately, ^{13}C NMR did not enable a qualitative measure to be made accurately of the fraction of monomer converted into cyclic oligomers. Thus we approximated to around 1-2 % of the converted monomer. Because of this, the polymerisation process initiated by the alkylating reagent associated with $[BF_4]^-$ can only be classified as *controlled polymerisation process* leading to linear increases of \overline{Mn} with conversion before and after polymer chain length expansion, large polydispersity ($\overline{Mw}/\overline{Mn} \approx 2$) and formation of cyclic oligomers (1-2 % of monomer are converted into cyclic oligomers) at high monomer conversion.

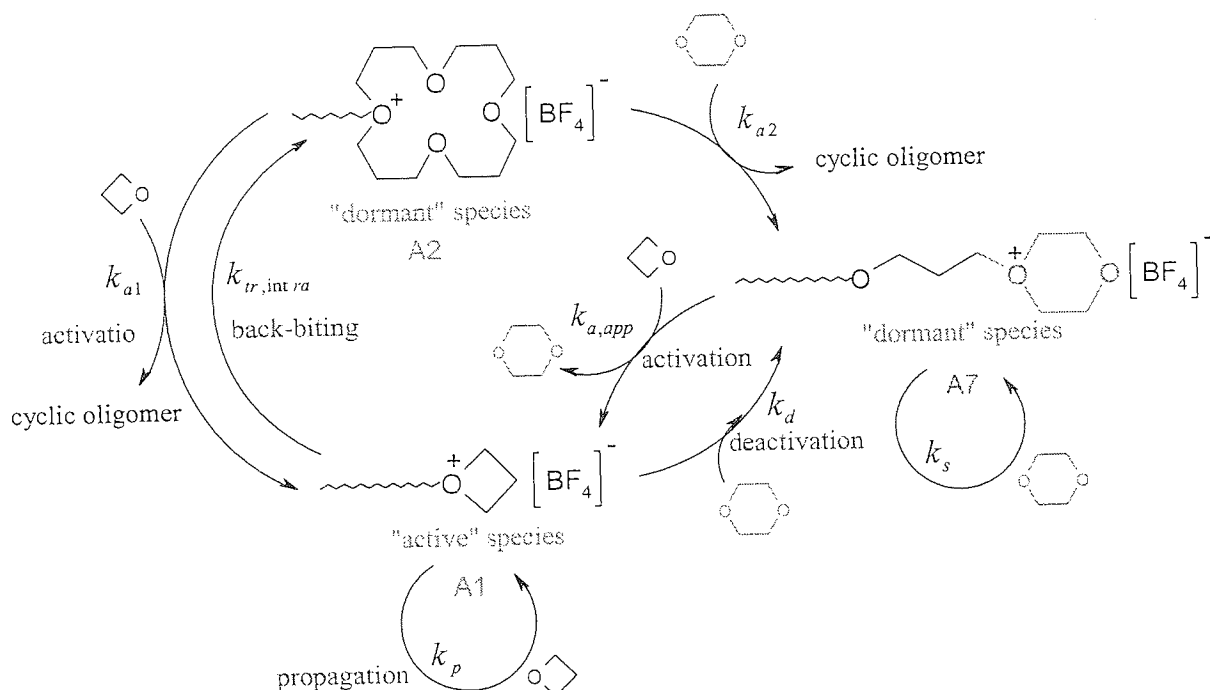


Figure 6. 6: Mechanism of controlled polymerisation of oxetane in 1,4-dioxane initiated by $\text{CH}_3\text{CH}_2\text{O}^+(\text{C}_2\text{H}_4)_2\text{O}; [\text{BF}_4]^-$.

As illustrated in the above scheme, such apparent control of polymerisation can only be explained if the living "active" species coexists in dynamic equilibrium with two "dormant" species. One from the reversible deactivation of the growing centres by 1,4-dioxane and the other one issue from the back-biting reactions. The linear dependence \overline{Mn} conversion before and after monomer addition seems to indicate that the use of 1,4-dioxane as solvent prevent intermolecular transfer reactions from occurring. Therefore, α and β_t the fraction of "dormant" species in the form end-cap by a molecule of 1,4-dioxane ($\beta_t = [\text{A7}]/\{(1-\alpha_t)\cdot c_0\}$), then $(1-\alpha_t)\cdot c_0$, $(1-\alpha_t)\cdot\beta_t\cdot c_0$ and $(1-\alpha_t)\cdot(1-\beta_t)\cdot c_0$ represent respectively the instantaneous concentration of A1, A7 and A2. Therefore the rate of monomer consumption can be written as follow:

$$-\frac{d[\text{Ox}]}{dt} = (k_{a,app} + (k_p - k_{a,app})\cdot\alpha_t)\cdot c_0 \cdot [\text{Ox}] \quad \text{E : 6.17}$$

with

$$k_{a,app} = k_{a1} + (k_a - k_{a1})\cdot\beta_t \quad \text{E: 6.18}$$

6.2.2.4 Study of the CROP of oxetane initiated by $H^+; [CH_3O:BF_3]^-$.

Because Friedel Craft reagents with protogens, (here $BF_3:MeOH$) induce a slow initiation of the polymerisation of oxetane in relation to the propagation, \overline{Mn} did not increase linearly with conversion and the produced polymers were characterised by broad molecular weight distribution ($1.7 < \overline{Mw}/\overline{Mn} < 3$). Surprisingly, the second monomer addition experiments show a linear increase of \overline{Mn} after almost full monomer conversion of the added monomer and the produced polymer showed narrower polydispersity. This apparent linear extension of the polymer chains after monomer addition needs more investigations knowing that the initiator ($BF_3:MeOH$) is probably not fully converted into growing polymers chains and that cyclic oligomer formation is not totally prevented (5 % of the added monomer are still converted into cyclic oligomers). Because \overline{Mn} increases throughout the polymerisation and after monomer addition, the polymerisation of oxetane initiated in 1,4-dioxane at 35 °C can be classified as *controlled polymerisation process* even if the polymerisation is characterised by a slow initiation process and by the formation of cyclic oligomers. Because protonic initiators generate nucleophilic hydroxyl end groups, a process of cyclic oligomer formation by end-biting reactions might also occur in parallel to the polymerisation process for the growing species that do not reach a sufficiently high chain length to entropically disfavour end to end polymer chains reactions. This could explain why $BF_3:MeOH$ produces more cyclic oligomers than $CH_3O^+(C_2H_4)_2O; [BF_4]^-$. Therefore the mechanism of polymerisation can be represented as follow:

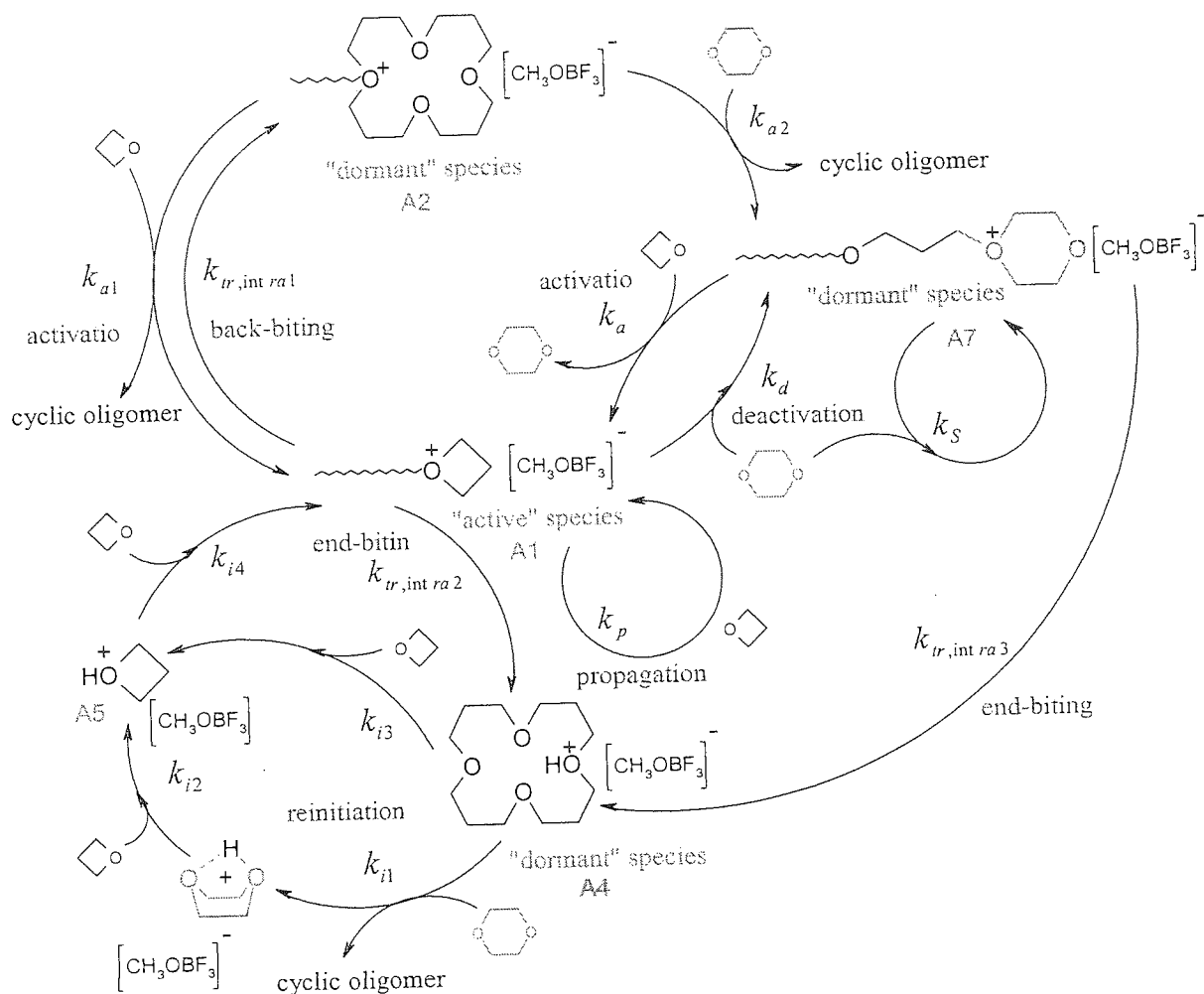
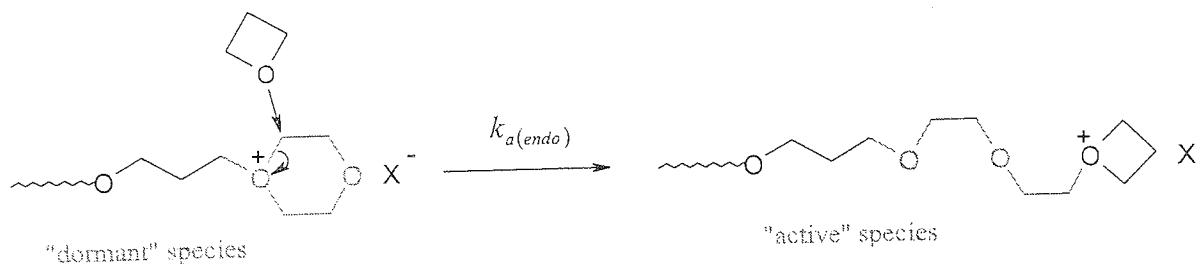


Figure 6.7: Mechanism of controlled polymerisation of oxetane in 1,4-dioxane initiated by $\text{H}^+; [\text{CH}_3\text{O:BF}_3]^-$.

6.2.2.5 Effect of the counter-ion on the copolymerisation of 1,4-dioxane with oxetane.

Surprisingly, the analysis of polymers by ^{13}C NMR showed that the strain free 1,4-dioxane that does not homopolymerise can be copolymerised and this depended on the size of the counter-ions. Indeed, with small and/or asymmetric counter-ion ($[\text{BF}_4]^-$, $[\text{MeOBF}_3]^-$), the composition of polymer in 1,4-dioxane reaches a maximum value around 4-5 % as soon as 5 to 10 % of monomer was consumed while with $[\text{SbF}_6]^-$ the copolymerisation starts at high oxetane conversion (conversion > 70 %), and then reaches a maximum value of 1-2% at about 80% oxetane conversion.

a) copolymerisation of 1,4-dioxane by oxetane



b) Substitution Nucleophile 2 of 1,4-dioxane by oxetane

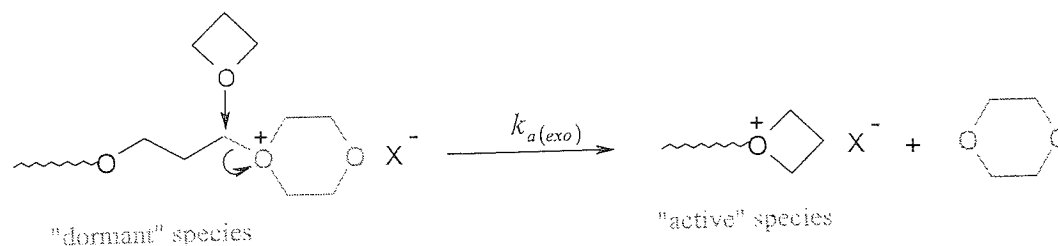


Figure 6. 8: Mechanism of reactivation of "dormant" species by oxetane via S_N2 process.

Therefore, if $p_{a(endo)}$ and $p_{a(exo)}$ represent respectively the probability that oxetane attacks the endo-cyclic and exo-cyclic electron deficient carbon atom in the α -position of the oxonium site, the apparent rate constant of activation can then be expressed as follow,

$$k_{a,app} = k_{a(endo)} + (k_{a(exo)} - k_{a(endo)}) \cdot p_{a(exo)} \quad \text{E: 6.19}$$

with

$$p_{a(endo)} + p_{a(exo)} = 1 \quad \text{E: 6.20}$$

It must be noted that $p_{a(endo)}$ and $p_{a(exo)}$ are constant during the entire course of the polymerisation and dependent also on the nature of the counter-ion. This unexpected result is believed to be due to the nature of the associated ions pairs. Indeed, with $[\text{SbF}_6]^-$, the counter-ion is believed to sterically disfavour the reactivation of the "dormant" species by copolymerisation. With smaller and/or asymmetrical counter-ions, the steric hindrance on the process of reactivation of the "dormant" species appears then to be reduced. Because the dissociation of tight ion pairs is favoured by an increase of the polarity of the medium and a decrease of the size of the counter-ions, it cannot be excluded that the decrease of the size of

the counter-ions or the use of asymmetric counter-ions could favour the dissociation of ion-pairs into less stereoselective loose ion-pairs. This could explain the lack of control of the polymerisation as we go from large $[\text{SbF}_6]^-$ to smaller $[\text{BF}_4]^-$ or asymmetric counter-ions $[\text{CH}_3\text{OBF}_4]^-$. So far in cationic polymerisation, there is no clear evidence in the literature on whether the growing centre exists in the form of tight or/and loose ion-pairs when the polymerisation is performed in a poor solvating medium. In this present study, it appears that the size of the counter-ion really affects the chemoselectivity of the propagating species towards propagation and intramolecular transfer reactions. Intermolecular transfer reactions are suppressed due to the presence of 1,4-dioxane.

6.2.3 CROP of oxetane in tetrahydropyran.

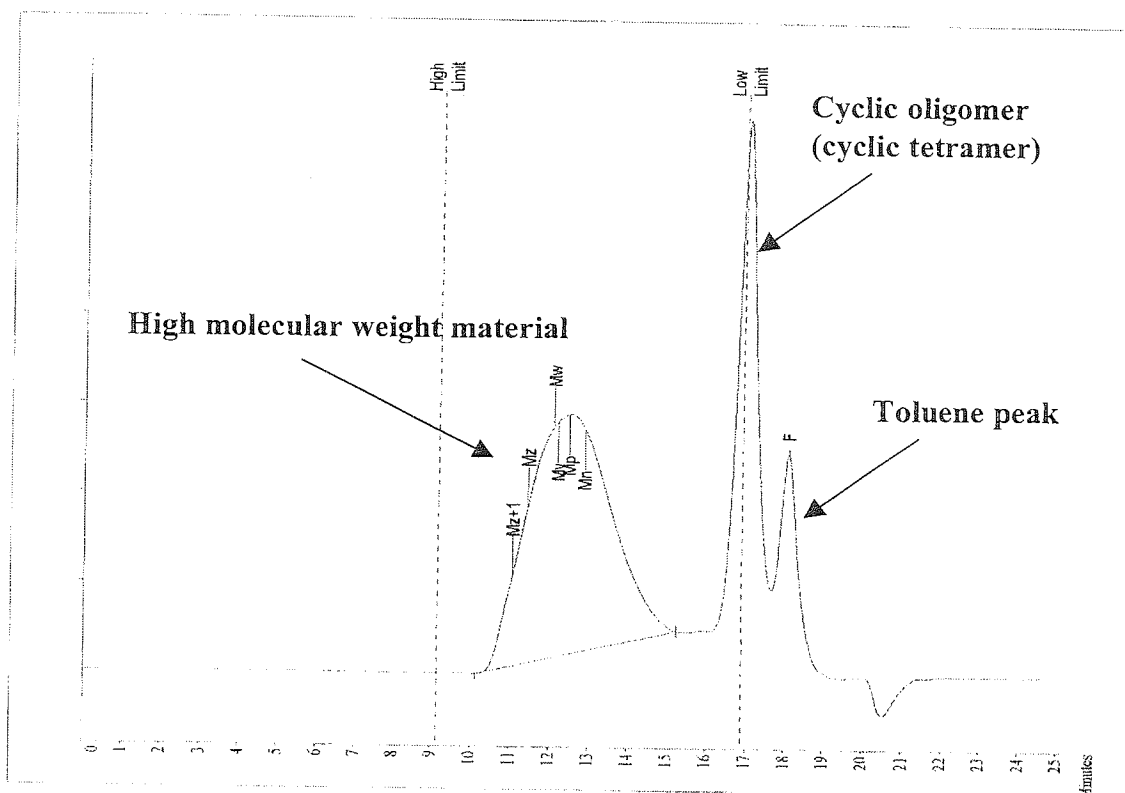
The use of *tetrahydropyrane* instead of 1,4-dioxane also led to the development of control polymerisation process over \overline{Mn} and $\overline{Mw}/\overline{Mn}$. As for 1,4-dioxane the reduction of cyclic oligomer formation was improved by using alkylating reagents instead of protonic reagents. However, because tetrahydropyran is a highly polar solvent, the reactivity of the "active" and "dormant" species were found to be unaffected by the size of the counter-ions and the reactivity of THP towards the copolymerisation with oxetane was found to be superior to the reactivity of 1,4-dioxane. It must be noted that the use of alkylating reagents associated $[\text{SbF}_6]^-$ did not prevent cyclic oligomer formation from occurring. Besides, the plot of $\overline{Mn}_{(\text{SEC})}$ against expected $\overline{Mn}^{(13\text{H},\text{NMR})}$ showed that the initiation was quantitative and that the initiator do not associate into aggregates. Here, this is the copolymerisation process that is believed to be responsible for the continuous increase of the polydispersity ($1.18 < \overline{Mw}/\overline{Mn} < 1.56$) when "living monomeric polyoxetane" initiator (I4) is used as fast initiator.

6.3 Further work

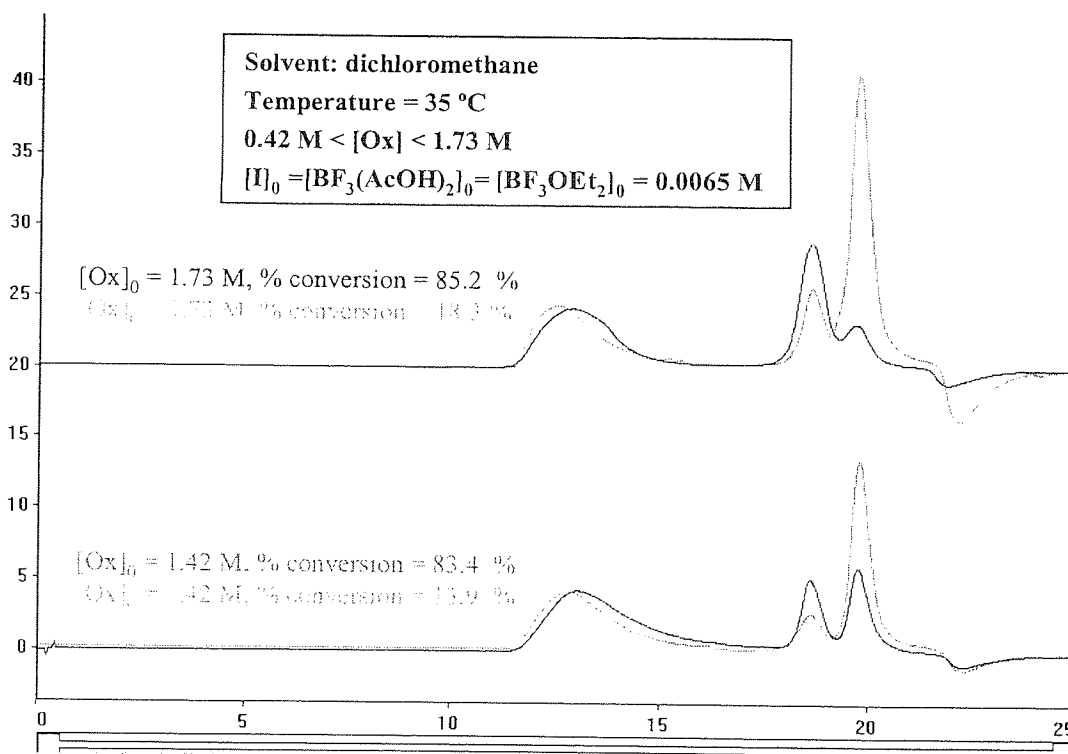
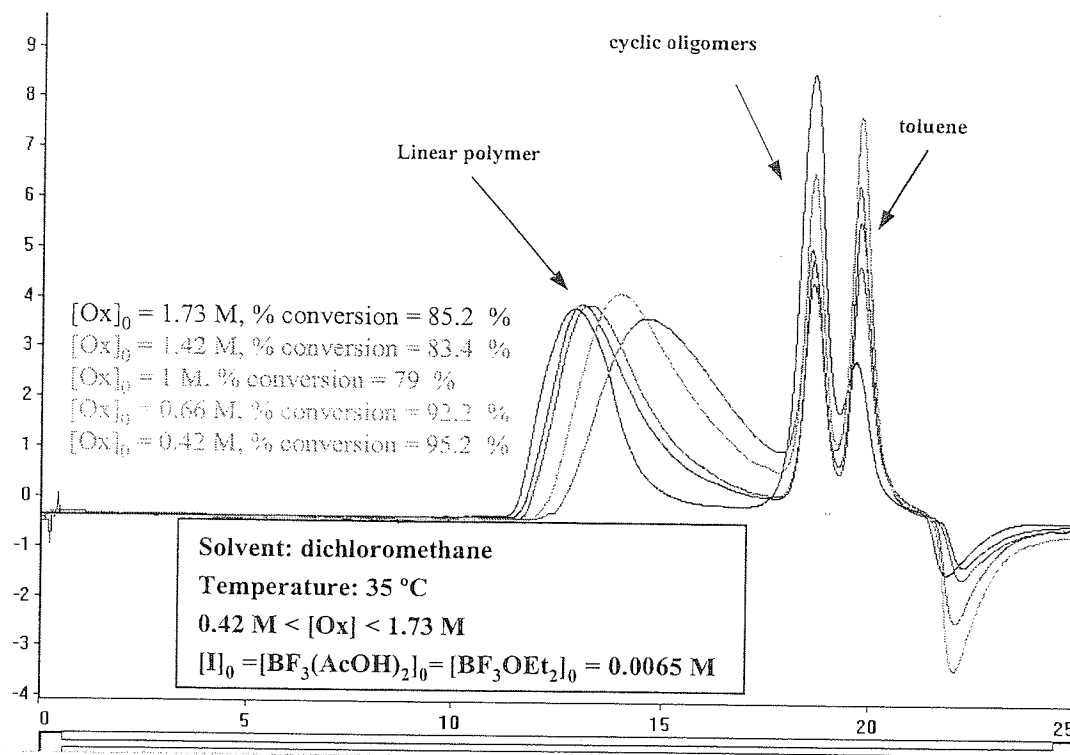
In summary, the C.R.O.P of oxetane in 1,4-dioxane is the first recorded quasiliving polymerisation process in which the concentration of "active" and "dormant" species are dependent on the remaining concentration of monomer. This is also the first cationic polymerisation system that enable by A.C.E mechanism the preparation in "living" manner of poly(oxetane) with predictable molecular weight and narrow molecular weight distribution.

The living character of the polymerisation process was demonstrated by the fact that the exiting polymer chains can be expanded correspondingly after monomer addition. However, there is a need for further work such as trying to improve the initiator efficiency and the spontaneous character of the initiation process. The control over $\overline{M}_w/\overline{M}_n$ should also be improved ($\overline{M}_w/\overline{M}_n < 1.2$) by slowing down the rate of propagation over the rate of interconversion between "active" and "dormant" species. This may be achieved by increasing the ratio $[Dox]_0/[Ox]_0$. Because 2-methyl oxetane fails to polymerise in presence of cationic initiator, the use of cyclic ether additive with one secondary carbon in the 2-position should prevent the process of reactivation by copolymerisation. Similarly the use of acyclic ether additive with one secondary carbon in the 2-position may also prevent during the reactivation of the dormant species, the transfer of the oxonium site from the polymer to the additive. More detailed kinetic study has to be carried out. Indeed, our investigation showed that depending on the nature of the counter-ion, linear dependence \overline{M}_n against conversion was not a criterion of livingness but one of control polymerisation. Moreover, the determinations of the rate constant of propagation (k_p), rate constant of deactivation (k_d) and rate constant of activation (k_a) have to be done to testify the quasiliving character of the polymerisation process. This supposes a mathematical resolution of the equation E: 6.15. Because the quasiliving CROP of oxetane generate living growing polymer chains, the end-functionalisation of polyoxetane should enable the preparation of well defined polymer such as start polymer, well-defined macromonomer as well as well-defined macroinitiator for control radical polymerisation (ATRP, RAFT/MADIX), living anionic polymerisation and coordination polymerisation of monomer more nucleophilic than oxygen atoms of the polyoxetane backbone. The extension of this quasiliving system to oxetane derivative monomers bearing side chains in the 3-position has to be investigated. Because cyclic ether monomers fail to polymerise in living manner using cationic initiator, this original quasiliving could be an alternative to control the polymerisation of oxirane, oxetane derivative, tetrahydrofuran and oxepane but also the preparation of block-copolymers and statistic copolymers. Similarly, this new concept of polymerisation could also be extended to others cyclic monomers such as thioethers, caprolactone, lactide, etc. Because a hydroxyl tail group is the stronger nucleophilic reagent in the polymerisation medium, it will be interesting to use this idea of end-capping the growing centre by an additive to prepare macrocyclic oligomers by end-biting reactions. Interesting results should be obtained by playing the ratio $[T]_0/[Ox]_0/[R-OH]_0$.

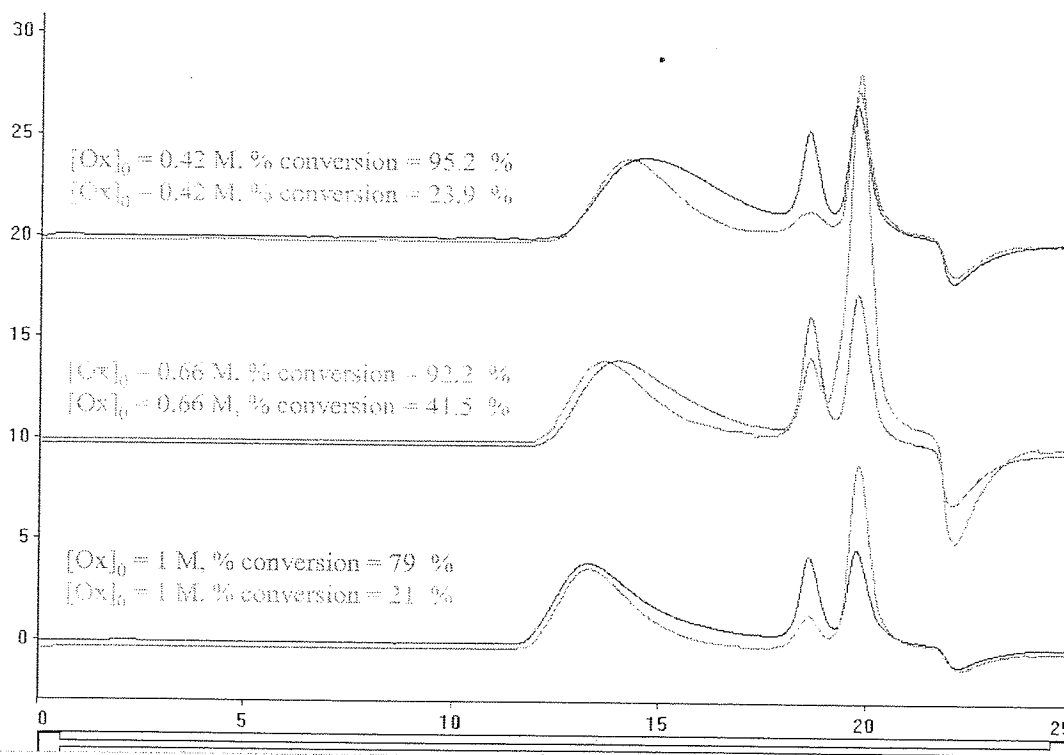
ANNEX



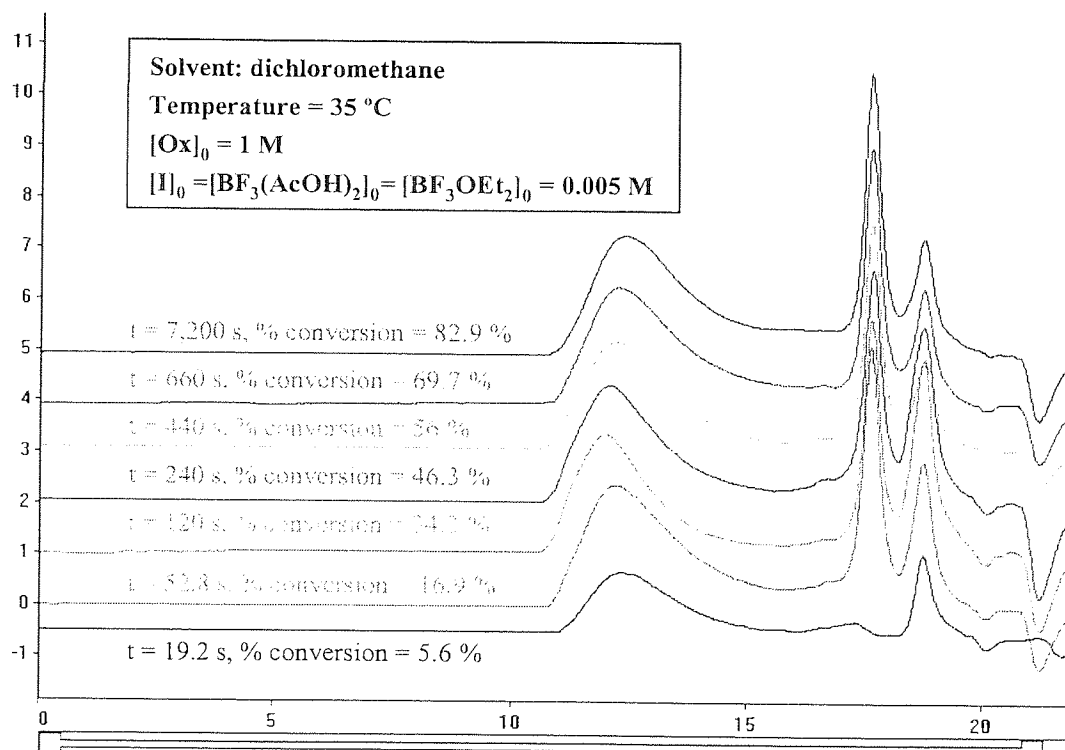
Annex 3. 1: Typical S.E.C chromatogram of polyoxetane - Bimodal distribution.



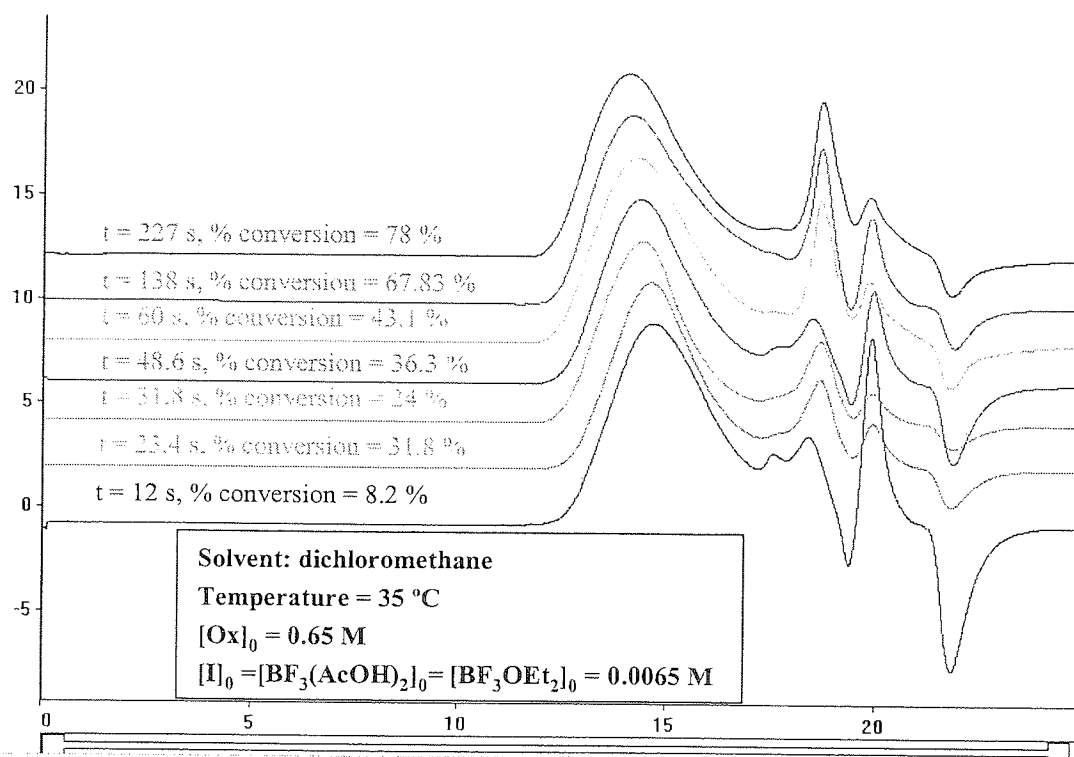
Annex 3. 2: S.E.C chromatogram of polyoxetane materials obtained at high monomer conversion for different concentration of oxetane. Polymerisation carried out in dichloromethane at 35 °C. $[BF_3(AcOH)_2]_0 = [BF_3OEt_2]_0 = 0.0065 \pm 0.005 \text{ M}$.



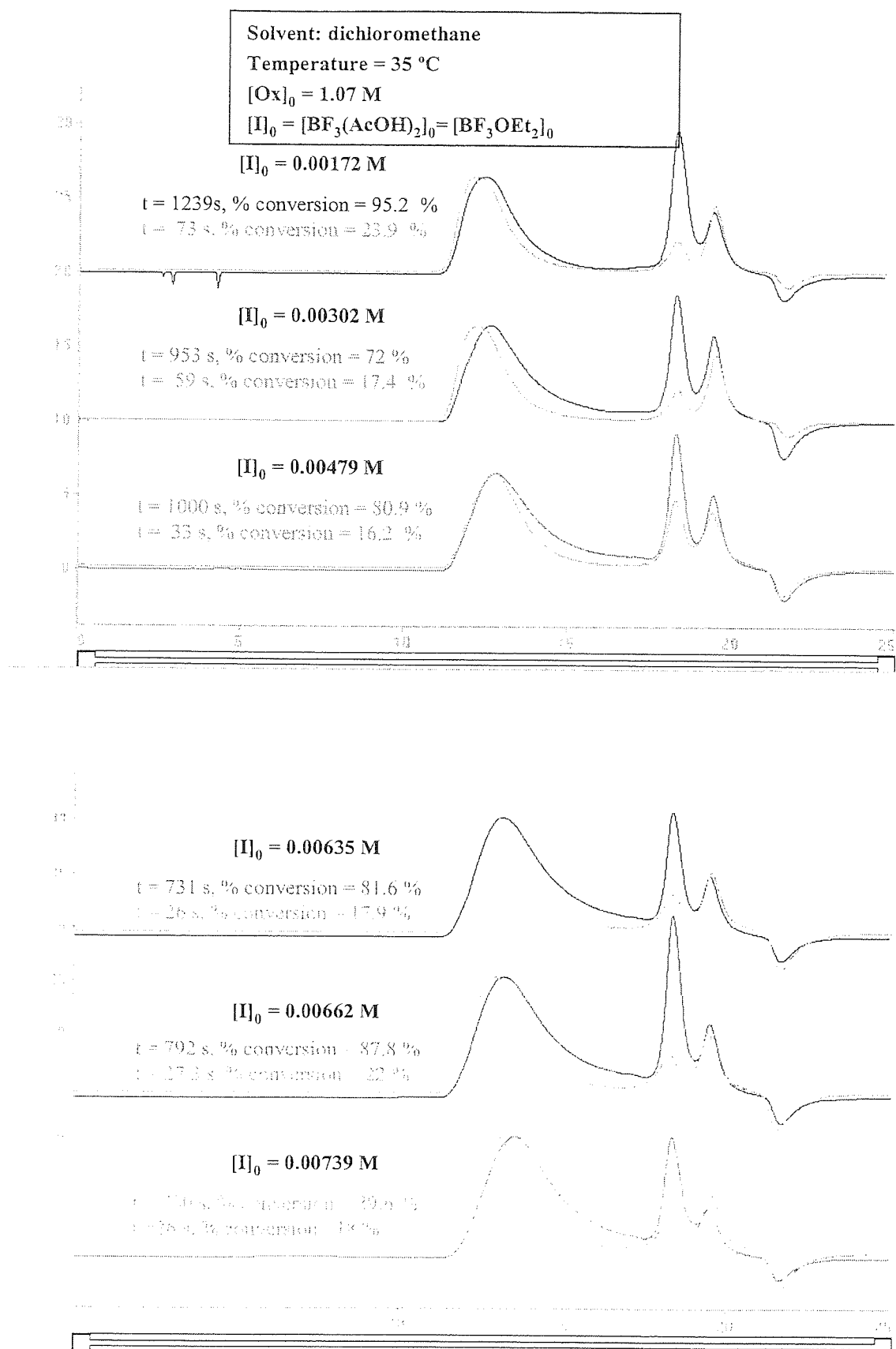
Annex 3. 3: S.E.C chromatogram of polyoxetane materials obtained at High and low monomer conversion for a different concentration of oxetane. Polymerisation carried out in dichloromethane at 35 °C. $[BF_3(AcOH)_2]_0 = [BF_3(AcOH)_2]_0 = 0.0065 \pm 0.005 \text{ M}$.



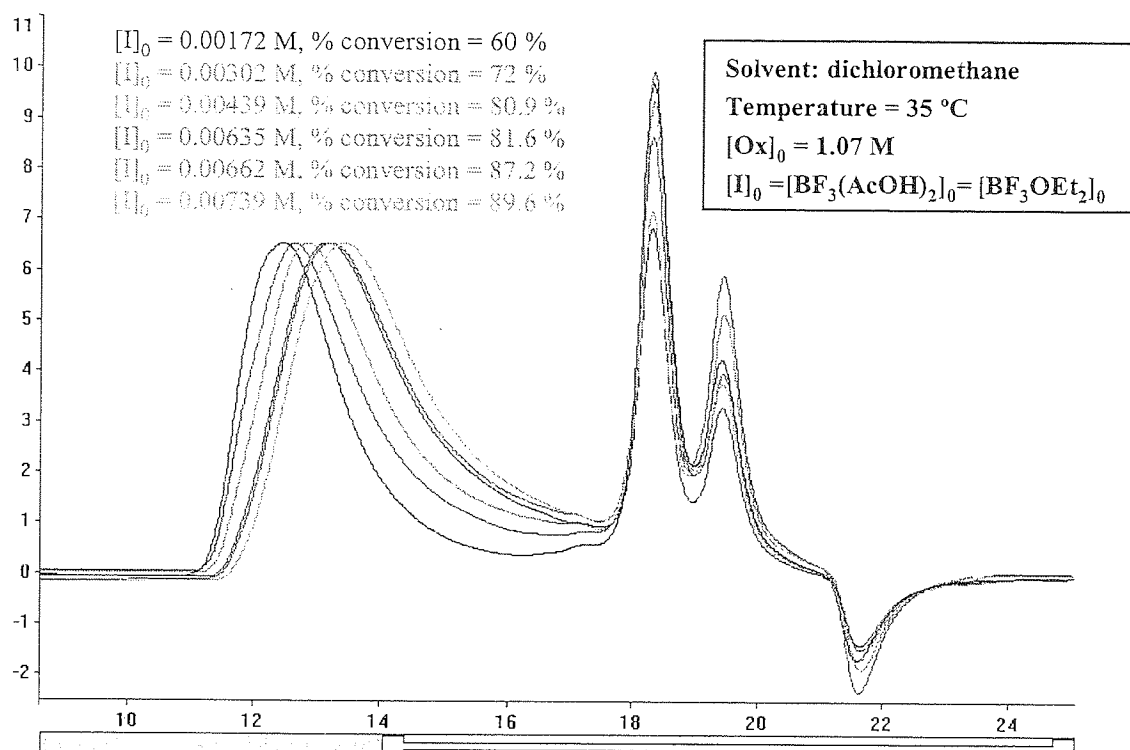
Annex 3. 4: S.E.C chromatogram of polymer obtained at different monomer conversion. Polymerisation carried in dichloromethane at 35°C. $[Ox]_0 = 1 \text{ M}$ and $[BF_3(AcOH)_2]_0 = [BF_3(AcOH)_2]_0 = 0.005 \text{ M}$ (table 3.5, series S 3.12).



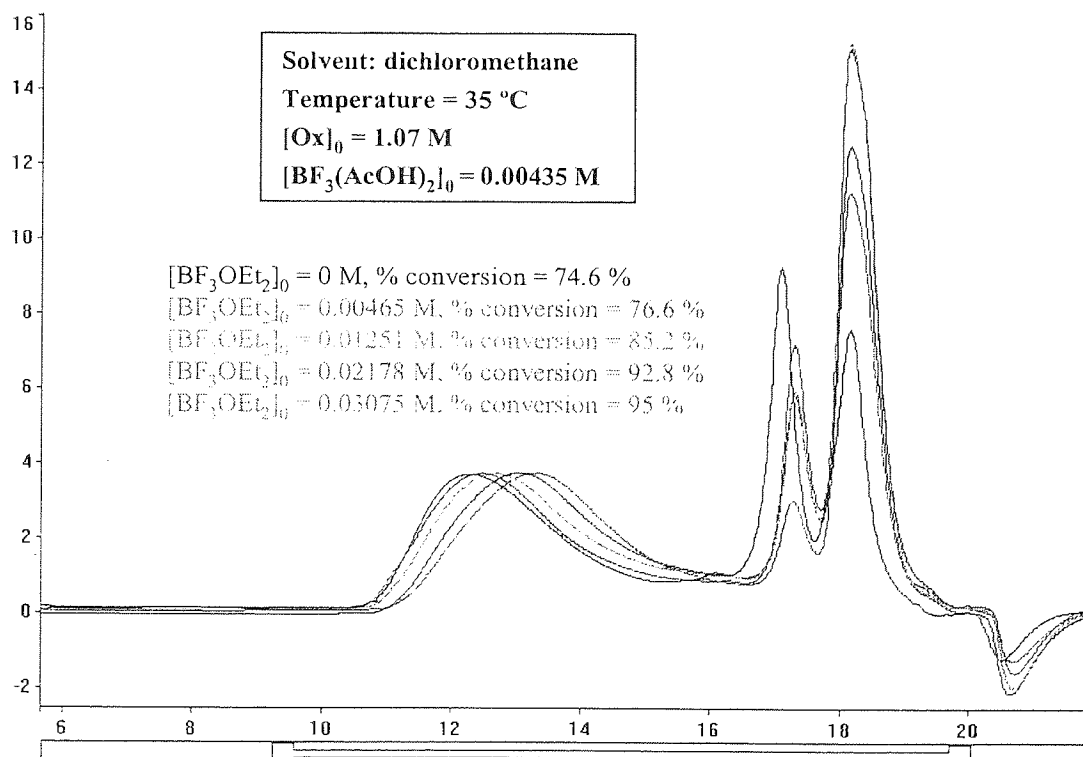
Annex 3. 5: S.E.C chromatogram of polymer obtained at different monomer conversion. Polymerisation carried in dichloromethane at 35°C. $[\text{Ox}]_0 = 0.65 \text{ M}$ and $[\text{BF}_3(\text{AcOH})_2]_0 = [\text{BF}_3(\text{AcOH})_2]_0 = 0.0065 \text{ M}$ (table 3.5, series S 3.13).



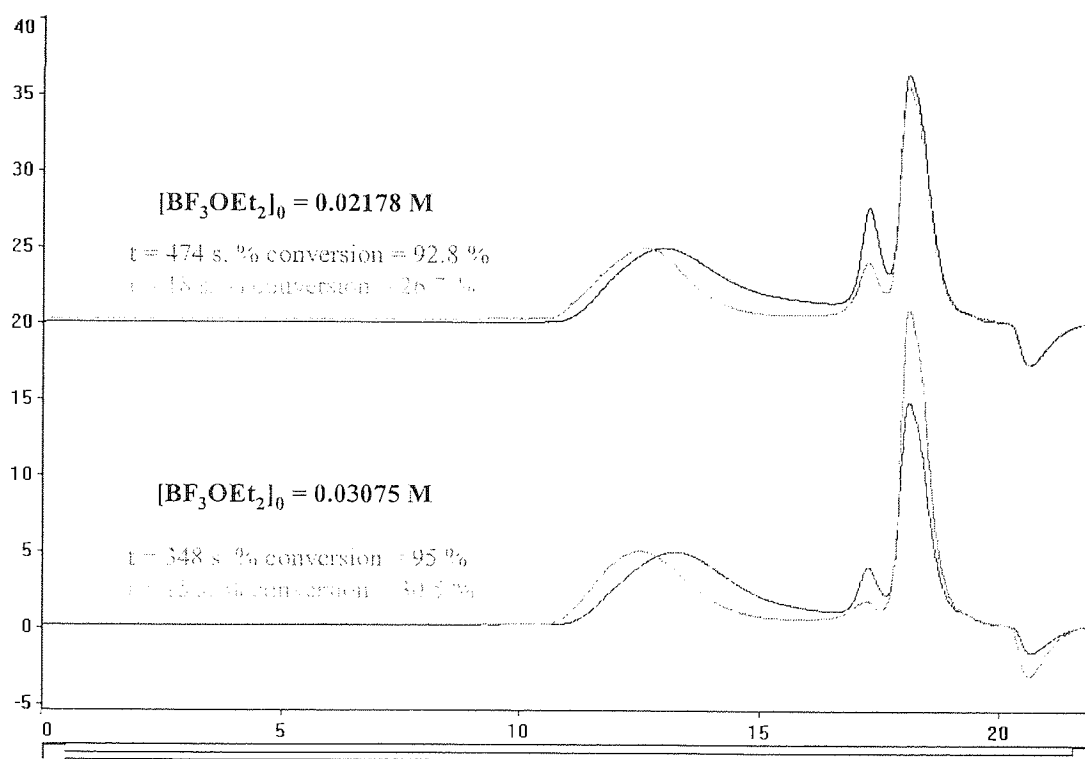
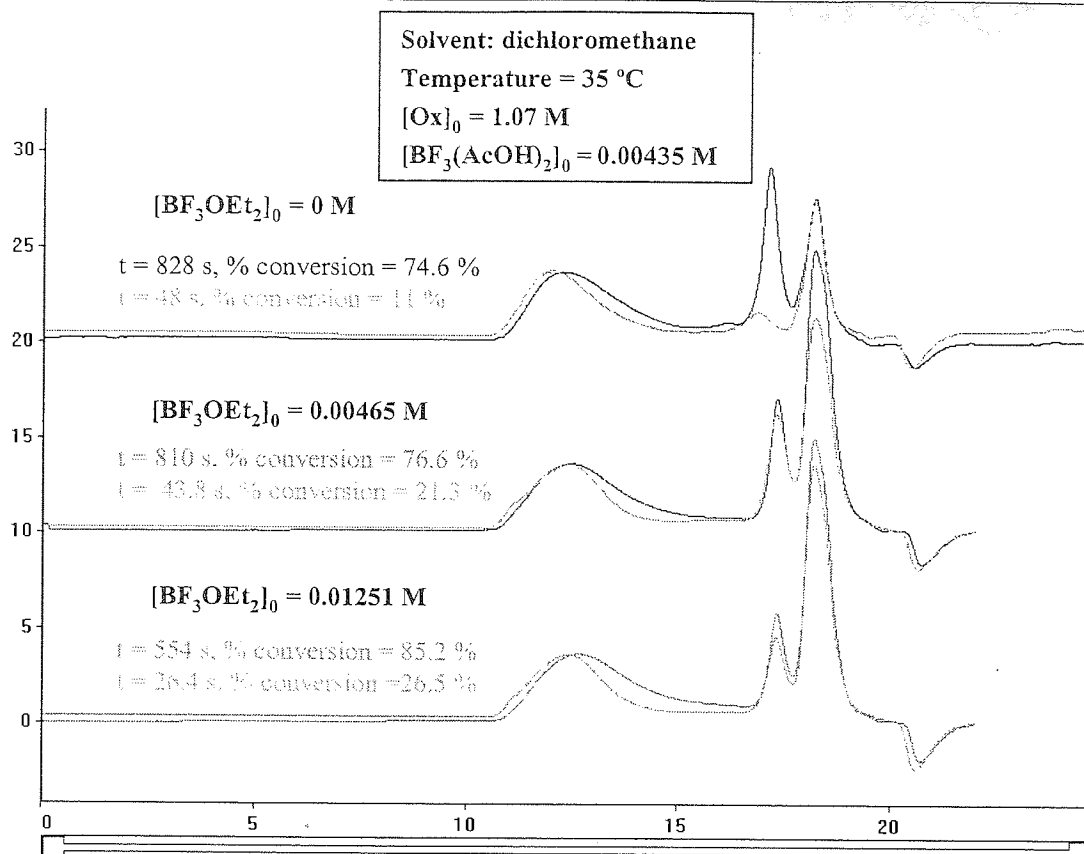
Annex 3. 6: S.E.C chromatogram of polyoxetane materials obtained at high and low monomer conversion for a different concentration of $\text{BF}_3(\text{CH}_3\text{COOH})_2/\text{BF}_3\text{OEt}_2$ (1/1). Polymerisation carried out in dichloromethane at 35 °C. $[\text{Ox}]_0 = 1.07 \text{ M}$ and $0.00171 < [\text{I}]_0 < 0.00739 \text{ M}$ (table 3.2, series S 3.6).



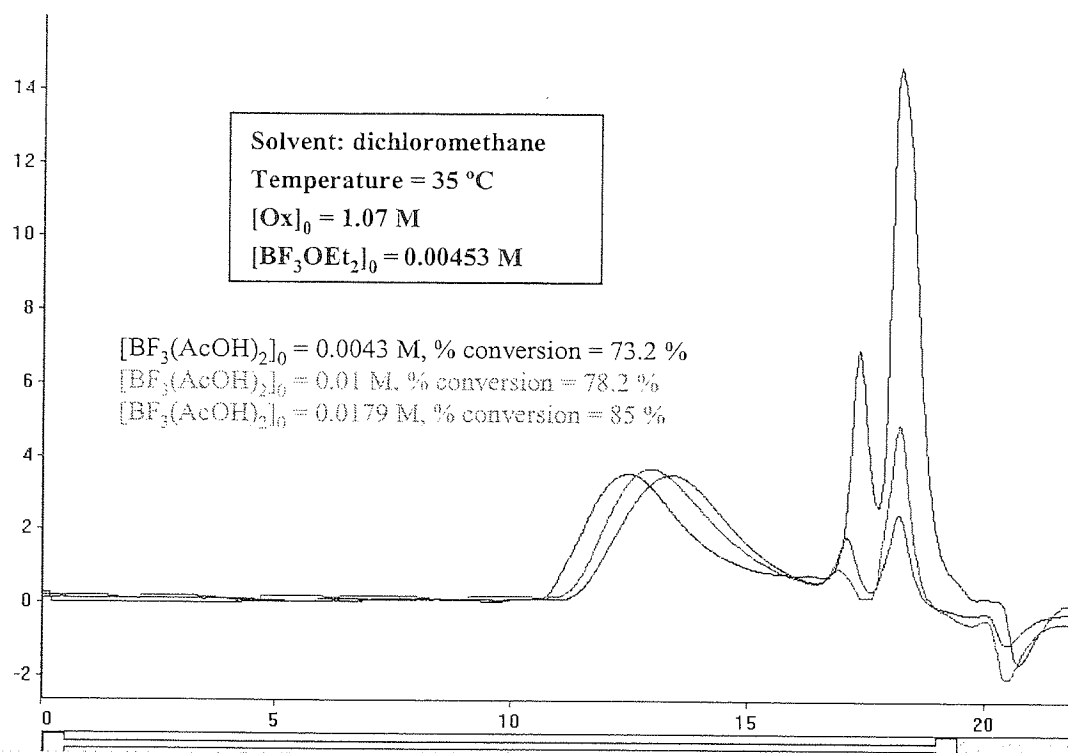
Annex 3. 7: S.E.C chromatogram of polymer obtained at high monomer conversion for a different concentration of $BF_3(CH_3COOH)_2/BF_3OEt_2$ (1/1). Polymerisation carried out in dichloromethane at 35 °C. $[Ox]_0 = 1.07 \text{ M}$ and $0.00171 < [I]_0 < 0.00739 \text{ M}$ (table 3.2, series S 3.6).



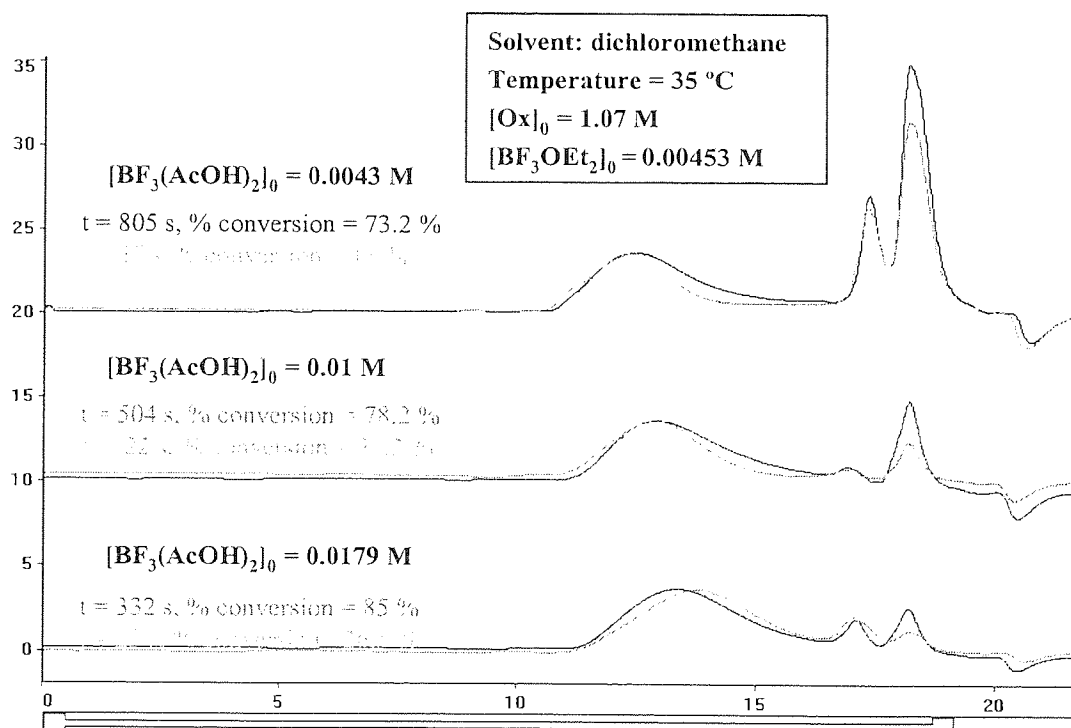
Annex 3. 8: S.E.C chromatogram of polymer obtained at high monomer conversion for a different concentration of BF_3OEt_2 . Polymerisation carried out in dichloromethane at 35 °C. $[Ox]_0 = 1.07 \text{ M}$, $[BF_3(AcOH)_2]_0 = 0.00435 \text{ M}$ and $0.00171 < [BF_3OEt_2]_0 < 0.00739 \text{ M}$ (table 3.2, series S 3.7).



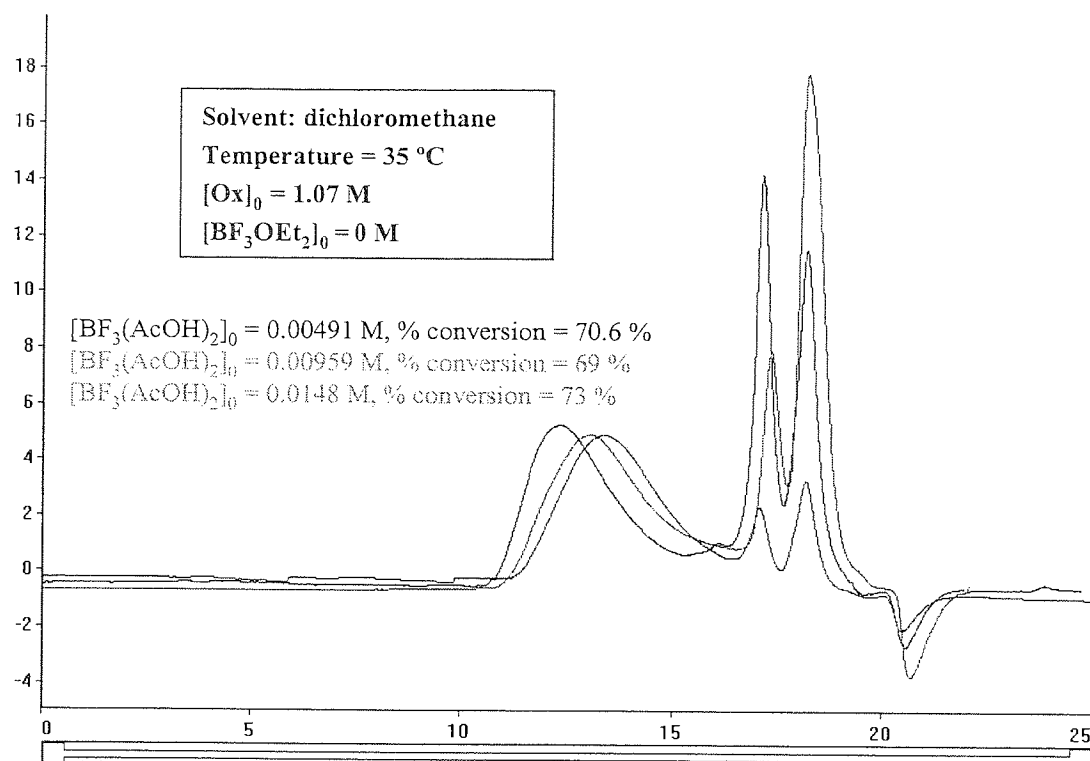
Annex 3. 9: S.E.C chromatogram of polymer obtained at high and low monomer conversion for a different concentration of BF₃OEt₂. Polymerisation carried out in dichloromethane at 35 °C. [Ox]₀ = 1.07 M, [BF₃(AcOH)₂]₀ = 0.00435 M and 0.00171 < [BF₃OEt₂]₀ < 0.00739 M (table 3.2, series S 3.7).



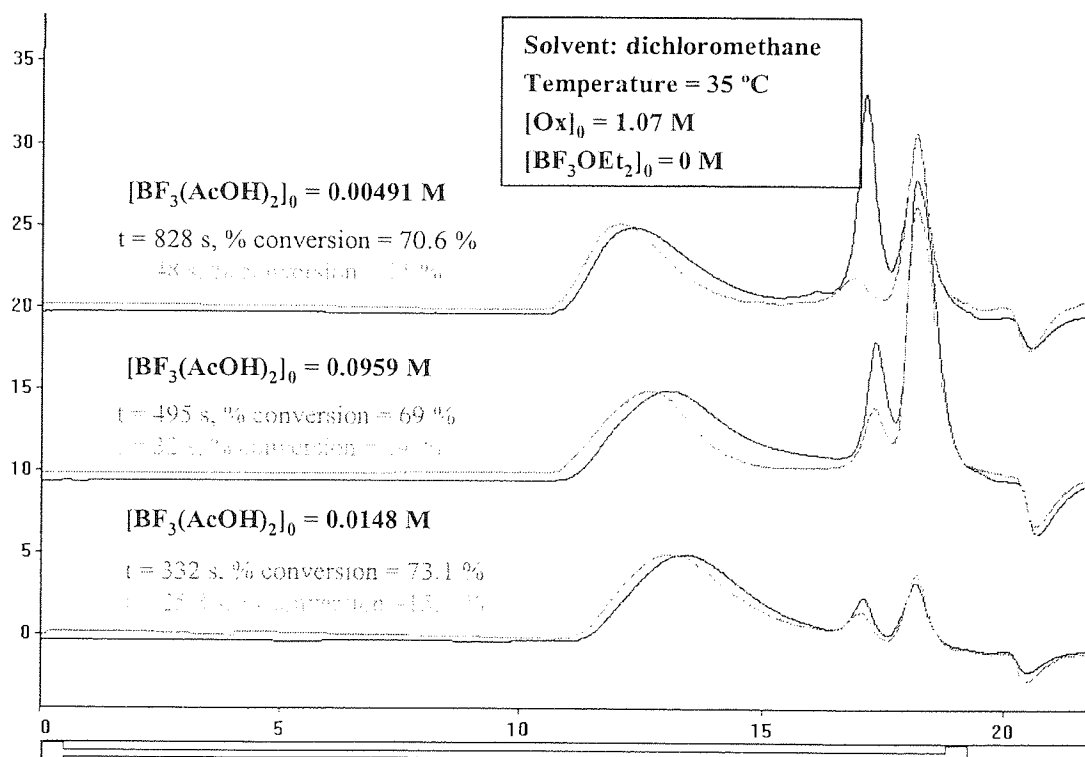
Annex 3. 10: S.E.C chromatogram of polyoxetane materials obtained at high monomer conversion for a different concentration of BF₃(AcOH)₂. Polymerisation carried out in dichloromethane at 35 °C. [Ox]₀ = 1.07 M, [BF₃OEt₂]₀ = 0.00453 M and 0.0043 < [BF₃(AcOH)₂]₀ < 0.00179 M (table 3.2, series S 3.8).



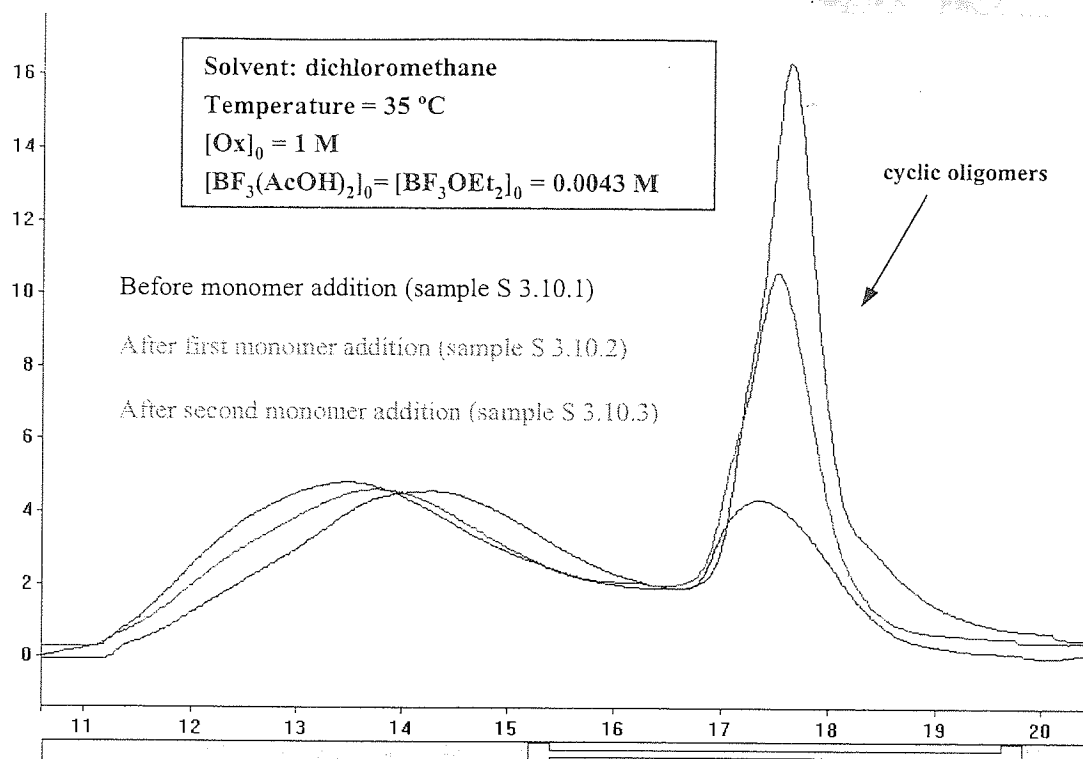
Annex 3. 11: S.E.C chromatogram of polyoxetane materials obtained at high monomer conversion for a different concentration of BF₃(AcOH)₂. Polymerisation carried out in dichloromethane at 35 °C. [Ox]₀ = 1.07 M, [BF₃OEt₂]₀ = 0.00453 M and 0.0043 < [BF₃(AcOH)₂]₀ < 0.00179 M (table 3.2, series S 3.8).



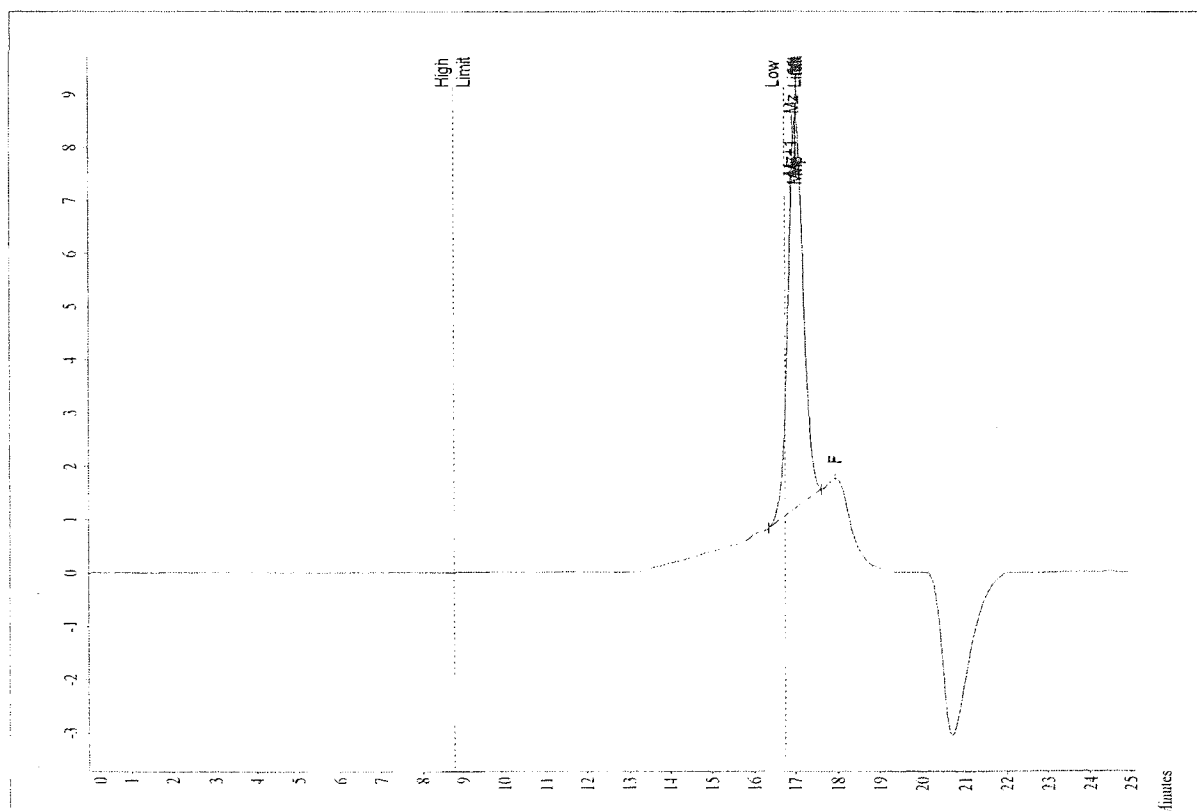
Annex 3. 12: S.E.C chromatogram of polyoxetane materials obtained at high monomer conversion for a different concentration of BF₃(AcOH)₂. Polymerisation carried out in dichloromethane at 35 °C. [Ox]₀ = 1.07 M, [BF₃OEt₂]₀ = 0 M and 0.0145 < [BF₃(AcOH)₂]₀ < 0.00491 M (table 3.2, series S 3.9).



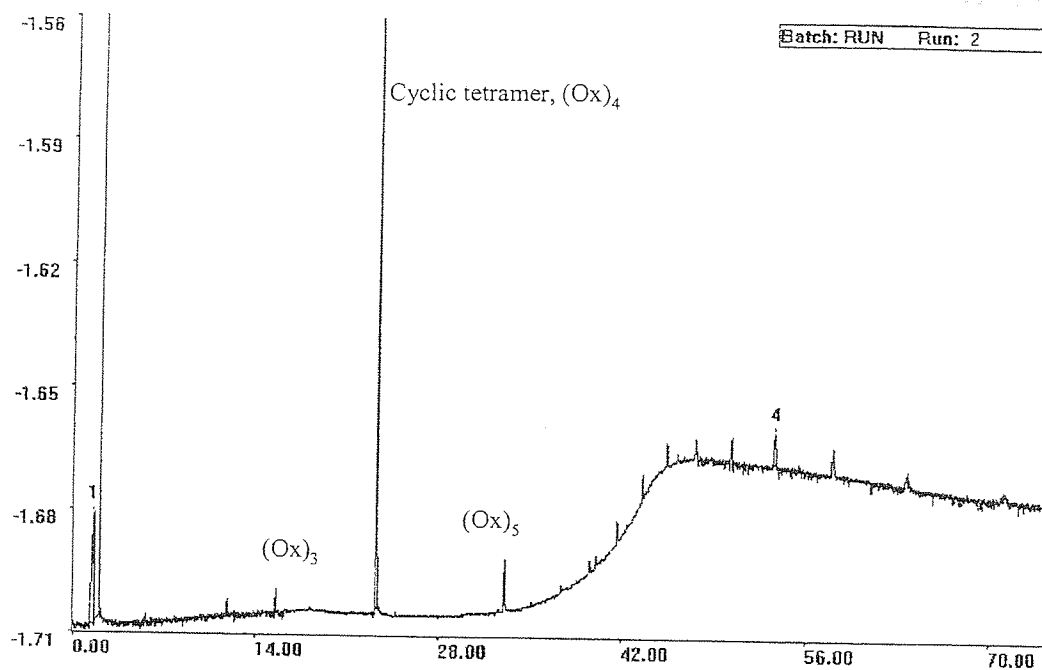
Annex 3. 13: S.E.C chromatogram of polyoxetane materials obtained at high and low monomer conversion for a different concentration of BF₃(AcOH)₂. Polymerisation carried out in dichloromethane at 35 °C. [Ox]₀ = 1.07 M, [BF₃OEt₂]₀ = 0 M and 0.0145 < [BF₃(AcOH)₂]₀ < 0.00491 M (table 3.2, series S 3.9).



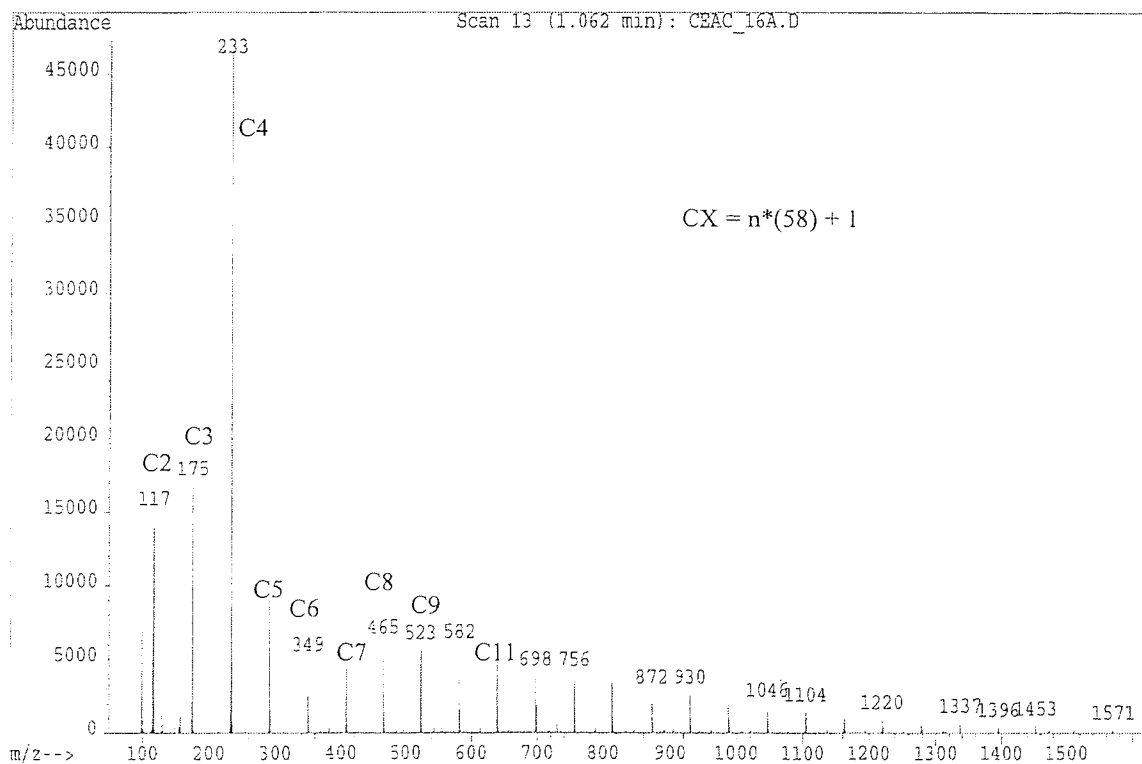
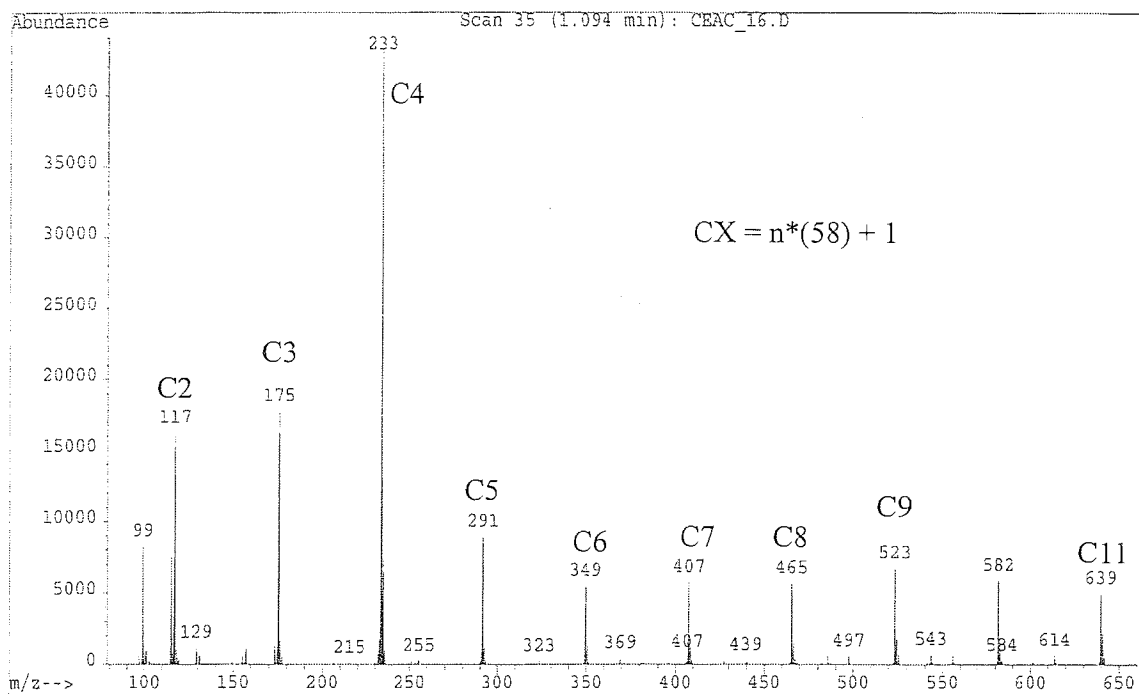
Annex 3. 14: SEC chromatogram of polyoxetane after a tentative of extension of polymer chain length by monomer addition on active polymer solution after full monomer conversion. Polymerisation carried out in dichloromethane at 35 °C (table 3.3, series S 3. 10 and S 3.11).



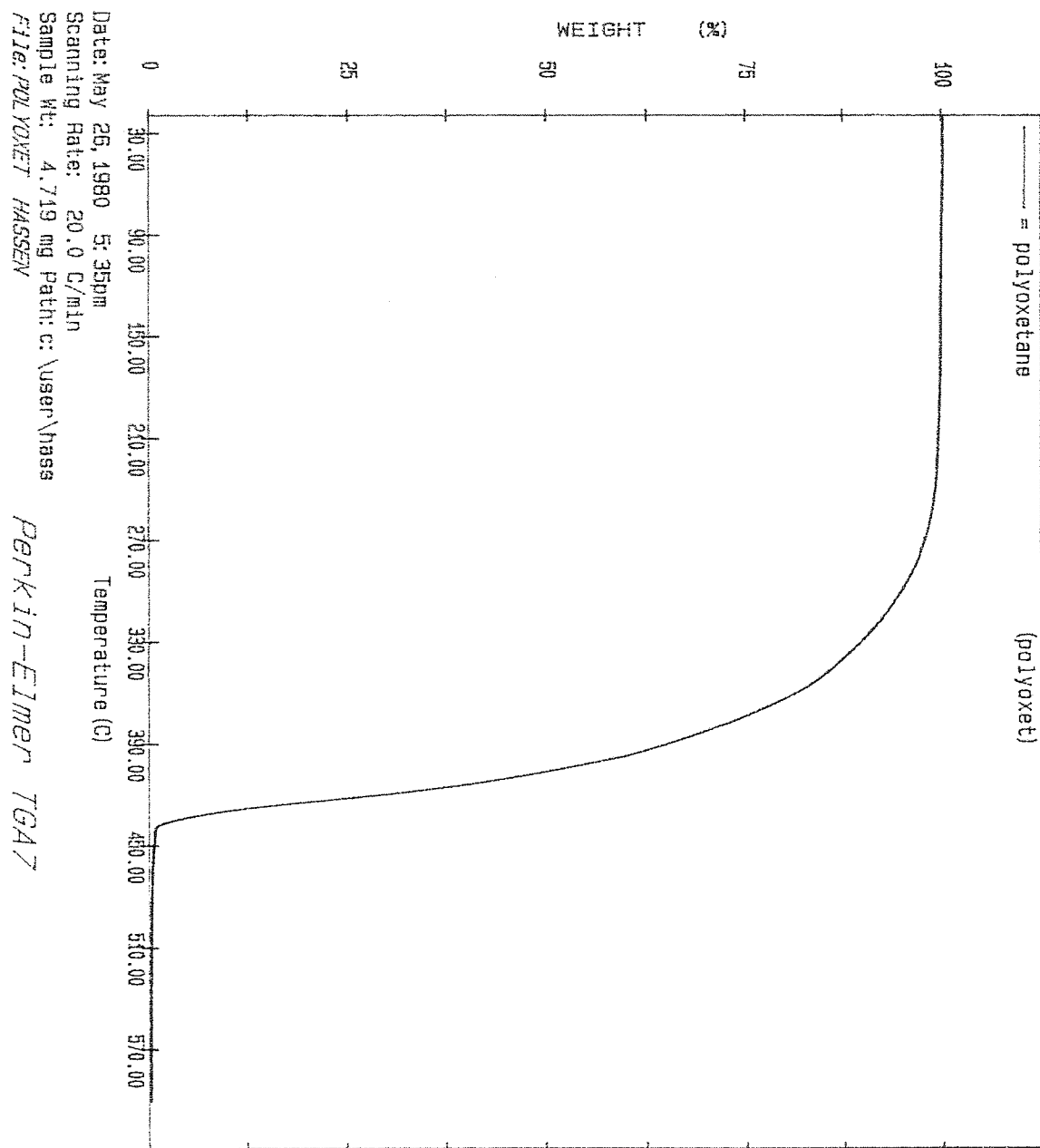
Annex 3. 15: SEC chromatogram of the extracted cyclic oligomers with cyclohexane.



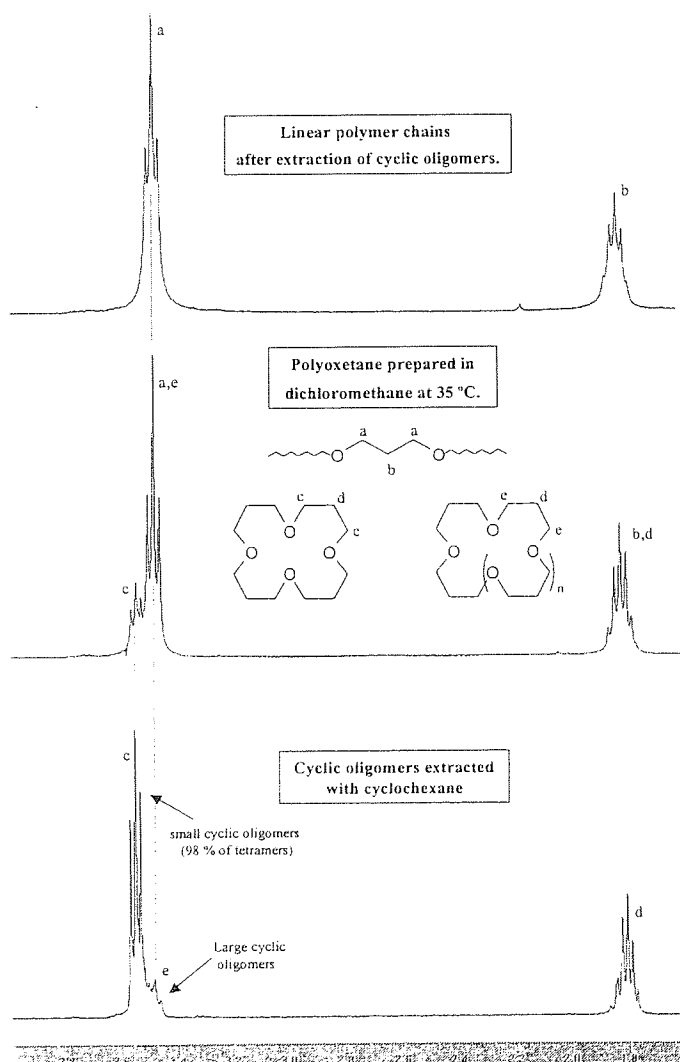
Annex 3. 16: GLC chromatogram of cyclic oligomers extracted with cyclohexane.



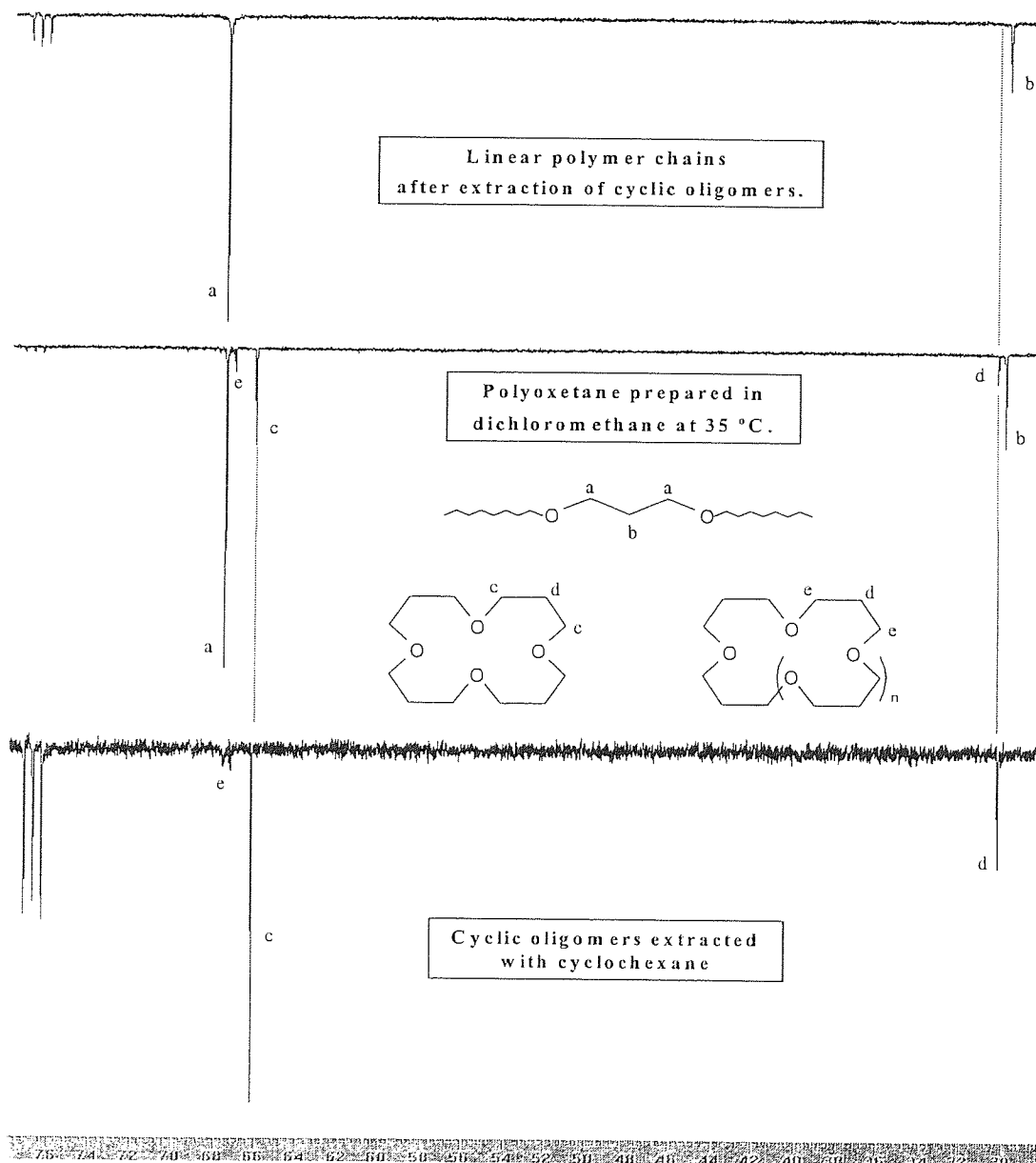
Annex 3. 17: MS of cyclic oligomers extracted with cyclohexane.



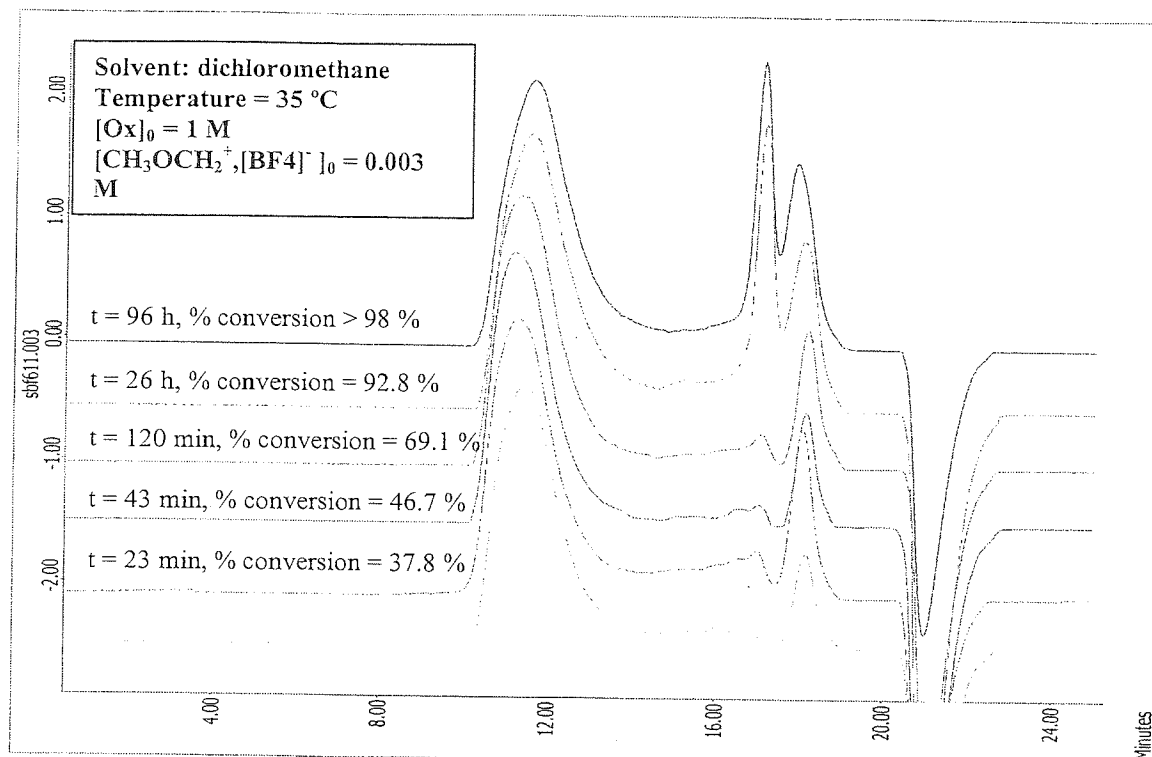
Annex 3. 18: TGA analysis of polyoxetane.



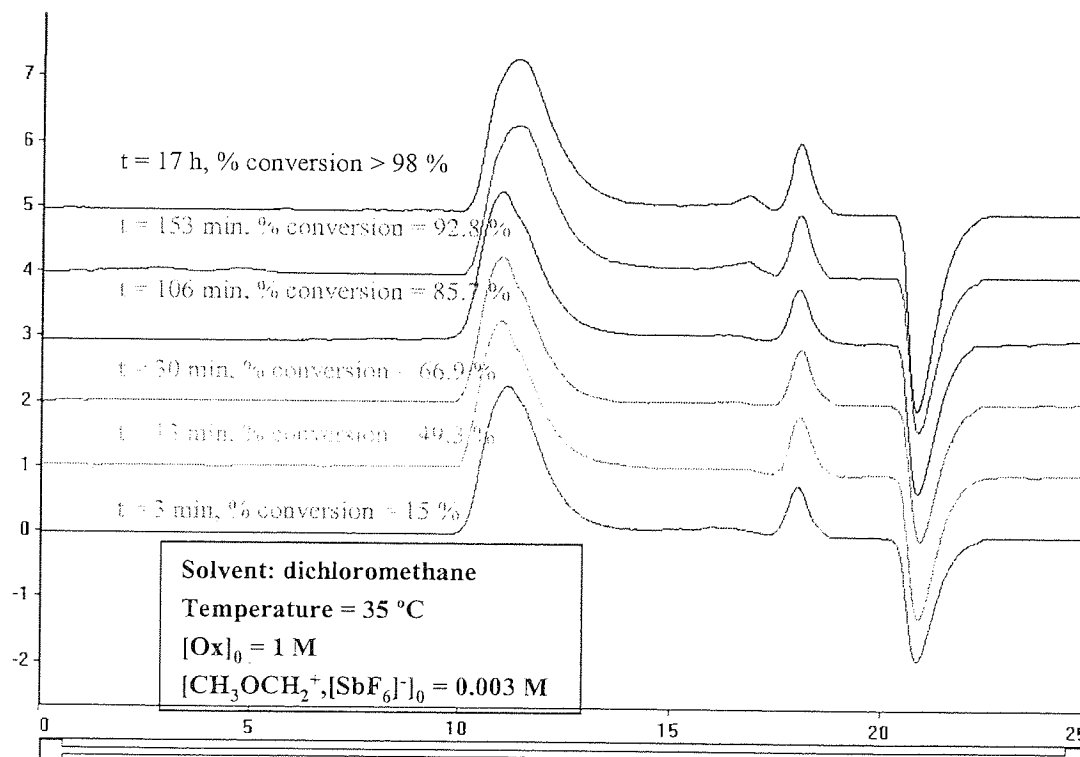
Annex 3. 19: ^1H NMR spectrum of cyclic oligomers extracted with cyclohexane. Polymer prepared in dichloromethane at 35 °C. $[\text{Ox}]_0 = 1 \text{ M}$ and $[\text{BF}_3(\text{AcOH})_2]_0 = [\text{BF}_3(\text{AcOH})_2]_0 = 0.005 \text{ M}$ (table 3.5, series S 3.11.7).



Annex 3. 20: ^{13}C NMR spectrum of cyclic oligomers extracted with cyclohexane. Polymer prepared in dichloromethane at 35 °C. $[\text{Ox}]_0 = 1 \text{ M}$ and $[\text{BF}_3(\text{AcOH})_2]_0 = [\text{BF}_3(\text{AcOH})_2]_0 = 0.005 \text{ M}$ (table 3.5, series S 3.11.7).

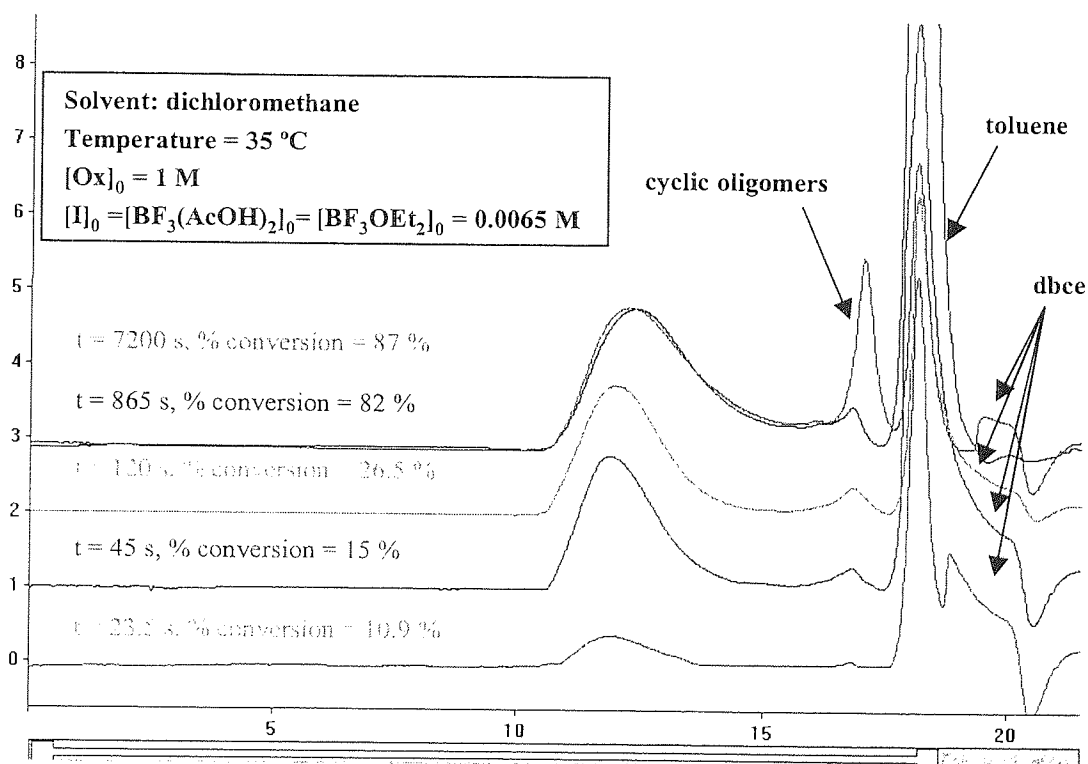


Annex 3. 21: S.E.C chromatogram of polymer obtained at different monomer conversion. Polymerisation carried in dichloromethane at 35°C. $[Ox]_0 = 1 \text{ M}$ and $[CH_3OCH_2^+, [BF_4]^-]_0 = 0.003 \text{ M}$ (table 3.6, series S 3.14).

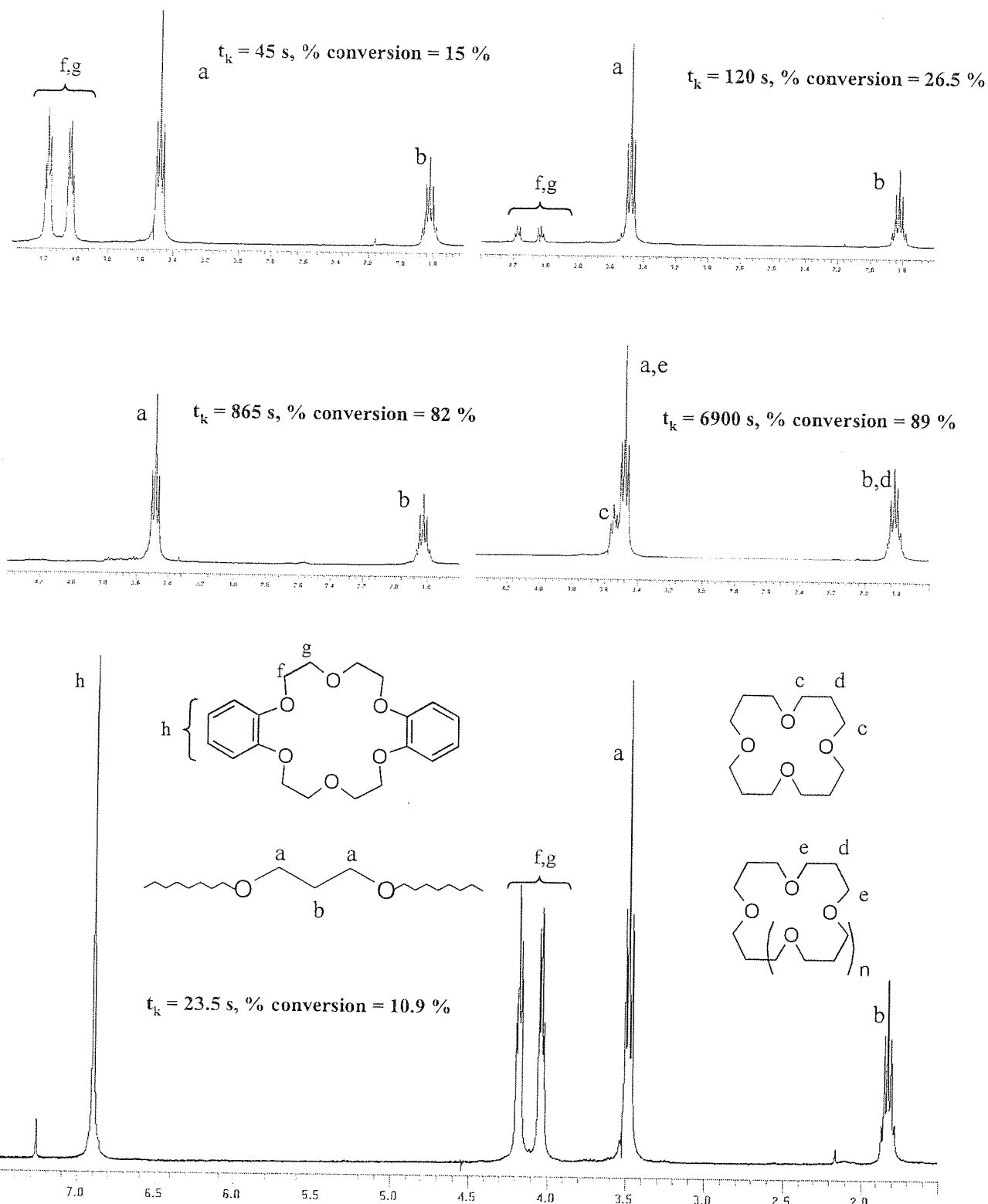


Annex 3. 22: S.E.C chromatogram of polymer obtained at different monomer conversion. Polymerisation carried in dichloromethane at 35°C. $[Ox]_0 = 1 \text{ M}$ and $[CH_3OCH_2^+, [SbF_6]^-]_0 = 0.003 \text{ M}$ (table 3.6, series S 3.15).

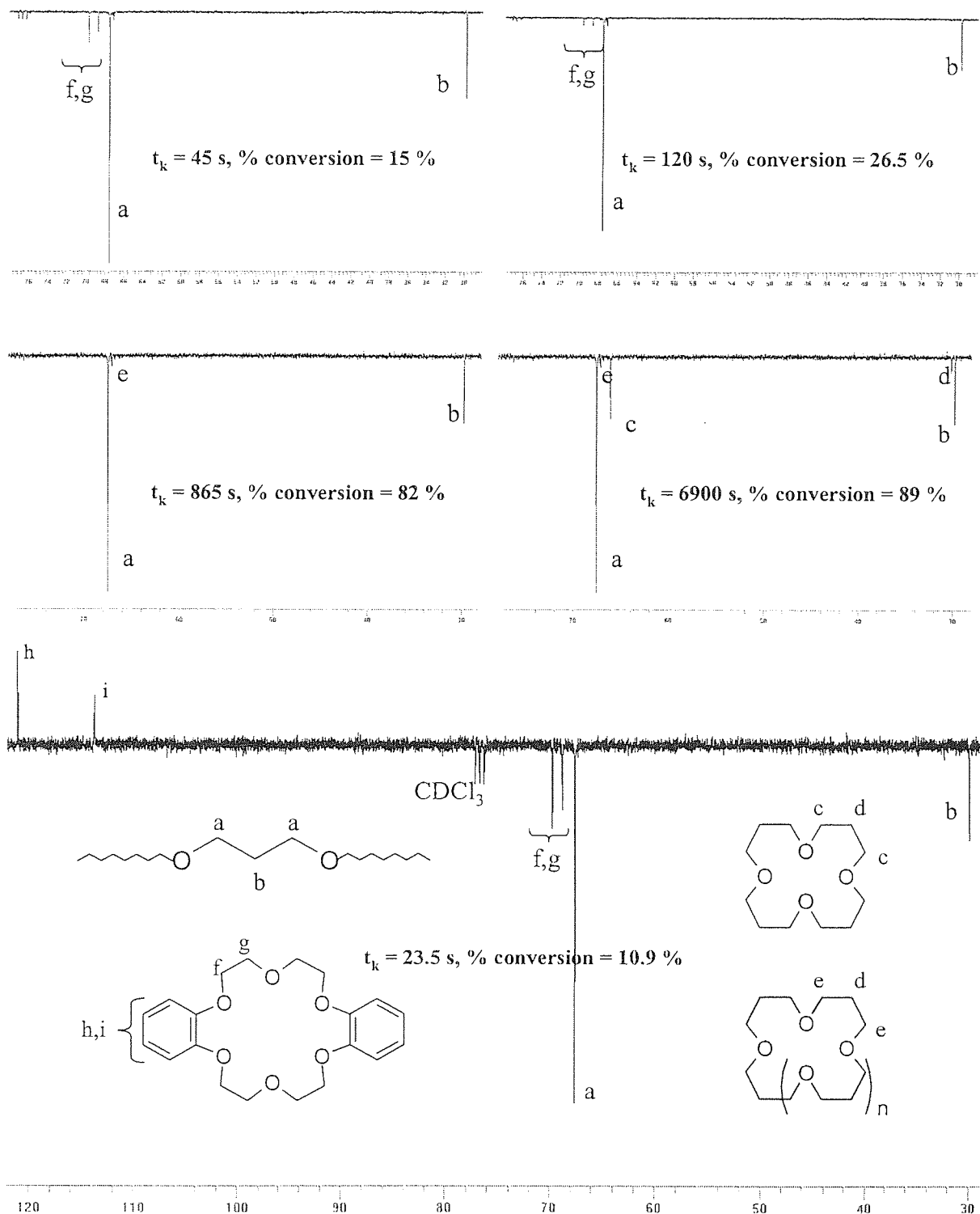
Annex 3. 23: SEC chromatograms of polyoxetane before and after degradation if pH is not neutralised when the polymerisation is terminated.



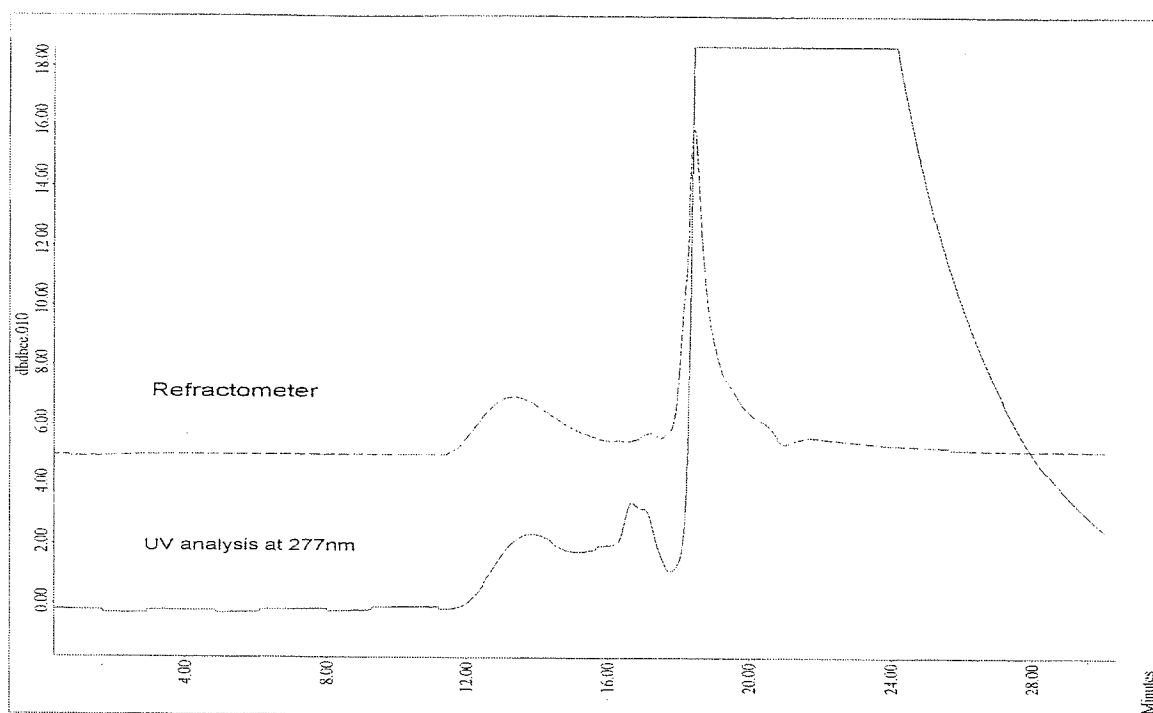
Annex 4. 1: S.E.C chromatogram of polymer obtained at different monomer conversion when dbce is used as co-initiator. Polymerisation carried in dichloromethane at 35°C. $[Ox]_0 = 1 \text{ M}$ and $[BF_3(AcOH)_2]_0 = [BF_3(AcOH)_2]_0 = 0.0065 \text{ M}$ and $[dbce]_0 = 0.1235$ (table 4.1, series S 4.3).



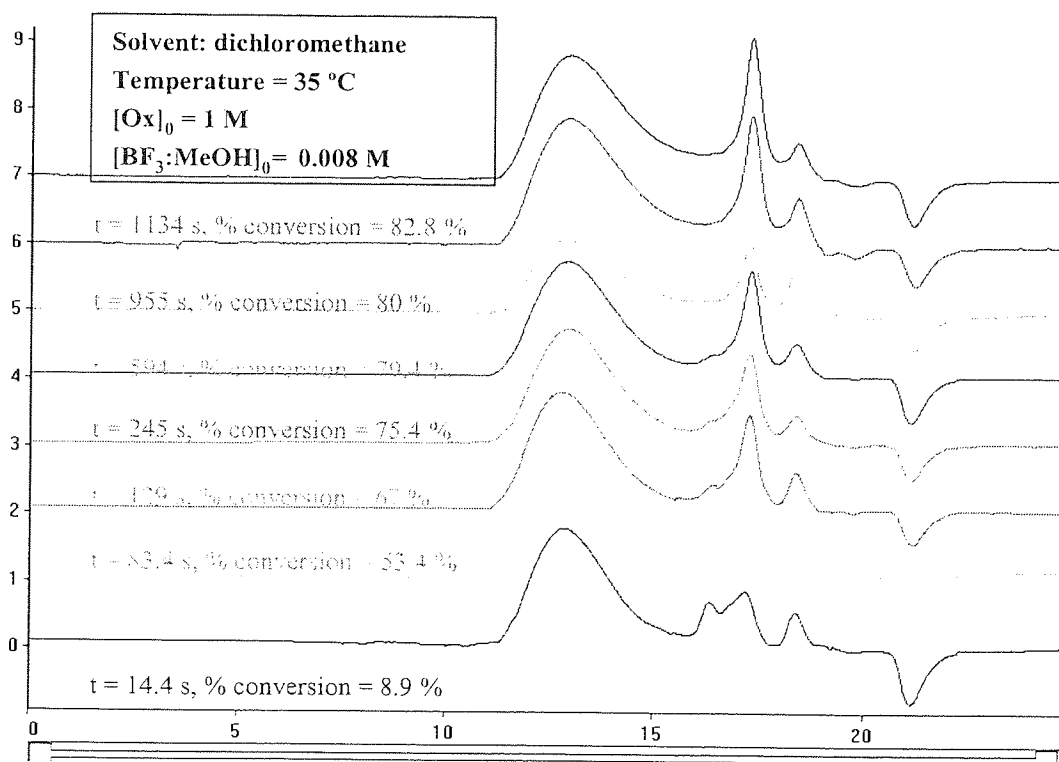
Annex 4. 2: ^1H NMR spectra of polymer obtained at different monomer conversion using dbce as co-initiator. Polymerisation carried in dichloromethane at 35°C . $[\text{Ox}]_0 = 1$ M and $[\text{BF}_3(\text{AcOH})_2]_0 = [\text{BF}_3(\text{AcOH})_2]_0 = 0.0065$ M and $[\text{dbce}]_0 = 0.1235$ (table 4.1, series S 4.3).



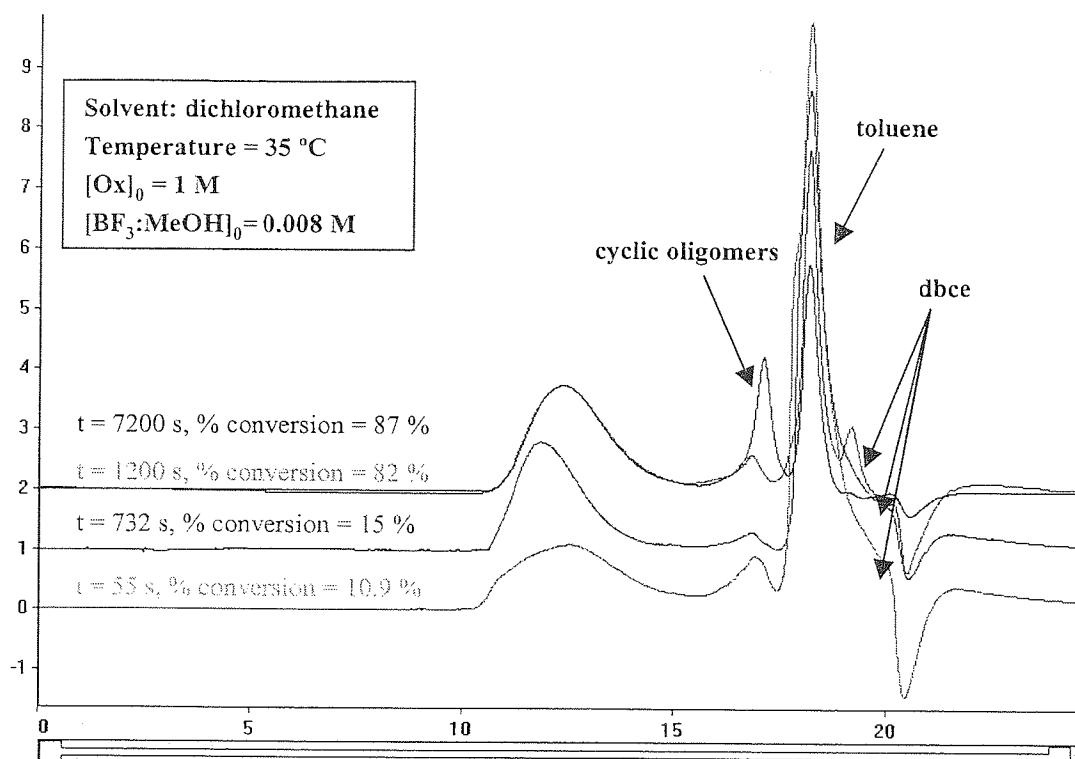
Annex 4. 3: ^{13}C NMR spectra of polymer obtained at different monomer conversion using dbce as co-initiator. Polymerisation carried in dichloromethane at 35°C . $[\text{Ox}]_0 = 1 \text{ M}$ and $[\text{BF}_3(\text{AcOH})_2]_0 = [\text{BF}_3(\text{AcOH})_2]_0 = 0.0065 \text{ M}$ and $[\text{dbce}]_0 = 0.1235$ (table 4.1, series S 4.3).



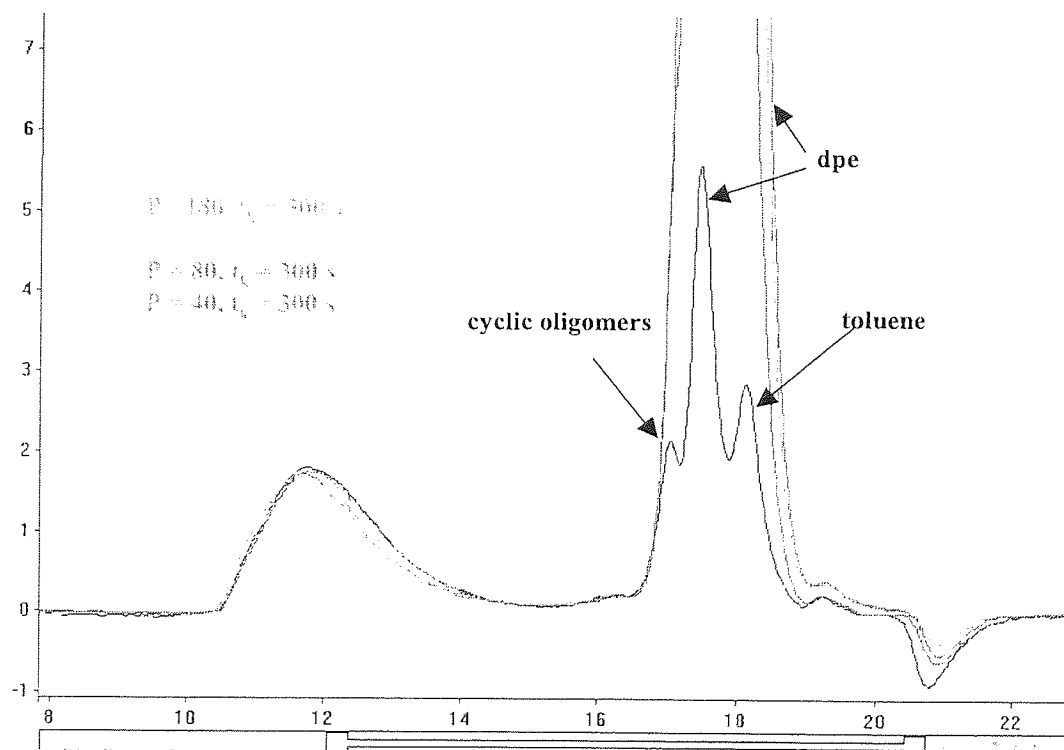
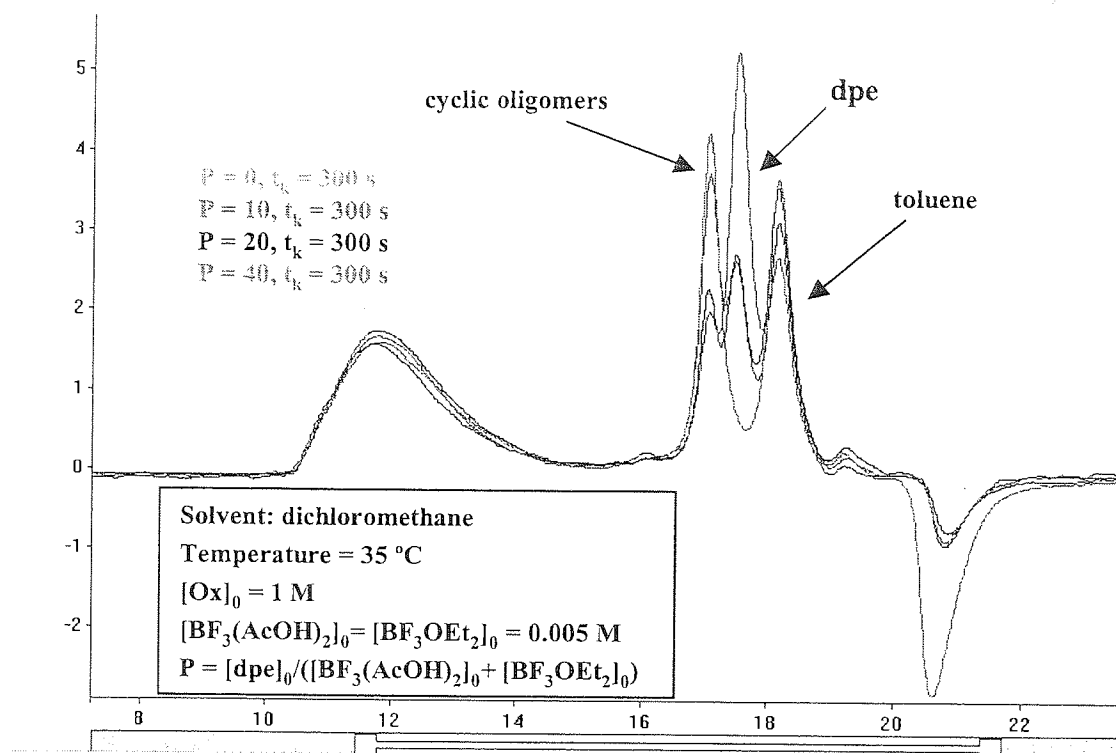
Annex 4. 4: S.E.C chromatogram of poly(oxetane-co-dbce) using UV detector at $\lambda = 277$ nm. Polymerisation carried in dichloromethane at 35°C using dbce as co-initiator. $[\text{Ox}]_0 = 1$ M and $[\text{BF}_3:\text{MeOH}]_0 = 0.008$ M and $[\text{dbce}]_0 = 0.0148$ M (table 4.2, series S 4.5).



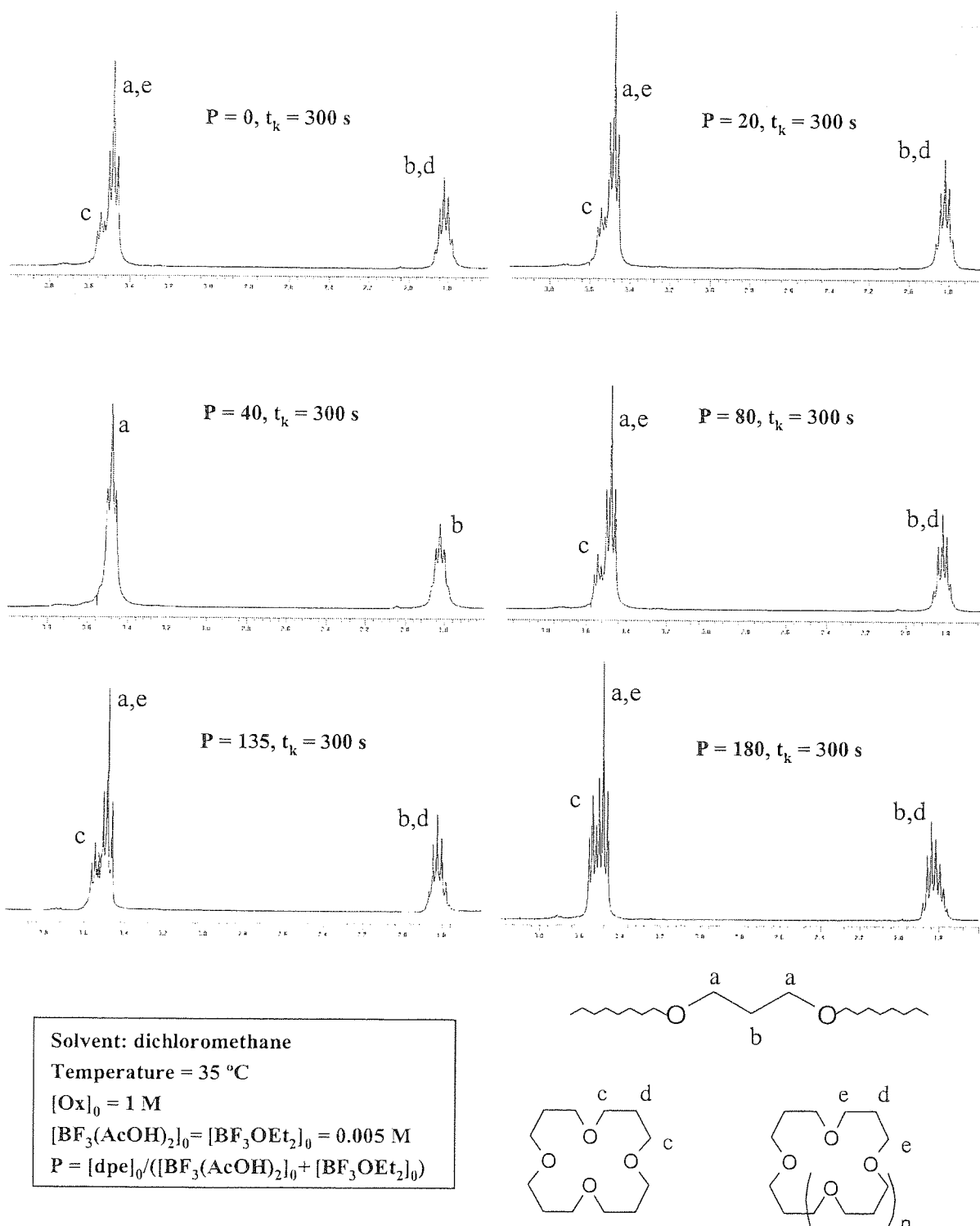
Annex 4. 5: S.E.C chromatogram of polymer obtained at different monomer conversion. Polymerisation carried in dichloromethane at 35°C . $[\text{Ox}]_0 = 1$ M and $[\text{BF}_3:\text{MeOH}]_0 = 0.008$ M (table 4.2, series S 4.4).



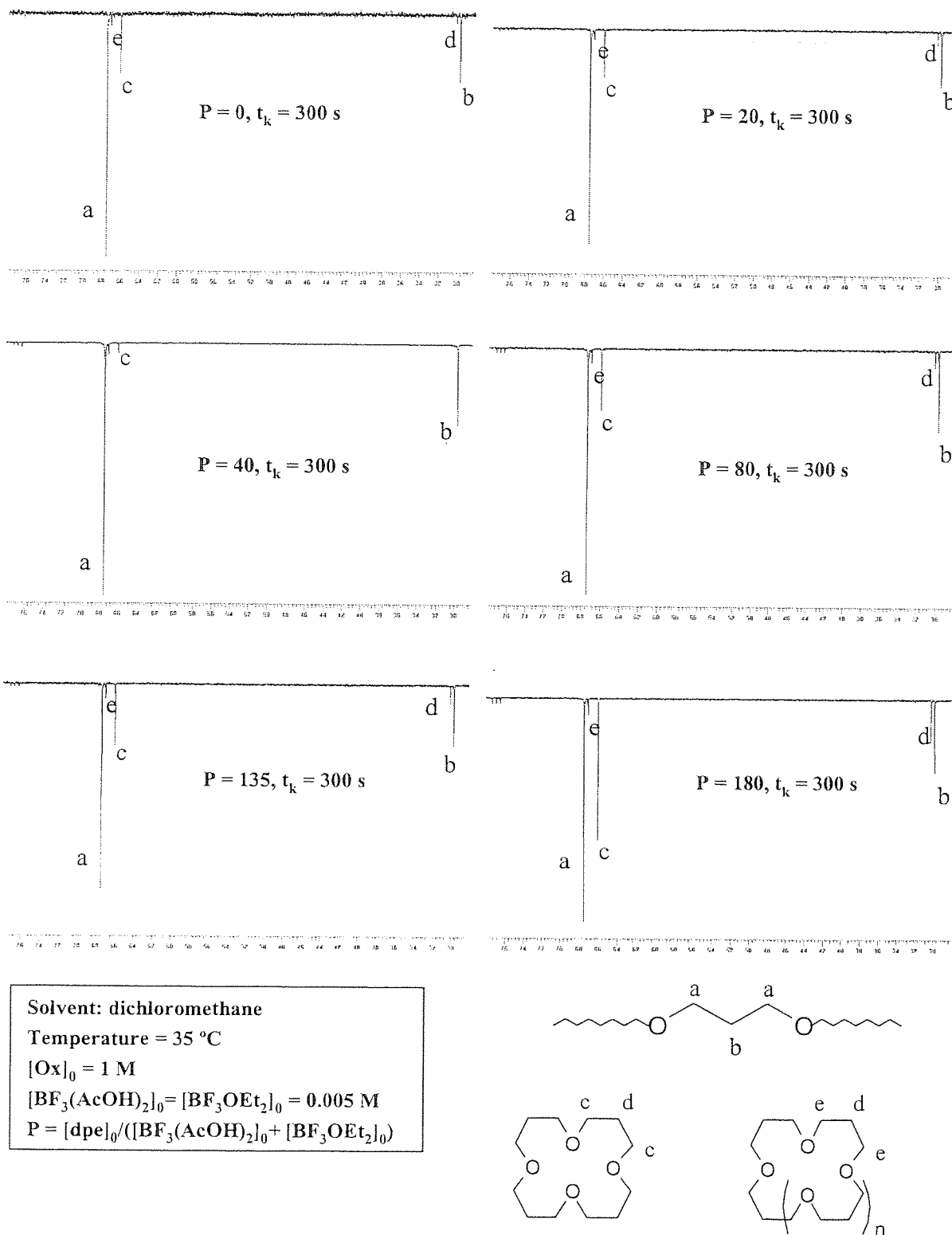
Annex 4. 6: S.E.C chromatogram of polymer obtained at different monomer conversion using dbce as co-initiator. Polymerisation carried in dichloromethane at 35°C. [Ox]₀ = 1 M and [BF₃:MeOH]₀ = 0.008 M and [dbce]₀ = 0.0148 M (table 4.2, series S 4.5).



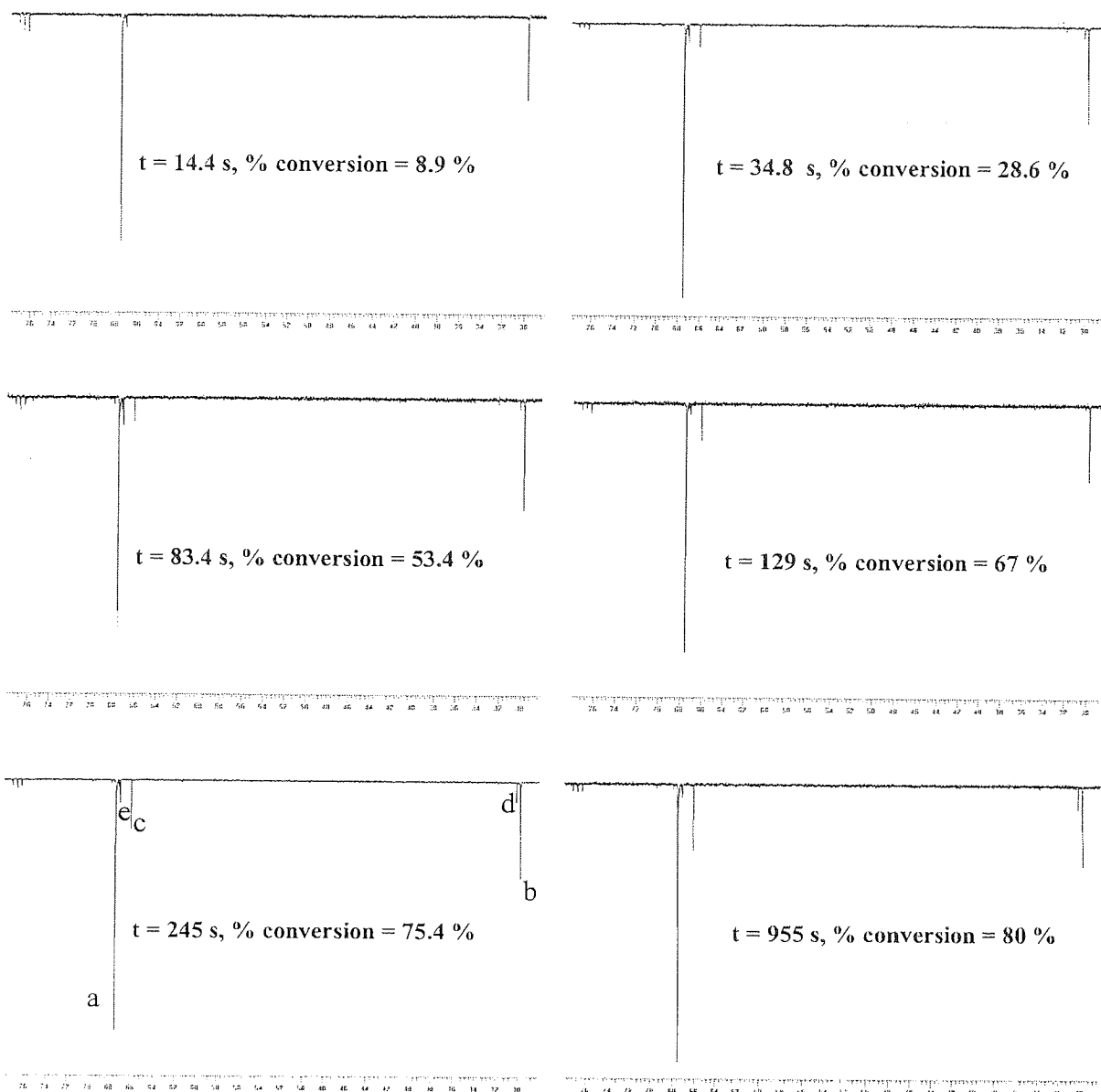
Annex 4. 7: S.E.C chromatogram of polymer obtained at various concentration of dpe. Polymerisation carried in dichloromethane at 35°C. $[\text{Ox}]_0 = 1 \text{ M}$ and $[\text{BF}_3:\text{MeOH}]_0 = 0.008 \text{ M}$ and $0.05 < [\text{dpe}]_0 < 0.9 \text{ M}$ (table 4.5, series S 4.8).



Annex 4. 8: ^1H NMR spectra of polymer obtained at various concentration of dpe. Polymerisation carried in dichloromethane at 35°C. Polymerisation carried in dichloromethane at 35°C. $[\text{Ox}]_0 = 1 \text{ M}$ and $[\text{BF}_3:\text{MeOH}]_0 = 0.008 \text{ M}$ and $0.05 < [\text{dpe}]_0 < 0.9 \text{ M}$ (table 4.5, series S 4.8).



Annex 4. 9: ^{13}C NMR spectra of polymer obtained at various concentration of dpe in dichloromethane at 35°C. $[Ox]_0 = 1 \text{ M}$ and $[BF_3 \cdot MeOH]_0 = 0.008 \text{ M}$ and $0.05 < [dpe]_0 < 0.9 \text{ M}$ (table 4.5, series S 4.8).

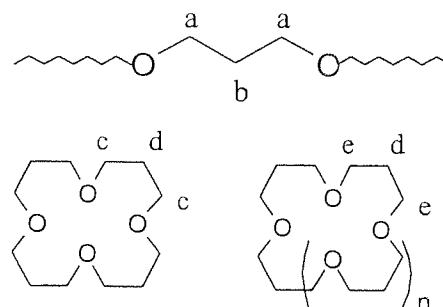


Solvent: dichloromethane

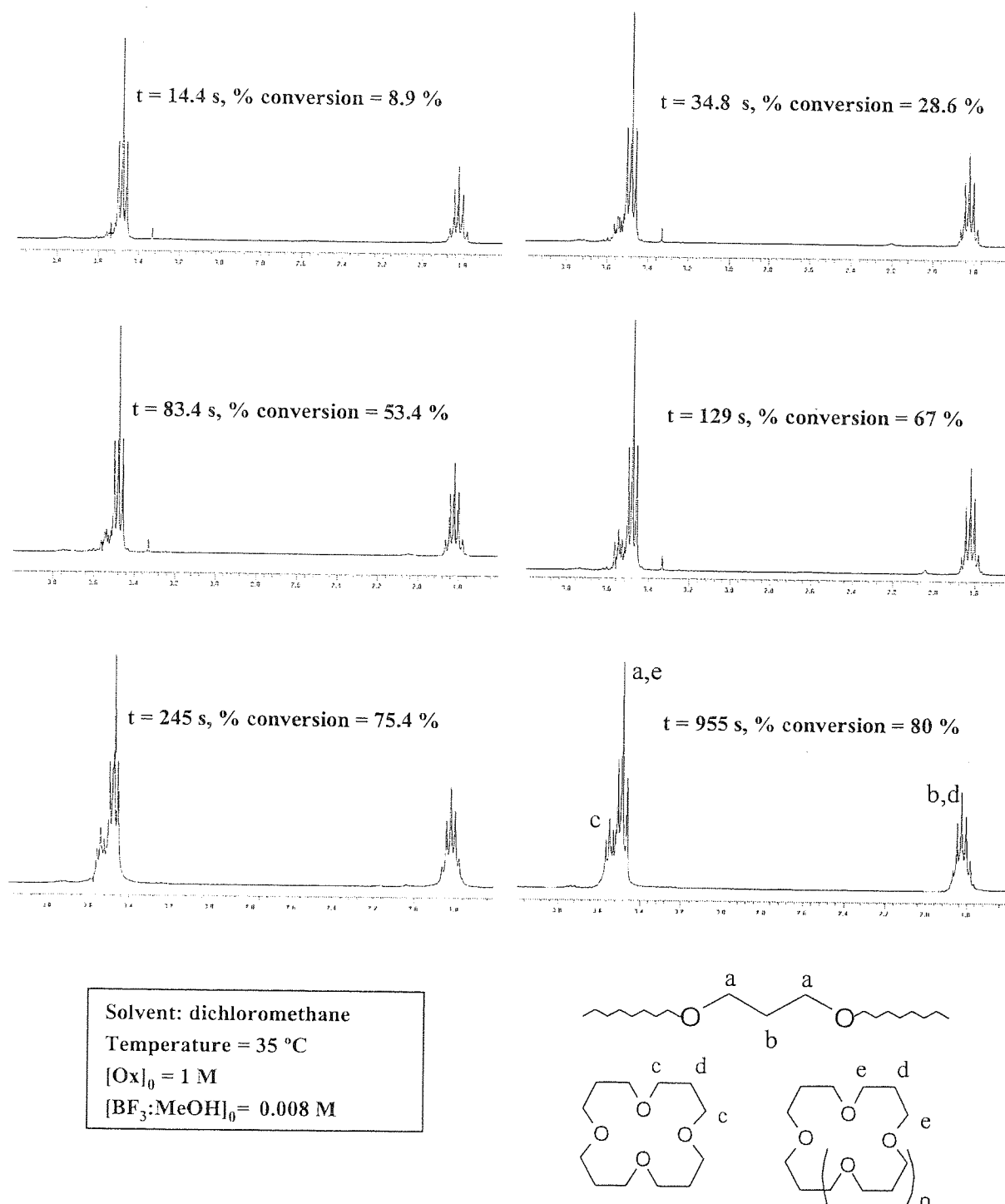
Temperature = 35 °C

$[\text{Ox}]_0 = 1 \text{ M}$

$[\text{BF}_3 \cdot \text{MeOH}]_0 = 0.008 \text{ M}$

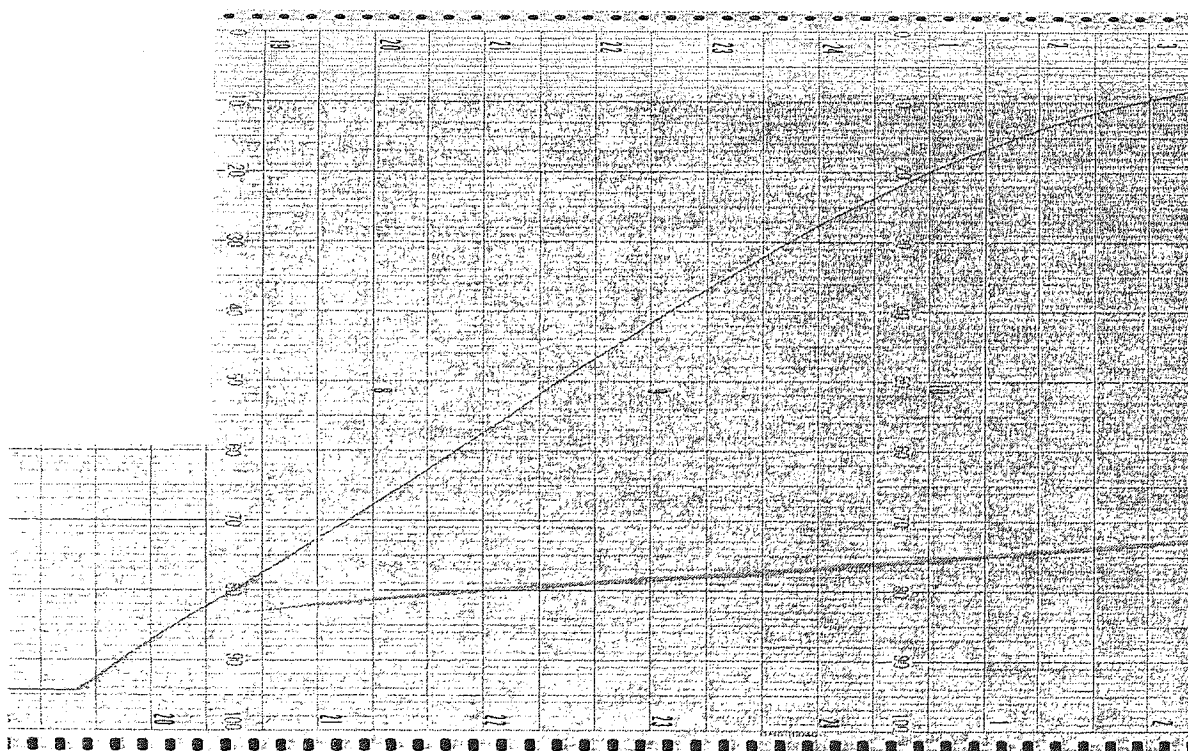


Annex 5.1 : ^{13}C NMR spectra of polymer obtained throughout the polymerisation in dichloromethane at 35°C. $[\text{Ox}]_0 = 1 \text{ M}$ and $[\text{BF}_3 \cdot \text{MeOH}]_0 = 0.008 \text{ M}$. Table 4.4 and 5.4, series S 4.4.

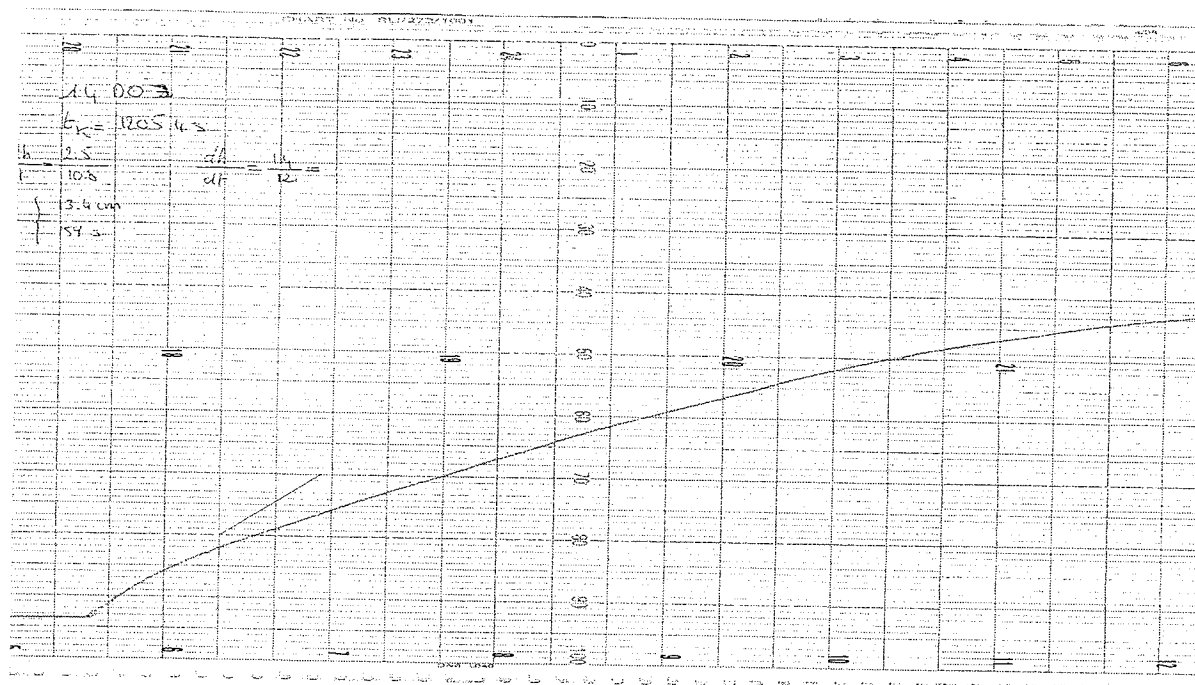


Annex 5. 2: ^1H NMR spectra of polymer obtained throughout the polymerisation in dichloromethane at 35°C. $[\text{Ox}]_0 = 1 \text{ M}$ and $[\text{BF}_3 \cdot \text{MeOH}]_0 = 0.008 \text{ M}$. Table 4.4 and 5.4, series S 4.4.

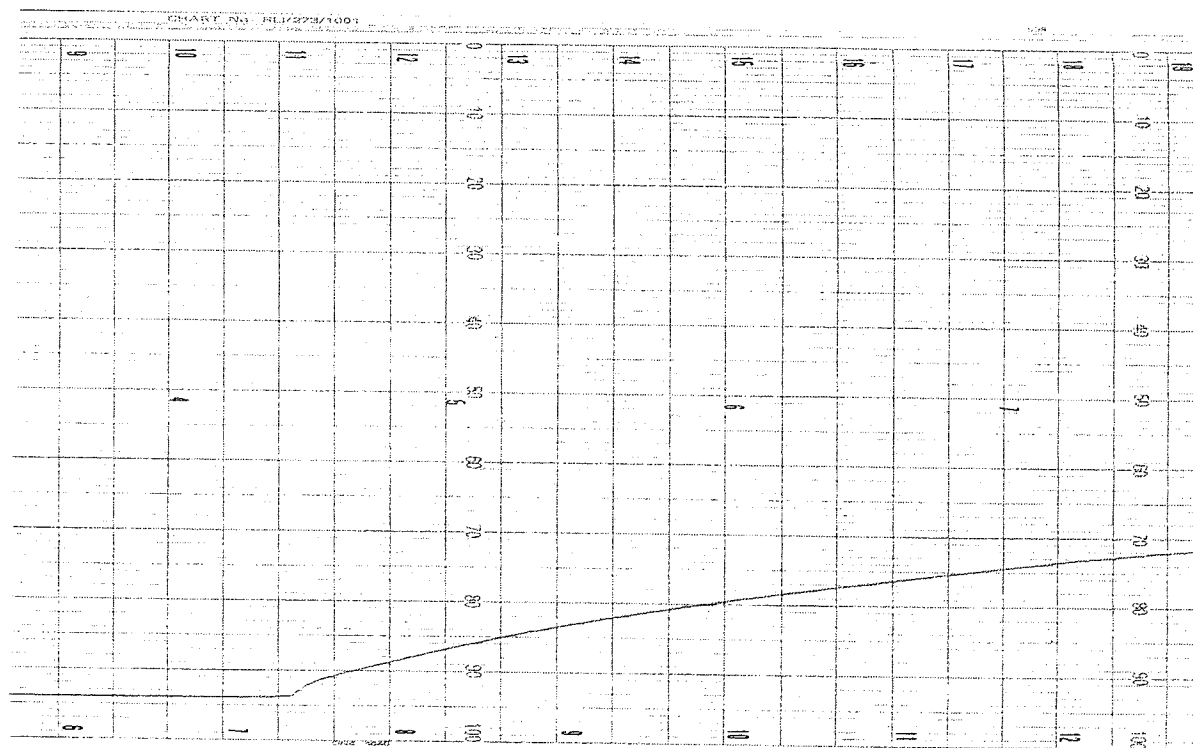
Annex 5. 3: SEC chromatogram of polyoxetane after a tentative of extension of polymer chain length by monomer addition on active polymer solution after full monomer conversion. Polymerisation carried out in dichloromethane at 35 °C. (table 5.2, series S 5. 1).



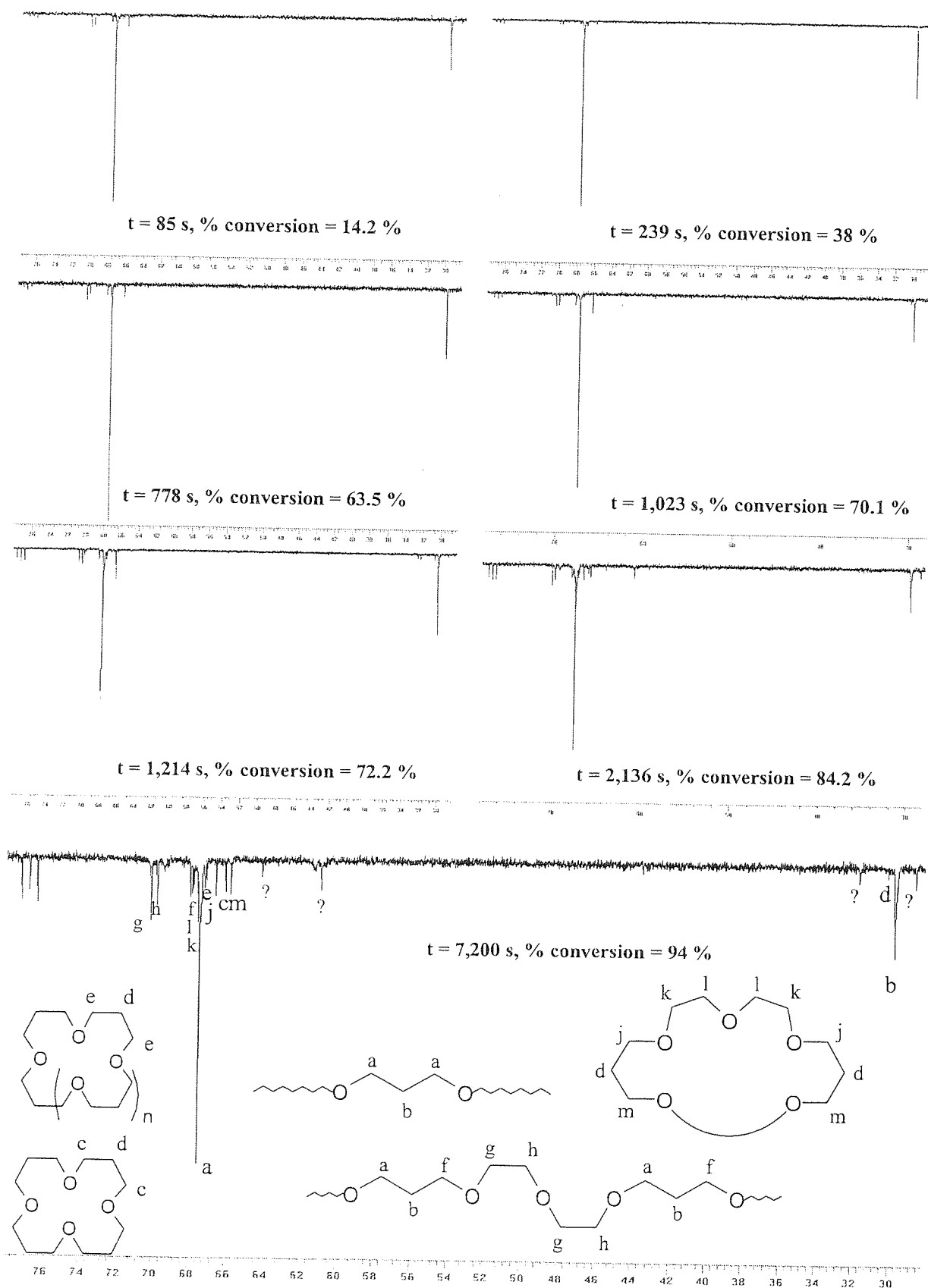
Annex 5. 4: Calorimetric analysis. Trace of deflection temperature against time when the polymerisation of oxetane proceeds in dichloromethane at 35 °C. $[Ox] = 1\text{ M}$ and $[BF_3MeOH] = 0.0077\text{ M}$.



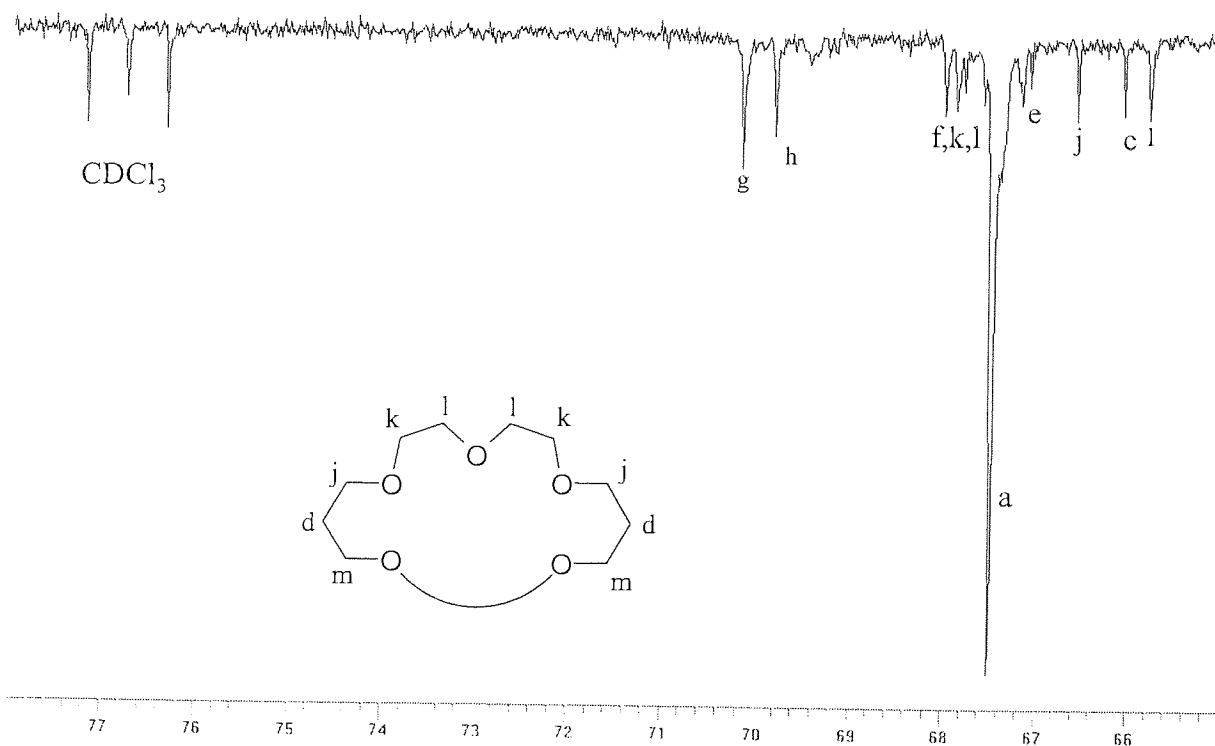
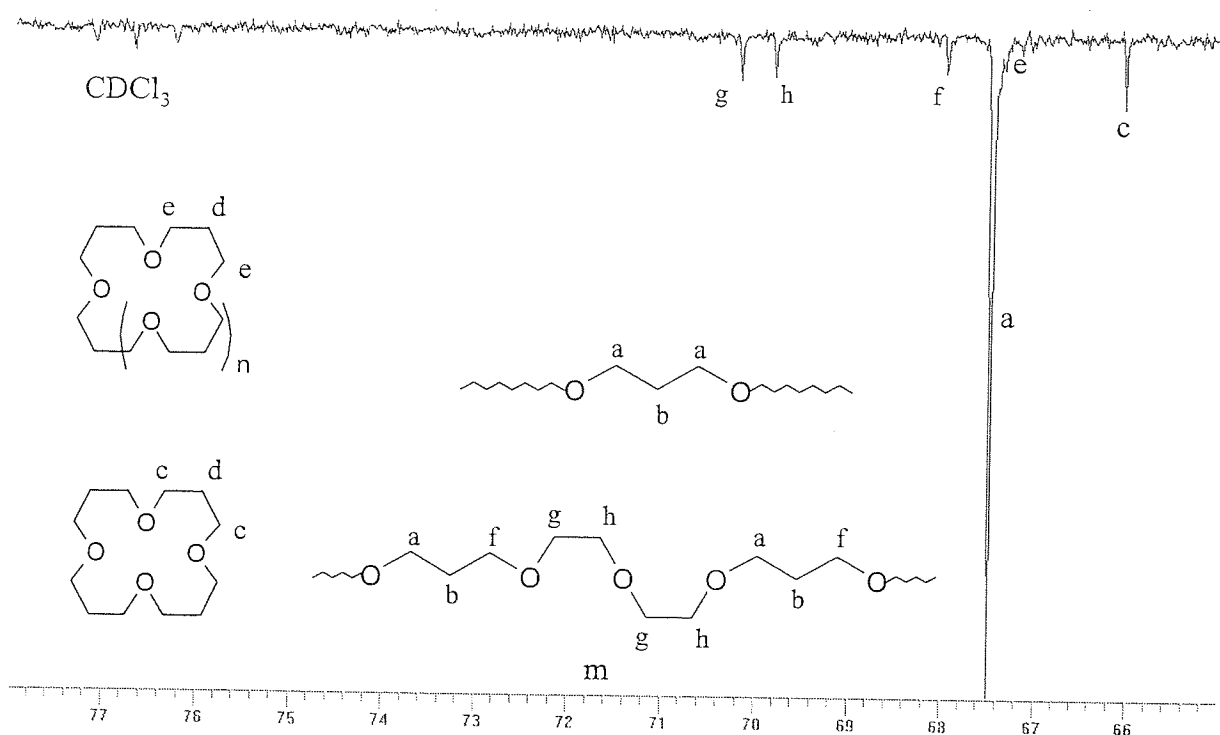
Annex 5. 5: Calorimetric analysis. Trace of deflection temperature against time when the polymerisation of oxetane proceeds in 1,4-dioxane at 35 °C. $[Ox] = 1$ M, $[Dox]/[Ox] = 9.45$ and $[BF_3MeOH] = 0.0077$ M.



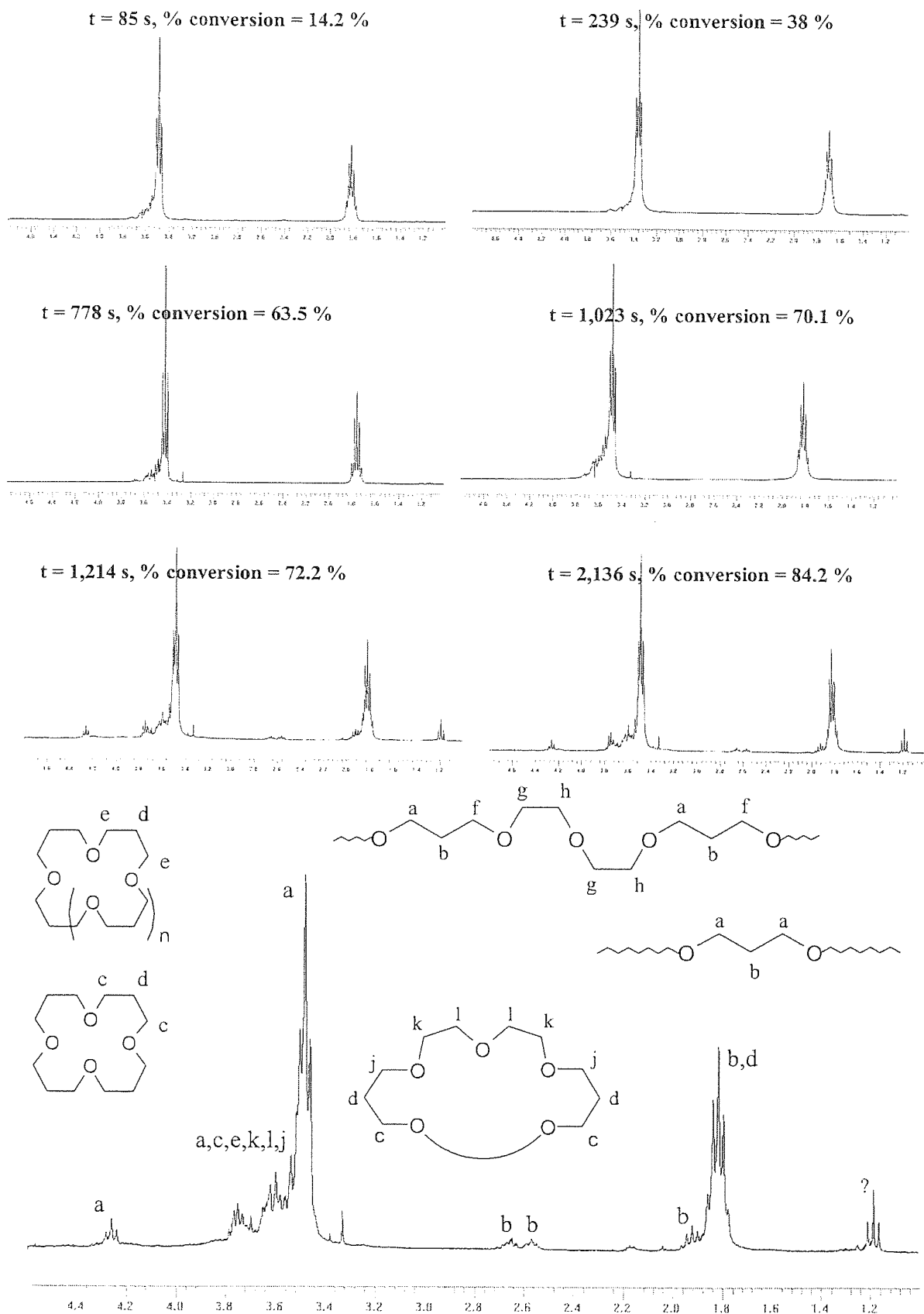
Annex 5. 6: Calorimetric analysis. Trace of deflection temperature against time when the polymerisation of oxetane proceeds in 1,4-dioxane at 35 °C. $[Ox] = 0.66$ M, $[Dox]/[Ox] = 15.95$ and $[BF_3MeOH] = 0.0077$ M.



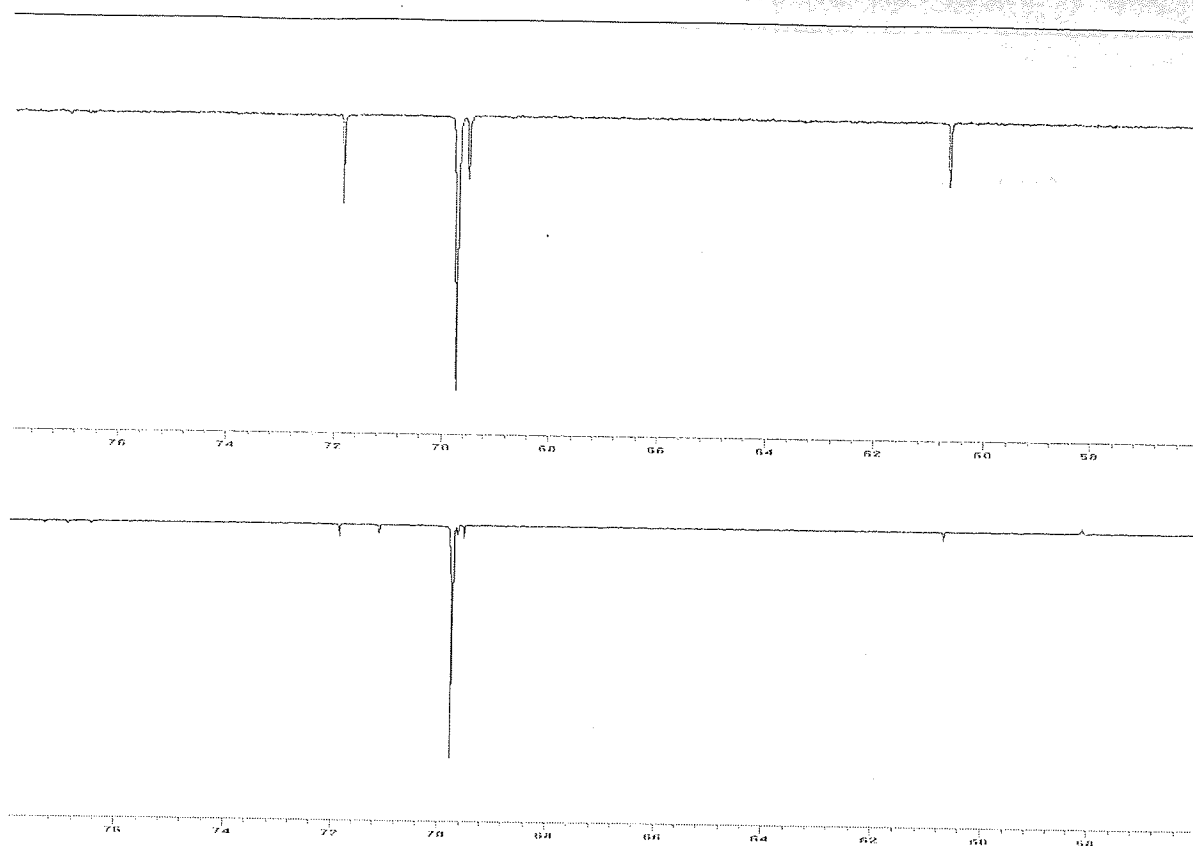
Annex 5. 7: ^{13}C NMR spectra of polymer obtained throughout the polymerisation in 1,4-dioxane at 35°C . $[\text{Ox}]_0 = 1 \text{ M}$, $[\text{BF}_3:\text{MeOH}]_0 = 0.0077 \text{ M}$ and $[\text{Dox}]/[\text{Ox}] = 9.45$. Table 5.4 series S 5.2.



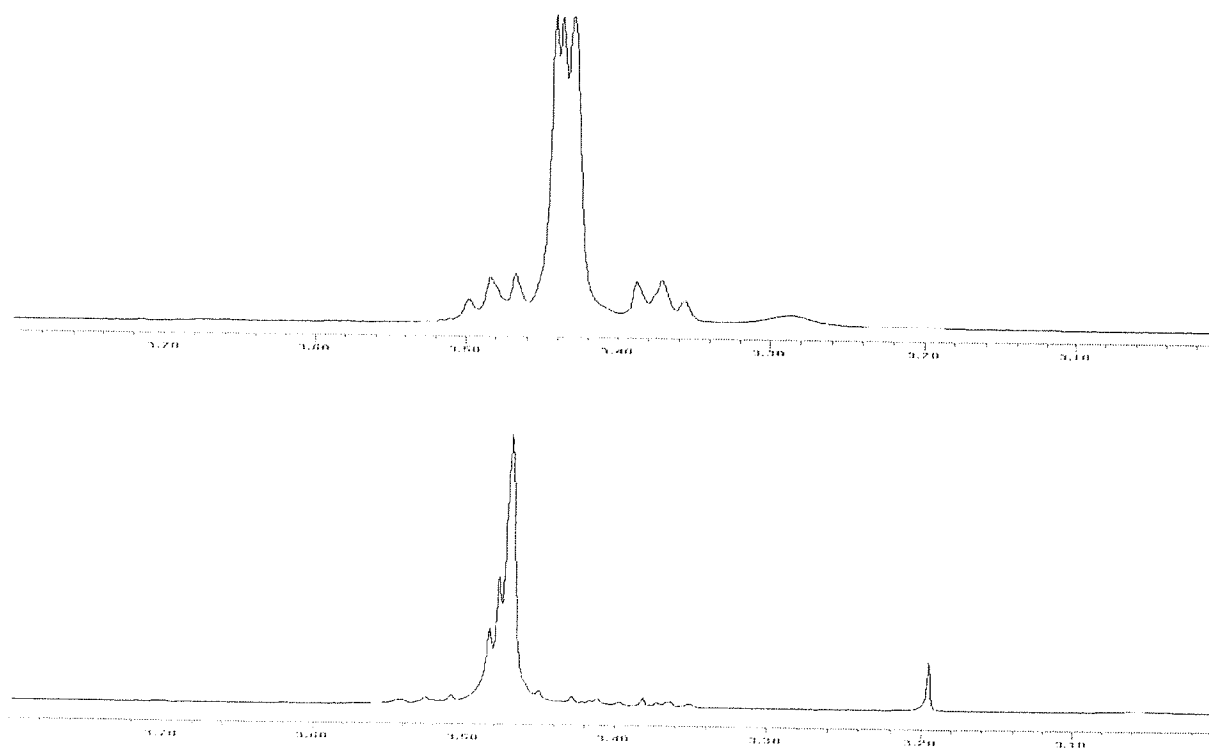
Annex 5. 8: ^{13}C NMR spectra of polymer obtained throughout the polymerisation in 1,4-dioxane at 35°C . $[\text{Ox}]_0 = 1 \text{ M}$, $[\text{BF}_3:\text{MeOH}]_0 = 0.0077 \text{ M}$ and $[\text{Dox}]/[\text{Ox}] = 9.45$. Table 5.4 series S 5.2.



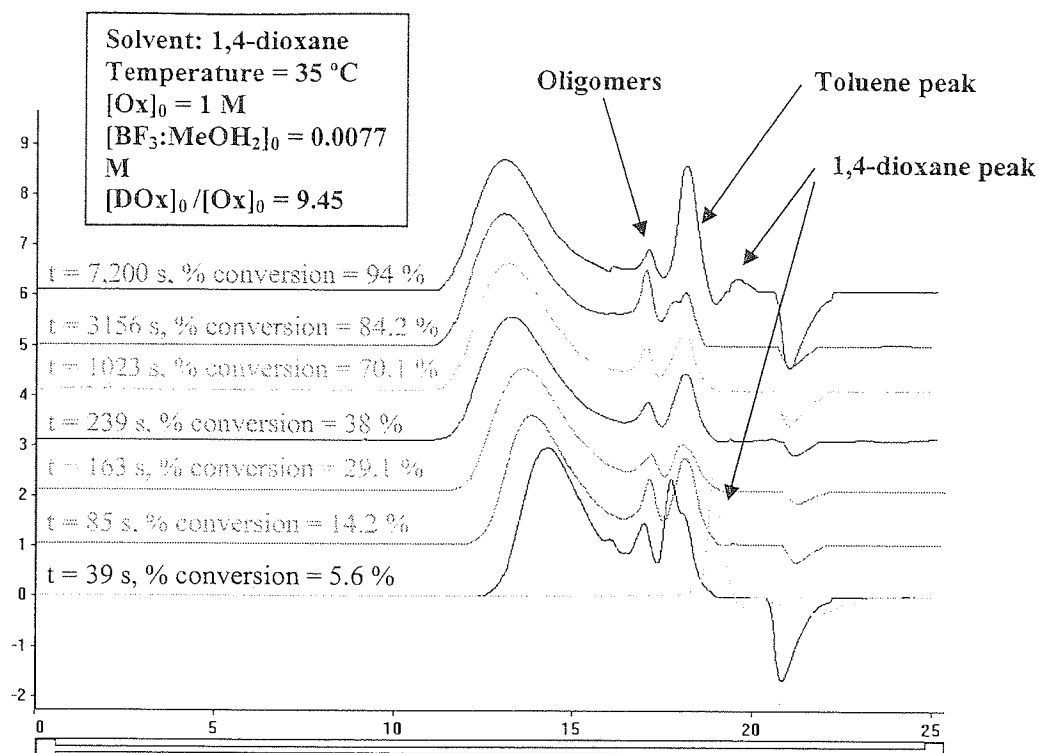
Annex 5. 9: ^1H NMR spectra of polymer obtained throughout the polymerisation in 1,4-dioxane at 35°C . $[\text{Ox}]_0 = 1 \text{ M}$, $[\text{BF}_3 \cdot \text{MeOH}]_0 = 0.0077 \text{ M}$ and $[\text{Dox}]/[\text{Ox}] = 9.45$. Table 5.4 series S 5.2.



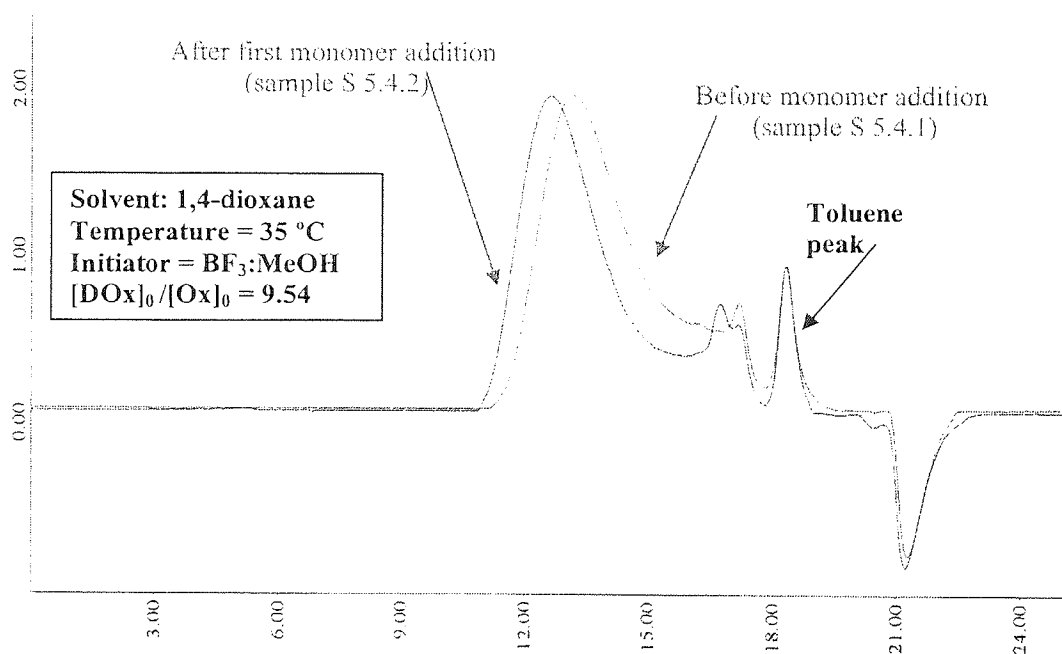
Annex 5. 10: ^{13}C NMR spectrum of poly(ethylene oxide).



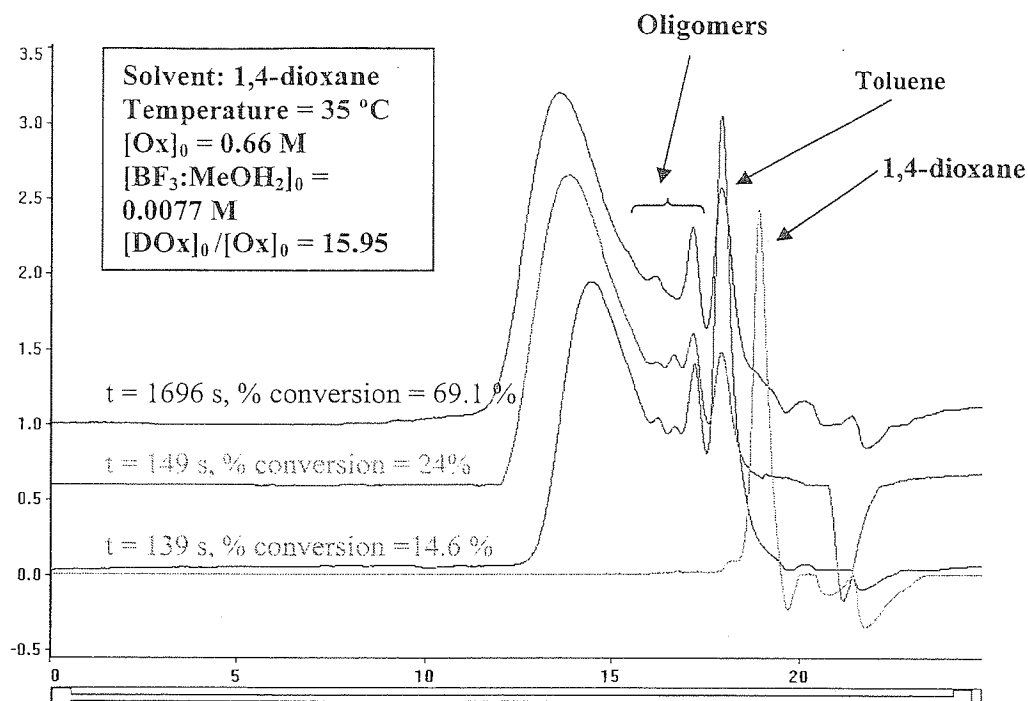
Annex 5. 11: ^1H NMR spectrum of poly(ethylene oxide).



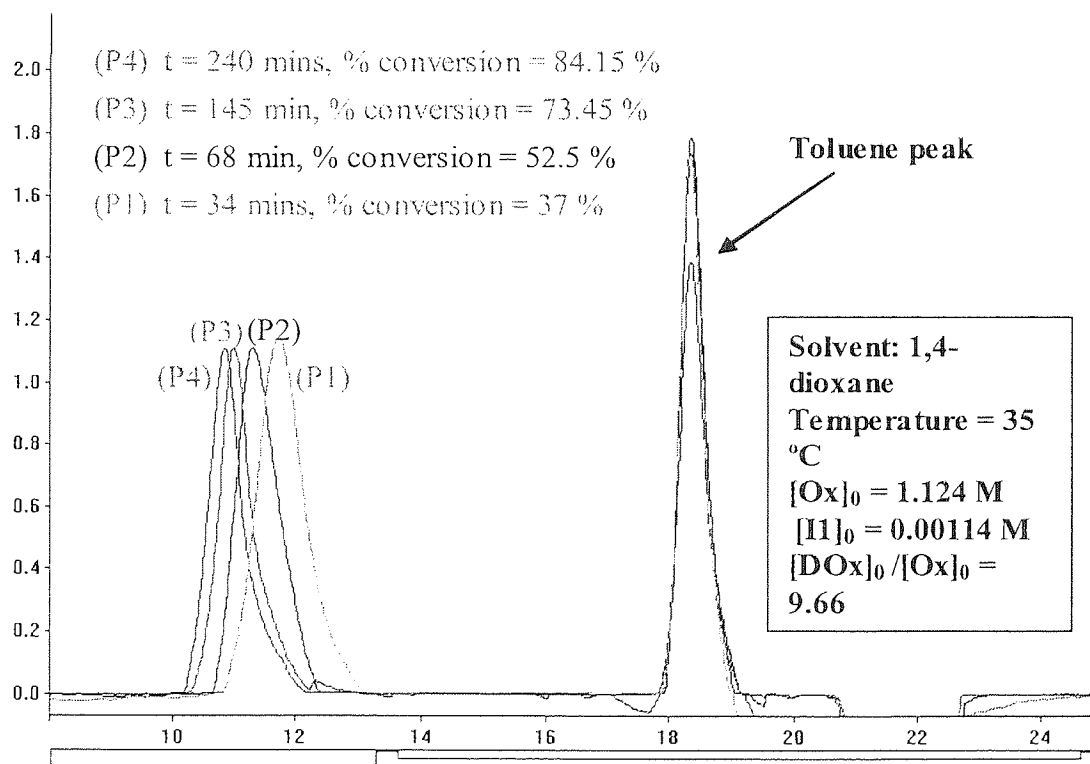
Annex 5. 12: SEC chromatogram of polyoxetane obtained throughout the polymerisation in 1,4-dioxane at 35°C. [Ox]₀ = 1 M, [BF₃:MeOH]₀ = 0.0077 M and [Dox]/[Ox] = 9.45. Table 5.4 series S 5.2.



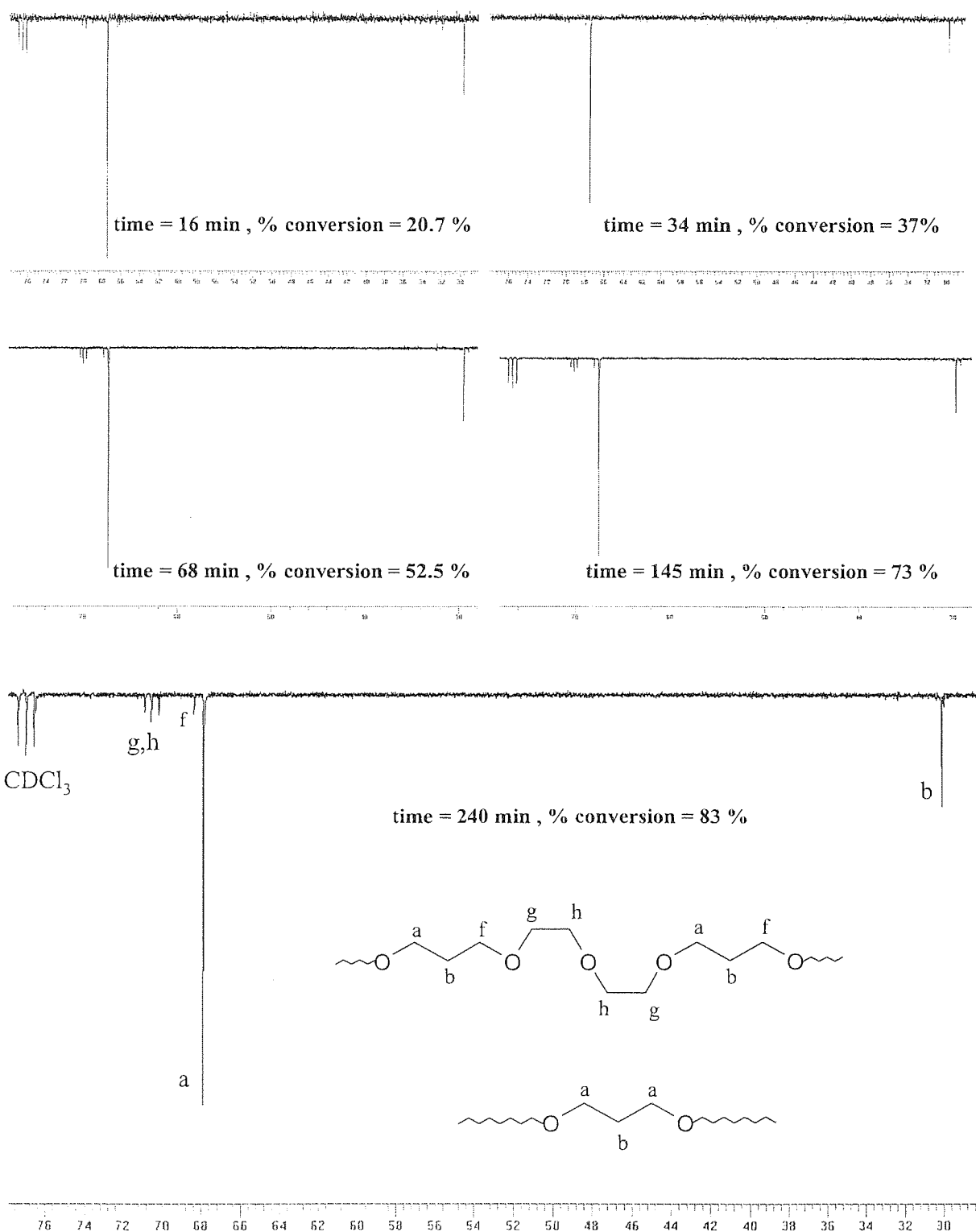
Annex 5. 13: SEC chromatogram of polyoxetane after a tentative of extension of polymer chain length by monomer addition on active polymer solution after full monomer conversion. Polymerisation carried out in 1,4-dioxane at 35 °C. Table 5.5 series S 5.4.



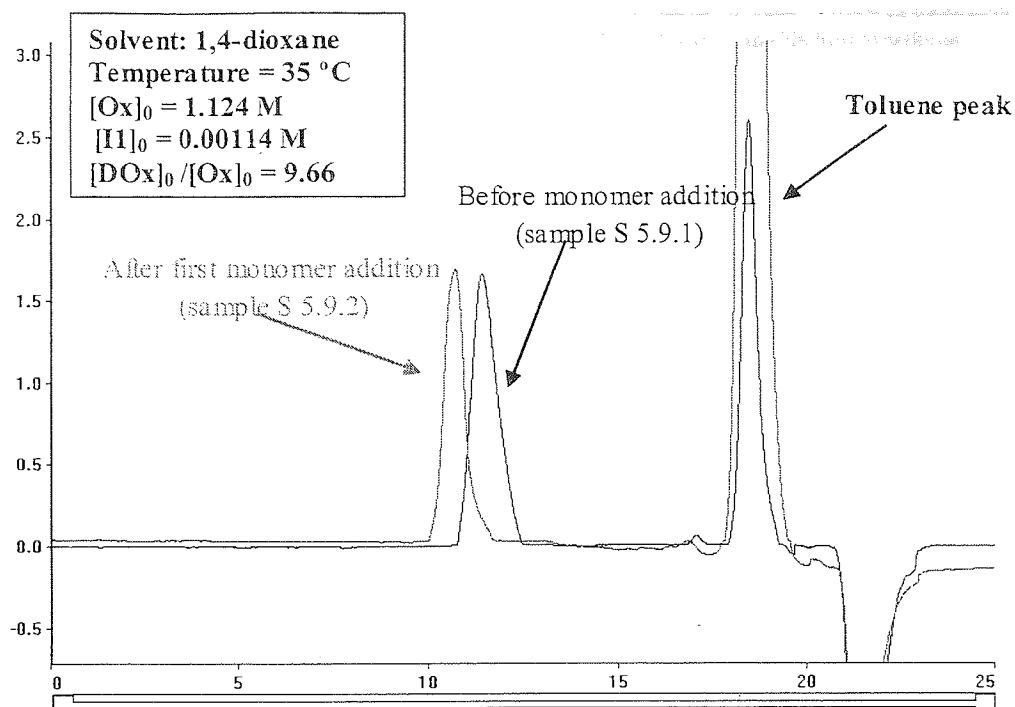
Annex 5. 14: SEC chromatogram of polyoxetane obtained throughout the polymerisation in 1,4-dioxane at 35°C. $[Ox]_0 = 0.66$ M, $[BF_3:MeOH_2]_0 = 0.0077$ M and $[DOx]/[Ox] = 15.95$. Table 5.4 series S 5.3.



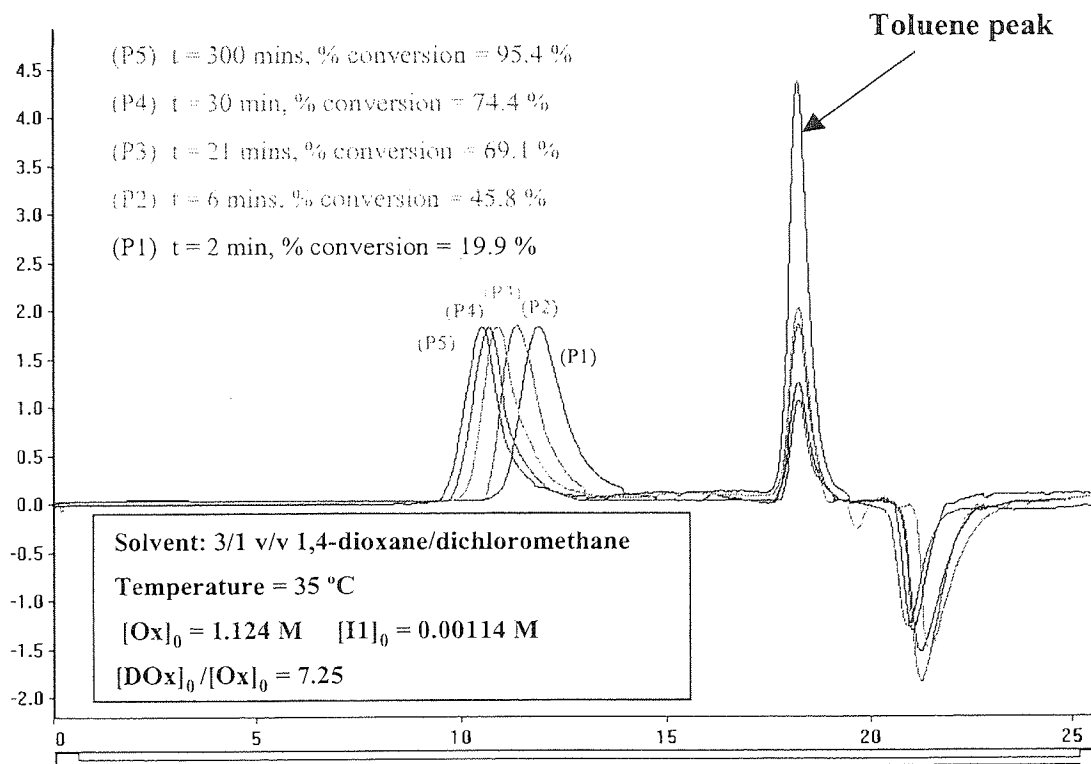
Annex 5. 15: SEC chromatogram of polymer obtained throughout the polymerisation in 1,4-dioxane at 35°C. $[Ox]_0 = 1.124$ M, $[I1]_0 = 0.00114$ M and $[DOx]/[Ox] = 9.66$. Table 5.6 series S 5.5.



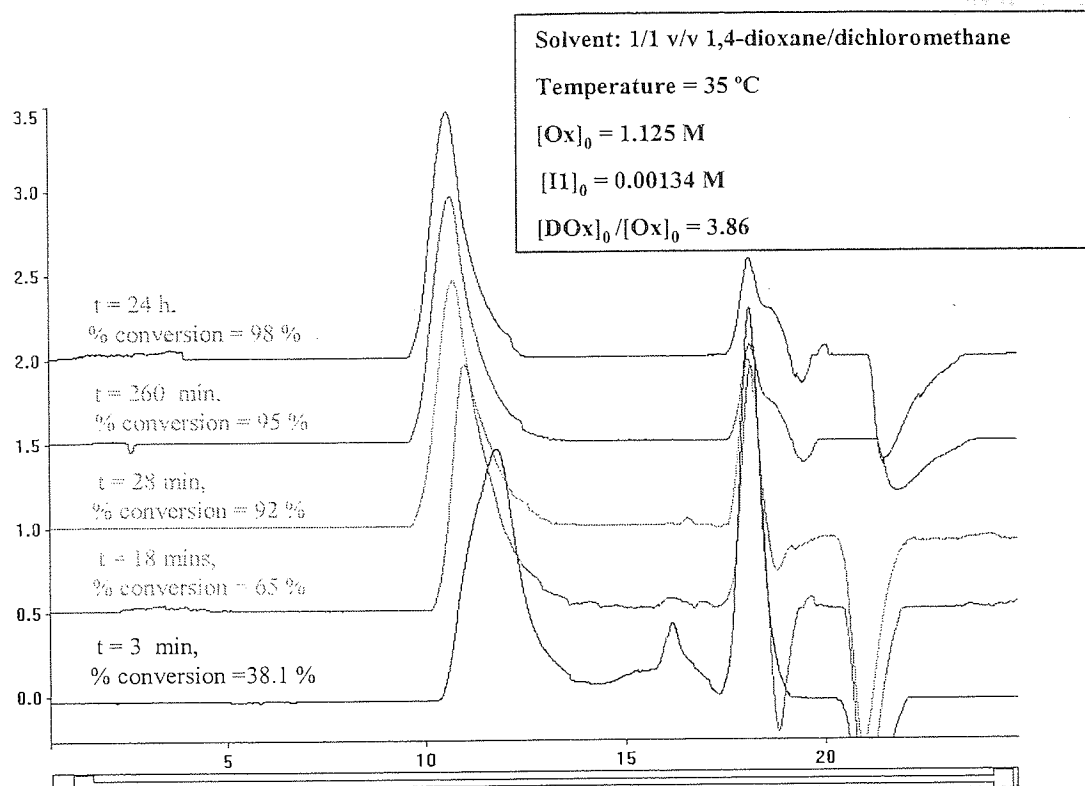
Annex 5. 16: ¹³C NMR spectra of polymer obtained throughout the polymerisation in 1,4-dioxane at 35°C. [Ox]₀ = 1.124 M and [I1]₀ = 0.00114 M. Table 5.6 series S 5.5.



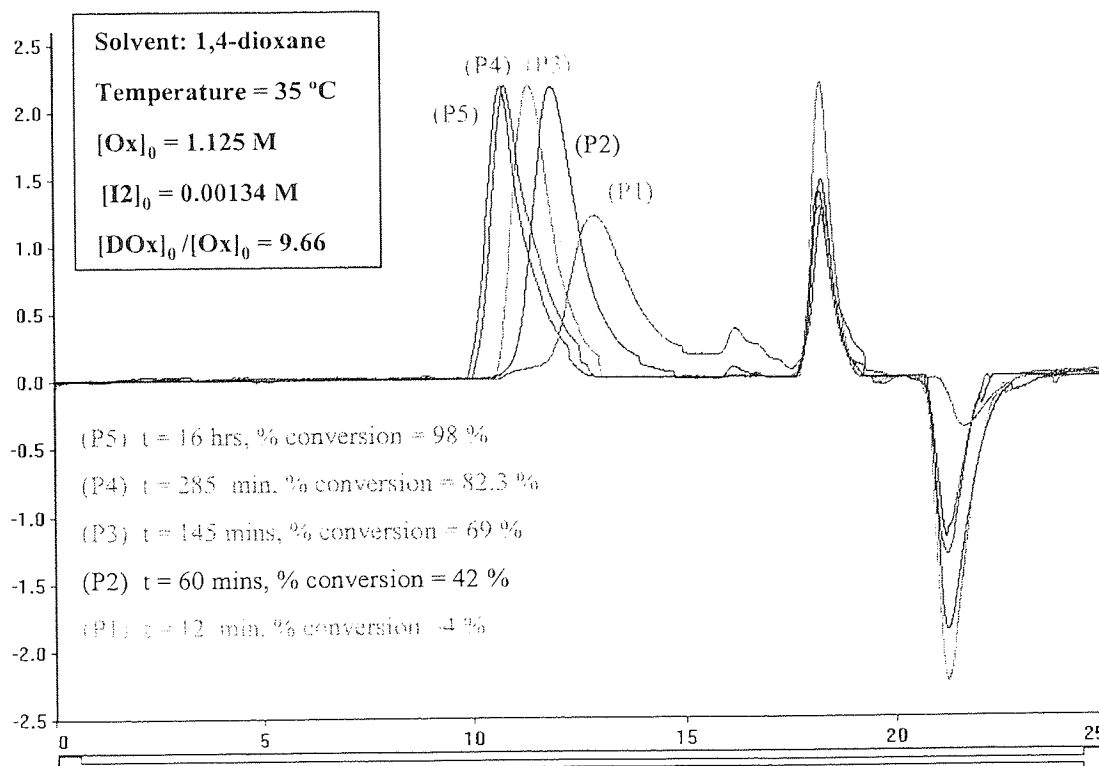
Annex 5. 18: SEC chromatogram of polyoxetane after extension of polymer chain length by monomer addition on active polymer solution after full monomer conversion. Polymerisation carried out using “living monomeric polyoxetane” initiator I1 in 1,4-dioxane at 35 °C. Table 5.7 series S 5.9.



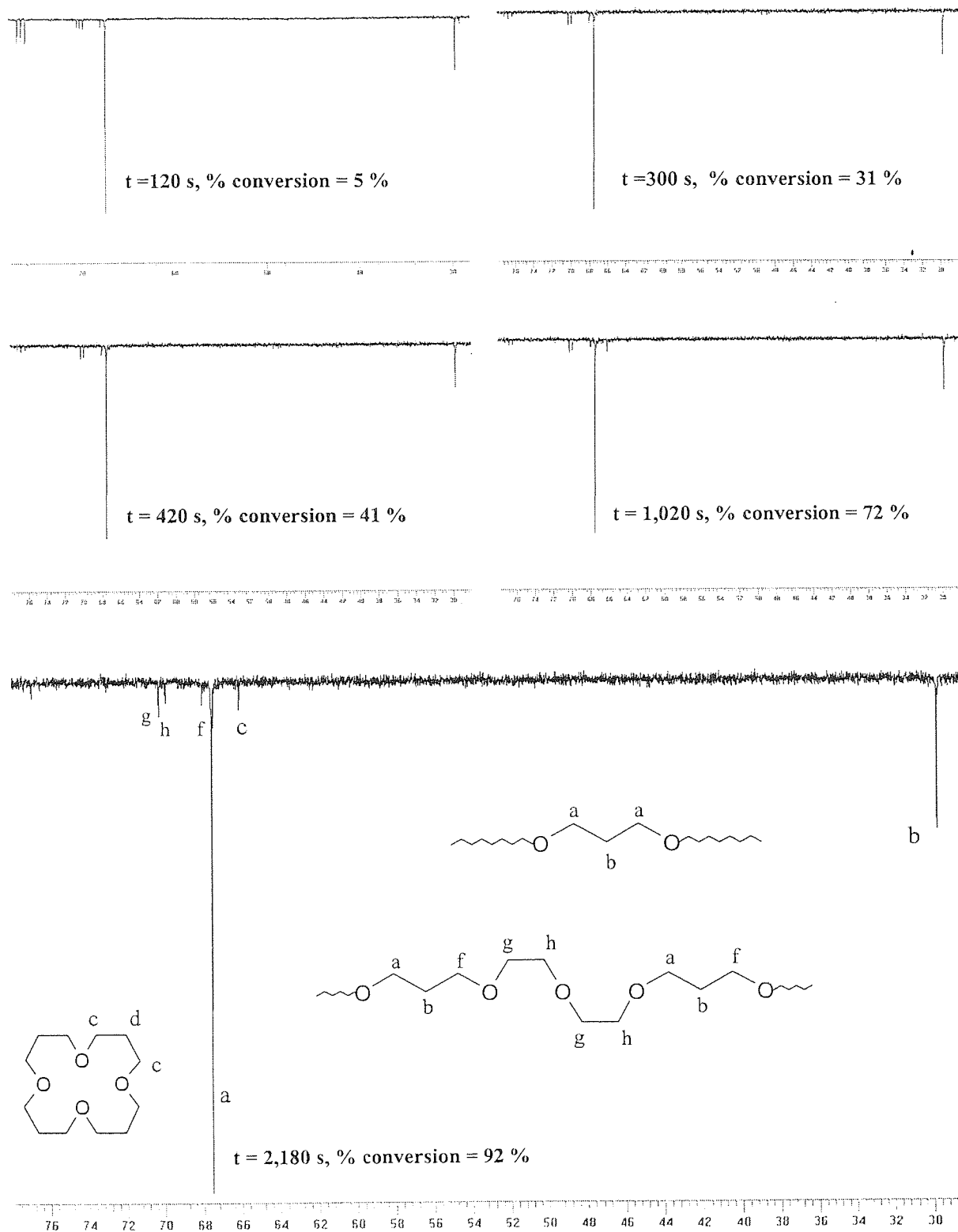
Annex 5. 19: SEC chromatogram of polyoxetane obtained throughout the polymerisation in 3:1 v/v 1,4-dioxane:dichloromethane at 35°C. $[Ox]_0 = 1.125 \text{ M}$, $[I1]_0 = 0.00114 \text{ M}$ and $[DOx]/[Ox] = 7.25$. Table 5.6 series S 5.7



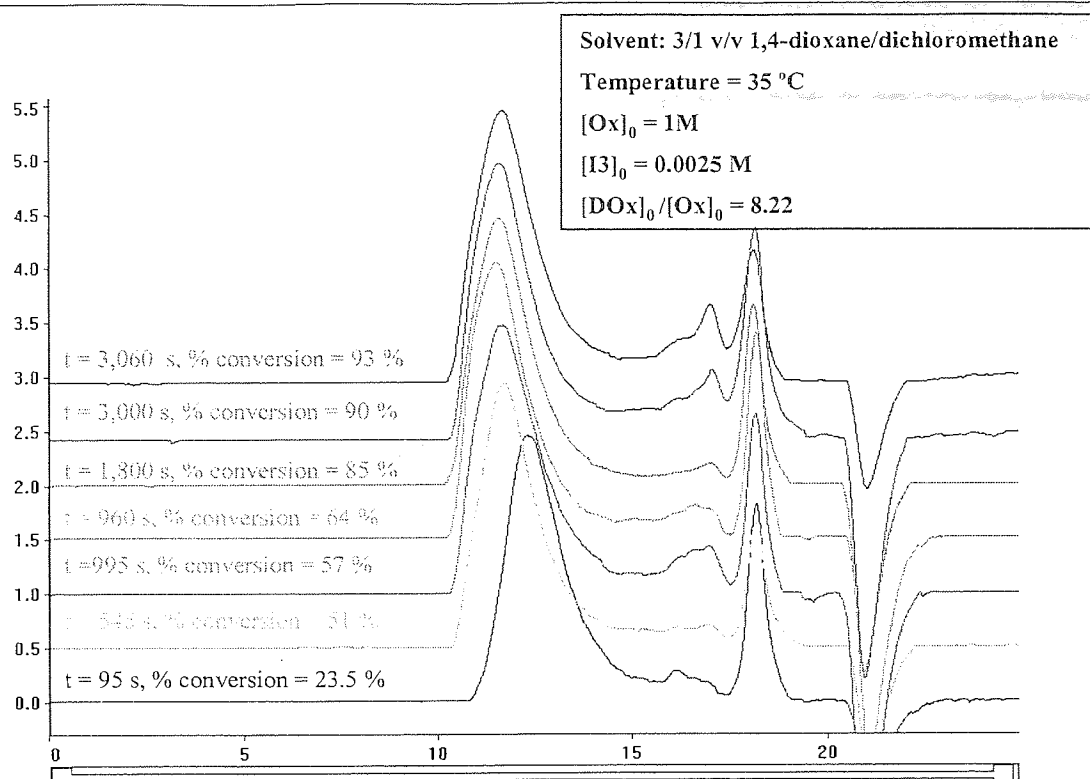
Annex 5. 20: SEC chromatogram of polyoxetane obtained throughout the polymerisation in 2:3 v/v 1,4-dioxane:dichloromethane at 35°C. $[Ox]_0 = 1.124 \text{ M}$, $[I1]_0 = 0.00114 \text{ M}$ and $[Dox]/[Ox] = 3.86$. Table 5.6 series S 5.8



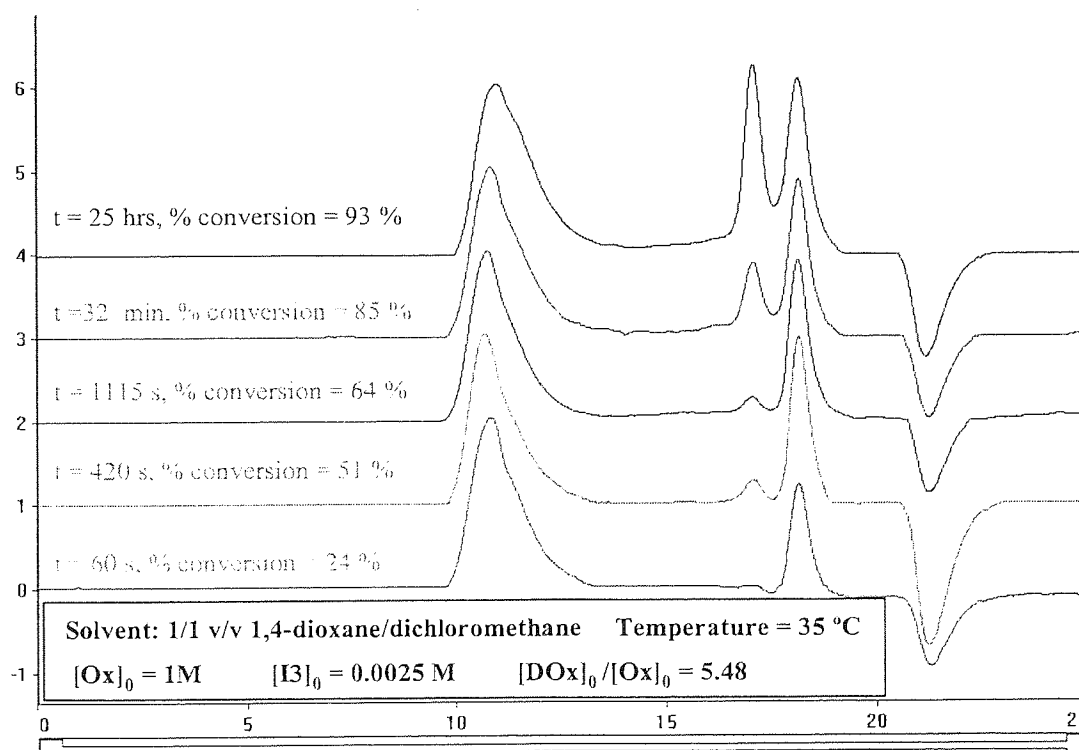
Annex 5. 21: SEC chromatogram of polyoxetane obtained throughout the polymerisation in 1,4-dioxane at 35°C. $[Ox]_0 = 1.125 \text{ M}$, $[I2]_0 = 0.00134 \text{ M}$ and $[Dox]/[Ox] = 9.66$. Table 5.6 series S 5.8.



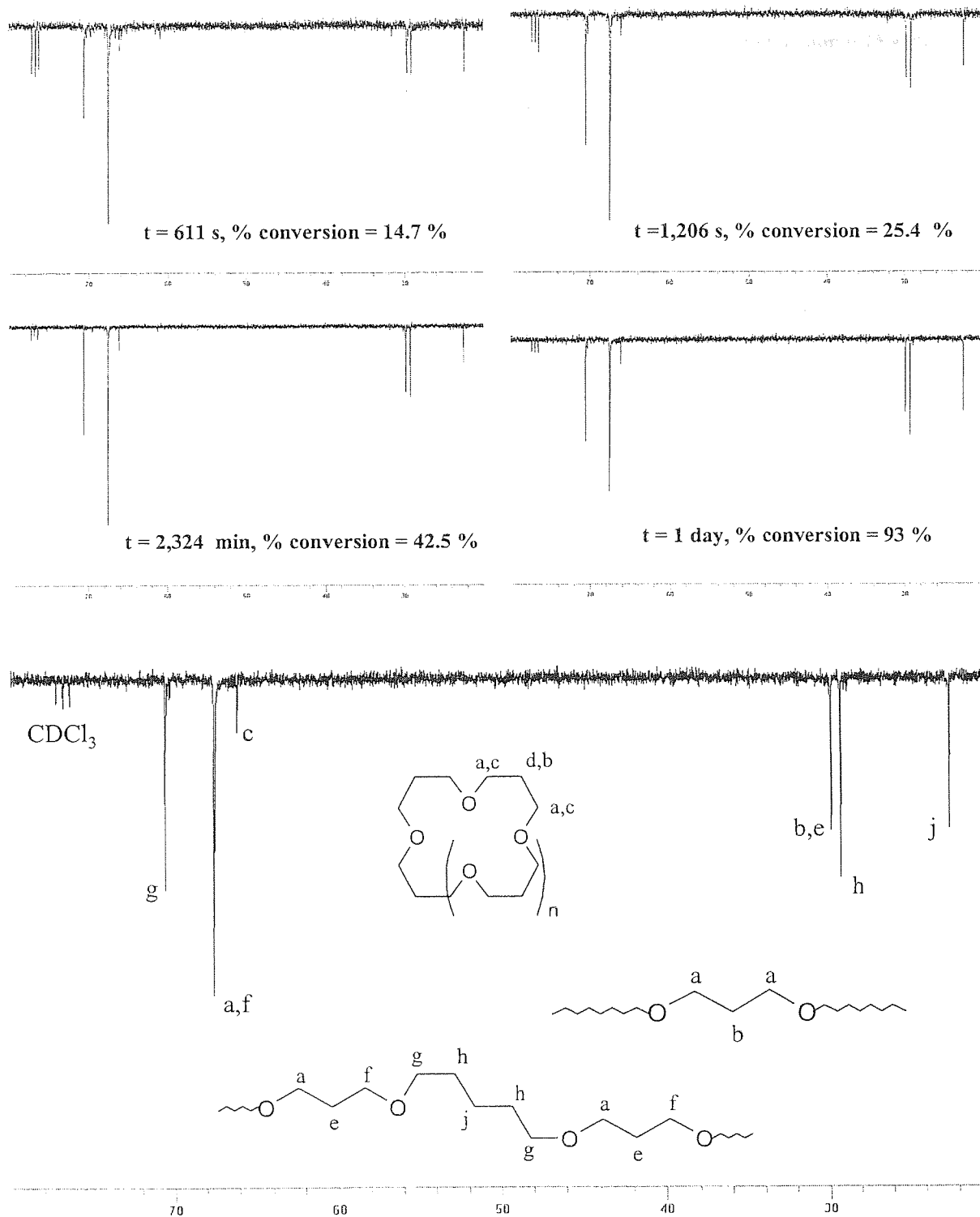
Annex 5. 22: ^{13}C NMR spectra of polymer obtained throughout the polymerisation in 1,4-dioxane at 35°C . $[\text{Ox}]_0 = 1 \text{ M}$, $[\text{I3}]_0 = 0.0025 \text{ M}$ and $[\text{Dox}]/[\text{Ox}] = 9.7$. Table 5.8 series S 5.10.



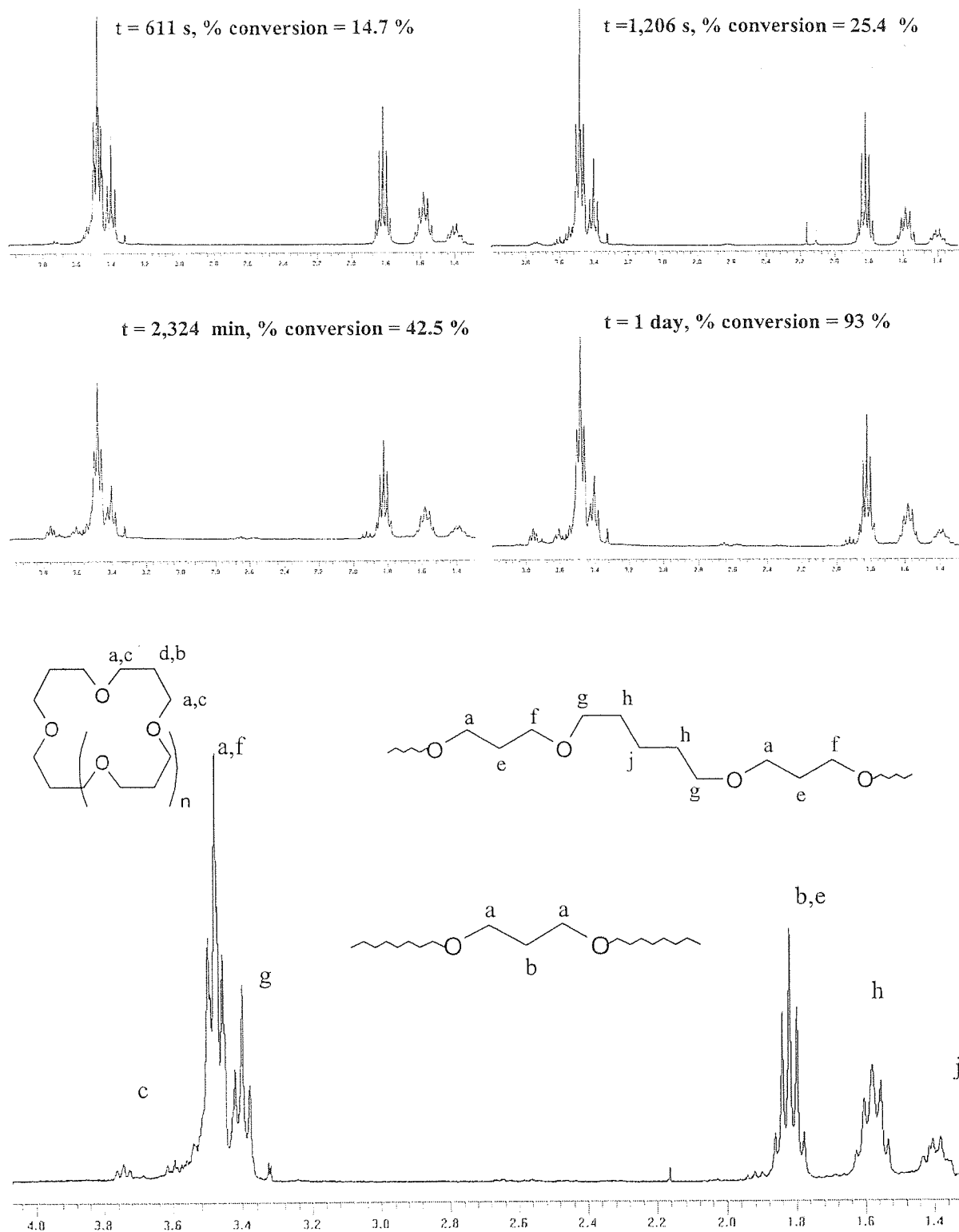
Annex 5. 23: SEC chromatogram of polyoxetane obtained throughout the polymerisation in 3/1 v/v 1,4-dioxane/dichloromethane at 35°C. $[Ox]_0 = 1 M$, $[I3]_0 = 0.0026 M$ and $[Dox]/[Ox] = 8.22$. Table 5.8 series S 5.11.



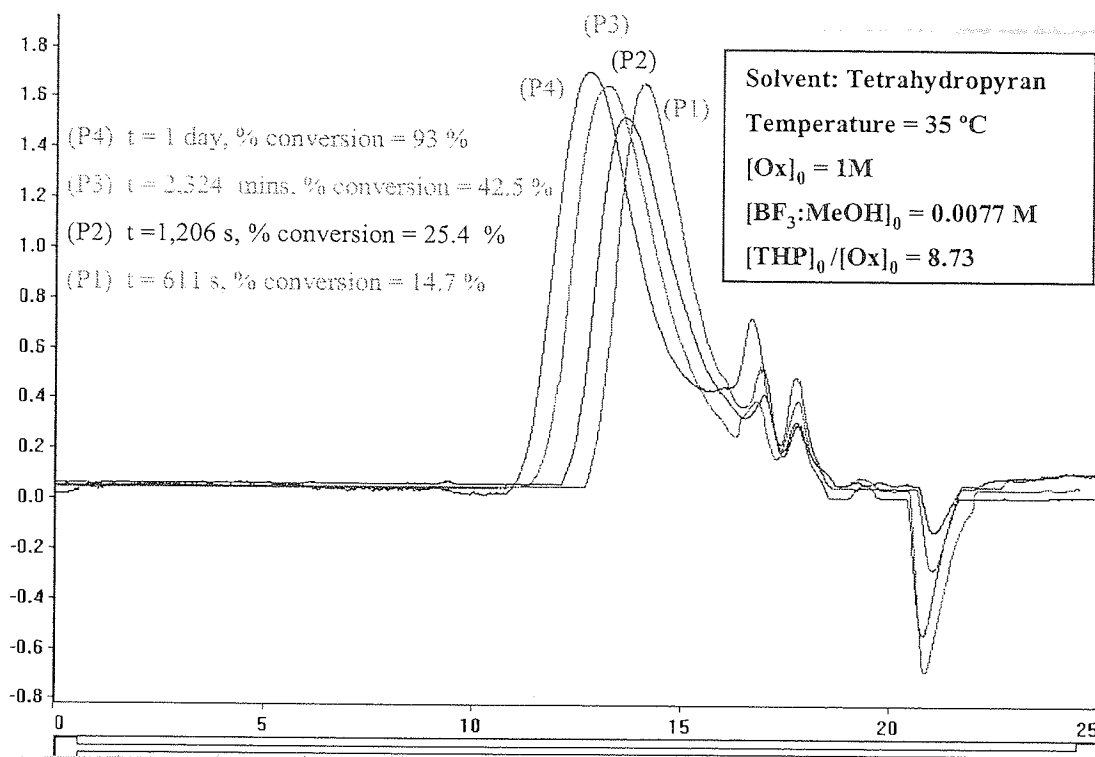
Annex 5. 24: SEC chromatogram of polyoxetane obtained throughout the polymerisation in 1,4-dioxane at 35°C. $[Ox]_0 = 1 M$, $[I3]_0 = 0.0026 M$ and $[Dox]/[Ox] = 5.48$. Table 5.8 series S 5.12.



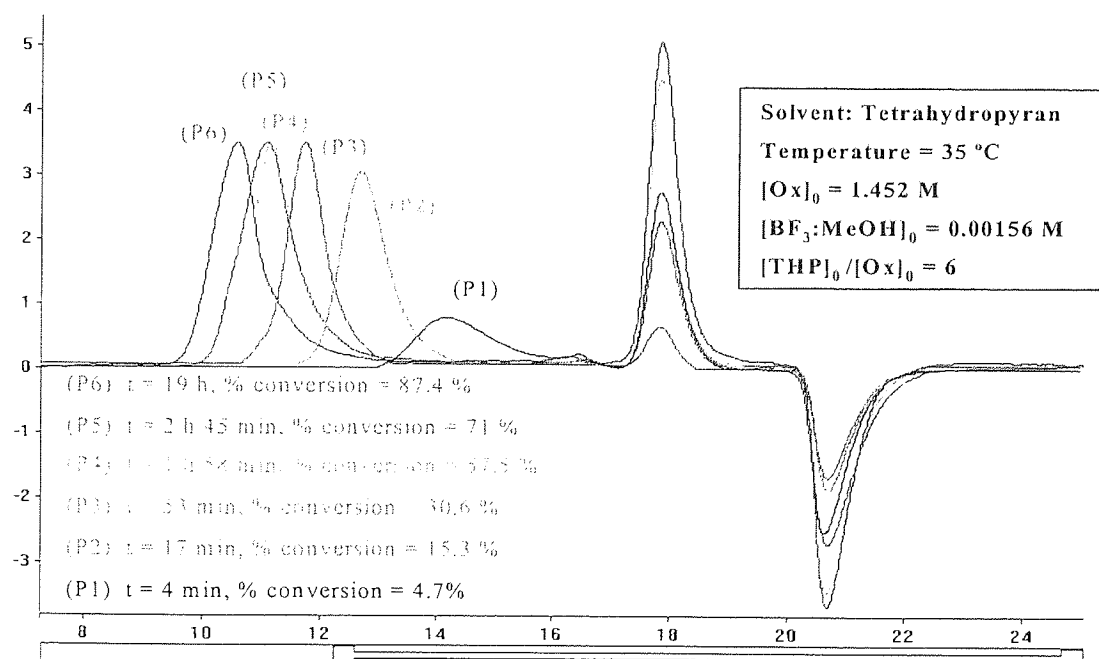
Annex 5. 25: ^{13}C NMR spectra of polymer obtained throughout the polymerisation in tetrahydropyran at 35°C . $[\text{Ox}]_0 = 1 \text{ M}$, $[\text{BF}_3:\text{MeOH}]_0 = 0.0077 \text{ M}$ and $[\text{THP}]/[\text{Ox}] = 8.73$. Table 5.10 series S 5.14.



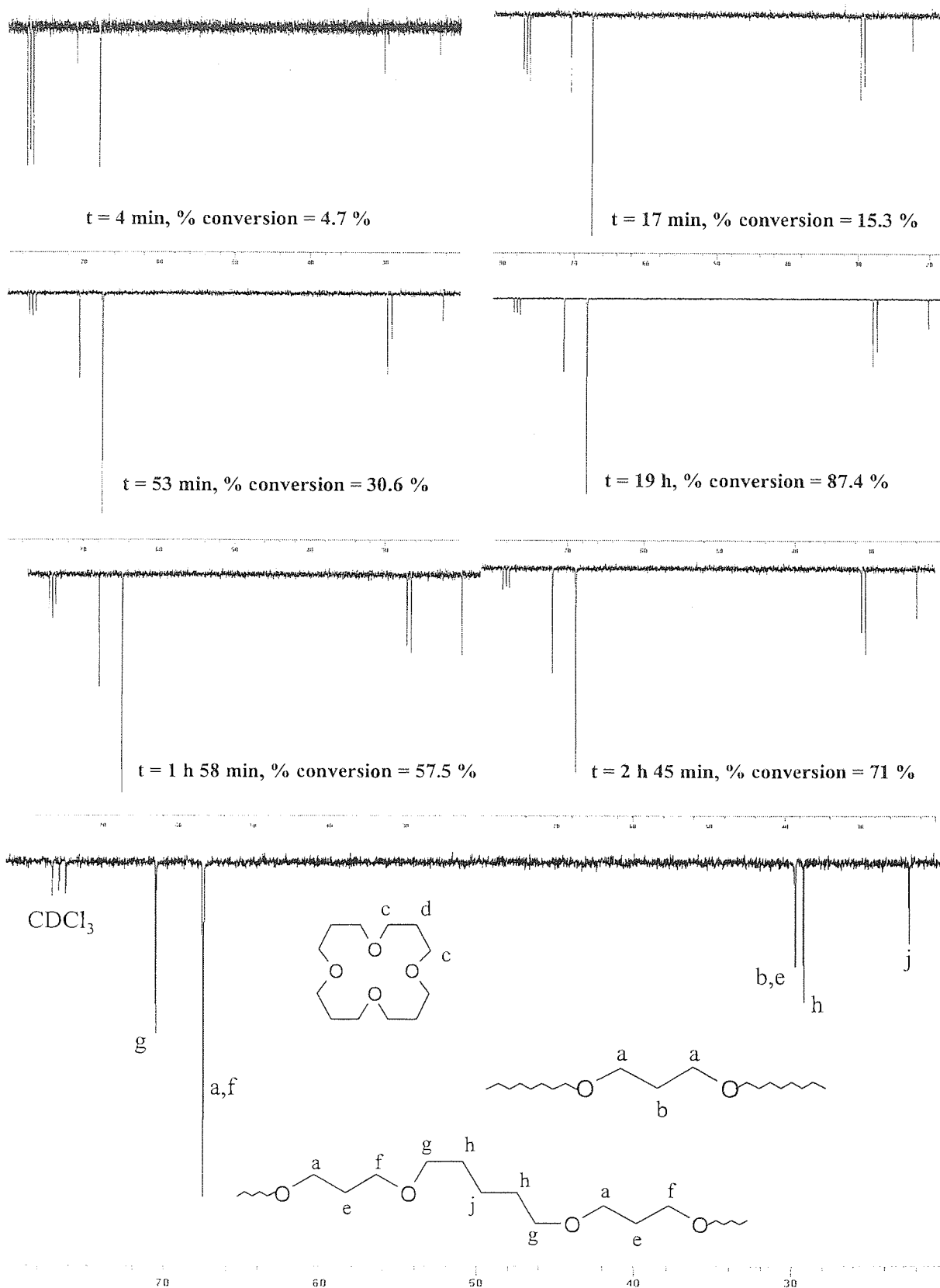
Annex 5. 26: ^1H NMR spectra of polymer obtained throughout the polymerisation in 1,4-dioxane at 35°C . $[\text{Ox}]_0 = 1 \text{ M}$, $[\text{BF}_3 \cdot \text{MeOH}]_0 = 0.0077 \text{ M}$ and $[\text{THP}]/[\text{Ox}] = 8.73$. Table 5.10 series S 5.14.



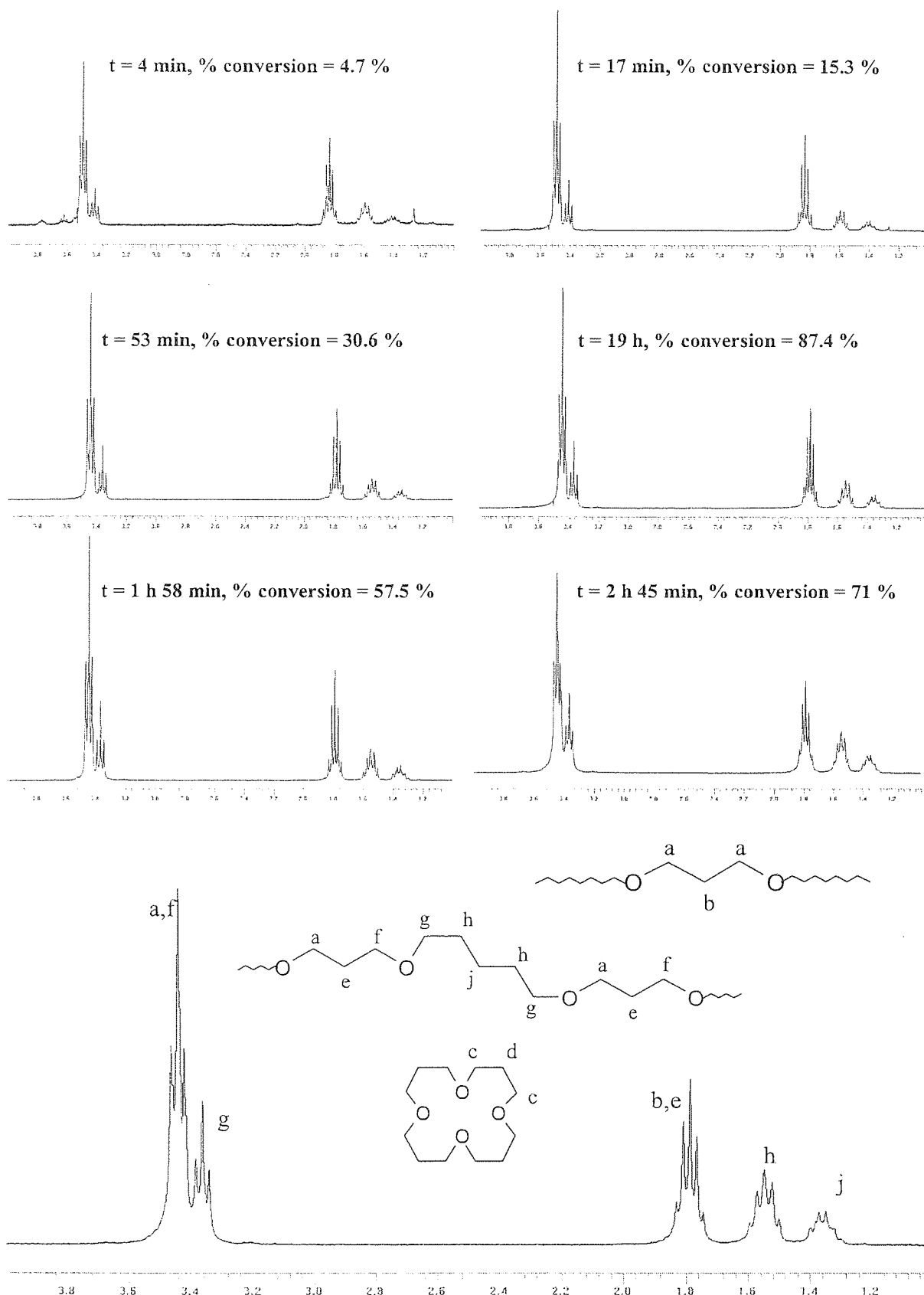
Annex 5. 27: SEC chromatogram of polyoxetane obtained throughout the polymerisation in tetrahydropyran at 35°C. $[Ox]_0 = 1 M$, $[BF_3:MeOH]_0 = 0.0077 M$ and $[THP]/[Ox] = 8.73$. Table 5.10 series S 5.14.



Annex 5. 28: SEC chromatogram of polyoxetane obtained throughout the polymerisation in tetrahydropyran at 35°C. $[Ox]_0 = 1.452 M$, $[I_2]_0 = 0.00156 M$ and $[THP]/[Ox] = 6$. Table 5.10 series S 5.15.



Annex 5. 29: ^{13}C NMR spectra of polymer obtained throughout the polymerisation in tetrahydropyran at 35°C . $[\text{Ox}]_0 = 1.452 \text{ M}$, $[\text{I}2]_0 = 0.00156 \text{ M}$ and $[\text{THP}]/[\text{Ox}] = 6$. Table 5.10 series S 5.15.



Annex 5. 30: ^1H NMR spectra of polymer obtained throughout the polymerisation in 1,4-dioxane at 35°C . $[\text{Ox}]_0 = 1.452 \text{ M}$, $[\text{I2}]_0 = 0.00156 \text{ M}$ and $[\text{THP}]/[\text{Ox}] = 6$. Table 5.10 series S 5.15.

REFERENCES

1. Jacqueline Akhavan, *the chemistry of explosives* 1998, Royal Society of Chemistry Paperbacks, UK.
2. J. B. Rose, *J. Chem. Soc.*, **1956**, 542, 546.
3. H. Cheradame, J. P. Andreolety, E. Rousset, *Makromol. Chem.*, **1991**, 192, 901.
4. H. Cheradame, J. P. Andreolety, E. Rousset, *Makromol. Chem.*, 1991, 192, 9198.
5. S. Penczek, P. Kubisa, and K. Matyjaszewski, *Adv. Polym. Sci.*, 1985, 68/69.
6. H. Cheradame, J. P. Andreolety, E. Rousset, *Makromol. Chem.*, **1991**, 192, 901.
7. M. A. H. Talukder, *Makromol. Chem.*, **1991**, 42/43, 501.
8. M. A. H. Talukder, G. A. Lindsay, G. A., *J. Polym. Sci. Part : A*, **1990**, 28, 2393.
9. B. Xu, Y. G. Lin. and Y. S. Chiu, *J. Appl. Polym. Sci.*, **1991**, 46, 1603.
10. Y. L. Hsiue, Y. G. Liu and Y. S. Chiu, *J. Polym. Sci. Chem. Ed.*, **1993**, 31, 3371.
11. Y. L. Hsiue, Y. G. Liu and Y. S. Chiu, *J. Polym. Sci. Chem. Ed.*, **1994**, 32, 2151.
12. Y. G. Liu, Y. L. Hsiue and Y. S. Chiu, *J. Appl. Polym. Sci.*, **1995**, 58, 579.
13. E. A. Murphy, T. Ntozakhe, C. J. Murphy, J. J., Fay, L. H. Sperling and G. E. Manse, *J. Appl. Polym. Sci.*, **1989**, 37, 267.
14. M. Wogtania, P. Kubisa and S. Penczek, *Makromol. Chem. Makromol. Symp.*, **1986**, 6, 201.
15. S. Penczek, *ACS Polym. Prepr.*, **1988**, 29, 38.
16. T. Saegusa, S. Matsumoto and Y. Hashimoto, *Macromolecules*, **1970**, 3, 377.
17. M. Morton, *Anionic polymerization: Principal and Practice*, Academic Press, **1983**.
18. H. F. Mark, N. M. Bikales, L. G. Overberger and Menges, in *Encyclopedia of Polymer Science and Engineering* (2nd Edn.), Wiley Interscience, 380,189.
19. W. H. Carothers, "Studies on polymerisation and ring formation. I. an introduction to the general theory of condensation polymer" *J. Am. Chem. Soc.*, **1929**, 51, 2578.
20. P. J. Flory, *Principles of polymer chemistry*, **1953**, Cornell University Press, Ithaca, New York.
21. J. A. Brydson, *Plastics materials*, Butterworth Heinemann (sixth Edition), 1995.
22. G. Moad and D. H. Solomon, *The chemistry of free radical polymerisation*, Pergamon, Elsevier Science Ltd, 1995; C. H. Bamford, "Radical polymerisation", *Encyclopaedia of Polymer Science and Engineering* 2nd Edition, 13, 708-867, John Wiley & sons, New York, (1988).
23. M. Szwarc, "Carbanion Living Polymers and Electron Transfer", Interscience, New York (1968); S. Bywater, "Anionic polymerisation", *Encyclopaedia of Polymer Science and Engineering* 2nd Edition, 2, 1-43, John Wiley & sons, New York, (1985).

24. P. H. Plesch, "Developments in the theory of Cationoid Polymerisations", Rapra Technology Ltd (2001); H. Cheradame, A. Gandidi, "Cationic polymerisation", Encyclopaedia of Polymer Science and Engineering 2nd Edition, 2, 729-814, John Wiley & sons, New York, (1985).
25. K. C. Frisch and S. Reegen (eds), "Ring-opening polymerisation", 1969, Marcel Dekker, New York.
26. F. Danusso and G. Natta (editors), "Stereoregular polymers and stereospecific polymerisation", Pergamon Press, Oxford, (1967).
27. K. J. Ivin, "Methathesis polymerisation.", Encyclopaedia of Polymer Science and Engineering 2nd Edition, 9, 643-668, John Wiley & sons, New York, (1985).
28. W. J. Brittain, Rubber Chemistry and Technology, 1992, 65, 580.
29. M. Szwarc, M. Levy, R. Milkowich, *J. Am. Chem. Soc.*, **1956**, 78, 2656; M. Szwarc, *Nature*, **1956**, 178, 1168.
30. K. Ziegler, *Angew. Chem.*, **1936**, 49, 499.
31. M. Szwarc and M. Van Beylen, "Ionic Polymerization and Living Polymers". Kluwer Academic Publishers, 1993.
32. M. Miyamoto, M., Sawamoto, and T. Higashimura, *Macromolecules*, **1984**, 17, 265.
33. W. J. Brittain, *Rubber Chemistry and Technology*, 1992, **65**, 580.
34. S. Bywater, *Prog. in Polym. Sci.*, **1994**, 19, 287.
35. J. E. Puskas, G. Kaszas, *Prog. Polym. Sci.*, **2000**, 25, 403.
36. W. B. Farnham, W. R. Hertler, T. V. Rajanbabu, D. Y. Sogah and O. W. Webster, "Group-transfer polymerisation", *J. Am. Chem. Soc.*, **1983**, 5706, 105.
37. V. Dragutan and R. Streck, Catalytic "Polymerization of Cycloolefins - Ionic, Ziegler-Natta and ring-opening metathesis polymerization", Elsevier Science Ltd, 2002.
38. W. Kurane, *Prog. Polym. Sci.*, **1998**, 23, 919.
39. D. Colombani, *Prog. Polym. Sci.*, **1997**, 22, 1649. D. Colombani, *Prog. Polym. Sci.*, **2000**, 25, 403.
40. T. Otsu, M. Yoshida, *Makromol. Chem. Rap. Commun.*, 1982, **3**, 127.
41. M. K. Georges, R. P. N. Veregin, P. M. Kazmaier and G. K. Hamer, *Macromolecules*, **1993**, 26, 2987.
42. M. Kato, M. Kamigaito, M. Sawamoto and T. Higashimura, *Macromolecules*, **1995**, 28, 1721.
43. J. S. Wong, D. Grestza, K. Matyjaszewski, *Macromolecules*, 1995, 28, **7901**.

44. a) T. Le, G. Moad, E. Rizzardo, S.H. Thang PCT Int. Appl. WO 9801478 (*Chem. Abstr.* **1998**, 128, 115390). S.H. Thang, G. Moad, E. Rizzardo PCT Int Appl WO9830601. J. Chiefari, R.T.A. Mayadunne, G. Moad, E. Rizzardo, S.H. Thang PCT Int Appl WO9931144. J. Chiefari, Y.K. Chong, F. Ercole, J. Krstina, J. Jeffery, T. Le, R. Mayadunne, G. Meijs, C. Moad, G. Moad, E. Rizzardo, S.H. Thang *Macromolecules*, **1998**, 31, 5559-5562.
- b) PCT. Int. Appl. WO 9935177 (1999), Rhodia chimie, ins.: P. Corporat, D. Charmot, S. Zard, X. Frank, G. Bouhadir.
45. P. J. Flory, *J. Am. Chem. Soc.* **1940**, 62, 1561.
46. C. F. H. Tipper and D. A. Walker, *J. Chem. Soc.*, **1959**, 1352.
47. H. K. Jr. Hall and P. J. Ykman, *J. Polym. Sci., Macro. Rev.*, **1976**, 11, 1.
48. G. Natta, G. Dall'Asta and G. Mazzanti, *Angew. Chem. Int. Edn.*, **1964**, 3, 723.
49. W. L. Truett, D. R., Johnson, I. N, Robindon and B. A. Montague, *J. Am. Chem. Soc.*, **1960**, 82, 2337.
50. T. Takahashi and I. Yamashita, *J. Polym. Sci.*, **1965**, B3, 251.
51. I. Cho and J. B. Kim, *J. Polym. Sci.*, **1980**, 18, 3053.
52. T. Takahashi, *J. Polym. Sci.*, A-1, **1968**, 6, 403.
53. C. G. Overberger and G. W. Halek, *J. Polym. Sci.*, A-1, **1970**, 8, 359.
54. H. K. Jr. Hall, H. Tsuchiya, P. J. Ykman, J. Otton, S. C. Snider and Deutschman, *Ring-opening polymerization* (ed. T ; Saegusa and Goethals) **1977**, American Chemical Society, Washington, P. 285.
55. P. G. Gassman, G. R. Meyer and F. J. Williams, *J. Am. Chem. Soc.*, **1972**, 94, 7741.
56. S. Perry and H. Hibbert, *Can. J. Res.*, **1933**, 8, 102; *J. Am., Chem. Soc.*, **1940**, 62, 2599.
57. H. Meerwein, German Patent, 741478 (**1933**), 8, 102; *J. Am. Chem. Soc.*, **1959**, 81, 3374.
58. T. Aida, Y. Maekawa, S. Asano and S. Inoue, *Macromol.*, **1988**, 21, 1195.
59. W. F. Gresham, US Patent 2856 370, Du Pont; *Chem. Abstr.*, **1946**, 40, 3022.
60. H. Sumitomo and M. Oakada, *Adv. Polym. Sci.*, **1978**, 28, 47.
61. A. Pictet, *Helv. Chem. Acta.*, **1918**, 1, 226.
62. S. Boileau and P. Sigwalt, *Bull. Soc. Chim. France*, **1968**, 1418.
63. La. A. Korotneva,, G. P. Belonovskaya,, J. D. Tchernova, Yu. P. Kouznetsov and B. A. Dolgoplosk, *Synthes Struktura i Svoistva Polimerov ANSRR*, **1970**, 15, 1971.

64. J. I. Lambert, D. Van Ooteghem and E. J. Goethals, *J. Polym. Sci.*, A-1, **1971**, 9, 3055.
65. W. G. Barb *J. Chem. Soc.*, **1955**, 2464 and 2577.
66. G. M. Lukovokin, V. S. Pshezhetsky, and G. A. Murtazaeva, *Europ. Polym. J.*; **1973**, 9, 559.
67. E. F. Razvodovskii, A. A. Berlin, A. V. Nekrasov, A. T. Ponomarenko, N. G. Puschkova and N. S. Enikolopyan, *Vyskomolek. Soedin.*, **1973**, A15, 2233.
68. R. H. Wiley and L. L. Jr. Bennett, *Chem. Rev.*, **1979**, 44, 447.
69. T. Saegusa, S. Kobayashi and M. Ishiguro, *Macromolecules*, **1974**, 7, 958.
70. A. Levy and M. Litt *Polym. Lett.*, **1967**, 5, 881.
71. S. W. Kantor, W. N. Gruu and R. C. Osthoff, *J. Am. Chem. Soc.*, **1954**, 76, 5190.
72. J. A. Semlyen and P. V. Wright, *Polymer*, **1969**, 10, 543.
73. H. Cherdron, H. Ohse and F. Korte, *Makromol. Chem.*, **1962**, 56, 179; **1962**, 56, 187.
74. Y. Etienne and N. Fisher (to kodfak Pathé) French Patent, 1231163 (1960); *Chem. Abstr.*, **1961**, 55, 19330f.
75. Y. Yamashita, T. Tsuda, M. Okada and S. Iwatsuki, *J. Polym. Sci.*, A-1, **1966**, 4, 2121.
76. A. Hamitou, T. Ouhadi, R. Jerome and P. Teyssie, *J. Polymer Sci.-Chem.*, **1977**, 15, 865.
77. C. G. Overberger and J. K. Weise, *J. Am. Chem. Soc.*, **1968**, 90, 3525, 3533 and 3538.
78. M. Szwarc, *Adv. Polym. Sci.*, **1964**, 4, 1.
79. R. M. Joyce and D. M. Ritter, US Patent 2,251,519 (1941) ; *J. Polym. Sci.*, **1948**, 3, 167.
80. H. K., Jr Hall, *J. Am. Chem Soc.*, **1958**, 80, 6404.
81. S. Barzakay, S., M. Levy and D. J. Vofsi, *J. Polym. Sci.*, A-1, **1966**, 4, 2211.
82. M. Rothe, H. Boenish, and D. Essig, *Makromol., Chem.*, **1966**, 91, 24.
83. R. Puffr and J. Sebenda, US Patent 3, 740, 379; *Chem. Abstr.*, **1973**, 79, 67085; R. Puffr and J. Sebenda, German Patent 2,508,564; *Chem. Abstr.*, **1975**, 83, 194094 R. Puffr and J. Sebenda, J., US Patent 4,111,869; *Chem. Abstr.*, **1979**, 90, 122271.
84. J. Sebenda, in : *Polymerisation of heterocyclics*, Vol 2 : *Ring opening polymerization* (Eds. K. C. Frish and S. L. Reegen), **1969**, Marcel Dekker, New-York, pp. 303-26.
85. T. Kodira, J. Stlechicek, and J. Sebenda, *Europ. Polym. J.*, **1970**, 6, 1451.
86. T. Kodira, J. Stlechicek, and J. Sebenda, *Europ. Polym. J.*, **1971**, 7, 97.

87. N. L. Cox and W. E. Hanford., US Patent 2,276,164 (1942); *Chem. Abst.*, **1942**, 36, 4637.
88. J. Libiszowsky, R. Kalunzynski and S. Penczek, *J. Polym. Sci., Polym. Chem.*, **1978**, 16, 1275; *Makromol. Chem.*, **1977**, 178, 2943.
89. G. Lapienis and S. Penczek, *Macromolecules*, **1974**, 7, 166; *Macromolecules*, **1977**, 10, 1301.
90. F. Fairbrother, G. Gee and G. T. Merrall, *J. Poly. Sci.*, **1955**, 16, 459.
91. A. V. Tobolsky and A. Eisenberg, *J. Colloid Sci.*, **1962**, 17, 49-65.
92. P. J. Flory, *Principles of polymer chemistry*, **1953**, Cornell University Press, Ithaca, New York.
93. K. J. Ivin and J. Leonard, *Polymer*, **1965**, 6, 621.
94. M. P. Dreyfuss and P. Dreyfuss, *J. Polym. Sci., A-1*, **1966**, 4, 2179-2200.
95. K. J. Ivin and J. Leonard, *Euro. Polym.*, **1970**, 6, 331.
96. F. S. Dainton and K. J. Ivin, *Quart. Rev. Chem. Soc.*, **1958**, 12, 61.
97. E. A. Ofstead and N. Calderon, *Makromol. Chem.*, **1972**, 154, 21-24.
98. J. D. Cox *Tetrahedron*, **1963**, 19, 1175.
99. K. J. Ivin and J. Leonard, *Eur. Polym.*, **1970**, 6, 331.
100. J. Leonard and L. Malhortra, *J. Polym. Sci., A-1*, **1971**, 9, 1983.
101. L. I. Kuzub, M. A. Markevich, A. A. Berlin and N. S. Yenikolopyan, *Polym. Sci. USSR*, **1968**, 10, 2332.
102. J. Leonard and D. Maheux, *J. Macromol. Sci.-Chem.*, **A7**, **1973**, 7, 1421.
103. S. Penczek and K. Matyjaszewski, *J. Polym. Sci. Polym. Symp.*, **1976**, 56, 255.
104. F. S. Dainton, T. R. E. Delvin and P. A. Small, *Trans. Faraday Soc.*, **1955**, 51, 1710.
105. G. Natta, G. Dall'Asta and L. Porri, *Makromol. Chem.*, **1965**, 81, 253.
106. T. J. Katz and N. Acton *Tetrahedron Lett.*, **1976**, 4251.
107. G. Dall'Asta, *J. Polym. Sci., A-1*, **1968**, 6, 2397.
108. Goodyear Tire and Rubber Co., *Chem. Abstr.*, **1977**, 86, 5893.
109. G. Natta, G. Dall'Asta, I. W. Bassi and G. Carrelà, *Makromol. Chem.*, **1966**, 91, 87.
110. G. Natta, G. Dall'Asta and G. Mazzanti, *Angew. Chem ; Int. Edn.*, **1964**, 3, 723.
111. P. A. Patton, C. P. Lillya and T. J. McCarthy, *Macromolecules*, **1986**, 19, 1266.
112. N. Calderon, E. A. Ofstead and W. A. Judy, Paper presented at the central regional Meeting, am. Chem. Soc., Akron, May, 1968.
113. G. Pruckmayer and T. K. Wu, *Macromolecules*, **1975**, 8, 954.
114. M. Rahman and K. E. Weale, *Polymer*, **1970**, 11, 122.

115. J. B. Rose, *J. Chem. Soc.*, **1956**, 542, 546.
116. A.S. Pell and G. Pilcher, *Trans. Faraday Soc.*, **1965**, 62, 71.
117. S. Penczek, P. Kubisa and K. Matyjaszewski, *Adv. Polym. Sci.*, **1980**, 37, 1.
118. S. Kobayashi, H. Danda and T. Saegusa, *Bull. Chem. Soc. Japan.*, **1974**, 7, 415.
119. T. Saegusa and S. Kobayashi, *J. Polym. Sci., Polym. Symp.*, **1976**, 56, 255.
120. K. c. Frisch and S. L. Reegen, *Ring-Opening Polymerizations*, Ed. by Marcel Decker Inc., New York, N. Y. (1969).
121. T. Saegusa and S. Kobayashi, *Pogress in Polymer Science Japan*, Vol.6, Ed. by Onogi, S. and K. Uno, Kodansha Scientific, Tokyo (1973), pp. 107-151.
122. T. Saegusa, H. Fujii, S. Kobayashi, S. Ando and R. Kawase, *Macromolecules*, **1973**, 6, 26.
123. D. J. Worsfold and A. M. Eastham, *J. Am. Chem. Soc.*, **1957**, 79, 900.
124. J. Dale, K. Daasvatn and T. Grønneberg, *Makromol. Chem.*, **1977**, 178, 873.
125. S. Kobayahsi, K. Morikawa, T. Saegussa, *Macromolmecules*, **1975**, 8, 952.
126. Y. Yamashita, K. Iwao and K. Ito, *Polym. Lett.*, **1979**, 17, 1.
127. K. Ito, N. Usami, and Y. Yamashita, *Polym. J.*, **1979**, 11, 171.
128. Y. Yamashita and K. Ito, *Polym.Bull.*, **1978**, 1, 73.
129. Y. Kawakami, A. Ogama and Y. Yamashita, *J. Org. Chem.*, **1972**, 44, 441.
130. Y. Kawakami, A. Ogama and Y. Yamashita, *J. Polym. Chem.*, **1979**, 17, 3785..
131. H. Sasaki, J. M. Rudzinski and T. Kakuchi, *J. Polym. Sc.: Part A: Polym. Chem. Ed.*, **1995**, 33, 1807.
132. W. M. Pasika, *J. Polym. Sci.*, **1965**, A3, 4287.
133. K. Brzezinska, K. Matyjaszewski and S. Penczek, *Makromol. Chem.*, **1978**, 179, 2387.
134. T. Saegusa and S. Matsumato, *J. Macromol. Sci.*, **1970**, A4, 870.
135. K. Matyjaszewski and S. Penczek, *J. Polym. Sci., Polym. Chem.*, **1974**, 12, 1905.
136. S. Kobayashi, H. Danda and T. Saegusa, *Bull. Chem. Soc. Japan.*, **1973**, 46, 3214.
137. S. Kobayashi, H. Danda and T. Saegusa, *Bull. Chem. Soc. Japan.*, **1974**, 47, 2699.
138. S. Kobayashi, K. Morikawa and T. Saegusa, *Macromolecules*, **1975**, 8, 952; Y. L. Liu, G. H. Hsiue and Y. C. Chiu, *J. Polym. Sci., Polym. Chem.*, **1994**, 32, 2543.
139. K. Matyjaszewski and S. Penczek, *J. Polym. Sci.*, **1974**, 12, 1905.
140. A. M. Eastham, *J. Am. Chem. Soc.*, **1956**, 78, 6040.
141. A. C. Farthing and R. J. Reynolds, *J. Polym. Sc.*, **1954**, 12, 503.
142. J. P. Kennedy and F. J. Y. Chen, *Polym. Bull.*, **1986**, 15, 201.

143. S. Penczek, P. Kubisa and K. Matyjaszewski, *Adv. Polym. Sci.*, **1980**, 37, 1.
144. M. P. Dreyfuss and P. Dreyfuss, *J. Polym. Sci., A-1*, **1966**, 4, 2179.
145. H. Meerwein and H. Morshel, *Angew. Chem.*, **1960**, 72, 927.
146. H. Meerwein, E. Battenburg, E. Gold, E. Hpfeil and G. J. Willfang, *Prakt. Chem.*, **1939**, 154, 83.
147. H. Meerwein, D. Delfs and R. J. Reynolds, *Angew. Chem.*, **1960**, 72, 927.
148. A. Stolarczyk, P. Kubissa and S. Penczek, *J. Macromol. Sci.-Chem.*, **1977**, 25, 627.
149. Y. Yamashita, K. Nobutaki, Y. Nakamura and M. Hirata, *Macromolecules*, **1971**, 4, 458.
150. P. Kubisa, *Bull. Acad. Polon. Sci., Ser. Sci. Chem.*, **1977**, 25, 627.
151. F. Afshar-Taromi, M. Scheer, P. Rempp and E. Franta, *Makromol. Chem.*, **1978**, 179, 849.
152. G. A. Olah, S. J. Kuhn, W. S. Tolgyeshi and E. B. Barker, *J. Am. Chem. Soc.*, **1962**, 84, 2733.
153. P. Kubisa and S. Penczek, *Makromol. Chem.*, **1978**, 179, 445.
154. K. Matyjaszewski and S. Penczek, *J. Polym. Sci., Polym. Chem.*, **1974**, 12, 1905.
155. S. Kobayashi, H. Danda and T. Saegusa, *Bull. Chem. Soc. Japan.*, **1973**, 46, 3214.
156. T. Saegusa and S. Kobayashi, *J. Polym. Sci., Polym. Symp.*, **1976**, 56, 241.
157. D. J. Worsfold and A. M. Eastham, *J. Am. Chem. Soc.*, **1957**, 79, 900.
158. T. Saegusa, H. Imai and J. Furukawa, *Makromol. Chem.*, **1962**, 54, 218.
159. T. Saegusa, T. Ueshima, H. Imai and J. Furukawa, *J., Makromol. Chem.*, **1964**, 79, 221.
160. T. Saegusa, T. Ueshima, and S. Tomita, *Makromol. Chem.*, **1967**, 107, 131.
161. H. Meerwein, D. Delfs and H. Morschel, *Angew. Chem.*, **1960**, 72, 927.
162. E. B. Ludvig, B. A. Rosenberg, T. M. Zvereva, A. R. Gantmakher and S. S. Medvedev, *Vyskomol. Soedin.*, **1965**, 7, 269 ; *Polym. Sci. USSR*, **1965**, 7, 296.
163. Kuntz, I., *J. Polym. Sc., Part A-1*, **1967**, 5, 193.
164. M. Dreyfuss, J. P. Westphal and P. Dreyfuss, *Macromol.*, **1968**, 1, 437.
165. P. Dreyfuss, in 'Poly(tetrahydrofuran)' Gordon and Breach, New York, 35, 1982.
166. T. G. Croucher and R. E. Wetton, *Polym. Sci., A-1*, **1976**, 17, 205.
167. J. V. Crivello, *Chemtech.*, **1980**, 624.
168. H. Sasaki and J. V. Crivello, *J. Macromol. Sci., Pure Appl. Chem.*, **1989**, A29(10), 915.

169. H. Sasaki, J. V. Crivello and H. Sasaki, *J. Macromol. Sci., Pure Appl. Chem.*, **1993**, A30(2&3), 173.
170. H. Sasaki, J. V. Crivello and H. Sasaki, *J. Macromol. Sci., Pure Appl. Chem.*, **1993**, A30(2&3), 189.
171. J. V. Crivello and H. J. W. Lam, *J. Polym. Sci. Polym. Chem. Ed.*, **1980**, 18, 2677.
172. J. V. Crivello, *Adv. Olym. Sci.*, **1984**, 64, 1.
173. G. Manivannan and J. P. Fouassier, *J. Polym. Sci : Part A: Polym. Chem. Ed.*, **1991**, 29, 1113.
174. J. V. Crivello and H. J. W. Lam, *J. Polym. Sci. Polym. Chem. Ed.*, **1980**, 18, 1021.
175. J. V. Crivello and H. J. W. Lam, *Macromol.*, **1981**, 14, 1141.
176. N. Yamazaki, *Adv. Polym. Sci.*, **1969**, 6, 377.
177. C. F. Heinz, *J. Polym. Sci., Polym. Lett.*, **1969**, 7, 625.
178. S. Hino, S. Nakahama and N. Yamazaky, *Polymer J.*, **1971**, 2, 56.
179. W. Strobel and R. C. Schulz, *Makromol. Chem.*, **1966**, 99, 103.
180. J. Dale and K. Daasvatn, *J. Chem. Soc., Chem ; Comm.*, 294, **1976**.
181. R. O. Colclough, G. Gee, W. C. E. Higginson, J. B. Jackson and M. Litt, *J. Polym. Sci.*, **1959**, 34, 171.
182. P. Dreyfuss and M. P. Dreyfuss, *Polym. J.*, **1976**, 8, 81.
183. G. Pruckmayr and T. K. Wu, *Macromolecules*, **1978**, 11, 265.
184. K. Matyjaszewski, S. Slomkoski and S. Penczek, *J. Polym. Sci.*, 1979, 17, 2413.
185. S. Penczek and K. Matyjaszewski, *J. Polym. Sci.*, **1976**, 56, 255.
186. D. Vofsi and A. V. Tobolsky, *J. Polym. Sci : Part A*, **1965**, 3, 3261.
187. P. Dreyfuss and m. P. Dreyfuss, *Polymer*, **1965**, 6, 93.
188. A. Sato, T. Hirano, M. Suga, and T. Tsuruta, *Polym. J.*, **1977**, 9, 209.
189. G. A. Latremouille, G. T. Merall and A. m. Eastham, *J. Am. Chem. Soc.*, **1960**, 82, 120.
190. J. Dale et al., *Chem. Tech.*, 3, **1975**.
191. Kobayahsi, S., Morikawa, K., Saegussa, T., *Polym. J.*, 405, 11, 1979.
192. I. M. Robinson and G. Pruckmayr, *Macromolecules*, 1979, 12, 1043.
193. R. O. Colclough and K. Wilkinson, *J. Polym. Sci., Part C*, **1966**, 4, 322.
194. J. L. Down, J. Lewis, B. Moore and K. Wilkinson, *J. Chem. Soc.*, 3771, **1959**.
195. J. M. Hammond, J. F. Hooper and W. G. P. Robertson, *J. Polym. Sci., A-1*, 281, 9, 281.

196. A. M. Eastham, in : *The chemistry of cationic polymerisation* (ed. P. H. Plesch), 1963 Pergamon Press, New York, Ch. 10.
197. E. J. Goethals, *Pure. Appl. Chem.*, **1976**, 38, 435; *Adv. Polym. Sci.*, **1977**, 23, 103.
198. M. R. Bucquoye and E. J. Goethals, *Polym. Bull.*, **1978**, 179, 1681.
199. M. R. Bucquoye and E. J. Goethals, *Polym. Bull.*, **1980**, 2, 713.
200. M. R. Bucquoye and E. J. Goethals, *Makromol. Chem.*, **1981**, 182, 3379.
201. Riat, PhD. Thesis, Aston University, UK.
202. K. Matyjaszewski, M. Zielinski, P. Kubisa, S. Slomkowski, J. Chjonowsky and S. Penczek, *Makromol. Chem.*, **1980**, 181, 146.
203. J. F. Brown, G. m. J. Slusarczuk, *J. Am. Chem. Soc.*, **1965**, 87, 931.
204. J. M. Andrew, F. R. Jones, J. A. Semlyen, *Polymer*, **1974**, 15, 420.
205. T. Kelen D. Schlotterbeck, V. Jaacks, XXIII Congress of IUPAC, Macromolecular Preprint, Boston, USA, Vol. II, p. 649;
J. M. Andrew, F. R. Jones, J. A. Semlyen, *Polymer*, **1972**, 13, 141.
206. N. Calderon, E. A. Ofstead and J. W. Judy, *Tetrahedron Lett.*, **1967**, 5, 2209.
207. J. A. Semlyen, *Adv. Polymer*, **1976**, 21, 41.
208. Y. Imanshi, K. Kugimiya and T. Higashimura, *Biopolymers*, **1973**, 12, 2643;
Biopolymers, **1974**, 13, 1205.
209. T. Saegusa, Y. Hashimoto and S. I. Matsumoto, *Macromolecules*, **1971**, 1, 4.
210. B. A. Rosenberg et al., *Vysokomol. Soed.*, **1977**, 19B, 510.
211. S. Penczek, *Polym. Prep.*, 1988, 2, 38.
212. S. Penczek, H. Sekiguchi, P. Kubisa, Activated monomer polymerisation of cyclic monomers. In : K. Hatada, T. Kitayama, O. Vogl, editors. *Macromolecular design of polymeric materials*. New York : Marcel Dekker, 1997.p.199.
213. S. Penczek and P. Kubisa, Cationic ring-opening polymerisation. In : Brunelle DJ, editor. *Ring-opening polymerisation*. Munich : Hanser Publishers, 1993.
214. S. Penczek, H. Sekiguchi, P. Kubisa, *Makromol. Chem. Makromol. Symp.*, **1986**, 3, 203.
215. P. Kubisa, *Makromol. Chem. Makromol. Symp.*, **1988**, 13/14, 203.
216. T. Biedron, R. Szysmanski, P. Kubisa and S. Penczek, *Makromol. Chem. Makromol. Symp.*, **1990**, 32, 155.
217. M. Bednarek, P. Kubisa and S. Penczek, *Makromol. Chem. Suppl.*, **1989**, 15, 49.
218. M. Bednarek, T. Biedron, P. Kubisa and S. Penczek, *Makromol. Chem. Suppl.*, **1991**, 42/43, 475.

219. M. Wojtania, P. Kubissa and S. Penczek, *Makromol. Chem. Symp.*, **1986**, 6, 201.
220. F. Lagarde, L. Reibel and E. Franta, *Makromol. Chem.*, **1992**, 193, 1087.
221. F. Lagarde, L. Reibel and E. Franta, E., *Makromol. Chem.*, 1992, 193, 1099.
222. F. Lagarde, L. Reibel and E. Franta, E., *Makromol. Chem.*, **1992**, 193, 1109.
223. Y. Okamoto, in *Ring Opening Polymerisation – Kinetics, Mechanism and systems*, J. E. Mc Grath, Ed., American Chemical Society, Washington, DC, Series 286 (25), 1985, p.361.
224. H. Desai, A. V. Cunliffe, M. J. Stewart and A. J. Amass, *Polymer*, **1993**, 34, 642.
225. J. A. Wojtowicz and J. R. Polak, *J. Org. Chem.*, **1973**, 38, 2061.
226. E. J. Vandenberg, J. C. Mullis, R. S. Juvet, T. Mullet and R. A. Nieman, *J. Polym. Sci. Part A*, **1989**, 27, 3113.
227. M. Bednarek, T. Biedron, J. Helinski, K. Kalunzynski, P. Kubisa, S. Penczek, *Macromol. Rapid Commun.*, 1999, 20, 369.
228. H. Magnusson, E. Malmstrom and A. Hult, *Macromol. Rapid Commun.*, **1999**, 20, 453.
229. E. J. Vandenberg, J. C. Mullis and R. S. Juvet Jr., T. Mullet and R. A. Nieman, R. A., *J. Polym. Sci. Part A*, **1989**, 27, 3083.
230. C. C. Price and D. D. Carmelite, *J. Am. Chem. Soc.*, **1966**, 88, 4039.
231. A. A. Solovyanov and K. K. Kasanskii, *Vysokomol. Soedin.*, 1974, **16A**, 595.
232. P. Sigwalt and S. Boileau, *J. Polym. Sci., Polym. Symp.*, **1978**, 62, 51.
233. J. C. Chang, R. F. Kiesel and T. E. Hogen-Esch, *J. Am. Chem. Soc.*, **1973**, 95, 8446.
234. S. Boileau, P. Hemery and J. C. Justice, *J. Solution Chem.*, **1975**, 4, 873.
235. K. S. Kazanski, A. A. Solovyanov and S. G. Entelis, *Europ. Polym. J.*, **1971**, 7, 1421.
236. I. Cabasso and A. Zilkha, *J. Macromol. Sci.-Chem.*, **1974**, A8, 587.
237. D. M. Simons and J. j. Verbanc, *J. Polym. Sci.*, **1960**, 44, 303.
238. A. Deffieux, P. Sigwalt and S. Boileau, *Eur. Polym. J.*, **1984**, 20, 77.
239. A. Deffieux and S. Boileau, *Polymer J.*, **1977**, 18, 1047.
240. M. E. Pruitt and J. M. Bagget, US Patent 2 706 181, 1955, assigned to Dow Chemical CO.
241. L. E. St Pierre and C. C. Price, *J. Am. Chem. Soc.*, **1956**, 78, 3432.
242. M. Osgan and C. C. Price, *J. Polym. Sci.*, **1959**, 34, 153.
243. J. Furukawa, T. Tsuruta, R. Sakata, T. Saegusa and A. Kawasaki, *Makromol. Chem.*, **1959**, 32, 90.
244. R. O. Colclough, G. Gee and A. H. Jagger, *J. Polym. Sci.*, **1960**, 48, 273.

245. E. J. Vandenberg, *J. Polym. Sci.*, 1960, 47, 486.
246. E. J. Vandenberg and A. E. Robinson, in *Polyether*, ed. E. J. Vandenberg, ACS Symp. Ser. 6, American Chemical Society, Washington, DC, 1975, pp101-119.
247. M. Ishimori, G. Hsue and T. Tsuruta, *Makromol. Chem.*, 1969, 128, 52.
248. E. J. Vandenberg and A. E. Robinson, *Polym. Prepr. Am. Chem. Soc., Div. Polym. Chem.*, 1974, 15, 208.
249. N. Oguni and J. Hyoda, *Macromolecules*, 1980, 13, 1687.
250. J. Kops and H. Spanggard, *Macromolecules*, 1982, 15, 1200.
251. E. J. Vandenberg, J. C. Mullis, *J. Polym. Sci. Part A*, 1991, 29, 1421.
252. S. Inoue, T. Tsuruta and J. Furukawa, *Makromol. Chem.*, 1962, 53, 215.
253. T. Tsuruta, S. Inoue, N. Yoshida and J. Furukawa, *Makromol. Chem.*, 1962, 55, 230.
254. N. Spasky, A. Le Borgne and M. Sepulchre, *Pure Appl. Chem.*, 1981, 53, 1735.
255. H. Kageyama, N. Kai, C. Susuki, N. Yoshino and T. Tsuruta, *Makromol. Chem. Rapid Commun.*, 1984, 5, 89.
256. M. Ishimori, T. Higawara, T. Tsuruta, Y. Kai, N. Yasuoka and N. Kasai, *Bull. Chem. Soc. Jpn*, 1976, 49, 1165.
257. M. Ishimori, T. Higawara and T. Tsuruta, *Makromol. Chem.*, 1978, 179, 2337.
258. M. Ishimori, T. Higawara and T. Tsuruta, *Makromol. Chem.*, 1981, 182, 501.
259. H. Hasegawa, K. Miki, N. Tanaka, N. Kasai, M. Ishimori, T. Heki, and T. Tsuruta, *Makromol. Chem. Rapid Commun.*, 1982, 3, 947.
260. T. Aida, S. Inoue, *Macromolecules*, 1981, 14, 1166.
261. S. Asano, T. Aida, S. Inoue, *Macromolecules*, 1985, 15, 2957.
262. T. Yasuda, T. Aida, S. Inoue *Bull. Chem. Soc. Jpn*, 1986, 49, 3931.
263. C. L. Jun, A. Le Borgne and N. Spasky, *J. Polym. Sci. Symp. D*, 1986, 74, 31.
264. S. Inoue, in *Catalysis in Polymer Synthesis*, eds. E. J. Vandenberg and J. C. Salamone, ACS Symp. Ser.496, American Chemical Society, Washington, DC, 1992, pp194-204.
265. S. Inoue and T. Aida, in *Ring Opening Polymerisation*, eds. D. J. Brunelle. Hanser Verlag, Munich, 1993, pp197-215.
266. A. J. Amass, M. C. Perry, D. S. Riat, B. J. Tighe, Colcough and M. J. Stewart, *Eur. Polym. J.*, 1994, 30, 641.
267. S. Inoue, IUPAC International on Ionic Polymerization, Istanbul, Turkey, 1995, Abstracts, p. 60.
268. D. Takeuchi, Y. Watanabe, T. Aida and S. Inoue, *Macromolecules*, 1995, 28, 651.

269. T. Aida, Y. Maekawa, S. Asano and S. Inoue, *Macromolecules*, **1988**, 21, 1195.
270. V. Vincens, A. Le Borgne and N. Spasky, in *Catalysis in Polymer Synthesis*, eds. E. J. Vandenberg and J. C. Salamone, ACS Symp. Ser.496, American Chemical Society, Washington, DC, 1992, pp 205-214.
271. S. G. Dzugan and V. L. Goedken, *Inorg. Chem.*, **1986**, 25, 2858.
272. W. Kuran, IUPAC *International Symposium in ionic polymerisation*, Istanbul, Turkey, 1995, Abstracts, p. 20.
273. W. Kuran, T. Listos and M. Abramczyk, IUPAC International Symposium in Ionic Polymerization, Istanbul, Turkey, 1995, Abstracts, p. 101.
274. W. Kuran, T. Listos and M. Abramczyk, *J. Macromol. Sci.-Pure Appl. Chem. A*, **1998**, 45, 427.
275. M. Kuroki, Y. Watanabe, T. Aida and S. Inoue, *J. Am. Chem. Soc.*, **1991**, 32, 5903.
276. Y. Watanabe, T. Aida and S. Inoue, *Macromolecules*, **1990**, 23, 2612.
277. S. Inoue and T. Aida, T., *Macromol. Symp.*, **1994**, 88, 117.
278. S. Inoue and T. Aida, *Chemtech.*, **1994**, 24, 28.
279. T. Saegusa, Y. Hashimoto and S. I. Matsumoto, *Macromolecules*, **1968**, 1, 442.
280. V. Perec, *Polym. Bull.*, **1981**, 5, 651.
281. H. Jakobson, W. H. Stockmayer, *J. Chem. Phys.*, **1950**, 18, 1600.
282. P. J. Flory, *J. Chem. Phys.*, **1949**, 17, 303.
283. H. J. Alkema and R. Van Helden, *Chem. Abstr.*, 1968, 69, 95906, 96 066.
284. H. Höcker and R. Musch, *Makromol. Chem.*, **1974**, 175, 1395.
285. K. W. Scott, N. Calderon, E. A. Ofstead, J. W. Judy and J. P. Ward, *Adv. Chem. Ser.*, **1969**, 91, 399.
286. V. M. Cherednichenko, *Polymer Sci U.S.S.R.*, **1979**, 20, 1225.
287. R. H. Biddulph, P. M. Plesh and P. Rutherford, *J. Chem. Soc.*, 274, 1964.
288. N. N. Greenwood and R. L. Martin, "*Boron trifluoride coordination compounds*", *Qt. Revs.* **1954**, 8, 1-39.
289. G. Olah (ed.), *Friedel-Craft and related reactions*, Interscience, New York, 1963 (4 volumes).
290. M. J. Dubreuil, N. G. Farcy and E. J. Goethals, *Macromol. Rapid Commun.*, **1999**, 20, 383.
291. R. Cotrel, G. Sauvet, J. P. Vairon and P. Sigwalt, *Macromolecules*, **1976**, 9, 931.
292. R. Cotrel, G. Sauvet, J. P. Vairon and P. Sigwalt, *Eur. Polym. J.*, **1974**, 10, 501.
293. Gouarderes PhD. Thesis, Aston University, UK.

294. J. Furukawa, *Polymer*, **1962**, 3, 487.
295. A. Ishigaki, T. Shono and Y. Hashiama, *Makromol. Chem.*, **1964**, 79, 170.
296. T. Tsuda, T. Nomura and Y. Yamashita, *Makromol. Chem.*, **1965**, 86, 301.
297. T. Tsuda and Y. Yamashita, *Makromol. Chem.*, **1966**, 99, 297.
298. M. Matsuda, F. Akiyama and Y. Hara, *Chem. Abstr.*, **1975**, 83, 206611x.
299. B.D. Coleman and T. G. Fox, *J. Am. Chem. Soc.*, **1963**, 85, 1241.
300. R. V. Figini, *Makromol. Chem.*, **1964**, 71, 193.
301. R. V. Figini, *Makromol. Chem.*, **1967**, 107, 170.
302. M. Szwarc and J. J. Hermans, *J. Polym. Sci. Part B*, **1964**, 2, 815.
303. L. L. Böhm, *Z. Phys. Chem. (Frankfurt)*, **1970**, 72, 199.
304. L. L. Böhm, *Z. Phys. Chem. (Frankfurt)*, **1974**, 88, 297.
305. S. Krause, L. Defonso and D. L. Glusker, *J. Polym. Sci. Part A*, **1965**, 3, 1617.
306. J. P. Kennedy, *J. Polym. Sci., Part A, Polym. Chem.*, **1999**, 37, 2285.
307. J. P. Kennedy, T. Kelen and F. Tudos, *J. Makromol. Sci., Chem A*, **1982-1983**, 18, 1189.
308. R. Faust, A. Fehervari and J. P. Kennedy, *J. Makromol. Sci., Chem A*, **1982-1983**, 18, 1209.
309. J. Puskas, G. Kasas, J. P. Kennedy, T. Kelen and F. Tudos, *J. Makromol. Sci., Chem A*, **1982-1983**, 18, 1245.
310. J. Puskas, G. Kasas, J. P. Kennedy, T. Kelen and F. Tudos, *J. Makromol. Sci., Chem A*, **1982-1983**, 18, 1229.
311. R. Faust, J. P. Kennedy, *J. Polym. Sci.: Part A: Polym. Chem.*, **1987**, 25, 1847.
312. J. M. Sawamoto and J. P. Kennedy, *J. Makromol. Sci., Chem A*, **1982-1983**, 18, 1275.
313. J. M. Sawamoto and J. P. Kennedy, *J. Makromol. Sci., Chem A*, **1982-1983**, 18, 1301.
314. S. Aoshima, H. Oda, E. Kobayashi, *J. Polym. Sci.: Polym. Chem.*, **1992**, 30, 2407.
315. S. Aoshima, S. Iwasa, E. Kobayashi, *Polym. J. (Tokyo)*, **1994**, 26, 912.
316. S. Asthana, S. Varanasi, R. m. Lemert, *J. Polym. Sci., Part A: Polym. Chem.*, **1996**, 34, 1993.
317. T. Hashimoto, T. Iwata, A. Minami, T. Kodaira, *J. Polym. Sci., Part A: Polym. Chem.*, **1998**, 26, 335.
318. T. Hashimoto, T. Iwata, N. Uchiyama, T. Kodaira, *J. Polym. Sci., Part A: Polym. Chem.*, **1999**, 15, 2923.

319. S. Aoshima, T. Fujisawa and E. Kobayashi, *J. Polym. Sci.: Part A: Polym. Chem.*, **1994**, 32, 1719.
320. T. Saegusa, Y. Hashimoto and S. Matsumoto, *Macromolecules*, **1971**, 1, 4.
321. A. A. Frost and R. G. Pearson. "*Kinetic and mechanism*", John Wiley & Sons, Inc., N. Y., **1961**.
322. T. Saegusa, F. Fujii, S. Kobayashi, H. Ando and R. Kawase, *Macromolecules*, **1973**, 6, 26.
323. J. A. Riddick and W. Bunger, "*Organic chemistry*", Wiley-Interscience, N. Y., **1970**.
324. C. K. Ingold, "*Structure and Mechanism in organic Chemistry*", (2nd Ed.), Cornell University Press, Ithaca, N. Y., **1969**, 457.
325. H. Sasaki, J. m. Rudzinski and T. Kakuci, *J. Polym. Sci.: Part A*, **1995**, 33, 1807.
326. S. Aoki, Y. Harita, Y. Tanaka, H. Mandai and T. Otsu, *J. Polym. Sci.: Part A-1*, **1968**, 6, 2585.
327. T. Kagiya, Y. Sumita and T. Inoue, *Polym. J.*, **1970**, 1, 312.
328. F. S. Dainton, T. R. E. Devlin and P. A. Small, *Trans Faraday Soc.*, **1955**, 51, 1710.
329. J. Furukawa, *Polymer*, **1962**, 3, 487.
330. A. Ledwith and D. C. Sherrington, *Adv. Poly. Sci.*, **1975**, 19, 1.
331. F. J. Burgess, A. V. Cunliffe, D. H. Richards and D.C. Sherrington, *J. Polym. Sci. Polym. Lett. Ed.*, **1976**, 14, 471.
332. F. J. Burgess, A. V. Cunliffe, J. R. MacCalum and D. H. Richards, *Polymer*, **1977**, 18, 719.
333. F. J. Burgess, A. V. Cunliffe, J. R. MacCalum and D. H. Richards, *Polymer*, **1977**, 18, 726.
334. F. J. Burgess, A. V. Cunliffe, J. V. Dawkins and D. H. Richards, *Polymer*, **1977**, 18, 733.
335. F. J. Burgess, A. V. Cunliffe, D. H. Richards and D. Thompson, *Polymer*, **1978**, 19, 334.
336. K. Boehkle, P. Weyland and V. Jaacks, XXIII IUPAC Congress, Boston 1971, Vol 2, p. 641.
337. G. Sauvet, J. p. Vairon and P. Sigwalt, *Eur. Polym. J.*, **1974**, 10, 501.
338. H. Mayr, R. Schneider and C. Schade, *Makromol. Chem. Symp.*, **1988**, 13-14, 43.